THE ROLE OF THE ENVIRONMENT IN AUTOIMMUNITY

EDITED BY: Allen Jay Rosenspire, Kenneth Michael Pollard and James J. Pestka
PUBLISHED IN: Frontiers in Immunology

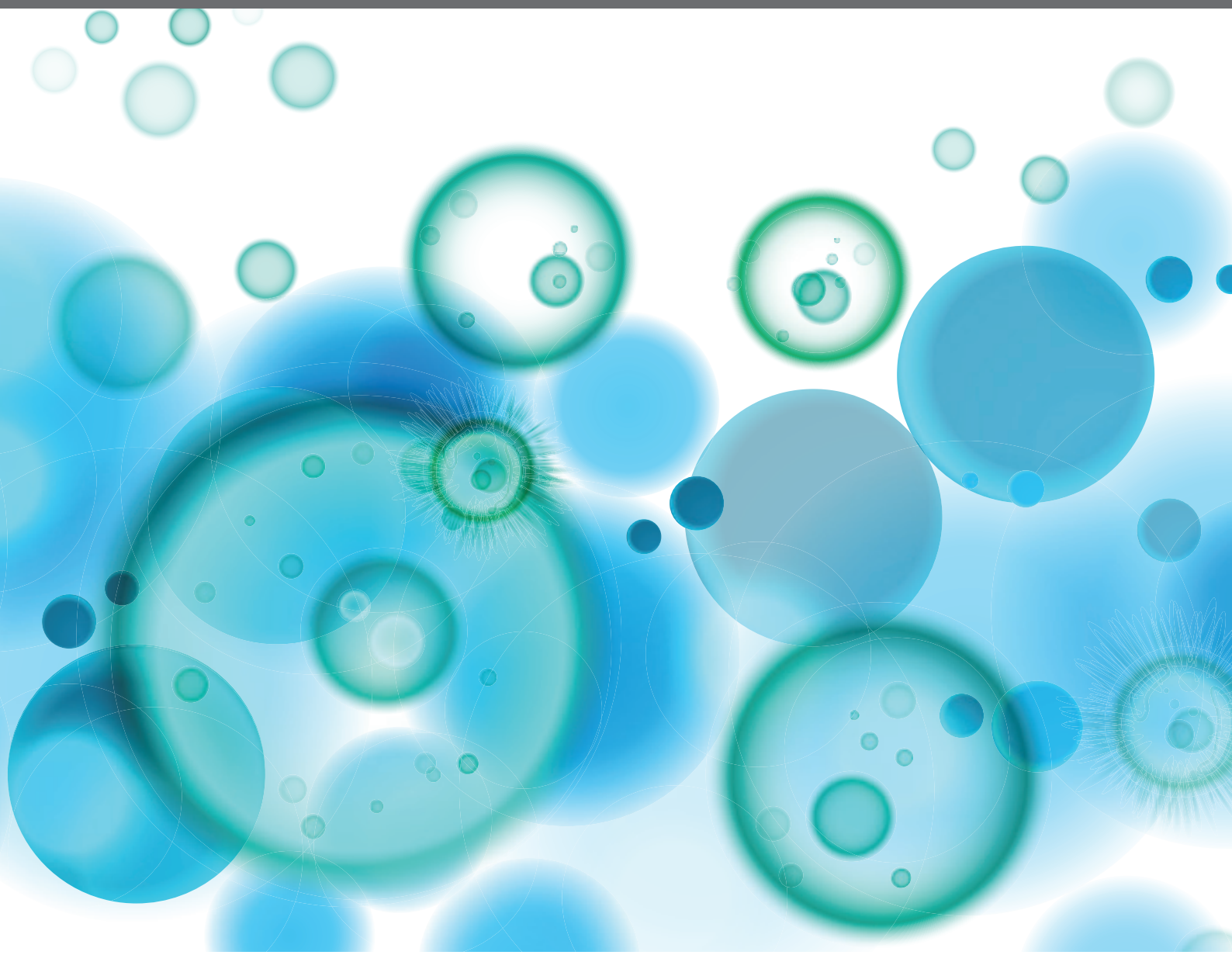

frontiers Research Topics

frontiers

ISSN 1664-8714
ISBN 978-2-88966-647-8
DOI 10.3389/978-2-88966-647-8

About Frontiers

Frontiers is more than just an open-access publisher of scholarly articles: it is a pioneering approach to the world of academia, radically improving the way scholarly research is managed. The grand vision of Frontiers is a world where all people have an equal opportunity to seek, share and generate knowledge. Frontiers provides immediate and permanent online open access to all its publications, but this alone is not enough to realize our grand goals.

Frontiers Journal Series

The Frontiers Journal Series is a multi-tier and interdisciplinary set of open-access, online journals, promising a paradigm shift from the current review, selection and dissemination processes in academic publishing. All Frontiers journals are driven by researchers for researchers; therefore, they constitute a service to the scholarly community. At the same time, the Frontiers Journal Series operates on a revolutionary invention, the tiered publishing system, initially addressing specific communities of scholars, and gradually climbing up to broader public understanding, thus serving the interests of the lay society, too.

Dedication to Quality

Each Frontiers article is a landmark of the highest quality, thanks to genuinely collaborative interactions between authors and review editors, who include some of the world's best academicians. Research must be certified by peers before entering a stream of knowledge that may eventually reach the public - and shape society; therefore, Frontiers only applies the most rigorous and unbiased reviews.
Frontiers revolutionizes research publishing by freely delivering the most outstanding research, evaluated with no bias from both the academic and social point of view. By applying the most advanced information technologies, Frontiers is catapulting scholarly publishing into a new generation.

What are Frontiers Research Topics?

Frontiers Research Topics are very popular trademarks of the Frontiers Journals Series: they are collections of at least ten articles, all centered on a particular subject. With their unique mix of varied contributions from Original Research to Review Articles, Frontiers Research Topics unify the most influential researchers, the latest key findings and historical advances in a hot research area! Find out more on how to host your own Frontiers Research Topic or contribute to one as an author by contacting the Frontiers Editorial Office: frontiersin.org/about/contact

THE ROLE OF THE ENVIRONMENT IN AUTOIMMUNITY

Topic Editors:
Allen Jay Rosenspire, Wayne State University, United States
Kenneth Michael Pollard, The Scripps Research Institute, United States
James J. Pestka, Michigan State University, United States

Citation: Rosenspire, A. J., Pollard, K. M., Pestka, J. J., eds. (2021). The Role of the Environment in Autoimmunity. Lausanne: Frontiers Media SA.
doi: 10.3389/978-2-88966-647-8

Table of Contents

frontiers in Immunology

EDITORIAL
published: 22 February 2021
doi: 10.3389/fimmu.2021.641171

Editorial: The Role of the Environment in Autoimmunity

James J. Pestka[1,2]*, *K. Michael Pollard*[3]* and *Allen J. Rosenspire*[4]*

[1] Department of Microbiology and Molecular Genetics, Michigan State University, East Lansing, MI, United States, [2] Institute for Integrative Toxicology, Michigan State University, East Lansing, MI, United States, [3] Department of Molecular Medicine, Scripps Research, La Jolla, CA, United States, [4] Department of Biochemistry, Microbiology and Immunology, Wayne State University, Detroit, MI, United States

Keywords: environment, trigger, toxicant, autoimmunity, inflammation, autoantibody, lupus (SLE), tolerance

Editorial on the Research Topic

The Role of the Environment in Autoimmunity

Preclinical and epidemiologic investigations reveal that environmental factors may impact multiple immune system checkpoints within the framework of an individual's unique genetics to potentiate or attenuate onset and/or flaring and drive the progression of autoimmunity. Examples of environmental factors include anthropogenic chemicals, pesticides, respirable particles, drugs, microbes, and diet. Here we present a themed collection containing five reviews, eight original research articles, and one opinion from leading scientists who have contributed to our current understanding of the role of environment on autoimmune disease. This compilation is dedicated to the memory of Dr. Noel Rose who passed away this past year (1, 2). Dr. Rose, universally recognized as the father of autoimmune research, stressed from the beginning the fundamentally intertwined roles of genetics and environment in autoimmune disease. He was a mentor and role model for countless immunologists including the guest associate editors.

A striking feature of environmental factors that affect autoimmunity is their astounding diversity. This Research Topic, although barely scratching the surface, discusses some of these factors currently under investigation. For instance, there is building evidence suggesting that atmospheric particulate matter (PM) exposures aggravate a range of autoimmune diseases. AHR, a ligand activated transcription factor, is activated by organic toxicants including those present in PM such as dioxins and polycyclic aromatic hydrocarbons. The comprehensive review by O'Driscoll and Mezrich focuses on the AHR as a potential mechanistic target for modulating T cell responses associated with PM-mediated autoimmune disease citing the most recent literature on the role of this transcription factor in autoreactive T cell function and autoimmune disease.

The industrial solvent trichloroethylene (TCE), a drinking water pollutant, has been implicated in $CD4^+$ T cell-mediated autoimmunity. In mice, these effects were sustained in adult mice after developmental and early life exposure to TCE. Byrum et al. determined whether these persistent effects are associated with epigenetic changes by assessing methylation of CpG sites in autosomal chromosomes in activated effector/memory $CD4^+$ T cells The investigators found that developmental exposure to TCE differentially methylated binding regions of polycomb group (PcG) proteins in effector/memory $CD4^+$ cells that lasted into adulthood.

Farming and pesticide use have been linked to systemic autoimmune diseases, however, the role of specific pesticides is unclear. In an elegant study, Parks et al. related serum antinuclear autoantibodies (ANAs) in 668 male farmers to lifetime use of 46 different pesticides. ANAs were

OPEN ACCESS

Edited and reviewed by:
Betty Diamond,
Feinstein Institute for Medical Research, United States

***Correspondence:**
James J. Pestka
pestka@msu.edu
K. Michael Pollard
mpollard@scripps.edu
Allen J. Rosenspire
arosenspire@wayne.edu

Specialty section:
This article was submitted to Autoimmune and Autoinflammatory Disorders, a section of the journal Frontiers in Immunology

Received: *13 December 2020*
Accepted: *02 February 2021*
Published: *22 February 2021*

Citation:
Pestka JJ, Pollard KM and Rosenspire AJ (2021) Editorial: The Role of the Environment in Autoimmunity. Front. Immunol. 12:641171. doi: 10.3389/fimmu.2021.641171

positively associated with exposure to the fumigant methyl bromide, the carbamate insecticide aldicarb, and combined use of four cyclodiene organochlorine insecticides but inversely associated with non-cyclodiene organochlorine insecticides. Accordingly, specific organochlorine insecticides might pose a risk of developing systemic autoimmunity.

Exposure to respirable crystalline silica in occupations such as construction, mining, and farming is associated with development of autoimmune diseases including systemic lupus erythematosus (lupus). In the lupus-prone female NZBWF1 mouse, weekly repeated airway exposure over 1 month to silica triggers pulmonary ectopic lymphoid neogenesis, systemic autoantibody elevation, and glomerulonephritis. Bates et al. report that within 1 week after silica exposure, increases in mRNAs associated with chemokine release, cytokine production, sustained interferon activity, complement activation, and adhesion molecules were evident in the lung that increased over the course of the 3-month long experiment. Aberrant expression of innate and adaptive immune genes was observed later in the spleen and kidney. These findings suggest that upon silica exposure, the lung functions as the central autoimmune nexus for launching systemic autoimmunity and ultimately, glomerulonephritis. In a related contribution, Foster et al. used normal C57BL/6 and lupus-prone BXSB, MRL, and NZB strains and mice carrying an autoantibody transgene on each of these backgrounds to elucidate how silica lung exposure affects B cell tolerance and unleashes autoreactive B cells. Their findings suggest that silica-induced lung injury has systemic effects that subtly influence autoreactive B cell regulation, perhaps modulating B cell anergy, and that can be revealed by exposure to TLR ligands or other immunostimulants.

Environmental encounters with microbes including viruses and bacteria can influence development of autoimmunity. Notably, exposure to Epstein-Barr virus (EBV) infection is a risk factor for multiple rheumatic diseases. Xuan et al. assessed the association of EBV antibodies with Sjögren's syndrome (SjS) and found that patients with SjS had both a significantly higher prevalence and titers to EBV early antigen and higher titers to EBV viral capsid antigen than case controls. Subsequent meta-analysis of 14 seroepidemiological studies found associations between SjS and antibodies to EBV early antigen and viral capsid antigen.

Antiphospholipid antibodies (aPL), a large family of heterogeneous autoantibodies with the affinity toward negatively charged phospholipids or protein-phospholipid complexes, potentially contribute to antiphopholipid syndrome (APS) leading to vascular thrombosis and miscarriage. The review by Martirosyan et al. focuses on how potential environmental triggers such as viruses, bacteria, fungi, parasite, vaccines, drugs, and other factors induce aPL and might contribute to APS in genetically susceptible individuals.

Gut microbiome dysbiosis has been linked to the onset of different autoimmune diseases. Khan and Wang review recent epidemiological and mechanistic evidence connecting environmental exposures with various autoimmune diseases. They additionally discuss how gut microbiome composition changes might influence disease pathogenesis, particularly in response to exposure to environmental chemicals.

In an Opinion paper, Frew extends the hygiene hypothesis by posing the provocative proposition, based on overlapping gene associations identified by GWAS, that pathogen-specific positive selection might explain disparate rates of autoimmune and allergic disease in different human populations.

Diet selection taken in the context of the underlying genetic background can exacerbate or delay the development of autoimmune diseases. Patients with lupus have increased prevalence of metabolic syndrome but the underlying mechanisms are unknown. Activation of TLR 7 by single stranded-RNA has a critical role in antimicrobial host defense and in the initiation and progression of lupus both in mice and humans. Hanna Kazazian et al. demonstrated that TLR7 signaling plays an essential role high fat diet-induced metabolic syndrome and exacerbation of lupus autoimmunity in TLR8-deficient mice. They further posit that this TLR might be a novel target in tailored therapy in lupus and metabolic diseases. Also related to diet, Song et al. provide a meta-analysis of 22 clinical studies to estimate the association of thyroid autoimmunity and dysfunction with obesity. They found that obesity was significantly correlated with positive thyroid peroxidase antibody and was associated with an increased risk of Hashimoto's thyroiditis, suggesting that prevention of obesity is crucial for thyroid disorders.

Preclinical studies suggest that consumption of ω-3 polyunsaturated fatty acids (PUFAs) found in fish oil might be used as an intervention against the development of autoimmune diseases. Li et al. reviewed clinical studies using ω-3 fatty acids as interventions against lupus, rheumatoid arthritis, type 1 diabetes (T1D) and multiple sclerosis. While many clinical studies found positive effects, some didn't. These discrepancies are likely related to different dose, source, and duration of ω-3 PUFAs treatments. A key limitation of many of these studies was the lack of data on blood concentrations of the ω-3s DHA and EPA of the enrolled patients, making it difficult to evaluate if the enrolled patients for their studies have indeed gained sufficient ω-3 PUFAs in their diet.

The anti-inflammatory and pro-resolving effects of ω-3 PUFAs are inextricably linked to their presence in membrane phospholipids which can be ready measured in red blood cells (RBCs) and reflected as two biomarkers- the ω-3 highly unsaturated fatty acid (HUFA, i.e., PUFA of $\geq$ C20) score and the Omega-3 Index (O3I). Using data from prior preclinical DHA supplementation studies in the silica-triggered NZBWF1 mouse model, Wierenga et al. found that increases in both the ω-3 HUFA score (>40%) and the O3I (>10%) were strongly associated with suppression of silica-triggered lupus. These ω-3 HUFA scores and O3I thresholds are attainable in humans and could be targeted in future ω-3 PUFA intervention studies for autoimmune diseases. Finally, at the mechanistic level, silica-induced inflammasome activation is believed to be a critical first step for autoimmune triggering. Wierenga et al. found that DHA pre-incubation suppressed

silica-induced inflammasome activation and release of IL-1β and IL-1α in macrophages and that these suppressive effects were linked to inhibition of LPS-induced *Nlrp3*, *Il1b*, and *Il1a* transcription, potentially through the activation of the transcription factor PPARγ.

In conclusion, this collection provides new perspectives on how selected environmental influences impact autoimmunity, particularly in genetically susceptible individuals. We hope that this topic will stimulate further advances in the field that can be translated into preventive and intervention strategies to counter autoimmune disease.

AUTHOR CONTRIBUTIONS

JP, KP, and AR contributed to writing and editing this editorial. All authors contributed to the article and approved the submitted version.

FUNDING

This research was funded in part by NIH ES027353 (JP), ES029581 (KP), NIH ES029484 (AR), USDA NIFA Hatch Project 1020129 (JP), and the Dr. Robert and Carol Deibel Family Endowment (JP).

REFERENCES

1. Watts G. Noel Richard Rose. *Lancet.* (2020) 396:880. doi: 10.1016/S0140-6736(20)31975-9
2. Scott DW, Caspi RR, Moudgil KD, Noel R. Rose 1927–2020. *Nat Immunol.* (2020) 21:1306. doi: 10.1038/s41590-020-0790-6

Conflict of Interest: The authors declare that the research was conducted in the absence of any commercial or financial relationships that could be construed as a potential conflict of interest.

frontiers in Immunology

HYPOTHESIS AND THEORY
published: 06 December 2018
doi: 10.3389/fimmu.2018.02833

The Aryl Hydrocarbon Receptor as an Immune-Modulator of Atmospheric Particulate Matter-Mediated Autoimmunity

Chelsea A. O'Driscoll[1,2] *and Joshua D. Mezrich*[1]*

[1] *Division of Transplantation, Department of Surgery, School of Medicine and Public Health, University of Wisconsin-Madison, Madison, WI, United States,* [2] *Molecular and Environmental Toxicology Center, School of Medicine and Public Health, University of Wisconsin-Madison, Madison, WI, United States*

This review examines the current literature on the effects of atmospheric particulate matter (PM) on autoimmune disease and proposes a new role for the aryl hydrocarbon receptor (AHR) as a modulator of T cells in PM-mediated autoimmune disease. There is a significant body of literature regarding the strong epidemiologic correlations between PM exposures and worsened autoimmune diseases. Genetic predispositions account for 30% of all autoimmune disease leaving environmental factors as major contributors. Increases in incidence and prevalence of autoimmune disease have occurred concurrently with an increase in air pollution. Currently, atmospheric PM is considered to be the greatest environmental health risk worldwide. Atmospheric PM is a complex heterogeneous mixture composed of diverse adsorbed organic compounds such as polycyclic aromatic hydrocarbons (PAHs) and dioxins, among others. Exposure to atmospheric PM has been shown to aggravate several autoimmune diseases. Despite strong correlations between exposure to atmospheric PM and worsened autoimmune disease, the mechanisms underlying aggravated disease are largely unknown. The AHR is a ligand activated transcription factor that responds to endogenous and exogenous ligands including toxicants present in PM, such as PAHs and dioxins. A few studies have investigated the effects of atmospheric PM on AHR activation and immune function and demonstrated that atmospheric PM can activate the AHR, change cytokine expression, and alter T cell differentiation. Several studies have found that the AHR modulates the balance between regulatory and effector T cell functions and drives T cell differentiation *in vitro* and *in vivo* using murine models of autoimmune disease. However, there are very few studies on the role of AHR in PM-mediated autoimmune disease. The AHR plays a critical role in the balance of effector and regulatory T cells and in autoimmune disease. With increased incidence and prevalence of autoimmune disease occurring concurrently with increases in air pollution, potential mechanisms that drive inflammatory and exacerbated disease need to be elucidated. This review focuses on the AHR as a potential mechanistic target for modulating T cell responses associated with PM-mediated autoimmune disease providing the most up-to-date literature on the role of AHR in autoreactive T cell function and autoimmune disease.

Keywords: atmospheric particulate matter, T cells, autoimmune disease, autoimmunity, aryl hydrocarbon receptor, polycyclic aromatic hydrocarbons

OPEN ACCESS

Edited by:
Kenneth Michael Pollard, The Scripps Research Institute, United States

Reviewed by:
David H. Sherr, Boston University, United States
Laura Mandik-Nayak, Lankenau Institute for Medical Research, United States

***Correspondence:**
Joshua D. Mezrich
mezrich@surgery.wisc.edu

Specialty section:
This article was submitted to Autoimmune and Autoinflammatory Disorders, a section of the journal Frontiers in Immunology

Received: *02 October 2018*
Accepted: *16 November 2018*
Published: *06 December 2018*

Citation:
O'Driscoll CA and Mezrich JD (2018) The Aryl Hydrocarbon Receptor as an Immune-Modulator of Atmospheric Particulate Matter-Mediated Autoimmunity. Front. Immunol. 9:2833. doi: 10.3389/fimmu.2018.02833

BACKGROUND

Currently, there are over 80 recognized autoimmune diseases (1). In the United States alone, autoimmune diseases are among the most prevalent diseases effecting 24.5 million people or approximately 8% of the population (1, 2). Both incidence and prevalence of autoimmune diseases have been increasing worldwide (3–5), however the reasons for these increases remain unknown (4). Autoimmune disease results from failure of cells and tissues to distinguish self from non-self leading to a loss of self-tolerance and autoimmune pathology. Autoreactive T cells play a critical role in development of autoimmune diseases such as type 1 diabetes (T1D), rheumatoid arthritis (RA), multiple sclerosis (MS), and systemic lupus erythematosus (SLE) (6–10). Genetic predispositions account for approximately 30% of autoimmune diseases, leaving environmental factors as a major contributor (11, 12). While genetic predispositions play a role in disease incidence (13), epidemiologic studies strongly support that high levels of air pollution, specifically, particulate matter (PM) in the atmosphere, increase the incidence and severity of autoimmune disease (1, 3).

PM, a component of air pollution, has emerged as the largest environmental risk factor for mortality worldwide (14). While many people equate exposure to inhaled PM with airway disease, its role in other systemic illnesses has also been well documented. Increases in incidence of autoimmune disease have occurred concurrently with increases in global air pollution (3, 4, 14, 15). Exposure to PM has been associated with aggravation of several autoimmune diseases including T1D, MS, RA, and SLE (16–32). Epidemiologic studies strongly suggest that exposure to PM can increase both incidence and severity of autoimmune diseases (33, 34).

Atmospheric PM is a complex mixture of solid particles and liquid droplets formed from a combination of primary sources, such as road transportation (diesel exhaust PM), stationary combustion (mainly domestic coal burning) and industrial processes (35), that emit PM directly into the atmosphere and secondary sources, such as gaseous vegetative emissions, motor vehicle emissions, and wood-smoke emissions (36), that emit gaseous PM precursors into the atmosphere and undergo oxidation reactions to form PM (35, 36). The diverse primary emission sources and secondary chemical reactions that lead to atmospheric PM components result in complex mixtures of PM components that include metals, nitrates, sulfates, and diverse organic compounds like polycyclic aromatic hydrocarbons (PAHs) (37, 38).

PM contains organic compounds such as PAHs and dioxins, among others, which are aryl hydrocarbon receptor (AHR) ligands, adsorbed to its surface (37–40). The AHR is ligand-activated transcription factor that responds to exogenous ligands, as well as endogenous ligands, and upregulates cytochrome P450 (CYP) metabolizing enzymes as well as other gene targets (40). The majority of high affinity AHR ligands are synthetic in nature and include 2,3,7,8-tetrachlorodibenzo-p-dioxin (TCDD), the prototypic AHR ligand, and PAHs, among others (41, 42). The most potent AHR ligands are more metabolically stable, like TCDD and dioxin-like compounds, whereas less potent ligands, like PAHs, are more metabolically labile (41). Early studies of the AHR focused on understanding the underlying mechanisms of TCDD toxicity. It was discovered that TCDD exposure caused severe toxicity and life-threatening manifestations such as progressive liver failure, emphysema, renal failure, and myocardial degeneration, among other pathologies (43). In addition to these manifestations, rodent studies described immune phenotypes of TCDD exposure revealing a role of AHR in the immune system. Following TCDD exposure, rodents suffered profound effects on the developing immune system as well as dose-dependent thymic involution, depletion of other lymphoid organs, and reduced circulating lymphocyte counts (43). The discovery of immune pathologies associated with TCDD exposure led immunologists to focus on the AHR.

The AHR has been studied in many aspects of immunology, but a major focus has been on regulatory and effector T cell differentiation and function. *Ahr* is expressed in most $CD4^+$ T cell subsets, with highest expression in T helper (Th)17, type 1 regulatory T cells (Tr1), forkhead box P3 $(FOXP3)^+$ regulatory T cells (Treg), followed by Th1 and Th2 (44, 45) and is critical in modulating the balance between Th17 and Treg cells (44, 46). TCDD has been associated with an increase in Treg cells and immunosuppression, whereas other ligands such as 6-formylindolo[3,2-b] carbazole (FICZ), a tryptophan breakdown product, has been associated with enhanced Th17 effector cells and inflammation (44, 46). In the context of autoimmune disease, TCDD has been shown to enhance Treg differentiation and suppress experimental autoimmune encephalomyelitis (EAE), a murine model of autoimmune disease, and FICZ has been shown to enhance Th17 differentiation and worsen EAE (44, 46).

This review summarizes the current research regarding the role of PM on development and/or progression of autoimmune disease. We first provide a brief overview of the role autoreactive T cells play in autoimmune diseases and summarize the evidence that PM impacts T cells and autoimmune disease. Given the numerous and extensive reviews on AHR ligands (40, 47), we only highlight PM-mediated AHR effects *in vitro* and *in vivo*. We then focus on the AHR as the receptor central to the mechanism behind modulating T cell responses in PM-mediated autoimmune disease. We chose to focus on four diseases, T1D, RA, MS, and SLE as strong correlations between PM exposure and worsened disease have been observed and the AHR has been linked to these diseases as well. We examine the data demonstrating the effects of organic constituents adhered to PM, specifically AHR ligands, on T cells and suggest the AHR pathway as a target for modulating PM-mediated autoimmune disease. We propose a novel hypothesis that AHR ligands present in atmospheric PM activate the AHR shifting the T cell balance from regulatory to effector ultimately leading to PM-mediated autoimmune disease.

THE ROLE OF AUTOREACTIVE T CELLS IN AUTOIMMUNE DISEASE

In an attempt to develop a rigorous immune system that can react quickly and decisively to outside insults and internal threats

(including bacteria, viruses, and dysfunctional/dysregulated cells), but at the same time to avoid autoimmune insults, multiple non-redundant checkpoints have evolved during the development of immune cells to delete self-reactive lymphocytes and generate self-tolerance (4). Central tolerance eliminates self-reactive T cells during their development by negative selection, however, this process is leaky and some self-reactive lymphocytes escape to the periphery (4, 48). Mechanisms of peripheral tolerance control these autoreactive T cells to avoid damage to cells and tissues through employment of anergy, immunological ignorance, and/or regulation (4). Suppression of autoreactive T cells by Tregs is one critical pathway in the induction of peripheral tolerance (4). Regulatory T cells suppress the actions of effector T cells and control the immune response through cell contact, secretion of inhibitor cytokines, and competition for growth factors (4, 49, 50). Tregs can become overwhelmed by persistent inflammation during an immune response or in some cases are dysfunctional resulting in unregulated effector responses and ultimately autoimmune disease (4, 49, 51–53). The complex development of lymphocytes and random rearrangement of adaptive lymphocyte receptors allows for immense diversity of antigen receptor specificity but comes at the cost of creating self-reactive T lymphocytes that escape to the periphery and evade or overcome peripheral tolerance mechanisms ultimately leading to autoimmune disease (54).

Autoreactive T cells play a role in the pathology of autoimmune disease by overcoming central and peripheral tolerance and rendering Tregs insufficient to dampen inflammatory responses. Genetic predispositions account for less than half of all autoimmune disease leaving environmental factors like PM as a potential contributor to the development of autoreactive T cells. Our studies focus on identifying the active component of PM that exacerbates autoimmune disease and elucidating the mechanism through which it acts. Currently, the focus is on understanding how PAHs present in PM act through the AHR to shift the T cell balance and alter autoimmune disease states.

PARTICULATE MATTER

Defining PM

PM is a complex mixture of solid particles and liquid droplets that vary in physical and chemical properties as well chemical composition and origin, over time and space (35, 55). PM is defined based on size, specifically aerodynamic equivalent diameter (AED) (56). AED is a measure of behavior of the particle in the air and is a function of particle diameter, density, shape, and surface characteristics (57). The particles are further subdivided into AED fractions based on how the particles are generated and their ability to penetrate and deposit in human airways: PM_{10} ($<10\,\mu M$), $PM_{2.5}$ ($<2.5\,\mu M$), $PM_{0.1}$ ($<0.1\,\mu M$) (56). It is important to appreciate that PM_{10} contains, ultrafine $PM_{0.1}$, fine $PM_{0.1-2.5}$, and coarse $PM_{2.5-10}$ fractions (56). By far, the greatest number of particles fall into the ultrafine size range, PM with an AED of $0.1\,\mu M$ or less ($PM_{0.1}$) (35). The total number and the total surface area of these particles increases exponentially as the diameter of the particle deceases, and as the diameter of the particle decreases, the total particle mass exponentially decreases (56). $PM_{0.1}$ ultrafine particles are inherently unstable in the atmosphere and coagulate and condensate to form larger particles (35). $PM_{2.5}$ fine particles also grow by coagulation and condensation in the atmosphere (35). PM_{10} coarse particles vary in size and while they contribute little to particle number, they contribute majorly to particle mass (35).

Composition and Sources of PM

Atmospheric PM is a complex mixture of solid particles and liquid droplets formed from a combination of primary sources that emit PM directly into the atmosphere and secondary sources that emit gaseous PM precursors into the atmosphere and undergo oxidation to form PM (35, 36). These complex mixtures of PM components include metals, nitrates, sulfates and diverse organic compounds like PAHs (37, 38). Anthropogenic primary sources include road transportation (diesel exhaust particulate matter), stationary combustion (mainly domestic coal burning) and industrial processes (35). The nature of the industrial particles depends on the process; however combustion particles are generally dominated by black or elemental carbon and heavy organic materials such as PAHs (58). Secondary sources emit PM precursors, which are gases that lead to PM formation through atmospheric reactions and include gaseous vegetative emissions, motor vehicle emissions, and wood-smoke emissions (36).

Particulate Matter-Mediated Autoimmune Disease

Increases in global air pollution have occurred concurrently with a dramatic increase in autoimmune incidence (3, 4, 14, 15). Exposure to air pollution, specifically PM, is associated with aggravation of various autoimmune diseases including T1D, RA, MS, and SLE (16–32). Epidemiologic studies strongly suggest that exposure to PM can increase both incidence and severity of autoimmune disease (33, 34).

PM and Autoreactive T Cells

Exposure to PM has been associated with aggravation of autoimmune diseases including T1D, RA, MS, and SLE, which will be the focus of this review (16–32). Pathology of autoimmune diseases can be mediated by autoreactive T cells and exposure to PM has been shown to alter effector T cell populations in healthy T cells as well as diseased. In human T cells from healthy donors, diesel exhaust particles (DEPs) from low emission diesel engines decreased expression of CD25, a marker for $FOXP3^+$ Tregs, on $CD4^+$ T cells and induced autophagic-lysosomal blockade *in vitro* which has been associated with pathogenic events of autoimmune disease (59). Using cells from atopy-prone mice, which are highly sensitive hosts, Nakamura et al. (60) showed that nanoparticle-rich DEP reduced cell viability and proliferation in a dose-related manner. Retinoic-acid receptor-related orphan receptor gamma t (RORγt) expression and subsequent IL-17A production/release by the cells was increased in the splenocytes in a dose-dependent manner implicating Th17 cells in PM-mediated immune responses. Additionally, $CD4^+$ and $CD8^+$ T cells exposed to $PM_{2.5}$ significantly elevated mRNA and protein

levels of inflammatory cytokine production in a macrophage-dependent manner (61). Furthermore, in a model of chronically inhaled $PM_{2.5}$ for 24–28 weeks, exposure to $PM_{2.5}$ resulted in increased T cell infiltration and increased activation of effector T cells in the lungs and indicates that $PM_{2.5}$ potentiates a proinflammatory Th1 response (62). In addition, van Voorhis et al. (63) demonstrated that a 3 day intranasal instillation of a standard reference material (SRM)1649b, an ambient urban dust PM sample, significantly upregulated IL-17 mRNA in the lung of C57BL/6 mice. Moreover, in a mixed leukocyte culture, using C57BL/6 splenocytes activated with Balb/c DCs, which creates an immune response, a significant increase in IL-17 protein was measured as well as IL-22 mRNA suggesting an increase in Th17 responses (63). Likewise, Castaneda et al. (64) demonstrated that PM enhances DC activation and primes naïve T cell differentiation toward a Th17-like phenotype *in vitro* and *in vivo*.

PM and T1D

T1D is an autoimmune disease resulting in targeting of islet cell autoantigens leading to a severe loss of pancreatic β cells (9, 65). T1D patients exhibit defects in peripheral tolerance including effector resistance to Treg suppression (66) and/or impaired Treg function (67). Incidence of T1D has been increasing by 2–5% worldwide (68) especially in children 0–4 years of age (69) and prevalence is approximately 1 in 300 in the U.S. by age 18 (68). Long-term exposure to $PM_{2.5}$ at low levels has been related to increased mortality attributable to T1D (17). Hathout et al. (20) found pre-diagnosis PM_{10} exposure was significantly higher in children diagnosed before 5 years of age compared to healthy controls. Likewise, a study from Chile found that $PM_{2.5}$ levels were associated with the onset of T1D in children (19). Beyerlein et al. (16) analyzed data from a population-based register monitoring incidence of diabetes in children and youths in Germany since 2009 and found that high exposure to the traffic-related air pollutants PM_{10}, NO_2, and possibly $PM_{2.5}$ accelerated the manifestation of T1D, but only in very young children. Additionally, children of mothers exposed to high levels of air pollution while pregnant had a higher risk of later developing T1D (21). Di Ciaula et al. (18) showed T1D incidence rate was significantly and positively correlated with mean yearly PM_{10} in Italy, however the correlation between T1D and PM_{10} air levels was more evident in children 10–14 years and 5–9 years than 0–4 years. Together, these data demonstrate an association between exposure to PM and diagnosis and exacerbation of T1D in children, mainly under the age of 5. On the other hand, a study in Southern California, demonstrated that pre-diagnosis PM_{10} exposure in children was not associated with increased odds of T1D (70). In adult disease, Michalska et al. (71) showed a relationship between the number of new T1D cases and mean annual concentration of PM_{10} in 2016, but not 2015 in Poland. Additionally, Yitshak et al. (72) showed that the 3-month average concentration of PM_{10} was associated with increases of serum glucose, HbA1c (average glucose concentration over 3 months and a marker for diabetic complications), low-density lipoprotein and triglycerides, and decrease of high-density lipoprotein with strongest associations observed among subjects with diabetes. Conversely, Lanzinger et al. (73) found no relationship between PM and T1D and no significant associations between HbA1c and PM_{10}. Overall, these data suggest exposure to PM may increase incidence, onset, and accelerate T1D in children and may be associated with worsened diabetes in adults.

PM and RA

RA is characterized by accumulation of inflammatory cells in the joints, leading to synovitis and severe tissue damage (74, 75). RA is a systemic autoimmune disease effecting approximately 1% of the adult population (76) and overall heritability of RA is estimated to be approximately 60% (77), leaving environmental pollutants, such as PM, as significant factors. Chang et al. (27) detected an increased risk of RA in participants exposed to $PM_{2.5}$ and there are several studies, including the Nurses' Health Study (76), that show an elevated risk of RA in people living less than or equal to 50 meters of major highways (76, 78). However, in the same population of nurses, adult exposures to specific air pollutants were not associated with an increased RA risk (79). Similarly, in the Swedish Epidemiological Investigation of Rheumatoid Arthritis, no evidence of an increased risk of RA with exposure to traffic pollutants, including PM_{10} was measured (80). Nonetheless, there are multiple studies that show an increased incidence of RA in urban areas compared to rural areas (81, 82) and living near air pollution emitters was associated with higher risks of developing RA and of producing RA-specific autoantibodies (82). Additionally, Gan et al. (83) showed that PM exposure was not associated with RA-related autoantibodies and joint signs among individuals without RA, but at an increased risk of developing RA.

Moreover, in children, case control studies indicated an increased relative risk for juvenile idiopathic arthritis (JIA), also known as juvenile rheumatoid arthritis, in American children $<$5.5 years of age was found with increasing $PM_{2.5}$ exposure, but evidence was less clear for links between exposure to air pollutants and development of RA (84). Furthermore, Zeft et al. (85) demonstrated that increased concentrations of $PM_{2.5}$ in the preceding 14 days of diagnosis were associated with significantly elevated risk of JIA onset in preschool aged children but not older children. Additionally, Zeft et al. (86) showed the most positive associations of short-term $PM_{2.5}$ exposure with systemic JIA were in children younger than 5.5 years. Together these data suggest a strong relationship between exposure to PM and risk of developing RA in both adults and children, however the link between PM exposure and exacerbation of RA is less clear. Overall, these data suggest a potential role of PM exposure in development and/or exacerbation of juvenile and adult onset RA.

PM and MS

MS is a demyelinating inflammatory disorder of the central nervous system (CNS) mediated by pathogenic T cells against myelin antigens (87). Like other autoimmune diseases, MS has a multifactorial etiology and likely results from an interaction between genetic predispositions, like mutations in the class II major histocompatibility genomic region, as well as environmental factors, like PM_{10} and $PM_{2.5}$. A strong link between risk of MS relapse or hospitalization and concentrations

of PM_{10} has been established world-wide (22, 24–26, 88, 89). Additionally, Gregory II et al. (23) found strong associations between total MS prevalence rates as well as individual female and male prevalence rates with mobile sources of $PM_{2.5}$ and PM_{10}. Moreover, a significant spatial correlation between the clustering of MS cases and patterns of PM_{10} was found in Tehran, Iran in that significantly higher yearly averages of PM_{10} existed in regions where MS patients lived compared to healthy controls (90). In pediatric MS, poor air quality was related to increased odds of developing MS in the pediatric population (91). For those pediatric patients living less than 20 miles from a recruitment center, the odds for MS increased by 4 as the air quality worsened and similarly, for those living more than 20 miles from the recruitment centers, the odds for MS doubled as air quality worsened (91). To understand how PM may be aggravating MS, Bergamaschi et al. (92) investigated the relationship between PM_{10} levels and inflammatory lesions in the brains of patients with MS using MRI data with gadolinium (Gd), which marks blood brain barrier breakdown and inflammatory lesions, in Italy. They found that PM_{10} levels in the 5, 10, 15, 20, and 25 days before brain MRIs were higher with reference to MRIs of patients with Gd enhanced lesions (Gd+) vs. patients with MRIs having no Gd enhanced lesions (Gd-) and there was a significant association between Gd+ MRI and PM_{10} levels. This suggests that PM exposure may be linked to increased inflammatory lesions and blood brain barrier leakiness and breakdown associated with MS. Furthermore, Klocke et al. (93, 94) exposed pregnant mice to PM and characterized endpoints after birth. Gestational exposure to concentrated ambient fine and ultrafine particles at levels consistent with environmental levels near California freeways altered neuropathology (93). These data suggest that gestational PM exposure alters the developing brain.

Contrarily, using the Nurses' Health Study, there was no relationship found between PM exposure and MS risk for women in the U.S (95). Similarly, Chen et al. (96) found no association between living near a major roadway in MS in patients in Ontario, Canada in a population-based cohort study. In Madrid, Spain no associated was found between PM_{10} or $PM_{2.5}$ and MS emergency room admissions across the period analyzed (97). Despite these studies that did not find an associated between PM and MS risk or exacerbation, a large body of evidence exists suggesting that PM contributes to both onset and exacerbation. Cumulatively, these data demonstrate a potential role of PM exposure in the development and exacerbation of MS, however the specific mechanisms remain unknown.

PM and SLE

SLE is a caused by an aberrant autoimmune response to unknown autoantigens by both autoreactive T cells and autoantibodies that effect vital organs such as brain and kidney (98). PM exposure has been linked to SLE in both adult and pediatric patients (28–32, 99). In adults, Bernatsky et al. (29) showed that antibodies against double-stranded DNA (anti-dsDNA) and urinary casts, markers of disease related to SLE, were significantly associated with $PM_{2.5}$ levels averaged over 24 or 48 h before clinical visits in Montreal, Canada. Moreover, Bernatsky et al. (30) also demonstrated the odds of having a systemic autoimmune rheumatic disease (SARD), which includes SLE, increased with $PM_{2.5}$ levels (30). Additionally, in two different Canadian provinces, Alberta and Quebec, the odds of being diagnosed with SARDs increased with $PM_{2.5}$ levels (31). Similarly, Fernandes et al. (32) observed a significant increased risk of juvenile-onset SLE disease activity 13 and 16 days after exposure to PM_{10}. On days where PM levels exceeded the World Health Organization (WHO) air quality standard (50 mg/m^3), the risk of juvenile-onset SLE activity was 79.0% higher than it was on days with levels below the standard (32). Together these data suggest a potential role of PM in the development and exacerbation of SLE.

Summary

Several studies from around the world demonstrate an association between the risk of development and/or exacerbation of autoimmune diseases and exposure to PM, and a few do not (**Table 1**). While the epidemiological data is strong, the mechanistic understanding of how PM increases the risk of developing autoimmune disease or exacerbates autoimmune disease remains largely unknown. The lack of mechanistic understanding of the components of PM responsible for the epidemiologic correlations as well as the pathways in which the components act, make understanding the contradictory data difficult. Despite the contradictory data, several studies establish clear correlations between exposure to PM and autoimmune diseases. Based on the data presented, one possible mechanism is that PM exposure increases inflammation and exacerbates autoimmune disease, however the specific pathways and mechanisms that are targeted to cause the inflammatory responses are unclear. Identifying components of PM and specific pathways associated with PM-mediated autoimmune disease will allow for targeted therapies to delay onset and ameliorate symptoms caused by PM exposure.

The Relationship Between PM and the AHR

Epidemiologic data provides strong associations between PM and autoimmune diseases, however the mechanisms in which PM elicits its negative health impacts are largely unknown. PM contains AHR ligands such as PAHs, dioxins, and polychlorinated biphenyl (PCBs) congeners, among others adsorbed to its surface. Andrysik et al. (120) found that the organic extract of SRM1649a, ambient urban dust PM containing dioxins, PCBs, and PAHs, which are present at the highest concentration of AHR ligands adhered to the sample, as well as its neutral and polar fractions, were potent inducers of AHR-mediated responses. These responses occurred at doses one order of magnitude lower than DNA damage and included induction of AHR-mediated transcription of CYP1A1 and CYP1B1 and AHR-dependent cell proliferation (120). PAHs were major contributors to overall AHR-mediated activity (120). Additionally, extracts of real-world PM_{10} samples obtained from southwest United States and Mexico were rich in PAHs and had significant activity in an ethoxyresorufin-*O*-deethylase (EROD) which measures CYP1A1 induction, and in a luciferase assay, which measures AHR activation (121).

TABLE 1 | Summary of the effects of PM and AHR agonists on autoimmunity.

		Treatment	Immunosuppressive	Immunostimulatory	No effect on autoimmunity
Pre-clinical	PM	DEP PM		(100)	
		DEP OF	(100)	(100)	
		Ambient PM	(101)	(63, 64)	
		Ambient OF			
	AHR agonists	TCDD	(46, 102, 103)	(104–106)	
		FICZ	(102)	(46, 106, 107)	
		10-Cl-BBQ	(108)		
		Norisoboldine	(109)		
		Tetrandrine	(110)		
		Sinomenine	(111)		
		Laquinimod	(112)		
		ITE	(113)		
		I3C	(107, 114)		
		DIM	(107, 114)		
	AHR knockout		(115–117)		
Clinical	PM			(16, 18–21, 23, 27, 59, 71, 72, 76, 78, 81–86, 90, 92)	(70, 71, 73, 79, 80, 83, 85, 95–97)
	AHR antagonists	GNF351	(118, 119)		

This table summarizes the effects of PM and other AHR ligands in preclinical and clinical studies based on whether the treatment led to an immunosuppressive or immunostimulatory outcome. Preclinical studies include in vivo animal studies whereas the clinical studies include epidemiology studies as well as studies using human cells or tissue. Most of the studies using AHR agonists led to an immunosuppressive effect whereas PM had both immunosuppressive and immunostimulatory effects. Route of exposure and extent and duration of AHR activation contribute to the effects of AHR ligands on autoimmunity and may explain the differential responses observed in these studies. Several clinical epidemiology data suggest that PM exposure leads to immunostimulatory responses while some suggest it does not have an effect on autoimmunity. Together, these data led to the novel hypothesis that PAHs adhered to PM activate the AHR, shift the T cell balance, and lead to PM-mediated autoimmune disease.

Similarly, when looking at immune cells, den Hartigh et al. (122) examined the effects of PM collected from Fresno, California on activation of human monocytes and found that PM exposure increased CYP1A1 expression, and inhibition of the AHR reduced the CYP1A1 levels and inflammatory responses. Likewise, Jaguin et al. (123) showed that AHR and nuclear factor erythroid 2–related factor 2 (Nrf2) pathways were activated in human macrophages after DEP exposure. Specifically, AHR activation by DEP lowered the capacity of human macrophages to secrete inflammatory cytokines, IL-6 and IL-12p40 (123). van Voorhis et al. (63) demonstrated that a 3 day intranasal instillation of SRM1649b not only increased IL-17mRNA in the lung, but also significantly increased CYP1A1 mRNA *in vivo*. In addition, in a mixed leukocyte culture, where splenocytes from C57BL/6 mice are stimulated with DCs from Balb/c mice to generate an immune response, a significant increase in IL-17 protein levels were observed as well as an increase in CYP1A1 mRNA (63).

When examining the effects of intact PM vs. organic extracts, bioavailability of active components, such as PAHs, has been shown to alter biologic responses. PM samples from complete combustion provided a stronger response in the PAH-CALUX assay, which measures PAH-induced AHR activity, and PM from incomplete combustion provided a weaker response suggesting that PM contains organic components that strongly adsorb PAHs thereby reducing their bioavailability (124). These findings were found to be strongly associated with the amount of elemental carbon present in the PM samples with higher elemental carbon favoring less bioavailability of PAHs in PM (124). Additionally, Libalova et al. (125) demonstrated that exposure to extractable organic matter (EOM) induced significantly lower DNA adduct levels, while expression of AHR-dependent PAH-activating enzymes as well as other AHR target genes, was strongly enhanced compared to benzo[a]pyrene-treated cells. This suggests that the genotoxicity of benzo[a]pyrene is inhibited by other organic compounds bound to $PM_{2.5}$ but induction of AHR-dependent gene expression by benzo[a]pyrene is not inhibited by EOM constituents (125). Vondracek et al. (126) found that although PAHs are major contributors to the AHR-mediated activity of organic compounds associated with particles derived from diesel exhaust, polar compounds, which does include polar PAH derivatives generated through metabolism, present in these mixtures are more active in human cells, as compared with rodent cells. Misaki et al. (127) further demonstrated that polar fractions of DEP contribute significantly to AHR activation *in vitro*. Likewise, Palkova et al. (128) found that PAHs, as well as polar compounds contained within DEP, are important inducers of the AHR-mediated activity and contributed significantly to formation of stable DNA adducts, activation of DNA damage response signaling pathways, and induction of cell death. Together, these data suggest the AHR has the potential to be a modulator of PM-mediated disease.

In the context of exposure to PM and its derivatives, O'Driscoll et al. (100) demonstrated that exposure to standard reference material (SRM)1650b PM, which is from a 4-cylinder diesel truck engine, enhanced Th17 differentiation in an AHR-dependent manner and SRM2975, which is from a 2-cylinder diesel forklift engine, enhanced Th1 differentiation

in an AHR-dependent manner [**Figure 1** from O'Driscoll et al. (100)]. In addition, the chemically-extracted OF of SRM1650b and SRM2975 which contains AHR ligands, such as PAHs, enhanced Th17 differentiation in an AHR-dependent manner (100). Synthetic PAH mixtures which include 15 PAHs present in SRM1650b and SRM2975 enhanced Th17 differentiation, however SRM1650b synthetic PAH mixture required the AHR at high doses and at lower doses enhanced Th17 differentiation only in the absence of CYP enzymes (100). SRM2975 synthetic PAH mixture enhanced Th17 differentiation only in the absence of CYP enzymes suggesting that the inhibition of CYP enzymes prevents the breakdown of the active component allowing for the observed T cell effect [(**Figure 1** from O'Driscoll et al. (100)] (100). Similarly, O'Driscoll et al. (101) demonstrated that an ambient urban dust PM sample enhanced Th17 differentiation in an AHR-dependent manner. Likewise, Castaneda et al. (64) showed that PM enhanced DC activation and primed naïve T cells toward a Th17-like phenotype in an AHR-dependent manner *in vitro* and *in vivo*.

Aryl Hydrocarbon Receptor: an Environmental Sensor

The AHR is a member of the PER-ARNT-SIM (PAS) superfamily (129, 130) and is a ligand-activated transcription factor that in the absence of ligand is maintained as an inactive complex in the cytosol with two molecules of the chaperone heat shock protein (HSP) 90 (131, 132), as well as aryl hydrocarbon associated protein 9 (ARA9) (also known AIP1 or XAP2) (133, 134) and p23 (135). Together, these chaperones contribute to the cytosolic localization of unliganded AHR, protect it from degradation, and maintain a favorable state for ligand and DNA-binding (136–138). Upon ligand binding, the AHR-complex undergoes a conformational change that reveals its nuclear localization sequence (139). As a result of this conformational change, AHR sheds its cellular chaperones (140, 141), translocate to the nucleus, where it heterodimerizes with another bHLH-PAS protein, aryl hydrocarbon nuclear translocator (ARNT) (also known as HIF1β) (142). The ligand-activated AHR-ARNT complex is capable of binding to specific sequences of DNA (—TNGCGTGT—) known as aryl hydrocarbon response elements (AHREs) [also known as dioxin response elements (DREs) or xenobiotic response elements (XREs)] (143–145) and inducing transcription of target loci such as CYP1A1 (**Figure 2**) (146, 147). The AHR is a promiscuous receptor that it binds both exogenous ligands, such as TCDD and PAHs, and endogenous ligands, such as FICZ and 2-(1′H-indole-3′-carbonyl)-thiazole-4-carboxylic acid methyl ester (ITE), that are structurally diverse (40, 47, 148).

The AHR is subject to negative regulation. Following ligand-induced activation and nuclear export (141), the AHR is degraded via a 26S proteasome pathway (149–151). Another mechanism in which the AHR is negatively regulated is by the upregulation of the aryl hydrocarbon receptor repressor (AHRR), a bHLH-PAS protein that functions as a transcriptional

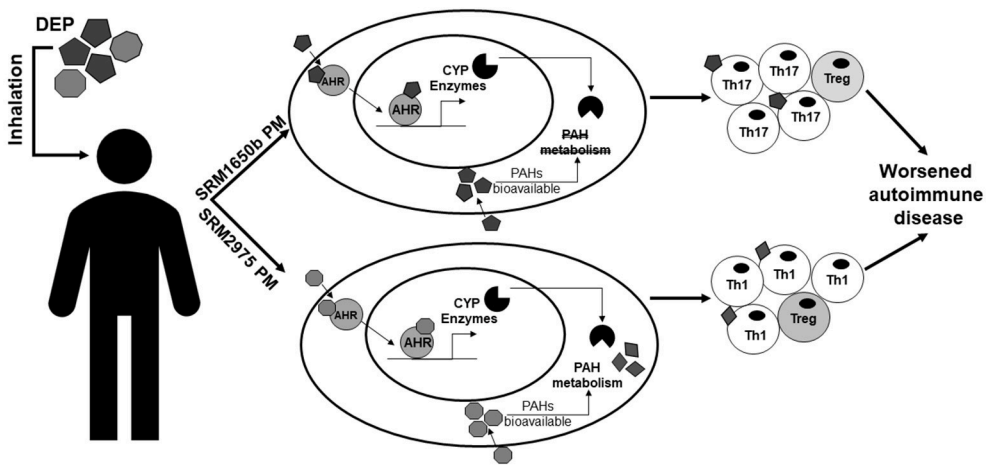

FIGURE 1 | Summary of the effects of DEP on T cells and autoimmune disease. This figure from O'Driscoll et al. (100) summarizes the differential effects of two DEPs, SRM1650b from a 4-cylinder diesel engine, and SRM2975 from a 2-cylinder diesel engine on T cell differentiation and autoimmune disease. SRM1650b enters the T cell, binds AHR, which then translocates to the nucleus and binds DNA, driving transcription of CYP enzymes (**top**). SRM1650b enhances Th17 differentiation in an AHR-dependent manner and worsens autoimmune disease (**top**). Based on the *in vivo* EAE data using the intact PM and chemically-extracted OF, SRM1650b requires the particle to aggravate autoimmune disease because of bioavailability of the PAHs and their ability to activate the AHR. Like SRM1650b, SRM2975 enters the T cell, binds AHR, translocates to the nucleus, binds DNA, and drives transcription of CYP enzymes (**bottom**). However, SRM2975 enhances Th1 differentiation in an AHR-dependent manner but still worsens autoimmune disease (**bottom**). Based on the *in vivo* EAE data demonstrating SRM2975 worsens autoimmune disease in PM and OF forms and the *in vitro* data showing a role of CYP enzymes in T cell differentiation, metabolism of SRM2975 plays a role in its ability to worsen autoimmune disease in that CYP metabolism of PAHs may lead to more potent intermediates that drive immune responses *in vivo*. Additionally, in the presence of PAHs and AHR activation, enhanced effector differentiation by both samples results in increase in Th17 or Th1 cells and a reduction in Treg cells. However, when PAHs are at much lower concentrations as with the low doses, enhanced effector differentiation is lost and Treg differentiation is enhanced. SRM, standard reference materials; DEPs, diesel exhaust particles; AHR, aryl hydrocarbon receptor; CYP, cytochrome P450; PAH, polycyclic aromatic hydrocarbons. This figure or a version of this figure was published in Particle and Fibre and Toxicology and is licensed under the Creative Commons Attribution 4.0 International Public License.

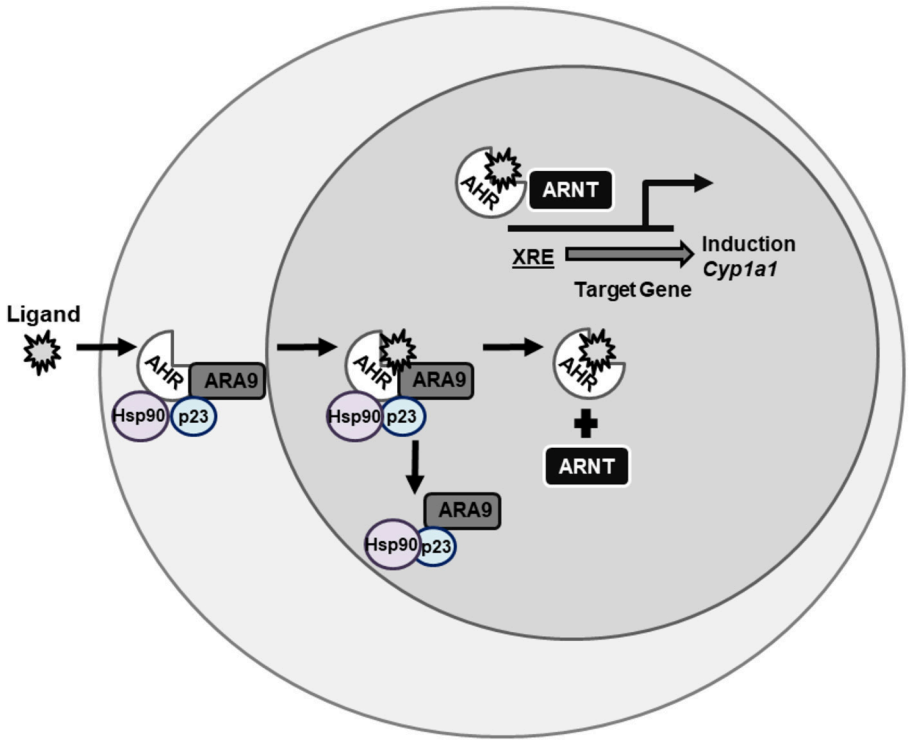

FIGURE 2 | AHR signaling pathway. AHR is a ligand-activated transcription factor the resides in the cytosol being held in conformation by chaperone proteins until bound by ligand. Once bound by ligand, AHR translocates to the nucleus, sheds its chaperone proteins, and binds ARNT. This complex then binds XREs on DNA and induces gene transcription of genes such as CYP1A1. AHR, aryl hydrocarbon receptor; ARNT, aryl hydrocarbon receptor nuclear translocator; XRE, xenobiotic response element; CYP, cytochrome P450.

repressor (152). The AHRR represses AHR transcriptional activity by competing with AHR for heterodimerization with ARNT and from AHRR-ARNT complex binding AHREs (152).

THE ROLE OF AHR IN T CELLS

AHR is critical in maintaining the balance between Th17 and Treg cells which play a major role in autoimmune disease. TCDD exposure, and subsequent AHR signaling, were shown to play a role in the generation of adaptive $CD4^+CD25^+$ Tregs early in an immune response (153). Additionally, the expression of AHR on T cells was shown to be critical in blocking the generation of peripheral Tregs in the lower gastrointestinal tract after a bone marrow transplant, suggesting the AHR on donor T cells is essential for pathogenesis in acute graft vs. host disease (154). Quintana et al. (46) demonstrated that AHR directly controls $FOXP3^+$ Treg generation, by binding AHR binding sites on the *Foxp3* gene. In addition, FICZ, in combination with Th17 promoting cytokines, enhanced Th17 differentiation in an AHR-dependent manner and interfered with the differentiation of Treg cells *in vitro* (46). Moreover, Veiga-Parga et al. (155) showed that a single administration of TCDD reduced severity of stromal keratitis lesions in the cornea by causing apoptosis of $FOXP3^-$ $CD4^+$ T cells but not $FOXP3^+$ $CD4^+$ Tregs. TCDD also decreased the proliferation of $FOXP3^-$ $CD4^+$ T cells resulting in an increase in the ratio of Tregs to T effectors. In addition, *in vitro* studies revealed that TCDD addition to anti-CD3/CD28 stimulated naïve $CD4^+$ T cells caused a significant induction of Tregs and inhibition of Th1 and Th17 differentiation (155).

In addition to TCDD, more natural AHR ligands, indole-3-carbinol (I3C), 3,3′-diindolylmethane (DIM), ITE, and kynurenine, among others have been shown to promote Tregs, and FICZ to promote Th17 cells (46, 107, 156–159). Veldhoen et al. (44) demonstrated that AHR is most highly expressed in Th17 cells and AHR ligation by FICZ promotes Th17 differentiation, measured by an increase in percent of IL-17a and IL-22 positive cells, in an AHR-dependent manner. Moreover, Mezrich et al. (156) demonstrated that tryptophan breakdown product kynurenine activates the AHR leading to AHR-dependent Treg generation and has no effect on the generation of Th17 cells (156). Singh et al. (107) showed that treatment of C57BL/6 mice with I3C or DIM attenuated delayed-type hypersensitivity (DTH) response and generation of Th17 cells and promoted Tregs, whereas FICZ exacerbated the DTH response and promoted Th17 cells. Treatment with I3C or DIM decreased the induction of IL-17 but promoted IL-10 and FOXP3 expression in an AHR-dependent manner (107). In addition, Liu et al. (160) demonstrated that FICZ increased Th17 cells and

decreased Treg cells, but naphthoflavone decreased Th17 and increased Treg cells.

One question that has emerged as a result of data showing different AHR ligands seem to have opposite effects on T cell differentiation, is whether the ability to elicit different effects is intrinsic to the ligand itself or specific to experimental features, such as route of exposure, AHR affinity, among others? Local administration of FICZ, combined in the emulsion with Complete Freund's adjuvant, worsened EAE (44, 46). However, Duarte et al. (102) demonstrated that systemic administration of FICZ by intraperitoneal injection resulted in partial inhibition of EAE, halfway to what was seen with TCDD. More recently, Erhlich et al. (161) used an acute alloresponse model and demonstrated that when dose and timing of administration of high-affinity AHR ligands was optimized for TCDD-equivalent *Cyp1A1* induction, all ligands tested suppressed the alloresponse and induced Tr1 cells early on and Treg cells later. However, a low dose of FICZ led to transient *Cyp1A1* mRNA expression, no suppression the alloresponse, and enhanced IL-17 production (161). Similar results were observed for low dose TCDD. Together these data demonstrate that route of exposure, dose and duration of AHR activation, and ligand affinity of AHR ligands drives the fate of T cell differentiation and leads to differential T cell effects *in vivo* (**Table 1**). This suggests that the differential immune responses observed are not intrinsic to each ligand, but rather a result of differential AHR activation.

In addition to $FOXP3^+$ Tregs and Th17 cells, AHR has been shown to play a role in Tr1 cells which are $FOXP3^-$ regulatory $CD4^+$ T cells that produce IL-10 and are generated by IL-27 and have non-redundant roles in the control of inflammation (162). IL-27 also suppresses the development of pathogenic IL-17-producing CD4+ T cells Th17 cells (162). In human PBMCs, AHR promotes the differentiation of Tr1 cells and production of IL-10 through granzyme B (163). Additionally, Mascanfroni et al. demonstrated that at later time points in differentiation AHR promotes hypoxia inducible factor 1-α (HIF1-α) degradation and controls Tr1 cell metabolism.

THE ROLE OF AHR IN AUTOIMMUNE DISEASE

In the context of autoimmunity, activation of AHR by exogenous and endogenous ligands modulates T cell differentiation as well as effector and regulatory T cell function, and contributes to antigen presenting cell responses, all of which alter autoimmune diseases. In addition, AHR has been shown to differentially regulate these effector and regulatory T cells through both AHRE-mediated pathways, primarily for Th17, as well as non-AHRE mediated pathways, which have been shown to regulate Tregs (164). Given the complexity of AHR signaling and the differential regulation of T cells, the AHR has been studied as a candidate target for autoimmune disease.

Ishimaru et al. (104) demonstrated that three low dose TCDD exposures in neonatal mice disrupted thymic selection, enhanced production of Th1 cytokines from splenic CD4+ T cells, and increased autoantibodies in the sera of TCDD-exposed mice compared with those in control mice indicating that early exposure to environmental contaminants and consequent AHR signaling in the neonatal thymus alters differentiation and/or development of T cells associated with autoimmunity (104). In addition, Boule et al. (105) found that developmental exposure to TCDD and subsequent activation of AHR via lactation accelerated disease in $Gnaq^{+/-}$ mice, which are mice that are heterozygous for the Gαq protein and have a genetic predisposition to develop an autoimmune disease with symptoms similar to SLE and RA, but are not guaranteed to develop disease. This accelerated disease correlated with increases in effector and regulatory $CD4^+$ T-cell populations in females as compared to males (105). Together these data imply a role of early environmental exposure with AHR-mediated autoimmune disease. It has been demonstrated that AHR ligands, including environmental toxicants, bind AHR and alter T cell development and function. In the context of autoimmune disease, AHR has been shown to play a role in T1D, RA, MS, and SLE by altering T cell functions.

AHR and T1D

One of the most commonly used mouse modes of type 1 diabetes is the non-obese diabetic (NOD) mouse, which develops spontaneous disease similar to humans, and females are most predominately affected (165). Diabetes in NOD mice is characterized by hyperglycemia and insulitis, leukocytic infiltration of the pancreatic islets, and decreases in pancreatic insulin (165, 166).Using NOD mice harboring a transgenic T cell receptor, Bellemore et al. (167) showed that IL-23 plus IL-6 driven Th17 differentiation of $CD4^+$ cells results in production of large amounts of IL-22 and these cells induce T1D in young NOD mice upon adoptive transfer. Th17 cells polarized with TGF-β plus IL-6 expressed AHR, IL-10, IL-21, and IL-9, and were able to suppress pathogenic Th17 cells in adoptive transfer experiments suggesting that regulatory $T_{reg}17$ cells induced by TGF-β plus IL-6 express high levels of AHR and are protective while Th17 cells with a very low level of AHR induced by IL-23 plus IL-6 are pathogenic.

Kerkvliet et al. (103) found that chronic treatment of NOD mice with TCDD suppressed the development of autoimmune T1D, reduced pancreatic islet insulitis, and resulted in an expanded population of $CD4^+CD25^+FOXP3^+$ cells in the pancreatic lymph nodes. However, when TCDD treatment was stopped after 15 weeks, mice exhibited lower number of Tregs and decreased activation of AHR associated with development of diabetes over the next 8 months after treatment was terminated (103). Similarly, Ehrlich et al. (108) discovered that repeated oral dosing with the AHR ligand, 10-Cl-BBQ, suppressed infiltration in islet cells of NOD mice without clinical toxicity in an AHR-dependent manner and this was associated with increased frequency of $FOXP3^+$ Tregs in the pancreas and pancreatic lymph nodes. Additionally, depletion of $FOXP3^+$ cells did not abrogate immune suppression observed with 10-Cl-BBQ exposure, but reduction of effector T cells was sufficient to suppress disease suggesting 10-Cl-BBQ acts independently of $FOXP3^+$ Tregs to suppress the development of pathogenic T cells (108). Additionally, Ehrlich et al. (117) discovered that in the

absence of AHR, female NOD mice have a significantly reduced onset of diabetes in comparison to wild-type mice. A similar trend was observed between knockout and wild-type male mice suggesting AHR is important in the onset of T1D in NOD mice (117).

AHR and RA

RA results in an inflammatory milieu which causes primary human fibroblast-like synoviocytes (FLS) to undergo hyperplasia and ultimately lead to joint destruction. Lahoti et al. (118) demonstrated that co-treatment of FLS with the AHR antagonist, GNF351, repressed IL-1β-induced cytokine and chemokine expression and inhibited the recruitment of AHR to the promoters of *IL-1β* and *IL-6*. In human FLS from patients with RA, the potent AHR antagonist, GNF351, attenuated IL-1β–induced growth factor expression, IL-1β–induced proliferation, protease-dependent invasion, and migration in RA-FLS in an AHR-dependent manner (119). Likewise, the percentage of AHR positive cells in PBMCs as well as AHR and CYP1A1 expression was higher in RA patients compared to healthy controls (168). Additionally, the percentage of $AHR^+CD4^+CD25^+$ T cell was significantly reduced in RA patients and the percentage of $AHR^+CCR6^+CD4^+$T cells was significantly increased in patients with RA (168).

Collagen-induced arthritis is a model of RA characterized by infiltration of macrophages and neutrophils into the joint, as well as T cell and B cell responses to type II collagen (169). The model involves immunizing genetically susceptible mice (DBA/1J) with a type II bovine collagen emulsion in complete Freund's adjuvant (CFA) or C57BL/6J mice with type II chicken collagen in CFA and giving a boost of type II bovine or type II chicken collagen in incomplete Freund's adjuvant (IFA) 21 days after the first injection (169). Mice typically develop disease 26 to 35 days after the initial injection (169). A rat model of collagen-induced arthritis involves immunizing with chicken type II collagen and CFA intradermally into the base of the tail on day 0 and a follow-up booster of chicken type II collagen in IFA on day 7 (170).

Isoquinoline alkaloids found in plants have been shown to have AHR activity and induce Tregs alleviating collagen-induced arthritis. Tong et al. (109) demonstrated that norisoboldine, an anti-arthritic isoquinoline alkaloid, functioned as an AHR ligand demonstrated by induction of CYP1A1 expression and activity, promotion of AHR/Hsp90 dissociation and AHR nuclear translocation, induction of AHRE reporter activity, and facilitation of AHR/AHRE binding and promoted intestinal Treg cell differentiation and function in an AHR-dependent manner. Additionally, adoptive transfer of Treg cells from norisoboldine treated mice alleviated arthritis in recipient collagen-induced arthritis mice (109). Similarly, tetrandrine, an alkaloid constituent, alleviated severity of arthritis, reduced serum levels of pro-inflammatory cytokines, and restored the Th17/Treg balance via the AHR, measured by serum levels of IL-17 and IL-10 respectively in collagen-induced arthritis mice (110). Likewise, Tong et al. (111) showed sinomenine, a plant alkaloid, induced the generation of intestinal Treg cells, and facilitated the immunosuppressive function of these Treg cells in collagen-induced arthritis mice. The induction of intestinal Treg cells and the anti-arthritic effect of sinomenine in collagen-induced arthritis mice was diminished by the AHR antagonist resveratrol (111).

Nakahama et al. (115) used a murine collagen-induced arthritis model of RA and showed that AHR deficiency ameliorated collagen-induced arthritis and AHR null mice immunized with collagen showed decreased serum levels of proinflammatory cytokines IL-1β and IL-6. In addition, Th17 cells were decreased in the lymph nodes of AHR null mice whereas Th1 cells in lymph nodes were increased. This loss of AHR specifically in T cells suppressed collagen-induced arthritis development. Further supporting a role for AHR in RA, Talbot et al. (116) demonstrated that cigarette smoke, which contains AHR ligands like PAHs, induces arthritis aggravation and increases the frequency of Th17 cells. Mice null for IL-17 or AHR were protected from cigarette-smoking induced arthritis and exposure to PAHs aggravated arthritis suggesting that AHR ligands in cigarette smoke drive Th17 responses *in vivo* (116).

In RA, the shared epitope (SE), a five amino acid sequence motif encoded by RA-associated *HLA-DRB1* is the most significant genetic risk factor. Fu et al. (106) showed that the SE and the AHR pathway exhibit a synergistic interaction dependent on nuclear factor kappa B (NF-kB) that results in osteoclast differentiation and Th17 polarization after exposure to FICZ or TCDD in bone marrow cells from transgenic mice carrying human SE-coding alleles. *In vivo*, exposure to FICZ or TCDD in transgenic mice carrying human SE-coding alleles resulted in a robust increase in arthritis severity, bone destruction, overabundance of osteoclasts, and infiltration of IL-17-expressing cells in the inflamed joints and draining lymph nodes of arthritic mice (106).

AHR and MS

Experimental autoimmune encephalomyelitis (EAE) is an inflammatory demyelinating disease of the CNS in rodents that has similar pathologic and clinical symptoms to human MS. In C57BL/6J mice, the disease is induced by myelin oligodendrocyte $(MOG)_{35-55}$ peptide and mediated by $CD4^+$ T cells and macrophages (171). Initially, EAE was thought to be mediated by an exaggerated Th1 response, however deficiency in IL-12, and thus IFNγ effector cells, exacerbated EAE (172). In contrast, mice deficient in IL-23, which promotes IL-17 effector cells, failed to develop EAE demonstrating IL-23, not IL-12 as the critical cytokine in autoimmune inflammation (172). Later, Park et al. (173) demonstrated that blocking IL-17 resulted in attenuation and delay of EAE and reversed the progression of active EAE and Harrington et al. (174) showed that IL-23-induced, IL-17 producing $CD4^+$ effector T cells have a distinct development program from Th1 or Th2 cells defining them as Th17 cells. Quintana et al. (46) demonstrated that intraperitoneal injection of TCDD shifts the balance toward Treg cells *in vitro* and *in vivo* and suppresses EAE whereas FICZ in the MOG_{35-55} emulsion drives Th17 responses *in vitro* and *in vivo* and worsens severity of EAE (44). However, Duarte et al. (102) demonstrated that intraperitoneal administration of TCDD and FICZ lessened severity of EAE. Using EAE as a model, Kaye

et al. (112) showed that laquinimod, an oral drug currently being evaluated for treatment of relapsing and remitting MS, induced genes associated with the AHR pathway such as *Cyp1a1* and *Ahrr* in both naive and EAE mice treated with laquinimod *in vitro* and *Cyp1a1 in vivo*. Laquinimod treatment resulted in an AHR-dependent expansion of Tregs and reduction of effector T cells in EAE (112). O'Driscoll et al. (100) demonstrated that intranasal exposure to diesel PM samples, shown to enhance T cell differentiation through the AHR, worsened severity of EAE, however exposure to its chemically-extracted OF resulted in one diesel OF worsening severity of EAE but the other lost this effect. O'Driscoll et al. (101) demonstrated that mice exposed intranasally to an ambient urban dust PM sample exhibited delayed disease onset and reduced severity of EAE and the delayed disease onset was AHR-dependent *in vivo*. Intranasal treatment to the ambient urban dust PM sample resulted in reduction of pathologic T cells in the CNS on day 10 after EAE induction and in a significant AHR-dependent reduction of IFNγ-producing T cells in an *in vitro* MOG-specific splenocyte assay (101). O'Driscoll et al. (101) identified the AHR pathway as a novel pathway through with PM can reduce Th1 responses in the CNS and although this suppression of Th1 cells may reduce severity of disease it opens the door for opportunistic infection if the immunosuppression in non-reversible. In humans, Rothhammer et al. (175) detected a global decrease of circulating AHR agonists in relapsing-remitting MS patients as compared to controls. However, increased AHR agonistic activity was observed during acute CNS inflammation in clinically isolated syndrome or active MS.

Tr1 cells are regulated by AHR and characterized as $FOXP3^{-}CD4^{+}$ T cells that require IL-27, produce IL-10, and have been shown to prevent autoimmune disease. Apetoh et al. (176) demonstrated that AHR activation increased the production of IL-10 and IL-21, which acts as an autocrine growth factor for Tr1 cells, and mice with impaired AHR signaling exhibited decreased production of IL-10 and resistance to IL-27-mediated inhibition of EAE (176). $FOXP3^{+}$ Tregs are also modulated by AHR and play a role in autoimmune disease. Quintana et al. (113) found that AHR signaling participates in $FOXP3^{+}$ Treg differentiation *in vivo* and treatment with the endogenous AHR ligand, ITE, given parenterally or orally induced $FOXP3^{+}$ Tregs that suppressed EAE. Rouse et al. (114) demonstrated that pretreatment of EAE-induced mice with the endogenous AHR ligands, I3C and DIM completely prevented clinical symptoms and cellular infiltration into the CNS and post-treatment of EA- induced mice with I3C or DIM reduced severity of disease. In addition, I3C or DIM promoted the generation of Tregs, while down-regulating the induction of MOG-specific Th17 cells (114).

AHR and SLE

Rekik et al. (177) demonstrated that transcription of TGF-β1 target genes are impaired in $CD3^{+}$ T cells of active SLE patients and this impaired response to TGF-β1 is associated with an overexpression of IL-22 in SLE patients suggesting that excessive activation of AHR pathway could inhibit the immunosuppressive effects of TGF-β1 leading to exacerbated SLE. Similarly, Dorgham et al. (178) showed a significant expansion of Th17 and Th22 cells in the peripheral blood of active SLE patients, compared to inactive patients and controls. In addition, propranolol, a potential lupus-inducing drug, induced stronger AHR activation in PBMCs of SLE patients than in those of controls and SLE patients also exhibited signs of AHR activation in cutaneous tissues that correlated with lesion expression (178). Moreover, Shinde et al. (179) showed that an enhanced AHR transcriptional signature correlated with disease in patients with SLE. In murine SLE, strength of the AHR signal correlated with disease progression and disease course could be altered by modulating AHR activity (179).

Summary: AHR Ligands and Autoimmune Disease

Some AHR ligands have been shown to ameliorate autoimmune disease and others to exacerbate disease *in vitro* and *in vivo* (**Table 1**), but despite these differences it is clear that AHR ligands shift the balance between effector and regulatory T cells determining autoimmune disease outcomes. One question that has been raised is what gives certain ligands the ability to exacerbate disease vs. ameliorate disease? Previously it was thought that AHR regulated Th17 and Treg differentiation *in vitro* and *in vivo* in a ligand-specific manner (44, 46). This created a paradigm that TCDD promotes immunosuppression whereas endogenous ligands like FICZ promote Th17 responses exacerbating immune responses. However, Duarte et al. (102) demonstrated that AHR ligands can upregulate the Th17 program *in vitro* depending on AHR affinity and there are no ligand intrinsic modes of action differentiating one ligand from another. Moreover, *in vivo* the timing and mode of application as well as the differential susceptibility to metabolism by different ligands contributes to the immune response observed (102). More recently, it has been shown that extent and duration of AHR activation contribute to the immune effects observed (161). More specifically, if AHR activation was normalized to TCDD CYP1A1 mRNA induction levels in a model of graft vs. host disease, all ligands tested reduced severity of disease, but if lower levels of TCDD were given, along with other AHR ligands, the exposure increased Th17 cells and started to make disease worse (161). Together, these data suggest that extent and duration of AHR activation determine the immune effect elicited by specific ligands and that ligand-specific responses do not determine the immune responses. Cumulatively, these data demonstrate a clear role of AHR in autoimmune disease and indicate a likely role of AHR ligands present in PM in autoimmune disease.

Linking PAHS and Autoimmune Disease

PM contains many organic constituents which are AHR ligands that have the potential to contribute to autoimmunity. van Voorhis et al. (63) demonstrated that an individual PAH, benzo[k]fluoranthene, enhanced Th17 differentiation in an AHR-dependent manner. Additionally, PM extracts and cigarette extracts, both of which contain PAHs, enhanced Th17 differentiation as well (63). Although this review focuses on the effects of PM and its constituents on autoimmune disease, it is worth noting that cigarette smoke also contains numerous PAHs

at varying levels and there are several epidemiological studies that demonstrate an increased risk of autoimmune diseases such as RA, MS, and SLE in individuals who smoke cigarettes (180–185) and using animal models, Talbot et al. (116) demonstrated that cigarette smoke, which contains AHR ligands like PAHs, aggravates arthritis and increases the frequency of Th17 cells. Furthermore, O'Driscoll et al. (100) demonstrated that synthetic PAH mixtures based on the milieu of 15 PAHs present in standard PM samples enhanced Th17 differentiation via the AHR and/or CYP metabolism. The combination of epidemiological data that associated PM, as well as cigarette smoke, with increased risk and/or exacerbated autoimmune diseases and the *in vitro* studies in mice that demonstrated PM and its chemically-extracted organic fraction (63, 100), cigarette smoke extract (63), individual PAHs (63), and synthetic PAH mixtures (100), enhanced Th17 differentiation suggest that PAHs present in PM are candidate components that may activate the AHR, shift T cell balances, and alter autoimmune disease status.

Closing the Gap

The incidence and prevalence of autoimmune diseases is continuing to rise and although a clear genetic component exists, environmental factors also contribute to autoimmune diseases. Epidemiologic studies strongly suggest that exposure to PM can increase both incidence and severity of autoimmune disease. Exposure to PM has been associated with aggravation of autoimmune diseases including T1D, MS, RA, and SLE. These autoimmune diseases also have a clear autoreactive T cell component to their pathology. Although a clear role for autoreactive T cells has been established, identifying specific exposures and mechanisms leading to autoimmune disease process has proven particularly difficult.

PM activates the AHR and induces the production of inflammatory cytokines in immune cells. The AHR can modulate T cells responses by shifting the balance between regulatory and effector responses. Both PM and the AHR have strong associations with autoreactive T cells and autoimmune disease (**Table 1**). Additionally, PM exposures act through the AHR altering T cell responses *in vitro* and *in vivo* changing autoimmune disease pathology (**Table 1**). The AHR responds to several environmental toxicants found in PM, such as PAHs, and PM exposures alter T cell balance and autoimmune disease via the AHR. Moreover, the contradictory epidemiologic data could be explained by differences in AHR ligands present in the PM and the extent and duration of activation of the AHR. This leads us to the novel hypothesis that AHR ligands present in PM activate the AHR, shift the T cell balance, and lead to PM-mediated autoimmune disease. We propose a hypothesis in which AHR ligands, such as PAHs, adhered to atmospheric PM activate the AHR and upregulate CYP enzymes [**Figure 3** adapted from O'Driscoll et al. (100)]. The extent and duration of AHR activation by AHR ligands adhered to PM shifts the T cell response resulting in an effector T cell response that is suppressed and ameliorates autoimmunity or enhanced and aggravates autoimmunity [**Figure 3** adapted from O'Driscoll et al. (100)]. Additionally, AHR ligands may become bioavailable either while adhered to the PM or after getting removed from the PM. Once bioavailable, the ligands have the capacity to get metabolized by CYP enzymes and this metabolism can play a role aggravating autoimmune disease [**Figure 3** adapted from

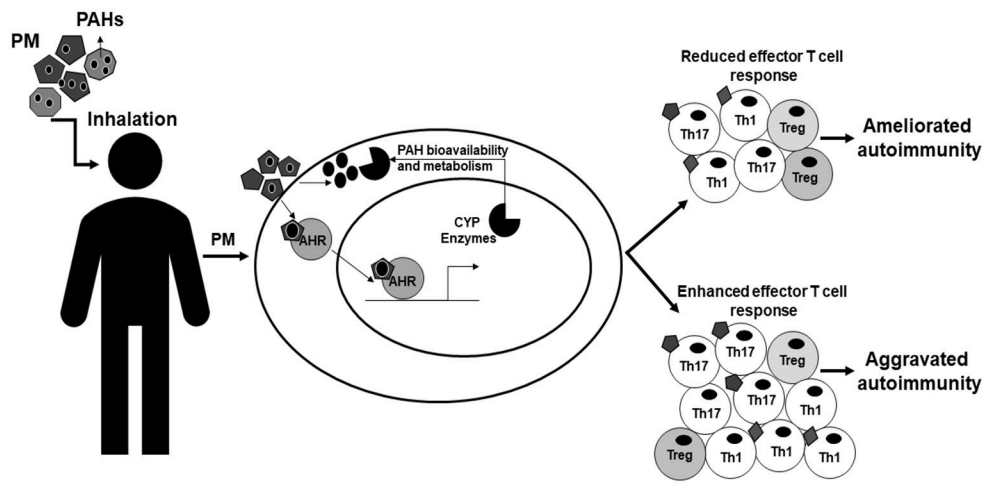

FIGURE 3 | Model of AHR modulation of PM-mediated autoimmunity. This figure is adapted from O'Driscoll et al. (100) and demonstrates how AHR may modulate PM-mediated autoimmunity. PM is inhaled by people and once inhaled is able to be taken-up and has the capacity to activate the AHR in cells within the body. AHR ligands, such as PAHs, adhered to atmospheric PM activate the AHR and cause the AHR to translocate to the nucleus and bind DNA elements such as XRE, inducing genes including CYP enzymes. The extent and duration of activation of AHR ligands shifts the immune balance enhancing effector T cells worsening autoimmunity or suppressing T cell responses and ameliorating autoimmunity. The AHR ligands adhered to the particulate have the potential to become bioavailable through metabolism or other mechanisms and then can be metabolized by CYP enzymes potentially causing other immune related effects or altering the immune responses. AHR, aryl hydrocarbon receptor; PM, particulate matter; PAHs, polycyclic aromatic hydrocarbons; XRE, xenobiotic response element; CYP, cytochrome P450. This figure or a version of this figure was published in Particle and Fibre and Toxicology and is licensed under the Creative Commons Attribution 4.0 International Public License.

O'Driscoll et al. (100)]. The identification of components of PM that activate the AHR and also specific AHR pathway targets that can shift the immune balance from inflammatory to regulatory are crucial for understanding the mechanisms through which the AHR contributes to PM-mediated autoimmune disease. PM contains multiple AHR ligands and thus understanding the specific ligands and pathways involved in autoimmune disease could lend insight into the environmental component of autoimmune pathology. Although the AHR is unlikely to be the whole story, it may be a start to identifying mechanisms to alleviate symptoms of autoimmune disease as well as prevent disease all together. Future studies should investigate (1) the AHR ligands present in PM and how they alter T cell response and (2) the specific AHR pathway components required for responses in order to generate therapies to decrease autoimmune disease and hopefully prevent disease onset secondary to PM exposure.

AUTHOR CONTRIBUTIONS

CO and JM wrote the manuscript. All authors read and approved the final manuscript.

FUNDING

This work was supported by the National Institute of Environmental Health Sciences (NIEHS). [RO1 ES023842 to JM, R21 ES025304 to JM], and [T32 ES007015 (CO)]. Its contents are solely the responsibility of the authors and do not necessarily represent the official views of the NIEHS.

REFERENCES

1. Miller FW, Alfredsson L, Costenbader KH, Kamen DL, Nelson LM, Norris JM, et al. Epidemiology of environmental exposures and human autoimmune diseases: findings from a National Institute of Environmental Health Sciences Expert Panel Workshop. *J Autoimmun.* (2012) 39:259–71. doi: 10.1016/j.jaut.2012.05.002
2. Cooper GS, Bynum MLK, Somers EC. Recent insights in the epidemiology of autoimmune diseases. Improved prevalence estimates and understanding of clustering of diseases. *J Autoimmun.* (2009) 33:197–207 doi: 10.1016/j.jaut.2009.09.008
3. Lerner A, Jeremias P, and Matthias, T. The world incidence and prevalence of autoimmune diseases is increasing. *Int J Celiac Dis.* (2015) 3:151–5. doi: 10.12691/ijcd-3-4-8
4. NIO Health. Progress in autoimmune disease research. In: *The Autoimmune Diseases Coordinating Committee*. Bethesda: National Institute of Health (2005). p. 1–146.
5. Cooper GS, Stroehla BC. The epidemiology of autoimmune diseases. *Autoimmun Rev.* (2003) 2:119–25. doi: 10.1016/S1568-9972(03)00006-5
6. Goverman J. Autoimmune T cell responses in the central nervous system. *Nat Rev Immunol.* (2009) 9:393. doi: 10.1038/nri2550
7. Suarez-Fueyo A, Bradley SJ, Tsokos GC. T cells in systemic lupus erythematosus. *Curr Opin Immunol.* (2016) 43:32–8. doi: 10.1016/j.coi.2016.09.001
8. Cope AP, Schulze-Koops H, Aringer M. The central role of T cells in rheumatoid arthritis. *Clin Exp Rheumatol.* (2007) 25:S4–11.
9. Pugliese A. Autoreactive T cells in type 1 diabetes *J Clin Invest.* (2017) 127:2881–91. doi: 10.1172/JCI94549
10. Fletcher JM, Lalor SJ, Sweeney CM, Tubridy N, Mills KHG. T cells in multiple sclerosis and experimental autoimmune encephalomyelitis. *Clin Exp Immunol.* (2010) 162:1–11. doi: 10.1111/j.1365-2249.2010.04143.x
11. Rosenblum MD, Remedios KA, Abbas AK. Mechanisms of human autoimmunity. *J Clin Invest.* (2015) 125:2228–33. doi: 10.1172/JCI78088
12. Vojdani A, Pollard KM, Campbell AW. Environmental triggers and autoimmunity. *Autoimmune Dis.* (2014) 2014:798029. doi: 10.1155/2014/798029
13. Seldin MF. The genetics of human autoimmune disease: a perspective on progress in the field and future directions. *J Autoimmun.* (2015) 64:1–12. doi: 10.1016/j.jaut.2015.08.015
14. Institute HE. State of Global Air 2018. In: *Health Effects Institute*, Boston, MA (2018).
15. Brauer M, Freedman G, Frostad J, van Donkelaar A, Martin RV, Dentener F, et al. Ambient air pollution exposure estimation for the global burden of disease 2013. *Environ Sci Technol.* (2016) 50:79–88. doi: 10.1021/acs.est.5b03709
16. Beyerlein A, Krasmann M, Thiering E, Kusian D, Markevych I, D'Orlando O, et al. Ambient air pollution and early manifestation of type 1 diabetes. *Epidemiology* (2015) 26:e31–2. doi: 10.1097/EDE.0000000000000254
17. Brook RD, Cakmak S, Turner MC, Brook JR, Crouse DL, Peters PA, et al. T. Long-term fine particulate matter exposure and mortality from diabetes in Canada. *Diabetes Care* (2013) 36:3313–20. doi: 10.2337/dc12-2189
18. Di Ciaula A. Type I diabetes in paediatric age in Apulia (Italy): Incidence and associations with outdoor air pollutants. *Diabetes Res Clin Pract.* (2016) 111:36–43. doi: 10.1016/j.diabres.2015.10.016
19. Gonzalez RN, Torres-Aviles F, Carrasco PE, Salas PF, Perez BF. [Association of the incidence of type 1 diabetes mellitus with environmental factors in Chile during the period 2000-2007]. *Rev Med Chil.* (2013) 141:595–601. doi: 10.4067/S0034-98872013000500007
20. Hathout EH, Beeson WL, Nahab F, Rabadi A, Thomas W, Mace JW. Role of exposure to air pollutants in the development of type 1 diabetes before and after 5 yr of age. *Pediatr Diabetes* (2002) 3:184–8. doi: 10.1034/j.1399-5448.2002.30403.x
21. Malmqvist E, Larsson HE, Jonsson I, Rignell-Hydbom A, Ivarsson SA, Tinnerberg H, et al. Maternal exposure to air pollution and type 1 diabetes–Accounting for genetic factors. *Environ Res.* (2015) 140:268–74. doi: 10.1016/j.envres.2015.03.024
22. Angelici L, Piola M, Cavalleri T, Randi G, Cortini F, Bergamaschi R, et al. Effects of particulate matter exposure on multiple sclerosis hospital admission in Lombardy region, Italy. *Environ Res.* (2016) 145:68–73. doi: 10.1016/j.envres.2015.11.017
23. Gregory AC, Shendell DG, Okosun IS, Gieseker KE. Multiple sclerosis disease distribution and potential impact of environmental air pollutants in Georgia. *Sci Total Environ.* (2008) 396:42–51. doi: 10.1016/j.scitotenv.2008.01.065
24. Oikonen M, Laaksonen M, Laippala P, Oksaranta O, Lilius EM, Lindgren S, et al. Ambient air quality and occurrence of multiple sclerosis relapse. *Neuroepidemiology* (2003) 22:95–9. doi: 10.1159/000067108
25. Roux J, Bard D, Le Pabic E, Segala C, Reis J, Ongagna JC, et al. Air pollution by particulate matter PM10 may trigger multiple sclerosis relapses. *Environ Res.* (2017) 156:404–10. doi: 10.1016/j.envres.2017.03.049
26. Vojinovic S, Savic D, Lukic S, Savic L, Vojinovic J. Disease relapses in multiple sclerosis can be influenced by air pollution and climate seasonal conditions. *Vojnosanit Pregl* (2015) 72:44–9. doi: 10.2298/VSP140121030V
27. Chang KH, Hsu CC, Muo CH, Hsu CY, Liu HC, Kao CH, et al. Air pollution exposure increases the risk of rheumatoid arthritis: A longitudinal and nationwide study. *Environ Int.* (2016) 94:495–9. doi: 10.1016/j.envint.2016.06.008
28. Vidotto JP, Pereira LA, Braga AL, Silva CA, Sallum AM, Campos LM, et al. Atmospheric pollution: influence on hospital admissions in paediatric rheumatic diseases. *Lupus* (2012) 21:526–33. doi: 10.1177/0961203312437806
29. Bernatsky S, Fournier M, Pineau CA, Clarke AE, Vinet E, Smargiassi A. Associations between ambient fine particulate levels and disease activity in

patients with systemic lupus erythematosus (SLE). *Environ Health Perspect.* (2011) 119:45–9. doi: 10.1289/ehp.1002123
30. Bernatsky S, Smargiassi A, Johnson M, Kaplan GG, Barnabe C, Svenson L, et al. Fine particulate air pollution, nitrogen dioxide, and systemic autoimmune rheumatic disease in Calgary, Alberta. *Environ Res.* (2015) 140:474–8. doi: 10.1016/j.envres.2015.05.007
31. Bernatsky S, Smargiassi A, Barnabe C, Svenson LW, Brand A, Martin RV, et al. Fine particulate air pollution and systemic autoimmune rheumatic disease in two Canadian provinces. *Environ Res.* (2016) 146:85–91. doi: 10.1016/j.envres.2015.12.021
32. Fernandes EC, Silva CA, Braga AL, Sallum AM, Campos LM, Farhat SC. Exposure to air pollutants and disease activity in juvenile-onset systemic lupus erythematosus patients. *Arthritis Care Res.* (2015) 67:1609–14. doi: 10.1002/acr.22603
33. Farhat SC, Silva CA, Orione MA, Campos LM, Sallum AM, Braga AL. Air pollution in autoimmune rheumatic diseases: a review. *Autoimmun Rev.* (2011) 11:14–21. doi: 10.1016/j.autrev.2011.06.008
34. Gawda A, Majka G, Nowak B, Marcinkiewicz J. Air pollution, oxidative stress, and exacerbation of autoimmune diseases. *Cent Eur J Immunol.* (2017) 42:305–12. doi: 10.5114/ceji.2017.70975
35. Kelly FJ, Fussell JC. Size, source and chemical composition as determinants of toxicity attributable to ambient particulate matter. *Atmospheric Environ.* (2012) 60:504–26. doi: 10.1016/j.atmosenv.2012.06.039
36. National Research Council. *Global Sources of Local Pollution: An Assessment of Long-Range Transport of Key Air Pollutants to and From the United States*. Washington, DC: TNA Press (2010).
37. Cheung K, Daher N, Kam W, Shafer MM, Ning Z, Schauer JJ, et al. Spatial and temporal variation of chemical composition and mass closure of ambient coarse particulate matter (PM10–2.5) in the Los Angeles area. *Atmos Environ.* (2011) 45:2651–62. doi: 10.1016/j.atmosenv.2011.02.066
38. Vincent R, Bjarnason SG, Adamson IY, Hedgecock C, Kumarathasan P, Guénette J, et al. Acute pulmonary toxicity of urban particulate matter and ozone. *Am J Pathol.* (1997) 151:1563–70.
39. USEP Agency. *Health Assessment Document for Diesel Engine Exhaust* (Final 2002). Washington, DC: US Environmental Protection Agency; National Center for Environmental Assessment; EPA, Washington Office (2002).
40. DeGroot D, He G, Fraccalvieri D, Bonati L, Pandini A, Denison M. AhR ligands: promiscuity in binding and diversity in response. In: Pohjanvirta R, editor. *The AH Receptor in Biology and Toxicology*. Hoboken, NJ: Wiley (2011).
41. Denison MS, Nagy SR. Activation of the aryl hydrocarbon receptor by structurally diverse exogenous and endogenous chemicals. *Annu Rev Pharmacol Toxicol.* (2003) 43:309–34. doi: 10.1146/annurev.pharmtox.43.100901.135828
42. White SS, Birnbaum LS. An overview of the effects of dioxins and dioxin-like compounds on vertebrates, as documented in human and ecological epidemiology. *J Environ Sci Health C Environ Carcinog Ecotoxicol Rev.* (2009) 27:197–211. doi: 10.1080/10590500903310047
43. Stockinger B, Di Meglio P, Gialitakis M, Duarte JH. The aryl hydrocarbon receptor: multitasking in the immune system. *Annu Rev Immunol.* (2014) 32:403–32. doi: 10.1146/annurev-immunol-032713-120245
44. Veldhoen M, Hirota K, Westendorf AM, Buer J, Dumoutier L, Renauld JC, et al. The aryl hydrocarbon receptor links TH17-cell-mediated autoimmunity to environmental toxins. *Nature* (2008) 453:106–9. doi: 10.1038/nature06881
45. Mascanfroni ID, Takenaka MC, Yeste A, Patel B, Wu Y, Kenison JE, et al. Metabolic control of type 1 regulatory T cell differentiation by AHR and HIF1-alpha. *Nat Med.* (2015) 21:638–46. doi: 10.1038/nm.3868
46. Quintana FJ, Basso AS, Iglesias AH, Korn T, Farez MF, Bettelli E, et al. Control of T(reg) and T(H)17 cell differentiation by the aryl hydrocarbon receptor. *Nature* (2008) 453:65–71. doi: 10.1038/nature06880
47. Nguyen LP, Bradfield CA. The search for endogenous activators of the aryl hydrocarbon receptor. *Chem Res Toxicol.* (2008) 21:102–16. doi: 10.1021/tx7001965
48. Griesemer AD, Sorenson EC, Hardy MA. The role of the thymus in tolerance. *Transplantation* (2010) 90:465–74. doi: 10.1097/TP.0b013e3181e7e54f
49. Charles J, Janeway A, Travers P, Walport M, Shlomchik MJ. *Self-Tolerance and Its Loss*. Garland Science (2001).
50. Sojka DK, Huang YH, Fowell DJ. Mechanisms of regulatory T-cell suppression – a diverse arsenal for a moving target. *Immunology* (2008) 124:13–22. doi: 10.1111/j.1365-2567.2008.02813.x
51. Dardalhon V, Korn T, Kuchroo VK, Anderson AC. Role of Th1 and Th17 cells in organ-specific autoimmunity. *J Autoimmun.* (2008) 31:252–6. doi: 10.1016/j.jaut.2008.04.017
52. Langrish CL, Chen Y, Blumenschein WM, Mattson J, Basham B, Sedgwick JD, et al. IL-23 drives a pathogenic T cell population that induces autoimmune inflammation. *J Exp Med.* (2005) 201:233–40. doi: 10.1084/jem.20041257
53. Komatsu N, Okamoto K, Sawa S, Nakashima TM, Oh-hora, KT, Tanaka S, et al. Pathogenic conversion of Foxp3+ T cells into TH17 cells in autoimmune arthritis. *Nat Med.* (2014) 20:62–8. doi: 10.1038/nm.3432
54. Burkett PR, Horste GMz, Kuchroo VK. Pouring fuel on the fire: Th17 cells, the environment, and autoimmunity. *J Clin Invest.* (2015) 125:2211–9. doi: 10.1172/JCI78085
55. Bell ML. *Assessment of the Health Impacts of Particulate Matter Characteristics*. Boston, MA: Health Effects Institute (2012).
56. Anderson JO, Thundiyil JG, Stolbach A. Clearing the air: a review of the effects of particulate matter air pollution on human health. *J Med Toxicol.* (2012) 8:166–75. doi: 10.1007/s13181-011-0203-1
57. DeCarlo PF, Slowik JG, Worsnop DR, Davidovits P, Jimenez JL. Particle Morphology and Density Characterization by Combined Mobility and Aerodynamic Diameter Measurements. Part 1: Theory. *Aerosol Sci Technol.* (2012) 38:1185–205. doi: 10.1080/027868290903907
58. Griffin RJ. The sources and impacts of tropospheric particulate matter. *Nat Educ Knowledge* (2013) 4:1.
59. Pierdominici M, Maselli A, Cecchetti S, Tinari A, Mastrofrancesco A, Alfe M, et al. Diesel exhaust particle exposure in vitro impacts T lymphocyte phenotype and function. *Part Fibre Toxicol.* (2014) 11:74. doi: 10.1186/s12989-014-0074-0
60. Nakamura R, Inoue K, Fujitani Y, Kiyono M, Hirano S, Takano. H. Effects of nanoparticle-rich diesel exhaust particles on IL-17 production *in vitro*. *J Immunotoxicol.* (2012) 9:72–6. doi: 10.3109/1547691X.2011.629638
61. Ma QY, Huang DY, Zhang HJ, Wang S, Chen XF. Exposure to particulate matter 2.5 (PM2.5) induced macrophage-dependent inflammation, characterized by increased Th1/Th17 cytokine secretion and cytotoxicity. *Int Immunopharmacol.* (2017) 50:139–45. doi: 10.1016/j.intimp.2017.06.019
62. Deiuliis JA, Kampfrath T, Zhong J, Oghumu S, Maiseyeu A, Chen LC, et al. Pulmonary T cell activation in response to chronic particulate air pollution. *Am J Physiol Lung Cell Mol Physiol.* (2012) 302:L399–409. doi: 10.1152/ajplung.00261.2011
63. van Voorhis M, Knopp S, Julliard W, Fechner JH, Zhang X, Schauer JJ, et al. Exposure to atmospheric particulate matter enhances Th17 polarization through the aryl hydrocarbon receptor. *PLoS ONE* (2013) 8:e82545. doi: 10.1371/journal.pone.0082545
64. Castaneda AR, Pinkerton KE, Bein KJ, Magana-Mendez A, Yang HT, Ashwood P, et al. Ambient particulate matter activates the aryl hydrocarbon receptor in dendritic cells and enhances Th17 polarization. *Toxicol Lett.* (2018) 292:85–96. doi: 10.1016/j.toxlet.2018.04.020
65. Atkinson MA, Eisenbarth GS, Michels AW. Type 1 diabetes. *Lancet* (2014) 383:69–82. doi: 10.1016/S0140-6736(13)60591-7
66. Schneider A, Rieck M, Sanda S, Pihoker C, Greenbaum C, Buckner JH. The effector T cells of diabetic subjects are resistant to regulation via CD4+ FOXP3+ regulatory T cells. *J Immunol.* (2008) 181:7350–5. doi: 10.4049/jimmunol.181.10.7350
67. Ferraro A, Socci C, Stabilini A, Valle A, Monti P, Piemonti L, et al. Expansion of Th17 cells and functional defects in T regulatory cells are key features of the pancreatic lymph nodes in patients with type 1 diabetes (2011) 60:2903–13. doi: 10.2337/db11-0090
68. Maahs DM, West NA, Lawrence JM, Mayer-Davis EJ. Chapter 1: epidemiology of type 1 diabetes. *Endocrinol Metab Clin North Am.* (2010) 39:481–97. doi: 10.1016/j.ecl.2010.05.011
69. Patterson CC, Dahlquist GG, Gyurus E, Green A, Soltesz G. Incidence trends for childhood type 1 diabetes in Europe during 1989–2003 and predicted new cases 2005–20: a multicentre prospective registration study. *Lancet* (2009) 373:2027–33. doi: 10.1016/S0140-6736(09)60568-7

70. Hathout EH, Beeson WL, Ischander M, Rao R, Mace JW. Air pollution and type 1 diabetes in children. *Pediatr Diabetes* (2006) 7:81–7. doi: 10.1111/j.1399-543X.2006.00150.x
71. Michalska M, Bartoszewicz M, Waz P, Kozaczuk S, Ben-Skowronek I, Zorena K. PM10 concentration and microbiological assessment of air in relation to the number of acute cases of type 1 diabetes mellitus in the Lubelskie Voivodeship. Preliminary report. *Pediatr Endocrinol Diabetes Metab.* (2017) 23:70–6. doi: 10.18544/PEDM-23.02.0076
72. Yitshak Sade M, Kloog I, Liberty IF, Schwartz J, Novack V. The association between air pollution exposure and glucose and lipids levels. *J Clin Endocrinol Metab.* (2016) 101:2460–7. doi: 10.1210/jc.2016-1378
73. Lanzinger S, Rosenbauer J, Sugiri D, Schikowski T, Treiber B, Klee D, et al. Impact of long-term air pollution exposure on metabolic control in children and adolescents with type 1 diabetes: results from the DPV registry. *Diabetologia* (2018) 61:1354–61. doi: 10.1007/s00125-018-4580-8
74. Feldmann M, Brennan FM, Maini RN. Rheumatoid arthritis. *Cell* (1996) 85:307–10. doi: 10.1016/S0092-8674(00)81109-5
75. Brennan FM, McInnes IB. Evidence that cytokines play a role in rheumatoid arthritis. *J Clin Invest.* (2008) 118:3537–45. doi: 10.1172/JCI36389
76. Hart JE, Laden F, Puett RC, Costenbader KH, Karlson EW. Exposure to traffic pollution and increased risk of rheumatoid arthritis. *Environ Health Perspect.* (2009) 117:1065–9. doi: 10.1289/ehp.0800503
77. Hoovestol RA, Mikuls TR. Environmental exposures and rheumatoid arthritis risk. *Curr Rheumatol Rep.* (2011) 13:431–9. doi: 10.1007/s11926-011-0203-9
78. De Roos AJ, Koehoorn M, Tamburic L, Davies HW, Brauer M. Proximity to traffic, ambient air pollution, and community noise in relation to incident rheumatoid arthritis. *Environ Health Perspect.* (2014) 122:1075–80. doi: 10.1289/ehp.1307413
79. Hart JE, Källberg H, Laden F, Costenbader KH, Yanosky JD, Klareskog L, et al. Ambient air pollution exposures and risk of rheumatoid arthritis in the Nurses' Health Study. *Arthritis Care Res.* (2013) 65:1190–6. doi: 10.1002/acr.21975
80. Hart JE, Kallberg H, Laden F, Bellander T, Costenbader KH, Holmqvist M, et al. Ambient air pollution exposures and risk of rheumatoid arthritis: results from the Swedish EIRA case-control study. *Ann Rheum Dis.* (2013) 72:888–94. doi: 10.1136/annrheumdis-2012-201587
81. Chiang YC, Yen YH, Chang WC, Cheng KJ, Chang WP, Chen HY. The association between urbanization and rheumatoid arthritis in Taiwan. *Int J Clin Pharmacol Ther.* (2016) 54:1–10. doi: 10.5414/CP202306
82. Sigaux J, Biton J, Andre E, Semerano L, Boissier MC. Air pollution as a determinant of rheumatoid arthritis. *Joint Bone Spine* (2018) doi: 10.1016/j.jbspin.2018.03.001
83. Gan RW, Deane KD, Zerbe GO, Demoruelle MK, Weisman MH, Buckner JH, et al. Relationship between air pollution and positivity of RA-related autoantibodies in individuals without established RA: a report on SERA. *Ann Rheum Dis.* (2013) 72:2002–5. doi: 10.1136/annrheumdis-2012-202949
84. Sun G, Hazlewood G, Bernatsky S, Kaplan GG, Eksteen B, Barnabe C. Association between air pollution and the development of rheumatic disease: a systematic review. *Int J Rheumatol.* (2016) 2016:5356307. doi: 10.1155/2016/5356307
85. Zeft AS, Prahalad S, Lefevre S, Clifford B, McNally B, Bohnsack JF, et al. Juvenile idiopathic arthritis and exposure to fine particulate air pollution. *Clin Exp Rheumatol.* (2009) 27:877–84.
86. Zeft AS, Prahalad S, Schneider R, Dedeoglu F, Weiss PF, Grom AA, et al. Systemic onset juvenile idiopathic arthritis and exposure to fine particulate air pollution. *Clin Exp Rheumatol.* (2016) 34:946–52.
87. Compston A, Coles A. Multiple sclerosis. *Lancet* (2008) 372:1502–17. doi: 10.1016/S0140-6736(08)61620-7
88. Oikonen MK, Eralinna JP. Beta-interferon protects multiple sclerosis patients against enhanced susceptibility to infections caused by poor air quality. *Neuroepidemiology* (2008) 30:13–9. doi: 10.1159/000113301
89. Jeanjean M, Bind MA, Roux J, Ongagna JC, de Seze J, Bard D, et al. Ozone, NO2 and PM10 are associated with the occurrence of multiple sclerosis relapses. Evidence from seasonal multi-pollutant analyses. *Environ Res.* (2018) 163:43–52. doi: 10.1016/j.envres.2018.01.040
90. Heydarpour P, Amini H, Khoshkish S, Seidkhani H, Sahraian MA, Yunesian M. Potential impact of air pollution on multiple sclerosis in Tehran, Iran. *Neuroepidemiology* (2014) 43:233–8. doi: 10.1159/000368553
91. Lavery AM, Waldman AT, Charles Casper T, Roalstad S, Candee M, Rose J, et al. Examining the contributions of environmental quality to pediatric multiple sclerosis. *Mult Scler Relat Disord.* (2017) 18:164–9. doi: 10.1016/j.msard.2017.09.004
92. Bergamaschi R, Cortese A, Pichiecchio A, Berzolari FG, Borrelli P, Mallucci G, et al. Air pollution is associated to the multiple sclerosis inflammatory activity as measured by brain MRI. *Mult Scler.* (2018) 24:1578–84. doi: 10.1177/1352458517726866
93. Klocke C, Allen JL, Sobolewski M, Mayer-Proschel M, Blum JL, Lauterstein D, et al. Neuropathological consequences of gestational exposure to concentrated ambient fine and ultrafine particles in the mouse. *Toxicol Sci.* (2017) 156:492–508. doi: 10.1093/toxsci/kfx010
94. Klocke C, Allen JL, Sobolewski M, Blum JL, Zelikoff JT, Cory-Slechta DA. Exposure to fine and ultrafine particulate matter during gestation alters postnatal oligodendrocyte maturation, proliferation capacity, and myelination. *Neurotoxicology* (2018) 65:196–206. doi: 10.1016/j.neuro.2017.10.004
95. Palacios N, Munger KL, Fitzgerald KC, Hart JE, Chitnis T, Ascherio A, et al. Exposure to particulate matter air pollution and risk of multiple sclerosis in two large cohorts of US nurses. *Environ Int.* (2017) 109:64–72. doi: 10.1016/j.envint.2017.07.013
96. Chen H, Kwong JC, Copes R, Tu K, Villeneuve PJ, van Donkelaar A, et al. Living near major roads and the incidence of dementia, Parkinson's disease, and multiple sclerosis: a population-based cohort study. *Lancet* (2017) 389:718–26. doi: 10.1016/S0140-6736(16)32399-6
97. Carmona R, Linares C, Recio A, Ortiz C, Diaz J. Emergency multiple sclerosis hospital admissions attributable to chemical and acoustic pollution: Madrid (Spain), 2001–2009. *Sci Total Environ.* (2018) 612:111–8. doi: 10.1016/j.scitotenv.2017.08.243
98. Tsokos GC. Systemic lupus erythematosus. *N Engl J Med.* (2011) 365:2110–21. doi: 10.1056/NEJMra1100359
99. Bernatsky S, Joseph L, Pineau CA, Tamblyn R, Feldman DE, Clarke AE. A population-based assessment of systemic lupus erythematosus incidence and prevalence–results and implications of using administrative data for epidemiological studies. *Rheumatology* (2007) 46:1814–8. doi: 10.1093/rheumatology/kem233
100. O'Driscoll CA, Owens LA, Gallo ME, Hoffmann EJ, Afrazi A, Han M, et al. Differential effects of diesel exhaust particles on T cell differentiation and autoimmune disease. *Part Fibre Toxicol.* (2018) 15:35. doi: 10.1186/s12989-018-0271-3
101. O'Driscoll CA, Owens LA, Hoffmann EJ, Gallo ME, Afrazi A, et al. Ambient urban dust particulate matter reduces pathologic T cells in the CNS and severity of EAE. *Environmental Res.* (2018) 168:178–92. doi: 10.1016/j.envres.2018.09.038
102. Duarte JH, Di Meglio P, Hirota K, Ahlfors H, Stockinger B. Differential influences of the aryl hydrocarbon receptor on Th17 mediated responses *in vitro* and *in vivo*. *PLoS ONE* (2013) 8:e79819. doi: 10.1371/journal.pone.0079819
103. Kerkvliet NI, Steppan LB, Vorachek W, Oda S, Farrer D, Wong CP, et al. Activation of aryl hydrocarbon receptor by TCDD prevents diabetes in NOD mice and increases Foxp3+ T cells in pancreatic lymph nodes. *Immunotherapy* (2009) 1:539–47. doi: 10.2217/imt.09.24
104. Ishimaru N, Takagi A, Kohashi M, Yamada A, Arakaki R, Kanno J, et al. Neonatal exposure to low-dose 2,3,7,8-tetrachlorodibenzo-p-dioxin causes autoimmunity due to the disruption of T cell tolerance. *J Immunol.* (2009) 182:6576–86. doi: 10.4049/jimmunol.0802289
105. Boule LA, Burke CG, Fenton BM, Thevenet-Morrison K, Jusko TA, Lawrence BP. Developmental activation of the AHR increases effector CD4+ T cells and exacerbates symptoms in autoimmune disease-prone Gnaq+/- Mice. *Toxicol Sci.* (2015) 148:555–66. doi: 10.1093/toxsci/kfv203
106. Fu J, Nogueira SV, van Drongelen V, Coit P, Ling S, Rosloniec EF, et al. Shared epitope–aryl hydrocarbon receptor crosstalk underlies the mechanism of gene–environment interaction in autoimmune arthritis. *Proc Natl Acad Sci USA.* (2018) 115:4755–60. doi: 10.1073/pnas.1722124115

107. Singh NP, Singh UP, Rouse M, Zhang J, Chatterjee S, Nagarkatti PS, et al. Dietary indoles suppress delayed-type hypersensitivity by inducing a switch from proinflammatory Th17 cells to anti-inflammatory regulatory T cells through regulation of microRNA. *J Immunol.* (2016) 196:1108–22. doi: 10.4049/jimmunol.1501727
108. Ehrlich AK, Pennington JM, Wang X, Rohlman D, Punj S, Lohr CV, et al. Activation of the Aryl hydrocarbon receptor by 10-Cl-BBQ prevents insulitis and effector T cell development independently of Foxp3+ regulatory T cells in nonobese diabetic mice. *J Immunol.* (2016) 196:264–73. doi: 10.4049/jimmunol.1501789
109. Tong B, Yuan X, Dou Y, Wu X, Chou G, Wang Z, et al. Norisoboldine, an isoquinoline alkaloid, acts as an aryl hydrocarbon receptor ligand to induce intestinal Treg cells and thereby attenuate arthritis. *Int J Biochem Cell Biol.* (2016) 75:63–73. doi: 10.1016/j.biocel.2016.03.014
110. Yuan X, Tong B, Dou Y, Wu X, Wei Z, Dai Y. Tetrandrine ameliorates collagen-induced arthritis in mice by restoring the balance between Th17 and Treg cells via the aryl hydrocarbon receptor. *Biochem Pharmacol.* (2016) 101:87–99. doi: 10.1016/j.bcp.2015.11.025
111. Tong B, Yuan X, Dou Y, Wu X, Wang Y, Xia Y, et al. Sinomenine induces the generation of intestinal Treg cells and attenuates arthritis via activation of aryl hydrocarbon receptor. *Lab Invest.* (2016) 96:1076–86. doi: 10.1038/labinvest.2016.86
112. Kaye J, Piryatinsky V, Birnberg T, Hingaly T, Raymond E, Kashi R, et al. Laquinimod arrests experimental autoimmune encephalomyelitis by activating the aryl hydrocarbon receptor. *Proc Natl Acad Sci USA*. (2016) 113:E6145–52. doi: 10.1073/pnas.1607843113
113. Quintana FJ, Murugaiyan G, Farez MF, Mitsdoerffer M, Tukpah AM, Burns EJ, et al. An endogenous aryl hydrocarbon receptor ligand acts on dendritic cells and T cells to suppress experimental autoimmune encephalomyelitis. *Proc Natl Acad Sci USA*. (2010) 107:20768–73. doi: 10.1073/pnas.1009201107
114. Rouse M, Singh NP, Nagarkatti PS, Nagarkatti M. Indoles mitigate the development of experimental autoimmune encephalomyelitis by induction of reciprocal differentiation of regulatory T cells and Th17 cells. *Br J Pharmacol.* (2013) 169:1305–21. doi: 10.1111/bph.12205
115. Nakahama T, Kimura A, Nguyen NT, Chinen I, Hanieh H, Nohara K, et al. Aryl hydrocarbon receptor deficiency in T cells suppresses the development of collagen-induced arthritis. *Proc Natl Acad Sci USA*. (2011) 108:14222–7. doi: 10.1073/pnas.1111786108
116. Talbot J, Peres RS, Pinto LG, Oliveira RDR, Lima KA, Donate PB, et al. Smoking-induced aggravation of experimental arthritis is dependent of aryl hydrocarbon receptor activation in Th17 cells. *Arthritis Res Ther.* (2018) 20:119. doi: 10.1186/s13075-018-1609-9
117. Ehrlich A, Pennington J, Greer R, Shulzhenko N, Kerkvliet N. Characterization of the microbiome in association with reduced diabetes incidence in AhR deficient NOD mice. *J Immunol.* (2016) 196:118.22.
118. Lahoti TS, John K, Hughes JM, Kusnadi A, Murray IA, Krishnegowda G, Amin et al. Aryl hydrocarbon receptor antagonism mitigates cytokine-mediated inflammatory signalling in primary human fibroblast-like synoviocytes. *Ann Rheum Dis.* (2013) 72:1708–16. doi: 10.1136/annrheumdis-2012-202639
119. Lahoti TS, Hughes JM, Kusnadi A, John K, Zhu B, Murray IA, et al. Aryl hydrocarbon receptor antagonism attenuates growth factor expression, proliferation, and migration in fibroblast-like synoviocytes from patients with rheumatoid arthritis. *J Pharmacol Exp Ther.* (2014) 348:236–45. doi: 10.1124/jpet.113.209726
120. Andrysik Z, Vondracek J, Marvanova S, Ciganek M, Neca J, Pencikova K, et al. Activation of the aryl hydrocarbon receptor is the major toxic mode of action of an organic extract of a reference urban dust particulate matter mixture: the role of polycyclic aromatic hydrocarbons. *Mutat Res.* (2011) 714:53–62. doi: 10.1016/j.mrfmmm.2011.06.011
121. Arrieta DE, Ontiveros CC, Li WW, Garcia JH, Denison MS, McDonald JD, et al. Aryl hydrocarbon receptor-mediated activity of particulate organic matter from the Paso del Norte airshed along the U.S.-Mexico border. *Environ Health Perspect.* (2003) 111:1299–305. doi: 10.1289/ehp.6058
122. den Hartigh LJ, Lame MW, Ham W, Kleeman MJ, Tablin F, Wilson DW. Endotoxin and polycyclic aromatic hydrocarbons in ambient fine particulate matter from Fresno, California initiate human monocyte inflammatory responses mediated by reactive oxygen species. *Toxicol In Vitro* (2010) 24:1993–2002. doi: 10.1016/j.tiv.2010.08.017
123. Jaguin M, Fardel O, Lecureur V. Exposure to diesel exhaust particle extracts (DEPe) impairs some polarization markers and functions of human macrophages through activation of AhR and Nrf2. *PLoS ONE* (2015) 10:e0116560 doi: 10.1371/journal.pone.0116560
124. Gauggel-Lewandowski S, Heussner AH, Steinberg P, Pieterse B, van der Burg B, Dietrich DR. Bioavailability and potential carcinogenicity of polycyclic aromatic hydrocarbons from wood combustion particulate matter *in vitro*. *Chem Biol Interact.* (2013) 206:411–22. doi: 10.1016/j.cbi.2013.05.015
125. Libalova H, Krckova S, Uhlirova K, Milcova A, Schmuczerova J, Ciganek M, et al. Genotoxicity but not the AhR-mediated activity of PAHs is inhibited by other components of complex mixtures of ambient air pollutants. *Toxicol Lett.* (2014) 225:350–7. doi: 10.1016/j.toxlet.2014.01.028
126. Vondracek J, Pencikova K, Neca J, Ciganek M, Grycova A, Dvorak Z, et al. Assessment of the aryl hydrocarbon receptor-mediated activities of polycyclic aromatic hydrocarbons in a human cell-based reporter gene assay. *Environ Pollut.* (2017) 220(Pt A), 307–16. doi: 10.1016/j.envpol.2016.09.064
127. Misaki K, Suzuki M, Nakamura M, Handa H, Iida M, Kato T, et al. Aryl hydrocarbon receptor and estrogen receptor ligand activity of organic extracts from road dust and diesel exhaust particulates. *Arch Environ Contam Toxicol.* (2008) 55:199–209. doi: 10.1007/s00244-007-9110-5
128. Palkova L, Vondracek J, Trilecova L, Ciganek M, Pencikova K, Neca J, et al. The aryl hydrocarbon receptor-mediated and genotoxic effects of fractionated extract of standard reference diesel exhaust particle material in pulmonary, liver and prostate cells. *Toxicol In Vitro* (2015) 29:438–48. doi: 10.1016/j.tiv.2014.12.002
129. Burbach KM, Poland A, Bradfield CA. Cloning of the Ah-receptor cDNA reveals a distinctive ligand-activated transcription factor. *Proc Natl Acad Sci USA* (1992) 89:8185–9. doi: 10.1073/pnas.89.17.8185
130. Ema M, Sogawa K, Watanabe N, Chujoh Y, Matsushita N, Gotoh O, et al. cDNA cloning and structure of mouse putative Ah receptor. *Biochem Biophys Res Commun.* (1992) 184:246–53. doi: 10.1016/0006-291X(92)91185-S
131. Perdew GH. Association of the Ah receptor with the 90-kDa heat shock protein. *J Biol Chem.* (1988) 263:13802–5.
132. Denis M, Cuthill S, Wikstrom AC, Poellinger L, Gustafsson JA. Association of the dioxin receptor with the Mr 90,000 heat shock protein: a structural kinship with the glucocorticoid receptor. *Biochem Biophys Res Commun.* (1988) 155:801–7. doi: 10.1016/S0006-291X(88)80566-7
133. Carver LA, Bradfield CA. Ligand-dependent interaction of the Aryl hydrocarbon receptor with a novel immunophilin homolog *in vivo*. (1997) *J Biol Chem*. 272:11452–6. doi: 10.1074/jbc.272.17.11452
134. Ma Q, Whitlock JP Jr. A novel cytoplasmic protein that interacts with the Ah receptor, contains tetratricopeptide repeat motifs, and augments the transcriptional response to 2,3,7,8-tetrachlorodibenzo-p-dioxin. *J Biol Chem.* (1997) 272:8878–84. doi: 10.1074/jbc.272.14.8878
135. Kazlauskas A, Poellinger L, Pongratz I. Evidence that the co-chaperone p23 regulates ligand responsiveness of the dioxin (Aryl hydrocarbon) receptor. *J Biol Chem.* (1999) 274:13519–24. doi: 10.1074/jbc.274.19.13519
136. Pongratz I, Mason GG, Poellinger L. Dual roles of the 90-kDa heat shock protein hsp90 in modulating functional activities of the dioxin receptor. Evidence that the dioxin receptor functionally belongs to a subclass of nuclear receptors which require hsp90 both for ligand binding activity and repression of intrinsic DNA binding activity. *J Biol Chem.* (1992) 267:13728–34.
137. Soshilov A, Denison MS. Ligand displaces heat shock protein 90 from overlapping binding sites within the aryl hydrocarbon receptor ligand-binding domain (2011) *J Biol Chem.* 286:35275–82. doi: 10.1074/jbc.M111.246439
138. Henry EC, Gasiewicz TA. Transformation of the aryl hydrocarbon receptor to a DNA-binding form is accompanied by release of the 90 kDa heat-shock protein and increased affinity for 2,3,7,8-tetrachlorodibenzo-p-dioxin (1993) 294(Pt 1):95–101.
139. Bunger MK, Moran SM, Glover E, Thomae TL, Lahvis GP, Lin BC, et al. Resistance to 2,3,7,8-tetrachlorodibenzo-p-dioxin toxicity and abnormal liver development in mice carrying a mutation in the nuclear localization

sequence of the aryl hydrocarbon receptor. *J Biol Chem.* (2003) 278:17767–74. doi: 10.1074/jbc.M209594200
140. Wilhelmsson A, Cuthill S, Denis M, Wikstrom AC, Gustafsson JA, Poellinger L. The specific DNA binding activity of the dioxin receptor is modulated by the 90 kd heat shock protein. *EMBO J* (1990) 9:69–76. doi: 10.1002/j.1460-2075.1990.tb08081.x
141. Ikuta T, Eguchi H, Tachibana T, Yoneda Y, Kawajiri K. Nuclear localization and export signals of the human aryl hydrocarbon receptor. *J Biol Chem.* (1998) 273:2895–904. doi: 10.1074/jbc.273.5.2895
142. Reyes H, Reisz-Porszasz S, Hankinson O. Identification of the Ah receptor nuclear translocator protein (Arnt) as a component of the DNA binding form of the Ah receptor. *Science* (1992) 256:1193–5. doi: 10.1126/science.256.5060.1193
143. Dolwick KM, Swanson HI, Bradfield CA. *In vitro* analysis of Ah receptor domains involved in ligand-activated DNA recognition. *Proc Natl Acad Sci USA.* (1993) 90:8566–70. doi: 10.1073/pnas.90.18.8566
144. Lusska A, Shen E, Whitlock JP Jr. Protein-DNA interactions at a dioxin-responsive enhancer. Analysis of six bona fide DNA-binding sites for the liganded Ah receptor. *J Biol Chem.* (1993) 268:6575–80.
145. Shen ES, Whitlock JP Jr. Protein-DNA interactions at a dioxin-responsive enhancer. Mutational analysis of the DNA-binding site for the liganded Ah receptor. *J Biol Chem.* (1992) 267:6815–9.
146. Hankinson O. Role of coactivators in transcriptional activation by the aryl hydrocarbon receptor. *Arch Biochem Biophys.* (2005) 433:379–86. doi: 10.1016/j.abb.2004.09.031
147. Tukey RH, Hannah RR, Negishi M, Nebert DW, Eisen HJ. The Ah locus: correlation of intranuclear appearance of inducer-receptor complex with induction of cytochrome P1–450 mRNA. *Cell* (1982) 31:275–84. doi: 10.1016/0092-8674(82)90427-5
148. Mezrich JD, Nguyen LP, Kennedy G, Nukaya M, Fechner JH, Zhang X, et al. SU5416, a VEGF receptor inhibitor and ligand of the AHR, represents a new alternative for immunomodulation. *PLoS ONE* (2012) 7:e44547. doi: 10.1371/journal.pone.0044547
149. Davarinos NA, Pollenz RS. Aryl hydrocarbon receptor imported into the nucleus following ligand binding is rapidly degraded via the cytosplasmic proteasome following nuclear export. *J Biol Chem.* (1999) 274:28708–15. doi: 10.1074/jbc.274.40.28708
150. Pollenz RS. The aryl-hydrocarbon receptor, but not the aryl-hydrocarbon receptor nuclear translocator protein, is rapidly depleted in hepatic and nonhepatic culture cells exposed to 2,3,7,8-tetrachlorodibenzo-p-dioxin. *Mol Pharmacol.* (1996) 49:391–8.
151. Roberts BJ, Whitelaw ML. Degradation of the basic helix-loop-helix/Per-ARNT-Sim homology domain dioxin receptor via the ubiquitin/proteasome pathway. *J Biol Chem.* (1999) 274:36351–6. doi: 10.1074/jbc.274.51.36351
152. Mimura J, Ema M, Sogawa K, Fujii-Kuriyama Y. Identification of a novel mechanism of regulation of Ah (dioxin) receptor function. *Genes Dev.* (1999) 13:20–5. doi: 10.1101/gad.13.1.20
153. Funatake CJ, Marshall NB, Steppan LB, Mourich DV, Kerkvliet NI. Cutting Edge. Activation of the aryl hydrocarbon receptor by 2,3,7,8-Tetrachlorodibenzo-p-dioxin generates a population of CD4+CD25+ cells with characteristics of regulatory T Cells *J Immunol.* (2005) 175:4184–8. doi: 10.4049/jimmunol.175.7.4184
154. Dant TA, Lin KL, Bruce DW, Montgomery SA, Kolupaev OV, Bommiasamy H, et al. T-cell expression of AhR inhibits the maintenance of pTreg cells in the gastrointestinal tract in acute GVHD. *Blood* (2017) 130:348–59. doi: 10.1182/blood-2016-08-734244
155. Veiga-Parga T, Suryawanshi A, Rouse BT. Controlling viral immuno-inflammatory lesions by modulating aryl hydrocarbon receptor signaling. *PLoS Pathog.* (2011) 7:e1002427. doi: 10.1371/journal.ppat.1002427
156. Mezrich JD, Fechner JH, Zhang X, Johnson BP, Burlingham WJ, Bradfield CA. An interaction between kynurenine and the aryl hydrocarbon receptor can generate regulatory T cells. *J Immunol.* (2010) 185:3190–8. doi: 10.4049/jimmunol.0903670
157. Abron JD, Singh NP, Mishra MK, Price RL, Nagarkatti M, Nagarkatti PS, et al. An endogenous aryl hydrocarbon receptor (AhR) ligand, ITE induces regulatory T cells (Tregs) and ameliorates experimental colitis. *Am J Physiol Gastrointest Liver Physiol.* (2018) 315:G220–30. doi: 10.1152/ajpgi.00413.2017
158. Julliard W, De Wolfe TJ, Fechner JH, Safdar N, Agni R, Mezrich JD. Amelioration of clostridium difficile infection in mice by dietary supplementation with Indole-3-carbinol. *Ann Surg.* (2017) 265:1183–91. doi: 10.1097/SLA.0000000000001830
159. Julliard W, Fechner JH, Owens L, O'Driscoll CA, Zhou L, Sullivan JA, et al. Modeling the effect of the aryl hydrocarbon receptor on transplant immunity. *Transplant Direct* (2017) 3:e157. doi: 10.1097/TXD.0000000000000666
160. Liu X, Hu H, Fan H, Zuo D, Shou Z, Liao Y, et al. The role of STAT3 and AhR in the differentiation of CD4+ T cells into Th17 and Treg cells. *Medicine* (2017) 96:e6615. doi: 10.1097/MD.0000000000006615
161. Ehrlich AK, Pennington JM, Bisson WH, Kolluri SK, Kerkvliet NI. TCDD, FICZ, and other high affinity AhR ligands dose-dependently determine the fate of CD4+ T cell differentiation. *Toxicol Sci.* (2018) 161:310–20. doi: 10.1093/toxsci/kfx215
162. Pot C, Apetoh L, Awasthi A, Kuchroo VK. Induction of regulatory Tr1 cells and inhibition of T(H)17 cells by IL-27. *Semin Immunol.* (2011) 23:438–45. doi: 10.1016/j.smim.2011.08.003
163. Gandhi R, Kumar D, Burns EJ, Nadeau M, Dake B, Laroni A, et al. Activation of the aryl hydrocarbon receptor induces human type 1 regulatory T cell-like and Foxp3(+) regulatory T cells. *Nat Immunol.* (2010) 11:846–53. doi: 10.1038/ni.1915
164. Mohinta S, Kannan AK, Gowda K, Amin SG, Perdew GH, August A. Differential regulation of Th17 and T regulatory cell differentiation by aryl hydrocarbon receptor dependent xenobiotic response element dependent and independent pathways. *Toxicol Sci.* (2015) 145:233–43. doi: 10.1093/toxsci/kfv046
165. Pearson JA, Wong FS, Wen L. The importance of the Non Obese Diabetic (NOD) mouse model in autoimmune diabetes. *J Autoimmun.* (2016) 66:76–88. doi: 10.1016/j.jaut.2015.08.019
166. Delovitch TL, Singh B. The nonobese diabetic mouse as a model of autoimmune diabetes: immune dysregulation gets the NOD. *Immunity* (1997) 7:727–38. doi: 10.1016/S1074-7613(00)80392-1
167. Bellemore SM, Nikoopour E, Schwartz JA, Krougly O, Lee-Chan E, Singh B. Preventative role of interleukin-17 producing regulatory T helper type 17 (Treg 17) cells in type 1 diabetes in non-obese diabetic mice. *Clin Exp Immunol.* (2015) 182:261–9. doi: 10.1111/cei.12691
168. Cheng L, Qian L, Tan Y, Wang GS, Li XM, Li XP, et al. Unbalanced expression of aryl hydrocarbon receptor in peripheral blood CCR6(+)CD4(+) and CD4(+)CD25(+)T cells of rheumatoid arthritis. *Rev Bras Reumatol.* (2017) 57:190–6. doi: 10.1016/j.rbr.2016.04.003
169. Pietrosimone KM, Jin M, Poston B, Liu P. Collagen-induced arthritis: a model for murine autoimmune arthritis. *Bio Protoc.* (2015) 5:e1626. doi: 10.21769/BioProtoc.1626
170. Tong B, Yu J, Wang T, Dou Y, Wu X, Kong L, et al. Sinomenine suppresses collagen-induced arthritis by reciprocal modulation of regulatory T cells and Th17 cells in gut-associated lymphoid tissues. *Mol Immunol.* (2015) 65:94–103. doi: 10.1016/j.molimm.2015.01.014
171. Gold R, Linington C, Lassmann H. Understanding pathogenesis and therapy of multiple sclerosis via animal models: 70 years of merits and culprits in experimental autoimmune encephalomyelitis research. *Brain* (2006) 129(Pt 8):1953–71. doi: 10.1093/brain/awl075
172. Cua DJ, Sherlock J, Chen Y, Murphy CA, Joyce B, Seymour B, et al. Interleukin-23 rather than interleukin-12 is the critical cytokine for autoimmune inflammation of the brain. *Nature* (2003) 421:744–8. doi: 10.1038/nature01355
173. Park H, Li Z, Yang XO, Chang SH, Nurieva RY, Wang H, et al. A distinct lineage of CD4 T cells regulates tissue inflammation by producing interleukin 17. *Nature Immunol.* (2005) 6:1133. doi: 10.1038/ni1261
174. Harrington LE, Hatton RD, Mangan PR, Turner H, Murphy TL, Murphy KM, et al. Interleukin 17-producing CD4+ effector T cells develop via a lineage distinct from the T helper type 1 and 2 lineages. *Nat Immunol.* (2005) 6:1123–32. doi: 10.1038/ni1254
175. Rothhammer V, Borucki DM, Garcia Sanchez MI, Mazzola MA, Hemond CC, Regev K, et al. Dynamic regulation of serum aryl hydrocarbon receptor agonists in MS. *Neurol Neuroimmunol Neuroinflamm.* (2017) 4:e359. doi: 10.1212/NXI.0000000000000359

176. Apetoh L, Quintana FJ, Pot C, Joller N, Xiao S, Kumar D, et al. The aryl hydrocarbon receptor interacts with c-Maf to promote the differentiation of type 1 regulatory T cells induced by IL-27. *Nat Immunol.* (2010) 11:854–61. doi: 10.1038/ni.1912
177. Rekik R, Smiti Khanfir M, Larbi T, Zamali I, Beldi-Ferchiou A, Kammoun O, et al. Impaired TGF-beta signaling in patients with active systemic lupus erythematosus is associated with an overexpression of IL-22. *Cytokine* (2018) 108:182–9. doi: 10.1016/j.cyto.2018.04.011
178. Dorgham K, Amoura Z, Parizot C, Arnaud L, Frances C, Pionneau C, et al. Ultraviolet light converts propranolol, a nonselective beta-blocker and potential lupus-inducing drug, into a proinflammatory AhR ligand. *Eur J Immunol.* (2015) 45:3174–87. doi: 10.1002/eji.201445144
179. Shinde R, Hezaveh K, Halaby MJ, Kloetgen A, Chakravarthy A, Medina TdS, et al. Apoptotic cell–induced AhR activity is required for immunological tolerance and suppression of systemic lupus erythematosus in mice and humans. *Nat Immunol.* (2018) 19:571. doi: 10.1038/s41590-018-0107-1
180. Zhang P, Wang R, Li Z, Wang Y, Gao C, Lv X, et al. The risk of smoking on multiple sclerosis: a meta-analysis based on 20,626 cases from case-control and cohort studies. *PeerJ* (2016) 4:e1797. doi: 10.7717/peerj.1797
181. Poorolajal J, Bahrami M, Karami M, Hooshmand E. Effect of smoking on multiple sclerosis: a meta-analysis. *J Public Health* (2018) 39:312–20. doi: 10.1093/pubmed/fdw030
182. Costenbader KH, Kim DJ, Peerzada J, Lockman S, Nobles-Knight D, Petri M, et al. Cigarette smoking and the risk of systemic lupus erythematosus: a meta-analysis. *Arthritis Rheum.* (2004) 50:849–57. doi: 10.1002/art.20049
183. Chang K, Yang SM, Kim SH, Han KH, Park SJ, Shin JI. Smoking and rheumatoid arthritis. *Int J Mol Sci.* (2014) 15:22279–95. doi: 10.3390/ijms151222279
184. Perricone C, Versini M, Ben-Ami D, Gertel S, Watad A, Segel MJ, et al. Smoke and autoimmunity. The fire behind the disease. *Autoimmun Rev.* (2016) 15:354–74. doi: 10.1016/j.autrev.2016.01.001
185. Harel-Meir M, Sherer Y, Shoenfeld Y. Tobacco smoking and autoimmune rheumatic diseases. *Nat Clin Pract Rheumatol.* (2007) 3:707–15. doi: 10.1038/ncprheum0655

Conflict of Interest Statement: The authors declare that the research was conducted in the absence of any commercial or financial relationships that could be construed as a potential conflict of interest.

frontiers in Immunology

OPINION
published: 06 March 2019
doi: 10.3389/fimmu.2019.00388

The Hygiene Hypothesis, Old Friends, and New Genes

*John W. Frew**

Laboratory of Investigative Dermatology, The Rockefeller University, New York, NY, United States

Keywords: autoimmunity, infection—immunology, genetics, allegy, monoclonal antibodies (immunology)

Allergic and autoimmune diseases such as asthma, psoriasis, rheumatoid arthritis, and inflammatory bowel disease vary in prevalence within human populations (1, 2). The hygiene hypothesis and more recently the "old friends" hypothesis have been quoted (3) to explain this disparity of prevalence, particularly between nations in the developed and developing world. Proposed etiological mechanisms include the absence of once-common childhood infections, as well as a reduction in exposure to a variety of commensal microorganisms in childhood (3). Exposure to such organisms is proposed to educate the immune system to appropriately respond to either innocuous and dangerous stimuli. Aberrant response to innocuous stimuli results in the development of allergic and autoimmune disease (3). However, these hypotheses alone do not fully account for the variability in prevalence of allergic and autoimmune disease (2, 4, 5). Certain populations exhibit an elevated risk to autoimmune and allergic disease above the background rate of individual human populations.

The advent of Genome Wide Association Studies (GWAS) have enabled identification of predisposing genetic variants to allergic and autoimmune disease (4, 5). They have also confirmed the association of previous loci identified in linkage studies. Genetic predisposition is a *"sine qua non"* for the development of allergic or autoimmune disease (4, 5) due to the ongoing evolutionary battle of protection against infectious disease whilst maintaining an acceptable risk of autoimmune disease which may impact upon reproductive capacity. In the identification of allergy and autoimmune disease-associated loci, multiple overlapping loci have been identified with pathogen-induced positive selection loci (6–12) (**Table 1**) (In this context, positive selection refers to genomic or Darwinian selection). A commonly known example of pathogen-induced positive selection is the increased prevalence of hemoglobin variants (HbS) causing sickle cell disease in populations with high previous malaria incidence, giving partial protection to severe malarial infection (10). In autoimmune and inflammatory disease, identified overlapping genes involve the activation and function of T cells, monocytes, NK cells, and dendritic cells as well as aspects of the major histocompatibility complex and transcription factors (13–17) (**Table 1**). Infectious agents associated with identified genes include *M. Leprae*, *M. Tuberculosis*, Y. *Pestis*, diarrheal illness, and *Plasmodium* sp. (4, 5, 8, 9, 11, 12) (**Table 1**). The presence of gene variants was associated with partial protection against the development of severe disease. Existing data is skewed by ascertainment bias with the majority of allergy and autoimmune GWAS have been undertaken in European populations. Also, GWAS for infectious disease require cohorts experiencing active infection, hence past endemic organisms with a high likelihood of producing positive selection (i.e., smallpox) are unable to be evaluated. Additionally, infectious agents with near saturation and multiple strains (i.e., *M. Tuberculosis*) indicate strong selective pressure (10), but due to the lack of comparison cohorts, positively selected genes are difficult to identify.

OPEN ACCESS

Edited by:
James J. Pestka,
Michigan State University,
United States

Reviewed by:
Kenneth Michael Pollard,
The Scripps Research Institute,
United States

***Correspondence:**
John W. Frew
jfrew@rockefeller.edu
orcid.org/0000-0001-5042-3632

Specialty section:
This article was submitted to Autoimmune and Autoinflammatory Disorders, a section of the journal Frontiers in Immunology

Received: *05 November 2018*
Accepted: *14 February 2019*
Published: *06 March 2019*

Citation:
Frew JW (2019) The Hygiene Hypothesis, Old Friends, and New Genes. Front. Immunol. 10:388. doi: 10.3389/fimmu.2019.00388

TABLE 1 | List of identified genes identified in Autoimmune/Allergic Disease by GWAS overlapping with implicated pathogen-associated positive selection loci.

Population	Candidate gene	Gene function	Allergic/autoimmune disease	Infection in which gene provides protective effect	References
European	FUT2	Cell-cell interaction Cell-microbe interaction	Psoriasis Crohn's Disease	Viral diarrhoea	(5, 10, 11, 13)
European/African	TRIM65	Zinc ion binding Autophagy	Psoriasis	*Yersinia pestis*	(8)
European	HLA-DRB1	Major histocompatability complex	Atopic dermatitis	*Plasmodium falciparum* HBV persistance HCV Persistance	(4)
European	IFN-Gamma	Innate and adaptive immunity	Atopic dermatitis	*Mycobacterial* sp.	(11)
European	IL-12B	Inducer of Th1 immunity	Rheumatoid arthritis Multiple sclerosis	*M. Leprae*	(4, 10)
European	IL-21R	Proliferation of T, B, and NK Cells	Allergy (IgE Phenotype)	*M. Leprae*	(4, 5, 10)
European	IL-23R	Activation dendritic cells, monocytes, T cells and NK cells	Crohn's Ankylosing spondylitis	*Plasmodium* sp. *M. Leprae*	(4, 7)
European	TLR5	Pathogen recognition and innate immunity	Systemic lupus erythematosis	Salmonella	(4, 10)
European	TYK2	Innate and adaptive immune signaling	Rheumatoid arthritis Psoriasis Systemic lupus erythematosis Multiple sclerosis Type 1 diabetes	Protozoal infection	(4, 7, 10)
European	SNRPC	U1 small nuclear ribosome	Systemic lupus erythematosis	*M. Tuberculosis*	(10)
European	UHRF1BP1	Negative regulator of cell growth	Systemic lupus erythematosis	*M. Tuberculosis*	(4, 5, 10)
European/ African	IL12RB2	Inducer of Th1 immunity	Crohn's disease	*Plasmodium* sp.	(12)
Chinese	NOD2	Innate immune function	Crohn's disease	*M. Leprae*	(5, 10)
European	HLA-DQB1	Major histocompatability complex	Ulcerative colitis	*M. Leprae*	(4, 5, 7, 10)
European/ African	STAT4	Transcription factor T-cell maturation and function	Rheumatoid arthritis	Salmonella	(4, 7)
African Americans	APOL1	Serum apolipoprotein	SLE collapsing glomerulopathy	Tryptosomiasia	(10)

The corollary therefore is that for specific human population groups, historical exposure to infectious pathogens have positively selected for protective variants to improve survival and reproduction (6). One could hypothesize that, in the absence of infectious disease, these variants predispose to aberrant immune activation which, in the setting of appropriate environmental stimuli (such as a loss of "old friends" as well as smoking, metals, particulates, etc.) may manifest as allergy and autoimmune disease.

The implications of this correlation extend beyond population genetics to pharmacogenetics and emerging infectious diseases. The efficacy of monoclonal antibodies for control of autoimmune and allergic disease has associations with patient genetic variants (18) which have differing prevalence in various human populations. This could lead to targeted pharmacogenomic screening prior to treatment initiation. In the future this may become pertinent in emerging economies of East Asia [given the known high prevalence of NOD2 in Han Chinese, and the impact of NOD2 variants on therapy in Crohn's Disease (19)] and the Americas [in a similar vein to G6PD deficiency in Latin America (20)]. The re-emergence of vector-borne infectious diseases (such as malaria) secondary to climate change (21), may place individuals with autoimmune or allergic disease, who are being actively treated with immunomodulating therapies, at risk of infection. This risk may be greatest in those individuals where the therapy actively suppresses an inflammatory pathway known to be protective against the infectious agent. A relevant modern-day corollary is the risk of *M. Tuberculosis* reactivation during psoriasis treatment with TNF-alpha inhibitors in individuals of European ancestry [given the proposed mechanism of ancestral *Mycobacterium* sp. positively selecting for European psoriasis-associated genetic variants (22)]. This causal hypothesis requires validation in epidemiologic and functional studies.

In summary, the presence of overlapping gene associations identified by GWAS, as well as the evidence of pathogen-specific positive selection is an extension of the "hygiene/old friends" hypothesis which integrates findings from population genetics to explain disparate rates of autoimmune and allergic disease in different human populations. It also suggests avenues

for further research in pharmacogenomics and susceptibility to emerging pathogens.

AUTHOR CONTRIBUTIONS

The author confirms being the sole contributor of this work and has approved it for publication.

ACKNOWLEDGMENTS

Supported in part by grant # UL1 TR001866 from the National Center for Advancing Translational Sciences (NCATS), National Institutes of Health (NIH) Clinical and Translational Science Award (CTSA) program.

REFERENCES

1. Rees, F, Doherty M, Grainge MJ, Lanyon P, Zhang W. The worldwide incidence and prevalence of systemic lupus erythematosus: a systematic review of epidemiological studies. *Rheumatol.* (2017) 56:1945–61. doi: 10.1093/rheumatology/kex260
2. Ng SC, Shi HY, Hamidi N, Underwood FE, Tang W, Benchimoi EI, et al. Worldwide incidence and prevalence of inflammatory bowel disease in the 21st century: a systematic review of population-based studies. *Lancet*. (2017) 390:2769–78. doi: 10.1016/S0140-6736(17)32448-0
3. Daley D. The evolution of the hygiene hypothesis: the role of early-life exposures to viruses and microbes and their relationship to asthma and allergic diseases. *Curr Opin Allergy Clin Immunol.* (2014) 14:390–6. doi: 10.1097/ACI.0000000000000101
4. Ramos PS. Population genetics and natural selection in rheumatic disease. *Rheum Dis Clin North Am.* (2017) 43:313–26. doi: 10.1016/j.rdc.2017.04.001
5. Raj T, Kuchroo M, Replogle JM, Raychaudhuri S, Stranger BE, De Jager PL. Common risk alleles for inflammatory diseases are targets of recent positive selection. *Am J Hum Genet.* (2013) 92:517–29. doi: 10.1016/j.ajhg.2013.03.001
6. Hill AVS. Evolution, revolution and heresy in the genetics of infectious disease susceptibility. *Phil Trans R Soc B.* (2012) 367:840–9. doi: 10.1098/rstb.2011.0275
7. Ellinghaus D, Jostins L, Spain SL, Cortes A, Bethune J, Han B, et al. Analysis of five chronic inflammatory diseases identifies 27 new associations and highlights disease-specific patterns at shared loci. *Nat Genet.* (2016) 48:510–8. doi: 10.1038/ng.3528
8. Corona E, Wang L, Ko D, Patel CJ. Systematic detection of positive selection in the human genome. *PLoS ONE*. (2018) 13:e0196676. doi: 10.1371/journal.pone.0196676
9. Withrock, IC. Anderson SJ, Jefferson MA, McCormack GR, Mlynarczyk GSA, Nakama A, et al. Genetic diseases conferring resistance to infectious diseases. *Genes Dis.* (2015) 2:247–54. doi: 10.1016/j.gendis.2015.02.008
10. Karlsson EK, Kwiatkowski DP, Sabeti PC. Natural selection and Infectious diseases in human populations. *Nat Rev Genet.* (2014) 15:379–93. doi: 10.1038/nrg3734
11. Casanova JL, Abel L. Human genetics of infectious disease: a unified theory. *EMBO J.* (2007) 26:915–22. doi: 10.1038/sj.emboj.7601558
12. Frodsham AJ, Hill AVS. Genetics of infectious disease. *Hum Mol Genet.* (2004) 13:R187–94. doi: 10.1093/hmg/ddh225
13. Bustamante M, Standl M, Bassat Q, Vilor-Tejedor N, Medina-Gomez C, Bonilla C, et al. A genome-wide association meta-analysis of diarrhoeal disease in young children identifies FUT2 locus and provides plausible biological pathways. *Hum Mol Genet.* (2016) 25:4127–42. doi: 10.1093/hmg/ddw264
14. Tsoi LC, Stuart PC, Tian C, Gudjonsson JE, Das S, Zawistowski M, et al. Large scale meta-analysis characterizes genetic architecture for common psoriasis associated variants. *Nat Commun.* (2017) 8:15382. doi: 10.1038/ncomms 15382
15. Romagnani S. Immunological influences on allergy and the TH1/TH2 balance. *J Allerg Clin Immunol.* (2004) 113:395–400. doi: 10.1016/j.jaci.2003.11.025
16. Vicente CT, Revez JA, Ferreira MAR. Lessions from 10 years of genome-wide association studies of asthma. *Clin Transl Immunol.* (2017) 6:e165. doi: 10.1038/cti.2017.54
17. Lin YH, Machner MP. Exploitation of the host cell ubiquitin machinery by microbial effector proteins. *J Cell Sci.* (2017) 130:1985–96. doi: 10.1242/jcs.188482
18. Hueber W, Sands BE, Lewitzky S, Vandemeulebroecke M, Reinisch W, Higgins PD, et al. Secukinumab, a human anti-IL-17A monoclonal antibody, for moderate to severe Crohn's disease: unexpected results of randomized, double placebo-controlled trial. *Gut*. (2012) 61:1693–700. doi: 10.1136/gutjnl-2011-301668
19. Kennedy NA, Lamb CA, Berry SH. The impact of NOD2 variants on fecal microbiota in Crohn's disease and controls without gastrointestinal disease. *Inflamm Bowel Dis.* (2018) 24:583–92. doi: 10.1093/ibd/izx061
20. Valencia SH, Ocampo ID, Arce-Plata MI. Glucose-6-Phosphate dehydrogenase deficiency prevalence and genetic variants in malaria endemic areas of Columbia. *Malar J.* (2016) 15:291. doi: 10.1186/s12936-016-1343-1
21. Medlock JM, Leach SA. Effect of climate change on vector-borne disease risk in the UK. *Lancet Infect Dis.* (2015) 15:721–30. doi: 10.1016/S1473-3099(15)70091-5
22. Brinkworth JF, Barreiro LB. The contribution of natural selection to present-day susceptibility to chronic inflammatory and autoimmune disease *Curr Opin Immunol.* (2014) 31:66–78. doi: 10.1016/j.coi.2014 .09.008

Conflict of Interest Statement: The author declares that the research was conducted in the absence of any commercial or financial relationships that could be construed as a potential conflict of interest.

frontiers in Immunology

ORIGINAL RESEARCH
published: 29 March 2019
doi: 10.3389/fimmu.2019.00632

Mapping of Dynamic Transcriptome Changes Associated With Silica-Triggered Autoimmune Pathogenesis in the Lupus-Prone NZBWF1 Mouse

Melissa A. Bates[1,2], Abby D. Benninghoff[3], Kristen N. Gilley[1], Andrij Holian[4], Jack R. Harkema[5] and James J. Pestka[1,2,6]**

[1] Department of Food Science and Human Nutrition, Michigan State University, East Lansing, MI, United States, [2] Institute for Integrative Toxicology, Michigan State University, East Lansing, MI, United States, [3] Department of Animal, Dairy and Veterinary Sciences and the School of Veterinary Medicine, Utah State University, Logan, UT, United States, [4] Department of Biomedical and Pharmaceutical Sciences, Center for Environmental Health Sciences, University of Montana, Missoula, MT, United States, [5] Department of Pathobiology and Diagnostic Investigation, Michigan State University, East Lansing, MI, United States, [6] Department of Microbiology and Molecular Genetics, Michigan State University, East Lansing, MI, United States

OPEN ACCESS

Edited by:
J. Michelle Kahlenberg, University of Michigan, United States

Reviewed by:
Jillian M. Richmond, University of Massachusetts Medical School, United States
Jason Weinstein, Rutgers Biomedical and Health Sciences, United States

***Correspondence:**
Abby D. Benninghoff
abby.benninghoff@usu.edu
James J. Pestka
pestka@msu.edu

Specialty section:
This article was submitted to Autoimmune and Autoinflammatory Disorders, a section of the journal Frontiers in Immunology

Received: 29 November 2018
Accepted: 08 March 2019
Published: 29 March 2019

Citation:
Bates MA, Benninghoff AD, Gilley KN, Holian A, Harkema JR and Pestka JJ (2019) Mapping of Dynamic Transcriptome Changes Associated With Silica-Triggered Autoimmune Pathogenesis in the Lupus-Prone NZBWF1 Mouse. Front. Immunol. 10:632. doi: 10.3389/fimmu.2019.00632

Crystalline silica ($cSiO_2$) is a widely recognized environmental trigger of autoimmune disease. In the lupus-prone female NZBWF1 mouse, airway exposure to $cSiO_2$ triggers pulmonary ectopic lymphoid neogenesis, systemic autoantibody elevation, and glomerulonephritis. Here we tested the hypothesis that upregulation of adaptive immune function genes in the lung precedes $cSiO_2$-triggering of autoimmune disease in this model. The study include three groups of mice, as follows: (1) necropsied 1 d after a single intranasal instillation of 1 mg $cSiO_2$ or vehicle, (2) necropsied 1 d after four weekly single instillations of 1 mg $cSiO_2$ or vehicle, or (3) necropsied 1, 5, 9, or 13 weeks after four weekly single instillations of 1 mg $cSiO_2$ or vehicle. NanoString nCounter analysis revealed modest transcriptional changes associated with innate and adaptive immune response as early as 1 d after a single $cSiO_2$ instillation. These responses were greatly expanded after four weekly $cSiO_2$ instillations. Concurrent with ectopic lymphoid neogenesis, dramatic increases in mRNAs associated with chemokine release, cytokine production, sustained interferon activity, complement activation, and adhesion molecules were observed. As disease progressed, expression of these genes persisted and was further amplified. Consistent with autoimmune pathogenesis, the time between 5 and 9 weeks post-instillation reflected an important transition period where considerable immune gene upregulation in the lung was observed. Upon termination of the chronic study (13 weeks), $cSiO_2$-induced changes in transcriptome signatures were similarly robust in kidney as compared to the lung, but more modest in spleen. Transcriptomic signatures in lung and kidney were indicative of infiltration and/or expansion of neutrophils, macrophages, dendritic cells, B cells, and T cells that corresponded with accelerated

autoimmune pathogenesis. Taken together, airway exposure to $cSiO_2$ elicited aberrant mRNA signatures for both innate and adaptive immunity that were consistent with establishment of the lung as the central autoimmune nexus for launching systemic autoimmunity and ultimately, kidney injury.

Keywords: autoimmunity, NanoString, lung, systemic lupus erythematosus, silica, transcriptome

INTRODUCTION

Systemic lupus erythematosus (lupus) is a devastating autoimmune disease (AD) with a multifaceted etiology and widely variable disease manifestations. The initiating event in lupus is loss of tolerance to self-antigens which elicits production of autoreactive antibodies and formation of circulating immune complexes [reviewed in Pons-Estel et al. (1)]. These complexes deposit in tissues where they promote infiltration and activation of circulating mononuclear cells. Importantly, deposition of these immune complexes in the kidney results in glomerulonephritis that can advance to end-stage renal failure—a major cause of death in lupus patients.

Ectopic lymphoid structures (ELS) are hallmarks of AD that reflect the interface between unresolved inflammation and loss of self-tolerance. Unlike secondary lymphoid organs, ELS are induced at sites of unresolved inflammation, and thus, not found in pre-programmed places of the body. Their *de novo* formation facilitates accelerated initiation of an adaptive immune response by promoting antigen presentation and rapid activation of naïve B- and T-cells to remediate the offending agent at the site of inflammation (2–4). When organized within follicular dendritic cell (FDC) networks, ELS contain functional germinal centers that yield autoantibody-secreting plasma cells and promote AD.

Lupus and other ADs are strongly associated with an individual's genome. However, low concordance rates among monozygotic twins indicate that heredity is not the sole disease determinant (5). Recent studies suggest that the exposome (i.e., cumulative lifetime environmental exposures) is an understudied contributor to AD heterogeneity (6). Crystalline silica ($cSiO_2$) is a widely recognized environmental trigger of autoimmunity. Over 2.3 million Americans are employed in occupations with high potential exposure to airborne $cSiO_2$ particles, such as construction, stone cutting, foundries, and hydraulic fracturing (7). Epidemiological studies have established an etiological link between occupational exposure to $cSiO_2$ and ADs, including lupus, rheumatoid arthritis, Sjögren's syndrome, scleroderma, and systemic vasculitis (8–12).

In lupus-prone female NZBWF1 mice, intranasal $cSiO_2$ instillation triggered autoimmunity and glomerulonephritis 3 months earlier than vehicle-instilled controls (13, 14). Extensive inflammatory perivascular and peribronchial leukocyte infiltrates were evident in the lungs that contained numerous B cells and T cells corresponding to ectopic lymphoid neogenesis. Concomitant with pulmonary inflammation and ELS formation, bronchoalveolar lavage fluid (BALF) from $cSiO_2$-exposed mice contained large numbers of neutrophils and macrophages as well as elevated concentrations of IgG, autoantibodies, IL-1β, IL-6, TNF-α, and B cell activating factor (BAFF). The latter responses were similarly reflected in the plasma and, therefore, indicate concomitant systemic autoimmunity. Collectively, these observations suggest that ELS in the lung might be central autoimmune triggering by $cSiO_2$.

Recently, we characterized ELS development and autoimmunity over time in NZBWF1 mice that were intranasally instilled with $cSiO_2$ weekly for 4 weeks and then sacrificed 1, 5, 9, or 13 weeks later (15). By week 1, inflammation comprising of B and T cells was observed in lungs of $cSiO_2$-treated mice; these responses were continually amplified at 5, 9, and 13 weeks. Marked FDC networking appeared at 9 and 13 weeks PI. IgG^+ plasma cells suggestive of mature germinal centers were evident at 13 weeks. Anti-dsDNA IgG in bronchial lavage fluid and plasma increased over the course of the experiment. $cSiO_2$-induced glomerulonephritis with concomitant B-cell accumulation in the renal cortex was evident at 13 weeks PI. Accordingly, $cSiO_2$ sequentially induced ectopic lymphoid neogenesis, germinal center development, systemic autoantibody elevation, and resultant glomerulonephritis in this unique preclinical model of environment-triggered lupus.

Little is known about how acute or chronic $cSiO_2$ exposures impact global immune gene expression. To address this, we tested the hypothesis that upregulation of adaptive immune function genes in the lung precedes $cSiO_2$-triggering of autoimmune disease in the NZBWF1 mouse. The NanoString nCounter platform is a targeted multiplex approach that enables measurement of up to 800 genes in a single reaction with high sensitivity and linearity across a broad dynamic range (16–18). Based on direct digital detection of mRNA molecules utilizing target-specific, color-coded probe pairs, this method bridges the gap between RNAseq and targeted RT-PCR expression profiling. Herein, we employed the nCounter platform to: (1) relate temporal changes in immune-related transcriptome signatures in the lung following acute and short-term repeated intranasal $cSiO_2$ exposure to ELS development and autoimmune pathogenesis in female NZBWF1 mice and (2) compare the terminal transcriptome signatures in the lung to those in the spleen and kidney.

MATERIALS AND METHODS

Animals and Diets

Experimental protocols were approved by the Institutional Animal Care and Use Committee at Michigan State University in accordance with the National Institutes of Health guidelines (AUF #01/15-021-00). Female 6-week-old lupus-prone NZBWF1 mice were provided by Jackson Laboratories (Bar Harbor, ME) and randomized into experimental groups. Mice were housed

four per cage and fed AIN-93G diet (Dyets Inc., Bethlehem, PA) as described previously (13, 15). Mice had free access to food and water and were kept at constant temperature (21–24°C) and humidity (40–55%) under a 12/h light/dark cycle.

$cSiO_2$

$cSiO_2$ (Min-U-Sil-5, 1.5–2.0 μm average particle size, Pennsylvania Sand Glass Corporation, Pittsburgh, PA) was acid washed and dried before addition of sterile phosphate buffered saline (PBS). Stock suspensions were prepared fresh in PBS prior to exposure and suspensions sonicated and vortexed for 1 min before intranasal instillation.

Experimental Design

Figure 1 depicts the experimental design for this study. To model acute response to a single dose of $cSiO_2$, (Acute.1x) groups of 8-week-old mice ($n = 8$/gp) were anesthetized with 4% isoflurane and intranasally instilled with 1.0 mg $cSiO_2$ in 25 μl PBS or 25 μl PBS vehicle (VEH) as described previously (13). To capture the acute response to short-term repeated exposure to $cSiO_2$, a second cohort of mice received 1.0 mg $cSiO_2$ or VEH once weekly for 4 weeks (Acute.4x). Each cohort was sacrificed 24 h after final instillation. The caudal lung lobe was removed, held in RNAlater (Thermo Fisher Scientific, Wilmington, DE) overnight at 4°C, and then stored at −80°C for RNA multiplexing.

To visualize how $cSiO_2$ impacts autoimmune gene expression over the long term, we used tissues from our recently published investigation that focused on the histopathological changes over time in $cSiO_2$-treated NZBWF1 mice (15). In that study, beginning at 8 weeks of age, groups of mice on were exposed to VEH or $cSiO_2$ weekly for 4 weeks. Thereafter, cohorts of mice were sacrificed over time at 1, 5, 9, and 13 weeks post final $cSiO_2$ exposure. One mouse in the 5 week VEH group died of unknown causes during the course of the experiment; it did not show the typical signs of sickness including loss of body weight before death. Tissues were collected at stored in RNAlater (ThermoFisher Scientific). Lungs were analyzed at 1 (Lung.W1), 5 (Lung.W5), 9 (Lung.W9), and 13 (Lung.W13) weeks post $cSiO_2$ exposure, and spleen (Spleen.W13) and kidney (Kidney.W13) at 13 weeks. These time points were selected to coincide with pathological changes previously described in this model following $cSiO_2$ exposure prior to and during onset of glomerulonephritis (13–15).

Gene Expression Analysis With NanoString nCounter

Total RNA was extracted from lung, spleen, and kidney with TriReagent (Sigma Aldrich, St. Louis, MO) per manufacturer's instructions. Resultant RNA was further purified and genomic DNA removed by RNeasy Mini Kit with DNase treatment (Qiagen, Valencia, CA). RNA was dissolved in nuclease-free water and quantified using a NanoDrop-1000 (Thermo Fisher). Samples were then analyzed for RNA integrity using a LabChip Gx Analyzer (Caliper Life Sciences, Waltham, MA). Samples with RIN values >7.0 were included for gene expression analysis.

The NanoString nCounter (NanoString Technologies, Inc., Seattle WA) was used to assess the effects of $cSiO_2$ exposure on acute and chronic changes in immune gene expression. This method was selected over other targeted multiplex approaches because it (i) requires minimal sample preparation, (ii) does not require cDNA conversion or target amplification—both major sources of variation in conventional qRT-PCR approaches, (iii) has robust user software for gene analysis, and (iv) has been repeatedly demonstrated to correlate well other microarray platforms (19–21). Briefly, RNA (n =7–8/gp) was analyzed using the nCounter Mouse PanCancer Immune Profiling Panel (catalog # 115000142), which includes 770 immune-related genes, 40 housekeeping genes, and 6 positive controls. Assays were performed and quantified on the nCounter MAX system, sample preparation station, and digital analyzer (NanoString Technologies) according to the manufacturer's instructions. Briefly, reporter and capture probes were hybridized to target analytes for 16 h at 65°C. After hybridization, samples were washed to remove excess probes. Then, the purified target-probe complexes were aligned and immobilized onto the nCounter cartridge, and the transcripts were counted via detection of the fluorescent barcodes within the reporter probe. Probe annotations are provided in **Supplementary File 1**.

Raw gene expression data were analyzed using NanoString's software nSolver v3.0.22 with the Advanced Analysis Module v2.0. Background subtraction was performed using the eight included negative controls included with the module. Genes with counts below a threshold of 2σ of the mean background signal were excluded from subsequent analysis (**Supplementary Figures 1–3**). Data normalization was performed on background-subtracted samples using internal positive controls and selected housekeeping genes that were identified with the geNorm algorithm (https://genorm.cmgg.be/).

Ratios of transcript count data were generated for $cSiO_2$-treated mice vs. VEH control as follows: acute response in lung tissue of $cSiO_2$-treated (single dose) mice vs. dosing-matched vehicle controls 1 day post instillation (Acute.1x); acute response in lung tissue of $cSiO_2$-treated (four weekly doses) mice vs. dosing-matched control 1 day post instillation (Acute.4x); chronic response in lung tissue of $cSiO_2$-treated (four weekly doses) mice vs. dosing- and time-matched vehicle controls 1, 5, 9, or 13 weeks post instillation (Lung.W1, Lung.W5, Lung.W9, Lung.W13, respectively); chronic response in kidney tissue of $cSiO_2$-treated (four weekly doses) mice vs. dosing- and time-matched vehicle controls 13 weeks post instillation (Kidney.W13); chronic response in spleen tissue of $cSiO_2$-treated (four weekly doses) mice vs. dosing- and time-matched vehicle controls 13 weeks post instillation (Spleen.W13). Ratios were then $\log_2$ transformed for downstream analysis.

Data Analysis

Differential gene expression analyses were performed using nSolver, which employs several multivariate linear regression models to identify significant genes (mixture negative binomial, simplified negative binomial, or log-linear model) as outlined in **Supplementary Figure 4**. Resulting p values were adjusted using the Benjamini-Hochberg (BH) method to control the false

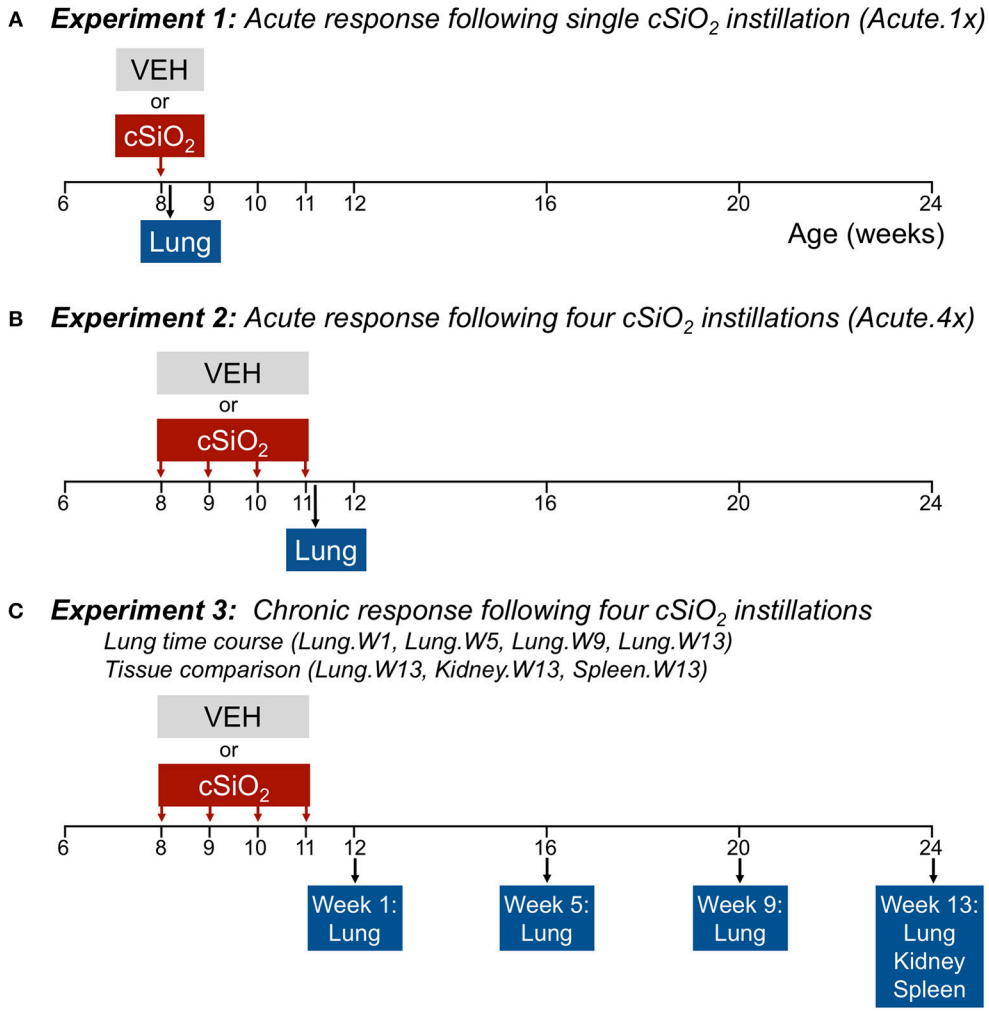

FIGURE 1 | Design of experiments. At 8 weeks of age, female NZBWF1 mice were dosed intranasally with 25 μl PBS (VEH) or 25 μl PBS containing 1.0 mg $cSiO_2$ once (**A**; experiment 1) or weekly for 4 weeks (**B,C**; experiments 2 and 3). Cohorts ($n = 7–8$) of mice were euthanized and necropsied 1 day (experiment 1 and 2) following the only/final instillation or 12, 16, 20, or 24 weeks of age corresponding to 1, 5, 9, or 13 weeks post the final instillation (experiment 3). Tissues obtained for nCounter digital transcript counting (NanoString PanCancer Immune Profiling gene set) are indicated above.

discovery rate. Statistically significant, differentially expressed genes were defined as those with expression levels corresponding to a $\log_2$ ratio >1 or <-1 and BH q value <0.05 for $cSiO_2$ treatments compared to the appropriate vehicle control group (**Supplementary Figure 5**). Outputs from nSolver differential expression analysis are provided in Supplementary File 2. Venn diagrams of significant differentially expressed genes in $cSiO_2$ groups were generated using BioVenn (22) or Venny v2.1 (23).

To assess impact of $cSiO_2$ treatment on annotated gene sets, global and directed significance scores were calculated for each pathway. The global significance score for each gene set was calculated as the square root of the mean squared t-statistic of genes, as determined by the differential gene expression analyses. The global score estimates the cumulative evidence for the differential expression of genes in a pathway. A directed significance score was also calculated by taking into account the sign of the t-statistics. Directed significance scores near zero may have many highly regulated genes, but no apparent tendency for those genes to be over- or under-expressed collectively. Pathway scores were used to summarize data from a pathway's genes into a single score. Pathway scores were calculated as the first principal component of the pathway genes' normalized expression and standardized by Z scaling. ClustVis (24) was used to perform unsupervised hierarchical cluster analyses (HCC) and principal components analyses (PCA) using $\log_2$ transcript count data. Supplementary Files 3–4 provide summary tables for all significance and pathway Z scores.

Immune Cell Profiling

A significant discovery feature of the NanoString platform is cell profiling, which uses marker genes expressed stably and specifically in immune cell types to estimate relative abundance in sample groups measured as the average log-scale expression of their characteristic genes (25). Note that this analysis does not provide information on the absolute number of immune cells in

a sample. Cell types and genes compatible with the PanCancer Immune Profiling Panel included leukocytes (*Ptprc*), B cells (*Ms4a1, Tnfrsf17*), T cells (*Cd3d, Cd3e, Cd3g, Cd6, Sh2d1a*), Th1 cells (*Tbx21*), T reg (*Foxp3*), CD8 T cells (*Cd8a, Cd8b1*), exhausted CD8 cells (*Cd244, Eomes, Lag3*), cytotoxic cells (*Ctsw, Gzma, Gzmb, Klrb1, Klrd1, Klrk1, Prf1*), dendritic cells (*Ccl2, Cd209e, Hsd11b1*), macrophages (*Cd163, Cd68, Cd84*), mast cells (*Ms4a2*), neutrophils (*Csf3r, Fcgr4*), and NK cells (*Ncr1, Xcl1*). The nCounter Advanced Analysis module reports *p* value confidence thresholds for reporting for cell types with multiple markers, though gene sets with high *p*-values may be useful if use of the biomarker genes is supported by prior studies. For this study, we report results for the immune cell types listed above, including those with threshold p values >0.05 as those data may be useful in future exploratory work. Supplementary File 5 provides the $\log_2$ scores for cell type profiling.

Network Analysis

Network analyses for interactions among significant genes were performed using STRING database version 10.5 (http://string-db.org/), which curates both experimental and predicted gene interactions. Only interactions among significant genes identified by the nSolver data analysis were considered with the confidence level for associations set at ≥ 0.7. Clusters were identified using the Markov Cluster (MCL) algorithm with inflation parameter of 1.5. Networks generated by STRING were visualized with Cytoscape v3.0, with nodes representing significant genes and edge width indicating the combined interaction score. Supplementary File 6 provides data for STRING-db networks and the predicted clusters.

Correlation Analysis

Spearman rank correlations were performed to examine overall patterns in the gene expression profiles compared to histopathological lesions in lung tissues and markers of immune cells. Correlation analysis was performed using *cor* and *corrplot* functions in R (www.R-project.org). Spearman ρ values were calculated using individual sample pathway Z scores and phenotype data: histopathology scores (lymphoid aggregates, ectopic lymphoid structures, alveolar proteinosis, alveolitis, type 2 cell hyperplasia, and mucus cell metaplasia) or percent positive staining (CD3, CD45R, and CD21/35) for lung tissues obtained from mice at 1, 5, 9, and 13 weeks post instillation (15). A significant correlation was inferred when $\rho > 0.5$ or <-0.5 and $p < 0.05$.

RESULTS

Acute mRNA Responses Following Single and Short Term $cSiO_2$ Exposure Indicate Innate and Adaptive Immune Activation

Five genes were differentially expressed in lung tissue 24 h after a single intranasal instillation of $cSiO_2$ (Acute.1x) whereas 56 genes were upregulated 24 h after four weekly $cSiO_2$ installations (Acute.4x) ($p < 0.05$) (**Figure 2A**, see **Supplementary Tables 1**, **2** for a full list of genes). Principal component analysis (PCA) plots (**Figure 2B**) indicated that distinct gene expression profiles distinguished the immediate immune response to a single exposure of $cSiO_2$ as compared to that after repeated $cSiO_2$ exposures.

Hierarchical clustering of the 56 genes differentially expressed in either exposure regimen revealed that the changes were more pronounced following four exposures to $cSiO_2$ than those elicited by a single exposure to $cSiO_2$ (**Figure 2C**). In general, these changes were associated with increased expression as relatively few genes were repressed. Clustering analysis also indicated that three out of eight mice exposed only once to $cSiO_2$ were strong responders whose transcriptomes mirrored the more severe responses observed all eight mice following four repeated $cSiO_2$ exposures.

To identify which immunological pathways were significantly altered and were upregulated or enhanced by $cSiO_2$ exposure, global and directed significance scores, respectively, were calculated as described above (**Figure 2D**). The resultant significance scores show broad scale activation of immune pathways. As indicated in heat maps of global and directed significance scores, the involvement of several immune pathways began after a single dose of $cSiO_2$ and was amplified upon repeated exposures. Importantly, the vast majority of immune pathways had potentiated expression, as opposed to attenuation, following a single or multiple exposures to $cSiO_2$. Network analyses of differentially expressed genes in lungs of mice with multiple $cSiO_2$ exposures revealed transcript groupings broadly associated with interferon (IFN) signaling, chemokine and cytokines, innate and adaptive immune response (**Supplementary Figure 6**).

To ascertain how different exposures to $cSiO_2$ influenced the overall gene expression, Z scores were calculated using expression values from all genes assigned a given pathway for each mouse in a treatment group, and the data were expressed as heat maps (**Figure 3A**). Again, strong responders in mice treated with one dose of $cSiO_2$ clustered closely and markedly reflected the gene response of mice instilled with multiple doses of $cSiO_2$. Importantly, immune pathways consistently activated in $cSiO_2$-treated mice were largely parallel with pathways known to influence the development of autoimmunity; these responses were absent in mice treated with vehicle alone (**Figure 3B**).

Based on previous studies by our group (15), we chose to elaborate on gene expression profiles with heat maps of the innate immune pathway (**Figure 4A**), the adaptive immune pathway (**Figure 4B**), B-cell functions (**Figure 4C**), T-cell functions (**Figure 4D**), chemokines and receptors (**Figure 4E**), cytokines and receptors (**Figure 4F**), and interferon (**Figure 4G**). When expression of representative genes of each of these pathways were plotted (**Figure 4**, dot plots to right of each heat map), upregulation of a number of genes in Acute.4x group were consistent with the Acute.1x high responders. Among the overlapping genes were the chemokines *Cxcl1*, *Cxcl5*, *Ccl2*, *Ccl3*, and *Ccl7* suggesting that leukocyte recruitment was a critical primary response 1 d after $cSiO_2$ instillation. Expression of these genes were considerably ramped up after short-term repeated exposure to the particle. Interestingly, a number of genes associated with netosis (26) were also upregulated by $cSiO_2$ including *C3ar, Ccl2, Ccl3, Cd14, Cd83, Cxcl, Ifit3, Il1a,*

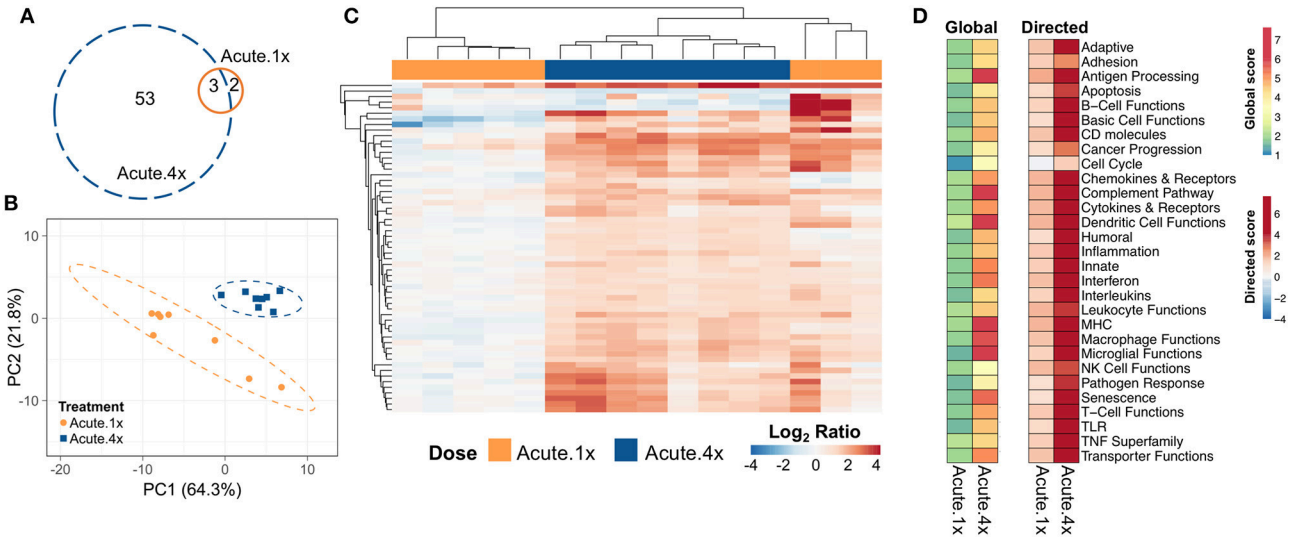

FIGURE 2 | Acute transcriptional response of immune-associated genes in lung tissues of mice that received either a single or four weekly instillations of $cSiO_2$. Mice received a single dose (Acute.1x) or four repeated weekly doses (Acute.4x) of $cSiO_2$ via intranasal instillation, and gene expression was determined in lung tissues obtained 1 day after the last dose. **(A)** Venn diagram depicting the number of genes identified as differentially expressed in lung tissue of mice that received a single $cSiO_2$ instillation (orange line) or four weekly $cSiO_2$ doses (blue dashed line) as compared to dosing-matched vehicle controls. **(B)** Principal components analysis of differentially expressed genes (BH $q < 0.05$, log_2 ratio >1 or <-1) in lung tissues of mice exposed to $cSiO_2$ once or four times compared to dosing-matched vehicle controls. PC1 and PC2 are shown with the 95% confidence interval bands (dashed ellipses). **(C)** Unsupervised, bidirectional hierarchical cluster analysis of lung immune pathway transcriptome data using the Euclidean distance method with average linkage. All genes differentially expressed in either the Acute.1x (orange) or Acute.4x (blue) treatment groups were included in the heatmap, which is colored by the log_2 ratio of transcript counts calculated with respect to average expression in dosing-matched vehicle controls. **(D)** Heatmaps depicting either global or directed significance scores for immune-related pathways (see Materials and Methods for details on calculation of significance scores).

Irf7, and Slc11a1 (**Figure 4**) as well as *Mmp9 and Rsad2* (**Supplementary Table 2**).

Using marker genes expressed stably and specifically in immune cell types, we estimated relative abundance in sample groups measured as the average log-scale expression of their characteristic genes. Congruent with chemokine effects, several immune cell populations were changed in lung tissue of mice following a single or multiple exposures to $cSiO_2$ (**Figure 5**). Notably, leukocytes, neutrophils, and T-cells were significantly increased following a single exposure to $cSiO_2$, indicating a rapid immune response with recruitment of circulating lymphocytes. After multiple exposures, mRNA signatures were suggestive of elevations in cells associated with the innate (macrophages, neutrophils, NK cells) and adaptive immune responses (dendritic cells, B cells, and various classes of T-cells including exhausted CD8 T-cells and Treg cells). Overall, the acute response data following single and short-term repeated exposures were suggestive of a nascent autoimmune response.

Short-Term Repeated $cSiO_2$ Exposure Induces Chronic Changes in Lung mRNA Signatures Consistent With a Vigorous Autoimmune Response

Many of the same genes that were induced in the lung 24 h after the fourth installation of $cSiO_2$ were also induced 1 week after the fourth exposure (**Figure 6A**). The number of differentially expressed genes in the lung increased over time: 77 genes at 1 week, 92 genes at 5 weeks, 110 genes at 9 weeks, and 108 genes at 13 weeks (**Figure 6B**); again, most of these genes were upregulated with a few repressed (**Supplementary Tables 3–6**).

PCA plots (**Figure 6C**) and hierarchical clustering heat maps (**Figure 6D**) revealed some variance in gene expression profiles over time as evidenced by less distinct clustering by time point, with most variance in individual mice observed at 9 and 13 weeks post exposure. Also, though a core set of 39 genes were commonly differentially regulated by $cSiO_2$ at all time points (**Figure 6B**), both PCA and HCC analyses suggest a shift in overall gene expression profiles over time such that the lung transcriptome during early disease was distinct from that at later disease stages. Global and directed significance scores highlight the dramatic involvement of several immune pathways that appear to be well-established by 5 weeks post final exposure to $cSiO_2$ (**Figure 6E**). Corresponding to 16 weeks of age, this time point may represent a critical transitional step for the establishment of diverse networks of immune pathways. Network visualization of differentially expressed genes in lungs over the course of disease development aligns well with the NanoString pathway analyses, as the resulting networks showed clear groupings of transcripts associated with innate and adaptive immunity, chemokine, cytokines interferon, and complement (**Supplementary Figures 7–10**).

Immune pathways in the lungs of individual mice treated with either $cSiO_2$ or VEH clearly segregated into distinct

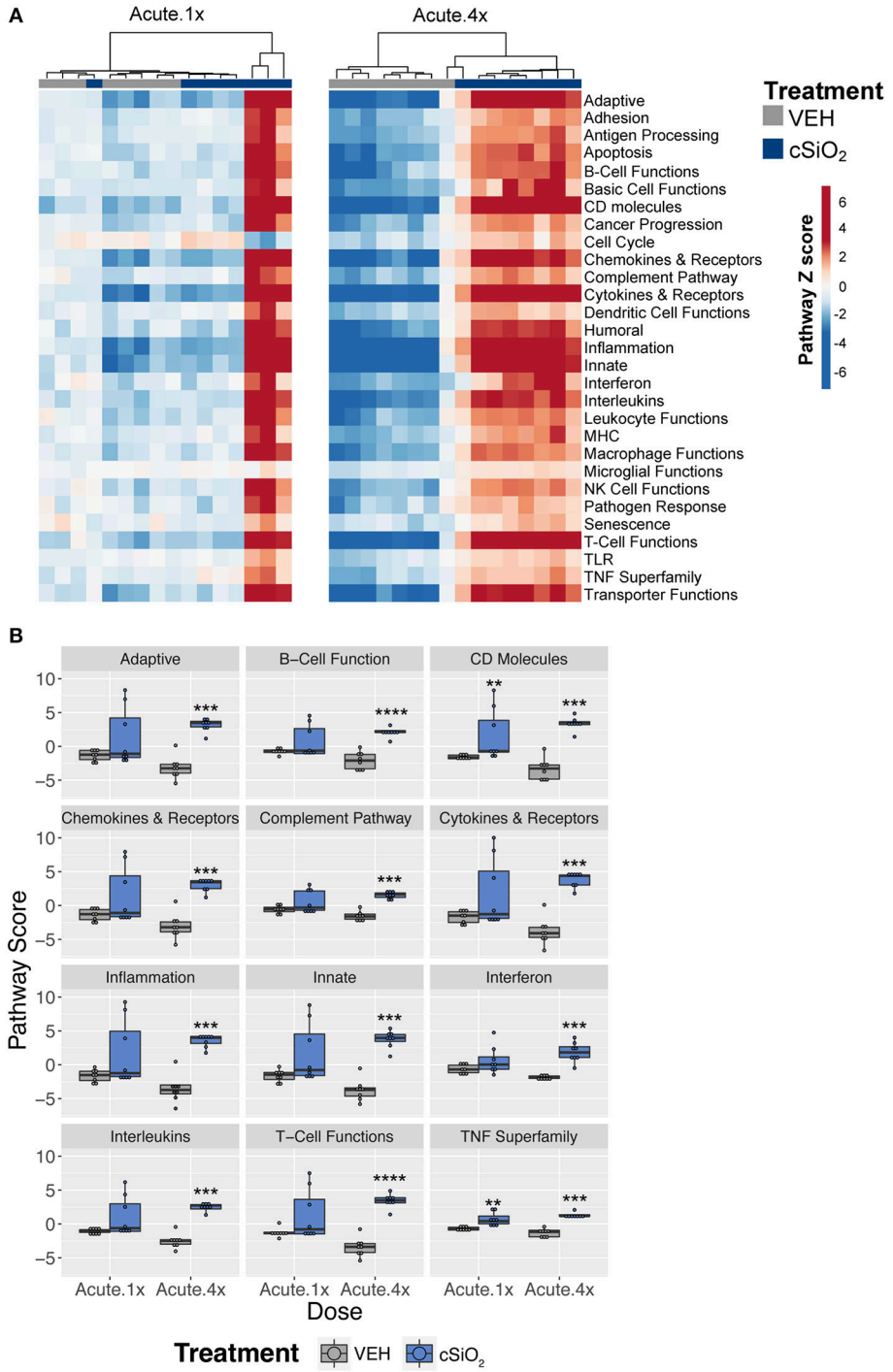

FIGURE 3 | Lung tissue gene expression pathway *Z* scores for mice that received either a single or four weekly instillations of $cSiO_2$. **(A)** Heatmap depicts individual pathway *Z* scores of each immune pathway for lung tissues obtained from vehicle (VEH) or $cSiO_2$-treated mice following a single (Acute.1x) or four weekly (Acute.4x) instillations. **(B)** Pathway *Z* scores are presented as Tukey box-plots ($n = 8$) for select immune pathways of interest. $^{**}p < 0.01$; $^{***}p < 0.001$, and $^{****}p < 0.0001$ compared to dosing-matched vehicle control as determined by the non-parametric Wilcoxon test.

clusters at each time point (**Figure 7A**). Notably, some pathways were responsive early on and then maintained consistent expression throughout the course of AD development (e.g., interferon, complement pathway, and TNF superfamily) whereas other pathways were modestly induced at early time points but markedly increased with progression of $cSiO_2$-induced

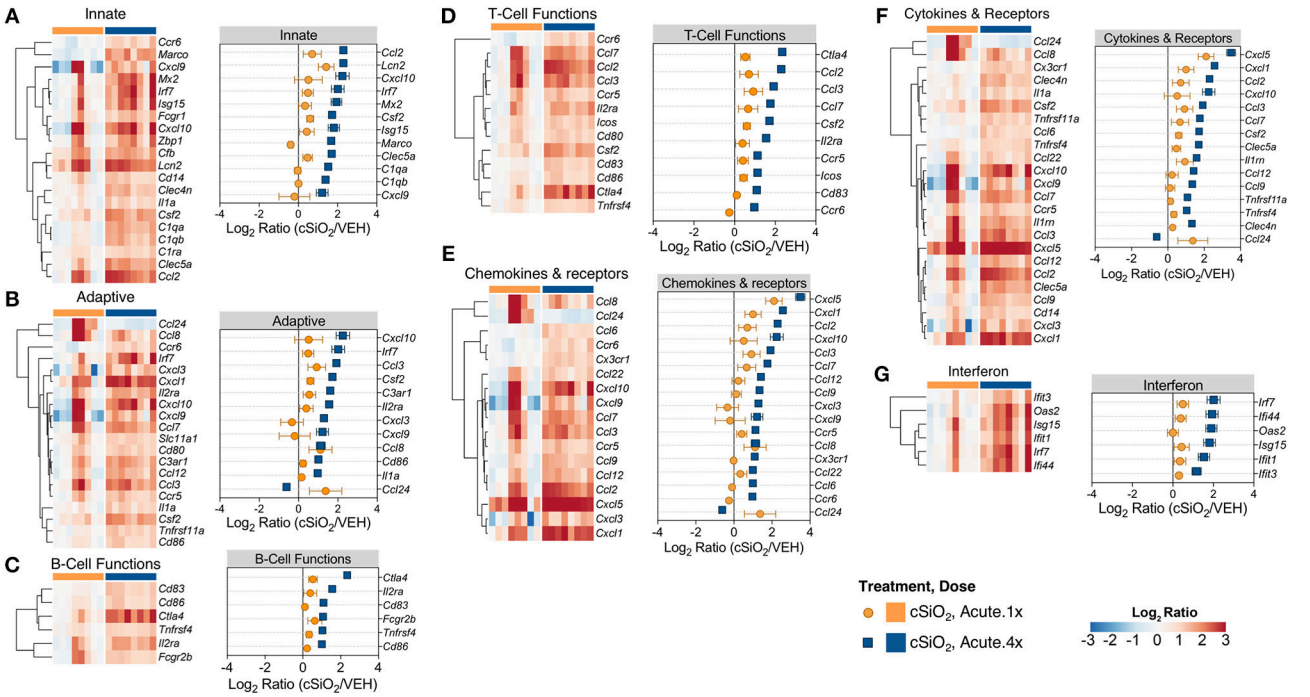

FIGURE 4 | Comparison of significant differentially expressed genes associated with immune response in lung tissues of mice that received either a single or four weekly instillations of $cSiO_2$. Gene expression data for **(A)** innate, **(B)** adaptive, **(C)** B-cell functions, **(D)** T-cell functions, **(E)** chemokines & receptors, **(F)** cytokines & receptors, and **(G)** interferon pathways were calculated as the $\log_2$ ratio of $cSiO_2$ with respect to dosing-matched vehicle (VEH) controls for mice that received a single (Acute.1x) or four weekly (Acute.4x) $cSiO_2$ instillations. For each pathway of interest, a heatmap with unsupervised clustering (Euclidian distance method) by gene is shown for all genes identified as significantly differentially expressed (BH $q < 0.05$, $\log_2$ ratio >1 or <−1) for either dosing protocol. Additionally, the mean $\log_2$ ratio values ± SEM for selected genes of interest are also shown for each panel. Note that some genes are associated with multiple immune response pathways, and thus, these genes appear in multiple panels.

autoimmunity (e.g., adaptive immunity, B-cell functions and T-cell functions) (**Figure 7B**).

Differentially expressed genes identified in immune pathways likely to be involved in the pathogenesis of $cSiO_2$-triggered autoimmunity are depicted in heat maps (**Figure 8**). Expression levels for selected genes representing these immunological pathways are also shown as line plots as a function of time to the right of these heat maps. Consistent with immune pathways, at least three trends were evident for these individual genes. Some genes were upregulated at 1 week post exposure and continued to increase over time (e.g., *Ccl2*, *Cxcl10*, *Cxcl13*, *Cxcl5*). Other sets of genes were modestly elevated at week 1 post exposure and remained so over the course of the experiment (e.g., *Marco*, *Cfb*, *Ctla4*, *Spp1*). Lastly, expression of a small number of genes (e.g., *Camp*, *Hamp*, *Txk*, *Cfd*, and *Il11ra1*) decreased over the length of the study. In addition, sequential comparisons over time were made to identify changes in gene expression as the disease progresses in the $cSiO_2$-exposed mice (**Supplementary Figure 11**). Upon comparing week 5 vs. week 1, week 9 vs. week 5, or week 13 vs. week 9, significant differences in relative expression >2-fold were identified for 17, 12, or 5 genes, respectively.

Immune cell type profiling in the lung based on expression of cell-specific mRNAs was carried out using NanoString software (**Figure 9**). Consistent with differential counts of bronchiolar lavage fluid carried out in the parent study (15), both macrophages and neutrophils increased in lungs of $cSiO_2$-exposed mice over time. Also, in accordance with our prior finding that $cSiO_2$ induced pulmonary ectopic lymphoid neogenesis, B-cell, T-cell, and dendritic cell mRNA signatures were increased in lungs of $cSiO_2$-treated mice. Intriguingly, Treg cells and exhausted CD8 T-cells were also increased in $cSiO_2$-treated mice.

Most pathways in individual lungs of $cSiO_2$-exposed lupus-prone mice correlated with pathological features the same lung tissues reported in the parent study (15) in a time-dependent manner (**Figure 10**). Again, the time between weeks 5 and 9 was particularly a critical period for transition.

Some, but Not All, $cSiO_2$-Induced mRNA Signatures in Lung Correlate With Those in Spleen and Kidney

To learn how the transcriptional responses in the lungs related to other organs associated with the autoimmunity, we compared lung mRNA signatures at 13 weeks after the final instillation of $cSiO_2$ to those in the spleen and kidney at the same time point. In spleen, 32 genes were altered and, strikingly, 168 were altered in the kidney (**Figure 11A**). Importantly, 55 genes were expressed

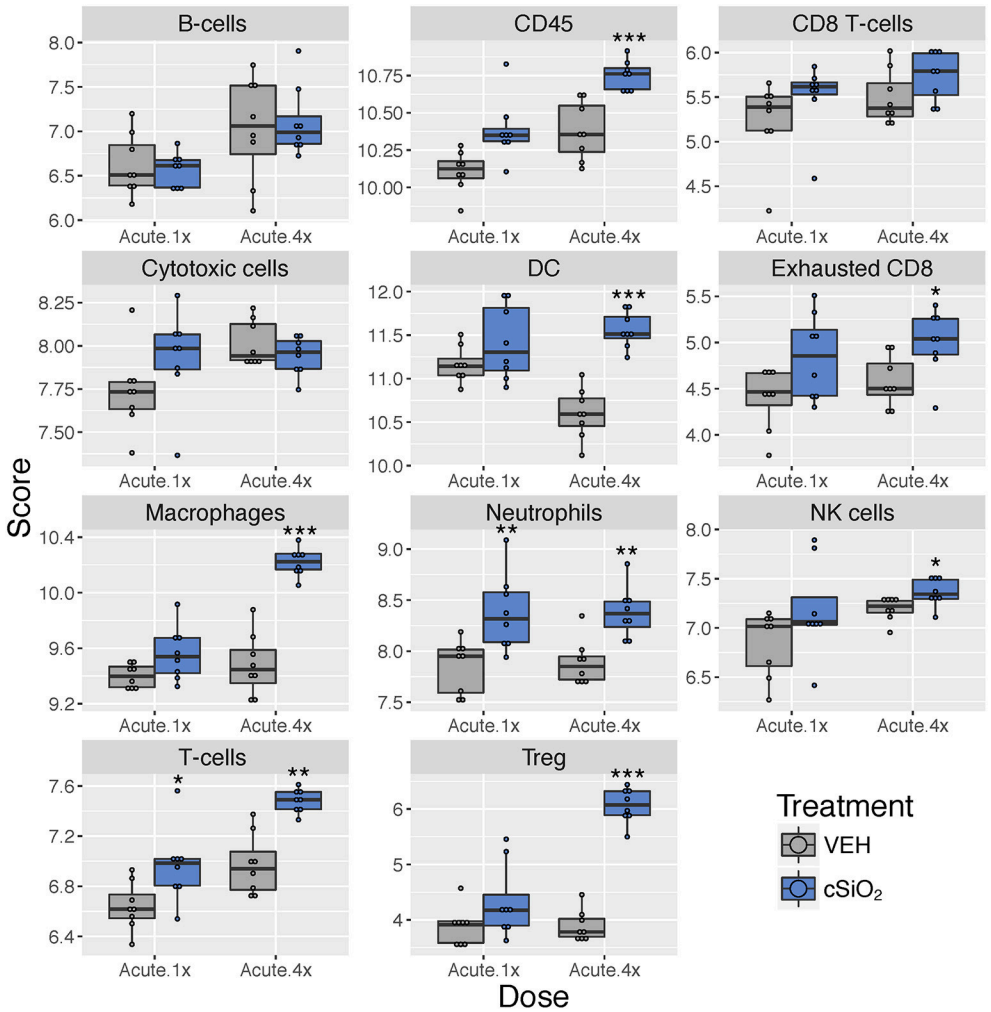

FIGURE 5 | Profiling of immune cell types in lung tissues obtained from mice that received either a single or four weekly instillations of $cSiO_2$ compared to non-exposed counterparts. Data shown are the log_2 cell type scores for mice for mice that received a single (Acute.1x) or four weekly (Acute.4x) instillations of $cSiO_2$ or saline vehicle (VEH). Scores may be compared within a cell type by dosing frequency to infer differences in abundance, but comparisons across cell types are not appropriate for this method of quantitation. $^{*}p < 0.05$; $^{**}p < 0.01$; and $^{***}p < 0.001$ compared to dosing-matched vehicle control as determined by the non-parametric Wilcoxon test.

both in the lung and kidney, and 11 genes were common to all tissues at 13 weeks post final exposure (**Supplementary Tables 7**, **8**). PCA indicated the expression profile of the lung clearly segregated from the kidney and spleen, although gene expression profiles for spleen and kidney could not be differentiated by the first two principal components (**Figure 11B**). Hierarchical clustering clearly demonstrated a substantial immune response in the kidney occurring as a result of intranasal $cSiO_2$ exposure, which paralleled closely with genes expressed in the lung and to a lesser extent, the spleen (**Figure 11C**). Significance scores in the kidney and spleen highlight that, as expected, the lung is the central affected organ at this time point (**Figure 11D**). However, all tissues have increased involvement of numerous immune pathways, with the kidney having a stronger response than the spleen at 13 weeks post final instillation of $cSiO_2$.

Further analysis of the immune pathways affected by intranasal $cSiO_2$ exposure in the spleen and kidney at 13 weeks reveal paralleled expression of a pathway within tissues of a given animal (**Figure 12A**). Like the lung, responses within the kidney were quite dramatic, whereas the involvement of the same pathways in the spleen were more modest. Despite the comparatively mild influence of $cSiO_2$ on the spleen, pathway scores were significantly increased in the spleen, as well as the lung and kidney, relative to VEH-treated mice (**Figure 12B**). A similar pattern was evident for the two network visualizations of differentially expressed transcripts in kidney and spleen. For kidney, the network was highly interconnected with major groupings of genes associated with interferon, chemokines and cytokines, TNF signaling, MHC molecules, adhesion, and CD molecules (**Supplementary Figure 12**). In contrast, the network for $cSiO_2$-responsive transcripts in spleen tissues was primarily limited to chemokines and cytokines, with small clusters of three genes associated with interferon or basic cell functions (**Supplementary Figure 13**).

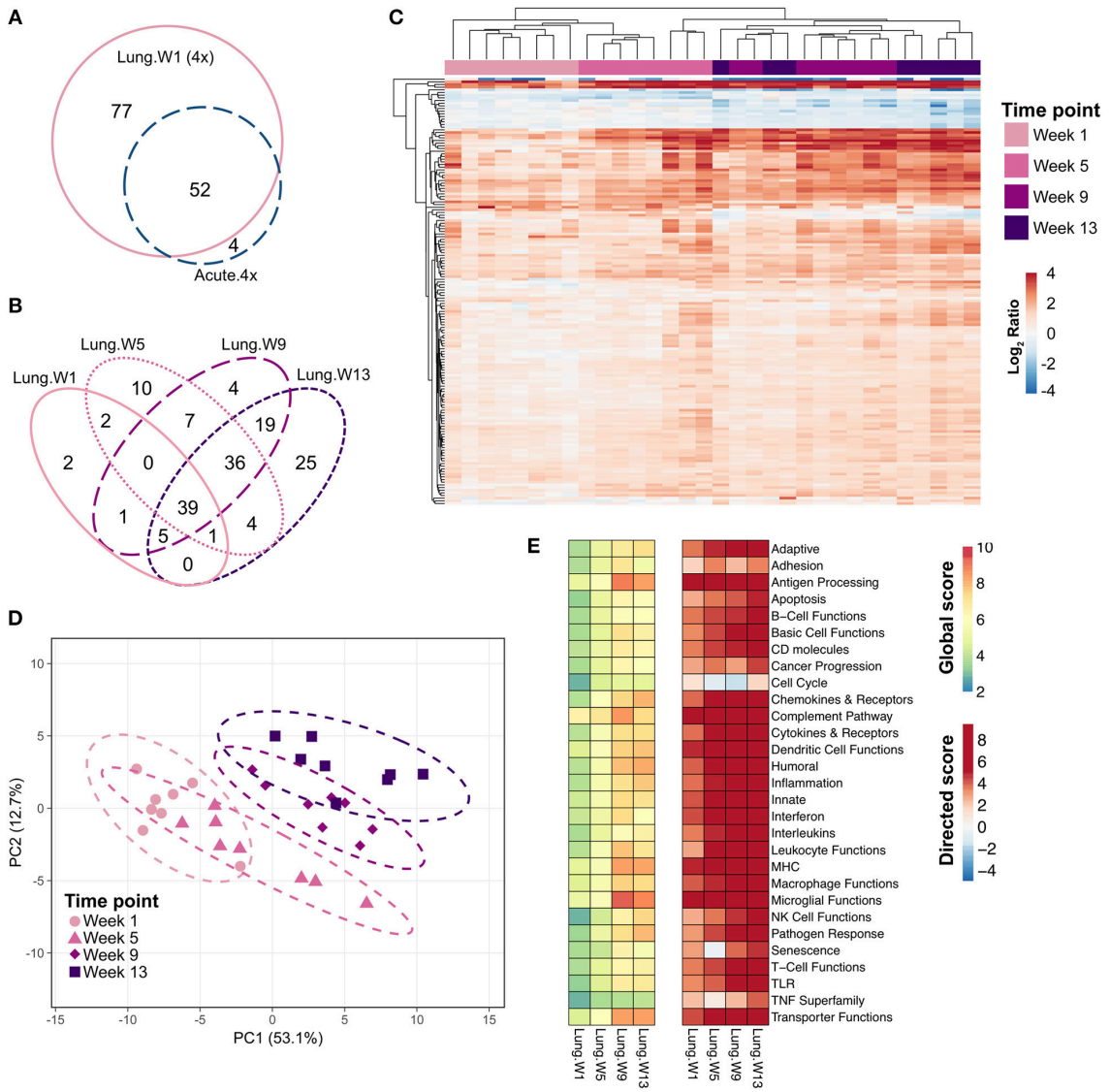

FIGURE 6 | Chronic transcriptional response of immune-associated genes in lung tissues of mice 1, 5, 9, or 13 weeks post $cSiO_2$ instillation. Mice received four repeated weekly doses of $cSiO_2$ or saline vehicle (VEH) via intranasal instillation, and gene expression was determined in lung tissues obtained 1, 5, 9, or 13 weeks post instillation. **(A)** Venn diagram depicting the number of genes identified as differentially expressed in lung tissue of mice 1 day (Acute.4x) or 1 week (Lung.W1) post $cSiO_2$ instillation compared to dosing-matched vehicle controls. **(B)** Venn diagram depicting the number of genes identified as differentially expressed in lung tissues over time as compared to time-matched, vehicle-exposed mice. **(C)** Principal components analysis of differentially expressed genes (BH $q < 0.05$, $\log_2$ ratio >1 or <-1) in lung tissues of mice exposed to $cSiO_2$ at 1, 5, 9, or 13 weeks post instillation compared to time-matched vehicle controls. PC1 and PC2 are shown with 95% confidence interval bands (dashed ellipses). **(D)** Unsupervised, bidirectional hierarchical cluster analysis of lung transcriptome data at weeks 1, 5, 9, or 13 using the Euclidean distance method with average linkage. All genes differentially expressed at any of the time points were included in the heatmap, which is colored by the $\log_2$ ratio calculated with respect to average expression in time-matched vehicle controls. **(E)** Heatmaps depicting either global or directed significance scores for immune-related pathways (see Materials and Methods for details on calculation of significance scores).

Figure 13 depicts selected tissue-specific gene responses within each immune signaling pathway. It is notable that a large number of genes associated with innate and T cell function were upregulated only in the kidney, such as *Tlr8*, *Ccl5*, and *Cxcr6* (**Figure 13A**) or *Itgal*, *Ccr2,* and *Cd48* (**Figure 13D**), respectively. In addition, two additional families of mRNA transcripts related to adhesion molecules and collagen deposition were present in the kidneys but not identified in the lungs following $cSiO_2$ exposure. The latter correlates with glomerulosclerosis.

Immune cell profiling indicated the involvement of cells of the innate and adaptive immune system in the transcriptional response of the spleen and kidney (**Figure 14**). As observed in the lung, leukocytes, dendritic cells, macrophages, neutrophils, and exhausted CD8 T-cells had statistically significant increased abundance in the spleen and kidney at 13 weeks post instillation.

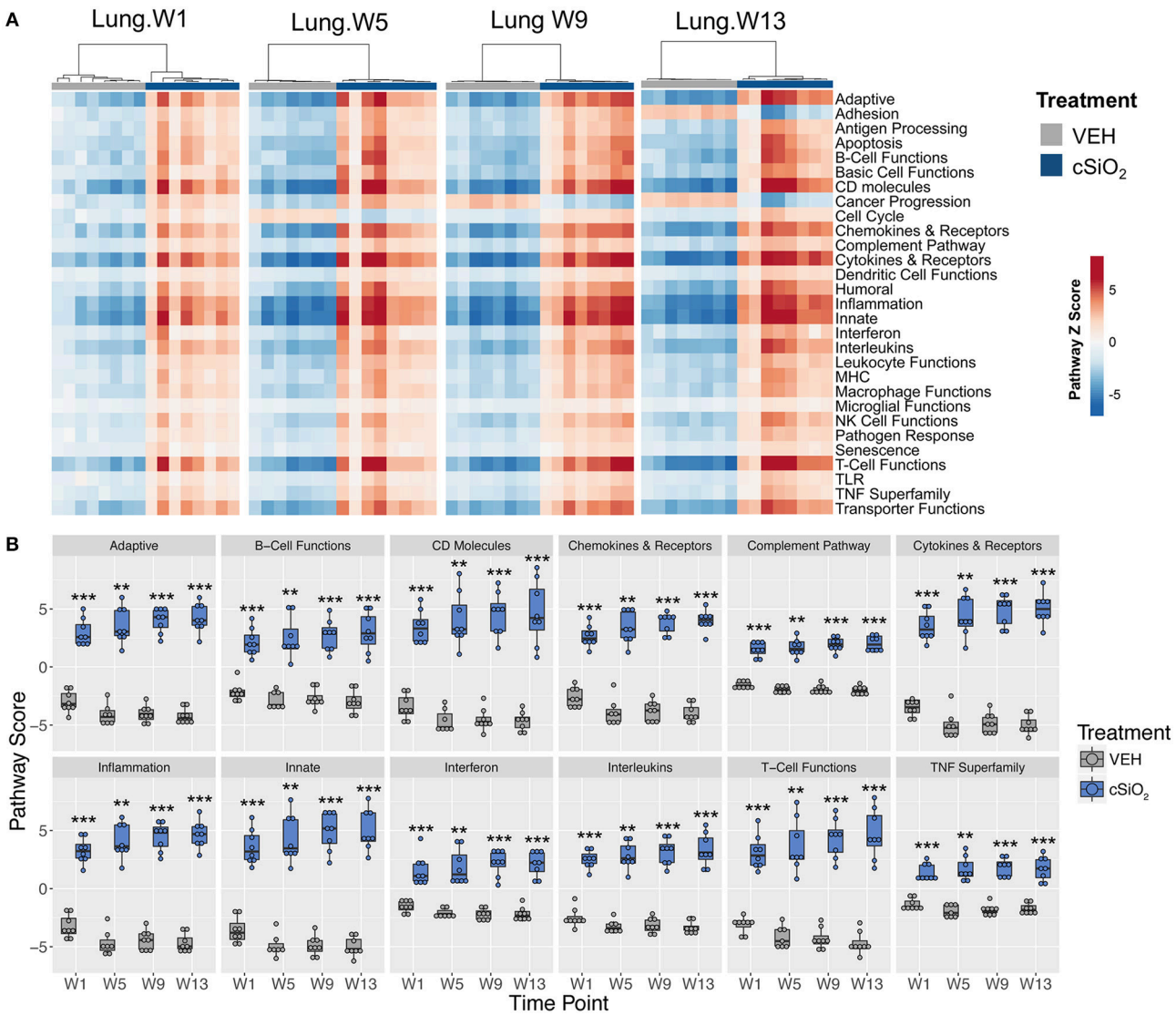

FIGURE 7 | Lung tissue gene expression pathway *Z* scores at 1, 5, 9, or 13 weeks post $cSiO_2$ instillation. **(A)** Heatmap depicts individual pathway *Z* scores of each immune pathway for lung tissues obtained from mice 1, 5, 9, or 13 weeks post instillation with $cSiO_2$ (four weekly doses) or time-matched vehicle (VEH) controls. **(B)** Pathway *Z* scores are presented as Tukey box-plots ($n = 7$–8) for select immune pathways of interest. $^{**}p < 0.01$; and $^{***}p < 0.001$ compared to time-matched vehicle control as determined by the non-parametric Wilcoxon test.

Additionally, like the lung, T-cells were increased in the kidney. The spleen had fewer cell types that achieved statistical significance possibly due to this tissue having higher basal expression of these markers which masked subtler effects of $cSiO_2$ in this tissue.

DISCUSSION

Identifying the critical genes associated with $cSiO_2$-triggered autoimmunity is of great importance because this particle has been linked to human AD. Furthermore, this response may model those of other exogenous particles (e.g., asbestos, carbon nanotubes) as well as endogenous particles (e.g., monosodium urate, cholesterol) (27). Targeted multiplex gene expression analysis with the nCounter provided a focused strategy to test the hypothesis that upregulation of adaptive immune function genes in the lung precedes $cSiO_2$-triggering in the NZBWF1 mouse. We found that $cSiO_2$ indeed induced wide scale adaptive immune gene upregulation and furthermore, these responses were intricately linked the particle's capacity to elicit an early and persistent inflammatory stimulus in the lung that promoted expression of mRNAs indicative both innate and adaptive immune pathways. Several novel findings were made in this investigation. First, relevant to lupus, dramatic increases were observed in mRNAs associated with chemokine release, cytokine production, sustained IFN activity,

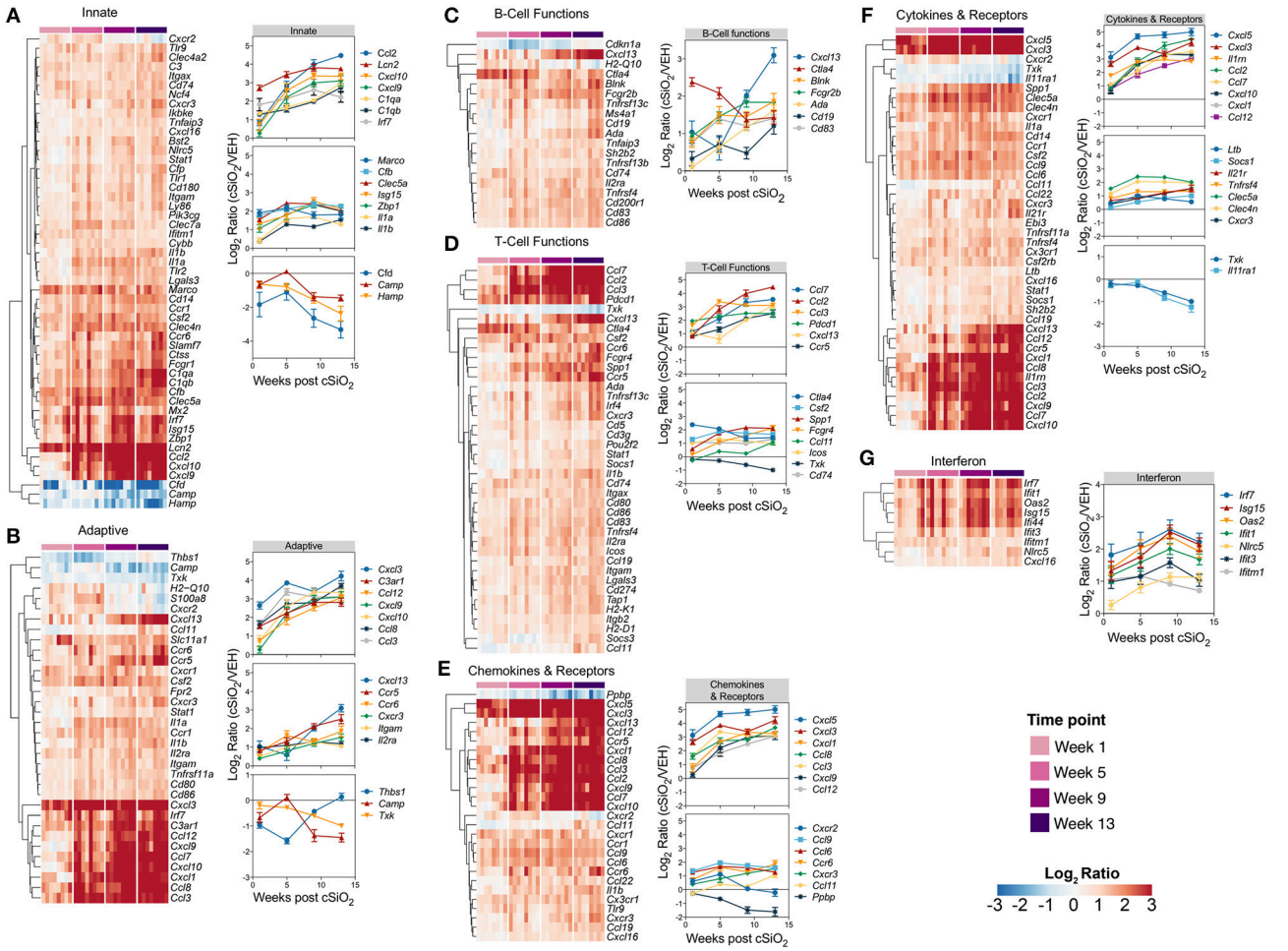

FIGURE 8 | Time course of significant differentially expressed genes associated with immune response in lung tissues of mice 1, 5, 9, or 13 weeks post instillation with $cSiO_2$. Gene expression data for **(A)** innate, **(B)** adaptive, **(C)** B-cell functions, **(D)** T-cell functions, **(E)** chemokines & receptors, **(F)** cytokines & receptors, and **(G)** interferon pathways were calculated as the log_2 ratio of expression values for $cSiO_2$-treated mice at 1, 5, 9, or 13 weeks PI with respect to time-matched vehicle controls. For each pathway of interest, a heatmap with unsupervised clustering (Euclidian distance method) by gene is shown for all genes identified as significantly differentially expressed (BH $q < 0.05$, log_2 ratio >1 or <-1) at any one of the indicated time points. The mean log_2 ratio values ± SEM for selected genes of interest are also shown for each panel. Note that some genes are associated with multiple immune response pathways, and thus, these genes appear in multiple panels.

complement activation, and adhesion molecule expression. Second, consistent with previously described histopathologic stages of $cSiO_2$-triggered autoimmune pathogenesis (15), the time between 5 and 9 weeks PI was an important transition period for gene upregulation in the lung. Third, at experiment termination, $cSiO_2$-induced changes in transcriptome signatures were equally robust in kidney but more modest in spleen. Finally, transcriptomic signatures in lung and kidney were indicative of expansion and/or activation of several leukocyte populations including neutrophils, macrophages, dendritic cells, B cells, and T cells that corresponded with accelerated autoimmune pathogenesis.

Both single and multiple $cSiO_2$ exposure protocols were employed here to map time-dependent changes in transcriptome signatures in the lung following $cSiO_2$ exposure. Regarding acute responses, mRNA signatures 24 h after a single dose of $cSiO_2$ (i.e., Acute.1x) were variable with three out of eight mice being extremely high responders and the remainder being low responders. Remarkably, signatures among these high responders were highly consistent with the less variable responses observed 24 h after short term repeated dosing (Acute.4x group). Variability in the single dose acute study might be attributable to use of intranasal instillation as the delivery route for $cSiO_2$. Particle suspensions deposited at the anterior nares can distribute into three sites in the mouse: (i) the upper respiratory tract, (ii) the lower respiratory tract, and (iii) the digestive system (28). Thus, variability might have resulted from slow and/or incomplete dissemination of the $cSiO_2$ particles in the lower airways of some mice at 1 d following a single dose (29). Comparatively, $cSiO_2$ dissemination might be more uniform after four dosages and longer time period than was achieved 24 h after a single installation.

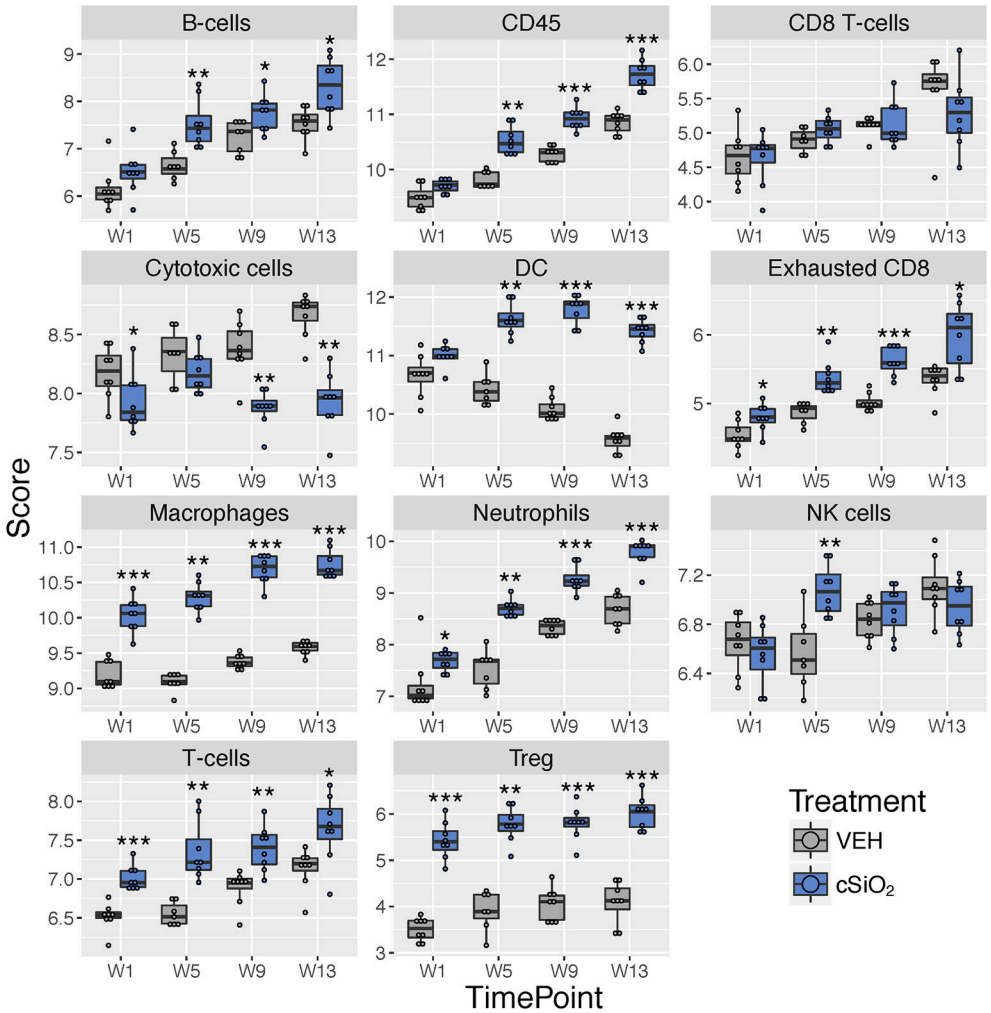

FIGURE 9 | Profiling of selected immune cell types in lung tissues at 1, 5, 9, or 13 weeks post $cSiO_2$ instillation. Data shown are the log_2 cell type scores for lung tissues obtained 1, 5, 9, or 13 weeks following four weekly instillations with $cSiO_2$ or saline vehicle (VEH). Scores may be compared within a cell type at each time point to infer differences in abundance, but comparisons across cell types are not appropriate for this method of quantitation. $^*p < 0.05$; $^{**}p < 0.01$; $^{***}p < 0.001$ compared to time-matched vehicle control as determined by the non-parametric Wilcoxon test.

Relative to short-term repeated exposures to $cSiO_2$, transcriptome signatures in the lung broadly reflected both activation of innate and adaptive pathways. While similar genes associated with disease pathways were significantly upregulated 1 d and 1, 5, 9, and 13 weeks after the final $cSiO_2$ instillation, both the numbers of genes and response intensity progressively increased. Notably, PCA analysis indicated that the most critical breakpoint in expression existed between weeks 5 and 9. This breakpoint corresponded to a massive expansion of ELS and appearance of follicular dendritic and plasma cells in the lung observed immunohistochemically at week 9 in the parent study, the source of the samples used here for the chronic study (15).

Once $cSiO_2$ enters the lung, it is largely retained at this site with miniscule amounts translocating to the mediastinal lymph node and thymus (30, 31). Thus, rather than being a direct effect of the particle, $cSiO_2$-driven gene responses observed in the kidney are more likely driven by autoantibodies arising in the lung. These autoantibodies likely enter into the systemic compartment in the unbound form or as immune complexes with autoantigens and subsequently deposit in distal tissues—most notably kidney. There they could elicit robust inflammatory responses resulting in glomerulonephritis. Thus, the transcriptome signatures observed in the kidney most likely reflect downstream effects of the ectopic lymphoid neogenesis in the lung.

Diverse chemokine genes were consistently upregulated in lung at all time points following $cSiO_2$ exposure. Chemokines are released from injured cells to recruit resident and circulating leukocytes to sites of inflammation by way of concentration gradients. Both C-X-C and C-C chemokines were identified in lung, kidney, and to a lesser extent spleen, thus implicating neutrophils, macrophages, B-cells, and T-cells in the progression

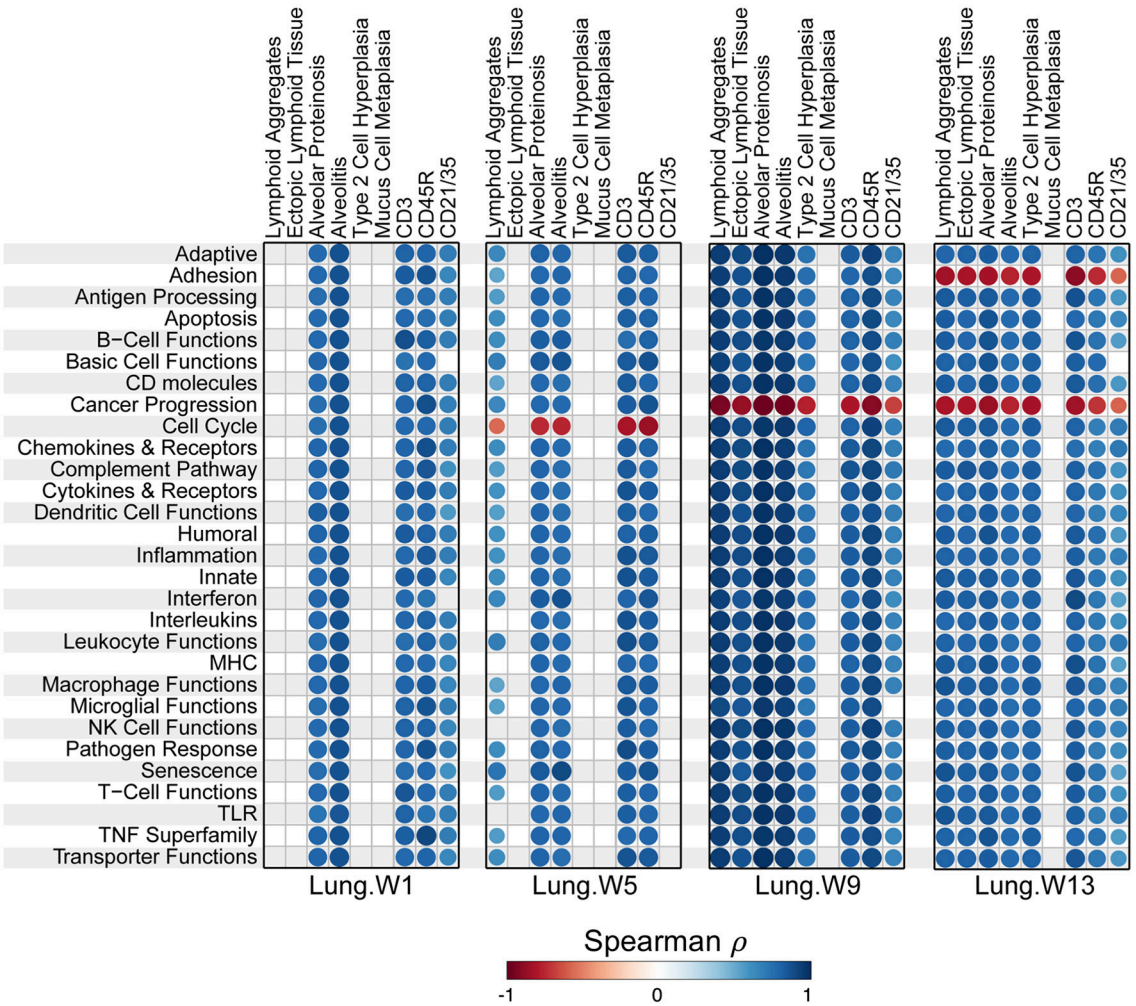

FIGURE 10 | Correlation analyses of immune-associated pathways and phenotypic endpoints assessed in lung tissues of mice collected 1, 5, 9, or 13 weeks post instillation with $cSiO_2$. Spearman ρ values were calculated using pathway Z scores and phenotype data (histopathology scores (lymphoid aggregates, ectopic lymphoid tissue, alveolar proteinosis, alveolitis, type 2 cell hyperplasia, and mucus cell metaplasia) or percent positive staining tissue (CD3, CD45R, and CD21/35). Significant correlation values ($p < 0.05$) are represented as circles colored by the correlation value (blue, positive; red, negative); non-significant correlations are indicated by blank cells.

of $cSiO_2$-triggered autoimmunity. These findings were highly consistent with immune cell profiles both identified using NanoString (**Figures 5**, **9**, **14**) and by differential staining of BALF and immunohistochemistry in the parent study (15). *Cxcl5* and *Cxcl3* were consistently among the most highly upregulated genes following $cSiO_2$ treatment. These chemokines predominately recruit neutrophils to sites of inflammation via the receptor Cxcr2. Degranulation of recruited neutrophils may release proteolytic enzymes into the extracellular space, thus resulting in bystander tissue injury and promoting lung inflammation (32–34). In addition, neutrophils at sites of inflammation can die by NETosis, a form of regulated cell death that releases neutrophil extracellular traps (NETs) consisting of nuclear material (e.g., dsDNA) that could be a source of autoantigen (35).

Other chemokines identified in this study were consistent with monocyte recruitment into inflamed tissues. These include *Ccl2*, *Ccl7*, *Ccl8*, and *Ccl12* which code for monocyte chemoattractant protein 1 (MCP-1), MCP-2, MCP-3, and MCP-5, respectively. In prior work, we have reported that $cSiO_2$ exposure promotes MCP-1 elevation in BALF and plasma (13). Importantly, increased MCP-1 in plasma is associated with increased disease severity in lupus patients (36, 37).

C-X-C motif chemokines that are chemoattractant for B and T cells were also found to be persistently upregulated by $cSiO_2$ in lung, spleen, and kidney. Of particular interest here, *Cxcl13* was highly expressed in the lung and kidneys of $cSiO_2$-treated mice. This chemokine, also known as B-lymphocyte chemoattractant (BLC), is preferentially produced by FDCs in B-cell follicles of lymphoid organs (38) and to some extent, by T follicular helper cells (39, 40) and Th17 cells (41). Relatedly, experimental anti-CXCL13 antibodies have shown promising results on murine models of autoimmune disease (42).

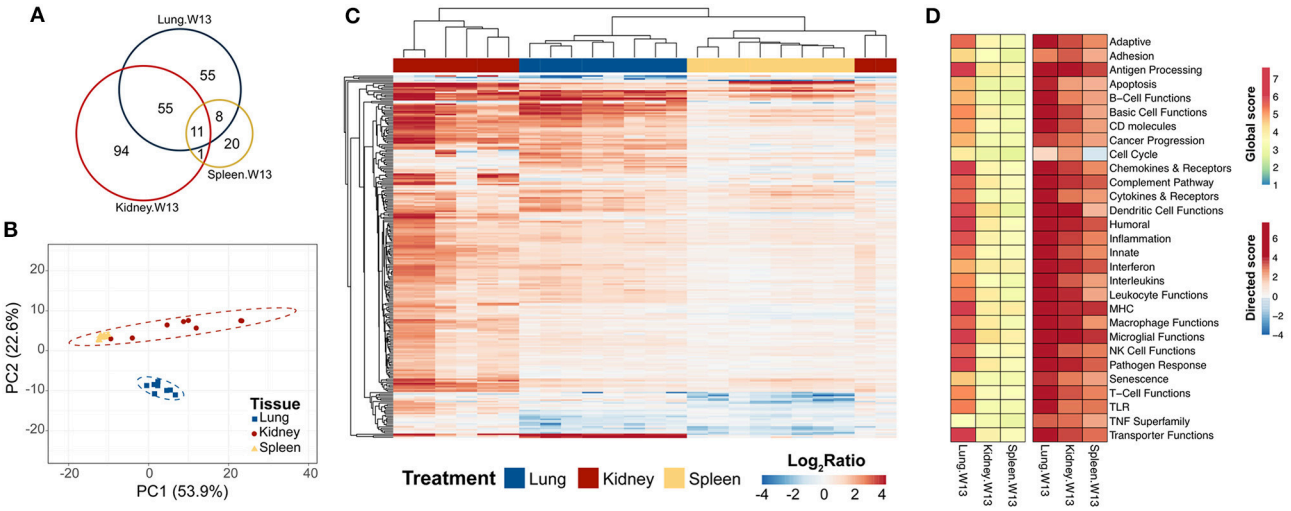

FIGURE 11 | Comparison of chronic transcriptional response of immune-associated genes in lung, kidney and spleen tissues of mice 13 weeks post instillation with $cSiO_2$. Mice received four repeated weekly doses of $cSiO_2$ or saline vehicle (VEH) via intranasal instillation, and gene expression was determined in lung, kidney and spleen tissues obtained 13 weeks post instillation. **(A)** Venn diagram depicting the number of genes identified as differentially expressed in lung, kidney, and spleen tissues 13 days post installation as compared to time-matched, vehicle-exposed mice. **(B)** Principal components analysis of differentially expressed genes (BH $q <$ 0.05, $\log_2$ ratio >1 or <-1) in lung, kidney, and spleen tissues of $cSiO_2$-exposed mice compared to time-matched vehicle controls. PC1 and PC2 are shown with 95% confidence intervals (dashed ellipses). **(C)** Unsupervised, bidirectional hierarchical cluster analysis of lung, kidney, and spleen immune pathway transcriptome data using the Euclidean distance method with average linkage. All genes differentially expressed in any one of the tissue types were included in the heatmap, which is colored by the $\log_2$ ratio as calculated with respect to average expression in time-matched vehicle controls. **(D)** Heatmaps depicting either global or directed significance scores for immune-related pathways (see Materials and Methods for details on calculation of significance scores).

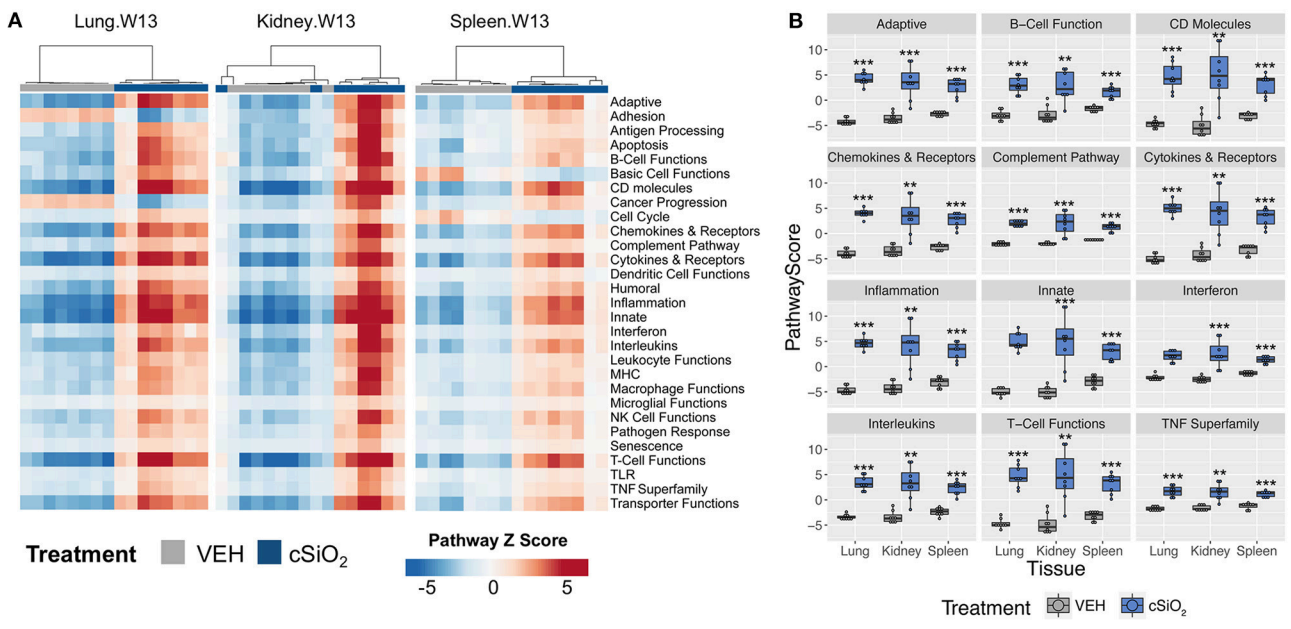

FIGURE 12 | Gene expression pathway *Z* scores for lung, kidney or spleen tissues obtained 13 weeks post $cSiO_2$ instillation. **(A)** Heatmap depicts individual pathway *Z* scores of each immune pathway for lung, kidney, or spleen tissues obtained from mice 13 weeks post instillation with $cSiO_2$ (four weekly doses) or the corresponding tissue-matched vehicle (VEH) control. **(B)** Pathway *Z* scores are presented as Tukey box-plots ($n = 8$) for select immune pathways of interest. $^{**}p <$ 0.01; and $^{***}p < 0.001$ compared to time-matched vehicle control as determined by the non-parametric Wilcoxon test.

Chemokines that recruit and direct the position of activated T-cells, namely *Cxcl9*, *Cxcl10*, *Cxcl11*, and *Cxcl16*, and receptors for these chemokines, *Cxcr3* and *Cxcr6*, were also highly expressed in the lungs of $cSiO_2$-exposed mice with similar effects being observed in the kidney. Notably, immune cell profiling revealed that both exhausted CD8

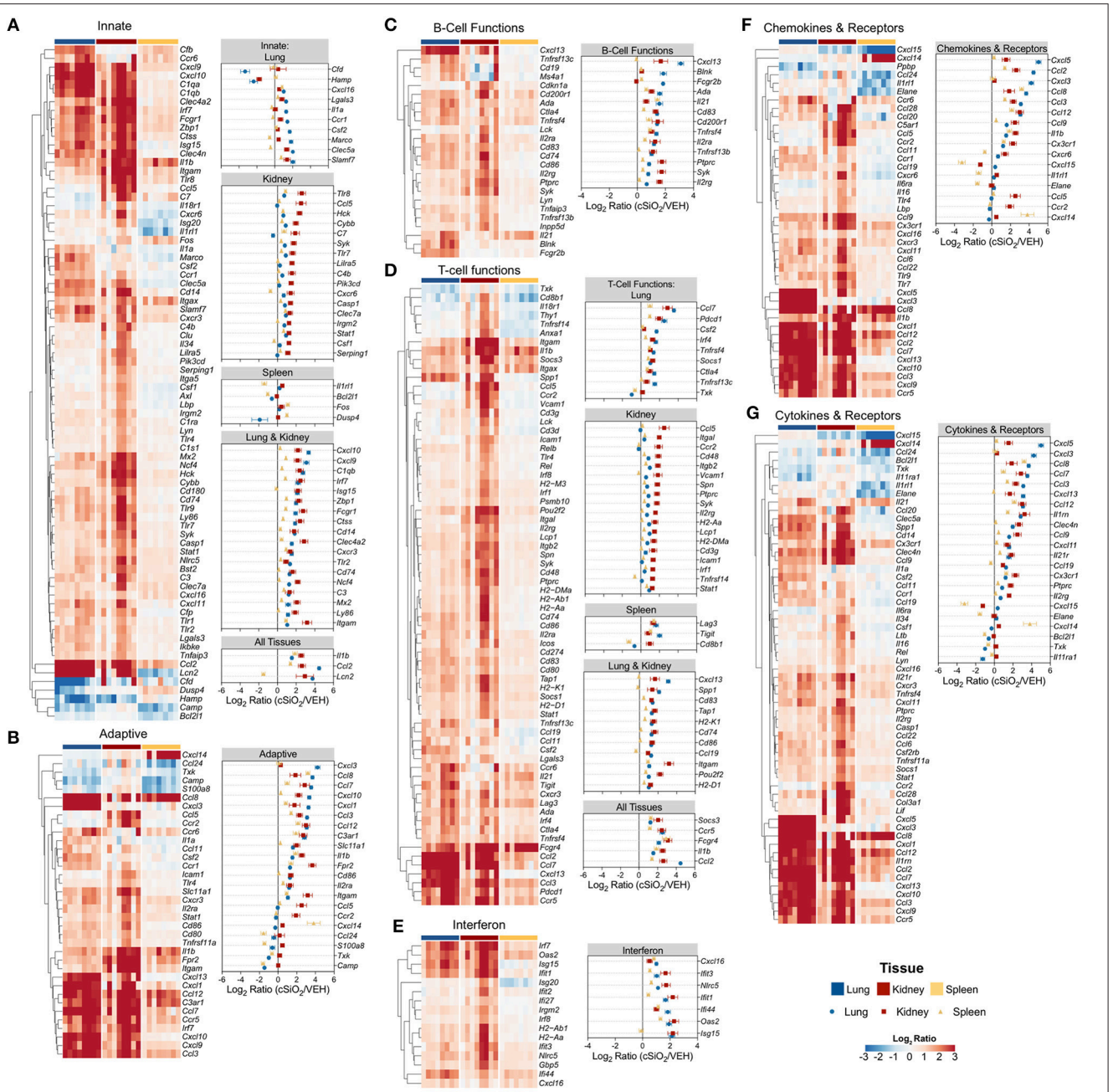

FIGURE 13 | Tissue comparison of significant differentially expressed genes associated with immune response in lung, kidney or spleen of mice 13 weeks post instillation with $cSiO_2$. Gene expression data for **(A)** innate, **(B)** adaptive, **(C)** B-cell functions, **(D)** T-cell functions, **(E)** chemokines & receptors, **(F)** cytokines & receptors, and **(G)** interferon pathways were calculated as the $\log_2$ ratio of expression values for $cSiO_2$-treated mice with respect to tissue-matched vehicle controls. For each pathway of interest, a heatmap with unsupervised clustering (Euclidian distance method) is shown for all genes identified as significantly differentially expressed (BH $q < 0.05$, $\log_2$ ratio >1 or <-1) in any one of the indicated tissues. The mean $\log_2$ ratio values ± SEM for selected genes of interest are also shown for each panel. Note that some genes are associated with multiple immune response pathways, and thus, these genes appear in multiple panels.

(lung, kidney, spleen) and regulatory T cells (lung, spleen) were upregulated in mice treated with $cSiO_2$ (**Figures 9**, **14**). These T cell phenotypes are associated with downregulation of the immune response and increased numbers have been associated with lupus and other autoimmune diseases (43, 44). Thus, their increased numbers observed here following $cSiO_2$ exposure likely reflect compensatory mechanisms to limit autoimmune pathogenesis.

Genes activated by the Type I and type II IFN constitute the "IFN signature," which is evident in 65% of patients with lupus and which correlates strongly with disease severity (45, 46). The panel of genes used to define the IFN signature varies by laboratory; however, we observed striking overlap in the IFN signature described by Li et al. (47). Type I IFNs (i.e., IFN-α and IFN-β) have been established to be pathogenic in lupus [reviewed in Crow (48)]. The main cellular source of Type I

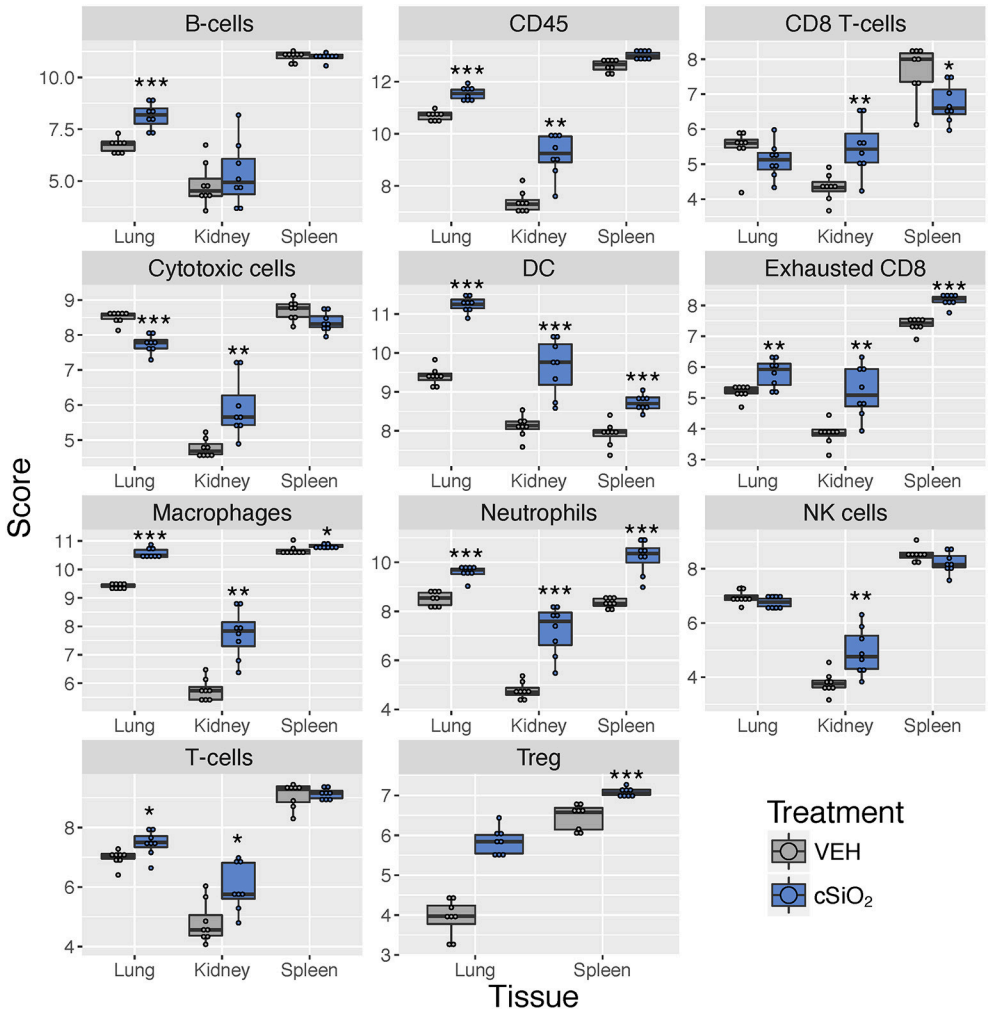

FIGURE 14 | Cell type profiling in lung, kidney and spleen tissues in mice 13 weeks post instillation with $cSiO_2$. Data shown are the log_2 cell type scores for lung, kidney and spleen tissues obtained 13 weeks after four weekly instillations with $cSiO_2$ or saline vehicle (VEH). Scores may be compared within a cell type for each tissue to infer differences in abundance, but comparisons across cell types are not appropriate for this method of quantitation. *$p < 0.05$; **$p < 0.01$; and ***$p < 0.001$ compared to dosing-matched vehicle control as determined by the non-parametric Wilcoxon test.

IFN is plasmacytoid dendritic cells, which are dependent on IRF4 activation of TLR7/9 (49, 50). Interestingly, NanoString immune cell profiling indicated that increased dendritic cells were evident in lungs, kidneys, and spleens of $cSiO_2$-treated mice. Additionally, the aforementioned genes were upregulated in lung (*Irf4*) and kidney (*Tlr7/9*) following $cSiO_2$ exposure. Both have been widely implicated in autoimmunity (50) and, of particular relevance here, in ELS during pristane-induced autoimmunity (51). Finally, exogenous administration of IFN-α to NZBWF1 mice accelerated disease onset (52, 53) and decreased the efficacy of pharmacological interventions (54). Type II IFN (i.e., IFN-γ) has also been implicated in lupus (55–57). Secreted predominately by NK and T-cells, IFN-γ heightened adaptive immunity by increased antigen presentation through enhanced expression of MHC II molecules (58) and immunoglobulin production (57). Exogenous administration of IFN-γ to lupus-prone NZBWF1 mice accelerated glomerulonephritis (59); whereas IFN-γ receptor deletion attenuated renal injury and autoantibody generation (52). Collectively, our findings are consistent with a possible pathogenic role for type I and/or type II IFN in $cSiO_2$-triggered autoimmunity.

The IL-1 superfamily is a key component of the innate immune system and functions to rapidly initiate inflammatory responses following toxic stimuli via several mechanisms. Consistent with the known actions of $cSiO_2$ and other particles [reviewed in Sayan and Mossman (60)], *Il1a*, *Il1b*, the decoy receptor *Il1r2*, and the receptor antagonist, *Il1rn*, were upregulated by exposure to $cSiO_2$ in lungs of NZBWF1 mice. Dying cells release IL-1α, which serves as an alarmin to alert the immune system of an inflammatory stimulus. Cells dying by pyroptosis in an NLRP3 inflammasome-dependent manner release IL-1β by way of caspase-1 activation. Caspase-1, IL-1 β and interleukin 1 receptor associated kinase 3 (IRAK3) were upregulated in the kidneys of $cSiO_2$-treated NZBWF1 mice in parallel with IL-1β in this study. Consistent with our findings, aberrant IL-1 signaling and inflammasome activation is suspected to contribute to the pathogenesis of ADs such as lupus [reviewed in Kahlenberg and Kaplan (61)].

Other genes for cytokines and cytokine receptors that potentially mediate formation and maintenance of lymphoid tissues were upregulated in lungs, spleen and kidney of $cSiO_2$-treated mice. These included *Lta* (lymphotoxin-α), *Il21*, *Il21r*, *Il6*, *Tnfsf11* (RANKL), *Tnfrsf11a* (RANK or TRANCE). Lymphotoxin-α, otherwise known as TNF-β, is induced by IL-21 and is critical to formation of lymphoid tissues (62). Mice deficient in lymphotoxin-α or RANKL fail to properly develop lymph nodes and Peyer's patches (63, 64). IL-21/IL-21R blockade is associated with decreased IL-6 and autoantibody production and has shown positive effects in preclinical trials in murine models of lupus and rheumatoid arthritis (65, 66).

Upregulation of genes for adhesion molecules that facilitate cellular infiltration are commonly observed in renal biopsies from individuals with lupus nephritis (67–69). Interestingly, expression of genes coding for adhesion were elevated in lupus-prone mice. Specifically, a number of adhesion molecule genes upregulated in the kidney by $cSiO_2$ exposure are expressed by infiltrating lymphocytes (*Itga4*, *Itgal*) and by endothelial cells (e.g., *Sele*, *Selplg*, *Vcam1*, *Icam1*). These might collectively promote cellular infiltration and facilitate enhanced development of glomerulonephritis in $cSiO_2$-treated NZBWF1 mice. It should be noted that ELS were negatively associated with adhesion molecule expression at 13 weeks post instillation (15).

Interestingly, cell cycle gene expression was negatively associated with features of ELS, notably lymphoid aggregates containing $CD3^+$ and $CD45R^+$ cells, at 5 weeks post instillation (**Figure 10**). Ectopic lymphoid neogenesis might have suppressed active cell proliferation until additional stimuli trigger their re-activation. In addition, genes associated with cancer progression (e.g., *Vegfr2*, *Angpt2*, and *Kdr*) were suppressed at 9 and 13 weeks post instillation. This may reflect the canon of immune surveillance and disease development: loss of immune tolerance results in autoimmunity, whereas overt immune tolerance results in cancer progression. In this case, active loss of tolerance (as occurs in our model of $cSiO_2$-triggered lupus) would effectively suppress pathways key to cancer progression.

$cSiO_2$ instillation induced large changes in immune genes in the lung and kidney, whereas responses in the spleen were relatively modest. Lung and kidney typically do not contain many immune cells, and the majority of cells that do persist within these tissues during inflammation are activated. Conversely, the spleen from these mice contain many more non-activated cells compared to the other two tissues which may dilute out the expression of inflammatory genes. Hence, one limitation of comparing differences in cell-specific genes among the tissues is that differences may be skewed due to drastic alterations in the number of activated to non-activated cells within each tissue.

Another limitation of this investigation is that targeted multiplex approaches, such as NanoString, focus on a subset of genes and, thus, do not capture genome-wide changes in mRNA abundance (20). As a result, analytical approaches designed for discovery, such as gene ontology, have limited utility in the identification of novel enriched genes. However, since we focused on immune pathways, a targeted approach was appropriate, as this method improves statistical power by querying a substantially smaller gene set. In addition, we recognize that transcriptomic profiling in whole tissue homogenates restricts the interpretation of results because mRNA signatures cannot be selectively attributed to a given cell type. Nevertheless, the targets discovered herein can be employed as endpoints in future studies that perform mRNA analyses on isolated populations obtained by cell sorting, cell separation columns, or laser dissection of lesions of interest from formalin-fixed paraffin sections (18).

CONCLUSION

Taken together, the early and dramatic impact of $cSiO_2$ exposure on immune gene expression in the lower respiratory tract promoted the establishment of the lung as the central nexus for launching systemic autoimmunity. Signatures consistent with persistent recruitment of neutrophils, monocytes/macrophages, lymphocytes, and antigen-presenting cells, including dendritic cells, were identified herein, implying that both innate and adaptive immune systems contribute largely to the onset and progression of $cSiO_2$-triggered autoimmunity. Future perspectives should include elucidation of the underlying modes of action of $cSiO_2$ in alveolar macrophages and neutrophils, two early responders to particles in the lung, as well as identifying novel interventions against this occupational toxicant.

DATA AVAILABILITY

The data output from nSolver analyses for this study can be found at https://doi.org/10.26078/9vtk-zg12. The raw data supporting the conclusions of this manuscript will be made available by the authors, without undue reservation, to any qualified researcher.

AUTHOR CONTRIBUTIONS

MB: study design, animal study coordination, $cSiO_2$ exposures, necropsy, RNA analysis, data analyses, interpretation, manuscript preparation, and project funding; AB: data analyses, interpretation, statistical analysis, figure preparation, and manuscript preparation/submission; KG: animal study coordination, RNA analysis, data analyses, and manuscript preparation; AH: experimental design, data interpretation, manuscript writing, and project funding; JH: study design, lung, kidney histopathology, morphometry, data analyses, manuscript preparation, and project funding; JP: planning, coordination, oversight, manuscript preparation, submission, and project funding.

FUNDING

Research was funded by NIH ES027353 (JP, JH, and AH), Lupus Foundation of America (MB, JP), and the Dr. Robert and Carol Deibel Family Endowment (JP).

ACKNOWLEDGMENTS

We would like to thank Dr. James Wagner, Dr. Ning Li, Dr. Daven Humbles-Jackson, Amy Freeland, Lysie Eldridge, and Ryan Lewandowski for their excellent technical support,

and Amy Porter and Kathy Joseph from the Michigan State University Histopathology Laboratory.

SUPPLEMENTARY MATERIAL

The Supplementary Material for this article can be found online at: https://www.frontiersin.org/articles/10.3389/fimmu.2019.00632/full#supplementary-material

Additional Supplementary Files are available at https://doi.org/10.26078/9vtk-zg12, including the following:

Supplementary File 1 | Customized probe annotation file for the Nanostring nCounter Mouse PanCancer Immune Profiling Panel.

Supplementary File 2 | Microsoft Excel document with output from nSolver for differential expression analyses.

Supplementary File 3 | Microsoft Excel document with output from nSolver for global and directed significance scores for immune pathways.

Supplementary File 4 | Microsoft Excel document with output from nSolver for immune pathway *Z* scores for pairwise comparisons.

Supplementary File 5 | Microsoft Excel document with output from nSolver for cell type profiling scores.

Supplementary File 6 | Microsoft Excel document with protein networks obtained from STRING database and clusters predicted by the MCL algorithm.

REFERENCES

1. Pons-Estel GJ, Ugarte-Gil MF, Alarcón GS. Epidemiology of systemic lupus erythematosus. *Exp Rev Clin Immunol.* (2017) 13:799–814. doi: 10.1080/1744666X.2017.1327352
2. Nacionales DC, Weinstein JS, Yan X-J, Albesiano E, Lee PY, Kelly-Scumpia KM, et al. B cell proliferation, somatic hypermutation, class switch recombination, and autoantibody production in ectopic lymphoid tissue in murine lupus. *J Immunol.* (2009) 182:4226–36. doi: 10.4049/jimmunol.0800771
3. Weinstein JS, Nacionales DC, Lee PY, Kelly-Scumpia KM, Yan X-J, Scumpia PO, et al. Colocalization of antigen-specific B and T cells within ectopic lymphoid tissue following immunization with exogenous antigen. *J Immunol.* (2008) 181:3259–67. doi: 10.4049/jimmunol.181.5.3259
4. Jones GW, Jones SA. Ectopic lymphoid follicles: inducible centres for generating antigen-specific immune responses within tissues. *Immunol.* (2016) 147:141–51. doi: 10.1111/imm.12554
5. Gulati G, Brunner HI. Environmental triggers in systemic lupus erythematosus. *Sem Arthritis Rheum.* (2017) 47:710–7. doi: 10.1016/j.semarthrit.2017.10.001
6. Parks CG, Miller FW, Pollard KM, Selmi C, Germolec D, Joyce K, et al. Expert panel workshop consensus statement on the role of the environment in the development of autoimmune disease. *Int J Mol Sci.* (2014) 15:14269–97. doi: 10.3390/ijms150814269
7. Anonymous. Occupational exposure to respirable crystalline silica. Final rule. *Fed Regist.* (2016) 81:16285–890. Available online at: https://www.govinfo.gov/content/pkg/FR-2016-03-25/pdf/2016-04800.pdf
8. Parks CG, Cooper GS, Nylander-French LA, Sanderson WT, Dement JM, Cohen PL, et al. Occupational exposure to crystalline silica and risk of systemic lupus erythematosus: a population-based, case–control study in the Southeastern United States. *Arthritis Rheum.* (2002) 46:1840–50. doi: 10.1002/art.10368
9. Vupputuri S, Parks CG, Nylander-French LA, Owen-Smith A, Hogan SL, Sandler DP. Occupational silica exposure and chronic kidney disease. *Ren Fail.* (2012) 34:40–6. doi: 10.3109/0886022X.2011.623496
10. Cooper GS, Parks CG. Occupational and environmental exposures as risk factors for systemic lupus erythematosus. *Curr Rheumatol Rep.* (2004) 6:367–74. doi: 10.1007/s11926-004-0011-6
11. Schleiff PL. Surveillance for silicosis — Michigan and New Jersey, 2003–2011. *MMWR Morb Mortal Wkly Rep.* (2016) 63:73–8. doi: 10.15585/mmwr.mm6355a7
12. Makol A, Reilly MJ, Rosenman KD. Prevalence of connective tissue disease in silicosis (1985-2006)-a report from the state of Michigan surveillance system for silicosis. *Am J Ind Med.* (2011) 54:255–62. doi: 10.1002/ajim.20917
13. Bates MA, Brandenberger C, Langohr I, Kumagai K, Harkema JR, Holian A, et al. Silica triggers inflammation and ectopic lymphoid neogenesis in the lungs in parallel with accelerated onset of systemic autoimmunity and glomerulonephritis in the lupus-prone NZBWF1 mouse. *PLoS ONE.* (2015) 10:e0125481. doi: 10.1371/journal.pone.0125481
14. Bates MA, Brandenberger C, Langohr II, Kumagai K, Lock AL, Harkema JR, et al. Silica-triggered autoimmunity in lupus-prone mice blocked by docosahexaenoic acid consumption. *PLoS ONE.* (2016) 11:e0160622. doi: 10.1371/journal.pone.0160622
15. Bates MA, Akbari P, Gilley KN, Wagner JG, Li N, Kopec AK, et al. Dietary docosahexaenoic acid prevents silica-induced development of pulmonary ectopic germinal centers and glomerulonephritis in the lupus-prone NZBWF1 mouse. *Front Immunol.* (2018) 9:2002. doi: 10.3389/fimmu.2018.02002
16. Mejia-Vilet JM, Parikh SV, Song H, Fadda P, Shapiro JP, Ayoub I, et al. Immune gene expression in kidney biopsies of lupus nephritis patients at diagnosis and at renal flare. *Nephrol Dial Transplant.* (2018). doi: 10.1093/ndt/gfy125. [Epub ahead of print].
17. Tsang HF, Xue VW, Koh SP, Chiu YM, Ng LP, Wong SC. NanoString, a novel digital color-coded barcode technology: current and future applications in molecular diagnostics. *Expert Rev Mol Diagn.* (2017) 17:95–103. doi: 10.1080/14737159.2017.1268533
18. Kulkarni MM. Digital multiplexed gene expression analysis using the NanoString nCounter system. *Cur Prot Mol Biol.* (2011) 25:Unit25B.10. doi: 10.1002/0471142727.mb25b10s94
19. Fassbinder-Orth CA. Methods for quantifying gene expression in ecoimmunology: from qPCR to RNA-Seq. *Int Comp Biol.* (2014) 54:396–406. doi: 10.1093/icb/icu023
20. Prokopec SD, Watson JD, Waggott DM, Smith AB, Wu AH, Okey AB, et al. Systematic evaluation of medium-throughput mRNA abundance platforms. *RNA.* (2013) 19:51–62. doi: 10.1261/rna.034710.112
21. Reis PP, Waldron L, Goswami RS, Xu W, Xuan Y, Perez-Ordonez B, et al. mRNA transcript quantification in archival samples using multiplexed, color-coded probes. *BMC Biotech.* (2011) 11:46. doi: 10.1186/1472-6750-11-46
22. Hulsen T, de Vlieg J, Alkema W. BioVenn - a web application for the comparison and visualization of biological lists using area-proportional Venn diagrams. *BMC Genomics.* (2008) 9:488. doi: 10.1186/1471-2164-9-488
23. Oliveros JC. Venny. *An Interactive Tool for Comparing Lists With Venn's diagrams. (2007-2015)*. Available online at: http://bioinfogp.cnb.csic.es/tools/venny/index.html.
24. Metsalu T, Vilo J. ClustVis: a web tool for visualizing clustering of multivariate data using Principal Component Analysis and heatmap. *Nucleic Acids Res.* (2015) 43:W566–70. doi: 10.1093/nar/gkv468
25. Danaher P, Warren S, Dennis L, D'Amico L, White A, Disis ML, et al. Gene expression markers of tumor infiltrating leukocytes. *J Immunther Cancer.* (2017) 5:18. doi: 10.1186/s40425-017-0215-8
26. Khan MA, Palaniyar N. Transcriptional firing helps to drive NETosis. *Sci Rep.* (2017) 7:41749. doi: 10.1038/srep41749
27. Nakayama M. Macrophage recognition of crystals and nanoparticles. *Front Immunol.* (2018) 9:103. doi: 10.3389/fimmu.2018.00103
28. Warawa J. Evaluation of surrogate animal models of melioidosis. *Front Microbiol.* (2010) 1:141. doi: 10.3389/fmicb.2010.00141
29. Lacher SE, Johnson C, Jessop F, Holian A, Migliaccio CT. Murine pulmonary inflammation model: a comparative study of anesthesia and instillation methods. *Inhal Toxicol.* (2010) 22:77–83. doi: 10.3109/08958370902929969
30. Absher MP, Hemenway DR, Leslie KO, Trombley L, Vacek P. Intrathoracic distribution and transport of aerosolized silica in the rat. *Exp Lung Res.* (1992) 18:743–57. doi: 10.3109/01902149209031705
31. Vacek PM, Hemenway DR, Absher MP, Goodwin GD. The translocation of inhaled silicon dioxide: an empirically derived compartmental model. *Fund Appl Toxicol.* (1991) 17:614–26. doi: 10.1016/0272-0590(91)90211-L

32. Korkmaz B, Horwitz MS, Jenne DE, Gauthier F. Neutrophil elastase, proteinase 3, and cathepsin G as therapeutic targets in human diseases. *Pharmacol Rev.* (2010) 62:726–59. doi: 10.1124/pr.110.002733
33. Kruger P, Saffarzadeh M, Weber ANR, Rieber N, Radsak M, Bernuth Hv, et al. Neutrophils: between host defence, immune modulation, and tissue injury. *PLoS Path.* (2015) 11:e1004651. doi: 10.1371/journal.ppat.1004651
34. Anderson BO, Brown JM, Harken AH. Mechanisms of neutrophil-mediated tissue injury. *J Surg Res.* (1991) 51:170–9. doi: 10.1016/0022-4804(91)90090-9
35. Yu Y, Su K. Neutrophil extracellular traps and systemic lupus erythematosus. *J Clin Cell Immunol.* (2013) 4:139. doi: 10.4172/2155-9899.1000139
36. Bauer JW, Petri M, Batliwalla FM, Koeuth T, Wilson J, Slattery C, et al. Interferon-regulated chemokines as biomarkers of systemic lupus erythematosus disease activity: a validation study. *Arthritis Rheum.* (2009) 60:3098–107. doi: 10.1002/art.24803
37. El-Shehaby A, Darweesh H, El-Khatib M, Momtaz M, Marzouk S, El-Shaarawy N, et al. Correlations of urinary biomarkers, TNF-like weak inducer of apoptosis (TWEAK), osteoprotegerin (OPG), monocyte chemoattractant protein-1 (MCP-1), and IL-8 with lupus nephritis. *J Clin Immunol.* (2011) 31:848–56. doi: 10.1007/s10875-011-9555-1
38. Vermi W, Lonardi S, Bosisio D, Uguccioni M, Danelon G, Pileri S, et al. Identification of CXCL13 as a new marker for follicular dendritic cell sarcoma. *J Pathol.* (2008) 216:356–64. doi: 10.1002/path.2420
39. Chtanova T, Tangye SG, Newton R, Frank N, Hodge MR, Rolph MS, et al. T follicular helper cells express a distinctive transcriptional profile, reflecting their role as non-Th1/Th2 effector cells that provide help for B cells. *J Immunol.* (2004) 173:68–78. doi: 10.4049/jimmunol.173.1.68
40. Gu-Trantien C, Migliori E, Buisseret L, de Wind A, Brohée S, Garaud S, et al. CXCL13-producing TFH cells link immune suppression and adaptive memory in human breast cancer. *JCI Insight*. 2:91487. doi: 10.1172/jci.insight.91487
41. Takagi R, Higashi T, Hashimoto K, Nakano K, Mizuno Y, Okazaki Y, et al. B cell chemoattractant CXCL13 is preferentially expressed by human Th17 cell clones. *J Immunol.* (2008) 181:186–9. doi: 10.4049/jimmunol.181.1.186
42. Klimatcheva E, Pandina T, Reilly C, Torno S, Bussler H, Scrivens M, et al. CXCL13 antibody for the treatment of autoimmune disorders. *BMC Immunol.* (2015) 16:6. doi: 10.1186/s12865-015-0068-1
43. Ohl K, Tenbrock K. Regulatory T cells in systemic lupus erythematosus. *Eur J Immunol.* (2015) 45:344–55. doi: 10.1002/eji.201344280
44. McKinney EF, Lee JC, Jayne DR, Lyons PA, Smith KG. T-cell exhaustion, co-stimulation and clinical outcome in autoimmunity and infection. *Nature.* (2015) 523:612–6. doi: 10.1038/nature14468
45. Baechler EC, Batliwalla FM, Karypis G, Gaffney PM, Ortmann WA, Espe KJ, et al. Interferon-inducible gene expression signature in peripheral blood cells of patients with severe lupus. *Proc Natl Acad Sci USA.* (2003) 100:2610–5. doi: 10.1073/pnas.0337679100
46. Bezalel S, Guri KM, Elbirt D, Asher I, Sthoeger ZM. Type I interferon signature in systemic lupus erythematosus. *Israel Med Assoc J.* (2014) 16:246–9. Available online at: https://www.ima.org.il/FilesUpload/IMAJ/0/77/38682.pdf
47. Li Q-Z, Zhou J, Lian Y, Zhang B, Branch VK, Carr-Johnson F, et al. Interferon signature gene expression is correlated with autoantibody profiles in patients with incomplete lupus syndromes. *Clin Exp Immunol.* (2010) 159:281–91. doi: 10.1111/j.1365-2249.2009.04057.x
48. Crow MK. Type I interferon in the pathogenesis of lupus. *J Immunol.* (2014) 192:5459–68. doi: 10.4049/jimmunol.1002795
49. Honda K, Yanai H, Negishi H, Asagiri M, Sato M, Mizutani T, et al. IRF-7 is the master regulator of type-I interferon-dependent immune responses. *Nature.* (2005) 434:772–7. doi: 10.1038/nature03464
50. Kim J-M, Park S-H, Kim H-Y, Kwok S-K. A plasmacytoid dendritic cells-type I interferon axis is critically implicated in the pathogenesis of systemic lupus erythematosus. *Int J Molec Sci.* (2015) 16:14158–70. doi: 10.3390/ijms160614158
51. Nacionales DC, Kelly KM, Lee PY, Zhuang H, Li Y, Weinstein JS, et al. Type I interferon production by tertiary lymphoid tissue developing in response to 2,6,10,14-tetramethyl-pentadecane (pristane). *Am J Pathol.* (2006) 168:1227–40. doi: 10.2353/ajpath.2006.050125
52. Liu Z, Bethunaickan R, Huang W, Lodhi U, Solano I, Madaio MP, et al. Interferon alpha accelerates murine SLE in a T cell dependent manner. *Arthr Rheum.* (2011) 63:219–29. doi: 10.1002/art.30087
53. Mathian A, Weinberg A, Gallegos M, Banchereau J, Koutouzov S. IFN-alpha induces early lethal lupus in preautoimmune (New Zealand Black x New Zealand White) F1 but not in BALB/c mice. *J Immunol.* (2005) 174:2499–506. doi: 10.4049/jimmunol.174.5.2499
54. Liu Z, Bethunaickan R, Huang W, Ramanujam M, Madaio MP, Davidson A. IFNα confers resistance of SLE nephritis to therapy in NZB/WF1 mice. *J Immunol.* (2011) 187:1506–13. doi: 10.4049/jimmunol.1004142
55. Munroe ME, Lu R, Zhao YD, Fife DA, Robertson JM, Guthridge JM, et al. Altered type II interferon precedes autoantibody accrual and elevated type I interferon activity prior to systemic lupus erythematosus classification. *Ann Rheum Dis.* (2016) 75:2014–21. doi: 10.1136/annrheumdis-2015-208140
56. Jackson SW, Jacobs HM, Arkatkar T, Dam EM, Scharping NE, Kolhatkar NS, et al. B cell IFN-γ receptor signaling promotes autoimmune germinal centers via cell-intrinsic induction of BCL-6. *J Exp Med.* (2016) 213:733–50. doi: 10.1084/jem.20151724
57. Pollard KM, Cauvi DM, Toomey CB, Morris KV, Kono DH. Interferon-γ and systemic autoimmunity. *Discovery Med.* (2013) 16:123–31.
58. Schoenborn JR, Wilson CB. Regulation of interferon-gamma during innate and adaptive immune responses. *Adv Immunol.* (2007) 96:41–101. doi: 10.1016/S0065-2776(07)96002-2
59. Jacob CO, van der Meide PH, McDevitt HO. *In vivo* treatment of (NZB X NZW)F1 lupus-like nephritis with monoclonal antibody to gamma interferon. *J Exp Med.* (1987) 166:798–803. doi: 10.1084/jem.166.3.798
60. Sayan M, Mossman BT. The NLRP3 inflammasome in pathogenic particle and fibre-associated lung inflammation and diseases. *Part Fibre Toxicol.* (2016) 13:15. doi: 10.1186/s12989-016-0162-4
61. Kahlenberg JM, Kaplan MJ. The inflammasome and lupus: another innate immune mechanism contributing to disease pathogenesis? *Cur Opin Rheum.* (2014) 26:475–81. doi: 10.1097/BOR.0000000000000088
62. Jang E, Cho S-H, Park H, Paik D-J, Kim JM, Youn J. A positive feedback loop of IL-21 signaling provoked by homeostatic CD4+CD25– T cell expansion is essential for the development of arthritis in autoimmune K/BxN mice. *J Immunol.* (2009) 182:4649–56. doi: 10.4049/jimmunol.0804350
63. Matsumoto M, Fu YX, Molina H, Chaplin DD. Lymphotoxin-alpha-deficient and TNF receptor-I-deficient mice define developmental and functional characteristics of germinal centers. *Immun Rev.* (1997) 156:137–44. doi: 10.1111/j.1600-065X.1997.tb00965.x
64. Dougall WC, Glaccum M, Charrier K, Rohrbach K, Brasel K, De Smedt T, et al. RANK is essential for osteoclast and lymph node development. *Genes Dev.* (1999) 13:2412–24. doi: 10.1101/gad.13.18.2412
65. Herber D, Brown TP, Liang S, Young DA, Collins M, Dunussi-Joannopoulos K. IL-21 has a pathogenic role in a lupus-prone mouse model and its blockade with IL-21R.Fc reduces disease progression. *J Immunol.* (2007) 178:3822–30. doi: 10.4049/jimmunol.178.6.3822
66. Young DA, Hegen M, Ma HLM, Whitters MJ, Albert LM, Lowe L, et al. Blockade of the interleukin-21/interleukin-21 receptor pathway ameliorates disease in animal models of rheumatoid arthritis. *Arthr Rheum.* (2007) 56:1152–63. doi: 10.1002/art.22452
67. Sabry A, Sheashaa H, El-Husseini A, El-Dahshan K, Abdel-Rahim M, Elbasyouni SR. Intercellular adhesion molecules in systemic lupus erythematosus patients with lupus nephritis. *Clin Rheumatol.* (2007) 26:1819–23. doi: 10.1007/s10067-007-0580-7
68. Daniel L, Sichez H, Giorgi R, Dussol B, Figarella-Branger D, Pellissier JF, et al. Tubular lesions and tubular cell adhesion molecules for the prognosis of lupus nephritis. *Kidney Int.* (2001) 60:2215–21. doi: 10.1046/j.1523-1755.2001.00055.x
69. Hauser IA, Riess R, Hausknecht B, Thüringer H, Sterzel RB. Expression of cell adhesion molecules in primary renal disease and renal allograft rejection. *Nephrol Dial Transplant.* (1997) 12:1122–31. doi: 10.1093/ndt/12.6.1122

Conflict of Interest Statement: The authors declare that the research was conducted in the absence of any commercial or financial relationships that could be construed as a potential conflict of interest.

frontiers in Immunology

REVIEW
published: 10 July 2019
doi: 10.3389/fimmu.2019.01609

Environmental Triggers of Autoreactive Responses: Induction of Antiphospholipid Antibody Formation

Anush Martirosyan[1,2], *Rustam Aminov*[3]* and *Gayane Manukyan*[1,2]*

[1] Laboratory of Molecular and Cellular Immunology, Institute of Molecular Biology, Yerevan, Armenia, [2] Russian-Armenian (Slavonic) University, Yerevan, Armenia, [3] School of Medicine, Medical Sciences and Nutrition, University of Aberdeen, Aberdeen, United Kingdom

Antiphospholipid antibodies (aPLs) comprise a diverse family of autoantibodies targeted against proteins with the affinity toward negatively charged phospholipids or protein-phospholipid complexes. Their clinical significance, including prothrombotic potential of anti-cardiolipin antibodies (aCLs), anti-β2-glycoprotein I antibodies (aβ2-GPIs), and lupus anti-coagulant (LA), is well-established. However, the ontogeny of these pathogenic aPLs remains less clear. While transient appearance of aPLs could be induced by various environmental factors, in genetically predisposed individuals these factors may eventually lead to the development of the antiphospholipid syndrome (APS). Since the first description of APS, it has been found that a wide variety of microbial and viral agents influence aPLs production and contribute to clinical manifestations of APS. Many theories attempted to explain the pathogenic potential of different environmental factors as well as a phenomenon termed molecular mimicry between β2-GPI molecule and infection-relevant structures. In this review, we summarize and critically assess the pathogenic and non-pathogenic formation of aPLs and its contribution to the development of APS.

Keywords: antiphospholipid antibodies, antiphospholipid syndrome, bacteria, viruses, vaccination, drugs

OPEN ACCESS

Edited by:
Kenneth Michael Pollard, The Scripps Research Institute, United States

Reviewed by:
Howard A. Young, National Cancer Institute at Frederick, United States
Laura Andreoli, University of Brescia, Italy

***Correspondence:**
Rustam Aminov
rustam.aminov@gmail.com
Gayane Manukyan
gaya.manukyan@gmail.com; g_manukyan@mb.sci.am

Specialty section:
This article was submitted to Autoimmune and Autoinflammatory Disorders, a section of the journal Frontiers in Immunology

Received: *28 March 2019*
Accepted: *27 June 2019*
Published: *10 July 2019*

Citation:
Martirosyan A, Aminov R and Manukyan G (2019) Environmental Triggers of Autoreactive Responses: Induction of Antiphospholipid Antibody Formation. Front. Immunol. 10:1609. doi: 10.3389/fimmu.2019.01609

INTRODUCTION

Antiphospholipid antibodies (aPL) comprise a diverse family of heterogeneous autoantibodies targeting proteins with the affinity toward negatively charged phospholipids or protein-phospholipid complexes. aPLs are increasingly being recognized as causative factors of antiphopholipid syndrome (APS) manifestations. Syndrome is defined by persistent aPL positivity accompanied by thromboembolic events and/or obstetrical complications (1).

While a broad spectrum of aPL exists, the presence of anti-β2 glycoprotein I (anti-β2GPI) antibodies, anticardiolipin (aCL), and lupus anticoagulant (LA) is accepted as independent risk factors for the episodes of vascular thrombosis and pregnancy loss in APS (2, 3). aPL are responsible for the alterations in the mechanisms of coagulation and fibrinolysis, leading to a proinflammatory, or hypercoagulable state. Beyond the heterogeneity of different aPL, it is widely accepted that they represent a bulk of natural antibodies (mainly IgG and IgM classes) with low affinity, generated for the most part by B1 cells (4). Pathogenic role of aPL was shown in animal studies (5, 6). In mice, the passive transfer of aPL produced features resembling human APS, that is, fetal loss and thrombotic events (7). Another evidence for the pathogenicity of autoantibodies was obtained in studies proving a substantial clinical improvement after the removal of autoantibodies by plasma exchange or plasmapheresis (8). Mechanistically, we demonstrated

the restoration of monocyte transcriptional activity in patients with APS after plasmapheresis (9).

The presence of aPL is not necessarily associated with the primary APS; they could be detected in a variety of clinical conditions, including different autoimmune diseases, infections, neoplasms, after vaccination or drug use, etc., and could also be transiently expressed in healthy individuals (3). In autoimmune disorders, aPL are mainly cofactor dependent and require the presence of phospholipid-binding proteins, such as β2GPI and prothrombin, which are their main targets, while aPL generated after infections are largely cofactor independent (10).

Based on the currently available clinical and experimental evidence, it is likely that in predisposed individuals, different environmental triggers may eventually lead to the production of aPL, which then can lead to the development of APS. Several theories tried to explain the pathogenic potential of different environmental factors as well as a phenomenon termed molecular mimicry between β2GPI molecule and infection-relevant structures. This review summarizes current findings on the origin and mechanisms of production of APS-associated antibodies and compiles the recent advances toward understanding the functional relevance of aPL to the development of APS.

VIRUSES

Among a wide range of infectious agents, which may contribute to the increase of aPL, human immunodeficiency virus (HIV) and hepatitis C virus (HCV) are among the most frequently reported. HIV infection, association of which with aCL antibodies has been first reported more than 30 years ago (11), currently remains the most frequent infectious cause for aPL production in adult and pediatric patients. A considerable diversity of aPL can be detected in HIV-infected individuals, including aCL, anti-β2GPI, LA, aPT, aPS, aPI, and aPC (12, 13). The aCL antibodies during HIV infection could be of both pathogenic type (β2GPI cofactor dependent) and post-infectious type (non-β2GPI dependent). The estimated incidence of IgG aCL among HIV-positive individuals is in the range of 7–94% (mean 46.5%) compared to 1.98% in control subjects (13). IgM aCL are less common and their clinical significance remains controversial (14). Both positive (15) and negative (14) associations between aCL and thromboembolic phenomena in patients were reported, although aPL-related clinical features are generally uncommon in HIV patients (16). The latter may be explained by the ability of β2GPI to inhibit the interaction between HIV-specific IgG aPL antibodies and CL, which was demonstrated in the competition study designed to delineate the true autoimmune and non-pathogenic aPL (17). Further assessment of the binding specificity and avidity of aPL antibodies in HIV showed low antibody avidity (18). Except for a low incidence of anti-β2GPI, the prevalence of aCL, aPS, aPI, and aPC antibodies in HIV-1 infection was comparable to that found in APS, indicating the tendency to recognize various phospholipids other than β2GPI (18). It is likely that the relatively low levels of anti-β2GPI and cofactor-independent nature of HIV-specific aPL, compared to the autoimmune one, accounts for the rare incidence of APS among HIV-positive individuals. The frequency and complications of LA may vary considerably among HIV-infected patients. Reported incidences are in the range of 0–72% (19), but the pathogenic association with thrombosis is somewhat exceptional (15).

Similarly to HIV, aCL antibodies are the most common type of aPL in HCV infection. A high prevalence of aCL in HCV patients compared to healthy controls has been reported (18.6% vs. 1.78%) (13). aCL from these patients showed no β2GPI dependency, and association with the thromboembolic events was weak (15). An earlier study demonstrated that aCL due to HCV exhibit features of natural polyspecific autoantibodies, suggesting their non-pathogenic nature (20). High incidence of LA presumably predispose the occurrence of thrombotic complications in a small subset of HCV-positive APS patients, since in an unselected cohort of HCV-infected individuals the presence of LA is a rare event (21). Albeit other hepatitis viruses were less intensively studied in term of aPL, occurrence of aCL in both HBV and HDV infection have been suggested to interfere with thrombotic incidence in patients with hepatitis-related hepatocellular carcinoma (22).

High frequency of HIV- and HCV-induced aPL in terms of a possible association with APS is highly attractive but also controversial. Analyses of the spectrum of clinical features related to APS (peripheral thrombosis, valvular heart disease, nephropathy, etc.) in patients with chronic HIV/HCV infections suggested that while in individual cases these infections may lead to the development of a true APS, in most cases the presence of aPL and relevant clinical manifestation might merely represent an epiphenomenon secondary to the chronic immune stimulation by the virus (21). In several documented cases, thrombotic episodes in HIV, or HCV-infected patients were linked to extrinsic causes (antiretroviral treatment and opportunistic infections), suggesting a limited role of aPL in these events (12). Analogously, HIV-associated vascular damage, endothelial dysfunction and pulmonary embolism may well mimic clinical presentation of APS. In the case of HCV, immunological markers of chronic infection such as ANA, cryoglobulins, hypocomplementemia, and rheumatoid factor may potentially contribute to the development of symptomatic features resembling APS.

In the light of remarkable similarities in the clinical manifestations of patients with parvovirus B19 infection, autoimmune systemic lupus erythematosus (SLE), and/or APS such as thrombosis, hemolytic anemia, spontaneous abortion, livedo reticularis, and arthritis, B19 infection is considered as an initial trigger for autoimmune processes (23). Development of pathogenic aPL has been often reported as being associated with this infection. In particular, over a quarter of children with rheumatic diseases were found to be positive for aPL and also had B19 parvovirus infection, presently or in the past (24). The most notable characteristic of aPL, detected in patients infected with parvovirus B19, is the enhanced antigen-binding ability in the presence of β2GPI as a cofactor (25). Antibodies present in the serum of B19-infected patients are predominantly of the IgG isotype, they are specific toward the negatively charged phospholipids, aCL and phosphatidyl serine (aPS) and, on rare occasions, to the neutral phospholipid phosphatidyl ethanolamine (aPE). Based on these observations,

it has been suggested that the nature of B19-induced aPL is markedly different from the antibodies generated in response to other viral infections. Their binding ability, isotype distribution, and cofactor dependence resemble those present in patients with autoimmune diseases, pointing to the potential role of B19 in triggering autoimmune events (25). To our knowledge, there have been at least two reported cases of thrombotic events associated with parvovirus B19 infection: a male patient who developed splenic infarction and a female patient with multiple pulmonary emboli (26, 27). Both cases were characterized by the transient presence of aPL antibodies of IgM or IgG isotypes. Mechanisms responsible for the aPL production during B19 infection are: cross-reactivity between anti-B19 IgG antibodies with multiple human autoantigens (cardiolipin, collagen II, keratin, angiotensin II type 1 receptor, and platelet membrane glycoprotein IIb/IIIa), presentation of apoptosis-associated self-antigens by infected cells (23), and phospholipase-A2-like activity observed in the VP1 unique region of the structural protein VP1 (24).

Viral agents that are less frequently reported as provoking a transient or permanent rise of aPL include the human herpesviruses such as cytomegalovirus (CMV), varicella-zoster virus (VZV), and Epstein-Barr virus (EBV) (28). They are common viral pathogens with the estimated seroprevalence among adult population >90% (29). These three viruses have been implicated in the presence of aPL and aPL-related clinical manifestations. An intriguing association between infection and aPL was revealed in pregnant women who underwent routine prenatal screening for toxoplasmosis, rubella, cytomegalovirus, and herpes simplex virus (TORCH panel). Substantial proportion of healthy pregnant women (52.2%) with false-positive TORCH appeared to be aPL positive (30). Another study has summarized the findings on thrombosis associated with CMV infection: among 97 patients who developed CMV-induced thrombosis 14 had transient or permanent APS (31). aPL-independent mechanisms responsible for CMV-triggered procoaguable state include activation of coagulation factors and platelets, adhesion of leukocytes as a sequel to the direct vascular endothelial damage by the virus (32), generation of thrombin or factor VIII, and/or down-regulation of physiological anticoagulant mechanisms (33). Another cross-sectional study, with 95 children enrolled, showed a transient increase of LA and aCL in 43 children following varicella infection (34). Moreover, a direct pathogenic role of VZV-induced transient increase of IgM/IgG aCL, IgM anti-b2GPI, or LA in the development of hypercoaguable state was suggested for a number of pediatric and adult cases with thrombotic or vascular complications (35–37). Exposure to EBV was associated with a lupus phenotype and promoted autoimmune processes (38). The main type of aPL detected in EBV infection was aCL IgG (39). In favor of pathogenic nature of aPL is the case described in the report by Delbos et al., who described CMV-induced thrombosis in a previously healthy woman with a pulmonary embolism in the presence of aPL (40).

Adenovirus infection is also associated with a significant increase of aCL. aCL-specific IgG and IgM classes were found in a half of children with respiratory disease caused by adenoviral infection (41). Transitory increase of LA, aCL, and antiphosphatidylserine-dependent antithrombin antibodies (aPS/PT) was observed in a 9-year-old girl following acute gastroenteritis (due to adenovirus) and pneumonia (due *Mycoplasma pneumoniae*) (42). Herpes simplex virus, dengue virus, human herpes virus 6, rubella, measles, chicken pox, and mumps infections are usually accompanied by a relatively low level of autoantibodies, which are often declined after the elimination of infection and are not associated with thrombosis incidences (28).

Initial encounter between a virus and a target cell occurs at the plasma membrane interface. Negatively charged phospholipids, along with low-density lipoprotein receptors and gangliosides, have been shown to play a role in the entry of numerous viruses (43). Most enveloped viruses, including retroviruses, acquire their lipid envelope by budding through the cellular membrane. For example, HIV uses phosphatidylserine (PS) as a cofactor for infection and acquires this phospholipid from lipid rafts during budding (44). A comprehensive survey of total lipid composition of retroviral envelopes revealed a considerable resemblance with that of the plasma membrane, unless they were highly enriched in specific negatively charged phosphoinositides, PIP and PIP2, which are phosphorylated derivatives of phosphatidylinositol (45). Additionally, viruses use the host lipids in the later stages of infection to promote intracellular trafficking, replication, viral assembly, and egress. RNA and DNA viruses that replicate in the cytosol tend to entail membranes of specific cellular compartments (e.g., endoplasmic reticulum, mitochondria, endosomes, lysosomes, or Golgi bodies) (46). Despite that the mitochondrial disturbances are prevalent among HIV-infected individuals, interaction of the virus with host mitochondrial CL has not been tested yet. However, demonstration of *in vitro* CL cross-reactivity with HIV–specific neutralizing antibodies (47) has inspired researchers to analyze the correlation between the occurrence of HIV-specific aCL and viral parameters. It was shown that aCL, detected in HIV patients, are strongly and independently associated with the level of virus replication, regardless of the disease stage (48). In another case report, initially high titers of aCL and anti-β2GPI in a HIV-positive man were shown to progressively decrease, in parallel with a viral load (49).

It seems that entangled and interactive relationships between the viral infection and the host immune system mediate diversity of aPL responses and related manifestations. Despite the mounting evidence supporting the contribution of infection agents to production of autoantibodies, aPL-related complications in the context of viral infection are rare. Thus, the development of true APS is exceptional, excluding the cases when autoimmunity is present prior infection. In this context, the assessment of β2GPI dependence could be helpful in differentiating the pathogenic autoimmune aPL from post-infectious one.

BACTERIA

It is a widely accepted view that pathogenesis of many autoimmune diseases is largely driven by inappropriate or inadequate immune responses toward bacterial agents (50, 51).

Similarly, a number of Gram-positive and Gram-negative bacteria are recognized as being linked to aPL production. Despite this, transitory increase of bacteria-induced aPL autoantibodies was only occasionally associated with thrombotic events (52).

M. pneumoniae and *Streptococcus* spp. infections, which are among the most prevalent bacterial infections in children and young adults, were linked to the occurrence of aPL. A significant increase in aCLof IgM and IgG classes was found in patients with *M. pneumoniae*, especially in those with severe infection or with cold hemagglutinins (53). Almost a half of patients with poststreptococcal glomerulonephritis were positive for aCL, with a long-term persistence of the antibodies in the majority of patients, but with no thromboembolic events (54). A case of childhood-onset autoimmune APS and several pediatric cases of aPL-related thromboembolic complications at various anatomical sites were all attributed to the pulmonary *M. pneumonia* infection (55–57). Two independent studies reported splenic infarctions secondary to aPL positivity due to *M. pneumoniae* or *Staphylococcus* spp. infection (58, 59).

Another evidence for aPL-mediated thrombosis as a consequence of microbial infection has been recently described in Lemierre syndrome (60). This a rare and potentially life-threatening condition characterized by thrombophlebitis of the internal jugular vein and pulmonary embolism (61). The syndrome is classically associated with an anaerobic bacterium *Fusobacterium necrophorum*, although a variety of other bacteria such as streptococci, staphylococci, and enterococci may be also responsible for the disease (61).

Examination of serum samples from leprosy patients demonstrated the presence of LA and aPT, with the prevalence of anti-β2GPI (62, 63), as well as the heterogeneity of aCL in regards to co-factor dependency (64). Some authors have suggested similarities between the leprosy-mediatedaPL with those found in patients with autoimmune diseases (65). Nevertheless, leprosy-specific aPL are infrequently associated with the thrombotic features. Several exceptional cases of microvascular thromboses, related to β2GPI-dependent aCL, were documented in patients who developed a rare Lucio's phenomenon on a background of diffuse lepromatous leprosy (66).

Although somewhat controversial, syphilis infection has also been associated with the production of aPL. The reported prevalence of syphilis-related aCL is wide-ranging, varying from 8 to 67%, which may be attributed to their cross-reactivity with treponemal cardiolipins (13). Nevertheless, the presence of anti-β2GPIand LA and thrombotic episodes are uncommon in this infection (13).

The pathogenic potential of aPL found in patients infected by *Mycobacterium tuberculosis*is contentious. Poly-reactive B1 cells were shown as the main source of non-specific anti-phospholipid IgM antibody produced in response to *M. tuberculosis* lipids which suggests non-pathogenic nature of these aPL (67). In support of this assertion no association of aPL levels with thrombotic events was reported. The increased levels of aCL-specific IgM and IgG isotypes were found in several population-based cohort studies (68–70). Elkayam et al. (71) were first to reveal the elevated level of anti-β2GPI in a substantial proportion of tuberculosis patients, which is declined following TB therapy (71). Similarly, the normalization of IgM class of aCL, antiphosphatidyl inositol (aPI), antiphosphatidyl ethanolamine (aPE), antiphosphatidyl choline (aPTC), and antisphingolipid (aSL) antibodies in the sera of tuberculosis patients following TB therapy was reported (72).

Presently it is widely accepted that infection by *Helicobacter pylori* is the most common cause of chronic gastritis (73). Both the pathogenic and protective roles for this infection in different autoimmune diseases were suggested (74). A first large-cohort study has been performed to estimate the prevalence of anti-*H. pylori* (anti-HP) antibodies in 1,290 patients diagnosed with 14 different autoimmune diseases, including 157 primary and secondary APS patients, and 385 matching healthy controls (75). All subjects were screened for the presence aPL. The study uncovered the highest frequency of anti-HP IgG and significantly elevated levels of aCL IgM among the patients with primary APS (75). Another study demonstrated a causal relationship between *H. pylori* infection and aCL of all isotypes IgA/IgM/IgG in 84 children, with a decline of autoantibody titers following eradication of *H. pylori* (76).

YEASTS AND FUNGI

The role of yeasts and fungi in APS has not gained too much attention and thus the cases of fungal-induced aPL are very rare in the literature (28). Recent findings have raised wariness regarding a pathogenic potential of food products prepared with the use of *Saccharomyces cerevisiae*, known as Brewer's and Baker's yeast (77). Anti-*S. cerevisiae* antibodies (ASCAs), directed against the phosphopeptidomannan, have been demonstrated to be prevalent among aPL-positive autoimmune patients, including those with Crohn's disease (78), SLE (79), RA (80), and APS (81). The presence of cross-reactive epitopes on β2GPI and *S. cerevisiae* (77, 81) and the fact that ASCAs tend to appear years before the fully developed autoimmune conditions (82) point to a possible pathogenic significance of ASCAs in APS.

COMMENSAL MICROBIOTA

Besides directly affecting the host, diet may exert indirect influence via modulating the composition and function of the gut microbial communities. Ingestion of probiotics, for instance, is considered to be beneficial for modulation and/or restoration of the gut microbiota, and it is capable of altering the course of autoimmune diseases and APS. For example, consumption of probiotic fermented milk products in β2GPI-immunized Balb/c mice resulted in a decline of serum anti-β2GPI titers and in the shift from Th2 type immune response toward Th1 (83). Based on above-mentioned observations, a role for commensal bacteria was hypothesized (84). Indeed, a report by Aguiar and coworkers has shown a specific change in the gut microbial composition in APS patients. Particularly, a decrease of bacteria belonging to the genus *Bilophila* and overgrowth of bacteria of the *Slackia* genus were shown

(85). Moreover, anti-domain I (DI) β2GPI IgG positivity in APS patients correlated significantly with the enrichment by *Slackia* spp. and by the lower abundance of butyrate-producing *Butyricimonas* (85). Reduction in microbe-derived butyrate, which has an anti-inflammatory and immunomodulatory activity (86), may enable a stronger T-cell proliferative response against β2GPI. Antigen-specific response toward gut microbiota was proven by the administration of broad-spectrum antibiotics in APS-prone (NZWxBXSB)F1 mice, which diminished the proliferation of β2GPI-reactive T cells but not of anti-CD3 (87). These microbiota-depleted animals showed a higher survival rate due to the prevention of thrombotic events and suppression of serum anti-β2GPI IgG titers. In further developments, a specific Gram-positive candidate bacterium, involved in immune cross-reactivity, has been identified based on *in silico* analysis. Common colonic butyrate-producing *Roseburia intestinalis* shared a high degree of sequence homology with both the major B and T cell epitopes to β2GPI (84). The evidences of the involvement of commensal microbiota in aPL production are sporadic and mainly published as preliminary results which does not allow us to fully estimate their contribution. Need to reiterate here though that under the normal conditions the epitopes of commensal bacteria are not usually exposed to the adaptive arm of the immune system. Response to the epitopes of commensal microbiota may appear only if the epithelial barrier function is compromised thus allowing elevated translocation of bacteria and the exposure of epitomes that are usually not encountered under the normal circumstances.

Commensal bacteria may act in several ways to modulate immune reactions. Initiation of an autoimmune reaction by gut commensals is likely to engage the mechanisms similar to that of pathogenic microbiota. Among the different potential scenarios, cross-reactivity triggered by commensal cardiolipin seems to be most intriguing. Cardiolipin is an ancient phospholipid universally found in energy transducing membranes of both prokaryotes and eukaryotes, albeit at different locations (88). In eukaryotes CL is found almost exclusively in mitochondria, while bacterial CL is found in the plasma membranes (89), which reflects the endosymbiotic origin of mitochondria. Given the fact that human CL is normally sequestered from the immune system but the aCL antibodies are broadly prevalent among infected/autoimmune patients, bacterial CL could be considered as a potential damage-associated molecular pattern (DAMP). Thus, it is reasonable to assume that CL-containing bacteria, among which Gram-positives are especially enriched with CL (90), can act as a source of persistent cross-reactive antigens in a genetically susceptible host with a compromised self-tolerance. Spectroscopic analysis has demonstrated a conformational change in β2GPI upon binding to CL, resulting in generation of highly immunogenic epitopes within β2GPI capable of mounting an autoimmune response (91). Therefore, it could be assumed that the initial pathology, which exposes the normally sequestered endogenous and bacterial CLs, may then lead to the recognition by the DAMP receptors and generation of different aPL subpopulations in respect to cofactor dependency.

VACCINES

Increased medical and public interest toward the safety of vaccination has been heightened following several reports of possible post-vaccination complications involving autoimmune reactions. Causal relationship between several vaccines and autoimmune responses has been reported in numerous studies, among which influenza vaccination is the most frequently reported in the context of aPL generation.

In two pediatric case reports a transient appearance of aPL following inactivated influenza vaccination was demonstrated. A 5-year-old boy and 5-year-old girl were both diagnosed with Henoch-Schönlein purpura (HSP), with the presence of aPL antibodies (92, 93). The involvement of bacterial and viral infections was excluded based on laboratory analyses. The girl presented with a palpable purpuric rash and severe abdominal pain about 12 days after immunization (93). Two months later, her blood was negative for aCL or LA. After 4 months, second immunological examination revealed elevated IgG aCL antibodies. Similar symptoms, accompanied by elevated anti-influenza A/H3N2 antibody, were presented in the boy on the second day after vaccination. Initial palpable purpura, abdominal and ankle pain was successfully improved after a month of oral corticosteroid therapy. Levels of aCL IgG antibody declined within a month, and LA disappeared 2 months after hospital discharge (92).

An association between influenza immunization and systemic autoimmune features was studied in 24 female patients with SLE (94). Six weeks after the vaccine administration, high titers of antibodies reacting with Sm, Sm/RNP, Ro, and La antigens were found, with a reduction in titers after 12 weeks follow-up. Another study of post-vaccination events in SLE patients, with and without former aPL positivity, revealed some mild clinical side-effects and increased levels of anti-β2GPI antibodies of IgG and IgM isotypes after repeated annual influenza vaccination (95). The findings suggested that in clinically stable SLE influenza vaccination may increase the risk of thrombotic manifestations (95). Kinetics of aCL, anti-β2GPI, LA, anti-ENA, and ANA autoantibodies, induced by seasonal influenza vaccination, was analyzed in a large group of healthy adults (96). Increased levels of autoantibodies were found in 15% of participants 1 month after the immunization (96). Six months later, increased levels of autoantibodies remained in 13% of participants suggesting potential long-term effects of influenza vaccination including the risk of thrombotic manifestations.

Although several reports suggested induction of aPL following seasonal and pandemic influenza vaccination, examination of the literature in this field revealed conflicting reports. Vista et al. (97) investigated a large cohort ($n = 101$) of SLE patients and matching controls ($n = 101$) at baseline and 2, 6, and 12 weeks after receiving seasonal influenza vaccination. The study showed a post-vaccination increase of aCL but without the increased onset of β2GPI (97). Another study, which employed a large panel of autoantibodies for screening, investigated 45 primary APS patients and 33 healthy controls after A/H1N1 non-adjuvant vaccine administration. In contrary to the previous study, they failed to find short- or long-term sequelae involving a significant

increase of aPL-related antibodies and thrombosis, suggesting that influenza vaccine, at least without adjuvant, is safe (98).

Several case reports raised concerns over a possible association between the vaccine-induced transitory autoimmune responses and the onset of neurological symptoms. An acute confusion state accompanied by severe headache, a middle cerebral artery occlusion, vasculitis, and thrombocytopenia were developed in a 55-years old woman, soon after receiving an influenza vaccine (99). This patient was diagnosed with SLE and secondary APS based on clinical findings and positive for anti-dsDNA, ANA, IgG aCL, and LA. Other two cases of elevated serum IgG anti-phosphatidylcholine antibodies were described in two female pediatric patients with a sudden onset of bilateral optic neuritis due to the administration of trivalent inactivated influenza vaccine (100).

There are only few indications of a possible effect of other types of vaccines on induction of aPL autoantibodies. Fluctuations of aCL, LA, and anti-β2GPI were seen in the minority of participants (n = 8/85) after a month following hepatitis B vaccination, with a decline of post-vaccination titers 5 months later (101). Manifestation of definitive APS was proven in a young male as a long-term consequence of diphtheria-tetanus toxoid vaccination (102). The patient experienced thrombotic event accompanied with the stable high LA titer over the next 3 months. Another clinically and serologically proven case of APS was a 13-year-old girl who received a quadrivalent human papillomavirus (HPV) vaccine (103). Acute thrombocytopenia and bleeding were rapidly improved although positive titers of aPL persisted for 6 months.

Among other vaccines, the strongest experimental evidence for post-vaccination development of aPL was revealed for tetanus toxoid (TTd) vaccine. In mouse models, APS manifestation was achieved by immunization of mice with TTd using different adjuvants (104, 105). In humans, an evidence of anti-β2GPI/anti-tetanus toxoid cross-reactive antibody generation after vaccination with TTd in two healthy men was reported (106).

Clearly, vaccines should share molecular patterns with pathogens to elicit protective immune responses. The overall reported frequency of aPL incidences after influenza immunization, however, is higher than after infection (our survey of the published literature). Whether this phenomenon is due to the better studied cohort of vaccinated individuals or to the increased sensitivity to concomitant stimuli such as adjuvants remains unknown. Recently, Shoenfeld and Agmon-Levin suggested to group several autoimmune conditions in a single entity called "ASIA"—Autoimmune (Autoinflammatory) Syndrome Induced by Adjuvants," which is triggered by external agents such as infections and vaccines (107). It has to be noted, however, that the effects of adjuvants could be significant only in genetically predisposed individuals, whilst less so in general population.

DRUGS

Evidence for a possible association of aPL production and drug administration was first described in 1945 in a patient, who developed a lupus-like syndrome presumably following sulphadiazine therapy (108). Currently a wide range of pharmacological agents used to treat arrhythmia, psychological disorders, hypertension, bacterial infections, epilepsy, or other convulsions, etc. could be implicated in the production of aPL and, in some cases, development of clinically significant APS manifestations (109). Pathogenic potential and clinical manifestations related to drugs-induced aPL are variable and largely dependent on the specific nature of a drug under question. The majority of the drug-induced aPL are usually considered to be fairly benign and disappear after the drug withdrawal (110). aPL induction by procainamide, adalimumab, interferon-α and several other drugs, however, may be linked to the development of thrombosis (111).

Antiarrhythmic agents, including procainamide, and quinidine have been frequently associated with the development of aPL, predominantly LA. Summarizing the relevant studies published between 1976 and 1998, Dlott and Roubey (109) have revealed the features suggestive or consistent with drug-induced LA in 13 of 42 reported cases. The authors highlighted the clinical presentation of thrombosis in 11 cases that could be associated with the underlying cardiac or vascular pathologies for which the patients were prescribed procainamide (109). Generation of β2GPI-dependent IgG aCL after the administration of procainamide resulted in thrombosis and, in one case, of the drug-induced APS (112). A number of studies demonstrated association between quinidine and its stereoisomer quinine and the occurrence of LA (113–115), while the occurrence of aCL was only rarely detected (116). Several mechanisms have been proposed to explain the link between antiarrhythmic drugs and aPL induction. The most plausible among these is a non-specific interaction of antiarrhythmic agents with membrane phospholipids, situated close to the sodium channels, which may trigger an initial event leading to self-reactivity (117).

Pharmacological efficiency of antipsychotic drugs is related to the toxic effects imposed by their non-specific interaction with the phospholipid bilayer, particularly with negatively charged lipids (118). Chlorpromazine (CPZ) is the agent most often implicated in cases of drug-induced aPL (109). LA, which is the main type of aPL antibodies found to be associated with CPZ, is rarely reported as the cause of thrombosis (109). Incidence of aCL alone or together with LA, following CPZ administration, was described in two separate studies (110, 119). Gharavi et al.(17) examined β2GPI-dependence of aPL, which is triggered by CPZ, and found its resemblance with autoimmune type antibodies (17). In another study, however, the presence of aCL, anti-β2GPI or LA was detected in patients with psychiatric diseases regardless of treatment by CPZ or other antipsychotics (120).

Besides antimicrobial activities, antibiotics may impose substantial interference with the host physiology and metabolism (121). Amoxicillin (111) and streptomycin (113) were the first antibiotics associated with the LA activity. In a later study, production of transient IgG aCL in response to sulfasalazine has been reported (122). There has been a renowned interest regarding the influence of antibiotics on aPL formation. Two studies reported the occurrence of LA, anti-β2GP1 and anti-phosphatidylethanolamine during the course of minocycline therapy (123, 124). The phenomenon of antibiotics-related aPL

is arguable as it may be a consequence of the infectious process itself.

Other drugs, including fluvastatin, propylthiouracil, carvedilol, adalimumab, infliximab, and thalidomide and chemical agents such as acrylamide and silicone are suspected as being associated with aPL production but there is only a limited number of studies available. At least 10 cases of aPL-mediated vasculitis and/or thrombotic manifestations were attributed to cocaine abuse (125–127). It was suggested that certain cocaine-related clinical presentations can be related to the toxic effect of adulterant levamisole (antihelminth agent) or their synergic action.

The exact mechanisms of the drug-induced autoimmune reactions are not definitely known. Several pharmacological agents, including procainamide, quinidine, valproic acid, and phenytoin inevitably destroy the integrity of phospholipid bilayer by passing through the cell membrane to reach their site of action (128). Membrane perturbations may be implicated in altered presentation of neo-antigens or cryptic epitopes resulting in the consequent autoimmune responses. Among others, individual acetylation status and hapten-like characteristics of a particular drug may be considered as possible mechanisms for drug-induced aPL.

OTHER ENVIRONMENTAL FACTORS

Resident gut microbiota, together with other environmental factors such as nutritional status and stress, can play a crucial role in immune homeostasis (129). Numerous experiments carried out to understand whether dietary manipulations can result in a loss of self-tolerance have revealed compelling effects of daily calories, proteins or fat intake on the development of autoimmune diseases (130, 131). In particular, the diets containing omega-3-rich linseed oil as a fat source have demonstrated a reduction in the serum levels of aCL and anti-dsDNA antibodies in BALB/c mice with experimentally induced lupus (130). The fatty acid composition of cell membrane scan be influenced by the phospholipids ingested. Alterations of membrane structure and fluidity, observed in response to dietary fats, might result in modulation of functional activities of macrophages, dendritic cells, or T lymphocytes (132). Another mechanism, attributed to the immunomodulatory effects of omega-3, is the reduction of eicosanoid synthesis, which is an important mediator regulating secretion of cytokines and inflammatory gene expression (133). In autoimmune and thrombosis-prone W/BF1 mice, feeding a calorie-restricted diet resulted in the reduction of aCL and anti-dsDNA and in protection against thrombogenesis (134). Mechanisms of protective effect of calorie restriction against autoimmunity remain debatable, though it appears that abrogation of free radical generation and inflammatory responses may be involved (135).

Several studies emphasized a possible association of low serum vitamin D levels and/or high frequency of vitamin D insufficiency with hypercoagulable state in APS patients (136). Besides, vitamin D may inhibit the anti-β2GPI-stimulated TF expression in human umbilical vein endothelial cells (HUVECs) has been shown (137). Vitamin D alone as well as in combination with low molecular weight heparin (LMWH) may exert an anti-inflammatory effect on aPL-stimulated trophoblasts (138). Thus, vitamin D supplements may warrant further investigation as a promising prophylactic agent for preventing aPL-related thrombotic and obstetric complications.

MECHANISMS OF APL PRODUCTION

A variety of mechanisms have been suggested to explain the origin of aPL. Production of aPL is a complex and largely unknown process, encompassing a multifactorial interaction of genetic susceptibility variants and environmental factors. Infectious agents may cause the development of aPL through antigen-dependent mechanisms such as molecular mimicry, or in antigen-independent manner such as breakdown of immune tolerance due to inflammation.

Currently molecular mimicry is considered to be as the most prevalent explanation for a frequent association of infections and aPL-related clinical manifestations and APS. Molecular mimicry represents a phenomenon of structure-and-function similarity between foreign and host antigens. As a result, the self-tolerance is compromised and the pathogen-specific immune response cross-reacts with self-antigens. There is a strong evidence for a significant homology between the bacterial and viral structures and peptides derived from β2GPI, which contribute to the selection of cross-reactive T and B cells. The molecular-mimicry hypothesis was tested in several animal model experiments designed to evaluate the pathogenic potential of infectious agents bearing membrane proteins similar to the main immunogenic epitopes targeted by anti-β2GPI antibodies. Induction of aPL in animals by heterologous β2GPI alluded that autoimmune reaction may be elicited by the immune complexes formed by host PL and PL-binding proteins derived from common infectious agents (139). Biopanning procedures identified synthetic peptides with high homology to the different regions of β2GPI, which, in *in vivo* and *in vitro* experiments, diminished endothelial cell activation, and adhesion properties of monocytes caused by patient-derived anti-β2GPI (140). This group further showed a significant rise of aCL and anti-β2GPI in mice immunized with *Haemophilus influenzae*, *Neisseria gonorrhoeae*, *Candida albicans,* or tetanus toxoid, which share structural homology with one of selected hexapeptides (TLRVYK) (141). As a confirmation to the earlier reports, APS-related clinical and serological manifestations were corroborated in naive mice passively infused with anti-TLRVYK antibodies from immunized mice (141). Similar results were obtained when mice were immunized with other synthetic peptides of bacterial or viral origin (adenovirus, CMV, *Bacillus subtilis*) that shared sequence and functional similarity with a 15 amino acid peptide "GDKV" in major phospholipid-binding region of β2GPI (139). Induction of aCL and anti-β2GPI in immunized mice supported the idea that certain viral and bacterial agents may trigger autoreactive aPL response via interaction of infection-derived PL-binding peptides with host β2GPI.

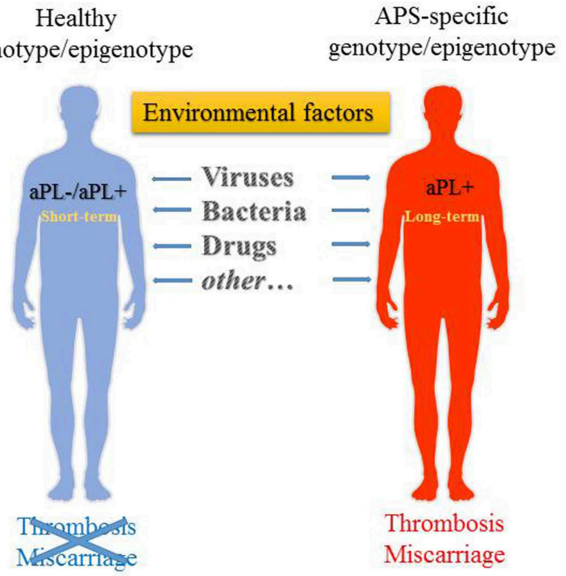

FIGURE 1 | Environmental factors that may trigger the generation of aPL. aPL generation can be triggered in both genetically susceptible as well as non-susceptible individuals, albeit it is transient in the latter. Long-term persistence of aPL in predisposed individuals may then lead to the development of APS.

Infection(s) can cause conformational changes in β2GPI resulting in anti-β2GPI formation. Particularly, β2GPI was shown to interact with *Streptococcus pyogenes* surface protein H, thereby exposing a cryptic epitope within domain I of β2GPI and triggering aPL response (142). Additionally, alteration of host antigenic determinants due to tissue injury and generation of neoepitopes may lead to molecular mimicry. Inflammation may play a role in modification of proteins, thus providing a source of neoepitopes that can be recognized by antibodies as a non-self. In the context of innate immune activation and a pro-inflammatory environment, interaction of β2GPI with anionic PL may result in the presentation of novel T cell epitopes, which are not observed in non-autoimmune individuals (143) and which appear as a result of modulation of presentation pathways (144). Among inflammatory cascades, oxidative stress is a key mechanism, which affects post-translational modification of proteins and/or alters membrane bilayers via lipid peroxidation (145). In addition, reactive species may enhance immunogenicity of β2GPI. Elevated levels of circulating complexes, which are formed by oxidatively modified low density lipoproteins (oxLDL) and β2GPI (oxLDL/β2GPI) and recognized by anti-β2GPI, were found to be associated with the increased risk of arterial thrombosis in APS and SLE patients (146).

In addition to the infection-induced β2GPI immunogenicity, certain conformational changes may lead to the exposure of the major B-cell binding site on domain I and of the major T-cell binding site on domain V that are required for aPL response (147). Each of the five β2GPI domains has been implicated in interaction with antibodies. The high immunogenicity and pathogenicity of antibodies with reactivity against DI of β2GPI, however, is a newly recognized circumstance. It is thought that β2GPI in the serum is present predominantly in a "closed" circular conformation, in which the interaction of domain I with domain V prevents the exposure of the G39-R43 epitope. Upon the conformational change, induced by the interaction of β2GPI with anionic surfaces ("open" conformation), domain I opens up thus exposing a hidden epitope and triggering the formation of autoantibodies (148). Multiple epidemiological studies have demonstrated that antibodies against DI correlate with a substantially increased risk of thrombosis and, to a lesser extent, of pregnancy complications (149–151). This is especially relevant for the patients with a triple aPL positivity, that confers the highest risk for thrombotic events and more severe forms of APS (152–154). One of the mechanisms responsible for the increased thrombosis rates is an anti-D1-mediated increase in monocytic TF expression (our unpublished data). A very recent study challenged the pathogenic value of antibodies to domain 1 or 4/5 of β2GPI in terms of risk stratification of APS-related complications *in-vitro*. Potent procoagulant properties of anti-D1 were demonstrated in LPS-primed rats, while anti-D5, similarly to negative control, was unable to promote clot formation (155). Despite this, there is still a controversy on whether the predictive power of classic aPL tests will benefit from anti-D1 screening (154) or not (153).

Anionic compounds with the ability to bind β2GPI appeared to be an interesting potential player in the pathogenic loop that supports continuous generation of anti-β2GPI in APS (144). The model proposed suggests that the FcγRI-mediated uptake of β2GPI/anti-β2GPI/anionic surface complexes by macrophages results in recognition and presentation of the β2GPI cryptic determinants. A subsequent activation of β2GPI-reactive CD4+ T cells triggers anti-β2GPI production by B cells thus establishing a self-sustained loop (144). Under physiological conditions, systemic oxLDL, which are phospholipids expressed on activated platelets or presented on apoptotic bodies, may potentially act as a source of anionic substrates that form stable complexes with β2GPI to drive aPL response via the mechanism described above. In a focused review by Andreoli and coworkers, pathogenic interplay between aPL and apoptotic processes was emphasized (156). The authors pointed out that apoptotic cells may act as immunogenic factors capable of triggering the aPL response. On the other hand, the persistent exposure of aPL target by dying cells may promote autoimmunity through the maintenance of inflammation, especially in the settings with the increased IFN signature (156).

Notwithstanding of the numerous mechanisms proposed, it is not clear how aPL antibodies induce thrombosis and obstetric complications. It was suggested that the sustained aPL titers and procoagulatory state "first hit" precipitate thrombotic events only in the presence of inflammatory "second hit" (157). Factors such as trauma, vascular injury, surgery, pregnancy, age, hypertension, diabetes, obesity, and infection may also potentiate thrombus formation (158, 159).

The etiology of APS is attributed to the interplay between genetic and environmental insults. Nevertheless, the impact of environment on disease risk is difficult to evaluate and the

TABLE 1 | Bacterial, viral, and parasitic agents linked to the aPL production and clinical manifestation.

	aCL	aβ2GPI	LA	Thrombosis	Structure	References
VIRAL INFECTIONS						
HIV	+	+	+	+	Enveloped	(12–15)
Hepatitis C	+	+	+	+	Enveloped	(13, 15, 21)
Parvovirus B19	+	+	+	+	Non-enveloped	(23–25, 63)
CMV	+	+	+	+	Enveloped	(31, 63)
Varicella zoster virus	+	+	+	+	Enveloped	(34–37, 63)
Epstein-Barr virus (EBV)	+	+	+	+	Enveloped	(13, 38, 39, 63)
Adenovirus	+	+	−	−	Non-enveloped	(15, 15, 63)
Hepatitis A	+	−	−	+	Non-enveloped	(63)
Influenza	−	−	−	+	Enveloped	(63)
Hepatitis B	+	−	−	−	Enveloped	(22, 63, 101)
Rubella	+	−	−	−	Enveloped	(28, 63)
Measles	−	−	−	−	−	(28)
Hepatitis D	+	+	+	−	Enveloped	(22)
Human T-lymphotropic virus 1	+	−	−	−	Enveloped	(12, 63)
Mumps	+	−	−	−	Enveloped	(28, 63)
BACTERIAL INFECTIONS						
Coxiella burnetii	+	−	+	−	Gram-negative	(28, 63)
Mycoplasma pneumonia	+	+	−	+	Gram-negative	(42, 53, 55–57, 63)
Streptococcus spp.	+	+	+	+	Gram-positive	(28, 52, 63)
Mycobacterium tuberculosis	+	+	−	+	Not classified	(28, 63)
Mycobacterium leprae	+	+	+	+	Gram-positive	(62–66)
Borrelia burgdorferi	+	+	+	+	Gram-positive	(125)
Staphylococcus spp.					Gram-negative	(28, 52, 58, 59)
Treponema pallidum	+	+	−	−	Gram-negative	(10, 13, 63)
Escherichia coli	+	+	−	+	Gram-negative	(28, 52, 63)
Salmonella spp.	+	+	+	+	Gram-negative	(28, 63)
Klebsiella spp.	+				Gram-negative	(10, 28)
Fusobacterium necrophorum	+	−	+	+	Gram-negative	(60, 63)
Chlamydiae	+	+	−	−	Gram-negative	(28, 63)
Helicobacter pylori	+	+	−	−	Gram-negative	(75, 76)
PARASITIC INFECTIONS						
Plasmodium malariae	+	+	−	+	Intracellular parasites	(12, 13, 63)
Plasmodium falciparum	+	−	−		Intracellular parasites	(68)
Leptospira spp.	+	+	−	−	Extracellular parasites	(63)

mechanisms involved remain pressing and enigmatic. Evidences accumulated over decades indicate that gene-environment interactions, mediated at the epigenetic level, may trigger autoimmune processes (160). Epigenetic alterations may regulate CD4, CD8 and B cell functions and appears to drive maturation of the high-affinity antibody response (161, 162). It is therefore intriguing to investigate the influence of particular environment factors on epigenetic landscape and following aPL response.

Our review includes the wide range of publications describing environmentally-triggered aPL generation including research papers, case reports, case-control studies, reviews, and clinical, epidemiological, population-based and big-cohort studies. Despite this, we are aware that the data in this review might be limited for several reasons. The first is the biased/heterogeneous or limited data of the relevant reviewed studies. The second limitation concerns the laboratory procedures for aPL detection, which still lack of standardization and interpretation strategies and may vary among laboratories. The possible variation arising from non-uniformity of results interpretation were not considered here.

CONCLUSION

In summary, the environmental triggers such as bacteria, viruses, commensal bacteria, vaccines, drugs, and other factors are potentially capable of inducing a variety of aPL and causing APS through a wide range of mechanisms in genetically susceptible individuals (**Figure 1**). These factors are also specified in **Table 1**. A most compelling evidence supporting the role of

environmental factors in induction of aPL is largely obtained from the epidemiological studies. The presence of aPL in healthy individuals points to the normal physiological role played by aPL. The post-infection increase of aPL is usually transient, and it is not accompanied by the manifestations of APS such as thrombosis. The main question remains, however, why in a genetically susceptible host the increase of aPL in response to the environmental stimuli is not resolved and results in the transition from low-affinity to high-affinity autoantibodies, with the increased pathogenic potential of aPL. Presently our understanding of mechanisms of inflammation resolution and self-tolerance is rather limited and cannot explain why in a subset of population initial adaptive immune response against foreign antigens is rerouted against self-antigens. Does it involve compromised innate immunity mechanisms ensuing continuous activation via the DAMP signaling? Or is adaptive immune response in the later stages involved that prevents clonal selection of T and B cells producing self-antibodies? Uncovering the mechanisms behind the generation of heterogeneous aPL that contribute to the development of APS will help to design the strategies for treatment and prevention of this disease.

AUTHOR CONTRIBUTIONS

All authors listed have made a substantial, direct and intellectual contribution to the work, and approved it for publication.

REFERENCES

1. Schreiber K, Sciascia S, de Groot PG, Devreese K, Jacobsen S, Ruiz-Irastorza G, et al. Antiphospholipid syndrome. *Nat Rev Dis Primers*. (2018) 11:17103. doi: 10.1038/nrdp.2017.103
2. Miyakis S, Lockshin MD, Atsumi I, Branch DW, Brey RL, Cervera R, et al. International concensus statement on an update of the classification criteria for definite antiphospholipid syndrome (APS). *J Thromb Haemost.* (2006) 4:295–306. doi: 10.1111/j.1538-7836.2006.01753.x
3. Willis R, Pierangeli SS. Pathophysiology of the antiphospholipid antibody syndrome. *Auto Immun Highlights*. (2011) 2:35–52. doi: 10.1007/s13317-011-0017-9
4. von Landenberg P, Doring Y, Modrow S, Lackner KJ. Are antiphospholipid antibodies an essential requirement for an effective immune response to infections? *Ann N Y Acad Sci*. (2007) 1108:578–83. doi: 10.1196/annals.1422.060
5. Salmon JE, de Groot PG. Pathogenic role of antiphospholipid antibodies. *Lupus*. (2008) 17:405–11. doi: 10.1177/0961203308090025
6. Pericleous C, Ruiz-Limón P, Romay-Penabad Z, Marín AC, Garza-Garcia A, Murfitt L, et al. Proof-of-concept study demonstrating the pathogenicity of affinity-purified IgG antibodies directed to domain I of β2-glycoprotein I in a mouse model of anti-phospholipid antibody-induced thrombosis. *Rheumatology*. (2015) 54:722–7. doi: 10.1093/rheumatology/keu360
7. Giannakopoulos B, Passam F, Rahgozar S, Krilis SA. Current concepts on the pathogenesis of the antiphospholipid syndrome. *Blood*. (2007) 109:422–30. doi: 10.1182/blood-2006-04-001206
8. Nakanishi T, Suzuki N, Kuragano T, Nagasawa Y, Hasuike Y. Current topics in therapeutic plasmapheresis. *Clin Exp Nephrol*. (2014) 18:41–9. doi: 10.1007/s10157-013-0838-0
9. Martirosyan A, Petrek M, Kishore A, Manukyan G. The immunomodulatory effects of therapeutic plasma exchange on monocytes in Antiphospholipid syndrome. *Exp Ther Med*. (2016) 12:1189–95. doi: 10.3892/etm.2016.3441
10. McNally T, Purdy G, Mackie IJ, Machin SJ, Isenberg DA. The use of an anti-beta2-glycoprotein-I assay for discrimination between anticardiolipin antibodies associated with infection and increased risk of thrombosis. *Br J Haematol*. (1995) 91:471–3. doi: 10.1111/j.1365-2141.1995.tb05324.x
11. Canoso RT, Zon LI, Groopman JE. Anticardiolipin antibodies associated with HTLV-III infection. *Br J Haematol*. (1987) 65:495–8. doi: 10.1111/j.1365-2141.1987.tb04157.x
12. Asherson RA, Cervera R. Antiphospholipid antibodies and infections. *Ann Rheum Dis*. (2003) 62:388–93. doi: 10.1136/ard.62.5.388
13. Sene D, Piette JC, Cacoub P. Antiphospholipid antibodies, antiphospholipid syndrome and infections. *Autoimmune Rev*. (2008) 7:272–7. doi: 10.1016/j.autrev.2007.10.001
14. Galrão L, Brites C, Atta ML, Atta A, Lima I, Gonzalez F, et al. Antiphospholipid antibodies in HIV-positive patients. *Clin Rheumatol*. (2007) 26:1825–30. doi: 10.1007/s10067-007-0581-6
15. Uthman IW, Gharavi AE. Viral infections and antiphospholipid antibodies. *Semin Arthritis Rheum*. (2002) 31:256–63. doi: 10.1053/sarh.2002.28303
16. Guglielmone H, Vitozzi S, Elbarcha O, Fernandez E. Cofactor dependence and isotype distribution of anticardiolipin antibodies in viral infections. *Ann Rheum Dis*. (2001) 60:500–4. doi: 10.1136/ard.60.5.500
17. Gharavi AE, Sammaritano LR, Wen J, Miyawaki N, Morse JH, Zarrabi MH, et al. Characteristics of human immunodeficiency virus and chlorpromazine induced antiphospholipid antibodies: effect of beta 2 glycoprotein I on binding to phospholipid. *J Rheumatol*. (1994) 21:94–9.
18. Petrovas C, Vlachoyiannopoulos PG, Kordossis T, Moutsopoulos HM. Anti-phospholipid antibodies in HIV infection and SLE with or without anti-phospholipid syndrome: comparisons of phospholipid specificity, avidity and reactivity with beta2-GPI. *J Autoimmun*. (1999) 13:347–55. doi: 10.1006/jaut.1999.0324
19. Bibas M, Biava G, Antinori A. HIV-associated venous thromboembolism. *Mediterr J Hematol Infect Dis*. (2011) 3:e2011030. doi: 10.4084/mjhid.2011.030
20. Giordano P, Galli M, Del Vecchio GC, Altomare M, Norbis F, et al. Lupus anticoagulant, anticardiolipin antibodies and hepatitis C virus infection in thalassaemia. *Br J Haematol*. (1998) 102:903–6. doi: 10.1046/j.1365-2141.1998.00853.x
21. Ramos-Casals M, Cervera R, Lagrutta M, Medina F, García-Carrasco M, de la Red G, et al. Clinical features related to antiphospholipid syndrome in patients with chronic viral infections (hepatitis C virus/HIV infection): description of 82 cases. *Clin Infect Dis*. (2004) 38:1009–16. doi: 10.1086/382537
22. Elefsiniotis IS, Diamantis ID, Dourakis SP, Kafiri G, Pantazis K, Mavrogiannis C. Anticardiolipin antibodies in chronic hepatitis B and chronic hepatitis D infection, and hepatitis B-related hepatocellular carcinoma. Relationship with portal vein thrombosis. *Eur J Gastroenterol Hepatol*. (2003) 15:721–6. doi: 10.1097/01.meg.0000059140.68845.74
23. Kerr JR. The role of parvovirus B19 in the pathogenesis of autoimmunity and autoimmune disease. *J Clin Pathol*. (2016) 69:279–91. doi: 10.1136/jclinpath-2015-203455
24. von Landenberg P, Lehmann HW, Knöll A, Dorsch S, Modrow S. Antiphospholipid antibodies in pediatric and adult patients with rheumatic disease are associated with parvovirus B19 infection. *Arthritis Rheum*. (2003) 48:1939–47. doi: 10.1002/art.11038
25. Loizou S, Cazabon JK, Walport MJ, Tait D, So AK. Similarities of specificity and cofactor dependence in serum antiphospholipid antibodies from patients with human parvovirus B19 infection and from those with systemic lupus erythematosus. *Arthritis Rheum*. (1997) 40:103–8. doi: 10.1002/art.1780400115
26. Asano Y, Sarukawa M, Idezuki T, Harada S, Kaji K, Nakasu I, et al. Multiple small pulmonary emboli associated with transient antiphospholipid syndrome in human Parvovirus B19 infection. *Clin Rheumatol*. (2006) 25:585–7. doi: 10.1007/s10067-005-0032-1
27. Kranidiotis G, Efstratiadis E, Kapsalakis G, Loizos G, Bilis A, Melidonis A. Splenic infarcts as a rare manifestation of parvovirus

B19 infection. *ID Cases*. (2016) 4:62–4. doi: 10.1016/j.idcr.2016.04.003
28. Abdel-Wahab N, Lopez-Olivo MA, Pinto-Patarroyo GP, Suarez-Almazor ME. Systematic review of case reports of antiphospholipid syndrome following infection. *Lupus*. (2016) 25:1520–31. doi: 10.1177/0961203316640912
29. Williams MV, Cox B, Ariza ME. Herpesviruses dUTPases: a new family of Pathogen-Associated Molecular Pattern (PAMP) proteins with implications for human disease. *Pathogens*. (2016) 6:2. doi: 10.3390/pathogens6010002
30. De Carolis S, Tabacco S, Rizzo F, Perrone G, Garufi C, Botta A, et al. Association between false-positive TORCH and antiphospholipid antibodies in healthy pregnant women. *Lupus*. (2018). 27:841–6. doi: 10.1177/0961203317741564
31. Justo D, Finn T, Atzmony L, Guy N, Steinvil A. Thrombosis associated with acute cytomegalovirus infection: a meta-analysis. *Eur J Intern Med*. (2011) 22:195–9. doi: 10.1016/j.ejim.2010.11.006
32. Rahbar A, Söderberg-Nauclér C. Human cytomegalovirus infection of endothelial cells triggers platelet adhesion and aggregation. *J Virol*. (2005) 79:2211–20. doi: 10.1128/JVI.79.4.2211-2220.2005
33. Squizzato A, Gerdes VE, Büller HR. Effects of human cytomegalovirus infection on the coagulation system. *Thromb Haemost*. (2005) 93:403–10. doi: 10.1160/TH04-08-0523
34. Josephson C, Nuss R, Jacobson L, Hacker MR, Murphy J, Weinberg A, et al. The varicella-autoantibody syndrome. *Pediatr Res*. (2001) 50:345–52. doi: 10.1203/00006450-200109000-00009
35. Viseux V, Darnige L, Carmi E, Chaby G, Poulain JF, Cevallos R, et al. Pulmonary embolism and transitory anti-beta2-GPI antibodies in an adult with chicken pox. *Lupus*. (2000) 9:558–60. doi: 10.1177/096120330000900716
36. Losurdo G, Giacchino R, Castagnola E, Gattorno M, Costabel S, Rossi A, et al. Cerebrovascular disease and varicella in children. *Brain Dev*. (2006) 28:366–70. doi: 10.1016/j.braindev.2005.11.002
37. Frontino G, Passoni A, Piscopo MA, Grechi E, Cammarata B, Pozzobon G. Bilateral cavo-ilio-femoral thrombosis in an adolescent with transient antiphospholipid antibodies and factor V heterozygous mutation: a case report. *Cases J*. (2009) 2:6830. doi: 10.4076/1757-1626-2-6830
38. Zandman-Goddard G, Berkun Y, Barzilai O, Boaz M, Blank M, Ram M, et al. Exposure to Epstein-Barr virus infection is associated with mild systemic lupus erythematosus disease. *Ann N Y Acad Sci*. (2009) 1173:658–63. doi: 10.1111/j.1749-6632.2009.04754.x
39. Ogawa J, Koike R, Sugihara T, Hagiyama H, Nishio J, Kohsaka H, et al. [An autopsied case of chronic active Epstein-Barr virus infection complicated in systemic lupus erythematosus and antiphospholipid antibody syndrome]. *Nihon Rinsho Meneki Gakkai Kaishi*. (2002) 25:458–65. doi: 10.2177/jsci.25.458
40. Delbos V, Abgueguen P, Chennebault JM, Fanello S, Pichard E. Acute cytomegalovirus infection and venous thrombosis: role of antiphospholipid antibodies. *J Infect*. (2008) 54:e47–50. doi: 10.1016/j.jinf.2006.03.031
41. Kratz C, Mauz-Körholz C, Kruck H, Körholz D, Göbel U. Detection of antiphospholipid antibodies in children and adolescents. *Pediatr Hematol Oncol*. (1998) 15:325–32. doi: 10.3109/08880019809014016
42. Shimizu T, Ishiguro A, Takayanagi T, Matsui T, Tonegawa N, Maekawa T, et al. [A case of lupus anticoagulant hypoprothrombinemia syndrome following adenovirus gastroenteritis and mycoplasma pneumonia]. *Nihon Rinsho Meneki Gakkai Kaishi*. (2014) 37:55–60. doi: 10.2177/jsci.37.55
43. Mazzon M, Mercer J. Lipid interactions during virus entry and infection. *Cell Microbiol*. (2014) 16:1493–502. doi: 10.1111/cmi.12340
44. Lorizate M, Sachsenheimer T, Glass B, Habermann A, Gerl MJ, Krausslich HG, et al. Comparative lipidomics analysis of HIV-1 particles and their producer cell membrane in different cell lines. *Cell Microbiol*. (2013) 15:292–304. doi: 10.1111/cmi.12101
45. Chan R, Uchil PD, Jin J, Shui G, Ott DE, Mothes W, et al. Retroviruses human immunodeficiency virus and murine leukemia virus are enriched in phosphoinositides. *J Virol*. (2008) 82:11228–38. doi: 10.1128/JVI.00981-08
46. de Armas-Rillo L, Valera MS, Marrero-Hernández S, Valenzuela-Fernández A. Membrane dynamics associated with viral infection. *Rev Med Virol*. (2016) 26:146–60. doi: 10.1002/rmv.1872
47. Haynes BF, Fleming J, St. Clair EW, Katinger H, Stiegler G, Kunert R, et al. Cardiolipin polyspecific autoreactivity in two broadly neutralizing HIV-1 antibodies. *Science*. (2005) 308:1906–8. doi: 10.1126/science.1111781
48. Martinez V, Diemert MC, Braibant M, Potard V, Charuel JL, Barin F, et al. Anticardiolipin antibodies in HIV infection are independently associated with antibodies to the membrane proximal external region of gp41 and with cell-associated HIV DNA and immune activation. *Clin Infect Dis*. (2009) 48:123–32. doi: 10.1086/595013
49. Diaz JS, Octavio JG, Fernandez-Guerrero ML. Antiphospholipid syndrome and acute HIV infection. *Emerg Infect Dis*. (2010) 16:360–1. doi: 10.3201/eid1602.090728
50. Martirosyan A, Petrek M, Navratilova Z, Blbulyan A, Boyajyan A, Manukyan G. Differential regulation of proinflammatory mediators following LPS- and ATP-induced activation of monocytes from patients with antiphospholipid syndrome. *Biomed Res Int*. (2015) 2015:292851. doi: 10.1155/2015/292851
51. Arleevskaya MI, Manukyan G, Inoue R, Aminov R. Editorial: microbial and environmental factors in autoimmune and inflammatory diseases. *Front Immunol*. (2017) 8:243. doi: 10.3389/fimmu.2017.00243
52. Cervera R, Asherson RA, Acevedo ML, Gómez-Puerta JA, Espinosa G, De La Red G, et al. Antiphospholipid syndrome associated with infections: clinical and microbiological characteristics of 100 patients. *Ann Rheum Dis*. (2004) 63:1312–7. doi: 10.1136/ard.2003.014175
53. Snowden N, Wilson PB, Longson M, Pumphrey RS. Antiphospholipid antibodies and *Mycoplasma pneumonia*e infection. *Postgrad Med J*. (1990) 66:356–62. doi: 10.1136/pgmj.66.775.356
54. Ardiles L, Ramirez P, Moya P, Caorsi I, Mezzano S. Anticardiolipin antibodies in acute poststreptococcal glomerulonephritis and streptococcal impetigo. *Nephron*. (1999) 83:47–52. doi: 10.1159/000045472
55. Espinosa G, Santos E, Cervera R, Piette JC, de la Red G, Gil V, et al. Adrenal involvement in the antiphospholipid syndrome: clinical and immunologic characteristics of 86 patients. *Medicine*. (2003) 82:106–18. doi: 10.1097/00005792-200303000-00005
56. Bakshi M, Khemani C, Vishwanathan V, Anand RK, Khubchandani RP. *Mycoplasma pneumonia* with antiphospholipid antibodies and a cardiac thrombus. *Lupus*. (2006) 15:105–6. doi: 10.1191/0961203306lu2258cr
57. Graw-Panzer KD, Verma S, Rao S, Miller ST, Lee H. Venous thrombosis and pulmonary embolism in a child with pneumonia due to *Mycoplasma pneumonia*e. *J Natl Med Assoc*. (2009) 101:956–8. doi: 10.1016/S0027-9684(15)31045-2
58. Witmer CM, Steenhoff AP, Shah SS, Raffini LJ. *Mycoplasma pneumonia*e, splenic infarct, and transient antiphospholipid antibodies: a new association? *Pediatrics*. (2007) 119:e292–5. doi: 10.1542/peds.2006-1340
59. Harada M, Nishi Y, Tamura S, Iba Y, Abe K, Yanbe Y, et al. [Infective endocarditis with a huge mitral vegetation related to atopic dermatitis and high serum level of infection-related antiphospholipid antibody: a case report]. *J Cardiol*. (2003) 42:135–40.
60. Goldenberg NA, Knapp-Clevenger R, Hays T, Manco-Johnson MJ. Lemierre's and Lemierre's-like syndromes in children: survival and thromboembolic outcomes. *Pediatrics*. (2005) 116:e543–8. doi: 10.1542/peds.2005-0433
61. Johannesen KM, Bodtger U. Lemierre's syndrome: current perspectives on diagnosis and management. *Infect Drug Resist*. (2016) 9:221–7. doi: 10.2147/IDR.S95050
62. Forastiero RR, Martinuzzo ME, de Larrañaga GF. Circulating levels of tissue factor and proinflammatory cytokines in patients with primary antiphospholipid syndrome or leprosy related antiphospholipid antibodies. *Lupus*. (2005) 14:129–36. doi: 10.1191/0961203305lu2048oa
63. Avcin T, Toplak N. Antiphospholipid antibodies in response to infection. *Curr Rheumatol Rep*. (2007) 9:212–8. doi: 10.1007/s11926-007-0034-x
64. Fiallo P, Travaglino C, Nunzi E, Cardo PP. Beta 2-Glycoprotein I-dependence of anticardiolipin antibodies in multibacillary leprosy patients. *Lepr Rev*. (1998) 69:376–81. doi: 10.5935/0305-7518.19980038
65. de Larrañaga GF, Forastiero RR, Martinuzzo ME, Carreras LO, Tsariktsian G, Sturno MM, et al. High prevalence of antiphospholipid antibodies in leprosy: evaluation of antigen reactivity. *Lupus*. (2000) 9:594–600. doi: 10.1191/096120300678828712
66. Levy RA, de Meis E, Pierangeli S. An adapted ELISA method for differentiating pathogenic from non-pathogenic aPL by a beta 2 glycoprotein

I dependency anticardiolipin assay. *Thromb Res*. (2004) 114:573–7. doi: 10.1016/j.thromres.2004.06.032
67. Ordoñez C, Savage HP, Tarajia M, Rivera R, Weeks-Galindo C, Sambrano D, et al. Both B-1a and B-1b cells exposed to *Mycobacterium tuberculosis* lipids differentiate into IgM antibody-secreting cells. *Immunology*. (2018) 154:613–23. doi: 10.1111/imm.12909
68. Adebajo AO, Charles P, Maini RN, Hazleman BL. Autoantibodies in malaria, tuberculosis and hepatitis B in a west African population. *Clin Exp Immunol*. (1993) 92:73–6. doi: 10.1111/j.1365-2249.1993.tb05950.x
69. Elkayam O, Caspi D, Lidgi M, Segal R. Auto-antibody profiles in patients with active pulmonary tuberculosis. *Int J Tuberc Lung Dis*. (2007) 11:306–10.
70. Shen CY, Hsieh SC, Yu CL, Wang JY, Lee LN, Yu CJ. Autoantibody prevalence in active tuberculosis: reactive or pathognomonic? *BMJ Open*. (2013) 26:7.doi: 10.1136/bmjopen-2013-002665
71. Elkayam O, Bendayan D, Segal R, Shapira Y, Gilburd B, Reuter S, et al. The effect of anti-tuberculosis treatment on levels of anti-phospholipid and anti-neutrophil cytoplasmatic antibodies in patients with active tuberculosis. *Rheumatol Int*. (2013) 33:949–53. doi: 10.1007/s00296-012-2487-0
72. Goodridge A, Cueva C, Lahiff M, Muzanye G, Johnson JL, Nahid P, et al. Anti-phospholipid antibody levels as biomarker for monitoring tuberculosis treatment response. *Tuberculosis*. 92:243–7. doi: 10.1016/j.tube.2012.02.004
73. Backert S, Neddermann M, Maubach G, Naumann M. Pathogenesis of *Helicobacter pylori* infection. *Helicobacter Suppl*. (2016) 1:19–25. doi: 10.1111/hel.12335
74. Smyk DS, Koutsoumpas AL, Mytilinaiou MG, Rigopoulou EI, Sakkas LI, Bogdanos DP. *Helicobacter pylori* and autoimmune disease: cause or bystander. *World J Gastroenterol*. (2014) 20:613–29. doi: 10.3748/wjg.v20.i3.613
75. Ram M, Barzilai O, Shapira Y, Anaya JM, Tincani A, Stojanovich L, et al. *Helicobacter pylori* serology in autoimmune diseases—fact or fiction? *Clin Chem Lab Med*. (2013) 51:1075–82. doi: 10.1515/cclm-2012-0477
76. Sarici SU, Gursel O, Kurekci E, Kesik V, Atay A, Okutan V, et al. Anticardiolipin antibodies in children with *Helicobacter pylori* infection. *Helicobacter*. (2015) 20:418–21. doi: 10.1111/hel.12226
77. Mankaï A, Layouni S, Ghedira I. Anti Saccharomyces cerevisiae antibodies in patients with anti-β2 glycoprotein I antibodies. *J Clin Lab Anal*. (2016) 30:818–22. doi: 10.1002/jcla.21942
78. Sipeki N, Davida L, Palyu E, Altorjay I, Harsfalvi J, Szalmas PA, et al. Prevalence, significance and predictive value of antiphospholipid antibodies in Crohn's disease. *World J Gastroenterol*. (2015) 21:6952–64. doi: 10.3748/wjg.v21.i22.6952
79. Mankaï A, Sakly W, Thabet Y, Achour A, Manoubi W, Ghedira I. Anti-Saccharomyces cerevisiae antibodies in patients with systemic lupus erythematosus. *Rheumatol Int*. (2013) 33:665–9. doi: 10.1007/s00296-012-2431-3
80. Dai H, Li Z, Zhang Y, Lv P, Gao XM. Elevated levels of serum IgA against *Saccharomyces cerevisiae* mannan in patients with rheumatoid arthritis. *Cell Mol Immunol*. (2009) 6:361–6. doi: 10.1038/cmi.2009.47
81. Krause I, Blank M, Cervera R, Font J, Matthias T, Pfeiffer S, et al. Cross-reactive epitopes on beta2-glycoprotein-I and Saccharomyces cerevisiae in patients with the antiphospholipid syndrome. *Ann N Y Acad Sci*. (2007) 1108:481–8. doi: 10.1196/annals.1422.051
82. Israeli E, Grotto I, Gilburd B, Balicer RD, Goldin E, Wiik A, et al. Anti-Saccharomyces cerevisiae and antineutrophil cytoplasmic antibodies as predictors of inflammatory bowel disease. *Gut*. (2005) 54:1232–6. doi: 10.1136/gut.2004.060228
83. Amital H, Gilburd B, Shoenfeld Y. Probiotic supplementation with *Lactobacillus casei* (Actimel) induces a Th1 response in an animal model of antiphospholipid syndrome. *Ann N Y Acad Sci*. (2007) 1110:661–9. doi: 10.1196/annals.1423.069
84. Ruff WE, Vieira SM, Kriegel MA. The role of the gut microbiota in the pathogenesis of antiphospholipid syndrome. *Curr Rheumatol Rep*. (2015) 17:472. doi: 10.1007/s11926-014-0472-1
85. Aguiar CL, Ruff W, Goodman A, Erkan D, Kriegel M. Cardiolipin-producing candidate commensals in the gut microbiome of antiphospholipid syndrome patients. *Arthritis Rheumatol*. (2016) 68 (Suppl. 10).
86. Furusawa Y, Obata Y, Fukuda S, Endo TA, Nakato G, Takahashi D, et al. Commensal microbe-derived butyrate induces the differentiation of colonic regulatory T cells. *Nature*. (2013) 19:446–50. doi: 10.1038/nature 12721
87. Vieira SM, Yu A, Pagovich OE, Tiniakou E, Sterpka J, Kriegel MA. Depletion of the gut microbiota prevents β2-glycoprotein I antibody production and mortality in a model of antiphospholipid syndrome. *Arthritis Rheum*. (2013) S1–1331.
88. Kagan VE, Tyurina YY, Tyurin VA, Mohammadyani D, Angeli JP, Baranov SV, et al. Cardiolipin signaling mechanisms: collapse of asymmetry and oxidation. *Antioxid Redox Signal*. (2015) 22:1667–80. doi: 10.1089/ars.2014.6219
89. Lewis RN, Mc Elhaney RN. The physicochemical properties of cardiolipin bilayers and cardiolipin-containing lipid membranes. *Biochim Biophys Acta*. (2009) 1788:2069–79. doi: 10.1016/j.bbamem.2009.03.014
90. Epand RM, Epand RF. Lipid domains in bacterial membranes and the action of antimicrobial agents. *Biochim Biophys Acta*. (2009) 1788:289–94. doi: 10.1016/j.bbamem.2008.08.023
91. Subang R, Levine JS, Janoff AS, Davidson SM, Taraschi TF, Koike T, et al. Phospholipid-bound beta 2-glycoprotein I induces the production of anti-phospholipid antibodies. *J Autoimmun*. (2000) 15:21–32. doi: 10.1006/jaut.2000.0382
92. Watanabe T, Onda H. Henoch-Schönleinpurpura with antiphospholipid antibodies following an influenza vaccination. *Pediatr Nephrol*. (2001) 16:458–9. doi: 10.1007/s004670100569
93. Mormile R, D'Alterio V, Treccagnoli G, Sorrentino P. Henoch-Schonleinpurpura with antiphospholipid antibodies after influenza vaccination: how fearful is it in children? *Vaccine*. (2004) 23:567–8. doi: 10.1016/j.vaccine.2004.07.029
94. Abu-Shakra M, Press J, Varsano N, Levy V, Mendelson E, Sukenik S, et al. Specific antibody response after influenza immunization in systemic lupus erythematosus. *J Rheumatol*. (2002) 29:2555–7.
95. Tarján P, Sipka S, Lakos G, Kiss E, Ujj G, Szegedi G. Influenza vaccination and the production of anti-phospholipid antibodies in patients with systemic lupus erythematosus. *Scand J Rheumatol*. (2006) 35:241–3. doi: 10.1080/03009740500474552
96. Toplak N, Kveder T, Trampuš-Bakija A, Subelj V, Cučnik S, Avčin T. Autoimmune response following annual influenza vaccination in 92 apparently healthy adults. *Autoimmun Rev*. (2008) 8:134–8. doi: 10.1016/j.autrev.2008.07.008
97. Vista ES, Crowe SR, Thompson LF, Air GM, Robertson JM, Guthridge JM, et al. Influenza vaccination can induce new-onset anticardiolipins but not β2-glycoprotein-I antibodies among patients with systemic lupus erythematosus. *Lupus*. (2012) 21:168–74. doi: 10.1177/09612033114 29554
98. de Medeiros DM, Silva CA, Bueno C, Ribeiro AC, Viana Vdos S, Carvalho JF, et al. Pandemic influenza immunization in primary antiphospholipid syndrome (PAPS): a trigger to thrombosis and autoantibody production? *Lupus*. (2014) 23:1412–6. doi: 10.1177/0961203314540351
99. Vainer-Mossel ED, Mekori YA, Mor A. Ischemic stroke in a patient with lupus following influenza vaccination: a questionable association. *Isr Med Assoc J*. (2009) 11:186–7.
100. Korematsu S, Miyahara H, Kakita A, Izumi T. Elevated serum anti-phosphatidylcholineIgG antibodies in patients with influenza vaccination-associated optic neuritis. *Vaccine*. (2014) 32:6345–8. doi: 10.1016/j.vaccine.2014.09.053
101. Martinuc Porobic J, Avcin T, Bozic B, Kuhar M, Cucnik S, Zupancic M, et al. Anti-phospholipid antibodies following vaccination with recombinant hepatitis B vaccine. *Clin Exp Immunol*. (2005) 142:377–80. doi: 10.1111/j.1365-2249.2005.02923.x
102. Meyer A, Rotman-Pikielny P, Natour A, Levy Y. Antiphospholipid syndrome following a diphtheria-tetanus vaccination: coincidence vs. causality. *Isr Med Assoc J*. (2010) 12:638–9.
103. Bizjak M, Bruck O, Kanduc D, Praprotnik S, Shoenfeld Y. Vaccinations and secondary immune thrombocytopenia with antiphospholipid antibodies by human papillomavirus vaccine. *Semin Hematol*. (2016) 53 (Suppl. 1):S48–50. doi: 10.1053/j.seminhematol.2016.04.014
104. Dimitrijević L, Živković I, Stojanović M, Petrušić V, Živančevi C, Simonović S. Vaccine model of antiphospholipid syndrome induced by tetanus vaccine. *Lupus*. (2012) 21:195–202. doi: 10.1177/0961203311429816

105. Zivkovic I, Petrusic V, Stojanovic M, Inic-Kanada A, Stojicevic I, Dimitrijevic L. Induction of decreased fecundity by tetanus toxoid hyper-immunization in C57BL/6 mice depends on the applied adjuvant. *Innate Immun*. (2012) 18:333–42. doi: 10.1177/1753425911407361
106. Blank M, Israeli E, Shoenfeld Y. When APS (Hughes syndrome) met the autoimmune/inflammatory syndrome induced by adjuvants (ASIA). *Lupus*. (2012) 21:711–4. doi: 10.1177/0961203312438115
107. Shoenfeld Y, Agmon-Levin N. 'ASIA'—autoimmune/inflammatory syndrome induced by adjuvants. *J Autoimmun*. (2011) 36:4–8. doi: 10.1016/j.jaut.2010.07.003
108. Hoffman BJ. Sensitivity to sufadiazine resembling acute disseminated lupus erythematosus. *Arch Derm Syphilol*. (1945) 51:190–2. doi: 10.1001/archderm.1945.01510210032007
109. Dlott JS, Roubey RA. Drug-induced lupus anticoagulants and antiphospholipid antibodies. *Curr Rheumatol Rep*. (2012) 14:71–8. doi: 10.1007/s11926-011-0227-1
110. Canoso RT, De Oliveira RM. Chlorpromazine-induced anticardiolipin antibodies and lupus anticoagulant: absence of thrombosis. *Am J Hematol*. (1988) 27:272–5. doi: 10.1002/ajh.2830270408
111. Triplett DA, Brandt JT, Musgrave KA, Orr CA. The relationship between lupus anticoagulants and antibodies to phospholipid. *JAMA*. (1988) 259:550–4. doi: 10.1001/jama.1988.03720040042024
112. Kameda H, Mimori T, Kaburaki J, Fujii T, Takahashi T, Akaishi M, et al. Systemic sclerosis complicated by procainamide-induced lupus and antiphospholipid syndrome. *Br J Rheumatol*. (1998) 37:1236–9. doi: 10.1093/rheumatology/37.11.1236
113. Gastineau DA, Kazmier FJ, Nichols WL, Bowie EJ. Lupus anticoagulant: an analysis of the clinical and laboratory features of 219 cases. *Am J Hematol*. (1985) 19:265–75. doi: 10.1002/ajh.2830190308
114. Walker TS, Triplett DA, Javed N, Musgrave K. Evaluation of lupus anticoagulants: antiphospholipid antibodies, endothelium associated immunoglobulin, endothelial prostacyclin secretion, and antigenic protein S levels. *Thromb Res*. (1988) 51:267–81. doi: 10.1016/0049-3848(88)90104-1
115. Bird MR, O'Neill AI, Buchanan RR, Ibrahim KM, Des PJ. Lupus anticoagulant in the elderly may be associated with both quinine and quinidine usage. *Pathology*. (1995) 27:136–9. doi: 10.1080/00313029500169742
116. Rosa-Re D, García F, Gascon J, Angrill J, Cervera R. Quinine induced lupus-like syndrome and cardiolipin antibodies. *Ann Rheum Dis*. (1996) 55:559–60. doi: 10.1136/ard.55.8.559-b
117. Suwalsky M, Sánchez I, Bagnara M, Sotomayor CP. Interaction of antiarrhythmic drugs with model membranes. *Biochim Biophys Acta*. (1994) 1195:189–96. doi: 10.1016/0005-2736(94)90255-0
118. Nussio MR, Sykes MJ, Miners JO, Shapter JG. Kinetics membrane disruption due to drug interactions of chlorpromazine hydrochloride. *Langmuir*. (2009) 25:1086–90. doi: 10.1021/la803288s
119. Lillicrap DP, Pinto M, Benford K, Ford PM, Ford S. Heterogeneity of laboratory test results for antiphospholipid antibodies in patients treated with chlorpromazine and other phenothiazines. *Am J Clin Pathol*. (1990) 93:771–5. doi: 10.1093/ajcp/93.6.771
120. Delluc A, Rousseau A, Le Galudec M, Canceil O, Woodhams B, Etienne S, et al. Prevalence of antiphospholipid antibodies in psychiatric patients users and non-users of antipsychotics. *Br J Haematol*. (2014) 164:272–9. doi: 10.1111/bjh.12627
121. Aminov RI. Biotic acts of antibiotics. *Front Microbiol*. (2013) 4:241. doi: 10.3389/fmicb.2013.00241
122. Vyse T, So AK. Sulphasalazine induced autoimmune syndrome. *Br J Rheumatol*. (1992) 31:115–6. doi: 10.1093/rheumatology/31.2.115
123. Graham LE, Bell AL. Minocycline-associated lupus-like syndrome with ulnar neuropathy and antiphospholipid antibody. *Clin Rheumatol*. (2001) 20:67–9. doi: 10.1007/s100670170108
124. Risse J, Vieira M, Beuret F, Petitpain N, Zuily S, Wahl D. Reversible drug-induced antiphospholipid syndrome. *Lupus*. (2018) 27:333–5. doi: 10.1177/0961203317712463
125. Gross RL, Brucker J, Bahce-Altuntas A, Abadi MA, Lipoff J, Kotlyar D, et al. A novel cutaneous vasculitis syndrome induced by levamisole-contaminated cocaine. *Clin Rheumatol*. (2011) 30:1385–92. doi: 10.1007/s10067-011-1805-3
126. Magro CM, Wang X. Cocaine-associated retiformpurpura: a C5b-9-mediated microangiopathy syndrome associated with enhanced apoptosis and high levels of intercellular adhesion molecule-1 expression. *Am J Dermatopathol*. (2013) 35:722–30. doi: 10.1097/DAD.0b013e31827eaf0b
127. Souied O, Baydoun H, Ghandour Z, Mobarakai N. Levamisole-contaminated cocaine: an emergent cause of vasculitis and skin necrosis. *Case Rep Med*. (2014) 2014:434717. doi: 10.1155/2014/434717
128. Lúcio M, Lima JL, Reis S. Drug-membrane interactions: significance for medicinal chemistry. *Curr Med Chem*. (2010) 17:1795–809. doi: 10.2174/092986710791111233
129. Calder PC. Feeding the immune system. *Proc Nutr Soc*. (2013) 72:299–309. doi: 10.1017/S0029665113001286
130. Reifen R, Blank M, Afek A, Kopilowiz Y, Sklan D, Gershwin ME, et al. Dietary polyunsaturated fatty acids decrease anti-dsDNA and anti-cardiolipin antibodies production in idiotype induced mouse model of systemic lupus erythematosus. *Lupus*. (1998) 7:192–7. doi: 10.1191/096120398678919985
131. Vojdani A. A potential link between environmental triggers and autoimmunity. *Autoimmune Dis*. (2014) 2014:437231. doi: 10.1155/2014/437231
132. Wolowczuk I, Verwaerde C, Viltart O, Delanoye A, Delacre M, Pot B, et al. Feeding our immune system: impact on metabolism. *Clin Dev Immunol*. (2008) 2008:639803. doi: 10.1155/2008/639803
133. Marion-Letellier R, Savoye G, Ghosh S. Polyunsaturated fatty acids and inflammation. *IUBMB Life*. (2015) 67:659–67. doi: 10.1002/iub.1428
134. Mizutani H, Engelman RW, Kinjoh K, Kurata Y, Ikehara S, Matsuzawa Y, et al. Calorie restriction prevents the occlusive coronary vascular disease of autoimmune (NZW x BXSB)F1 mice. *Proc Natl Acad Sci USA*. (1994) 91:4402–6. doi: 10.1073/pnas.91.10.4402
135. Anderson RM, Weindruch R. Metabolic reprogramming, caloric restriction and aging. *Trends Endocrinol Metab*. (2010) 21:134–41. doi: 10.1016/j.tem.2009.11.005
136. Riancho-Zarrabeitia L, Cubería M, Muñoz P, López-Hoyos M, García-Canale S, García-Unzueta M, et al. Vitamin D and antiphospholipid syndrome: a retrospective cohort study and meta-analysis. *Semin Arthritis Rheum*. (2018) 47:877–82. doi: 10.1016/j.semarthrit.2017.10.007
137. Agmon-Levin N, Blank M, Zandman-Goddard G, Orbach H, Meroni PL, Tincani A, et al. Vitamin D: an instrumental factor in the anti-phospholipid syndrome by inhibition of tissue factor expression. *Ann Rheum Dis*. (2011) 70:145–50. doi: 10.1136/ard.2010.134817
138. Gysler SM, Mulla MJ, Stuhlman M, Sfakianaki AK, Paidas MJ, Stanwood NL, et al. Vitamin D reverses aPL-induced inflammation and LMWH-induced sFlt-1 release by human trophoblast. *Am J Reprod Immunol*. (2015) 73:242–50. doi: 10.1111/aji.12301
139. Gharavi EE, Chaimovich H, Cucurull E, Celli CM, Tang H, Wilson WA, et al. Induction of antiphospholipid antibodies by immunization with synthetic viral and bacterial peptides. *Lupus*. (1999) 8:449–55. doi: 10.1177/096120339900800607
140. Blank M, Shoenfeld Y, Cabilli S, Heldman Y, Fridkin M, Katchalski-Katzir E. Prevention of experimental antiphospholipid syndrome and endothelial cell activation by synthetic peptides. *Proc Natl Acad Sci USA*. (1999) 96:5164–8. doi: 10.1073/pnas.96.9.5164
141. Blank M, Krause I, Fridkin M, Keller N, Kopolovic J, Goldberg I, et al. Bacterial induction of autoantibodies to beta2-glycoprotein- I accounts for the infectious etiology of antiphospholipid syndrome. *J Clin Invest*. (2002) 109:797–804. doi: 10.1172/JCI0212337
142. van Os GM, Meijers JC, Agar Ç, Seron MV, Marquart JA, Åkesson P, et al. Induction of anti-β2 -glycoprotein I autoantibodies in mice by protein H of Streptococcus pyogenes. *J Thromb Haemost*. (2011) 9:2447–56. doi: 10.1111/j.1538-7836.2011.04532.x
143. Kuwana M, Matsuura E, Kobayashi K, Okazaki Y, Kaburaki J, Ikeda Y, et al. Binding of beta 2-glycoprotein I to anionic phospholipids facilitates processing and presentation of a cryptic epitope that activates pathogenic autoreactive T cells. *Blood*. (2005) 105:1552–7. doi: 10.1182/blood-2004-08-3145
144. Yamaguchi Y, Seta N, Kaburaki J, Kobayashi K, Matsuura E, Kuwana M. Excessive exposure to anionic surfaces maintains autoantibody response to beta(2)-glycoprotein I in patients with antiphospholipid syndrome. *Blood*. (2007) 110:4312–8. doi: 10.1182/blood-2007-07-100008

145. Ryan BJ, Nissim A, Winyard PG. Oxidative post-translational modifications and their involvement in the pathogenesis of autoimmune diseases. *Redox Biol*. (2014) 2:715–24. doi: 10.1016/j.redox.2014.05.004
146. Matsuura E, Lopez LR. Are oxidized LDL/beta2-glycoprotein I complexes pathogenic antigens in autoimmune-mediated atherosclerosis? *Clin Dev Immunol*. (2004) 11:103–11. doi: 10.1080/10446670410001722186
147. Giannakopoulos B, Krilis SA. The pathogenesis of the antiphospholipid syndrome. *N Engl J Med*. (2013) 14:1033–44. doi: 10.1056/NEJMra1112830
148. de Laat B, van Berkel M, Urbanus RT, Siregar B, de Groot PG, Gebbink MF, et al. Immune responses against domain I of β(2)-glycoprotein I are driven by conformational changes: domain I of β(2)-glycoprotein I harbors a cryptic immunogenic epitope. *Arthritis Rheum*. (2011) 63:3960–8. doi: 10.1002/art.30633
149. Iverson GM, Reddel S, Victoria EJ, Cockerill KA, Wang YX, Marti-Renom MA, et al. Use of single point mutations in domain I of b2-glycoprotein I to determine fine antibody specificity of antiphospholipid autoantibodies. *J Immunol*. (2002) 169:7097–103. doi: 10.4049/jimmunol.169.12.7097
150. Ioannou Y, Pericleous C, Giles I, Latchman DS, Isenberg DA, Rahman A. Binding of antiphospholipid antibodies to discontinuous epitopes on domain I of human beta(2)-glycoprotein I: mutation studies including residues R39 to R43. *Arthritis Rheum*. (2007) 56:280–90. doi: 10.1002/art.22306
151. de Laat B, Pengo V, Pabinger I, Musial J, Voskuyl AE, Bultink IE, et al. The association between circulating antibodies against domain I of beta2-glycoprotein I and thrombosis: an international multicenter study. *J Thromb Haemost*. (2009) 7:1767–73. doi: 10.1111/j.1538-7836.2009.03588.x
152. Pengo V, Ruffatti A, Tonello M, Cuffaro S, Banzato A, Bison E. Antiphospholipid syndrome: antibodies to Domain 1 of β2-glycoprotein 1 correctly classifypatients at risk. *J Thromb Haemost*. (2015) 13:782–7. doi: 10.1111/jth.12865
153. Iwaniec T, Kaczor MP, Celinska-Löwenhoff M, Polanski S, Musiał J. Clinical significance of anti-domain 1 β2-glycoprotein I antibodies in antiphospholipid syndrome. *Thromb Res*. (2017) 153:90–4. doi: 10.1016/j.thromres.2017.02.019
154. Guo H, Zhang Y, Li A, Wang C, Yang S, Zhang Y, et al. Anti-domain 1 of beta2-glycoprotein I aids risk stratification in lupus anticoagulant-positive patients. *Clin Exp Med*. (2019). doi: 10.1007/s10238-019-00555-w. [Epub ahead of print].
155. Durigutto P, Grossi C, Borghi MO, Macor P, Pregnolato F, Raschi E, et al. New insight into antiphospholipid syndrome: antibodies to β2glycoprotein I-domain 5 fail to induce thrombi in rats. *Haematologica*. (2019) 104:819–26. doi: 10.3324/haematol.2018.198119
156. Andreoli L, Fredi M, Nalli C, Franceschini F, Meroni PL, Tincani A. Antiphospholipid antibodies mediate autoimmunity against dying cells. *Autoimmunity*. (2013) 46:302–6. doi: 10.3109/08916934.2013.783025
157. Shoenfeld Y, Blank M, Cervera R, Font J, Raschi E, Meroni PL. Infectious origin of the antiphospholipid syndrome. *Ann Rheum Dis*. (2006) 65:2–6. doi: 10.1136/ard.2005.045443
158. Hansen KE, Kong DF, Moore KD, Ortel TL. Risk factors associated with thrombosis in patients with antiphospholipid antibodies. *J Rheumatol*. (2001) 28:2018–24.
159. Girón-González JA, García del Río E, Rodríguez C, Rodríguez-Martorell J, Serrano A. Antiphospholipid syndrome and asymptomatic carriers of antiphospholipid antibody: prospective analysis of 404 individuals. *J Rheumatol*. (2004) 31:1560–7.
160. Aslani S, Mahmoudi M, Karami J, Jamshidi AR, Malekshahi Z, Nicknam MH. Epigenetic alterations underlying autoimmune diseases. *Autoimmunity*. (2016) 49:69–83. doi: 10.3109/08916934.2015.1134511
161. Schmidl C, Delacher M, Huehn J, Feuerer M. Epigenetic mechanisms regulating T-cell responses. *J Allergy Clin Immunol*. (2018) 142:728–43. doi: 10.1016/j.jaci.2018.07.014
162. Wu H, Deng Y, Feng Y, Long D, Ma K, Wang X, et al. Epigenetic regulation in B-cell maturation and its dysregulation in autoimmunity. *Cell Mol Immunol*. (2018) 15:676–84. doi: 10.1038/cmi.2017.133

Conflict of Interest Statement: The authors declare that the research was conducted in the absence of any commercial or financial relationships that could be construed as a potential conflict of interest.

frontiers in Immunology

ORIGINAL RESEARCH
published: 11 July 2019
doi: 10.3389/fimmu.2019.01476

Lifetime Pesticide Use and Antinuclear Antibodies in Male Farmers From the Agricultural Health Study

Christine G. Parks[1], Aline de Souza Espindola Santos[2], Catherine C. Lerro[3], Curt T. DellaValle[4], Mary H. Ward[3], Michael C. Alavanja[3], Sonja I. Berndt[3], Laura E. Beane Freeman[3], Dale P. Sandler[1] and Jonathan N. Hofmann[3]*

[1] Epidemiology Branch, National Institute of Environmental Health Sciences, Research Triangle Park, Durham, NC, United States, [2] Institute in Collective Health Studies, Federal University of Rio de Janeiro, Rio de Janeiro, Brazil, [3] Occupational and Environmental Epidemiology Branch, Division of Cancer Epidemiology and Genetics, National Cancer Institute, Bethesda, MD, United States, [4] All of Us Research Program, Office of the Director, National Institutes of Health, Bethesda, MD, United States

Farming and pesticide use have been associated with systemic autoimmune diseases, and while certain organochlorine insecticides and other pesticides are suspected to influence risk, the role of specific pesticides in the development of systemic autoimmunity is not known. We measured serum antinuclear autoantibodies (ANA) by immunofluorescence on Hep-2 cells in 668 male farmers in the study of Biomarkers of Exposure and Effect in Agriculture (BEEA; 2010–2013), an Agricultural Health Study (AHS) subcohort. We examined ANA in relation to lifetime use of 46 pesticides first reported at AHS enrollment (1993–1997) and updated at intervals through BEEA enrollment. Odds ratios (OR) and 95% confidence intervals (CI) were estimated after adjusting for age, state, education, season of blood draw, current pesticide use, and correlated pesticides. Having ANA antibodies (3 or 4+ intensity at a 1:80 dilution, 21% of study participants) was associated with a reported history of seeking medical care due to exposure to pesticides (OR 2.15; 95%CI 1.17, 3.95), use of the fumigant methyl bromide (OR 3.16; 95%CI 1.05, 9.5), and use of petroleum oil/distillates (OR 1.50; 95%CI 1.00, 2.25). Using a higher threshold (3 or 4+ at a 1:160 dilution, 9%) ANA positivity was associated with the carbamate insecticide aldicarb (OR 4.82; 95%CI 1.33, 17.5) and greater combined use of four cyclodiene organochlorine insecticides (top tertile of intensity-weighted lifetime days vs. no use; OR $_{T3}$ 3.20; 95%CI 1.10, 9.27). By contrast, greater use of non-cyclodiene organochlorine insecticides was inversely associated with ANA (1:80 dilution 3 or 4+, OR $_{T3}$ 0.24; 95%CI 0.08, 0.72). Specific autoantibodies (to extractable nuclear antigens and anti-dsDNA), measured on those with ANA detected at the 1:80 dilution 3 or 4+, were seen in 15 individuals (2%), and were associated with use of two or more cyclodiene organochlorine insecticides and several other pesticides (e.g., carbofuran, ethylene dibromide). These findings suggest that specific pesticide exposures may have long-term effects on ANA prevalence and support the hypothesis that certain organochlorine insecticides may increase the risk of developing systemic autoimmunity.

Keywords: epidemiology–analytic (risk factors), autoantibodies, pesticides, occupational epidemiology, cohort study (or longitudinal study)

OPEN ACCESS

Edited by:
Kenneth Michael Pollard, The Scripps Research Institute, United States

Reviewed by:
Ian P. Giles, University College London, United Kingdom
Marvin Fritzler, University of Calgary, Canada

****Correspondence:***
Christine G. Parks
parks1@mail.nih.gov

Specialty section:
This article was submitted to Autoimmune and Autoinflammatory Disorders, a section of the journal Frontiers in Immunology

Received: *29 March 2019*
Accepted: *13 June 2019*
Published: *11 July 2019*

Citation:
Parks CG, Santos AdSE, Lerro CC, DellaValle CT, Ward MH, Alavanja MC, Berndt SI, Beane Freeman LE, Sandler DP and Hofmann JN (2019) Lifetime Pesticide Use and Antinuclear Antibodies in Male Farmers From the Agricultural Health Study. Front. Immunol. 10:1476. doi: 10.3389/fimmu.2019.01476

INTRODUCTION

Farming occupation and pesticide use have been associated with elevated risk of systemic autoimmune diseases (1–9), but the role of specific pesticide exposures in the development of systemic autoimmunity is not known. Systemic autoimmunity, as measured by anti-nuclear antibodies (ANA; based on an intensity of 3+ or 4+ at the 1:80 titer), is estimated to occur in 12 to 16% of the US population ages 12 and older, with higher rates in women and older adults (10). Overall ANA positivity, including lower levels of ANA (i.e., at the 1:40 titer), is even more common, seen in almost a third of healthy adults (11). By contrast, higher level ANA (i.e., 1:160 titer and higher) are considered more likely to be clinically relevant; elevated ANA are typically present in patients with systemic lupus erythematosus, an uncommon autoimmune disease, and ANA prevalence is often elevated in family members and patients with other systemic autoimmune diseases (12, 13).

Various pesticides have immunotoxic effects and case series have suggested associations with autoantibodies (14). Only a few epidemiologic studies have examined ANA in relation to specific agricultural pesticides. In a cross-sectional study of Canadian farmers, ANA prevalence was significantly higher in association with use of some, but not all organochlorine insecticides (15). In another similar study from the same region, both positive and inverse associations were seen for ANA with the recent use of different herbicides and fungicides, though estimates were imprecise due to small sample size (16). Other studies have examined serum levels of organochlorine pesticides in relation to ANA, with inconsistent findings (17–19).

In the current study, we examined associations of lifetime pesticide use with ANA in a sample of male farmers from the Biomarkers of Exposure and Effect in Agriculture (BEEA) study in the Agricultural Health Study (AHS) (20), a large prospective cohort that includes farmers in Iowa and North Carolina (21). Cross-sectional studies show that ANA prevalence rises slowly with age over several decades (10, 22, 23). In theory, the loss of immune tolerance enabling the production of antibodies to self-antigens may occur at any time in the past, thereby conferring life-long potential to produce ANA. Therefore, our analyses focused on the association of ANA with lifetime exposures to pesticides, with a specific focus on the organochlorine insecticides.

METHODS

Study Population and Sample

The design and methodology for enrollment and specimen collection in the AHS and BEEA study have been described (20, 21). BEEA participants were recruited from among the male private pesticide applicators in the AHS who were ≥50 years of age, resided in Iowa or North Carolina, had completed the AHS enrollment questionnaire as well as two follow-up interviews (in 1999–2003 and 2005–2010), and had never been diagnosed with cancer (other than non-melanoma skin cancer). In the current investigation, we assessed ANA and other markers of autoimmunity in 699 participants enrolled in BEEA between June 2010 and September 2013. Because a diagnosis of autoimmune disease might have influenced pesticide use or reporting, we excluded 31 individuals who reported a doctor diagnosis of systemic autoimmune disease at AHS enrollment, for a final analysis sample of 668 participants. The study was approved by Institutional Review Boards at the National Cancer Institute and other participating institutions, and all participants provided written informed consent.

Questionnaire Data

Lifetime history of 50 specific pesticides was assessed based on participant report at AHS enrollment in 1993–1997. Pesticide use was updated in two follow-up surveys in 1999–2003 and 2005–2010, and at BEEA enrollment. All participants completed these four questionnaires, and 62% ($N = 410$) also completed a "take-home" questionnaire at AHS enrollment that solicited additional detailed information on the use of 28 of the pesticides, including organochlorine insecticides. The enrollment questionnaire also ascertained information about days per year and years of use pesticides overall, along with mixing and application practices, use of protective equipment, and repairing equipment. Data were updated in the follow-up surveys and used to derive intensity-weighted lifetime days of use (24). In the enrollment questionnaire, participants were also asked whether they had ever sought medical care or been hospitalized due to pesticide exposure, and in the take home questionnaire they were asked about high pesticide exposure events (HPEE) and whether they ever had ever been diagnosed with pesticide poisoning (25). Data on HPEE, medical treatment and pesticide poisoning were updated in follow-up surveys and combined as a single variable with three levels: (1) any medical treatment due to pesticides or pesticide poisoning diagnosis, (2) HPEE without medical treatment, and (3) neither. A health history, including diagnosis with rheumatoid arthritis and systemic lupus erythematosus, was collected at enrollment and throughout follow-up. BEEA enrollment questionnaires also collected data on current medication use, which were used to identify use of disease modifying antirheumatic drugs (DMARDs) and non-steroidal anti-inflammatory drugs. Questionnaires are available at https://aghealth.nih.gov/collaboration/questionnaires.html; the primary DMARD medications reported included methotrexate and hydroxychloroquine, as well as leflunomide, sulfasalazine, azathioprine, mycophenolate mofetil, cyclosporine, and biologics, but not steroids.

Assays

Non-fasting blood specimens were collected in the participant's home and transported and shipped cold via overnight delivery before processing, aliquoting, and storage at −80°C. Antinuclear antibodies (ANA) were measured by the gold standard immunofluorescence assay for serum samples under a standardized protocol in a clinical rheumatology laboratory with prior experience with high-throughput testing in epidemiologic studies (26); in brief, ANA were detected using HEp-2 cell slides (Kallestad, Bio-Rad Laboratories, Hercules, CA), incubated with a 1:80 dilution of sera, then washed and incubated with the burro anti-human polyvalent immunoglobulin FITC conjugate (Kallestad) read using fluorescent microscopy (Leitz

Fluorescence Scope, 50/1.0 magnification). Samples with a positive ANA (3 or 4+ at the 1:80 dilution) were subsequently tested for extractable nuclear autoantibodies (ENA), including RNP, SM, SSA (combined 52 and 60 kDa) and SSB (QUANTA Lite, Inova Diagnostics, San Diego, CA; RNP/SM/SSB—ochterlony; SSA—ELISA) and anti-dsDNA antibodies (EIA, Kallenstad). Anti-citrullinated peptide (anti-CCP) antibodies, specific for rheumatoid arthritis (27), were measured by second-generation ELISA; any detectable anti-CCP were seen in 2.3% of the study sample and <1% were positive based on a clinical cut-point of 25 AU/ml, within the expected prevalence in the general population (27). Testing for anti-TPO antibodies was previously described, with antibodies seen in 9% of the study sample (28). Coefficients of variation were <10% for all assays. Frequencies are shown in **Supplemental Table 1**.

Analyses

Three cut-points for ANA positivity were considered: first, ANA prevalence was based on a rating of 3+ or 4+ at 1:80 dilution, similar to recently published population-level data on ANA (10). We then lowered the cut-point, by including lower-level ANA, i.e., those with a rating of 2+ at 1:80 dilution, similar to a positive reading at the 1:40 dilution used in prior studies. Finally, we raised the cut-point in analyses limited to those with higher titer ANA based on having 3+ or 4+ intensity rating at the 1:160 dilution. Only five individuals had a positive reading (3+) at the 1:320 level (one with anti-dsDNA antibodies), so these were not considered separately. These groups are labeled as "Any" (≥1:80 2+), "Moderate-higher" (≥1:80 3+) and Higher (≥1:160 3+), to indicate the increasing threshold for positivity. Three sets of models were run comparing the different definitions of ANA positives to those with no detectable ANA, using logistic regression to calculate odds ratios (OR) and 95% confidence intervals (CIs), adjusting for age and other covariates at BEEA enrollment (i.e., BMI, state, education, season of blood draw, and use of agricultural pesticides in the past 12 months). We considered a p-value of <0.05 to be statistically significant, and a value of 0.05 to <0.10 as suggestive. Associations were estimated for lifetime use of pesticides (overall, and for use of 46 specific pesticides with at least five ANA positive participants exposed). We also adjusted for correlated pesticides (Spearman's rho ≥0.40 in the sample, **Supplemental Table 2**) when confounding was observed, i.e., inclusion in the model changed the effect estimate by at least 10%.

We explored intensity-weighted lifetime days for individual organochlorine insecticides (**Supplemental Table 3**), but numbers were smaller due to a lack of data on those who did not complete the take-home questionnaire, and we saw no clear exposure-response patterns. To increase statistical power, we also grouped the OCs into two groups based on similarities in structure and function. We then tested the hypothesis that ANA was related to use of certain organochlorine insecticides, examining exposure-response relationships across cumulative intensity-weighted lifetime days for two groups of insecticides, summing the intensity-weighted lifetime days for each individual pesticide in the group: cyclodienes (aldrin, dieldrin, chlordane, and heptachlor) and other organochlorines (DDT, toxaphene, and lindane). These two groups were correlated (rho = 0.53 for any use), so they were run in a mutually adjusted model. Finally, we explored the frequency of disease-specific autoantibodies (i.e., ENA and anti-dsDNA autoantibodies) by pesticide use, including combined organochlorine variables (e.g., none, 1, or 2 or more cyclodienes used), and estimated age-adjusted ORs to describe these associations. Sensitivity analyses excluded potential incident cases of autoimmune disease, i.e., based on self-reported rheumatoid arthritis or other autoimmune disease, DMARD use, or the presence of anti-thyroid or anti-citrullinated peptide autoantibodies identified during AHS follow-up or at BEEA enrollment.

RESULTS

Of 668 samples tested, 282 (42%) had detectable ANA: 143 (21%) had any detectable ANA (i.e., ≥1:80 dilution at 2+ intensity reading), 139 (21%) had ANA detected at ≥1:80 3 or 4+ and 60 (9%) had ANA detectable at 1:160 3 or 4+. Sample characteristics by ANA status are shown in **Table 1**. Participants with ANA were older: those over age 60 years had two to three times the odds of having moderate to higher-levels of ANA (at ≥1:80 3 or 4+) compared with those ages 50–55 years. After adjusting for age, no associations were noted for smoking status, BMI, state, current farming status and season at the time of blood draw. During follow-up or at BEEA enrollment, 44 participants reported an incident diagnosis of an autoimmune disease, which was associated with overall ANA (OR 3.62; 95%CI 1.87, 6.98) (**Supplemental Table 1**). Among those with moderate to high level ANA, 15 (2% of the total sample) had disease-specific autoantibodies, i.e., ENA ($n = 6$) or anti-dsDNA ($n = 11$).

Neither lifetime years nor average days per year of any pesticide use at AHS enrollment was associated with ANA positivity (**Table 2**). However, having sought medical care due to pesticide exposure was associated with having moderate to high level ANA (OR 2.15; 95%CI 1.17, 3.95). In analyses of specific pesticides (**Table 3**), we saw suggestive associations of high ANA with lifetime use of the organochlorine insecticide heptachlor (OR 1.93; 95%CI 0.96, 3.90) and the organophosphate insecticide diazinon (OR 1.64; 95%CI 0.92, 2.92), and a significant association with the carbamate insecticide aldicarb (OR 4.82; 95%CI 1.33, 17.5). Moderate to high level ANA were associated with the fumigant methyl bromide (OR 3.16; 95%CI 1.05 to 9.50), and suggestively associated with use of petroleum oil/distillates as an herbicide (OR 1.50; 95%CI 1.00, 2.25). By contrast, overall ANA (low, moderate, or high) were inversely associated with the organophosphate insecticides fonofos (OR 0.72; 95%CI 0.50, 1.00) and malathion (OR 0.62; 95%CI 0.42, 0.91), and the herbicide butylate (OR 0.72; 95%CI 0.52, 0.99).

We examined the relationship of ANA with intensity-weighted lifetime days of use for organochlorines grouped as cyclodienes (heptachlor, chlordane, aldrin, and dieldrin) and non-cyclodienes (DDT, lindane, toxaphene), in a mutually adjusted model (**Table 4**). Prevalence of high ANA was associated

TABLE 1 | Participant characteristics and age-adjusted associations with ANA.

Characteristics[3]	ANA Level[1]				Age-adjusted OR (95% CI)[2]		
	Negative *N* = 386	1:80 2+ *N* = 143	1:80 3/4+ *N* = 79	1:160 3/4+ *N* = 60	Any ANA (≥1:80 2+) vs. none	Moderate-higher ANA (≥1:80 3/4+) vs. none	Higher ANA (≥1:160 3/4+) vs. none
	N (%)						
Age (years)							
50–55	84 (22)	24 (17)	12 (15)	7 (12)	Referent	Referent	Referent
56–60	102 (26)	34 (24)	14 (18)	5 (8)	1.02 (0.62, 1.67)	0.82 (0.41, 1.66)	0.59 (0.18, 1.92)
61–70	107 (28)	39 (27)	28 (35)	24 (40)	1.66 (1.05, 2.64)	2.15 (1.18, 3.91)	2.69 (1.11, 6.55)
70+	93 (24)	46 (32)	25 (32)	24 (40)	2.00 (1.25, 3.18)	2.33 (1.27, 4.27)	3.10 (1.27, 7.56)
Smoked							
Past	120 (31)	53 (37)	30 (38)	36 (60)	1.21 (0.86, 1.70)	1.15 (0.76, 1.77)	1.06 (0.59, 1.92)
Current	14 (4)	8 (6)	4 (5)	3 (5)	1.74 (0.82, 3.67)	1.73 (0.68, 4.45)	NA
BMI							
Overweight	166 (43)	74 (52)	38 (48)	24 (42)	1.38 (0.89, 2.16)	1.47 (0.82, 2.64)	1.06 (0.49, 2.32)
Obese	150 (39)	44 (31)	32 (41)	25 (42)	1.17 (0.74, 1.86)	1.58 (0.87, 2.87)	1.32 (0.60, 2.89)
Used agricultural pesticides, past year	288 (75)	100 (70)	54 (68)	39 (65)	0.90 (0.63, 1.30)	0.91 (0.58, 1.44)	0.92 (0.49, 1.71)
Spring/summer[4]	206 (53)	76 (53)	39 (49)	37 (62)	1.03 (0.75, 1.40)	1.07 (0.72, 1.58)	1.44 (0.82, 2.54)
State (NC)	54 (14)	18 (13)	11 (14)	9 (15)	0.93 (0.57, 1.34)	0.88 (0.55, 1.55)	0.88 (0.40, 1.93)

NC, North Carolina; NA, not applicable due to fewer than five exposed cases.

[1]ANA Level shows four exclusive categories of ANA positivity based on highest reading observed; Negative, none detected at 1:80 dilution.

[2]Odds Ratios (ORs) and 95% Confidence Intervals (CI) were calculated by logistic regression models adjusted for age at interview; "Any ANA," "Moderate-higher ANA," and "Higher ANA" indicate increasing thresholds for positivity used for modeling.

[3]All were current at BEEA enrollment, except for state at AHS study enrollment.

[4]Blood collected in spring or summer, compared to fall or winter.

with being in the top tertile of intensity-weighted lifetime days of combined cyclodiene use vs. no use (OR_{T3} 3.20; 95%CI 1.10, 9.27). By contrast, greater use of non-cyclodiene organochlorines was inversely associated with moderate to high ANA (OR_{T3} 0.24; 95%CI 0.08, 0.72), which was similar to the association with greater DDT use (OR 0.35; 95%CI 0.13, 0.99, above the median intensity-weighted lifetime days; **Supplemental Table 3**).

In age adjusted models, having specific ENA or anti-dsDNA autoantibodies was associated with using two or more cyclodiene organochlorine insecticides, and with fonofos, cyanazine, and ethylene dibromide (**Table 5**). Because these comparisons are based on only a small number of participants with ENA or anti-dsDNA autoantibodies, confidence limits were wide, and we did not adjust these models for other covariates or correlated pesticides. All but one of the participants with disease-specific autoantibodies used carbofuran ($p = 0.002$). We also saw suggestive associations of disease-specific autoantibodies with aldicarb and methyl bromide, and an inverse association with malathion. Sensitivity analyses showed no substantial impact of excluding participants with a potential autoimmune disease during follow-up or at BEEA enrollment, i.e., who reported an incident diagnosis of an autoimmune disease since enrollment, or used disease-specific antirheumatic drugs, or were positive for thyroid or anti-CCP autoantibodies (not shown).

DISCUSSION

Our findings provide evidence that moderate to higher level ANA are associated with past use of specific pesticides and a history of seeking medical care for pesticide exposures in male farmers. Further, our results support the hypothesis that certain types of organochlorine insecticides may increase risk of developing autoimmunity. Two other pesticides, the carbamate insecticide aldicarb, and fumigant methyl bromide, were associated with increased odds of having moderate or higher-level ANA. By contrast, two of more commonly used organophosphate insecticides (in this sample), malathion and fonofos, and the herbicide butylate, were related to lower overall ANA. Together, these results suggest complex and lasting effects of some pesticides on autoimmunity.

Systemic autoimmune diseases are more common in reproductive age women, so past studies have been interested in the potential endocrine-disrupting effects of organochlorine pesticides on autoimmunity. Experimental and epidemiologic studies suggest a nuanced relationship. For example, the insecticide chlordecone (a cyclodiene) accelerated in a dose-dependent fashion the development of disease-specific anti-dsDNA autoantibodies in ovariectomized female mice in the NZB X NZW(F1) model of lupus (29). However, these effects did not appear to be mediated by estrogen-related mechanisms and did not extend to DDT. A recent study of a U.S. population

TABLE 2 | ANA associations with lifetime pesticide use and high pesticide exposure events.

Overall pesticide use	ANA Level[1]				Adjusted OR (95% CI)[2]		
	Negative *N* = 386	1:80 2+ *N* = 143	1:80 3/4+ *N* = 79	1:160 3/4+ *N* = 60	Any ANA (≥1:80 2+) vs. none	Moderate-higher (≥1:80 3/4+) ANA vs. none	Higher ANA (≥1:80 3/4+) vs. none
	N (%)						
MIXED OR APPLIED PESTICIDES – ENROLLMENT							
Years							
≤10	65 (18)	22 (16)	12 (16)	9 (15)	Referent	Referent	Referent
11–20	128 (35)	53 (38)	21 (27)	16 (27)	1.07 (0.66, 1.73)	0.88 (0.47, 1.65)	0.92 (0.38, 2.23)
21-30	130 (35)	47 (33)	33 (43)	26 (43)	1.04 (0.64, 1.69)	1.11 (0.61, 2.03)	1.11 (0.48, 2.58)
30+	47 (13)	19 (14)	11 (14)	9 (15)	0.78 (0.41, 1.55)	0.68 (0.31, 1.53)	0.60 (0.20, 1.81)
Average days/year							
<10	155 (42)	56 (40)	33 (43)	31 (53)	Referent	Referent	Referent
10–19	125 (34)	49 (35)	11 (14)	13 (15)	0.90 (0.62, 1.31)	0.70 (0.43, 1.14)	0.52 (0.26, 1.05)
20+	89 (24)	36 (25)	18 (23)	15 (25)	1.07 (0.71, 1.60)	0.95 (0.57, 1.57)	0.91 (0.45, 1.81)
HIGH EXPOSURE EVENTS/MEDICAL CARE/POISONING[3]							
Yes, but did not seek care	47 (12)	24 (17)	11 (14)	6 (10)	1.37 (0.86, 2.18)	1.22 (0.66, 2.25)	0.94 (0.37, 2.35)
Sought medical care	29 (8)	9 (6)	15 (18)	7 (12)	1.47 (0.85, 2.52)	**2.15 (1.17, 3.95)**	1.41 (0.58, 3.46)

NA, not applicable due to fewer than five ANA positive individuals who were exposed.

[1]ANA Level shows four exclusive categories of ANA positivity based on highest reading observed.

[2]Odds Ratios (ORs) and 95% Confidence Intervals (CI) were calculated by multivariable logistic regression models adjusted for age at interview, state, overweight/obese, ever smoked, spring, or summer season, current occupational pesticides use. Bold shows ORs that are statistically significant at $p < 0.05$.

[3]Ever had a high pesticide exposure event (without seeking medical care for pesticides), or were diagnosed with pesticide poisoning, hospitalized or saw a doctor due to pesticide exposure; referent group is those who did not report a high pesticide exposure event or seeking medical care for pesticide use.

sample ($N = 4{,}340$; National Health and Examination Survey, 1999–2004) reported no significant associations of measured organochlorines with moderate or higher ANA (3+ or 4+ at the 1:80 titer) after adjusting for multiple comparisons (17); in men, however, ANA was negatively associated with the DDT metabolite, DDE, and oxychlordane (a chlordane metabolite) at the $p < 0.05$ level. By contrast, in a small sample of African-American male farmers, higher DDE levels were suggestively (but non-significantly) associated with ANA (1:40 titer, equivalent to "overall" in the current study) (19). This later sample was selected from the population of rural eastern North Carolina as an add-on study to the AHS (non-overlapping with the current study sample); participants had an average of 2.2 (SD 5.5) years of DDT use and 12.3 (SD 13.4) years of overall pesticide use. In the current study sample, prevalence of high or moderate ANA was associated with greater intensity-weighted lifetime days using any of the four cyclodiene organochlorine insecticides (i.e., aldrin, dieldrin, chlordane, and heptachlor), and inversely associated with greater use of the non-cyclodiene organochlorine insecticides (especially DDT). Notably, DDT and the cyclodiene insecticides are no longer in use in the U.S., but our results suggest persistent effects on immunity decades later.

Our analyzing cyclodienes separately from the other organochlorines had both empirical and theoretical rationale. In analyses of ever-use of the individual organochlorine insecticides, we saw suggestive positive associations with heptachlor and chlordane, but not with DDT. This was consistent with results by Rosenberg et al. who reported that ANA prevalence was associated with lifetime organochlorine use, *excluding* DDT and methoxychlor in a sample of 322 rural adults (15). Organochlorine insecticides share a chlorinated hydrocarbon structure and physical properties such as lipid solubility and environmental persistence. Their toxic effects on insects are due to hyperexcitation of nerve cells. The DDT-type chemicals work by perturbing sodium gates, while the cyclodiene insecticides impact the γ-aminobutyric acid (GABA) receptor, impairing chlorine influx (30). While GABA is best known as a neurotransmitter, emerging evidence suggests an important role in immune function and innate immunity (31, 32). The closely related cyclodienes, chlordane, and heptachlor, have been associated with ANA in case series (33). Similar studies of aldrin and its breakdown product, dieldrin, were not identified in the autoimmunity literature, but there is some evidence of immunosuppressive effects of aldrin/dieldrin across different studies (34–36). In our data, having used two or more of these pesticides was also associated with having any of the disease-specific autoantibodies (e.g., anti-dsDNA autoantibodies). Together, these findings suggest these pesticides may increase the risk of developing clinically relevant autoimmunity. Lindane, a cyclohexane, also impacts GABA receptor function, but we saw limited evidence of an association with ANA. Besides their neurotoxicity, organochlorine pesticides can have other effects, for example endocrine disruption through estrogen or pregnane X receptors (37, 38), so targeted research is needed to identify which pathways may impact autoimmunity.

TABLE 3 | Antinuclear antibodies and lifetime use of insecticides.

Pesticide name	ANA Level[1]				Adjusted OR (95% CI)[2]		
	Negative *N* = 386	1:80 2+ *N* = 140	1:80 3/4+ *N* = 79	1:160 3/4+ *N* = 60	Any ANA (≥1:80 2+) vs. none	Moderate-higher (≥1:80 3/4+) vs. none	Higher (≥1:160 3/4+) vs. none
	N (%)						
INSECTICIDES							
Organochlorines							
Cyclodienes							
Aldrin[3]	81 (22)	32 (23)	23 (30)	21 (36)	0.96 (0.61, 1.50)	1.21 (0.70, 2.09)	1.08 (0.51, 2.28)
Chlordane	103 (27)	40 (29)	27 (35)	24 (41)	1.16 (0.81, 1.67)	1.35 (0.86, 2.11)	1.44 (0.78, 2.65)
Dieldrin[3]	31 (8)	19 (14)	7 (9)	8 (14)	1.06 (0.59, 1.91)	0.81 (0.39, 1.71)	0.89 (0.34, 2.33)
Heptachlor[3]	70 (19)	37 (27)	18 (24)	20 (35)	1.50 (0.98, 2.29)	1.50 (0.88, 2.54)	1.93 (0.96, 3.90)
Others							
DDT[3]	86 (23)	37 (26)	20 (27)	16 (28)	0.79 (0.51, 1.23)	0.68 (0.39, 1.20)	0.55 (0.25, 1.18)
Lindane	110 (29)	43 (30)	24 (30)	20 (33)	1.04 (0.74, 1.48)	1.07 (0.69, 1.65)	1.12 (0.64, 2.04)
Toxaphene[3]	57 (15)	21 (15)	15 (20)	10 (18)	0.95 (0.58, 1.55)	0.96 (0.53, 1.57)	0.78 (0.48, 1.81)
Organophosphates							
Phosphorothioates							
Chlorpyrifos	211 (55)	79 (55)	47 (60)	35 (58)	1.17 (0.85, 1.61)	1.32 (0.87, 1.98)	1.35 (0.76, 2.40)
Coumaphos	39 (10)	16 (11)	9 (11)	8 (13)	1.18 (0.72, 1.95)	1.24 (0.67, 2.31)	1.38 (0.60, 3.16)
Diazinon	112 (29)	50 (35)	22 (28)	26 (43)	1.25 (0.88, 1.76)	1.18 (0.77, 1.83)	1.64 (0.92, 2.92)
Phosphorodithioates							
Dichlorvos	66 (17)	23 (16)	10 (13)	11 (18)	0.85 (0.55, 1.30)	0.80 (0.46, 1.39)	1.02 (0.50, 2.11)
Fonofos	136 (35)	39 (27)	24 (30)	21 (35)	0.72 (0.50, 1.00)	0.80 (0.52, 1.24)	0.93 (0.51, 1.70)
Parathion	53 (14)	20 (14)	10 (13)	6 (11)	0.80 (0.49, 1.28)	0.66 (0.35, 1.22)	0.53 (0.21, 1.33)
Malathion	318 (82)	99 (69)	66 (84)	46 (77)	**0.62 (0.42, 0.91)**	0.87 (0.53, 1.45)	0.67 (0.34, 1.30)
Phorate	158 (41)	57 (40)	30 (38)	21 (35)	0.83 (0.59, 1.16)	0.76 (0.50, 1.17)	0.70 (0.38, 1.27)
Terbufos	212 (55)	70 (49)	42 (53)	29 (48)	0.82 (0.59, 1.14)	0.89 (0.59, 1.34)	0.82 (0.46, 1.46)
Carbamates							
Carbofuran	144 (37)	42 (29)	29 (37)	24 (40)	0.79 (0.57, 1.10)	0.95 (0.63, 1.44)	1.02 (0.58, 1.79)
Carbaryl	204 (53)	72 (50)	43 (54)	35 (58)	0.95 (0.69, 1.31)	1.05 (0.70, 1.58)	1.12 (0.63, 1.99)
Aldicarb[3]	20 (5)	7 (5)	6 (8)	7 (12)	1.44 (0.65, 3.18)	2.33 (0.89, 6.11)	**4.82 (1.33, 17.5)**
Pyrethroids							
Permethrin	145(38)	55 (39)	34 (43)	16 (27)	1.03 (0.74, 1.44)	1.00 (0.66, 1.53)	0.66 (0.35,1.24)
HERBICIDES							
Phenoxy							
2,4-D	338 (88)	120 (84)	68 (86)	56 (93)	0.84 (0.52, 1.37)	1.10 (0.57, 2.11)	1.84 (0.61, 5.54)
2,4,5-T	102 (26)	38 (27)	32 (41)	19 (32)	1.10 (0.77, 1.57)	1.33 (0.86, 2.06)	0.97 (0.52, 1.80)
2,4,5-TP	39 (10)	18 (13)	13 (17)	6 (10)	1.27 (0.77, 2.07)	1.27 (0.69, 2.34)	0.81 (0.32, 2.06)
Triazines							
Atrazine	331 (86)	125 (88)	71 (90)	54 (90)	1.28 (0.78, 2.07)	1.48 (0.77, 2.84)	1.51 (0.60, 3.84)
Cyanazine	207 (54)	76 (53)	37 (47)	35 (58)	0.91 (0.65, 1.26)	0.88 (0.58, 1.34)	1.20 (0.66, 2.17)
Metribuzin[3]	209 (54)	76 (53)	44 (56)	33 (55)	1.19 (0.82, 1.72)	1.15 (0.72, 1.83)	0.86 (0.44, 1.66)
Other							
Chlorimuron ethyl	150 (46)	68 (48)	34 (48)	28 (47)	1.23 (0.89, 1.69)	1.05 (0.70, 1.58)	0.91 (0.51, 1.62)
Metolachlor	221 (57)	78 (54)	41 (52)	38 (63)	0.98 (0.71, 1.35)	1.05 (0.7, 1.58)	1.43 (0.80, 2.58)
Alachlor	247 (64)	88 (62)	56 (71)	41 (68)	1.10 (0.79, 1.53)	1.37 (0.89, 2.10)	1.34 (0.73, 2.43)
EPTC	82 (21)	27 (19)	11 (14)	14 (23)	0.86 (0.58, 1.28)	0.84 (0.50, 1.40)	1.19 (0.61, 2.33)
Butylate	190 (49)	57 (40)	31 (39)	34 (57)	**0.72 (0.52, 0.99)**	0.83 (0.55, 1.25)	1.21 (0.68, 2.15)
Imazethapyr	178 (46)	71 (49)	38 (48)	28 (47)	1.04 (0.74, 1.46)	1.00 (0.65, 1.53)	0.98 (0.53, 1.78)
Dicamba	268 (69)	99 (69)	58 (73)	53 (72)	1.11 (0.75, 1.64)	1.33 (0.79, 2.22)	1.33 (0.64, 2.75)
Paraquat	87 (23)	28 (20)	19 (24)	12 (20)	0.88 (0.59, 1.31)	0.93 (0.57, 1.52)	0.80 (0.39, 1.63)

(Continued)

TABLE 3 | Continued

Pesticide name	ANA Level[1]				Adjusted OR (95% CI)[2]		
	Negative *N* = 386	1:80 2+ *N* = 140	1:80 3/4+ *N* = 79	1:160 3/4+ *N* = 60	Any ANA (≥1:80 2+) vs. none	Moderate-higher (≥1:80 3/4+) vs. none	Higher (≥1:160 3/4+) vs. none
	N (%)						
Glyphosate	353 (92)	129 (90)	73 (92)	54 (90)	0.99 (0.57, 1.73)	1.08 (0.53, 2.21)	0.88 (0.34, 2.26)
Trifluralin	208 (54)	73 (51)	36 (46)	35 (58)	0.84 (0.61, 1.15)	0.81 (0.54, 1.22)	1.05 (0.59, 1.87)
Pendimethalin	193 (50)	70 (49)	44 (56)	29 (48)	1.02 (0.75, 1.41)	1.11 (0.74, 1.66)	0.92 (0.43, 1.62)
Petroleum Oil/Distillates	204 (53)	83 (58)	50 (63)	38 (63)	1.34 (0.97, 1.84)	1.50 (1.00, 2.25)	1.48 (0.83, 2.62)
FUNGICIDES AND FUMIGANTS							
Ethylene dibromide[3]	13 (3)	8 (6)	3 (4)	3 (5)	2.06 (0.84, 5.08)	1.93 (0.61, 6.10)	NA
Maneb/Mancozeb[3]	25 (6)	11 (8)	6 (7)	2 (3)	0.85 (0.40, 1.79)	0.50 (0.18, 1.40)	NA
Methyl bromide[3]	25 (6)	9 (6)	8 (10)	7 (12)	1.94 (0.82, 4.60)	**3.16 (1.05, 9.50)**	3.61 (0.79, 16.6)
Aluminum phosphide	23 (6)	16 (11)	4 (5)	3 (5)	1.38 (0.75, 2.53)	0.81 (0.34, 1.96)	NA
Benomyl[3]	26 (7)	10 (7)	4 (5)	2 (3)	0.55 (0.25, 1.21)	0.42 (0.14, 1.22)	NA
Captan	53 (14)	21 (15)	14 (18)	7 (12)	1.06 (0.68, 1.66)	1.08 (0.62, 1.88)	0.79 (0.34, 1.84)
Metalaxyl[3]	74 (19)	25 (18)	16 (20)	12 (20)	0.92 (0.59, 1.44)	0.94 (0.54, 1.64)	0.94 (0.43, 2.05)

NA, not applicable due to fewer than five ANA positive individuals who were exposed.

[1]ANA Level shows four exclusive categories of ANA positivity based on highest reading observed.

[2]Reported ever use at AHS enrollment (1993–1997) based on list of 50 specific pesticides, with updated use throughout follow-up and BEEA enrollment; included in table if at least five ANA positive individuals exposed to individual pesticides.

[3]Odds Ratios (ORs) and 95% Confidence Intervals (CI) were calculated by multivariable logistic regression models adjusted for age at interview, state, overweight/obese, ever smoked, spring or summer season, current occupational pesticides use. Bold shows ORs that are statistically significant at $p < 0.05$.

*[4]Mutually adjusted for correlated pesticides (see **Supplemental Table 2**).*

The carbamate insecticide aldicarb was the only other insecticide associated with high ANA; although it has a high acute toxicity, its immune effects are not well-known (39–41). The other carbamate insecticides, carbaryl and carbofuran, were not associated with elevated ANA. However, all but one of the participants with disease-specific autoantibodies had used carbofuran. High ANA was suggestively associated with the organophosphate insecticide diazinon, and we noted increased ORs for the two other phosphorothioates, chlorpyrifos, and coumaphos, though neither was statistically significant. These chemicals have documented immunotoxic effects (42–45). Conversely, the phosphoro*di*thioate insecticides fonofos and malathion were inversely associated with overall ANA, and the other phosphoro*di*thioate insecticides also showed inverse, though not statistically significant, associations with overall ANA. There is some evidence of immunosuppression by malathion (46), while other studies (including in a MRL-lpr lupus mouse model) suggest that malathion may stimulate and accelerate the onset and intensity of the autoimmune response (47, 48). Immune effects of fonofos are not described in the literature, and our findings seem somewhat paradoxical; while inversely associated with overall ANA, fonofos was positively associated with disease-specific autoantibodies in those with moderate to high ANA compared with no ANA detected. The primary mechanism of action for organophosphate and carbamate insecticides is blocking acetylcholinesterase enzyme. Given cholinergic receptors on human lymphocytes, pesticides may influence the immune response through acetylchlolinergic pathways, though the direction of effects may depend on the activated pathway (49, 50). The phosphoro*di*thioates require oxidative activation *in vivo*. However, it is unclear how this would differentially influence immune-related mechanisms of action compared with the other organophosphates and carbamates.

We also saw an association of high or moderate level ANA with the fumigant methyl bromide. Ethylene dibromide was also associated with disease-specific autoantibodies. Immune-related mechanisms of these highly toxic chemicals are not well-described in the literature, although one study suggested a similar threshold for immune modulation and the level at which acute toxicity occurred (51, 52). Along with aldicarb and carbofuran, methyl bromide and ethylene dibromide are often used against nematodes. Many participants with elevated ANA and disease-specific autoantibodies used more than one of these chemicals, but we did not have sufficient sample size to examine them independently. Use of petroleum oil or distillates was also associated with high or moderate ANA. Petroleum oil is a plausible candidate for inducing systemic autoimmunity, given the model of pristane-induced lupus (53). Pristane is a byproduct of petroleum distillation and induces lupus-like autoantibodies and clinical disease in mice. Petroleum distillates in the past may also have included other contaminants such as benzene or xylene. Overall ANA prevalence was inversely associated with butylate, a thiocarbamate herbicide, linked to lymphohematopoetic cancers and NHL in the AHS (54), but immune effects are not described in the literature. Interestingly, past use of butylate and recent use of malathion were associated with shorter leukocyte telomere length, a potential marker of immune aging, in a different subsample of AHS participants (55).

TABLE 4 | ANA associations with intensity-weighted lifetimes days of organochlorine use.

Intensity weighted lifetime days[2]	ANA Level[1]				Adjusted OR (95% CI)[3]		
	Negative *N = 227*	1:80 2+ *N = 88*	1:80 3/4+ *N = 51*	1:160 3/4+ *N = 40*	Any ANA (≥1:80 2+) vs. none	Moderate-higher (≥1:80 3/4+) vs. none	Higher (≥1:160 3/4+) vs. none
	N (%)						
Cyclodienes[4]							
None	151 (66)	57 (65)	32 (63)	20 (50)	1.0 (referent)	1.0 (referent)	1.0 (referent)
Tertile 1	23 (10)	13 (15)	8 (16)	4 (10)	1.29 (0.66, 2.49)	1.40 (0.62, 3.17)	1.27 (0.38, 4.24)
Tertile 2	29 (13)	10 (11)	4 (8)	6 (14)	0.76 (0.38, 1.51)	0.84 (0.36, 1.99)	1.14 (0.38, 3.42)
Tertile 3	24 (11)	8 (9)	7 (14)	10 (25)	1.33 (0.64, 2.75)	**2.58 (1.09, 6.09)**	**3.20 (1.10, 9.27)**
Other OC[3]							
None	147 (65)	55 (63)	35 (69)	26 (65)	1.0 (referent)	1.0 (referent)	1.0 (referent)
Tertile 1	22 (10)	13 (15)	9 (18)	3 (8)	1.23 (0.63, 2.41)	1.14 (0.50, 2.60)	0.62 (0.16, 2.40)
Tertile 2	29 (13)	8 (9)	5 (10)	7 (17)	0.78 (0.41, 1.51)	0.82 (0.37, 1.79)	0.95 (0.35, 2.57)
Tertile 3	29 (13)	12 (14)	2 (4)	4 (10)	0.58 (0.28, 1.23)	**0.24 (0.08, 0.72)**	0.26 (0.07, 1.03)

NA, not applicable due to fewer than five exposed cases.

[1]ANA Level shows four exclusive categories of ANA positivity based on highest reading observed.

[2]Limited to applicators who completed the take-home questionnaire with information on frequency and duration of use.

[3]Odds Ratios (ORs) and 95% Confidence Intervals (CI) were calculated by multivariable models adjusted for age at interview, state, overweight/obese, ever smoked, spring or summer season, current occupational pesticides use. Bold shows ORs that are statistically significant at $p < 0.05$.

[4]ORs for tertiles of cyclodienes (aldrin, chlordane, dieldrin, or heptachlor) and other organochlorines (OCs, DDT, lindane, or toxaphene), mutually adjusted.

Our results also suggest that seeking medical care due to pesticide exposure (i.e., seeing a doctor or being hospitalized due to pesticide exposure, or being diagnosed with pesticide poisoning) was associated with having moderate or high ANA. The reasons for seeking medical care for pesticide exposure included high pesticide exposure events (HPEE) and presumably pesticide-related symptoms, however we did not analyze ANA in relation to symptoms data. We also saw an elevated OR for overall ANA with HPEE in those who experienced an event but did not seek medical care (OR 1.37). Prior AHS research suggests those reporting high pesticide exposure events used pesticides for more days per year and had certain practices that might increase personal exposures, such as storing pesticides in the home or spraying pesticides with open cab windows, and that many do not seek medical care for HPEE and exposure-related symptoms (56). In our study, among ANA positive individuals, only 21 (3% of the total) reported both HPEE and seeking medical care, while 39 (6%) sought medical care without reporting HPEE, and 88 (13%) reported only HPEE (not shown in tables). Thus, the actual exposures underlying our findings remain undetermined. The AHS collected data on specific pesticides involved in some high pesticide exposure events, but we had insufficient sample size to take advantage of these data.

Diverse and interrelated pathways lead to dysregulation of the immune response and development of autoimmunity. In healthy individuals, ANA may reflect increased exposure to self-antigens and dysregulation of various pathways, some of which are shared and others distinctive from patterns seen in autoimmune disease patients (57, 58). Pesticides may influence both the generation of autoimmunity and the strength of the immune response. Our study used the gold standard assay, which is sensitive to lower levels of ANA at the 1:40 dilution level while providing increased specificity at higher titers (e.g., 1:160). ANA are thought to arise as an immune response to nuclear antigens released from apoptotic cells. The interpretation of ANA detection at different thresholds for positivity varies by context: although detection at the 1:80 dilution of 3 or 4+ intensity has recently been specified among the constellation of clinical criteria for systemic lupus erythematosus, higher levels may be seen in lupus and sometimes associated with other clinical autoimmune diseases (59). Interestingly, we only saw positive associations for moderate or higher-level ANA, while inverse associations were seen only with having any detectable ANA (including lower levels, at least 2+ intensity at the 1:80 dilution).

A positive response to the HEp-2 ANA assay does not imply an association with clinical disease. The pattern of nuclear antibody staining is emerging as a key means to differentiate the origins and relevance of ANA in clinical and healthy populations, especially the dense fine speckled pattern and the associated anti-DFS70 antibody (60–62). Our analyses did not consider the fluorescence pattern, as the vast majority of ANA were identified as fine speckled, which at the time of the study was not differentiated from dense fine speckled and speckled. Antibodies to DFS70 may be a promising marker, as they appear to be more common in the general population and may even help to rule-out specific autoimmune diseases (60); had use of this marker been more common and validated at the time of the original testing, it would have been considered. We focused on specific disease-associated autoantibodies commonly examined in clinical assessments for SLE, but our results support further investigation of other types of antibodies as well, such as anti-histone and chromatin, which have been linked with certain

TABLE 5 | ENA and anti-dsDNA autoantibodies by lifetime pesticide use[1].

	ANA Negative (*N* = 386)		ENA/anti-dsDNA (*N* = 15)		Age-adjusted odds ratio (95% CI)[2]		
	N	%	*N*	%			*p*-value
ORGANOCHLORINE INSECTICIDES							
Cyclodienes							
Aldrin	81	22	9	60	3.39	(0.98, 11.7)	0.054
Chlordane	103	28	8	53	1.72	(0.55, 5.36)	0.350
Dieldrin	31	8	5	33	3.29	(0.88, 12.3)	0.076
Heptachlor	70	19	7	47	2.86	(0.80, 10.2)	0.106
Only one	78	21	2	13	1.39	(0.21, 9.08)	0.729
2 or more	74	20	10	67	**6.48**	**(1.45, 29.0)**	0.015
Others							
DDT	87	23	7	47	1.06	(0.29, 3.84)	0.934
Lindane	110	29	8	53	2.27	(0.77, 6.71)	0.140
Toxaphene	57	15	3	21	0.76	(0.18, 3.19)	0.708
One	103	27	2	13	0.45	(0.08, 2.41)	0.352
2 or more	65	17	7	47	1.74	(0.47, 6.43)	0.403
OTHER INSECTICIDES							
Chlorpyrifos	211	55	5	33	0.45	(0.14, 1.39)	0.166
Coumaphos	39	10	1	7	0.57	(0.07, 4.74)	0.607
Diazinon	112	29	6	40	1.20	(0.39, 3.71)	0.746
DDVP	66	17	5	33	2.12	(0.64, 7.01)	0.218
Fonofos	136	35	9	60	**3.70**	(**1.01, 13.5**)	0.048
Parathion	53	14	3	20	0.88	(0.22, 3.55)	0.863
Malathion	318	82	9	60	0.31	(0.10, 0.95)	0.041
Phorate	158	41	9	60	2.63	(0.70, 9.88)	0.152
Terbufos	212	55	10	67	3.32	(0.87, 12.6)	0.078
Carbofuran	144	37	14	93	**30.0**	(**3.59, 251**)	0.002
Carbaryl	204	53	10	67	1.41	(0.44, 4.55)	0.562
Aldicarb	20	5	3	20	5.28	(0.95, 29.5)	0.058
Permethrin	145	38	3	20	0.41	(0.11, 1.56)	0.190
HERBICIDES							
2, 4-D	338	88	14	93	1.77	(0.21, 15.2)	0.604
2, 4, 5-T	102	26	7	47	1.47	(0.47, 4.63)	0.512
Atrazine	331	86	14	93	2.44	(0.28, 21.4)	0.421
Cyanazine	207	54	12	80	**5.34**	(**1.12, 25.4**)	0.035
Metribuzin	209	54	9	60	1.21	(0.37, 3.89)	0.754
Chlorimuron ethyl	150	39	7	47	1.23	(0.41, 3.67)	0.713
Metolachlor	221	57	9	60	1.20	(0.39, 3.66)	0.745
Alachlor	247	64	10	67	1.47	(0.44, 4.96)	0.532
EPTC	82	21	5	33	2.42	(0.73, 8.06)	0.149
Trifluralin	208	54	9	60	1.09	(0.35, 3.42)	0.882
Butylate	190	49	9	60	1.77	(0.56, 5.60)	0.330
Imazethapyr	178	46	9	60	3.02	(0.79, 11.6)	0.107
Dicamba	268	69	11	73	1.78	(0.37, 8.55)	0.474
Paraquat	87	23	4	27	0.95	(0.27, 3.31)	0.941
Glyphosate	353	92	12	80	0.41	(0.10, 1.65)	0.209
Pendimethalin	193	50	9	60	2.02	(0.66, 6.24)	0.220
Petroleum_oil	204	53	10	67	1.82	(0.56, 5.90)	0.321
FUNGICIDES, FUMIGANTS							
Benomyl	26	7	3	20	1.92	(0.42, 8.73)	0.397
Captan	53	14	3	20	1.61	(0.42, 6.18)	0.489

(Continued)

TABLE 5 | Continued

	ANA Negative (*N* = 386)		ENA/anti-dsDNA (*N* = 15)		Age-adjusted odds ratio (95% CI)[2]		
	N	%	*N*	%			*p*-value
Metalaxyl	74	19	5	33	1.74	(0.52, 5.88)	0.372
Methyl bromide	25	6	3	20	16.6	(0.92, 299)	0.057
Aluminum Phosphide	23	6	2	13	2.20	(0.44, 11.0)	0.337
Ethylene Dibromide	13	3	3	20	**5.07**	(**1.10**, **23.4**)	0.038

ENA (Extractable Nuclear Antigens) measured on those ANA read as 3 or 4+ at 1:80 dilution; ANA Negative = none detected at 1:80 dilution.

[1]*Reported ever use at AHS enrollment (1993–1997) based on list of 50 specific pesticides, with updated use throughout follow-up and BEEA enrollment.*

[2]*Odds Ratios (ORs) and 95% Confidence Intervals (CI) were calculated by multivariable logistic regression models adjusted for age at interview.*

drug- and xenobiotic exposures and may help to identify the underlying role of specific exposures (63–66).

Half of the ANA-positive individuals in our study sample were positive only at the lowest-level (2+ at a 1:80 dilution); this threshold was used to enable comparisons with studies using a lower dilution (i.e., 1:40). The implications of having lower-level ANA are not well-understood. Most research on autoimmunity in the absence of autoimmune diseases has been based on cross-sectional and clinical samples; however, a few longitudinal studies showing that individuals with low level ANA are more likely to revert to seronegative status over time compared to those at lower titers (22, 62, 67). Notably, in a sample of rural residents and farmers, Semchuk observed that ANA prevalence at higher titers (3+ or 4+ at 1:80 and 1:160) was similar in the summer and winter, with similar rates of seroconversion and reversion across the seasons (16). On the other hand, lower level ANA (at the at 1:40 dilution, but not higher) were elevated in summer, supporting the idea that changing exposures by season may account for transient expression of ANA in some individuals. Although we adjusted for season in our statistical models, we saw no strong or consistent differences in ANA frequency for participants sampled at different times of year. Smoking history and BMI at the time of sampling were non-significantly associated with ANA and were included in our multivariable models along with other covariates as they generally increased the precision of observed associations. The causal relationship of specific pesticides with BMI is unknown; however, adjusting for BMI did not appear to explain any of the observed pesticide associations. Odds ratios approximate the relative risk for rare outcomes (<10%), for example with high ANA and ENA, but overestimate the relative risk for more common outcomes (i.e., overall ANA or high/moderate ANA). Our estimated ORs, therefore, may most accurately reflect the relative risks for high ANA. On the other hand, small numbers may inflate the OR and confidence limits, for example, in the analyses of uncommon pesticides and disease-specific autoantibodies.

We excluded prevalent cases of autoimmune diseases (e.g., rheumatoid arthritis and lupus) to reduce potential recall or reporting bias, or changes in exposures due to health conditions; in follow-up, some participants reported incident autoimmune diseases, which were associated with ANA as expected (**Supplemental Table 1**). Overall ANA (i.e., including low level ANA) was also associated with anti-TPO autoantibodies. Autoimmune thyroid diseases occur more often in those with systemic autoimmune diseases (68), and anti-TPO autoantibodies have been previously associated with ANA in healthy controls (57). Prevalence of anti-CCP autoantibodies, specific for rheumatoid arthritis, was not associated with ANA in our sample, and levels were similar to the general population (69–71), despite evidence that rheumatoid arthritis may be associated with agricultural work and pesticide use in the AHS and other studies (1–9). Sensitivity analyses showed no substantial changes after excluding possible new cases of autoimmune diseases and those specific autoantibodies (i.e., anti-CCP, anti-TPO, and disease specific ENA and anti-dsDNA autoantibodies) (not shown).

The BEEA study provides an opportunity to investigate the long-term health effects of pesticides and other agricultural exposures on autoimmunity. The study sample is representative of men who were actively farming at AHS enrollment in the mid-1990s, most of whom did not have a diagnosis of RA or other autoimmune diseases. Women in the AHS, mostly spouses of the licensed applicators, were not included in the BEEA sample. Spouses reported less pesticide use than the applicators, but potential associations of pesticides with ANA in spouses may be relevant given the higher prevalence of ANA in women generally. Farmers are a unique population, with diverse exposures to agricultural pesticides and other physical or chemical factors, so results may not be generalizable to the general population. Further research is warranted to investigate ANA in relation to other agricultural factors, for example to solvents and fertilizers, recently associated with rheumatoid arthritis in the AHS (72). Our study addresses several limitations of prior studies on pesticides and ANA, with data on lifetime exposure to over 40 specific agricultural pesticides. However, despite having a larger sample than most studies, we had low statistical power to examine associations with uncommon pesticides and disease-specific autoantibodies, and for testing exposure-response gradients. Non-differential exposure misclassification is a possibility due to errors in recall of past exposures. Evaluation of self-reported data in the AHS has established the reliability of recall for specific pesticides; further, an intensity-weighting algorithm developed for the study (integrating across multiple determinants of exposure

intensity) has shown good correlation with measurement data in an exposure sub-study, and may reduce the potential for non-differential misclassification to bias results toward the null in analyses of dose-response (24, 73, 74).

Our analyses are based on prospectively collected exposure data, but temporal ambiguity relative to ANA incidence is inherent to our study design focused on lifetime exposures. We cannot know whether exposures occurred prior to or after the development of ANA, or whether ANA appeared in the past and became non-detectable at the time they were measured. While the natural history of ANA in the general population is not well-understood, ANA prevalence typically increases with age, suggesting increasing incidence of ANA over time. Presumably, pesticides may influence two processes that contribute to the observed ANA at a single time point: (1) the breach of immune tolerance and initial production of autoantibodies, and (2) external factors impacting the production of measurable levels at the time of sampling. Further research is needed to investigate the associations of ANA with contemporary use of specific pesticides and the time since last use. Autoantibodies can precede the development of autoimmune diseases for a decade or longer (75), so other factors are likely to contribute to the development of pathology and disease.

Altogether our findings provide evidence that past pesticide use may influence the development of autoimmunity in middle age and older farmers, consistent with prior findings of elevated ANA with some organochlorine insecticides. The presence of disease-specific autoantibodies was also related to certain organochlorines, supporting the need to further explore these persistent pesticides as potential causal agents in development of autoimmune diseases. Future research should focus on the role of recent exposure and the evaluation of less common pesticides in larger studies or in targeted populations with greater use of these chemicals.

DATA AVAILABILITY

Due to ethical restrictions imposed in the interest of protecting participant confidentiality, the datasets for this study are available upon request to interested, qualified researchers. Requests to access the datasets should be directed to JH (hofmannjn@mail.nih.gov).

ETHICS STATEMENT

The study was approved by Institutional Review Boards at the National Cancer Institute and other participating institutions, and all participants provided written informed consent.

AUTHOR CONTRIBUTIONS

CP conceived of the research question, obtained funding for assays, performed analyses, evaluated results, and wrote the manuscript. AS assisted with planning analyses, evaluated results, and contributed to the manuscript. SB, MW, and CL assisted with planning analyses, evaluating results, and editing the manuscript. JH, DS, MA, CD, and LB obtained funding and generated data for the AHS and BEEA sub-cohort, assisted with planning analyses, evaluated results, and edited the manuscript.

FUNDING

This work was supported by the Intramural Research Program of the NIH, National Institute of Environmental Health Sciences (Z01-ES049030) and National Cancer Institute (Z01-CP010119).

ACKNOWLEDGMENTS

The authors thank Stuart Long, Westat, for programming support, and Fred Miller and Srishti Shrestha for helpful reviews of manuscript drafts. We would also like to thank Amy Miller, Kate Torres, Sandor Balogh, Marsha Dunn, and other staff at Westat, Inc. (Rockville, Maryland) and Charles Lynch, Debra Lande, Debra Podaril, and Jennifer Hamilton (University of Iowa) for study coordination, data management, and field research efforts. We also thank Kevin Deane (University of Colorado) for assay support, as well as Anne Taylor and Peter Hui (Information Management Services, Rockville, Maryland) for data management and analytic support. The authors gratefully acknowledge the ongoing participation of the Agricultural Health Study participants that made this work possible.

SUPPLEMENTARY MATERIAL

The Supplementary Material for this article can be found online at: https://www.frontiersin.org/articles/10.3389/fimmu.2019.01476/full#supplementary-material

REFERENCES

1. Gold LS, Ward MH, Dosemeci M, De Roos AJ. Systemic autoimmune disease mortality and occupational exposures. *Arthritis Rheum.* (2007) 56:3189–201. doi: 10.1002/art.22880
2. Lundberg I, Alfredsson L, Plato N, Sverdrup B, Klareskog L, Kleinau S. Occupation, occupational exposure to chemicals and rheumatological disease. A register based cohort study. *Scand J Rheumatol.* (1994) 23:305–10. doi: 10.3109/03009749409099278
3. Milham S Jr. Using multiple cause of death coding in occupational mortality studies. *Am J Ind Med.* (1988) 14:341–4. doi: 10.1002/ajim.4700140311
4. Khuder SA, Peshimam AZ, Agraharam S. Environmental risk factors for rheumatoid arthritis. *Rev Environ Health.* (2002) 17:307–15. doi: 10.1515/REVEH.2002.17.4.307
5. Li X, Sundquist J, Sundquist K. Socioeconomic and occupational risk factors for rheumatoid arthritis: a nationwide study based on hospitalizations in Sweden. *J Rheumatol.* (2008) 35:986–91.
6. Lee E, Burnett CA, Lalich N, Cameron LL, Sestito JP. Proportionate mortality of crop and livestock farmers in the United States, 1984–1993. *Am J Ind Med.* (2002) 42:410–20. doi: 10.1002/ajim.10131
7. Olsson AR, Skogh T, Wingren G. Occupational determinants for rheumatoid arthritis. *Scand J Work Environ Health.* (2000) 26:243–9. doi: 10.5271/sjweh.538

8. Meyer A, Sandler DP, Beane Freeman LE, Hofmann JN, Parks CG. Pesticide exposure and risk of rheumatoid arthritis among licensed male pesticide applicators in the Agricultural Health Study. *Environ Health Perspect*. (2017) 125:077010. doi: 10.1289/EHP1013
9. Parks CG, Hoppin JA, De Roos AJ, Costenbader KH, Alavanja MC, Sandler DP. Rheumatoid arthritis in Agricultural Health Study Spouses: associations with pesticides and other farm exposures. *Environ Health Perspect*. (2016) 124:1728–34. doi: 10.1289/EHP129
10. Satoh M, Chan EK, Ho LA, Rose KM, Parks CG, Cohn RD, et al. Prevalence and sociodemographic correlates of antinuclear antibodies in the United States. *Arthritis Rheum*. (2012) 64:2319–27. doi: 10.1002/art.34380
11. Tan EM, Feltkamp TE, Smolen JS, Butcher B, Dawkins R, Fritzler MJ, et al. Range of antinuclear antibodies in "healthy" individuals. *Arthritis Rheum*. (1997) 40:1601–11. doi: 10.1002/art.1780400909
12. Munroe ME, Young KA, Kamen DL, Guthridge JM, Niewold TB, Costenbader KH, et al. Discerning risk of disease transition in relatives of systemic lupus erythematosus patients utilizing soluble mediators and clinical features. *Arthritis Rheumatol*. (2017) 69:630–42. doi: 10.1002/art.40004
13. Elnady BM, Kamal NM, Shaker RH, Soliman AF, Hasan WA, Alghamdi HA, et al. Prevalence and clinical significance of nonorgan specific antibodies in patients with autoimmune thyroiditis as predictor markers for rheumatic diseases. *Medicine*. (2016) 95:e4336. doi: 10.1097/MD.0000000000004336
14. Corsini E, Sokooti M, Galli CL, Moretto A, Colosio C. Pesticide induced immunotoxicity in humans: a comprehensive review of the existing evidence. *Toxicology*. (2013) 307:123–35. doi: 10.1016/j.tox.2012.10.009
15. Rosenberg AM, Semchuk KM, McDuffie HH, Ledingham DL, Cordeiro DM, Cessna AJ, et al. Prevalence of antinuclear antibodies in a rural population. *J Toxicol Environ Health A*. (1999) 57:225–36. doi: 10.1080/009841099157674
16. Semchuk KM, Rosenberg AM, McDuffie HH, Cessna AJ, Pahwa P, Irvine DG. Antinuclear antibodies and bromoxynil exposure in a rural sample. *J Toxicol Environ Health A*. (2007) 70:638–57. doi: 10.1080/15287390600974593
17. Dinse GE, Jusko TA, Whitt IZ, Co CA, Parks CG, Satoh M, et al. Associations between selected xenobiotics and antinuclear antibodies in the national health and nutrition examination survey, 1999–2004. *Environ Health Perspect*. (2016) 124:426–36. doi: 10.1289/ehp.1409345
18. McConnachie PR, Zahalsky AC. Immune alterations in humans exposed to the termiticide technical chlordane. *Arch Environ Health*. (1992) 47:295–301. doi: 10.1080/00039896.1992.9938365
19. Cooper GS, Martin SA, Longnecker MP, Sandler DP, Germolec DR. Associations between plasma DDE levels and immunologic measures in African-American farmers in North Carolina. *Environ Health Perspect*. (2004) 112:1080–4. doi: 10.1289/ehp.6892
20. Hofmann JN, Beane Freeman LE, Lynch CF, Andreotti G, Thomas KW, Sandler DP, et al. The biomarkers of exposure and effect in agriculture (BEEA) study: rationale, design, methods, and participant characteristics. *J Toxicol Environ Health A*. (2015) 78:1338–47. doi: 10.1080/15287394.2015.1091414
21. Alavanja MC, Sandler DP, McMaster SB, Zahm SH, McDonnell CJ, Lynch CF, et al. The Agricultural Health Study. *Environ Health Perspect*. (1996) 104:362–9. doi: 10.1289/ehp.96104362
22. Xavier RM, Yamauchi Y, Nakamura M, Tanigawa Y, Ishikura H, Tsunematsu T, et al. Antinuclear antibodies in healthy aging people: a prospective study. *Mech Ageing Dev*. (1995) 78:145–54. doi: 10.1016/0047-6374(94)01532-Q
23. Guo YP, Wang CG, Liu X, Huang YQ, Guo DL, Jing XZ, et al. The prevalence of antinuclear antibodies in the general population of china: a cross-sectional study. *Curr Ther Res Clin Exp*. (2014) 76:116–9. doi: 10.1016/j.curtheres.2014.06.004
24. Coble J, Thomas KW, Hines CJ, Hoppin JA, Dosemeci M, Curwin B, et al. An updated algorithm for estimation of pesticide exposure intensity in the agricultural health study. *Int J Environ Res Public Health*. (2011) 8:4608–22. doi: 10.3390/ijerph8124608
25. Alavanja MC, Sandler DP, McDonnell CJ, Mage DT, Kross BC, Rowland AS, et al. Characteristics of persons who self-reported a high pesticide exposure event in the Agricultural Health Study. *Environ Res*. (1999) 80:180–6. doi: 10.1006/enrs.1998.3887
26. Kuller LH, Mackey RH, Walitt BT, Deane KD, Holers VM, Robinson WH, et al. Determinants of mortality among postmenopausal women in the women's health initiative who report rheumatoid arthritis. *Arthritis Rheumatol*. (2014) 66:497–507. doi: 10.1002/art.38268
27. Jorgensen KT, Wiik A, Pedersen M, Hedegaard CJ, Vestergaard BF, Gislefoss RE, et al. Cytokines, autoantibodies and viral antibodies in premorbid and postdiagnostic sera from patients with rheumatoid arthritis: case-control study nested in a cohort of Norwegian blood donors. *Ann Rheum Dis*. (2008) 67:860–6. doi: 10.1136/ard.2007.073825
28. Lerro CC, Beane Freeman LE, DellaValle CT, Kibriya MG, Aschebrook-Kilfoy B, Jasmine F, et al. Occupational pesticide exposure and subclinical hypothyroidism among male pesticide applicators. *Occup Environ Med*. (2018) 75:79–89. doi: 10.1136/oemed-2017-104431
29. Sobel ES, Gianini J, Butfiloski EJ, Croker BP, Schiffenbauer J, Roberts SM. Acceleration of autoimmunity by organochlorine pesticides in (NZB x NZW)F1 mice. *Environ Health Perspect*. (2005) 113:323–8. doi: 10.1289/ehp.7347
30. Coats JR. Mechanisms of toxic action and structure-activity relationships for organochlorine and synthetic pyrethroid insecticides. *Environ Health Perspect*. (1990) 87:255–62. doi: 10.1289/ehp.9087255
31. Kim JK, Kim YS, Lee HM, Jin HS, Neupane C, Kim S, et al. GABAergic signaling linked to autophagy enhances host protection against intracellular bacterial infections. *Nat Commun*. (2018) 9:4184. doi: 10.1038/s41467-018-06487-5
32. Wu CY, Gagnon DA, Sardin JS, Barot U, Telenson A, Arratia PE, et al. Enhancing GABAergic transmission improves locomotion in a caenorhabditis elegans model of spinal muscular atrophy. *eNeuro*. (2018) 5. doi: 10.1523/ENEURO.0289-18.2018. Available online at: http://www.eneuro.org/content/5/6/ENEURO.0289-18.2018.long
33. Holsapple MP. Autoimmunity by pesticides: a critical review of the state of the science. *Toxicol Lett*. (2002) 127:101–9. doi: 10.1016/S0378-4274(01)00489-1
34. Loose LD, Silkworth JB, Charbonneau T, Blumenstock F. Environmental chemical-induced macrophage dysfunction. *Environ Health Perspect*. (1981) 39:79–92. doi: 10.2307/3429282
35. Hugo P, Bernier J, Krzystyniak K, Potworowski EF, Fournier M. Abrogation of graft-versus-host reaction by dieldrin in mice. *Toxicol Lett*. (1988) 41:11–22. doi: 10.1016/0378-4274(88)90003-3
36. Fournier M, Chevalier G, Nadeau D, Trottier B, Krzystyniak K. Virus-pesticide interactions with murine cellular immunity after sublethal exposure to dieldrin and aminocarb. *J Toxicol Environ Health*. (1988) 25:103–18. doi: 10.1080/15287398809531192
37. Briz V, Molina-Molina JM, Sanchez-Redondo S, Fernandez MF, Grimalt JO, Olea N, et al. Differential estrogenic effects of the persistent organochlorine pesticides dieldrin, endosulfan, and lindane in primary neuronal cultures. *Toxicol Sci*. (2011) 120:413–27. doi: 10.1093/toxsci/kfr019
38. Coumoul X, Diry M, Barouki R. PXR-dependent induction of human CYP3A4 gene expression by organochlorine pesticides. *Biochem Pharmacol*. (2002) 64:1513–9. doi: 10.1016/S0006-2952(02)01298-4
39. Thomas PT, Ratajczak HV. Assessment of carbamate pesticide immunotoxicity. *Toxicol Ind Health*. (1988) 4:381–90. doi: 10.1177/074823378800400310
40. Hajoui O, Flipo D, Mansour S, Fournier M, Krzystyniak K. Immunotoxicity of subchronic versus chronic exposure to aldicarb in mice. *Int J Immunopharmacol*. (1992) 14:1203–11. doi: 10.1016/0192-0561(92)90056-Q
41. Thomas P, Ratajczak H, Demetral D, Hagen K, Baron R. Aldicarb immunotoxicity: functional analysis of cell-mediated immunity and quantitation of lymphocyte subpopulations. *Fundam Appl Toxicol*. (1990) 15:221–30. doi: 10.1093/toxsci/15.2.221
42. Duramad P, Tager IB, Leikauf J, Eskenazi B, Holland NT. Expression of Th1/Th2 cytokines in human blood after *in vitro* treatment with chlorpyrifos, and its metabolites, in combination with endotoxin LPS and allergen Der p1. *J Appl Toxicol*. (2006) 26:458–65. doi: 10.1002/jat.1162
43. Thrasher JD, Heuser G, Broughton A. Immunological abnormalities in humans chronically exposed to chlorpyrifos. *Arch Environ Health*. (2002) 57:181–7. doi: 10.1080/00039890209602934
44. Alluwaimi AM, Hussein Y. Diazinon immunotoxicity in mice: modulation of cytokines level and their gene expression. *Toxicology*. (2007) 236:123–31. doi: 10.1016/j.tox.2007.04.004
45. Neishabouri EZ, Hassan ZM, Azizi E, Ostad SN. Evaluation of immunotoxicity induced by diazinon in C57bl/6 mice. *Toxicology*. (2004) 196:173–9. doi: 10.1016/j.tox.2003.08.012

46. Banerjee BD, Pasha ST, Hussain QZ, Koner BC, and Ray A, A comparative evaluation of immunotoxicity of malathion after subchronic exposure in experimental animals. *Indian J Exp Biol*. (1998) 36:273–82.
47. Johnson VJ, Rosenberg AM, Lee K, Blakley BR. Increased T-lymphocyte dependent antibody production in female SJL/J mice following exposure to commercial grade malathion. *Toxicology*. (2002) 170:119–29. doi: 10.1016/S0300-483X(01)00515-7
48. Rodgers KE. Effects of oral administration of malathion on the course of disease in MRL-lpr mice. *J Autoimmun*. (1997) 10:367–73. doi: 10.1006/jaut.1997.0145
49. Fujii T, Mashimo M, Moriwaki Y, Misawa H, Ono S, Horiguchi K, et al. Expression and function of the cholinergic system in immune cells. *Front Immunol*. (2017) 8:1085. doi: 10.3389/fimmu.2017.01085
50. Bosmans G, Shimizu Bassi G, Florens M, Gonzalez-Dominguez E, Matteoli G, Boeckxstaens GE. Cholinergic modulation of type 2 immune responses. *Front Immunol*. (2017) 8:1873. doi: 10.3389/fimmu.2017.01873
51. Bulathsinghala AT, Shaw IC. The toxic chemistry of methyl bromide. *Hum Exp Toxicol*. (2014) 33:81–91. doi: 10.1177/0960327113493299
52. Ratajczak HV, Aranyi C, Bradof JN, Barbera P, Fugmann R, Fenters JD, et al. Ethylene dibromide: evidence of systemic and immunologic toxicity without impairment of *in vivo* host defenses. *In Vivo*. (1994) 8:879–84.
53. Freitas EC, de Oliveira MS, Monticielo OA. Pristane-induced lupus: considerations on this experimental model. *Clin Rheumatol*. (2017) 36:2403–14. doi: 10.1007/s10067-017-3811-6
54. Lynch SM, Mahajan R, Beane Freeman LE, Hoppin JA, Alavanja MC. Cancer incidence among pesticide applicators exposed to butylate in the Agricultural Health Study (AHS). *Environ Res*. (2009) 109:860–8. doi: 10.1016/j.envres.2009.06.006
55. Andreotti G, Hoppin JA, Hou L, Koutros S, Gadalla SM, Savage SA, et al. Pesticide use and relative leukocyte telomere length in the agricultural health study. *PLoS ONE*. (2015) 10:e0133382. doi: 10.1371/journal.pone.0133382
56. Payne K, Andreotti G, Bell E, Blair A, Coble J, Alavanja M. Determinants of high pesticide exposure events in the agricultural health cohort study from enrollment (1993–1997) through phase II (1999–2003). *J Agric Saf Health*. (2012) 18:167–79. doi: 10.13031/2013.41955
57. Li QZ, Karp DR, Quan J, Branch VK, Zhou J, Lian Y, et al. Risk factors for ANA positivity in healthy persons. *Arthritis Res Ther*. (2011) 13:R38. doi: 10.1186/ar3271
58. Slight-Webb S, Lu R, Ritterhouse LL, Munroe ME, Maecker HT, Fathman CG, et al. Autoantibody-positive healthy individuals display unique immune profiles that may regulate autoimmunity. *Arthritis Rheumatol*. (2016) 68:2492–502. doi: 10.1002/art.39706
59. Leuchten N, Hoyer A, Brinks R, Schoels M, Schneider M, Smolen J, et al. Performance of antinuclear antibodies for classifying systemic lupus erythematosus: a systematic literature review and meta-regression of diagnostic data. *Arthritis Care Res*. (2018) 70:428–38. doi: 10.1002/acr.23292
60. Conrad K, Rober N, Andrade LE, Mahler M. The clinical relevance of Anti-DFS70 autoantibodies. *Clin Rev Allergy Immunol*. (2017) 52:202–16. doi: 10.1007/s12016-016-8564-5
61. Mahler M, Andrade LE, Casiano CA, Malyavantham K, Fritzler MJ. Implications for redefining the dense fine speckled and related indirect immunofluorescence patterns. *Expert Rev Clin Immunol*. (2019) 15:447–8. doi: 10.1080/1744666X.2019.1596802
62. Mariz HA, Sato EI, Barbosa SH, Rodrigues SH, Dellavance A, Andrade LE. Pattern on the antinuclear antibody-HEp-2 test is a critical parameter for discriminating antinuclear antibody-positive healthy individuals and patients with autoimmune rheumatic diseases. *Arthritis Rheum*. (2011) 63:191–200. doi: 10.1002/art.30084
63. Pollard KM, Lee DK, Casiano CA, Bluthner M, Johnston MM, Tan EM. The autoimmunity-inducing xenobiotic mercury interacts with the autoantigen fibrillarin and modifies its molecular and antigenic properties. *J Immunol*. (1997) 158:3521–8.
64. Pollard KM, Pearson DL, Hultman P, Deane TN, Lindh U, Kono DH. Xenobiotic acceleration of idiopathic systemic autoimmunity in lupus-prone bxsb mice. *Environ Health Perspect*. (2001) 109:27–33. doi: 10.1289/ehp.0110927
65. Pfau JC, Barbour C, Black B, Serve KM, Fritzler MJ. Analysis of autoantibody profiles in two asbestiform fiber exposure cohorts. *J Toxicol Environ Health A*. (2018) 81:1015–27. doi: 10.1080/15287394.2018.1512432
66. Erdei E, Shuey C, Pacheco B, Cajero M, Lewis J, Rubin RL. Elevated autoimmunity in residents living near abandoned uranium mine sites on the Navajo Nation. *J Autoimmun*. (2019) 99:15–23. doi: 10.1016/j.jaut.2019.01.006
67. Hayashi N, Koshiba M, Nishimura K, Sugiyama D, Nakamura T, Morinobu S, et al. Prevalence of disease-specific antinuclear antibodies in general population: estimates from annual physical examinations of residents of a small town over a 5-year period. *Mod Rheumatol*. (2008) 18:153–60. doi: 10.1007/s10165-008-0028-1
68. Cooper GS, Bynum ML, Somers EC. Recent insights in the epidemiology of autoimmune diseases: improved prevalence estimates and understanding of clustering of diseases. *J Autoimmun*. (2009) 33:197–207. doi: 10.1016/j.jaut.2009.09.008
69. Kakumanu P, Yamagata H, Sobel ES, Reeves WH, Chan EK, Satoh M. Patients with pulmonary tuberculosis are frequently positive for anti-cyclic citrullinated peptide antibodies, but their sera also react with unmodified arginine-containing peptide. *Arthritis Rheum*. (2008) 58:1576–81. doi: 10.1002/art.23514
70. Avouac J, Gossec L, Dougados M. Diagnostic and predictive value of anti-cyclic citrullinated protein antibodies in rheumatoid arthritis: a systematic literature review. *Ann Rheum Dis*. (2006) 65:845–51. doi: 10.1136/ard.2006.051391
71. Fischer A, Solomon JJ, du Bois RM, Deane KD, Olson AL, Fernandez-Perez ER, et al. Lung disease with anti-CCP antibodies but not rheumatoid arthritis or connective tissue disease. *Respir Med*. (2012) 106:1040–7. doi: 10.1016/j.rmed.2012.03.006
72. Parks CG, Meyer A, Beane Freeman LE, Hofmann JN, Sandler DP. Farming tasks and the development of rheumatoid arthritis in the agricultural health study. *Occup Environ Med*. (2019) 76:243–9. doi: 10.1136/oemed-2018-105361
73. Blair A, Tarone R, Sandler D, Lynch CF, Rowland A, Wintersteen W, et al. Reliability of reporting on life-style and agricultural factors by a sample of participants in the Agricultural Health Study from Iowa. *Epidemiology*. (2002) 13:94–9. doi: 10.1097/00001648-200201000-00015
74. Blair A, Thomas K, Coble J, Sandler DP, Hines CJ, Lynch CF, et al. Impact of pesticide exposure misclassification on estimates of relative risks in the Agricultural Health Study. *Occup Environ Med*. (2011) 68:537–41. doi: 10.1136/oem.2010.059469
75. Ma WT, Chang C, Gershwin ME, Lian ZX. Development of autoantibodies precedes clinical manifestations of autoimmune diseases: a comprehensive review. *J Autoimmun*. (2017) 83:95–112. doi: 10.1016/j.jaut.2017.07.003

Conflict of Interest Statement: The authors declare that the research was conducted in the absence of any commercial or financial relationships that could be construed as a potential conflict of interest.

frontiers in Immunology

ORIGINAL RESEARCH
published: 28 August 2019
doi: 10.3389/fimmu.2019.02016

Continuous Developmental and Early Life Trichloroethylene Exposure Promoted DNA Methylation Alterations in Polycomb Protein Binding Sites in Effector/Memory CD4$^+$ T Cells

Stephanie D. Byrum[1†], *Charity L. Washam*[1†], *John D. Patterson*[2], *Kanan K. Vyas*[3], *Kathleen M. Gilbert*[4] *and Sarah J. Blossom*[3*]

[1] Department of Biochemistry and Molecular Biology, Arkansas Children's Research Institute, University of Arkansas for Medical Sciences, Little Rock, AR, United States, [2] College of Medicine, University of Arkansas for Medical Sciences, Little Rock, AR, United States, [3] Department of Pediatrics, Arkansas Children's Research Institute, University of Arkansas for Medical Sciences, Little Rock, AR, United States, [4] Department of Microbiology and Immunology, Arkansas Children's Research Institute, University of Arkansas for Medical Sciences, Little Rock, AR, United States

OPEN ACCESS

Edited by:
Randy Q. Cron,
University of Alabama at Birmingham,
United States

Reviewed by:
B. Paige Lawrence,
University of Rochester, United States
James J. Pestka,
Michigan State University,
United States

***Correspondence:**
Sarah J. Blossom
blossomsarah@uams.edu

[†]These authors have contributed equally to this work

Specialty section:
This article was submitted to Autoimmune and Autoinflammatory Disorders, a section of the journal Frontiers in Immunology

Received: 24 January 2019
Accepted: 08 August 2019
Published: 28 August 2019

Citation:
Byrum SD, Washam CL, Patterson JD, Vyas KK, Gilbert KM and Blossom SJ (2019) Continuous Developmental and Early Life Trichloroethylene Exposure Promoted DNA Methylation Alterations in Polycomb Protein Binding Sites in Effector/Memory CD4$^+$ T Cells. Front. Immunol. 10:2016. doi: 10.3389/fimmu.2019.02016

Trichloroethylene (TCE) is an industrial solvent and drinking water pollutant associated with CD4$^+$ T cell-mediated autoimmunity. In our mouse model, discontinuation of TCE exposure during adulthood after developmental exposure did not prevent immunotoxicity. To determine whether persistent effects were linked to epigenetic changes we conducted whole genome reduced representation bisulfite sequencing (RRBS) to evaluate methylation of CpG sites in autosomal chromosomes in activated effector/memory CD4$^+$ T cells. Female MRL+/+ mice were exposed to vehicle control or TCE in the drinking water from gestation until ∼37 weeks of age [postnatal day (PND) 259]. In a subset of mice, TCE exposure was discontinued at ∼22 weeks of age (PND 154). At PND 259, RRBS assessment revealed more global methylation changes in the continuous exposure group vs. the discontinuous exposure group. A majority of the differentially methylated CpG regions (DMRs) across promoters, islands, and regulatory elements were hypermethylated (∼90%). However, continuous developmental TCE exposure altered the methylation of 274 CpG sites in promoters and CpG islands. In contrast, only 4 CpG island regions were differentially methylated (hypermethylated) in the discontinuous group. Interestingly, 2 of these 4 sites were also hypermethylated in the continuous exposure group, and both of these island regions are associated with lysine 27 on histone H3 (H3K27) involved in polycomb complex-dependent transcriptional repression via H3K27 tri-methylation. CpG sites were overlapped with the Open Regulatory Annotation database. Unlike the discontinuous group, continuous TCE treatment resulted in 129 DMRs including 12 unique transcription factors and regulatory elements; 80% of which were enriched for one or more polycomb group (PcG) protein binding regions (i.e., SUZ12, EZH2, JARID2, and MTF2). Pathway analysis of the DMRs indicated that TCE primarily altered the methylation of genes associated with regulation

of cellular metabolism and cell signaling. The results demonstrated that continuous developmental exposure to TCE differentially methylated binding sites of PcG proteins in effector/memory CD4$^+$ cells. There were minimal yet potentially biologically significant effects that occurred when exposure was discontinued. These results point toward a novel mechanism by which chronic developmental TCE exposure may alter terminally differentiated CD4$^+$ T cell function in adulthood.

Keywords: polycomb, trichloroethylene, CD4$^+$ T cell, DNA methylation, developmental exposure

INTRODUCTION

As many as 5–7% of Americans suffer from a group of disorders consisting of over 100 different diseases collectively called immune-mediated inflammatory diseases (IMIDs) that include hypersensitivity disorders and autoimmune diseases (1). These chronic, incurable disorders disproportionately affect females, and are among the leading causes of death among young and middle-age women (2). Although these diseases result in different types of tissue damage, they appear to share some common inflammatory pathways. In many cases this includes sustained T cell activation. While it is not known what causes IMIDs, the increased prevalence and incidence rates of autoimmune disease parallel the documented increase chemicals that pollute the environment. Thus, pollutants common to industrialized nations are increasingly being recognized as possible triggers for immunotoxicity and autoimmunity (3). One potential environmental risk factor is trichloroethylene (TCE) (4–7). TCE is an organic solvent best known for its use as an industrial chemical and metal degreaser. Because of improper disposal over the years, TCE has contaminated many water systems in the US. Based on likelihood of exposure and an increasing appreciation of its toxicity, TCE is on the list of the top 90 chemicals selected from ∼85,000 in the Toxic Substances Control Act (TSCA) Inventory as having the highest potential for exposure and hazard (8).

The mechanisms behind TCE's ability to promote autoimmunity and hypersensitivity is not known. However, studies have shown that CD4$^+$ T cells are especially sensitive to TCE's effects, and even if overt disease is not diagnosed, altered numbers of peripheral blood CD4$^+$ T cells are often found in humans exposed to TCE (9–11). Expansion of peripheral blood CD4$^+$ T cells is a biomarker for patients with occupational TCE hypersensitivity syndrome (12). As shown by ourselves and others, chronic adult TCE exposure in mice modulates the percentage of IFN-γ- and IL-17-secreting effector/memory CD4$^+$ T cells in mice that went on to develop autoimmune hepatitis (13–15). Such effector/memory CD4$^+$ T cell subsets have been shown to be important in promoting idiopathic and experimental autoimmune disease (16, 17).

Prevention of TCE-mediated autoimmune disease depends on a better understanding mechanisms responsible for disease initiation or progression. Effector/memory CD4$^+$ T cells are the main drivers of autoimmune diseases due to their persistence and diverse contributions to pathology. In recent years it has been reported that the autoreactivity of effector/memory CD4$^+$ T cells may be regulated at the level of DNA methylation. T cell methylation abnormalities are common in autoimmune disease, and widely documented in lupus patients and lupus mouse models. In lupus, disease progression was reportedly accompanied by global DNA hypomethylation, presumably by favoring expression of proinflammatory genes (18). However, both hypomethylated and hypermethylated CpGs have been documented in lupus T cells in several genome-wide DNA methylation studies (19, 20). Along these lines, administration of 5-azacytidine, a potent DNA methylation inhibitor, both promoted and suppressed autoimmunity in lupus prone mice (21, 22). These studies underscore the complexities associated with DNA methylation events associated with T cells in autoimmunity, and it is not surprising that both hypomethylation of inflammatory elements and hypermethylation of regulatory elements have been reported to occur in T cells during the course of disease (23, 24).

In our mouse model, we previously reported that TCE exposure altered DNA methylation in activated effector/memory cells, and this effect was not observed in naïve CD4s. In addition, unlike in naïve CD4s, both chronic and sub-chronic adult-only TCE exposure *in vivo* altered global and gene-specific DNA methylation in effector/memory CD4$^+$ T cells using targeted bisulfite next-generation sequencing [(NGS) (25–27)]. More recently, genome-wide reduced representation bisulfite sequencing [RRBS) was used to interrogate activated effector/memory CD4$^+$ T cells isolated from adult female MRL+/+ mice exposed to TCE for 40 weeks (28). A majority of the differentially methylated CpG regions (DMRs) significantly altered by TCE were regions associated with polycomb group (PcG) proteins. PcG-mediated epigenetic gene regulation requires the action of 2 different polycomb repressive protein complexes (PRCs): PRC1 and PRC2. PRC2 consists of core components JARID2 (Jumonji and AT-Rich Interaction Domain containing 2), SUZ12 (Suppressor of Zeste 12 protein Homolog), EED (Embryonic Ectoderm Development, and either Enhancer of Zeste Homolog (EZH) 2 or EZH1. The EZH paralogs have methyltransferase activity and are the only enzymes known to trimethylate histone H3 at lysine 27 *in vivo*. Trimethylated histone H3K27 (H3K27me3) is a PcG-specific chromatin modification that is widely present in the promoter regions of silenced genes and thought to provide PRC2 with a role in transcriptional repression (29). In T cells, PcG proteins are important in modulating regulatory T cell (T reg) function and effector cell differentiation and function (30, 31).

While our previous RRBS study revealed important new information for a potential role for PcG proteins in TCE-induced immunotoxicity, the experiment was conducted in mice exposed to TCE during adulthood. Because sensitivity to immunotoxicants is thought to be greater in animal models if exposure occurred during development compared to adulthood, we hypothesized that methylation changes in activated effector/memory CD4s would be more robust if exposure occurred during development and/or early life. Additionally, we have shown autoimmune pathology and a number of altered immunological effects were sustained in adult mice after developmental exposure after TCE was removed from the drinking water 15 weeks prior to study terminus (32, 33). Thus, we predicted that at least some of the DNA methylation patterns would be maintained after exposure cessation to provide mechanistic insight into the persistence of TCE's effects.

MATERIALS AND METHODS

Mice and TCE Exposure

This study was conducted at ACRI under an approved Animal Use Protocol by the Animal Care and Use Committee at the University of Arkansas for Medical Sciences. Eight weeks old lupus-prone female MRL+/+ mice were purchased from Jackson Laboratories, Bar Harbor, ME, USA. Randomized mice were paired with age-matched male MRL +/+ mice as described (32, 33). Mice were divided into groups that were given ultrapure unchlorinated drinking water (MilliQ) with vehicle only or 500 μg/ml TCE (10 females per group). Vehicle controls were given water containing only 1% Alkamuls EL-620, the reagent used to solubilize the TCE. The drinking water bottles were changed 3 times/week to offset degradation of TCE. The level of direct TCE exposure in offspring (μg/kg/d) from weaning to PND 154 was based totally on ingestion (e.g., average body weight over time and average consumption of water). Female offspring were weighed weekly and water consumption was monitored. TCE exposure (μg/kg/day) was based on the average amount of TCE-containing water consumed per cage divided by the average mouse weight per cage and a previously calculated 20% degradation of TCE in water bottles. On average, the mice that were directly exposed to TCE (continuous exposure) were exposed on average to <100 mg/kg/day, which approximates the current US Occupational Safety and Health Administration (OSHA) Permissible Exposure Limit at 100 ppm or ∼76 mg/kg/day (34).

Study Design

As shown in **Figure 1**, offspring derived from 8 dams/treatment group were exposed both directly and indirectly to TCE beginning at gestational day (GD) 0 to postnatal day (PND) 0 *in utero*, and then from PND 1 to PND 21 via lactation. Female pups were weaned at PND 21 and further exposed to TCE directly in their drinking water until PND 154 (∼22 weeks of age) after which they were administered ultrapure drinking water without TCE until PND 259 (discontinuous group) as described (32). A subset of pups remained on TCE-containing water for an additional 15 weeks until study terminus [PND 259 (continuous group)]. A third group of mice were exposed to vehicle only for the duration of the experiment. PND 259 (∼37 weeks of age) was chosen as the endpoint based on previous studies where mice at approximately this age after chronic adult only exposure developed autoimmune pathology and global DNA methylation alterations in $CD4^+$ T cells (27). The period for stopping the exposure at PND 154 (∼22 weeks of age) was selected based on a previous study that documented a persistence in TCE-induced changes in ∼27 week old mice after ∼17 weeks of exposure cessation (35).

Isolation of Effector/Memory $CD4^+$ T Cells

Splenic effector memory ($CD62L^{lo}$) $CD4^+$ T cells were collected from euthanized mice at study terminus using Dynabeads FlowComp Mouse CD4 kit (Invitrogen) as described (28). The $CD4^+$ T cells were then further separated into naïve or effector/memory $CD4^+$ T cell populations using Dynabeads M-280 Streptavidin (Invitrogen) conjugated with biotinylated anti-CD62L antibody (eBiosciences, 13-0621-85). The resulting $CD62L^{lo}$ $CD4^+$ T cells were stimulated with immobilized anti-CD3 antibody and anti-CD28 antibody overnight and the activated cells were frozen for examination of DNA methylation. To ensure sufficient cells for use in all the assays, each sample of $CD4^+$ T cells used in the study originated in an equal number of pooled spleen cells from 2 to 3 female mice per litter resulting in 3–4 samples each from individual litters per each treatment group (3 control samples, 3 discontinuous samples, and 4 continuous samples).

DNA Methylation Analysis by Reduced Representation Bisulfite Sequencing (RRBS)

DNA from the $CD4^+$ T cells was isolated as described (28) using PureLink Genomic DNA Mini Kit (Thermo Fisher Scientific). Purity was examined on the NanoDrop 2000c for an A260/A280 range of 1.8–2.0. DNA quality confirmed using standard gel electrophoresis. The DNA was then restriction digested, end-repaired, purified, and ligated with barcode adapters. The RRBS libraries were generated, bisulfite converted, PCR enriched, size selected, purified, and sequenced (2 × 100 paired end) using Illumina HiSeq sequencer.

The Illumina fastq files were first checked for quality using Babraham Bioinformatics *FastQC* (version 0.11.7). Sequencing adaptors, low quality reads (Q < 20), and the ends were trimmed using *Trim Galore* (https://www.bioinformatics.babraham.ac.uk/projects/trim_galore/) and the quality was confirmed using *FastQC*. Bisulfite treated reads were aligned to the m10 reference genome and cytosine methylation sites were called using *Bismark* (https://github.com/FelixKrueger/Bismark). The alignment was performed using bismark with bowtie2 and methylation calls were performed using bismark methylation extractor. The bismark methylation extractor was run with the parameter—no_overlap to ensure that overlapping reads from the paired reads were not measured twice in the final analysis. The bismark coverage files were then imported into R for further analysis.

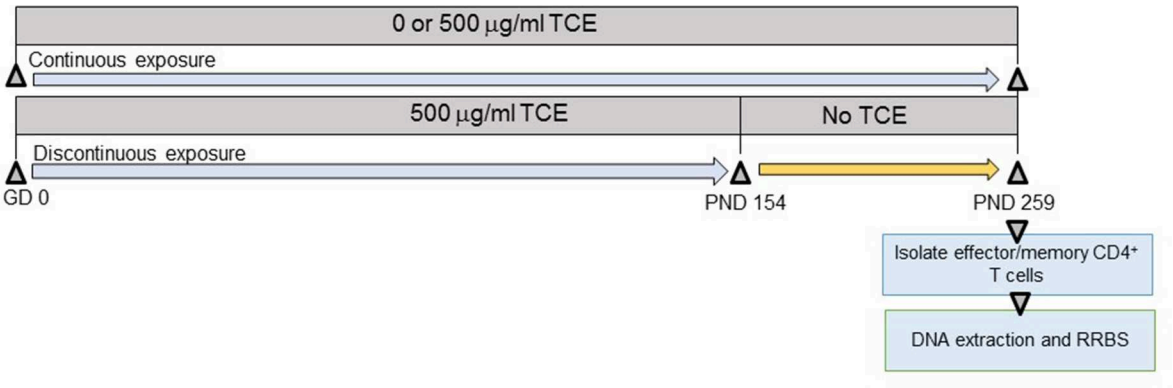

FIGURE 1 | Experimental design. Prior to breeding, female MRL+/+ mice were randomly assigned to treatment groups consisting of (1) vehicle control; (2) 500 μg/ml TCE. Female offspring were exposed continuously during development during gestation, lactation, and directly via the drinking water during early life. At PND 154 TCE was removed from the drinking water from a subset of the offspring. The remaining mice continued vehicle or TCE in the drinking water until PND 259 when all animals were euthanized. $CD4^+$ T cells were purified into effector/memory subsets and subjected to DNA extraction and RRBS analysis as described in the methods.

Bioinformatics Analysis and Assessment of Global and Differentially Methylated Regions

Methylation levels were also investigated based on the distance to the nearest transcriptional start site (TSS) and plotted using the lowess function in R. The overall global methylation patterns were averaged over all genes. Negative distances correspond to CpG sites downstream of gene TSS. The coefficients of the glmLRT models generated for each comparison were used to assess changes in methylation patterns relative to control as described (36).

The bismark coverage bed files for each sample were generated from Bismark methylation extractor and imported into R in order to identify differentially methylated regions (DMRs) between the control sample TCE dose (continuous), and between the control sample and the TCE dose that was discontinued at PND154 (discontinuous). The analysis was performed as described using the *edge*R Bioconductor package (36, 37) *edge*R is based on the negative binomial distribution and models the variation between biological replicates through the negative binomial dispersion parameter. As opposed to other methylation sequencing data analysis methods, this workflow keeps the counts for methylated and unmethylated reads as separate observations and does not limit analysis to percent methylation. Linear models are then used to fit the total read count (methylated plus unmethylated or M+U) at each genomic locus and methylated reads are modeled indirectly as an over-dispersed binomial distribution. DMRs are assessed by generalized linear models with likelihood ratio tests using edgeR generalized linear model likelihood ratio test (glmLRT). The *p*-values were corrected using the false discovery rate.

The total counts matrix was created by identifying CpG sites present in at least one sample and extracting the read counts of both methylated and unmethylated Cs at each CpG site within each sample. The data was analyzed for individual CpG sites as well as grouping the sites by CpG islands, promoter regions, and by regulatory elements based on the UCSC oregano track. The data was then filtered by requiring a CpG site to have a total count (M+U) of at least 8 across all the samples before it was included in the analysis. CpG islands, promoters, and regulatory elements were required to have a total count of at least 20, 50, and 30 total counts across all of the samples, respectively. The count matrix was then normalized so that the methylated and unmethylated reads were treated as a single unit, and the library sizes were set to be equal for each pair of libraries (average of the methylated and unmethylated library sizes). Both β-values (M/M+U) and M-values (log2 M/U) were calculated for each sample and compared. shinyCircos was used to generate a circos heatmap for the log2 fold-change values in order to visually represent the changes in methylation of promoters and regulatory elements (38).

Annotation of CpG Sites and Pathway Analysis

Several genomic regions of interest, including CpG islands, promoters, and regulatory elements were analyzed between the different sample groups by annotating with different UCSC genome browser tracks. Individual CpG islands were annotated with the gene with the nearest TSS. Promoters were analyzed using Bioconductor Open Source Software for Bioinformatics Annotation Package (*TxDb.Mmusculus.UCSC.mm10.knownGene package).* We defined the promoter of a gene as the region from 2 kb upstream to 1 kb downstream of the transcription start site (TSS) of that gene. We also analyzed regulatory elements including transcription factor binding sites, RNA binding sites, regulatory variants, and other regulatory elements utilizing the Open Regulatory Annotation database [(ORegAnno) (39)]. Once the counts matrix was annotated by each track and region of interest, the GLM-likelihood ratio test was applied to identify significantly differentially methylated regions in the continuous and discontinuous TCE dose samples. DMRs were considered

significant by a FDR adjusted p-value ≤ 0.05 and fold change > 2. GO terms overrepresentation analysis for molecular function and biological process of the significant promoter regions used the groupGO function of the clusterProfiler R package The KEGG pathway analysis was performed using clusterProfiler's gseKEGG function with default parameters (40).

RESULTS

Assessment of Global Methylation Patterns

As shown in **Figure 1** and described in the methods section, we performed RRBS analysis of purified effector/memory ($CD44^{hi}/CD62L^{lo}$) $CD4^+$ T cells from female MRL+/+ mice exposed to TCE as described previously (32, 33). All mice were euthanized at PND 259. The RRBS DNA methylation data was quality checked and filtered prior to differential analysis. Global methylation patterns in effector/memory $CD4^+$ T cells were analyzed using fry gene set analysis to identify differences in the methylation patterns at the TSS between continuous or discontinuous exposures compared to the control group. Overall, 288,894 CpG sites were assessed in the analysis. The methylated cytosine counts were summed across all genomic regions. **Figures 2A–C** shows histogram plots of global methylation patterns across all genes ± 20,000 bp of the TSS for each group. The plots showed that regardless of treatment, the basic shape of the methylation distribution did not differ among the groups **(Figure 2A)**. The histogram also revealed that most of the methylated CpG regions were furthest from the TSS, and a majority of the unmethylated CpGs were closest to the TSS regardless of TCE exposure. This pattern was similar when CpG islands, promoters, regulatory elements, and chromosomes were assessed individually (data not shown). Thus, CpG methylation levels in effector/memory $CD4^+$ T cells on a global scale were similar among all groups.

Global changes in methylation with continuous exposure (**Figure 2B**) or discontinuous exposure (**Figure 2C**) relative to controls are presented in histogram plots. The results revealed that effector/memory $CD4^+$ T cells have greater differences in methylation when TCE exposure was continuous. In marked contrast, there was very little change in the levels of methylation relative to controls in $CD4^+$ T cells isolated from mice whose TCE was removed from the drinking water ∼15 weeks before study terminus. While the greatest changes in methylation occurred in regions closest to the TSS in both groups, this effect was more evident in the continuous exposure group implying increased potential for altered gene expression.

Assessment of Differentially Methylated Regions in Promoters and CpG Islands

Several genomic regions of interest, including CpG islands, promoters, and ORegAnno regulatory elements were analyzed between the different sample groups by annotating with different UCSC genome browser tracks. Each genomic regions provides unique insight into how DNA methylation alterations regulate gene expression as either individual CpG sites or as a region. For instance, CpG methylation in promoter regions is often associated with silencing of transcription and gene expression. The methylation count data was analyzed using edge R glmLRT as described in the methods section to identify differentially methylated regions (DMRs) associated with each of the UCSC genome browser tracks.

First, we assessed the methylation of CpG islands in each exposure group. CpG sites overlapped with 15,788 of the 16,023 CpG islands in the mouse genome. After filtering for low counts, 13,084 CpG islands (82.9%) remained for DMR analysis. **Figure 3**, represents mean difference (MD) plots of the DMRs in CpG islands, promoter regions, and regulatory elements. Regions found to be significantly hypermethylated or hypomethylated in the exposure group compared to controls are depicted in red and blue, respectively. As shown in **Figure 3A** and in **Table 1**, a majority of the DMRs in both the continuous and discontinuous groups in CpG islands were hypermethylated (69%) relative to controls. Fourteen CpG island regions were significantly hypermethylated, and nine CpG islands were hypomethylated with continuous TCE exposure. In the discontinuous group, only four CpG island regions were significantly hypermethylated relative to controls. As shown in **Table 1**, among the four hypermethylated CpG islands in the discontinuous group, two regions were also hypermethylated in the continuous exposure group; namely, CpG 69 on chromosome 8 (3.72- vs. 3.88-fold; continuous vs. discontinuous, respectively), and CpG 24 on chromosome 9 (4.52- vs. 5.12-fold; continuous vs. discontinuous, respectively). Interestingly, both of these island regions have been previously linked to PcG-mediated H3K27 tri-methylation, an epigenetic repressive mark (41).

In the discontinuous group, two additional CpG islands were hypermethylated relative to controls that were not altered in the continuous group (**Table 1**). One region, CpG 32 on Chr11 encodes matrix metalloproteinase 28 (epilysin) or MMP-28. Although not thoroughly studied in T cells, MMP-28 has been shown to be a key regulatory of inflammation and macrophage differentiation (42). The other distinct island region, CpG 30 on Chr7, is a binding site for the transcription factor, Bhlhe40, known to control cytokine production by T cells and has been identified as a critical regulator of autoreactive T cell pathology (43).

In the promoter regions 2,080,592 CpG sites overlapped with 23,711 of the 24,044 promoter regions in the UCSC knownGenes track. After quality filtering, 13,322 promoter regions were analyzed. In the continuous exposure group, 252 CpGs were significantly differentially methylated compared to controls (**Figure 3B**). Out of these CpGs, 239 (95%) were hypermethylated and only 13 (5%) were hypomethylated relative to control. In contrast, none of the promoter regions were significantly altered relative to controls in the discontinuous group.

Differentially Methylated Regions Regulatory Elements Were Enriched for Polycomb Protein Binding Sites

We assessed regulatory elements included in the ORegAnno database. After filtering regions with low counts, 13,500 of the 415,390 elements were included in DMR analysis. As shown in **Figure 3C**, removal of the TCE from the drinking water did

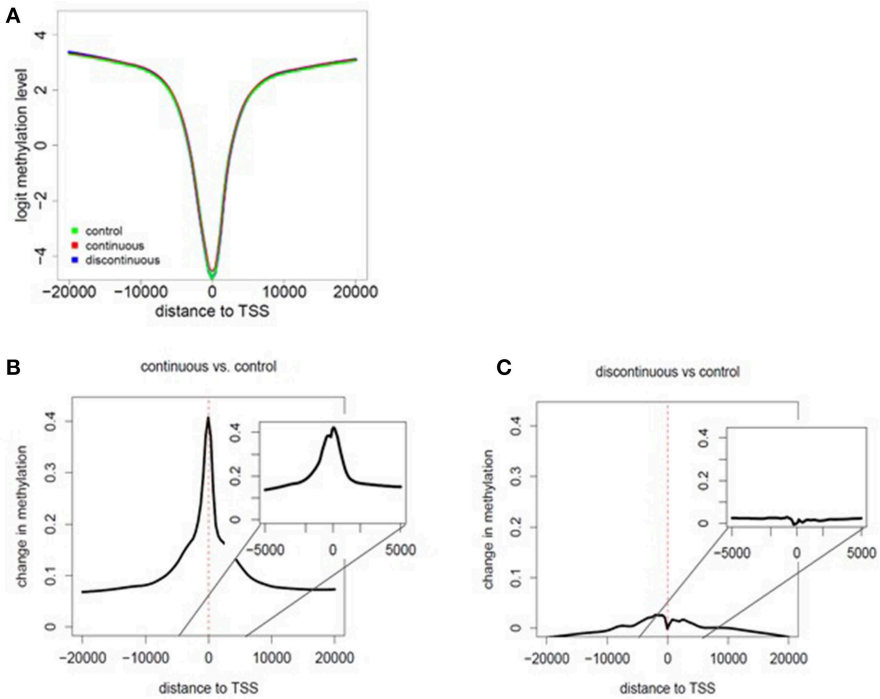

FIGURE 2 | Assessment of global methylation patterns. **(A)** Methylation levels averaged over all genes were investigated based on the distance to the nearest TSS (± 20,000 bp of the TSS for each group). The data in the histogram overlay depicts the methylation level from each exposure group. **(B,C)** Global changes in methylation with continuous exposure **(B)** or discontinuous exposure **(C)** relative to controls are presented in histogram plots. The inset shows the average change in methylation ± 5,000 bp around the TSS. Negative distances correspond to CpG sites downstream of gene TSS. The coefficients of the glmLRT models generated for each comparison were used to assess change in methylation patterns relative to control.

not significantly alter the methylation pattern of the $CD4^+$ T cells compared to control. However, continuous TCE treatment resulted in 113 hypermethylated and 16 hypomethylated elements. These binding sites included 12 unique transcription factors and regulatory elements. Interestingly, 80% of these DMRs included binding sites for PcG proteins associated with PRC2, namely; SUZ12, EZH2, JARID2, and MTF2. A majority of these PcG enriched DMRs were hypermethylated ($n = 99$) and only 6 were hypomethylated ($n = 6$). **Figure 4A** shows the number of hypermethylated vs. hypomethylated DMRs for each PcG protein binding region. **Figure 4B** breaks down the six hypomethylated regions according to gene and chromosome location. The *klhl4* gene on chromosome nine was linked to two PcG protein binding sites, SUZ12 and MTF2. Based on this finding, we analyzed the other 99 hypermethylated DMRs associated with PcG protein binding to see if any of the genes were linked to a shared region. **Figure 5** shows that among these regions, 16 unique genes linked to 44 DMRs were associated with more than one PcG protein binding site.

The other statistically significant DMRs included transcription factors representing 12 sites including; EBF1 (Early B Cell Factor 1), GATA1 (GATA Binding Protein 1), FOXA2 (Forkhead Box A2), STAT1 (Signal Transducer and Activator of Transcription), ATOH1 (Atonal BHLH Transcription Factor 1), ESR1 (Estrogen Receptor 1), KLF1 (Kruppel Like Factor 1), and EGR2 (Early Growth Response 2) (**Table 2**). Although there were fewer significant DMRs in transcription factor binding sites compared to PcG binding regions; a greater percentage of the DMRs in the transcription factor binding sites were hypomethylated; 14 of the transcription factor binding sites were hypermethylated and 10 regions were hypomethylated. Depending on the chromosomal location, five transcription binding sites were both hyper- and hypomethylated (GATA1, FOXA2, EBF1, and STAT1). ATOH1 was only hypermethylated (on chr7 and chr5), and three transcription factors (KLF1, ESR1, and EGR2) were exclusively hypomethylated.

A circos heatmap of the log2 fold change values in the continuous treatment compared to controls was generated to summarize the data. **Figure 6** depicts regional location and chromosomal location of hyper- and hypo-methylated DMRs in both promoters (outer ring) and regulatory elements (inner ring). Overall, the DMRs were predominantly hypermethylated (red) as opposed to only a few blue regions indicating hypomethylation. Thus, based on the overall hypermethylation of genes in regulatory elements and promoters, continuous TCE treatment may favor overall suppression of transcription compared to controls. The complete list of genes and chromosomal location for all DMRs linked to promoters and regulatory regions are found in **Supplementary Table 1**.

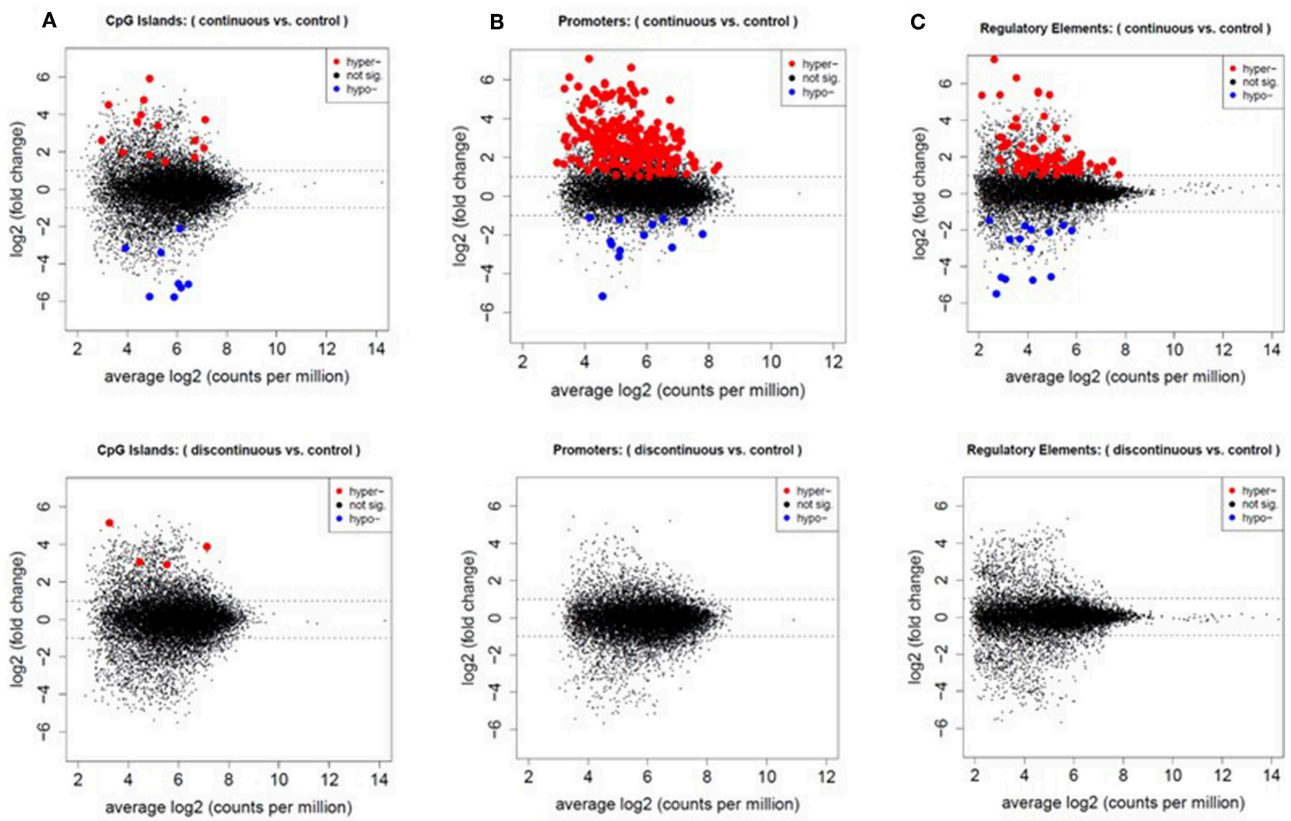

FIGURE 3 | Increased number of differentially methylated regions in the continuous exposure group. CpG sites were grouped by CpG islands **(A)**, promoter regions **(B)**, and regulatory elements **(C)** as described in the methods. Differentially methylated regions were analyzed using edgeR glmLRT. Graphs of the MD-plots represent the fold change (log2) between either continuous vs. control or discontinuous vs. control. DMRs were considered significant with an FDR-adjusted $p \leq 0.05$ and fold change > 2.

Pathways and Genes Associated With DMRs

Pathway analysis of the CpG sites differentially methylated by continuous TCE exposure in promoter regions revealed that, in terms of biological processes (**Figure 7A**), TCE primarily altered the methylation of genes associated with regulation of cellular metabolism, catabolism, and biosynthesis. Focusing in on the molecular function category, TCE effects were associated with transferase/hydrolase and cataloytic activity that were in turn, enriched for genes associated with various functions including cellular signaling pathways (**Figures 7B,C**). Taken together, TCE altered DNA methylation in a manner that seemed primed to impact downstream gene expression.

DISCUSSION

Sensitivity to immunotoxicants has been shown to be greater in animal models if exposure occurred during development compared with adulthood (44). In humans, it is not uncommon for IMIDs to manifest during childhood or adolescence suggesting developmental origins (45). These effects are believed to be due, in part, to epigenetic alterations including aberrant DNA methylation (46–50). DNA methylation is crucial for normal functioning of T cells during development. For example, CpG demethylation is important during T cell maturation in the thymus related to TCR function (51). In early life, the phenotype of $CD4^+$ T cell subsets that have differentiated in response to antigen are normally controlled by carefully maintained levels of DNA methylation in pertinent regulatory genes (52, 53). Throughout the lifespan, regulation of Th subset differentiation and expansion of effector/memory $CD4^+$ T cells is DNA methylation dependent (54). Thus, any event that perturbs the methylome may have important consequences for $CD4^+$ T cell function and disease. Aside from TCE, a role for environmental chemical exposures during development including mercury, dioxin, and bisphenol-A have been shown to alter DNA methylation and promote autoimmunity (55).

In the current study, it was predicted that a continuous exposure to TCE administered during development and early life would have a greater impact on the DNA methylation patterns of activated effector/memory $CD4^+$ T cells compared to adult-only exposure (28). Overall, TCE-mediated effects reported in this study and our previous study were strikingly similar. Apparently, TCE exposure, regardless of whether it began during development or adulthood, was associated

TABLE 1 | DMRs in CpG islands.

Chr	ID	Start	End	#CpG	%CpG	#Gc	%Gc	Fold change (log2)	FDR
Continuous									
Chr19	35	61266505	61266971	466	15	242	51.9	5.932811	0.012014
Chr15	61	76904006	76904671	665	18.3	404	60.8	4.784853	1.69E-05
Chr9	24	78427458	78427765	307	15.6	185	60.3	4.521959	0.005407
Chr9	18	58247028	58247256	228	15.8	138	60.5	4.004769	0.029688
Chr8	69	19784572	19785241	669	20.6	454	67.9	3.72208	1.69E-05
Chrx	128	6172298	6173448	1150	22.3	716	62.3	3.621685	0.014121
Chr9	83	1.09E+08	1.09E+08	929	17.9	570	61.4	3.406221	0.020168
Chr6	45	1.13E+08	1.13E+08	422	21.3	285	67.5	2.611359	0.014121
Chr9	233	95405215	95407761	2546	18.3	1698	66.7	2.602433	0.017659
Chr19	62	8888448	8889270	822	15.1	462	56.2	2.215014	0.029688
Chr2	23	75981547	75981815	268	17.2	162	60.4	1.970652	0.051439
Chr7	93	97325217	97326011	794	23.4	564	71	1.842948	0.020168
Chr5	43	1.24E+08	1.24E+08	365	23.6	252	69	1.735225	0.005407
Chrx	52	36111947	36112448	501	20.8	363	72.5	1.472045	0.012014
Chr6	53	1.41E+08	1.41E+08	367	28.9	258	70.3	−5.7822	0.005281
Chr2	54	34870778	34871358	580	18.6	370	63.8	−5.73915	0.004199
Chr1	81	1.61E+08	1.61E+08	887	18.3	564	63.6	−5.27595	0.029688
Chr15	94	76080388	76081110	722	26	512	70.9	−5.0925	0.048491
Chr3	37	27182877	27183286	409	18.1	262	64.1	−5.06582	0.031513
Chr18	53	74267931	74268512	581	18.2	383	65.9	−3.37984	0.038562
Chr5	17	1.35E+08	1.35E+08	226	15	140	61.9	−3.15186	0.026914
Chr10	70	22273321	22274267	946	14.8	582	61.5	−2.11188	0.051439
Discontinuous									
Chr9	24	78427445	78427765	307	15.6	185	60.3	5.159825	0.000668
Chr8	69	19784572	19785241	669	20.6	454	67.9	3.886291	0.000102
Chr11	32	83444820	83445050	230	27.8	157	68.3	3.056442	0.020591
Chr7	30	5125832	5126107	275	21.8	188	68.4	2.931381	0.028506

Pink represents hypermethylation and blue represents hypomethylation.

with enrichment of regions of the genome linked to PcG group binding in effector/memory $CD4^+$ T cells. Another consistent finding between the two studies was that CpG methylation in activated effector/memory $CD4^+$ T cells favored hypermethylation rather than hypomethylation. Thus, the results of two independent studies involving chronic low-level TCE exposure were relatively consistent.

In addition to global changes we focused on specific genomic regions of interest, including CpG islands, promoters, and ORegAnno regulatory elements by annotating with different UCSC genome browser tracks to understand how alterations in DNA methylation may regulate gene expression on an individual CpG level or as a region. When these regions were assessed, a total of 403 significant DMRs were identified in the continuous exposure group relative to controls after quality filtering; almost twice as many significant DMRs identified than in our previous investigation (28).

The complex interplay between DNA methylation and PRC2 binding and its functional consequences in T cells are only beginning to be studied. Among the PRC2 components that regulate PcG function, EZH2 is perhaps the most widely studied in T cells where it is highly expressed (56). Loss of EZH2, which enables functional inactivation of PRC2 and reduction of H3K27me3 levels, has been shown to promote autoimmune pathology commensurate with a reduction in T reg numbers (57) Three independent groups reported decreased IFN-γ production from PRC2/EZH2 deficient T cells cultured under Th1 polarizing conditions (31, 58, 59). One other report showed that EZH2 increased the stability of T-bet, an important Th1 transcription factor (60). Together, these reports underscore the importance of PcG proteins in Th1 differentiation, and suggest that a TCE-mediated alteration in PRC2 binding and downstream upregulation of proinflammatory Th1 cytokines could play a role in the ability of TCE to promote autoimmunity.

Additional work is needed to understand how TCE exposure modulates EZH2 and other associated PcG proteins in the PRC2 complex (e.g., SUZ12, MTF2) whose binding to DNA due to TCE-mediated DNA hypermethylation may be compromised. Indeed stability of PRC2 is dependent on several different components. PRC2 is stably recruited by MTF2 with JARID2, and are important in establishing repressive domains across the genome. In *mtf2* knockout cells, EZH2 catalytic subunit is abrogated, resulting in greatly reduced H3K27me3 deposition (61). Recently, a live imaging study underscored the importance

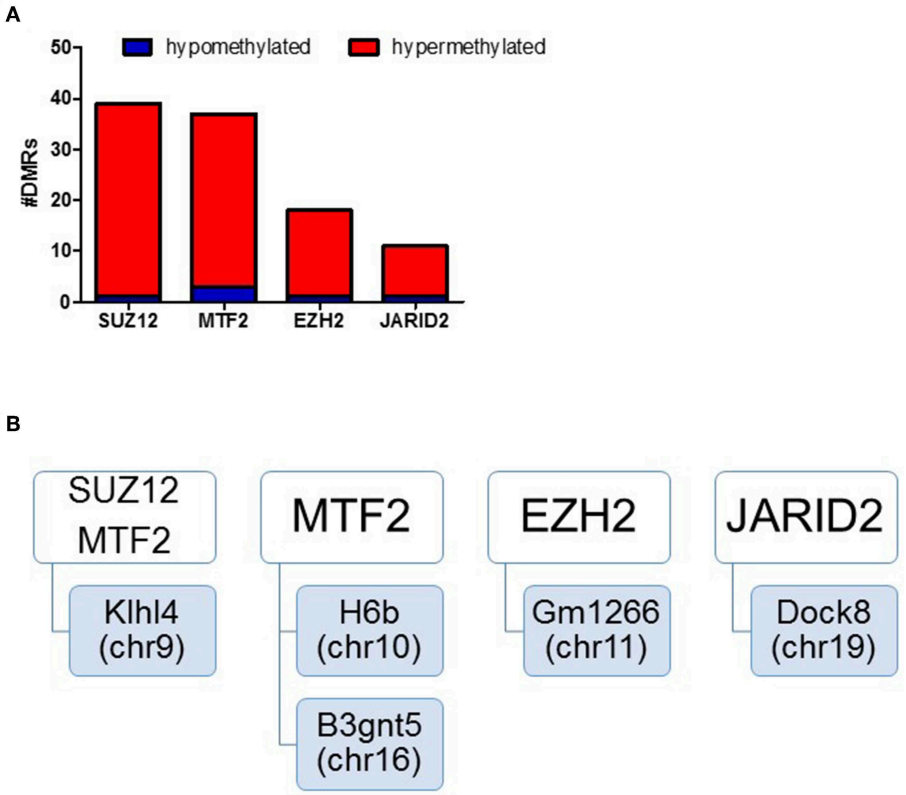

FIGURE 4 | DMRs of PcG binding sites in continuous exposure group are predominantly hypermethylated. RRBS analysis of effector memory $CD4^+$ T cells from control and continuous TCE exposure. **(A)** Regulatory elements included in the ORegAnno database were assessed. The number of hypermethylated vs. hypomethylated DMRs for each PcG protein binding region are shown. **(B)** Represents a summary of the few hypomethylated regions according to gene and chromosome location.

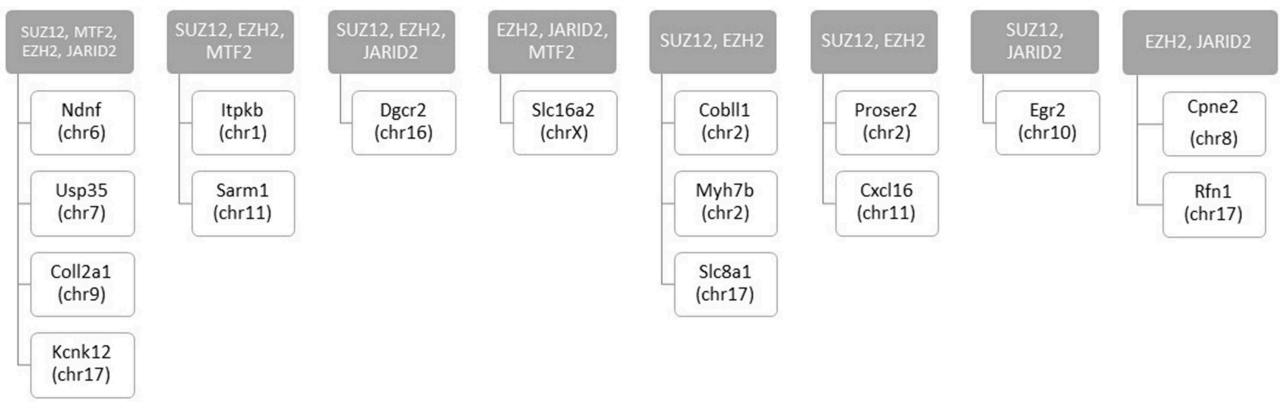

FIGURE 5 | Number of hypermethylated DMRs that are linked to more than one PcG binding sites with continuous exposure. RRBS analysis of effector memory $CD4^+$ T cells from control and continuous TCE exposure revealed 129 statistically significant DMRs from regulatory elements based on ORegAnno database. The hypermethylated DMRs associated with PcG group binding sites ($n = 99$) were linked to 16 unique genes associated with more than 1 PcG protein binding site.

of SUZ12 interaction with several accessory proteins for PRC2 chromatin binding *in vivo* (62). Thus, it is apparent that these PcG proteins are all indispensable functionally for PRC2. Our finding that many of the DMRs associated with TCE exposure bound more than one PcG binding site underscores a need to further study the complex interplay between TCE-induced DNA methylation events and PcG proteins.

In addition to PcG protein binding regions, in the remaining 20% of DMRs, 12 transcription factors were identified as being differentially methylated in the continuous exposure group. All

TABLE 2 | Transcription factors associated with DMRs from regulatory regions in the continuous exposure group.

Oreg ID	TF binding site	Gene	Chr	Start site	Fold change (log2)	FDR
OREG1667709	GATA1	Got1	chr19	43524408	5.400330	0.0378661
OREG1667084	GATA1	Ntpcr	chr8	125734385	5.3773777	0.0531756
OREG0071054	FOXA2		chr2	155050089	4.223175	0.001133
OREG1562375	EBF1	Ryr1	chr7	29040109	3.087317	0.0300861
OREG1666877	GATA1	Cyb5b	chr8	107150438	3.0108383	0.0451529
OREG1201127	ATOH1	Gm12764	chr7	34390804	2.130084	0.00403
OREG1559800	EBF1	Btd	chr14	31660270	1.797766	0.028670
OREG1564020	EBF1	Vps33a	chr5	123572681	1.742096	0.000369
OREG0048798	FOXA2	Gfil	chr5	107687900	1.460722	0.0328458
OREG1864590	STAT1	Gfi1	chr5	107688001	1.423059	0.0300861
OREG1199817	ATOH1	Gfi1	chr5	107688015	1.422497	0.024385
OREG0048387	FOXA2		chr4	150889206	1.3308524	0.0406727
OREG1665142	GATA1	Pde4dip	chr3	97767156	1.271897	0.021289
OREG1562020	EBF1	Cnksr3	chr10	7158580	1.2246290	0.0514763
OREG1760351	KLF1	Fig4	chr10	41204944	−5.4811978	0.0298196
OREG1668792	GATA1	Fig4	chr10	41204856	−5.4811978	0.0298196
OREG1563191	EBF1	Flcn	chr11	59809474	−4.7241132	0.0201386
OREG0042314	FOXA2	Ddx42	chr11	106216425	−4.6945932	0.0153887
OREG1863898	STAT1	Ddx42	chr11	106216435	−4.5741675	0.0221824
OREG0035646	ESR1		chr11	116199352	−4.54767328	0.0270150
OREG0598482	EGR2		chr2	144599905	−3.01723545	0.0286700
OREG1869968	STAT1	Eif4ebp3	chr18	36663812	−2.50431736	0.0300861
OREG0037174	ESR1	Eif4ebp3	chr18	36663725	−2.50431736	0.0300861
OREG1561198	EBF1	Slc1a1	chr12	80998351	−1.46607522	0.0220945

Pink represents hypermethylation and blue represents hypomethylation.

of these transcription factor binding sites have been shown to potentially alter T cells and/or affect subset differentiation, and some have been implicated in autoimmunity. For example, FOXA2 is has been shown to regulate T cell differentiation in the thymus to promote positive selection of $CD4^+$ T cells while downregulating Tregs (63). FOXA2 modulated the production of Th2 cytokines in mouse atopic dermatitis model via its action on T regs (64). In the current study, FOXA2 was both hypermethylated and hypomethylated in different regions. In fact, we showed that, unlike the PcG sites, there were almost as many hypomethylated regions as hypermethylated regions including 3 transcription factor binding sites that were exclusively hypomethylated (e.g., KLF1, ESR1, and EGR2) with continuous exposure. Although the significance of this finding is not clear, all 3 of these transcription factors have been shown to impact some aspect of T cell differentiation and autoimmunity (65–67).

The study also included an evaluation of activated effector/memory $CD4^+$ T cells isolated from mice after TCE was removed for a period of 15 weeks prior to study terminus. Persistence of functional effects in adult mice after developmental exposure followed by removal of TCE from the drinking water has been reported in previous studies (35, 68) including the mice that were used for a source of effector/memory $CD4^+$ T cell DNA for RRBS in the current study (32, 33). These results indicated a unique programming effect of TCE after discontinuation of the dose. Because epigenetic changes are often associated with maintenance of phenotypic effects, we expected to find DNA methylation events would be maintained and perhaps unique methylation profiles linked to these sustained phenotypes would be revealed. However, based on the global methylation pattern and DMR results, very little significant changes in methylation were found in the discontinuous group. It is not clear why the phenotypical effects observed in the same animals did not translate to DNA methylation effects. It is plausible that organ pathology occurred well before the TCE was removed, and events may have been irreversible based on some other mechanism including direct toxicant-induced direct damage or by disrupting repair or anti-oxidant systems designed to promote regeneration and recovery.

Despite the seemingly modest results in the discontinuous group, one interesting finding was the 2 shared hypermethylated DMRs in CpG islands in both the continuous and discontinuous group. The significance of this finding is not clear, but these shared CpG island regions have been associated with histone H3K27 tri-methylation (41). Mammalian PRC2 binding sites in CpG islands have primarily been described in embryonic stem cells where these island regions are generally unmethylated but remain transcriptionally active via H3K27, and have been identified as an important mechanism for expression of tumor suppressor genes (69). In contrast, PRC2 binding does not appear to be restricted to CpG islands in somatic

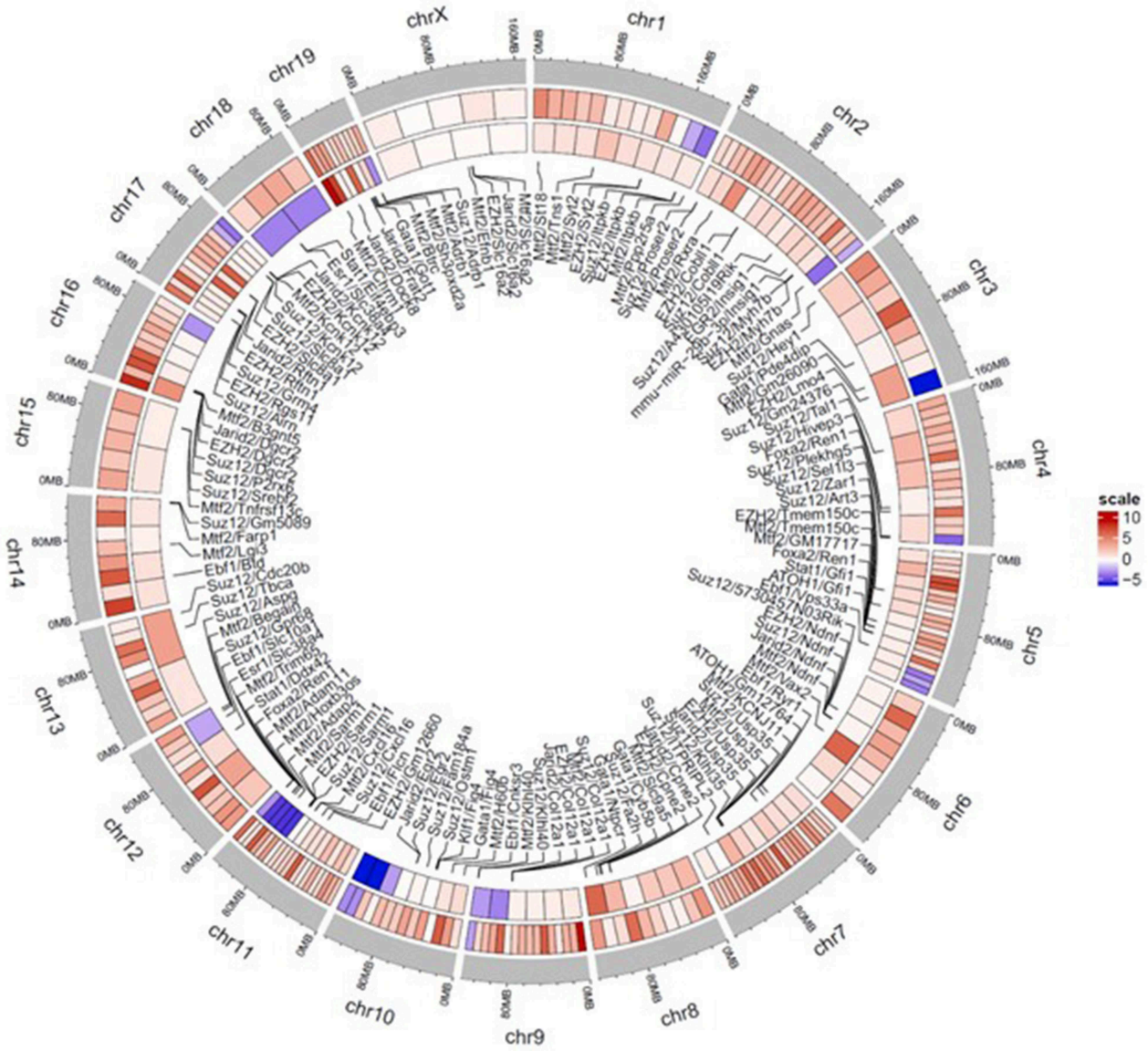

FIGURE 6 | Circos plot heatmap showing gene promoter and regulatory element regions that were significantly hyper or hypo-methylated with continuous TCE exposure. The heatmap indicates the average Log 2 fold change values for the statistically significant DMRs of promoters (outer ring) and regulatory elements (innermost ring). The outer most ring (gray) shows the chromosome and location. The lines point to associated regulatory element and chromosome location. Red indicates hypermethylation and blue indicates hypomethylation relative to controls.

cell types where there is a complex interplay between PRC2 binding and DNA methylation that is not well understood (70). Promoter regions with methylated H3K27 are more likely to gain DNA methylation by PRC2 recruitment of DNA methyltransferases during differentiation (71–73). Taken together, our result would suggest that certain PcG protein-related functions may be impaired due to increased methylation of these regions with continuous exposure. It is possible that at least some of these PcG-mediated functions could be maintained over time after removal of TCE from the drinking water. A closer look at these island regions may indicate a potential mechanism involved in the maintenance of immunotoxicity and autoimmune disease progression in our model.

Limitations of the study included the use of *ex vivo* stimulated CD4s without additional comparisons including assessment of effector/memory CD4 cells that were not stimulated with anti-CD3/CD28. Such an assessment would have provided useful baseline responses. However, this limitation does not affect the significance of the findings of the current study that was designed to directly compare TCE's effects on genome-wide DNA methylation patterns in our published study using only activated effector/memory CD4s from mice that were exposed during development vs. adulthood (28).

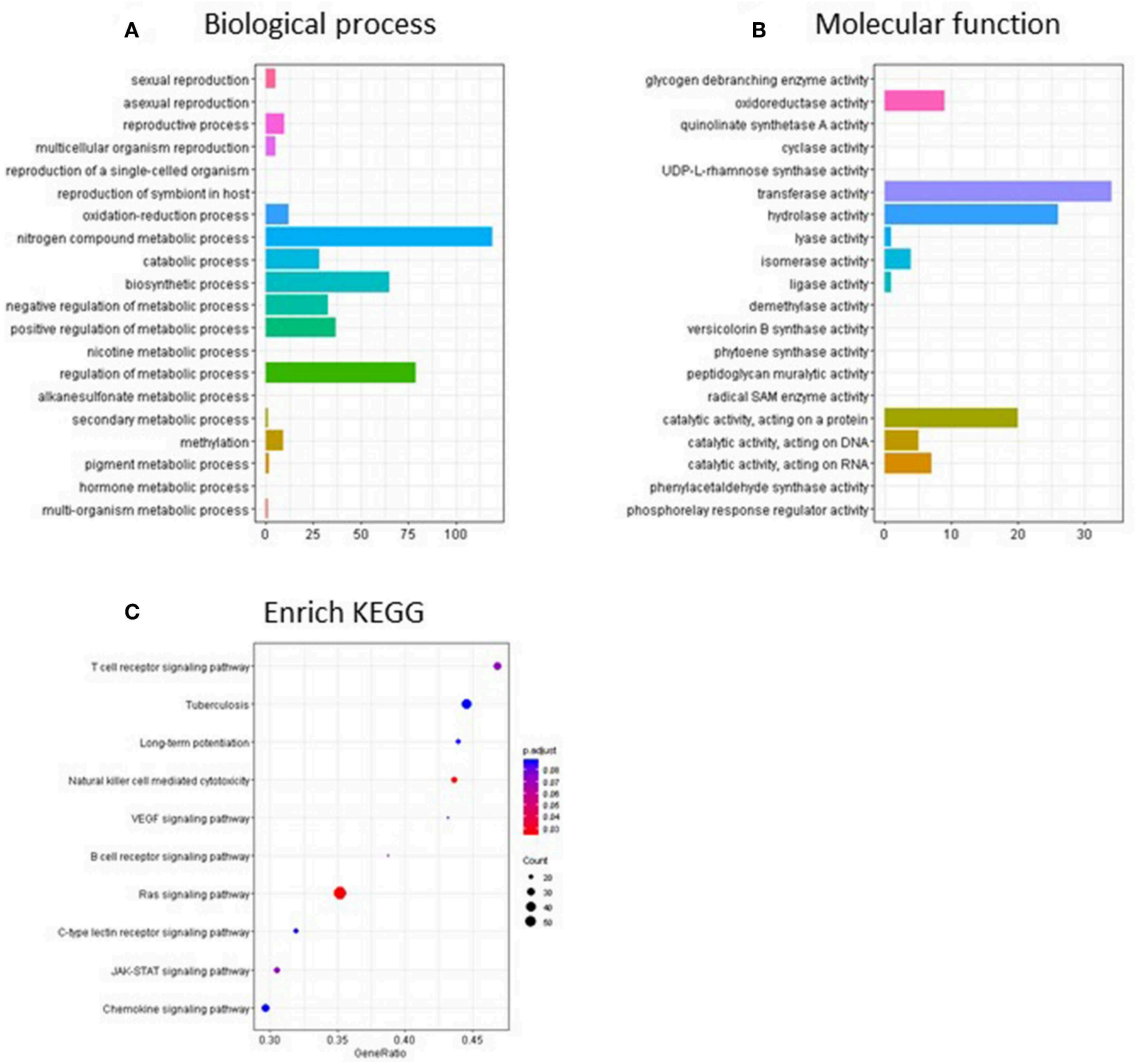

FIGURE 7 | Go terms and KEGG enriched pathways in the promoter regions of the continuous TCE group compared to control. GO terms overrepresentation analysis for **(A)** biological process and **(B)** molecular function of the significant promoter regions used the groupGO function of the clusterProfiler R package as described in the methods. **(C)** The KEGG pathway analysis was performed using clusterProfiler's gseKEGG function with default parameters.

Although we expected to observe even more robust changes following a developmental exposure compared to adult only exposure, this study was conducted in already differentiated, activated effector memory $CD4^+$ T cells. It is known that epigenetic modifications are more likely to accompany $CD4^+$ T cell differentiation, and these dynamic events are difficult to recapitulate *in vivo*. Thus a different approach that includes examining the time-dependent events that accompany $CD4^+$ T cell differentiation is necessary to distinguish whether enrichment of PcG proteins in the current study are associated with alterations and corresponding gene in actively differentiating cells. Our results highlight the possibility that similarities observed between continuous developmental vs. adult-only exposure represent marks of a terminally differentiated cell rather than some alteration that is unique to the timing of the exposure. Despite the limitations, the current study demonstrated that TCE regulated PcG binding sites in effector/memory $CD4^+$ T cells when exposure occurred continuously throughout development and early life. Future research will continue to explore how these DNA methylation alterations in PcG proteins may promote TCE-induced immunotoxicity with implications for autoimmune disease mechanisms in humans.

ETHICS STATEMENT

This study was carried out in accordance with the recommendations of Animal Welfare Act and PHS Policy on Humane Care and Use of Laboratory Animals. The protocol was approved by the University of Arkansas for Medical Sciences Institutional Animal Care and Use Committee.

AUTHOR CONTRIBUTIONS

SBy contributed to the manuscript by overseeing all aspects of data analysis and assisted in writing the manuscript. CW conducted data analysis, assisted in writing of the manuscript, and generated many of the figures presented in the manuscript. JP assisted with organization and analysis of the data. KV conducted animal exposures and prepared the T cells for DNA extraction and library preparation. KG implemented the experimental design and conducted initial data analysis. SBl contributed to the manuscript by implementing the experimental design, interpreting the results, and writing the manuscript.

FUNDING

This work was supported by grants from the National Institutes of Health (NIEHS-R01ES021484 and K02ES024387) and by the Center for Translational Pediatric Research (CTPR) NIH Center of Biomedical Research Excellence Award (P20 GM121293).

ACKNOWLEDGMENTS

The authors acknowledge the Arkansas Children's Research Institute Genomics Core and the Systems Biology Bioinformatics Core. We also thank Craig A. Cooney, PhD for insightful discussion and assistance with the initial planning and implementation of this project.

SUPPLEMENTARY MATERIAL

The Supplementary Material for this article can be found online at: https://www.frontiersin.org/articles/10.3389/fimmu.2019.02016/full#supplementary-material

REFERENCES

1. El-Gabalawy H, Guenther LC, Bernstein CN. Epidemiology of immune-mediated inflammatory diseases: incidence, prevalence, natural history, and comorbidities. *J Rheumatol Suppl*. (2010) 85:2–10. doi: 10.3899/jrheum.091461
2. Walsh SJ, Rau LM. Autoimmune diseases: a leading cause of death among young and middle-aged women in the United States. *Am J Public Health*. (2000) 90:1463–6. doi: 10.2105/AJPH.90.9.1463
3. Parks CG, Miller FW, Pollard KM, Selmi C, Germolec D, Joyce K, et al. Expert panel workshop consensus statement on the role of the environment in the development of autoimmune disease. *Int J Mol Sci*. (2014) 15:14269–97. doi: 10.3390/ijms150814269
4. Cooper GS, Makris SL, Nietert PJ, Jinot J. Evidence of autoimmune-related effects of trichloroethylene exposure from studies in mice and humans. *Environ Health Perspect*. (2009) 117:696–702. doi: 10.1289/ehp.11782
5. Huang Y, Xia L, Wu Q, Zeng Z, Huang Z, Zhou S, et al. Trichloroethylene hypersensitivity syndrome is potentially mediated through its metabolite chloral hydrate. *PLoS ONE*. (2015) 10:e0127101. doi: 10.1371/journal.pone.0127101
6. Parks CG, De Roos AJ. Pesticides, chemical and industrial exposures in relation to systemic lupus erythematosus. *Lupus*. (2014) 23:527–36. doi: 10.1177/0961203313511680
7. Zhao JH, Duan Y, Wang YJ, Huang XL, Yang GJ, Wang J. The influence of different solvents on systemic sclerosis: an updated meta-analysis of 14 case-control studies. *J Clin Rheumatol*. (2016) 22:253–9. doi: 10.1097/RHU.0000000000000354
8. EPA. *TSCA Work Plan for Chemical Assessments: 2014 Update* (2014).
9. Bassig BA, Zhang L, Vermeulen R, Tang X, Li G, Hu W, et al. Comparison of hematological alterations and markers of B-cell activation in workers exposed to benzene, formaldehyde and trichloroethylene. *Carcinogenesis*. (2016) 37:692–700. doi: 10.1093/carcin/bgw053
10. Hosgood HD III, Zhang L, Tang X, Vermeulen R, Qiu C, Shen M, et al. Decreased numbers of CD4(+) naive and effector memory T cells, and CD8(+) naive T cells, are associated with trichloroethylene exposure. *Front Oncol*. (2012) 1:53. doi: 10.3389/fonc.2011.00053
11. Lan Q, Zhang L, Tang X, Shen M, Smith MT, Qiu C, et al. Occupational exposure to trichloroethylene is associated with a decline in lymphocyte subsets and soluble CD27 and CD30 markers. *Carcinogenesis*. (2010) 31:1592–6. doi: 10.1093/carcin/bgq121
12. Yi J, Teng YX, Zang D, Zhou W, Dong HY, Niu Y, et al. [Analysis of subgroups of lymphocyte in peripheral blood among dermatitis medicamentosa-like of trichloroethylene patients and healthy exposed workers]. *Zhonghua Yu Fang Yi Xue Za Zhi*. (2011) 45:1017–21. doi: 10.3760/cma.j.issn.0253-9624.2011.11.014
13. Gilbert KM, Przybyla B, Pumford NR, Han T, Fuscoe J, Schnackenberg LK, et al. Delineating liver events in trichloroethylene-induced autoimmune hepatitis. *Chem Res Toxicol*. (2009) 22:626–32. doi: 10.1021/tx800409r
14. Griffin JM, Gilbert KM, Lamps LW, Pumford NR. CD4(+) T-cell activation and induction of autoimmune hepatitis following trichloroethylene treatment in MRL+/+ mice. *Toxicol Sci*. (2000) 57:345–52. doi: 10.1093/toxsci/57.2.345
15. Wang G, Wang J, Ma H, Ansari GA, Khan MF. N-Acetylcysteine protects against trichloroethene-mediated autoimmunity by attenuating oxidative stress. *Toxicol Appl Pharmacol*. (2013) 273:189–95. doi: 10.1016/j.taap.2013.08.020
16. Kawakami N, Odoardi F, Ziemssen T, Bradl M, Ritter T, Neuhaus O, et al. Autoimmune $CD4^+$ T cell memory: lifelong persistence of encephalitogenic T cell clones in healthy immune repertoires. *J Immunol*. (2005) 175:69–81. doi: 10.4049/jimmunol.175.1.69
17. Oling V, Reijonen H, Simell O, Knip M, Ilonen J. Autoantigen-specific memory $CD4^+$ T cells are prevalent early in progression to Type 1 diabetes. *Cell Immunol*. (2012) 273:133–9. doi: 10.1016/j.cellimm.2011.12.008
18. Zhang Y, Zhao M, Sawalha AH, Richardson B, Lu Q. Impaired DNA methylation and its mechanisms in CD4(+)T cells of systemic lupus erythematosus. *J Autoimmun*. (2013) 41:92–9. doi: 10.1016/j.jaut.2013.01.005
19. Chung SA, Nititham J, Elboudwarej E, Quach HL, Taylor KE, Barcellos LF, et al. Genome-wide assessment of differential DNA methylation associated with autoantibody production in systemic lupus erythematosus. *PLoS ONE*. (2015) 10:e0129813. doi: 10.1371/journal.pone.0129813
20. Jeffries MA, Dozmorov M, Tang Y, Merrill JT, Wren JD, Sawalha AH. Genome-wide DNA methylation patterns in $CD4^+$ T cells from patients with systemic lupus erythematosus. *Epigenetics*. (2011) 6:593–601. doi: 10.4161/epi.6.5.15374
21. Li H, Tsokos MG, Bickerton S, Sharabi A, Li Y, Moulton VR, et al. Precision DNA demethylation ameliorates disease in lupus-prone mice. *JCI Insight*. (2018) 3:120880. doi: 10.1172/jci.insight.120880
22. Strickland FM, Li Y, Johnson K, Sun Z, Richardson BC. CD4(+) T cells epigenetically modified by oxidative stress cause lupus-like autoimmunity in mice. *J Autoimmun*. (2015) 62:75–80. doi: 10.1016/j.jaut.2015.06.004
23. Hirahara K, Nakayama T. $CD4^+$ T-cell subsets in inflammatory diseases: beyond the Th1/Th2 paradigm. *Int Immunol*. (2016) 28:163–71. doi: 10.1093/intimm/dxw006
24. Ivanova EA, Orekhov AN. T helper lymphocyte subsets and plasticity in autoimmunity and cancer: an overview. *Biomed Res Int*. (2015) 2015:327470. doi: 10.1155/2015/327470
25. Gilbert KM, Blossom SJ, Erickson SW, Broadfoot B, West K, Bai S, et al. Chronic exposure to trichloroethylene increases DNA methylation

of the Ifng promoter in CD4$^+$ T cells. *Toxicol Lett.* (2016) 260:1–7. doi: 10.1016/j.toxlet.2016.08.017
26. Gilbert KM, Blossom SJ, Erickson SW, Reisfeld B, Zurlinden TJ, Broadfoot B, et al. Chronic exposure to water pollutant trichloroethylene increased epigenetic drift in CD4(+) T cells. *Epigenomics.* (2016) 8:633–49. doi: 10.2217/epi-2015-0018
27. Gilbert KM, Nelson AR, Cooney CA, Reisfeld B, Blossom SJ. Epigenetic alterations may regulate temporary reversal of CD4(+) T cell activation caused by trichloroethylene exposure. *Toxicol Sci.* (2012) 127:169–78. doi: 10.1093/toxsci/kfs093
28. Gilbert KM, Blossom SJ, Reisfeld B, Erickson SW, Vyas K, Maher M, et al. Trichloroethylene-induced alterations in DNA methylation were enriched in polycomb protein binding sites in effector/memory CD4(+) T cells. *Environ Epigenet.* (2017) 3:6. doi: 10.1093/eep/dvx013
29. Margueron R, Reinberg D. The Polycomb complex PRC2 and its mark in life. *Nature.* (2011) 469:343–9. doi: 10.1038/nature09784
30. Dobenecker MW, Park JS, Marcello J, McCabe MT, Gregory R, Knight SD, et al. Signaling function of PRC2 is essential for TCR-driven T cell responses. *J Exp Med.* (2018) 215:1101–13. doi: 10.1084/jem.20170084
31. Yang XP, Jiang K, Hirahara K, Vahedi G, Afzali B, Sciume G, et al. EZH2 is crucial for both differentiation of regulatory T cells and T effector cell expansion. *Sci Rep.* (2015) 5:10643. doi: 10.1038/srep10643
32. Gilbert KM, Bai S, Barnette D, Blossom SJ. Exposure cessation during adulthood did not prevent immunotoxicity caused by developmental exposure to low-level trichloroethylene in drinking water. *Toxicol Sci.* (2017) 157:429–37. doi: 10.1093/toxsci/kfx061
33. Khare S, Gokulan K, Williams K, Bai S, Gilbert KM, Blossom SJ. Irreversible effects of trichloroethylene on the gut microbial community and gut-associated immune responses in autoimmune-prone mice. *J Appl Toxicol.* (2019) 39:209–20. doi: 10.1002/jat.3708
34. Lee KM, Zhang L, Vermeulen R, Hu W, Bassig BA, Wong JJ, et al. Alterations in immune and renal biomarkers among workers occupationally exposed to low levels of trichloroethylene below current regulatory standards. *Occup Environ Med.* (2019). 76:376–81. doi: 10.1136/oemed-2018-105583
35. Blossom SJ, Fernandes L, Bai S, Khare S, Gokulan K, Yuan Y, et al. Opposing actions of developmental trichloroethylene and high-fat diet coexposure on markers of lipogenesis and inflammation in autoimmune-prone mice. *Toxicol Sci.* (2018) 164:313–27. doi: 10.1093/toxsci/kfy091
36. Robinson MD, McCarthy DJ, Smyth GK. edgeR: a Bioconductor package for differential expression analysis of digital gene expression data. *Bioinformatics.* (2010) 26:139–40. doi: 10.1093/bioinformatics/btp616
37. McCarthy DJ, Chen Y, Smyth GK. Differential expression analysis of multifactor RNA-Seq experiments with respect to biological variation. *Nucleic Acids Res.* (2012) 40:4288–97. doi: 10.1093/nar/gks042
38. Yu Y, Ouyang Y, Yao W. shinyCircos: an R/Shiny application for interactive creation of Circos plot. *Bioinformatics.* (2018) 34:1229–31. doi: 10.1093/bioinformatics/btx763
39. Lesurf R, Cotto KC, Wang G, Griffith M, Kasaian K, Jones SJ, et al. ORegAnno 3.0: a community-driven resource for curated regulatory annotation. *Nucleic Acids Res.* (2016) 44:D126–32. doi: 10.1093/nar/gkv1203
40. Yu G, Wang LG, Han Y, He QY. clusterProfiler: an R package for comparing biological themes among gene clusters. *OMICS.* (2012) 16:284–7. doi: 10.1089/omi.2011.0118
41. Koppens MA, Bounova G, Gargiulo G, Tanger E, Janssen H, Cornelissen-Steijger P, et al. Deletion of polycomb repressive complex 2 from mouse intestine causes loss of stem cells. *Gastroenterology.* (2016) 151:684–97 e12. doi: 10.1053/j.gastro.2016.06.020
42. Long ME, Gong KQ, Volk JS, Eddy WE, Chang MY, Frevert CW, et al. Matrix metalloproteinase 28 is regulated by TRIF- and type I IFN-dependent signaling in macrophages. *Innate Immun.* (2018) 24:357–65. doi: 10.1177/1753425918791024
43. Lin CC, Bradstreet TR, Schwarzkopf EA, Sim J, Carrero JA, Chou C, et al. Bhlhe40 controls cytokine production by T cells and is essential for pathogenicity in autoimmune neuroinflammation. *Nat Commun.* (2014) 5:3551. doi: 10.1038/ncomms4551
44. Dietert RR. Role of developmental immunotoxicity and immune dysfunction in chronic disease and cancer. *Reprod Toxicol.* (2011) 31:319–26. doi: 10.1016/j.reprotox.2010.09.006
45. Kappelman MD, Galanko JA, Porter CQ, Sandler RS. Association of paediatric inflammatory bowel disease with other immune-mediated diseases. *Arch Dis Child.* (2011) 96:1042–6. doi: 10.1136/archdischild-2011-300633
46. Alisch RS, Barwick BG, Chopra P, Myrick LK, Satten GA, Conneely KN, et al. Age-associated DNA methylation in pediatric populations. *Genome Res.* (2012) 22:623–32. doi: 10.1101/gr.125187.111
47. Colebatch AN, Edwards CJ. The influence of early life factors on the risk of developing rheumatoid arthritis. *Clin Exp Immunol.* (2011) 163:11–6. doi: 10.1111/j.1365-2249.2010.04263.x
48. Dietert RR. Developmental immunotoxicity, perinatal programming, and noncommunicable diseases: focus on human studies. *Adv Med.* (2014) 2014:867805. doi: 10.1155/2014/867805
49. Edmiston E, Ashwood P, Van de Water J. Autoimmunity, autoantibodies, and autism spectrum disorder. *Biol Psychiatry.* (2017) 81:383–90. doi: 10.1016/j.biopsych.2016.08.031
50. Sun B, Hu L, Luo ZY, Chen XP, Zhou HH, Zhang W. DNA methylation perspectives in the pathogenesis of autoimmune diseases. *Clin Immunol.* (2016) 164:21–7. doi: 10.1016/j.clim.2016.01.011
51. Rodriguez RM, Suarez-Alvarez B, Mosen-Ansorena D, Garcia-Peydro M, Fuentes P, Garcia-Leon MJ, et al. Regulation of the transcriptional program by DNA methylation during human alphabeta T-cell development. *Nucleic Acids Res.* (2015) 43:760–74. doi: 10.1093/nar/gku1340
52. Hashimoto S, Ogoshi K, Sasaki A, Abe J, Qu W, Nakatani Y, et al. Coordinated changes in DNA methylation in antigen-specific memory CD4 T cells. *J Immunol.* (2013) 190:4076–91. doi: 10.4049/jimmunol.1202267
53. Komori HK, Hart T, LaMere SA, Chew PV, Salomon DR. Defining CD4 T cell memory by the epigenetic landscape of CpG DNA methylation. *J Immunol.* (2015) 194:1565–79. doi: 10.4049/jimmunol.1401162
54. Schmidl C, Delacher M, Huehn J, Feuerer M. Epigenetic mechanisms regulating T-cell responses. *J Allergy Clin Immunol.* (2018) 142:728–43. doi: 10.1016/j.jaci.2018.07.014
55. Blossom SJ, Gilbert KM. Epigenetic underpinnings of developmental immunotoxicity and autoimmune disease. *Curr Opin Toxicol.* (2018) 10:23–30. doi: 10.1016/j.cotox.2017.11.013
56. Onodera A, Tumes DJ, Watanabe Y, Hirahara K, Kaneda A, Sugiyama F, et al. Spatial interplay between polycomb and trithorax complexes controls transcriptional activity in T lymphocytes. *Mol Cell Biol.* (2015) 35:3841–53. doi: 10.1128/MCB.00677-15
57. Sarmento OF, Svingen PA, Xiong Y, Sun Z, Bamidele AO, Mathison AJ, et al. The role of the histone methyltransferase enhancer of zeste homolog 2 (EZH2) in the pathobiological mechanisms underlying inflammatory bowel disease (IBD). *J Biol Chem.* (2017) 292:706–22. doi: 10.1074/jbc.M116.749663
58. Tumes DJ, Onodera A, Suzuki A, Shinoda K, Endo Y, Iwamura C, et al. The polycomb protein Ezh2 regulates differentiation and plasticity of CD4(+) T helper type 1 and type 2 cells. *Immunity.* (2013) 39:819–32. doi: 10.1016/j.immuni.2013.09.012
59. Zhang Y, Kinkel S, Maksimovic J, Bandala-Sanchez E, Tanzer MC, Naselli G, et al. The polycomb repressive complex 2 governs life and death of peripheral T cells. *Blood.* (2014) 124:737–49. doi: 10.1182/blood-2013-12-544106
60. Tong Q, He S, Xie F, Mochizuki K, Liu Y, Mochizuki I, et al. Ezh2 regulates transcriptional and posttranslational expression of T-bet and promotes Th1 cell responses mediating aplastic anemia in mice. *J Immunol.* (2014) 192:5012–22. doi: 10.4049/jimmunol.1302943
61. Perino M, van Mierlo G, Karemaker ID, van Genesen S, Vermeulen M, Marks H, et al. MTF2 recruits polycomb repressive complex 2 by helical-shape-selective DNA binding. *Nat Genet.* (2018) 50:1002–10. doi: 10.1038/s41588-018-0134-8
62. Youmans DT, Schmidt JC, Cech TR. Live-cell imaging reveals the dynamics of PRC2 and recruitment to chromatin by SUZ12-associated subunits. *Genes Dev.* (2018) 32:794–805. doi: 10.1101/gad.311936.118
63. Lau CI, Yanez DC, Solanki A, Papaioannou E, Saldana JI, Crompton T. Foxa1 and Foxa2 in thymic epithelial cells (TEC) regulate medullary TEC and regulatory T-cell maturation. *J Autoimmun.* (2018) 93:131–8. doi: 10.1016/j.jaut.2018.07.009

64. Ahmed MS, Kang MH, Lee E, Park Y, Jeong Y, Bae YS. SH2 domain-containing adaptor protein B expressed in dendritic cells is involved in T-cell homeostasis by regulating dendritic cell-mediated Th2 immunity. *Clin Exp Vaccine Res*. (2017) 6:50–60. doi: 10.7774/cevr.2017.6.1.50
65. Mohammad I, Starskaia I, Nagy T, Guo J, Yatkin E, Vaananen K, et al. Estrogen receptor alpha contributes to T cell-mediated autoimmune inflammation by promoting T cell activation and proliferation. *Sci Signal*. (2018) 11:eaap9415. doi: 10.1126/scisignal.aap9415
66. Taefehshokr S, Key YA, Khakpour M, Dadebighlu P, Oveisi A. Early growth response 2 and Egr3 are unique regulators in immune system. *Cent Eur J Immunol*. (2017) 42:205–9. doi: 10.5114/ceji.2017.69363
67. Teruya S, Okamura T, Komai T, Inoue M, Iwasaki Y, Sumitomo S, et al. Egr2-independent, Klf1-mediated induction of PD-L1 in CD4(+) T cells. *Sci Rep*. (2018) 8:7021. doi: 10.1038/s41598-018-25302-1
68. Blossom SJ, Melnyk SB, Li M, Wessinger WD, Cooney CA. Inflammatory and oxidative stress-related effects associated with neurotoxicity are maintained after exclusively prenatal trichloroethylene exposure. *Neurotoxicology*. (2017) 59:164–74. doi: 10.1016/j.neuro.2016.01.002
69. Bae MG, Kim JY, Choi JK. Frequent hypermethylation of orphan CpG islands with enhancer activity in cancer. *BMC Med Genomics*. (2016) 9 (suppl. 1):38. doi: 10.1186/s12920-016-0198-1
70. Rose NR, Klose RJ. Understanding the relationship between DNA methylation and histone lysine methylation. *Biochim Biophys Acta*. (2014) 1839:1362–72. doi: 10.1016/j.bbagrm.2014.02.007
71. Mohn F, Weber M, Rebhan M, Roloff TC, Richter J, Stadler MB, et al. Lineage-specific polycomb targets and de novo DNA methylation define restriction and potential of neuronal progenitors. *Mol Cell*. (2008) 30:755–66. doi: 10.1016/j.molcel.2008.05.007
72. Schlesinger Y, Straussman R, Keshet I, Farkash S, Hecht M, Zimmerman J, et al. Polycomb-mediated methylation on Lys27 of histone H3 pre-marks genes for *de novo* methylation in cancer. *Nat Genet*. (2007) 39:232–6. doi: 10.1038/ng1950
73. Vire E, Brenner C, Deplus R, Blanchon L, Fraga M, Didelot C, et al. The Polycomb group protein EZH2 directly controls DNA methylation. *Nature*. (2006) 439:871–4. doi: 10.1038/natur e04431

Conflict of Interest Statement: The authors declare that the research was conducted in the absence of any commercial or financial relationships that could be construed as a potential conflict of interest.

frontiers in Immunology

ORIGINAL RESEARCH
published: 04 September 2019
doi: 10.3389/fimmu.2019.02015

Lupus Autoimmunity and Metabolic Parameters Are Exacerbated Upon High Fat Diet-Induced Obesity Due to TLR7 Signaling

*Noël Hanna Kazazian, Yawen Wang, Annie Roussel-Queval, Laetitia Marcadet†, Lionel Chasson, Caroline Laprie, Benoit Desnues†, Jonathan Charaix, Magali Irla and Lena Alexopoulou**

Aix Marseille University, CNRS, INSERM, CIML, Marseille, France

Systemic lupus erythematosus (SLE) patients have increased prevalence of metabolic syndrome but the underlying mechanisms are unknown. Toll-like receptor 7 (TLR7) that detects single stranded-RNA plays a key role in antimicrobial host defense and also contributes to the initiation and progression of SLE both in mice and humans. Here, we report the implication of TLR7 signaling in high fat diet (HFD)-induced metabolic syndrome and exacerbation of lupus autoimmunity in TLR8-deficient (TLR8ko) mice, which develop spontaneous lupus-like disease due to increased TLR7 signaling by dendritic cells (DCs). The aggravated SLE pathogenesis in HFD-fed TLR8ko mice was characterized by increased overall immune activation, anti-DNA autoantibody production, and IgG/IgM glomerular deposition that were coupled with increased kidney histopathology. Moreover, upon HFD TLR8ko mice developed metabolic abnormalities, including liver inflammation. In contrast, upon HFD TLR7/8ko mice did not develop SLE and both TLR7ko and TLR7/8ko mice were fully protected from metabolic abnormalities, including body weight gain, insulin resistance, and liver inflammation. Interestingly, HFD led to an increase of TLR7 expression in WT mice, that was coupled with increased TNF production by DCs, and this phenotype was more profound in TLR8ko mice. Our study uncovers the implication of TLR7 signaling in the interconnection of SLE and metabolic abnormalities, indicating that TLR7 might be a novel approach as a tailored therapy in SLE and metabolic diseases.

Keywords: systemic lupus erythematosus (SLE), toll-like receptor 7 (TLR7), metabolic syndrome, obesity, animal model, innate immunity, dendritic cells

OPEN ACCESS

Edited by:
Allen Jay Rosenspire, Wayne State University, United States

Reviewed by:
Åsa Andersson, Halmstad University, Sweden
Vanja Sisirak, UMR5164 Immunologie Conceptuelle, Expérimentale et Translationnelle (Immuno ConcEpT), France

***Correspondence:**
Lena Alexopoulou
alexopoulou@ciml.univ-mrs.fr

†Present address:
Laetitia Marcadet, Centre de Recherche CHU de Québec Axe Neurosciences - Université Laval Québec, Quebec City, QC, Canada
Benoit Desnues, Aix-Marseille Univ, IRD, APHM, MEPHI, IHU-Méditerranée Infection, Marseille, France

Specialty section:
This article was submitted to Autoimmune and Autoinflammatory Disorders, a section of the journal Frontiers in Immunology

Received: *15 February 2019*
Accepted: *08 August 2019*
Published: *04 September 2019*

Citation:
Hanna Kazazian N, Wang Y, Roussel-Queval A, Marcadet L, Chasson L, Laprie C, Desnues B, Charaix J, Irla M and Alexopoulou L (2019) Lupus Autoimmunity and Metabolic Parameters Are Exacerbated Upon High Fat Diet-Induced Obesity Due to TLR7 Signaling. Front. Immunol. 10:2015. doi: 10.3389/fimmu.2019.02015

INTRODUCTION

Epidemiological data provide evidence of a significant increase of autoimmune diseases in the last 30 years and growing attention has focused on the role of environmental factors, especially the western dietary habits that have led to the parallel rise in obesity (1). A link between obesity, metabolic syndrome and autoimmune diseases, including systemic lupus erythematosus (SLE), and the associated chronic inflammation has been suggested, but the underlying mechanisms are still unknown (2, 3).

SLE is a chronic systemic autoimmune disease predominantly affecting young women, during their reproductive years, and is characterized by the presence of autoantibodies against self-nucleic acids and associated proteins (4). Self-nucleic acids released by dying cells are recognized by the autoantibodies and form immune complexes, which accumulate in different organs, leading to increased inflammation and tissue damage. SLE pathogenesis derives from the combination of genetic, environmental, hormonal, and epigenetic factors (4). Current standard of care treatments for SLE are mainly non-selective immunosuppressants. However, not all patients respond to these treatments, and one major side effect of the systemic immunosuppression is the increased incidence of infection (5). Thus, better understanding of the pathogenesis of SLE is pivotal for the development of new treatments.

Metabolic syndrome is characterized by several risk factors that include central obesity, insulin resistance, dyslipidemia, increased blood pressure, and endothelial dysfunction (6). It is highly linked to SLE and is associated with cumulative organ damage (7, 8). Metabolic syndrome is also common in young patients with recently diagnosed SLE. These patients present higher levels of inflammatory markers, than SLE subjects without metabolic syndrome (9). In childhood-onset SLE increased serum tumor necrosis factor (TNF) levels are associated with obesity and body fat content (10). The white adipose tissue is a crucial site for the generation of soluble mediators most of which carry pro-inflammatory activity. These include classical cytokines such as tumor necrosis factor alpha (TNF), interleukin 6 (IL-6), and adipokines such as leptin, adiponectin, and resistin (11). By their pro-inflammatory action, these molecules contribute to low-grade inflammation in obese subjects. Dysfunctional adipose tissue lipid metabolism leads to increased circulating fatty acids that initiates inflammatory signaling cascades in the population of infiltrating cells (11). A feedback loop of pro-inflammatory cytokines exacerbates this pathological state driving further immune infiltration and cytokine secretion and disrupts the insulin signaling cascade. In addition to adipose tissue, other metabolically critical sites, particularly the liver, are also involved during the course of the disease. Fatty liver is characterized by excessive triglyceride deposition as lipid droplets in hepatocytes that trigger mitochondrial oxidative stress and hepatic inflammation with increased TNF, IL-6, and IL-1β, cytokine production, which are considered as critical factors leading to the progression from benign hepatic steatosis to advanced steatohepatitis or even fibrosis and cirrhosis (12). All together, these events lead to what is termed a sterile inflammatory response, which if not appropriately resolved, can lead to the development of chronic inflammation that underlies or exacerbates autoimmunity.

Little is known about the early molecular events that lead to immune cell infiltration and inflammatory cytokine production in adipose tissue or liver. Nevertheless, the Toll-like receptor (TLR) family has recently emerged as a critical link between inflammation and a contributor to obesity and insulin resistance, both in mice and in humans (13–15). Among the 10 human TLR members, TLR2, TLR4, TLR5, and TLR9 have been reported as regulators of metabolic inflammation and insulin resistance in liver and adipose tissue (16–19). TLRs are evolutionary conserved transmembrane receptors that play a critical role in driving innate and adaptive immunity through the recognition of various microbial components and the activation of signaling pathways critical for the induction of inflammatory responses (20). In addition to sensing exogenous microbial ligands, TLRs also detect endogenous molecules released from damaged tissues or dead cells and regulate many sterile inflammatory processes (21). Mammalian endosomal TLRs (TLR3, TLR7, TLR8, and TLR9) and especially TLR7 play an important role in the development of SLE both in humans (22–24) and in mice (25–28). TLR7 and TLR8 are phylogenetically similar and both sense single stranded RNA (ssRNA) in humans, while in the mouse only TLR7 senses ssRNA (29–31). Despite the fact that murine TLR8 does not seem to have a ligand (32, 33), we previously demonstrated that it plays an important biological role by controlling TLR7-mediated lupus. Indeed, TLR8-deficiency in mice on the C57BL/6 background leads to lupus development due to increased TLR7 expression and signaling by DCs (26–28). Hence, tight control and regulation of TLR7 is pivotal for avoiding SLE and inflammatory pathology.

The implication of TLR7 in the chronic inflammation of SLE in the context of obesity or metabolic syndrome has never been reported to date. Given the increased risk of metabolic syndrome in SLE patients and the fact that TLR7 is implicated in SLE development we hypothesized that TLR7 might be the connecting link between metabolic syndrome and SLE. Thus, in the current study we evaluated the impact of high fat diet (HFD) on the development of SLE and metabolic syndrome in TLR8-deficient mice (TLR8ko) that spontaneously develop SLE due to increased TLR7 signaling by DCs (26–28). Our data revealed that in TLR8ko mice HFD exacerbated the development of SLE, and increased the occurrence of metabolic abnormalities. The elevated disease course in HFD-fed TLR8ko mice was accompanied by increased TLR7 expression and signaling in DCs. In contrast to TLR8ko mice, TLR7/8ko mice were fully protected from SLE and metabolic syndrome. Hence, TLR7 signaling is implicated in the connection between SLE and metabolic disease.

MATERIALS AND METHODS

Mice

TLR7ko, TLR8ko, and double TLR7/8ko mice were generated as described previously (26, 31, 34). All three TLR-deficient mouse lines were backcrossed on the C57BL/6 background for more than 10 generations. Familiar transmission shapes the distinct intestinal microbiota of TLR-deficient mice (35). Therefore, in order to normalize the microbiota between the TLR-deficient mice and WT controls and because the TLR7 and TLR8 genes are both located in the X chromosome, female age-matched TLR-deficient mice and their respective WT control mice were derived by mating littermate TLR-heterozygous female mice with WT or TLR-deficient male mice (e.g., $TLR8^{X+X-}$ x $TLR8^{X+Y}$,

Abbreviations: BWF1, (NZB x NZW) F1; DC, dendritic cell; HFD, high fat diet; pDC, plasmacytoid dendritic cell; SD, standard diet; TLR, Toll-like receptor.

or TLR8^{X-Y}). Mice were allowed to consume water and pellet shew *ad libitum*. For the HFD-induced obesity model, mice received either HFD (Research Diets, D12492; 60% of kcals from fat and 20% of kcals from carbohydrate) or standard diet (SD) (Research Diets, D12450J; 10% of kcals from fat, 70% of kcals from carbohydrate) beginning at 3 months of age. Mice were housed under specific pathogen-free conditions at the Center d'Immunologie de Marseille-Luminy and experiments were conducted in accordance with institutional guidelines for animal care and with protocols approved by the Comité National de Réflexion Ethique sur l'Expérimentation Animale (protocol number 13.325).

Reagents

R848, LPS from *E. coli* 0111-B4, CpG ODN 1826 and poly I:C were purchased from Invivogen.

RNA Isolation and Q-PCR

Total RNA was isolated with TRIzol reagent (Ambion, Life Technologies). RNA was reversed transcribed with Superscript II reverse transcriptase (Invitrogen) and Q-PCR for TLR7, TNF, IL-6, IL-1β, IL-10, Foxp3, and β-actin was performed as described previously (26). Primers are listed in **Table S1**.

Serological Analysis

Evaluation of IgM, and IgG autoantibodies against DNA and RNA on serum samples were performed as described previously (26).

Glucose Tolerance Test

Mice fed HFD or SD were injected intraperitonially with D-glucose (1 g/kg body weight) after 6 h fast. Blood was collected from tail tip at the indicated time points and glycemia was determined using a glucometer (ACCU-CHEK, Roche).

Flow Cytometric Analysis

Mice were euthanized, perfused with 10 ml sterile PBS solution to remove blood cells and then spleen, liver, or adipose tissue were extracted. Spleen was passed through a 200-gauge nylon mesh to obtain a single cell suspension followed by erythrocyte lysis. Splenocytes were digested with digestion solution (RPMI medium containing 2% FCS, 7 mg/ml Collagenase II and 1 mg/ml DNase I) for 20 min at 37°C. Following enzymatic digestion, cell suspension was passed through a 70 μm cell strainer and splenocytes were collected by centrifugation. Isolation of hepatic lymphocytes with mechanical dissection was carried out as follows: liver was cut in small pieces by scissors, suspended in digestion solution, incubated at 37°C for 20 min, cell suspension was passed through a 100 μm cell strainer, centrifuged, and erythrocytes were lysed. After centrifugation the cell pellet was resuspend in 80% Percoll solution, overlaid by a layer of 40% Percoll solution followed by centrifugation at 1,500 g for 20 min, the cells were aspirated from the Percoll interface and harvested by centrifugation. Stromal vascular fraction cells from adipose tissue were isolated with an adipose tissue dissociation kit from Miltenyi Biotec using manufacturer's instructions.

Cell suspensions were incubated with 24G2 hybridoma supernatant and then stained using fluorochrome-labeled antibodies against the following antigens: CD45.2, B220, CD3, NK1.1, CD11b, Ly6G, CD44, CD62L, CD38, CD138, GL7 from BD Biosciences, F4/80, CD4, CD8, IA/IE (MHC class II) from eBioscience and CD11c, CD64, SiglecH, CD69 from Biolegend. For intracellular staining of TLR7 and TNF, cells were fixed with Cytofix (BD Biosciences), permeabilized with 0.1% saponin containing staining buffer and stained in saponin buffer using immunofluorescence labeled antibodies for TLR7 (A94B10 from BD Biosciences) and TNF (MP6-XT22 from BD Biosciences). For intracellular staining of Foxp3, cells were fixed, permeabilized and stained with a Foxp3 staining kit, according to the manufacturer's instructions (FJK-16s from eBioscience). Flow cytometry was conducted using an LSR2 (BD Biosciences) and data were analyzed with FlowJo (Tree Star). The gating strategies for the various cell populations are presented in **Figures S1**, **S2**.

Histology and Immunofluorescence

For histopathology studies, livers were fixed in formalin and embedded in paraffin. For light microscopy 3–4 μm thick tissue sections were stained with hematoxylin and eosin (H&E). To determine the extent of renal and liver damage, biopsies were analyzed by a pathologist. Typical glomerular active lesions of lupus nephritis were evaluated based on glomerular cellularity, glomerular deposits, and interstitial inflammation. At least 20 glomeruli per kidney were evaluated. Kidney scoring was from 0 to 4 corresponding to no, low, moderate, high and severe changes, respectively. Liver scoring was from 0 to 3 [0, no inflammation; 1, mild inflammation (<5% of section area); 2 moderate inflammation (5–10% of section area); and 3 marked inflammation (more than 10% of section area)]. For cryostat sections, livers, and kidneys were embedded in OCT-compound and frozen in liquid nitrogen. Sections were cut on a cryostat at 10 μm, thaw-mounted on gelatinized slides, and immunofluorescence IgG and IgM staining on kidney sections and Oil red O staining on liver sections were performed as described previously (26, 36).

Statistical Analysis

Statistics were done using Prism 7 (GraphPad Software). In **Figures 1A,B**, **3G** comparisons were done only between two groups (SD-fed WT vs. TLR8ko mice, or HFD-fed WT vs. TLR8ko mice) and the statistics were done using Wilcoxon rank sum test. Statistics in **Figures 1C–F**, **2**, **3A–F**, **4**, **5**, **6A,B** were done by Kruskal-Wallis test followed by Wilcoxon rank sum tests and correction for multiple comparisons using the Benjamini-Hochberg method. *P*-values indicated throughout correspond to: $p < 0.05$ (*), $p < 0.01$ (**), $p < 0.001$ (***), $p < 0.0001$ (****).

RESULTS

HFD Aggravates the Lupus Phenotype of TLR8ko Mice

TLR8ko mice on the C57BL/6 background develop lupus due to increased TLR7 expression by DCs (26, 28). To evaluate the effect of high fat diet (HFD) on TLR7-dependent lupus, 3 months old female TLR8ko mice and their respective WT controls (see materials and methods) were fed on either standard diet (SD)

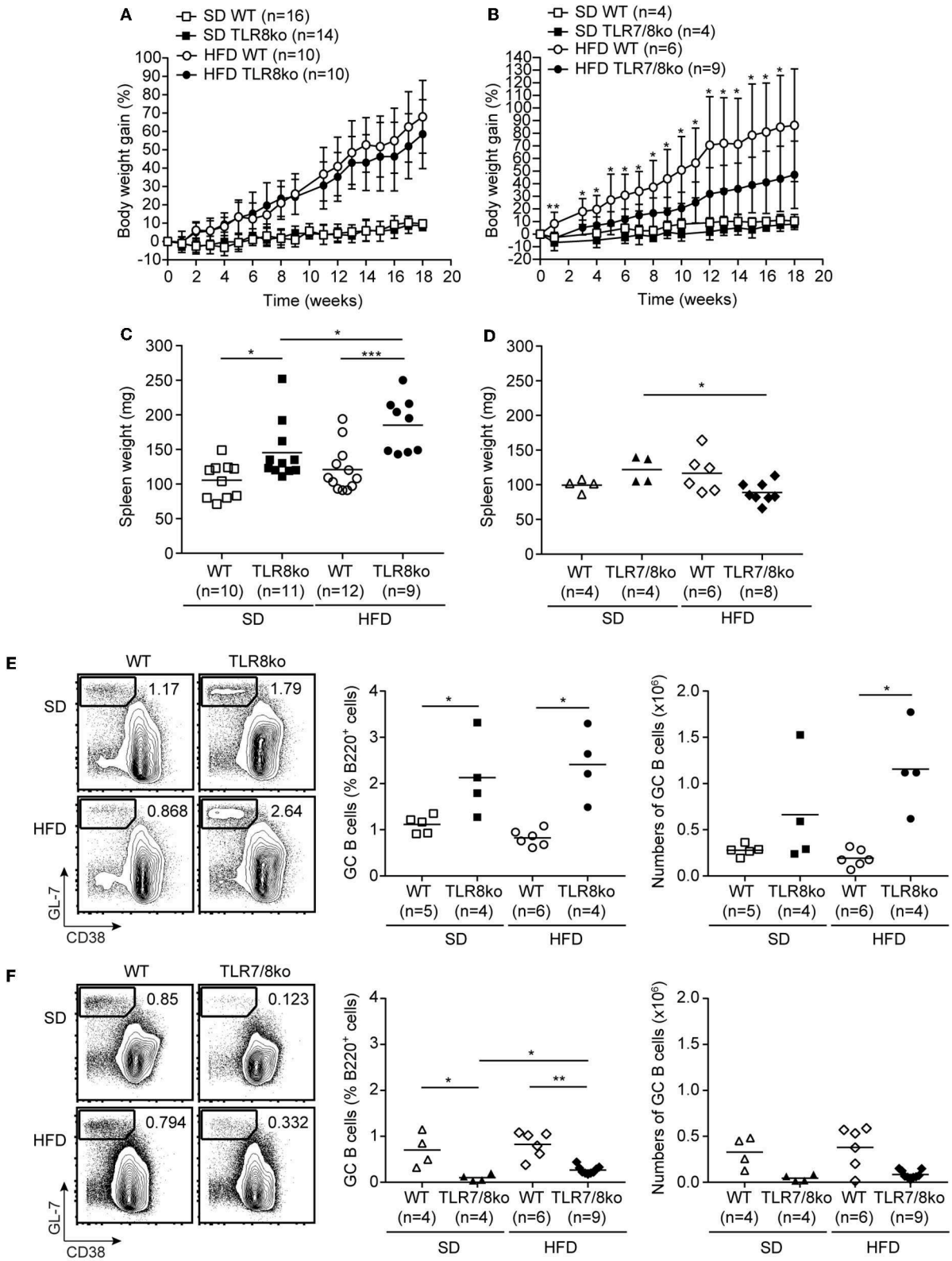

FIGURE 1 | Body weight gain over time of **(A)** TLR8ko or **(B)** TLR7/8ko mice and their respective WT control mice fed a standard diet (SD) or a high fat diet (HFD). Spleen weight of 8 months old female **(C)** TLR8ko or **(D)** TLR7/8ko mice and their WT controls fed-SD or -HFD. Representative flow cytometry plots (left) and

(Continued)

FIGURE 1 | graphical analysis (middle and right) of $B220^{+}GL7^{+}CD38^{-}$ GC B cells in splenocytes derived from 8 months old female **(E)** TLR8ko or **(F)** TLR7/8ko mice and their WT controls fed-SD or -HFD. In **(C,D)** and the right in **(E,F)**, each point represents the value obtained from one mouse and horizontal bars denote mean value. In **(A–D)** data are representative of 2 and 4 independent experiments for SD and HFD, respectively. In **(E,F)** data are representative of 2 independent experiments for each type of diet.

or HFD for a total period of 5 months. Total body weight mass was measured weekly after SD or HFD was initiated. HFD-fed mice gained more weight than SD-fed mice, but body weight gain was similar between TLR8ko and WT control mice (**Figure 1A**). In parallel, we also evaluated the body weight gain of TLR7/8ko and TLR7ko mice vs. their WT controls. Although, upon SD TLR7/8ko mice gained similar weight as their WT controls (**Figure 1B**), interestingly HFD-fed TLR7/8ko or TLR7ko mice showed reduced weight gain compared to their WT controls (**Figure 1B**, **Figure S3A**). The reduced weight gain was not due to differences in food consumption between the genotypes since the assessment of food intake of SD- and HFD-fed TLR8ko, TLR7/8ko, and their WT controls was similar (data not shown). Evaluation of liver, ovarian/uterus, and inguinal white adipose tissue weight, revealed increased fat accumulation in HFD-fed vs. SD-fed mice, but with no evident differences between TLR8ko and WT mice (**Figures S4A,B**, **Table S2**), while HFD-fed TLR7/8ko mice had reduced inguinal fat weight than their WT controls (**Figures S4C,D**, **Table S3**). These data suggest that upon HFD feeding TLR7-deficiency protects female mice from excess weight gain.

Since TLR8-deficiency in mice spontaneously leads to lupus that is accompanied by splenomegaly and altered splenic immune cell populations (26, 28), we next evaluated these parameters in the context of HFD. SD-fed TLR8ko mice developed splenomegaly compared to SD-fed WT controls, which is in accordance with our previous studies (26, 28), and this phenotype became even more profound in HFD-fed TLR8ko compared to SD-fed TLR8ko mice (**Figure 1C**, **Table S4**). On the contrary, SD- and HFD-fed TLR7/8ko and HFD-fed TLR7ko mice had normal spleen weight compared to their WT controls (**Figure 1D**, **Table S5**, **Figure S3B**). Thus, HFD exacerbates splenomegaly in TLR8ko mice and this phenotype is TLR7-dependent since it is abrogated in TLR7/8ko mice.

Flow cytometric analysis of the major immune splenic cell populations (cDCs, pDCs, $CD11c^{+}$ cells, NK, NKT, neutrophils, plasmablasts, B and T cells) revealed no major differences between SD-fed TLR8ko and WT mice (**Table S4**), except of increased percentages of germinal center (GC) B cells and $CD11c^{+}$ cells in TLR8ko mice (**Figure 1E**, **Table S4**), which is in agreement with our previous reports (26, 28). On the contrary, in SD-fed TLR7/8ko mice GC B cells were decreased while the percentages of $CD11c^{+}$ cells were normal, compared to their WT controls (**Figure 1F**, **Table S5**). HFD led to an increase of the total numbers of GC B cells in TLR8ko mice, but not in their WT controls (**Figure 1E**), while in HFD-fed TLR7/8ko or TLR7ko mice this population was similar to WT mice (**Figure 1F**, **Figure S3C**). Moreover, the percentages of cDCs were increased in HFD-fed TLR8ko mice, while HFD-fed TLR7/8ko mice had normal percentages (**Tables S4**, **S5**). Finally, HFD led to a dramatic reduction of $CD8^{+}$ T cells in TLR8ko, but not in TLR7/8ko mice (**Tables S4**, **S5**). Thus, HFD leads to a TLR7-dependent increase of cDCs and reduction of $CD8^{+}$ T cells in TLR8ko mice.

Next, we assessed serum levels of IgG autoantibodies against DNA and RNA, as well as IgM and found increased levels in SD-fed TLR8ko vs. WT mice (**Figure 2A**). Interestingly, HFD led to an increase of anti-DNA antibodies in HFD-fed TLR8ko vs. SD-fed TLR8ko mice, but that was not the case for anti-RNA antibodies or IgM levels (**Figure 2A**). In contrast, SD- or HFD-fed TLR7/8ko mice had reduced levels of IgM and IgG autoantibodies against DNA and RNA compared to their WT controls (**Figure 2B**). These results are in agreement with the differences that we observed in GC B cells in the three genotypes (**Figures 1E,F**) and strongly suggest that TLR7 is pivotal for autoantibody production.

For renal pathology evaluation, histopathological scoring of glomerular, and interstitial nephritis was performed. HFD-fed TLR8ko mice had increased total kidney and glomerulus score compared to SD-fed TLR8ko or HFD-fed WT mice, while HFD-fed TLR7/8ko mice did not develop any kidney pathology (**Figures 2C,D**, **Figure S5**, **Table S6**). Furthermore, we observed increased IgG and IgM glomerular deposition in HFD-fed TLR8ko mice vs. SD-fed TLR8ko or HFD-fed WT mice (**Figure 2C**). In contrast, HFD-fed TLR7/8ko and TLR7ko mice showed dramatically diminished glomerular deposition of IgM and IgG compared to HFD-fed WT mice (**Figure 2D**, **Figure S3D**). Taken together, these results demonstrate that HFD worsens anti-DNA autoantibody production and glomerular IgM and IgG immunodeposits in TLR8 deficient mice, and that both phenomena depend on TLR7 signaling.

HFD Exacerbates Liver Inflammation in TLR8ko Mice

Subclinical liver disease is common in SLE (37, 38), thus, in order to determine the effect of HFD and TLR7 expression on liver disease, histopathological evaluation was performed on hematoxylin/eosin and Oil Red O stained liver sections. HFD-fed TLR8ko mice showed an increased average hepatic inflammation with multifocal centrolobular and periportal lymphocytic infiltrates compared to SD-fed TLR8ko and HFD-fed WT mice (**Figure 3A**, **Figure S5**, **Table S6**). Interestingly, HFD-fed TLR7/8ko mice did not develop hepatic inflammation (**Figure 3B**, **Figure S5**, **Table S6**). Moreover, HFD led to a similar increase of the hepatic lipid content, in both TLR8ko and WT mice (**Figure 3C**), while in HFD-fed TLR7/8ko mice the hepatic lipid content was similar to WT controls (**Figure 3D**). The increased hepatic inflammation in HFD-fed TLR8ko mice was coupled with increased hepatic mRNA expression of the pro-inflammatory cytokines TNF and IL-6 compared to HFD-fed WT or SD-fed TLR8ko mice (**Figure 3E**). In contrast, both SD- and HFD-fed TLR7/8ko mice had similar hepatic TNF, IL-6 and IL-1β mRNA levels to their WT controls (**Figure 3E**). Evaluation by FACS analysis of the major hepatic immune cell

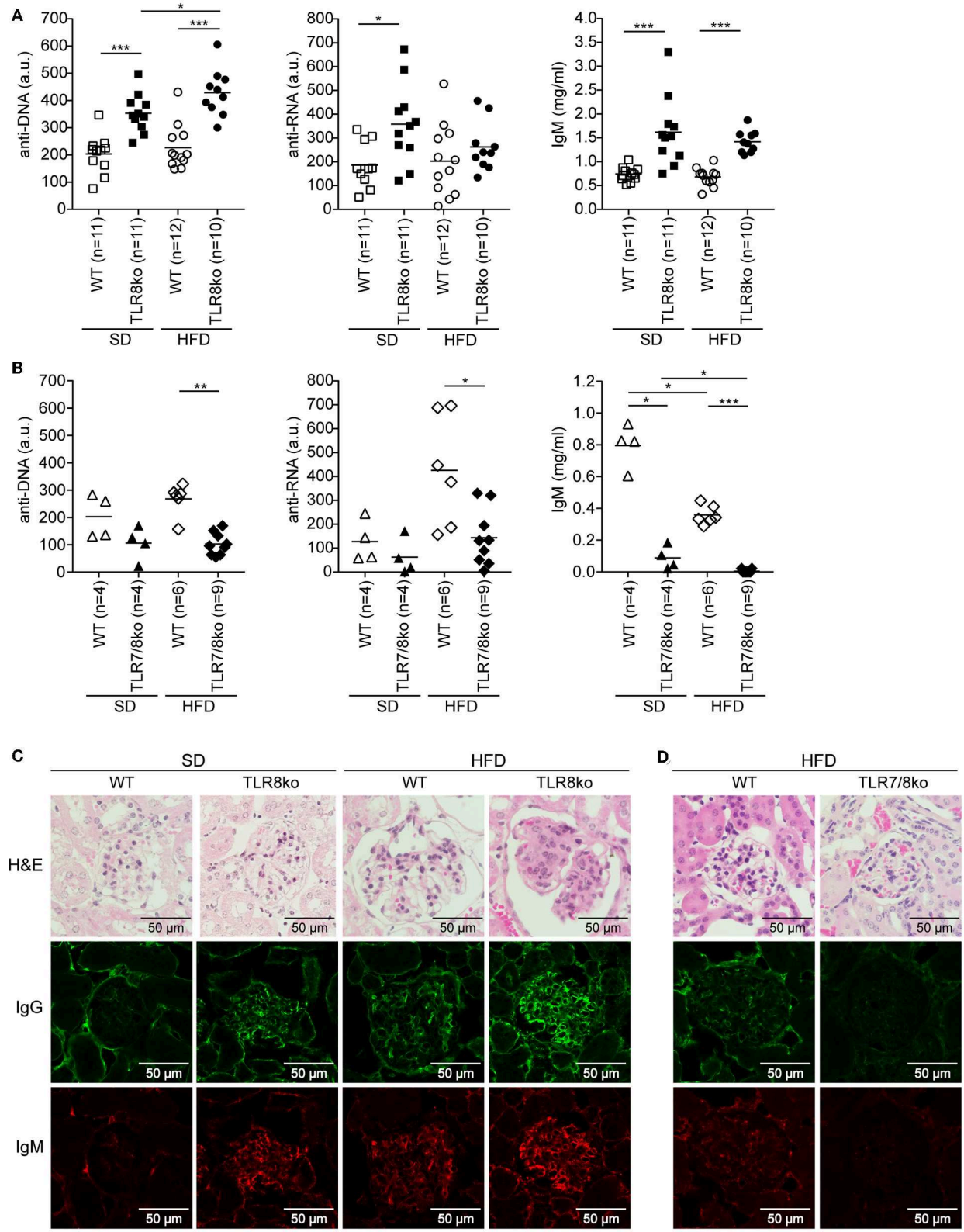

FIGURE 2 | Effect of HFD on serum levels of anti-DNA and anti-RNA autoantibodies and kidney pathology in TLR8ko, TLR7/8ko, and WT mice. Levels of anti-DNA and anti-RNA autoantibodies and IgM in sera of 8 months old female **(A)** TLR8ko or **(B)** TLR7/8ko mice and their WT controls upon SD or HFD were evaluated by

(Continued)

FIGURE 2 | ELISA. Each point represents the value of one mouse and horizontal bars denote mean. In **(A)** data are pooled from two independent experiments. Kidney sections from female 8 months old **(C)** SD or HFD-fed TLR8ko and WT or **(D)** HFD-fed TLR7/8ko and WT mice ($n = 6$, for each genotype) were stained with H&E, anti-IgM, or anti-IgG antibodies. In **(A,B)** data are representative of 2 and 4 independent experiments for SD and HFD, respectively. In **(C,D)** data are representative of 2 independent experiments for each type of diet.

populations revealed that HFD-fed TLR8ko mice had increased numbers of $CD11c^+$ cells and hepatic macrophages (defined as $CD45.2^+MHCII^+CD11b^+F4/80^+CD64^+$) compared to HFD-fed WT mice (**Table S2**, **Figure 3F**), while in HFD-fed TLR7/8ko mice the numbers of $CD11c^+$ cells and hepatic macrophages were normal (**Table S3**, **Figure 3F**). Evaluation of the activation status of the hepatic macrophages by the expression of CD11c or CD86 did not reveal obvious differences among the three genotypes (data not shown). Therefore, these data demonstrate that HFD consumption leads to a TLR7-dependent hepatic inflammation in lupic TLR8ko mice.

Since liver maintains glucose metabolism, we performed glucose tolerance test (GTT) in SD- and HFD-fed mice. TLR8ko and WT mice showed similar glucose kinetics (**Figure 3G**), while HFD-fed TLR7/8ko and TLR7ko mice showed improved glucose tolerance compared to their HFD-fed WT controls (**Figure 3G**, **Figure S3E**), suggesting that TLR7-deficiency protects from HFD-induced glucose intolerance.

Increased T Cell Activation and Foxp3$^+$ Regulatory T Cells in TLR8ko Mice

Since autoreactive $CD4^+$ T cells play an essential role in SLE and steatohepatitis, we next evaluated the percentages/numbers and status of splenic and hepatic T cells. HFD led to a reduction of splenic $CD4^+$ and $CD8^+$ T cells both in WT and TLR8ko mice compared to SD-fed mice (**Table S4**), while no differences were observed between SD- and HFD-fed TLR7/8ko mice (**Table S5**).

The percentages of splenic effector memory ($CD44^{hi}CD62L^-$) $CD4^+$ and $CD8^+$ T cells were increased in SD- and HFD-fed TLR8ko vs. WT controls (**Figure 4A**). On the contrary, the percentages of splenic effector memory $CD4^+$ and $CD8^+$ T cells were normal in SD-fed TLR7/8ko, whereas HFD induced an increase in WT but not in TLR7/8ko mice (**Figure 4B**). Accordingly, splenic naïve ($CD44^-CD62L^+$) $CD4^+$ and $CD8^+$ T cells were reduced in SD-fed TLR8ko vs. WT mice, whereas HFD led to an important reduction of these cell populations in both genotypes (**Figure 4A**). In contrast, in SD-fed TLR7/8ko mice, the percentages of splenic naïve $CD4^+$ and $CD8^+$ T cells were similar to WT mice, while HFD led to a reduction in WT, but not in TLR7/8ko mice (**Figure 4B**).

In the liver, the percentages of effector memory $CD4^+$ T cells were similar between TLR8ko, TLR7/8ko and WT mice (**Figure 4C**). On the contrary, hepatic effector memory $CD8^+$ T cells were increased both in SD- and HFD-fed TLR8ko mice compared to their WT controls (**Figure 4C**). In SD-fed TLR7/8ko mice hepatic effector memory $CD8^+$ T cells were similar to WT controls, whereas HFD led to an increase of effector memory $CD8^+$ T cells in WT, but not in TLR7/8ko mice (**Figure 4D**). Respectively, hepatic naïve $CD8^+$ T cells percentages were normal in SD-fed TLR7/8ko mice, while HFD induced a strong decrease in their WT controls, but not in HFD-fed TLR7/8ko mice (**Figure 4D**). Altogether, these data show that both in the spleen and liver HFD leads to an increase of effector memory and decrease of naïve $CD4^+$ and $CD8^+$ T cells in a TLR7-dependent manner.

$CD4^+$ forkhead box protein 3 $(Foxp3)^+$ regulatory T (Treg) cells maintain self-tolerance by suppressing autoreactive lymphocytes and are critical regulators of cellular metabolism and glucose homeostasis (39, 40). Considering that defects in Treg cells can contribute in SLE pathogenesis and steatohepatitis (41), we next evaluated splenic and hepatic Treg cells. SD- and HFD-fed TLR8ko mice had increased percentages of Treg cells compared to WT controls, both in the spleen (**Figure 5A**) and the liver (**Figure 5E**). The total number of splenic and hepatic Treg cells were similar in TLR8ko and WT mice upon SD (**Figures 5A,E**), while HFD led to a decrease of hepatic Treg cells in WT mice, but not in TLR8ko mice (**Figure 5E**). In contrast, TLR7/8ko mice had similar percentages and numbers of splenic and hepatic Treg cells to their WT controls, both upon SD or HFD (**Figures 5B,F**). In addition, both splenic and hepatic Treg cells where more activated in SD- and HFD-fed TLR8ko mice vs. WT controls (**Figures 5C,G**). In marked contrast, splenic and hepatic Treg cells of TLR7/8ko mice showed similar activation status to WT cells (**Figures 5D,H**). No substantial differences were observed regarding splenic or hepatic Foxp3 mRNA between TLR8ko, TLR7/8ko, TLR7ko, and their WT controls (**Figures 5I,J**, **Figure S3F**). Given that Treg-mediated suppression can be directly linked to IL-10 production (42), we next assessed splenic and hepatic expression of IL-10. We observed a 2-fold and 5-fold increase of IL-10 mRNA levels in the spleen and liver, respectively, of HFD-fed TLR8ko mice vs. WT controls (**Figures 5I,J**), while IL-10 levels were normal in TLR7/8ko and TLR7ko mice (**Figures 5I,J**, **Figure S3G**). Altogether these results indicate that splenic and hepatic Treg cells are increased in TLR8ko vs. WT mice, and upon HFD this increase is accompanied by elevated levels of the anti-inflammatory cytokine IL-10. Importantly, these phenomena are TLR7-dependent since they are abolished in TLR7/8ko mice.

HFD Induces a Profound Increase of TLR7$^+$TNF$^+$ DCs in TLR8ko DCs

To further determine whether exacerbated lupus and metabolic abnormalities observed in HFD- vs. SD-fed TLR8ko mice could be attributed to augmented TLR7 signaling, we next evaluated TLR7 expression levels. While HFD did not have an effect on splenic TLR7 mRNA expression (**Figure 6A**), it strongly increased of hepatic TLR7 mRNA levels in TLR8ko vs. WT mice (**Figure 6B**). In contrast, and as expected TLR7 mRNA was

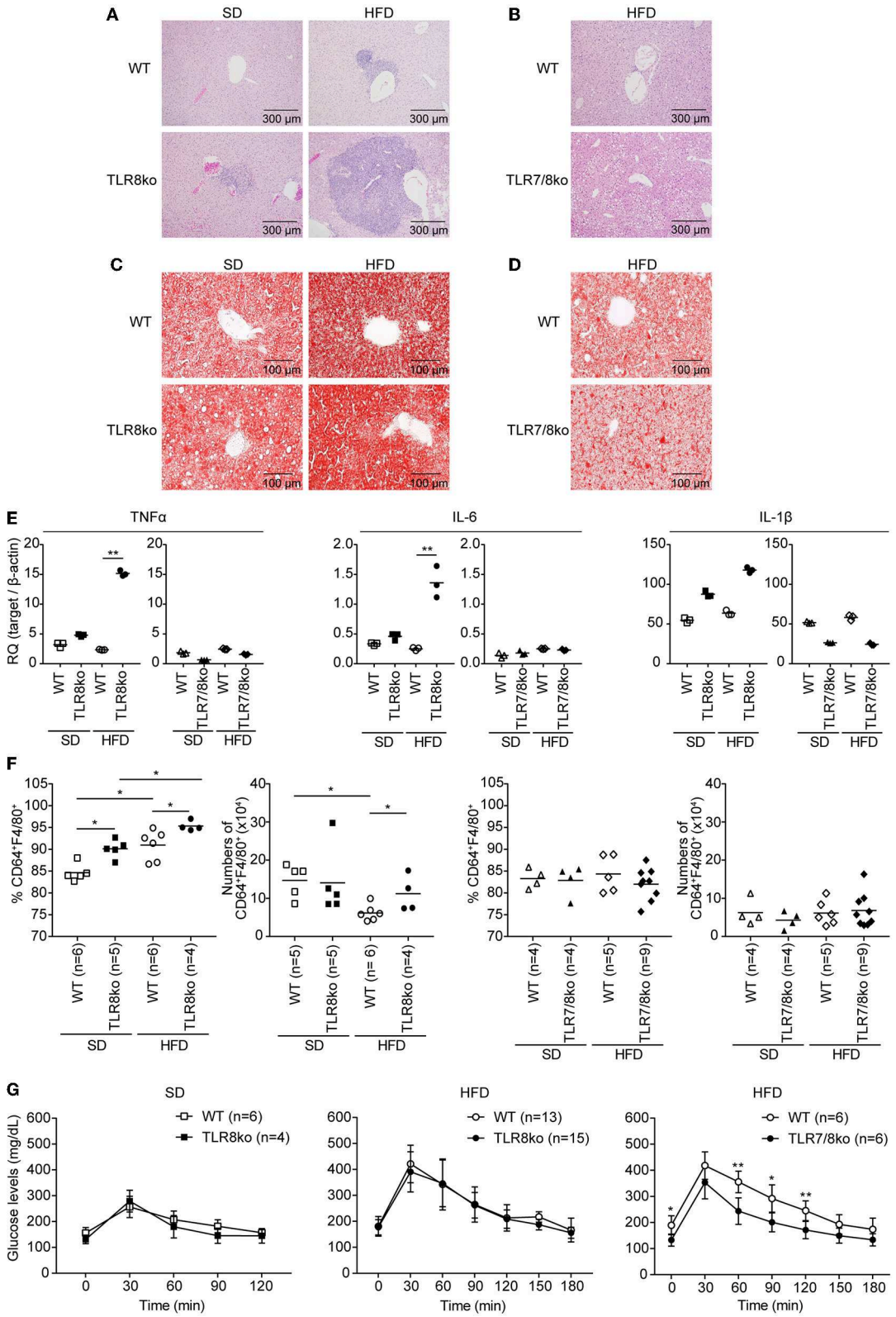

FIGURE 3 | Exacerbation of liver inflammation upon HFD is more profound in TLR8ko vs. WT mice, while TLR7/8ko mice are protected. Liver sections from 8-months-old SD- or HFD-fed TLR8ko or TLR7/8ko mice and their WT controls ($n = 6$ for each genotype) were stained with **(A,B)** H/E or **(C,D)** oil-red O. Data are

(Continued)

FIGURE 3 | representative of 2 to 3 independent experiments. **(E)** Expression of TNF, IL-6, and IL-1β mRNA levels was evaluated in the liver of SD- or HFD-fed TLR8ko, TLR7/8ko, or WT mice by Q-PCR. Plots represent mean ± SD of triplicates, with $n = 4$–6 mice combined per genotype. Data are representative of 2 independent experiments. **(F)** Frequency and total numbers of hepatic macrophages (defined as $CD45.2^+MHCII^+CD11b^+F4/80^+CD64^+$) from SD- or HFD-fed TLR8ko, TLR7/8ko, or WT mice were evaluated by FACS analysis. Data are representative of 2 independent experiments. **(G)** Glucose tolerance test (GTT) of 7-months-old SD- or HFD-fed TLR8ko or TLR7/8ko mice and their WT controls. Data are representative of 2–3 independent experiments.

undetectable in TLR7/8ko mice (**Figures 6A,B**). Furthermore, we evaluated TLR7 protein levels by FACS analysis in pDCs, cDCs and macrophages derived from the spleen, liver, and adipose tissue of TLR8ko and WT mice. Upon SD, TLR8ko mice showed higher TLR7 protein levels than WT mice in pDCs, cDCs, and macrophages in all three tissues (**Figures 6C,D**). Compared to SD-fed mice, HFD led to an increase of TLR7 expression in pDCs and cDCs in both genotypes, but again the HFD-TLR8ko-derived cells had higher TLR7 expression than HFD-WT cells in all three tissues (**Figures 6C,D**). In contrast, HFD did not affect TLR7 expression in macrophages (**Figures 6C,D**).

Next, in order to evaluate if the increased TLR7 expression resulted in altered cytokine production, we measured TNF and type I IFN protein levels by flow cytometry. The expression of type I IFN was quite low (data not shown) and difficult to interpret, thus we focused our analysis on TNF production by TLR7 expressing cells. Compared to SD-fed mice, HFD led to an increase of TNF expression mainly in $TLR7^+$ pDCs and cDCs derived from the spleen and liver, but not the inguinal fat (**Figure 6D**). Interestingly, SD-fed TLR8ko mice showed higher TNF expression in $TLR7^+$ pDCs and cDCs than SD-fed WT cells, and this difference become even more profound in HFD-fed mice (**Figure 6D**). However, in macrophages HFD did not increase TNF expression in $TLR7^+$ cells either in WT or in TLR8ko mice (**Figure 6D**). These results are in accordance with our previous findings that TLR8-deficiency in mice leads to increased TLR7 expression and signaling in DCs, but not in macrophages (26, 28). Overall, TLR8ko pDCs and cDCs have higher TLR7 expression than WT cells, whereas HFD-mediated obesity leads to an increase of $TLR7^+TNF^+$ pDCs and cDCs, and this is more profound in TLR8ko than in WT mice.

DISCUSSION

SLE patients have an increased prevalence of metabolic syndrome and this chronic inflammation seems to be associated with cumulative organ damage (7, 8). Mounting evidence suggest an important contribution of TLR7 signaling in lupus disease development both in mice (25–28, 43) and humans (44–47). However, its respective contribution to the metabolic abnormalities observed in the SLE setting is unknown. Using TLR8ko mice on the C57BL/6 background that develop lupus due to increased TLR7 expression and signaling by dendritic cells (26, 28), our data clearly demonstrate that HFD leads to exacerbation of lupus autoimmunity and metabolic parameters and these phenomena could be attributed to increased TLR7 expression and signaling (**Figure 7**).

Obesity leads to a breakdown of the body's protective self-tolerance, creating the optimal environment for autoimmune diseases, and generates a pro-inflammatory environment likely to worsen disease progression (3). Here, we demonstrated that HFD-induced obesity aggravated the severity of lupus in TLR8ko female mice. This was characterized by profound splenomegaly, kidney IgG and IgM immune-deposits, increased percentages and numbers of GC B cells, anti-DNA serum levels and liver inflammation. B cell-intrinsic TLR7 signaling is essential for the development of germinal centers (48). Indeed, in TLR7/8ko mice the percentages of GC B cells were decreased, while in HFD-fed TLR8ko mice both the percentages and numbers of GC B cells were increased and could explain the increased levels of anti-DNA autoantibodies in HFD-fed TLR8ko mice. Moreover, in accordance with our results previous studies in the female (NZB x NZW) F1 (BWF1) mouse model of SLE have shown that high dietary fat accelerates lupus nephritis and leads to shorter life span (49–51). In HFD-fed TLR8ko mice we did not observe any lethality up to 12 months of age (data not shown), since TLR8ko mice develop a rather mild lupus phenotype compared to BWF1 mice. Indeed, upon SD and up to 12 months TLR8ko mice have normal levels of proteinuria and a 100% survival rate (28), while by the age of 10 months 50% of BWF1 mice develop pathogenic levels of proteinuria and die (51). HFD-fed TLR8ko and WT mice exhibited similar accelerated weight gain, which was coupled with increased inguinal and ovarian fat weight compared to SD-fed control mice. However, female HFD-fed TLR7/8ko and TLR7ko mice showed reduced weight gain and had reduced inguinal fat weight compared to HFD-fed WT controls. This is in agreement with a previous study where upon HFD male TLR7ko mice had normal body weight, but reduced adipose fat pad weight compared to littermate WT mice (52). Strikingly, TLR7/8ko mice did not show any sign of lupus autoimmunity. Thus, TLR7 signaling contributes to the exacerbation of lupus autoimmunity in HFD-fed TLR8ko mice, as well as to the accelerated weight gain that was observed in HFD-fed WT vs. TLR7-deficient mice. Importantly, our study indicates that TLR8ko females provide an ideal mouse model to study the long-term effect of HFD-induced low grade-inflammation in the setting of SLE since mice have a 100% survival rate up to 12 months.

Despite the high heterogeneity in the literature regarding the prevalence of SLE-associated liver diseases, it is becoming apparent that liver is an important target of SLE (53). Subclinical liver disease is common in SLE, where 25–50% of patients with lupus develop abnormal liver function at some point (37, 38). We found that TLR8ko mice developed a TLR7-dependent hepatic inflammation that was accompanied by increased production

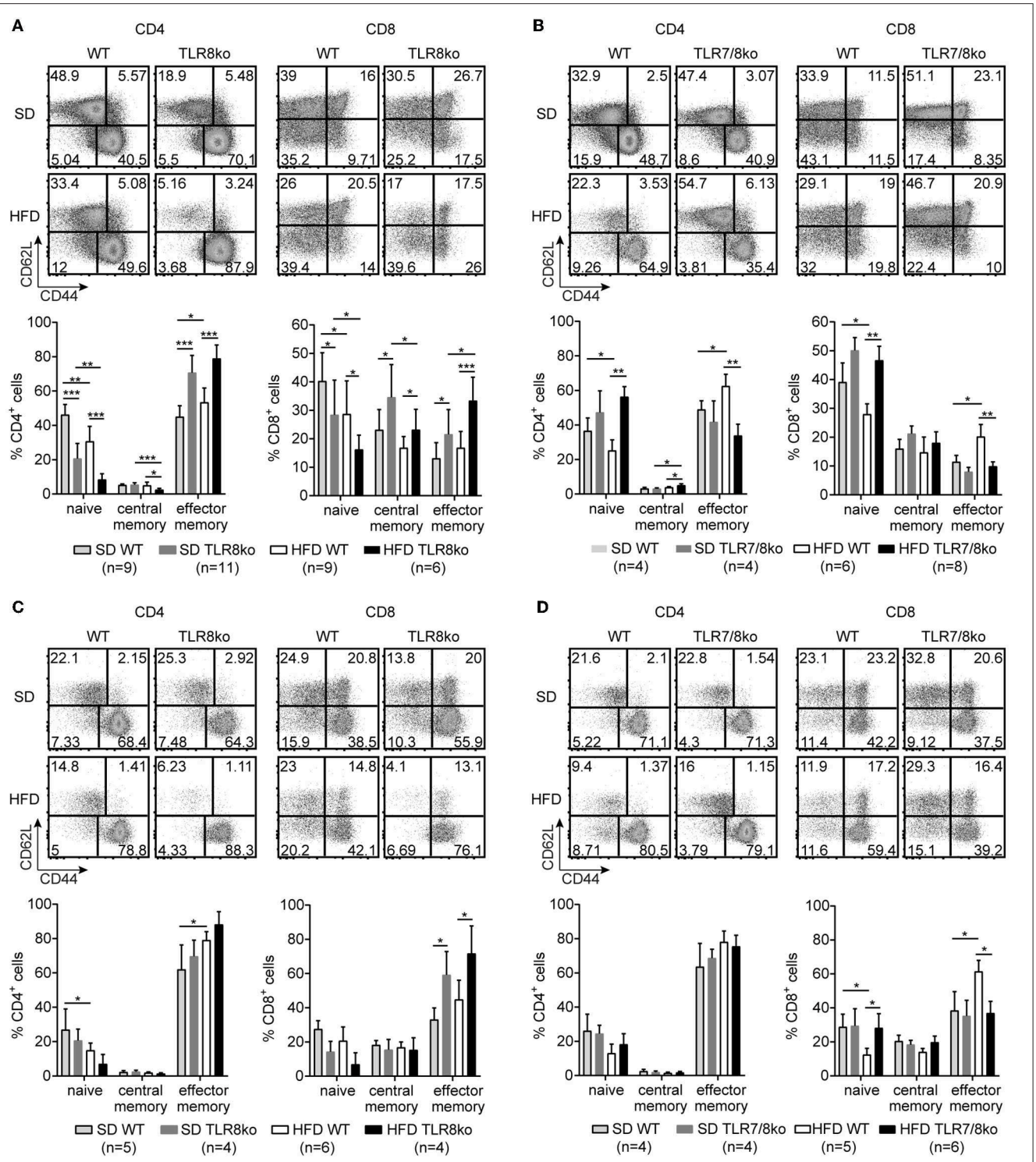

FIGURE 4 | TLR7-dependent increase of effector memory $CD4^+$ and $CD8^+$ T cells in TLR8ko mice. Representative flow cytometry plots (upper) and graphical analysis (lower) of **(A,B)** splenocytes and **(C,D)** hepatocytes from 8 months old SD- or HFD-fed TLR8ko or TLR7/8ko mice and their WT controls, analyzed for the expression of CD3, CD4, CD8, CD44, and CD62L. CD44/CD62L relative expression were used to identify naive ($CD44^{lo/-}CD62L^{hi}$), central memory ($CD44^{hi}CD62L^{hi}$), and effector memory ($CD44^{hi}CD62L^{lo}$) subpopulations. Plots represent mean ± SD. Data are representative of 2 and 3 independent experiments for SD and HFD, respectively.

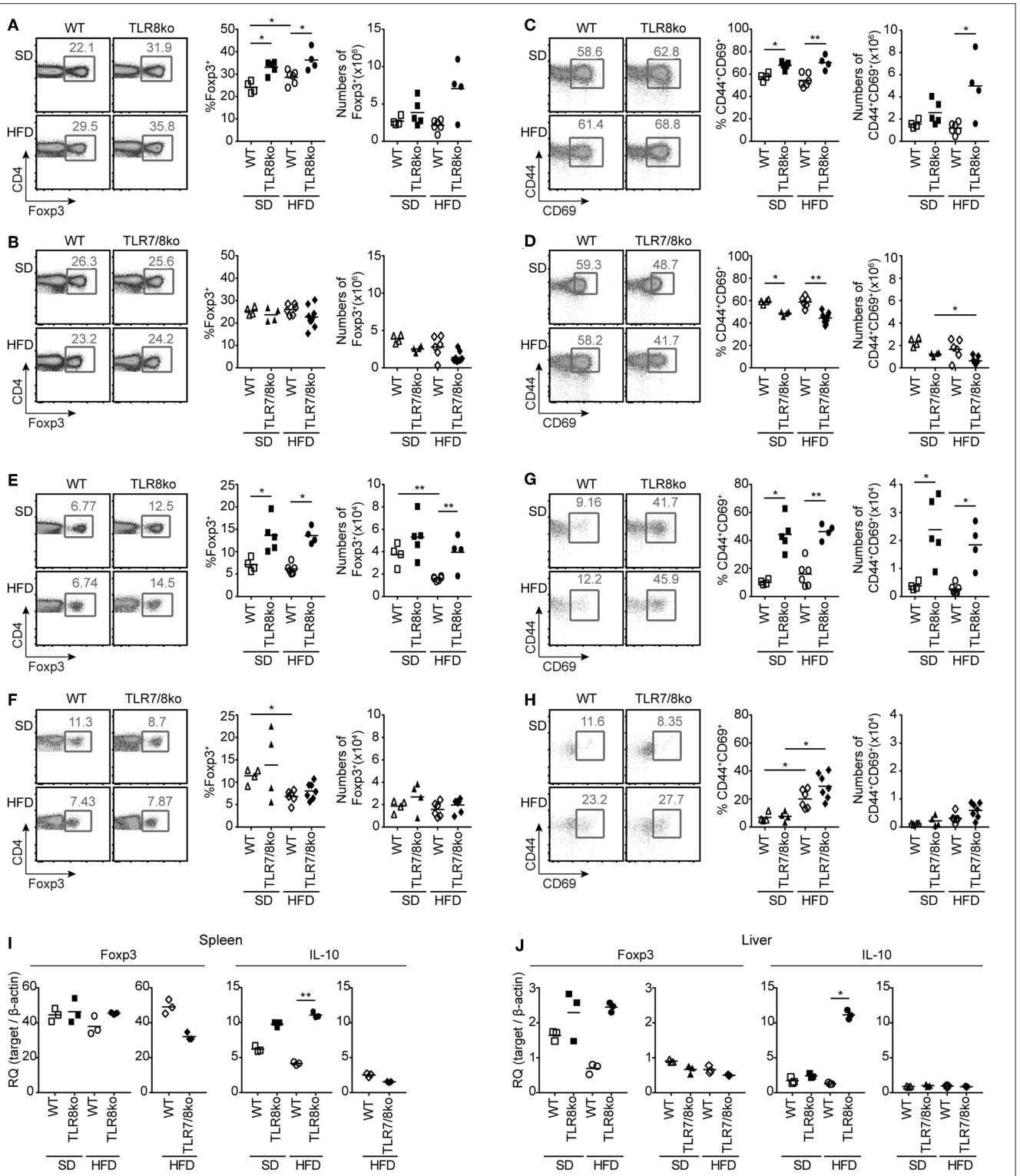

FIGURE 5 | Increased numbers and activation of Treg cells in HFD-fed TLR8ko mice are TLR7-dependent. Total **(A–D)** splenocytes and **(E–H)** hepatic lymphocytes were isolated from 8 months old TLR8ko (SD, $n = 5$; HFD, $n = 4$) and WT (SD, $n = 4$; HFD, $n = 6$) or TLR7/8ko (SD, $n = 4$; HFD, $n = 7$) and WT (SD, $n = 4$; HFD, $n = 6$) mice and analyzed by flow cytometry for **(A,B,E,F)** Treg cells ($CD4^+Foxp3^+$) and **(C,D,G,H)** their activation status ($CD44^+CD69^+$). Expression of Foxp3 and IL-10 mRNA levels were evaluated in the **(I)** spleen and **(J)** liver of SD- or HFD-fed TLR8ko, TLR7/8ko, or WT mice by Q-PCR in triplicates. Plots in **(I–J)** represent mean ± SD of triplicates, with $n = 4$–6 mice combined per genotype. Data in **(A–H)** and **(I,J)** are representative of 3 and 2 independent experiments, respectively.

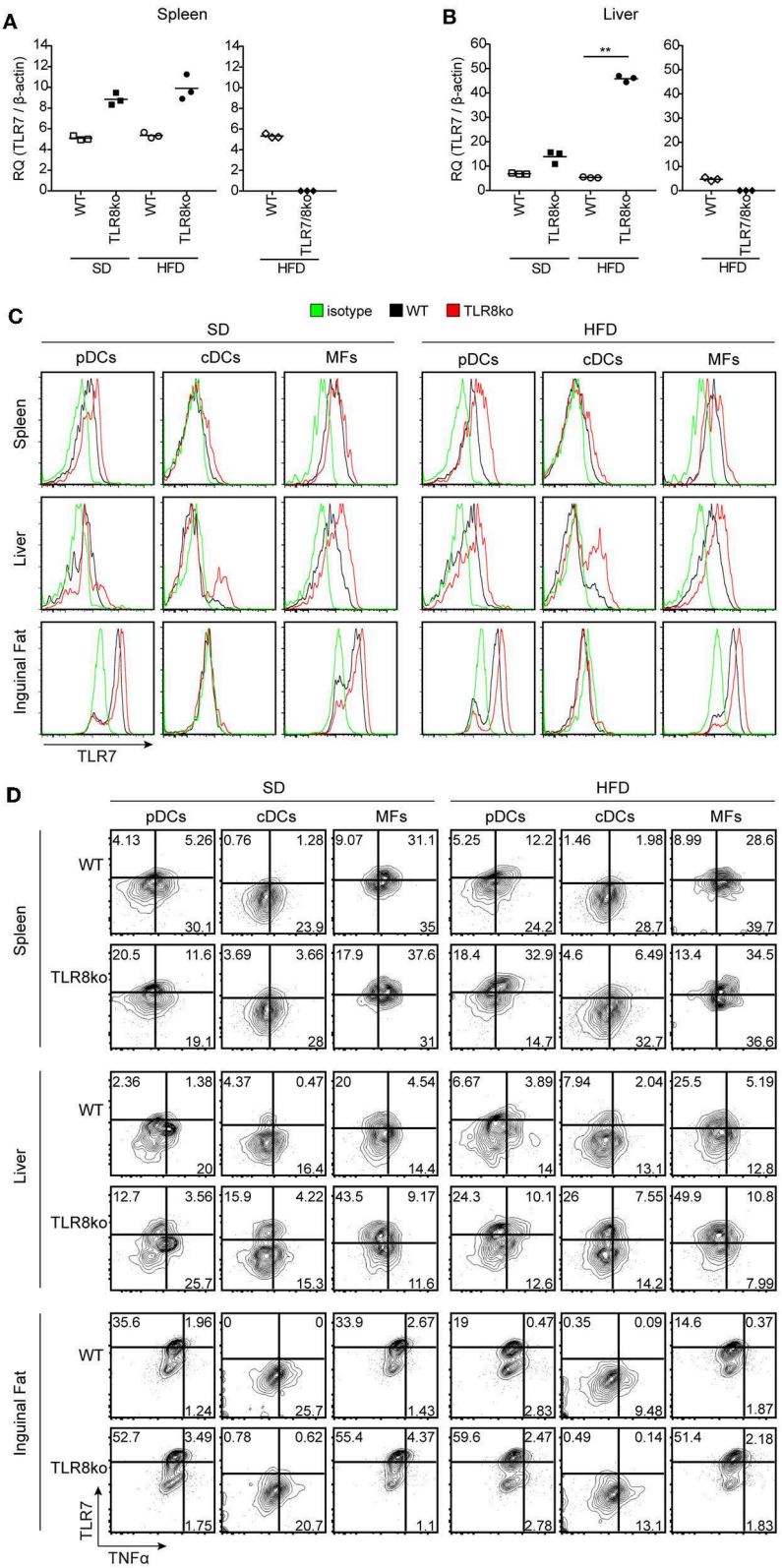

FIGURE 6 | HFD-induced obesity promotes TLR7 and TNF expression by pDCs and cDCs. Total RNA was extracted from **(A)** spleen and **(B)** liver of SD- or HFD-fed WT, TLR8ko, and TLR7/8ko mice and the expression of TLR7 was assessed by Q-PCR. Plots represent mean ± SD of triplicates, with $n = 4–6$ mice combined per

(Continued)

FIGURE 6 | genotype. FACS plots represent **(C)** TLR7 expression and **(D)** TLR7 vs. TNF expression on pDCs ($CD45.2^+CD11c^{int}SiglecH^+$), cDCs ($CD45.2^+CD11c^+MHCII^{hi}DC64^-$), and macrophages (MFs) ($CD45.2^+CD64^+CD11c^+CD11b^+$) derived from the spleen, liver, or inguinal adipose tissue of 8 months-old SD- or HFD-fed female WT and TLR8ko mice ($n = 3$ per genotype). In panel **(D)** gates have been placed relative to isotypes controls as shown in **Figure S1**. Data in **(A,B)** and **(C,D)** are representative of 2 and 3 independent experiments, respectively.

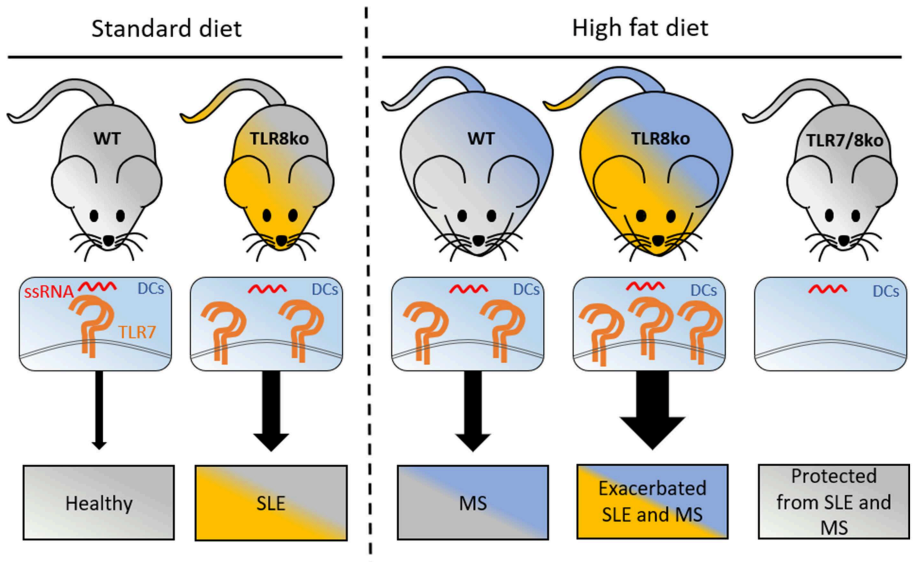

FIGURE 7 | Graphical abstract of how increased TLR7 signaling by DCs can lead to lupus and metabolic syndrome. Under standart diet (SD), TLR8ko mice develop spontaneous SLE due to increased TLR7 expression and signaling by DCs. High fat diet (HFD) leads to the development of MS in WT mice, and exacerbated SLE, and MS in TLR8ko mice, due to increased TLR7 signaling, compared to SD-fed mice. Deletion of TLR7 (TLR7/8ko mice) protects TLR8ko mice from HFD-induced exacerbation of SLE and MS development. DCs, dendritic cells; MS, metabolic syndrome; SLE, systemic lupus erythematosus; ssRNA, single stranded RNA; TLR7, Toll-like receptor 7.

of pro-inflammatory cytokines (TNF and IL-6), as well as lymphocytic and macrophage infiltrates. Moreover, HFD led to the worsening of the hepatic inflammation in TLR8ko mice. In accordance to our findings regarding the involvement of TLR7 signaling in hepatic inflammation, transgenic mice that overexpress TLR7 develop SLE and massive hepatic inflammation (54), while the contribution of TLR7 signaling in alcoholic hepatic inflammation both in mice and in humans has also been reported recently (55). Therefore, TLR7 signaling contributes to SLE-associated liver diseases.

Treg cells are a subset of $CD4^+$ T cells that maintain self-tolerance by suppressing autoreactive lymphocytes. Defects in Treg cells are therefore thought to contribute to SLE pathogenesis (41). Indeed, scurfy mice that are deficient in Treg cells develop generalized autoimmune disorder, including SLE (56). Nevertheless, the data regarding the numbers and function of Treg cells especially in human SLE are contradictory (41). The percentages and numbers of hepatic Treg cells and the activation status of splenic and hepatic Treg cells were increased in TLR8ko mice. These observations correlated with higher hepatic levels of IL-10 in HFD-fed TLR8ko than in HFD-fed WT mice. On the contrary, in TLR7/8ko mice the numbers and activation status of splenic and hepatic Treg cells, as well as hepatic IL-10 levels were normal. These results suggest that TLR7-expression by DCs is pivotal in controlling Treg numbers and their activation status in TLR8ko mice. Interestingly, increased percentages of splenic Treg cells have also been reported in 8 and 16 weeks old female BWF1 mice, which develop spontaneously SLE, hepatic steatosis, and metabolic syndrome (57). However, in the same study it was reported that by the age of 24 weeks the female BWF1 mice had normal percentages of splenic Treg cells, a decline of metabolic symptoms, while classical SLE symptoms increased progressively (57). The observation that Treg cells did not decrease in 8 months old (34 weeks old) TLR8ko mice and even increased upon HFD could be due to the fact that whole body homeostasis deterioration is slower in TLR8ko mice than in BWF1 mice. Indeed, a previous study using BWF1 female mice reported the appearance of lupus-related signs earlier and a 69% survival rate by week 36 (58), while in the study by Vila et al. survival was 100% by week 36 (57). Therefore, the TLR7-dependent increased numbers of Treg cells in TLR8ko mice might have a reparatory role, since Treg cells besides their role in suppressing the immune response are important in tissue protection and regeneration in various tissues (59). Thus, we could hypothesize that the numbers, activation status, heterogeneity, stability, and function of Treg cells can vary during the different stages of SLE progression (60). Furthermore, recent studies have uncovered novel subsets of Treg cells that have a pathogenic role, notably

through the secretion of the cytokine IL17A, in the setting of the autoimmune diseases, including SLE and arthritis (61, 62), which could also explain why the role of Treg cells in human SLE remains contradictory. We this could not rule out that Treg cells in HFD-fed TLR8ko mice contain pathogenic cells that contribute to the pathology.

Obesity-related inflammation of metabolic tissues, including liver and adipose tissue, are key elements in the development of metabolic inflammation and insulin resistance, but many of the contributing mechanisms remain ambiguous (63). Our data revealed that in WT mice HFD leads to an increased TLR7 expression that is coupled with increased TNF production especially by splenic and hepatic cDCs and pDCs. Importantly, increased TLR7 expression and signaling was even more profound in TLR8ko mice and correlated with dramatic increase of hepatic cytokines. In accordance with our findings that HFD leads to increased TLR7 expression, a previous study revealed that HFD upregulated the mRNA expression of all TLRs, including TLR7, in the murine adipose tissue, and this phenomenon was coupled by increased NF-κB signaling and cytokine expression (64). Moreover, Revelo et al., showed that HFD-induced obesity in male mice promotes excess release and diminished clearance of nucleic acids, in the form of extracellular traps, that can be detected by TLR7 and can lead to worsening of metabolic inflammation (52). Interestingly, upregulated adipose TLR7 expression and correlation with systemic inflammatory markers has also been reported in obese individuals (65). Thus, we can hypothesize that the increased TLR7 expression and response that we noticed upon HFD mainly in DCs could be the outcome of the activation of DCs either through direct detection of the increased amounts of the endogenous TLR7-ligand and/or increased inflammatory cytokines that lead to DC activation. Increased TLR7 expression coupled with increased TLR7 signaling has detrimental effects on accelerating systemic metabolic inflammation and SLE progression. In line to our findings, calorie restriction in mice delayed the development of kidney disease, age-related immune dysfunction and complications, and thus prolonged the life span in the BWF1 mouse model of lupus (66–68). Information regarding the impact of diet and caloric restriction on human SLE is yet insufficient (2, 69). Nevertheless, caloric restriction was proven to induce various benefits to the immune system (69), since this restriction also leads to changes in the gut microbiota, which act as guardians of a healthy immune system (70).

In conclusion, our data demonstrate that HFD-induced obesity increases TLR7 expression and signaling, that contributes to the acceleration of the progression of SLE and metabolic abnormalities. Since SLE is a systemic inflammatory autoimmune disease with a broad clinical and immunological phenotype, whereas the observed clinical heterogeneity reflects differences in underlying immunopathological process, treatment personalization should be done according to underlying molecular mechanisms (71). It is tempting to speculate that in certain SLE patients the molecular basis of the disease could be due to TLR7 overexpression and signaling, that if it is also coupled with obesity and/or metabolic syndrome this could have detrimental consequences for the initiation, exacerbation and progression of the SLE pathology. Therefore, interventions to reduce or reverse overweight and obesity could improve both symptoms and long-term outcomes of patients with lupus or systemic inflammation, and if this is not achievable then targeting TLR7 is expected to have beneficial effects both for SLE and for metabolic inflammation, especially in certain genetically predisposed individuals.

DATA AVAILABILITY

All datasets generated for this study are included in the manuscript and/or the **Supplementary Files**.

ETHICS STATEMENT

Experiments were conducted in accordance with institutional guidelines for animal care and with protocols approved by the Comité National de Réflexion Ethique sur l'Expérimentation Animale.

AUTHOR CONTRIBUTIONS

LA and NH designed the experiments and analyzed the data. NH, YW, AR-Q, LM, LC, CL, BD, and JC performed experiments and/or analyzed data. LA supervised the project, and wrote the manuscript with the help of NH and MI.

FUNDING

This work received funding from the European Foundation for the study of Diabetes (EFSD/Novo Nordisk) (NN2014_5) (to LA), the Fondation de France-Cardiovasculaire (OTP43032) (to LA), the Arthritis Fondation Courtin (to LA), the Agence Nationale de la Recherche (TollSOME project to LA), and the ARC Foundation (PJA20171206491) (to MI). NH was supported by fellowship from the Ministère de l'Enseignement Supérieur et de la Recherche and YW by fellowship from the China Scholarship Council (CSC 201706140151). We also acknowledge institutional support from CNRS, INSERM, and Aix-Marseille University.

ACKNOWLEDGMENTS

We thank Marc Barad, Sylvian Bigot, and Atika Zouine for technical support on flow cytometry, the personnel at the mouse facility and the PICSL imaging facility (ImagImm) of the CIML for technical assistance, and Lionel Spinelli for critical discussion and help with statistical analysis.

SUPPLEMENTARY MATERIAL

The Supplementary Material for this article can be found online at: https://www.frontiersin.org/articles/10.3389/fimmu.2019.02015/full#supplementary-material

REFERENCES

1. Moroni L, Bianchi I, Lleo A. Geoepidemiology, gender and autoimmune disease. *Autoimmun Rev*. (2012) 11:A386–92. doi: 10.1016/j.autrev.2011.11.012
2. Manzel A, Muller DN, Hafler DA, Erdman SE, Linker RA, Kleinewietfeld M. Role of "Western diet" in inflammatory autoimmune diseases. *Curr Allergy Asthma Rep*. (2014) 14:404. doi: 10.1007/s11882-013-0404-6
3. Versini M, Jeandel PY, Rosenthal E, Shoenfeld Y. Obesity in autoimmune diseases: not a passive bystander. *Autoimmun Rev*. (2014) 13:981–1000. doi: 10.1016/j.autrev.2014.07.001
4. Tsokos GC. Systemic lupus erythematosus. *N Engl J Med*. (2011) 365:2110–21. doi: 10.1056/NEJMra1100359
5. Tektonidou MG, Wang Z, Dasgupta A, Ward MM. Burden of serious infections in adults with systemic lupus erythematosus: a national population-based study, 1996–2011. *Arthritis Care Res.* (2015) 67:1078–85. doi: 10.1002/acr.22575
6. Deedwania PC, Gupta R. Management issues in the metabolic syndrome. *J Assoc Physicians India*. (2006) 54:797–810.
7. Demir S, Artim-Esen B, Sahinkaya Y, Pehlivan O, Alpay-Kanitez N, Omma A, et al. Metabolic syndrome is not only a risk factor for cardiovascular diseases in systemic lupus erythematosus but is also associated with cumulative organ damage: a cross-sectional analysis of 311 patients. *Lupus*. (2016) 25:177–84. doi: 10.1177/0961203315603140
8. Parker B, Urowitz MB, Gladman DD, Lunt M, Donn R, Bae SC, et al. Impact of early disease factors on metabolic syndrome in systemic lupus erythematosus: data from an international inception cohort. *Ann Rheum Dis*. (2015) 74:1530–6. doi: 10.1136/annrheumdis-2013-203933
9. Chung CP, Avalos I, Oeser A, Gebretsadik T, Shintani A, Raggi P, et al. High prevalence of the metabolic syndrome in patients with systemic lupus erythematosus: association with disease characteristics and cardiovascular risk factors. *Ann Rheum Dis*. (2007) 66:208–14. doi: 10.1136/ard.2006.054973
10. Sinicato NA, Postal M, Peres FA, Pelicari Kde O, Marini R, dos Santos Ade O, et al. Obesity and cytokines in childhood-onset systemic lupus erythematosus. *J Immunol Res*. (2014) 2014:162047. doi: 10.1155/2014/162047
11. Hotamisligil GS. Inflammation and metabolic disorders. *Nature*. (2006) 444:860–7. doi: 10.1038/nature05485
12. Cai D, Yuan M, Frantz DF, Melendez PA, Hansen L, Lee J, et al. Local and systemic insulin resistance resulting from hepatic activation of IKK-beta and NF-kappaB. *Nat Med*. (2005) 11:183–90. doi: 10.1038/nm1166
13. Fresno M, Alvarez R, Cuesta N. Toll-like receptors, inflammation, metabolism and obesity. *Arch Physiol Biochem*. (2011) 117:151–64. doi: 10.3109/13813455.2011.562514
14. Konner AC, Bruning JC. Toll-like receptors: linking inflammation to metabolism. *Trends Endocrinol Metab*. (2011) 22:16–23. doi: 10.1016/j.tem.2010.08.007
15. Wagner H. Endogenous TLR ligands and autoimmunity. *Adv Immunol*. (2006) 91:159–73. doi: 10.1016/S0065-2776(06)91004-9
16. Garcia-Martinez I, Santoro N, Chen Y, Hoque R, Ouyang X, Caprio S, et al. Hepatocyte mitochondrial DNA drives non-alcoholic steatohepatitis by activation of TLR9. *J Clin Invest*. (2016) 126:859–64. doi: 10.1172/JCI83885
17. Jialal I, Kaur H, Devaraj S. Toll-like receptor status in obesity and metabolic syndrome: a translational perspective. *J Clin Endocrinol Metab*. (2014) 99:39–48. doi: 10.1210/jc.2013-3092
18. Jin C, Flavell RA. Innate sensors of pathogen and stress: linking inflammation to obesity. *J Allergy Clin Immunol*. (2013) 132:287–94. doi: 10.1016/j.jaci.2013.06.022
19. Nishimoto S, Fukuda D, Higashikuni Y, Tanaka K, Hirata Y, Murata C, et al. Obesity-induced DNA released from adipocytes stimulates chronic adipose tissue inflammation and insulin resistance. *Sci Adv*. (2016) 2:e1501332. doi: 10.1126/sciadv.1501332
20. Kawai T, Akira S. The role of pattern-recognition receptors in innate immunity: update on Toll-like receptors. *Nat Immunol*. (2010) 11:373–84. doi: 10.1038/ni.1863
21. Lin Q, Li M, Fang D, Fang J, Su SB. The essential roles of Toll-like receptor signaling pathways in sterile inflammatory diseases. *Int Immunopharmacol*. (2011) 11:1422–32. doi: 10.1016/j.intimp.2011.04.026
22. Enevold C, Nielsen CH, Jacobsen RS, Hermansen ML, Molbo D, Avlund K, et al. Single nucleotide polymorphisms in genes encoding toll-like receptors 7, 8, and 9 in Danish patients with systemic lupus erythematosus. *Mol Biol Rep*. (2014) 41:5755–63. doi: 10.1007/s11033-014-3447-4
23. Kawasaki A, Furukawa H, Kondo Y, Ito S, Hayashi T, Kusaoi M, et al. TLR7 single-nucleotide polymorphisms in the 3' untranslated region and intron 2 independently contribute to systemic lupus erythematosus in Japanese women: a case-control association study. *Arthritis Res Ther*. (2011) 13:R41. doi: 10.1186/ar3277
24. Shen N, Fu Q, Deng Y, Qian X, Zhao J, Kaufman KM, et al. Sex-specific association of X-linked Toll-like receptor 7 (TLR7) with male systemic lupus erythematosus. *Proc Natl Acad Sci USA*. (2010) 107:15838–43. doi: 10.1073/pnas.1001337107
25. Deane JA, Pisitkun P, Barrett RS, Feigenbaum L, Town T, Ward JM, et al. Control of toll-like receptor 7 expression is essential to restrict autoimmunity and dendritic cell proliferation. *Immunity*. (2007) 27:801–10. doi: 10.1016/j.immuni.2007.09.009
26. Demaria O, Pagni PP, Traub S, de Gassart A, Branzk N, Murphy AJ, et al. TLR8 deficiency leads to autoimmunity in mice. *J Clin Invest*. (2010) 120:3651–62. doi: 10.1172/JCI42081
27. Desnues B, Macedo AB, Ordonez-Rueda D, Roussel-Queval A, Malissen B, Bruhns P, et al. The transcriptional repressor Gfi1 prevents lupus autoimmunity by restraining TLR7 signaling. *Eur J Immunol*. (2016) 46:2801–11. doi: 10.1002/eji.201646573
28. Desnues B, Macedo AB, Roussel-Queval A, Bonnardel J, Henri S, Demaria O, et al. TLR8 on dendritic cells and TLR9 on B cells restrain TLR7-mediated spontaneous autoimmunity in C57BL/6 mice. *Proc Natl Acad Sci USA*. (2014) 111:1497–502. doi: 10.1073/pnas.1314121111
29. Diebold SS, Kaisho T, Hemmi H, Akira S, Reis e Sousa C. Innate antiviral responses by means of TLR7-mediated recognition of single-stranded RNA. *Science.* (2004) 303:1529–31. doi: 10.1126/science.1093616
30. Heil F, Hemmi H, Hochrein H, Ampenberger F, Kirschning C, Akira S, et al. Species-specific recognition of single-stranded RNA via toll-like receptor 7 and 8. *Science*. (2004) 303:1526–9. doi: 10.1126/science.1093620
31. Lund JM, Alexopoulou L, Sato A, Karow M, Adams NC, Gale NW, et al. Recognition of single-stranded RNA viruses by Toll-like receptor 7. *Proc Natl Acad Sci USA*. (2004) 101:5598–603. doi: 10.1073/pnas.0400937101
32. Alexopoulou L, Desnues B, Demaria O. [Toll-like receptor 8: the awkward TLR]. *Med Sci*. (2012) 28:96–102. doi: 10.1051/medsci/2012281023
33. Cervantes JL, Weinerman B, Basole C, Salazar JC. TLR8: the forgotten relative revindicated. *Cell Mol Immunol*. (2012) 9:434–8. doi: 10.1038/cmi.2012.38
34. Valenzuela DM, Murphy AJ, Frendewey D, Gale NW, Economides AN, Auerbach W, et al. High-throughput engineering of the mouse genome coupled with high-resolution expression analysis. *Nat Biotechnol*. (2003) 21:652–9. doi: 10.1038/nbt822
35. Ubeda C, Lipuma L, Gobourne A, Viale A, Leiner I, Equinda M, et al. Familial transmission rather than defective innate immunity shapes the distinct intestinal microbiota of TLR-deficient mice. *J Exp Med*. (2012) 209:1445–56. doi: 10.1084/jem.20120504
36. Traub S, Demaria O, Chasson L, Serra F, Desnues B, Alexopoulou L. Sex bias in susceptibility to MCMV infection: implication of TLR9. *PLoS ONE*. (2012) 7:e45171. doi: 10.1371/journal.pone.0045171
37. Luangjaru S, Kullavanijaya P. Gastrointestinal and hepatobiliary manifestations in systemic lupus erythematosus. *J Med Assoc Thai*. (2005) 88:71–5.
38. van Hoek B. The spectrum of liver disease in systemic lupus erythematosus. *Neth J Med*. (1996) 48:244–53. doi: 10.1016/0300-2977(96)00003-4
39. Josefowicz SZ, Lu LF, Rudensky AY. Regulatory T cells: mechanisms of differentiation and function. *Annu Rev Immunol*. (2012) 30:531–64. doi: 10.1146/annurev.immunol.25.022106.141623
40. Matarese G, Procaccini C, De Rosa V, Horvath TL, La Cava A. Regulatory T cells in obesity: the leptin connection. *Trends Mol Med*. (2010) 16:247–56. doi: 10.1016/j.molmed.2010.04.002
41. Ohl K, Tenbrock K. Regulatory T cells in systemic lupus erythematosus. *Eur J Immunol*. (2015) 45:344–55. doi: 10.1002/eji.201344280
42. Chaudhry A, Samstein RM, Treuting P, Liang Y, Pils MC, Heinrich JM, et al. Interleukin-10 signaling in regulatory T cells is required for

suppression of Th17 cell-mediated inflammation. *Immunity*. (2011) 34:566–78. doi: 10.1016/j.immuni.2011.03.018
43. Pisitkun P, Deane JA, Difilippantonio MJ, Tarasenko T, Satterthwaite AB, Bolland S. Autoreactive B cell responses to RNA-related antigens due to TLR7 gene duplication. *Science*. (2006) 312:1669–72. doi: 10.1126/science.1124978
44. Jenks SA, Cashman KS, Zumaquero E, Marigorta UM, Patel AV, Wang X, et al. Distinct effector B cells induced by unregulated Toll-like receptor 7 contribute to pathogenic responses in systemic lupus erythematosus. *Immunity*. (2018) 49:725–39.e6. doi: 10.1016/j.immuni.2018.08.015
45. Lee YH, Choi SJ, Ji JD, Song GG. Association between toll-like receptor polymorphisms and systemic lupus erythematosus: a meta-analysis update. *Lupus*. (2016) 25:593–601. doi: 10.1177/0961203315622823
46. Murayama G, Furusawa N, Chiba A, Yamaji K, Tamura N, Miyake S. Enhanced IFN-alpha production is associated with increased TLR7 retention in the lysosomes of palasmacytoid dendritic cells in systemic lupus erythematosus. *Arthritis Res Ther*. (2017) 19:234. doi: 10.1186/s13075-017-1441-7
47. Souyris M, Mejia JE, Chaumeil J, Guery JC. Female predisposition to TLR7-driven autoimmunity: gene dosage and the escape from X chromosome inactivation. *Semin Immunopathol*. (2018) 41:153–64. doi: 10.1007/s00281-018-0712-y
48. Soni C, Wong EB, Domeier PP, Khan TN, Satoh T, Akira S, et al. B cell-intrinsic TLR7 signaling is essential for the development of spontaneous germinal centers. *J Immunol*. (2014) 193:4400–14. doi: 10.4049/jimmunol.1401720
49. Alexander NJ, Smythe NL, Jokinen MP. The type of dietary fat affects the severity of autoimmune disease in NZB/NZW mice. *Am J Pathol*. (1987) 127:106–21.
50. Gilbert EL, Ryan MJ. High dietary fat promotes visceral obesity and impaired endothelial function in female mice with systemic lupus erythematosus. *Gend Med*. (2011) 8:150–5. doi: 10.1016/j.genm.2011.03.006
51. Kelley VE, Izui S. Enriched lipid diet accelerates lupus nephritis in NZB x W mice. Synergistic action of immune complexes and lipid in glomerular injury. *Am J Pathol*. (1983) 111:288–97.
52. Revelo XS, Ghazarian M, Chng MH, Luck H, Kim JH, Zeng K, et al. Nucleic acid-targeting pathways promote inflammation in obesity-related insulin resistance. *Cell Rep*. (2016) 16:717–30. doi: 10.1016/j.celrep.2016.06.024
53. Bessone F, Poles N, Roma MG. Challenge of liver disease in systemic lupus erythematosus: clues for diagnosis and hints for pathogenesis. *World J Hepatol*. (2014) 6:394–409. doi: 10.4254/wjh.v6.i6.394
54. Sun X, Wiedeman A, Agrawal N, Teal TH, Tanaka L, Hudkins KL, et al. Increased ribonuclease expression reduces inflammation and prolongs survival in TLR7 transgenic mice. *J Immunol*. (2013) 190:2536–43. doi: 10.4049/jimmunol.1202689
55. Massey VL, Qin L, Cabezas J, Caballeria J, Sancho-Bru P, Bataller R, et al. TLR7-let-7 signaling contributes to ethanol-induced hepatic inflammatory response in mice and in alcoholic hepatitis. *Alcohol Clin Exp Res*. (2018) 42:2107–22. doi: 10.1111/acer.13871
56. Hadaschik EN, Wei X, Leiss H, Heckmann B, Niederreiter B, Steiner G, et al. Regulatory T cell-deficient scurfy mice develop systemic autoimmune features resembling lupus-like disease. *Arthritis Res Ther*. (2015) 17:35. doi: 10.1186/s13075-015-0538-0
57. Vila L, Roglans N, Baena M, Barroso E, Alegret M, Merlos M, et al. Metabolic alterations and increased liver mTOR expression precede the development of autoimmune disease in a murine model of lupus erythematosus. *PLoS ONE*. (2012) 7:e51118. doi: 10.1371/journal.pone.0051118
58. Alperovich G, Rama I, Lloberas N, Franquesa M, Poveda R, Goma M, et al. New immunosuppresor strategies in the treatment of murine lupus nephritis. *Lupus*. (2007) 16:18–24. doi: 10.1177/0961203306073136
59. Li J, Tan J, Martino MM, Lui KO. Regulatory T-cells: potential regulator of tissue repair and regeneration. *Front Immunol*. (2018) 9:585. doi: 10.3389/fimmu.2018.00585
60. Overacre AE, Vignali DA. T(reg) stability: to be or not to be. *Curr Opin Immunol*. (2016) 39:39–43. doi: 10.1016/j.coi.2015.12.009
61. Kluger MA, Nosko A, Ramcke T, Goerke B, Meyer MC, Wegscheid C, et al. RORgammat expression in Tregs promotes systemic lupus erythematosus via IL-17 secretion, alteration of Treg phenotype and suppression of Th2 responses. *Clin Exp Immunol*. (2017) 188:63–78. doi: 10.1111/cei.12905
62. Komatsu N, Okamoto K, Sawa S, Nakashima T. Oh-hora M, Kodama T, et al. Pathogenic conversion of Foxp3+ T cells into TH17 cells in autoimmune arthritis. *Nat Med*. (2014) 20:62–8. doi: 10.1038/nm.3432
63. Osborn O, Olefsky JM. The cellular and signaling networks linking the immune system and metabolism in disease. *Nat Med*. (2012) 18:363–74. doi: 10.1038/nm.2627
64. Kim SJ, Choi Y, Choi YH, Park T. Obesity activates toll-like receptor-mediated proinflammatory signaling cascades in the adipose tissue of mice. *J Nutr Biochem*. (2012) 23:113–22. doi: 10.1016/j.jnutbio.2010.10.012
65. Sindhu S, Wilson A, Akhter N, Shenouda S, Kochumon S, Behbehani K, et al. Increased adipose tissue expression of Toll-like receptor (TLR)-7 in obese individuals: significance in metabolic disease. *J Glycom Lipidom*. (2015) 5:1000136. doi: 10.4172/2153-0637.1000136
66. Fernandes G, Yunis EJ, Good RA. Influence of diet on survival of mice. *Proc Natl Acad Sci USA*. (1976) 73:1279–83. doi: 10.1073/pnas.73.4.1279
67. Jolly CA, Muthukumar A, Avula CP, Troyer D, Fernandes G. Life span is prolonged in food-restricted autoimmune-prone (NZB x NZW)F(1) mice fed a diet enriched with (n-3) fatty acids. *J Nutr*. (2001) 131:2753–60. doi: 10.1093/jn/131.10.2753
68. Muthukumar AR, Jolly CA, Zaman K, Fernandes G. Calorie restriction decreases proinflammatory cytokines and polymeric Ig receptor expression in the submandibular glands of autoimmune prone (NZB x NZW)F1 mice. *J Clin Immunol*. (2000) 20:354–61. doi: 10.1023/A:1006620130114
69. Constantin MM, Nita IE, Olteanu R, Constantin T, Bucur S, Matei C, et al. Significance and impact of dietary factors on systemic lupus erythematosus pathogenesis. *Exp Ther Med*. (2019) 17:1085–90. doi: 10.3892/etm.2018.6986
70. Rosser EC, Mauri C. A clinical update on the significance of the gut microbiota in systemic autoimmunity. *J Autoimmun*. (2016) 74:85–93. doi: 10.1016/j.jaut.2016.06.009
71. Banchereau R, Hong S, Cantarel B, Baldwin N, Baisch J, Edens M, et al. Personalized immunomonitoring uncovers molecular networks that stratify lupus patients. *Cell*. (2016) 165:551–65. doi: 10.1016/j.cell.2016.03.008

Conflict of Interest Statement: The authors declare that the research was conducted in the absence of any commercial or financial relationships that could be construed as a potential conflict of interest.

frontiers in Immunology

ORIGINAL RESEARCH
published: 20 September 2019
doi: 10.3389/fimmu.2019.02130

Docosahexaenoic Acid Suppresses Silica-Induced Inflammasome Activation and IL-1 Cytokine Release by Interfering With Priming Signal

*Kathryn A. Wierenga[1,2†], Josephine Wee[3†‡], Kristen N. Gilley[3], Lichchavi D. Rajasinghe[3], Melissa A. Bates[2,3], Mikhail A. Gavrilin[4], Andrij Holian[5] and James J. Pestka[2,3,6]**

[1] Department of Biochemistry and Molecular Biology, Michigan State University, East Lansing, MI, United States, [2] Institute for Integrative Toxicology, Michigan State University, East Lansing, MI, United States, [3] Department of Food Science and Human Nutrition, Michigan State University, East Lansing, MI, United States, [4] Division of Pulmonary, Critical Care and Sleep Medicine, Ohio State University, Columbus, OH, United States, [5] Department of Biomedical and Pharmaceutical Sciences, Center for Environmental Health Sciences, University of Montana, Missoula, MT, United States, [6] Department of Microbiology and Molecular Genetics, Michigan State University, East Lansing, MI, United States

Occupational exposure to respirable crystalline silica ($cSiO_2$) has been etiologically linked to human autoimmunity. Intranasal instillation with $cSiO_2$ triggers profuse inflammation in the lung and onset of autoimmunity in lupus-prone mice; however, dietary supplementation with the omega-3 polyunsaturated fatty acid docosahexaenoic acid (DHA) abrogates these responses. Inflammasome activation, IL-1 cytokine release, and death in alveolar macrophages following $cSiO_2$ exposure are early and critical events that likely contribute to triggering premature autoimmune pathogenesis by this particle. Here we tested the hypothesis that DHA suppresses $cSiO_2$-induced NLRP3 inflammasome activation, IL-1 cytokine release, and cell death in the macrophage. The model used was the murine macrophage RAW 264.7 cell line stably transfected with the inflammasome adapter protein ASC (RAW-ASC). Following priming with LPS, both the canonical activator nigericin and $cSiO_2$ elicited robust inflammasome activation in RAW-ASC cells, as reflected by IL-1β release and caspase-1 activation. These responses were greatly diminished or absent in wild-type RAW cells. In contrast to IL-1β, $cSiO_2$ induced IL-1α release in both RAW-ASC and to a lesser extent in RAW-WT cells after LPS priming. $cSiO_2$-driven effects in RAW-ASC cells were confirmed in bone-marrow derived macrophages. Pre-incubating RAW-ASC cells with 10 and 25 μM DHA for 24 h enriched this fatty acid in the phospholipids by 15- and 25-fold, respectively, at the expense of oleic acid. DHA pre-incubation suppressed inflammasome activation and release of IL-1β and IL-1α by nigericin, $cSiO_2$, and two other crystals – monosodium urate and alum. DHA's suppressive effects were linked to inhibition of LPS-induced *Nlrp3, Il1b,* and *Il1a* transcription, potentially through the activation of PPARγ. Finally, nigericin-induced death was inflammasome-dependent, indicative of pyroptosis, and could be inhibited by

OPEN ACCESS

Edited by:
Attila Mócsai,
Semmelweis University, Hungary

Reviewed by:
Rksubbarao Malireddi,
St. Jude Children's Research Hospital, United States
Ashley Mansell,
Hudson Institute of Medical Research, Australia

***Correspondence:**
James J. Pestka
pestka@msu.edu

[†] These authors have contributed equally to this work

[‡] Present address:
Josephine Wee,
Department of Food Science, The Pennsylvania State University, State College, PA, United States

Specialty section:
This article was submitted to Autoimmune and Autoinflammatory Disorders, a section of the journal Frontiers in Immunology

Received: *19 February 2019*
Accepted: *23 August 2019*
Published: *20 September 2019*

Citation:
Wierenga KA, Wee J, Gilley KN, Rajasinghe LD, Bates MA, Gavrilin MA, Holian A and Pestka JJ (2019) Docosahexaenoic Acid Suppresses Silica-Induced Inflammasome Activation and IL-1 Cytokine Release by Interfering With Priming Signal. Front. Immunol. 10:2130. doi: 10.3389/fimmu.2019.02130

DHA pretreatment. In contrast, $cSiO_2$-induced death was inflammasome-independent and not inhibited by DHA. Taken together, these findings indicate that DHA suppresses $cSiO_2$-induced inflammasome activation and IL-1 cytokine release in macrophages by acting at the level of priming, but was not protective against $cSiO_2$-induced cell death.

Keywords: macrophage, cell death, inflammasome, silica, omega-3 fatty acids, *in vitro*

INTRODUCTION

Occupational exposure to airborne crystalline silica ($cSiO_2$) has been linked to the prevalence of autoimmune disease (1). We have previously demonstrated that $cSiO_2$ triggers the early onset and progression of systemic autoimmunity and glomerulonephritis in lupus-prone female NZBWF1 mice (2). In this model, intranasal instillation with $cSiO_2$ induces profuse inflammation in the lung characterized by cytokine and chemokine secretion, lymphocyte infiltration, and autoantigen release. Collectively, these processes promote the development of pulmonary ectopic lymphoid structures (ELS) that drive autoimmune pathogenesis. Remarkably, supplementing the NZBWF1 mouse diets with the omega-3 polyunsaturated fatty acid (ω-3 PUFA) docosahexaenoic acid (C22:6 ω-3; DHA), a widely used dietary supplement extracted from cold-water fish, blocks $cSiO_2$-triggered inflammation, ectopic lymphoid neogenesis, systemic autoimmunity, and nephritis (3, 4). Accordingly, supplementation with DHA and other ω-3 PUFAs may be an effective intervention against triggering of lupus onset, flaring, and/or progression by environmental agents such as $cSiO_2$. However, the mechanisms behind DHA's suppression of $cSiO_2$-accelerated pulmonary and systemic autoimmunity are unclear.

Phagocytosis by alveolar macrophages (AMΦs) is a primary line of defense against respirable particles. After $cSiO_2$ is phagocytosed, it induces lysosomal membrane permeabilization that in turn elicits NLRP3 inflammasome oligomerization and caspase-1 activation (5–8). Caspase-1 selectively cleaves pro-IL-1β to mature IL-1β, and induces cell death via pyroptosis (9–11). The latter results in release of inflammatory mediators, alarmins, autoantigens, and reemergence of the $cSiO_2$ particles into the alveolar space. Continuous repetition of this sequence promotes recruitment and activation of additional leukocytes in the lung, culminating in chronic inflammation and autoimmunity (5). Other crystals, including monosodium urate (MSU) (12), alum (8), and cholesterol (13), have also been shown to activate the NLRP3 inflammasome.

NLRP3 inflammasome activation requires a priming signal such as the pathogen-associated lipopolysaccharide (LPS), which upregulates expression of inflammasome components and IL-1 cytokines (14). Importantly, cytokines (e.g., IL-1β, TNF-α, and IL-6) and endogenous danger signals such as alarmins can similarly elicit this priming effect. The canonical alarmin IL-1α is constitutively expressed in myriad cell populations, including macrophages under steady state conditions, but its expression can be upregulated by proinflammatory or stress-associated stimuli (15). Rabolli et al. (16) reported that macrophages are a main source of IL-1α in the lung and that $cSiO_2$ can induce release of this cytokine. Like IL-1β, IL-1α binds the IL-1R1 receptor on AMΦ, consequently activating NF-κB-driven expression of inflammasome proteins (15). Release of IL-1β and IL-1α in concert with the sustained presence of $cSiO_2$ (17) then allows a feed-forward loop of inflammasome activation and pyroptotic cell death within MΦs that is capable of perpetually activating inflammation and autoimmune pathogenesis.

Previous studies suggest that DHA and other ω-3 PUFAs potentially interfere with $cSiO_2$-induced NLRP3 inflammasome activation, release of IL-1 cytokines, and death of AMΦs (18–22). However, elucidation of how ω-3 PUFAs influence these responses is inherently difficult due to low numbers of AMΦs isolatable from animals or humans. The murine RAW 264.7 (RAW) cell line is a widely used MΦ model that has been cited in mechanism studies nearly 10,000 times since its discovery in 1977 by Raschke et al. (23). Importantly, the wild-type RAW (RAW-WT) cells lack the inflammasome adapter ASC (apoptosis-associated speck-like protein containing a CARD domain) that is crucial for NLRP3 inflammasome assembly (24). This can be rectified by transfection with the ASC gene thereby rendering this cell line capable of mounting an inflammasome response similar to primary AMΦs (25). Herein, we employed RAW-ASC and RAW-WT cells with and without inflammasome priming to test the hypothesis that DHA suppresses $cSiO_2$-induced NLRP3 inflammasome activation, IL-1 cytokine release, and cell death in the macrophage.

MATERIALS AND METHODS

RAW-WT and RAW-ASC MΦ Models

Murine-derived wild-type RAW 264.7 (RAW-WT) cells were purchased from the American Type Culture Collection (ATCC® TIB-71™). RAW-ASC cells were obtained by transfection with a fusion CFP-ASC protein. The open-reading frame of ASC was amplified from cDNA by PCR and inserted at the C-terminus of cyan fluorescent protein (CFP) of pLenti-CFP plasmid generated on the basis of pLenti6/V5 (Invitrogen Life Technologies, Carlsbad, CA) resulting in a fusion CFP-ASC protein, as described previously (26). Plasmid containing the fusion CFP-ASC protein (designated pLenti-CFP-ASC) was verified by Sanger sequencing. The lentiviral system was generated in the packaging cell line HEK293-FT (Invitrogen Life Technologies) and transfected with pLenti-CFP-ASC and helper plasmids pCMVΔR8.2 and pMD.G using Lipofectamine 2000 (Invitrogen Life Technologies). Cell culture medium containing virus was harvested at 48 and 72 h post-transfection, filtered, and

concentrated at 3,200 x g for 30 min in Centricon C-20 columns, 100,000 MWCO (Millipore Sigma, Burlington, MA) resulting in a titer of 1–2E7 TU/ml. To restore inflammasome function, RAW 264.7 lacking expression of endogenous ASC were transduced with CFP-ASC lentivirus at 2–5 multiplicity of infection (MOI) in the presence of 6 μg/ml polybrene. After lentiviral transduction, 10–15% cells expressed fluorescent protein. Stably transduced cells were then selected with 5 μg/ml of blasticidin (InvivoGen) for 10 days, resulting in 90% fluorescent cells as observed by fluorescent microscopy. Both cell types were cultured in phenol red-free RPMI 1640 medium (Thermo Fisher Scientific, Waltham, MA) supplemented with 10% FBS (Thermo Fisher Scientific) and 1% Penicillin-streptomycin (Invitrogen Life Technologies) and sub-cultured every 2–4 days (24, 27).

Preparation of Bone Marrow-Derived Macrophages (BMDMs)

All experimental protocols involving animals were reviewed and approved by the Institutional Animal Care and Use Committee at Michigan State University in accordance with the National Institutes of Health guidelines (AUF # PROTO201800113). Femurs were removed from 8 to 14 week old C57BL/6J mice and marrow was flushed from the bone with ice cold PBS. Cells were dissociated by pipetting and filtered through a 40 μm cell strainer. Cells were pelleted and resuspended in 1 mL red blood cell lysis buffer (Thermo Fisher Scientific) and incubated at room temperature for 10 min. An additional 10 mL PBS were added and cells were pelleted, counted, and plated at 5×10^6 cells per 100 mm petri dish in DMEM (Thermo Fisher Scientific) supplemented with 10% FBS, 1% Penicillin-streptomycin, and 20% L929 supernatant as previously described (28). Medium was refreshed every 2–3 days. Adherent macrophages were used in experiments at 7 days after isolation.

$cSiO_2$ and Other Crystals

$cSiO_2$ (Min-U-Sil-5, Pennsylvania Glass Sand Corp, Pittsburgh, PA) was prepared as previously described (29). Briefly, $cSiO_2$ was suspended in 1 M HCl and washed for 1 h at 100°C. Following cooling, $cSiO_2$ was washed 3 times with sterile water and dried at 200°C overnight. For treatments, acid washed $cSiO_2$ was suspended in fresh, sterile Dulbecco's phosphate-buffered saline (DPBS, pH 7.4). Similarly, MSU crystals (InvivoGen) were suspended in DPBS at 5 mg/mL per the manufacturer's instructions. A 20 mg/mL stock suspension of alum crystals (InvivoGen) was prepared in sterile water and diluted 1:4 with PBS before use. All crystal suspensions were stored at 4°C for no longer than 2 weeks. Prior to use, crystal suspensions were vortexed thoroughly, sonicated for 1 min and added dropwise to wells to achieve the desired concentrations.

DHA Preparation

DHA-bovine serum albumin (BSA) complexes were used to supplement cell culture media at physiologically relevant doses. The complexes were prepared as previously described (30, 31). Briefly, a 15% solution of fatty acid-free, endotoxin-, and fatty acid-free BSA (Millipore Sigma) was prepared in serum-free RPMI. Stocks of DHA (Cayman Chemical, Ann Arbor, MI) were diluted in EtOH to 11.76 mg/mL. A volume of the DHA corresponding to 20 mg DHA was transferred to glass tube and EtOH evaporated under a steady stream of N_2. DHA was then dissolved in 4 mL of 0.05 M Na_2CO_3 for a final concentration of 5 mg/mL. The tube was flushed with N_2 gas, vortexed, and incubated at room temperature for 1 h. DHA in Na_2CO_3 and 15% w/v BSA in RPMI were added to serum-free RPMI to obtain a final concentration of 2.5 mM DHA and 0.833 mM BSA (3:1 molar ratio). The tube was flushed with N_2 and gently mixed for 30 min. The DHA-BSA complex solution was filter sterilized and aliquoted. Complexes were capped with N_2 and stored at −20°C for no longer than 3 months.

Experimental Design

Approaches used for this study are summarized in **Figure 1**. Frequently used reagents can be found in **Table S1**. For comparison of RAW-WT or RAW-ASC MΦs, cells were plated at 3×10^5 cells/well in 12 well plates, 1.5×10^5 cells/well in 24 well plates, or 1.7×10^4 cells/well in 96 well plates in order to achieve 70–90% confluency at the time of treatment. Unless otherwise noted, cells were cultured for 24 h in complete RPMI (phenol red-free RPMI 1640, 10% FBS, 1% penicillin-streptomycin), washed once with sterile DPBS and primed for 2 h with 20 ng/mL LPS in serum deprived RPMI (phenol red-free RPMI 1640, 0.25% FBS, 1% penicillin-streptomycin). Following priming with LPS (from *Salmonella enterica* serotype typhimurium containing <1% protein impurities, Millipore Sigma), $cSiO_2$, nigericin (Millipore Sigma), MSU, alum, or vehicle (DPBS for $cSiO_2$ and <0.3% EtOH for nigericin) was added to cultures dropwise. Cells were incubated with nigericin for 30 to 120 min, with $cSiO_2$ for 1 to 4 h, and with MSU or alum for 8 h. Culture supernatants were collected for cytokine ELISAs and lactate dehydrogenase (LDH) assays, and cells were collected for RNA and protein extraction. For DHA supplementation studies, cells were seeded at 2.5×10^5 cells/well in 12 well plates or 1.25×10^5 cells/well in 24 well plates, as established in prior experiments to achieve 70–90% confluency at the time of treatment. Cells were grown 24 h in complete RPMI. Wells were then washed once with DPBS and media was replaced with RPMI containing 0.25% FBS and 10 or 25 μM DHA as a 3:1 complex with BSA (30, 32). Non-supplemented media (0 μM DHA) containing BSA was used as a vehicle control. After 24 h, wells were washed with DPBS and subjected to treatments as described above.

IL-1 Cytokine Analyses

IL-1β and IL-1α release was measured using the mouse IL-1β/IL-1F2 DuoSet® ELISA and mouse IL-1α/IL-1F1 DuoSet® ELISA (R&D Systems, Minneapolis, MN) per the manufacturer's instructions.

Caspase-1 Activity

Caspase-1 activation was determined in LPS-primed and unprimed RAW-ASC cells using the FAM-FLICA *in vitro* Caspase-1 kit (ImmunoChemistry Technologies, LLC, Bloomington, MN). This kit employs the fluorescent inhibitor probe FAM-YVAD-FMK to label active caspase-1 enzyme in living cells. To investigate the effect of $cSiO_2$ on caspase-1 activation in RAW-ASC cells, 1.5 x 10^5 cells per well were seeded in complete RPMI medium in a clear bottomed, black

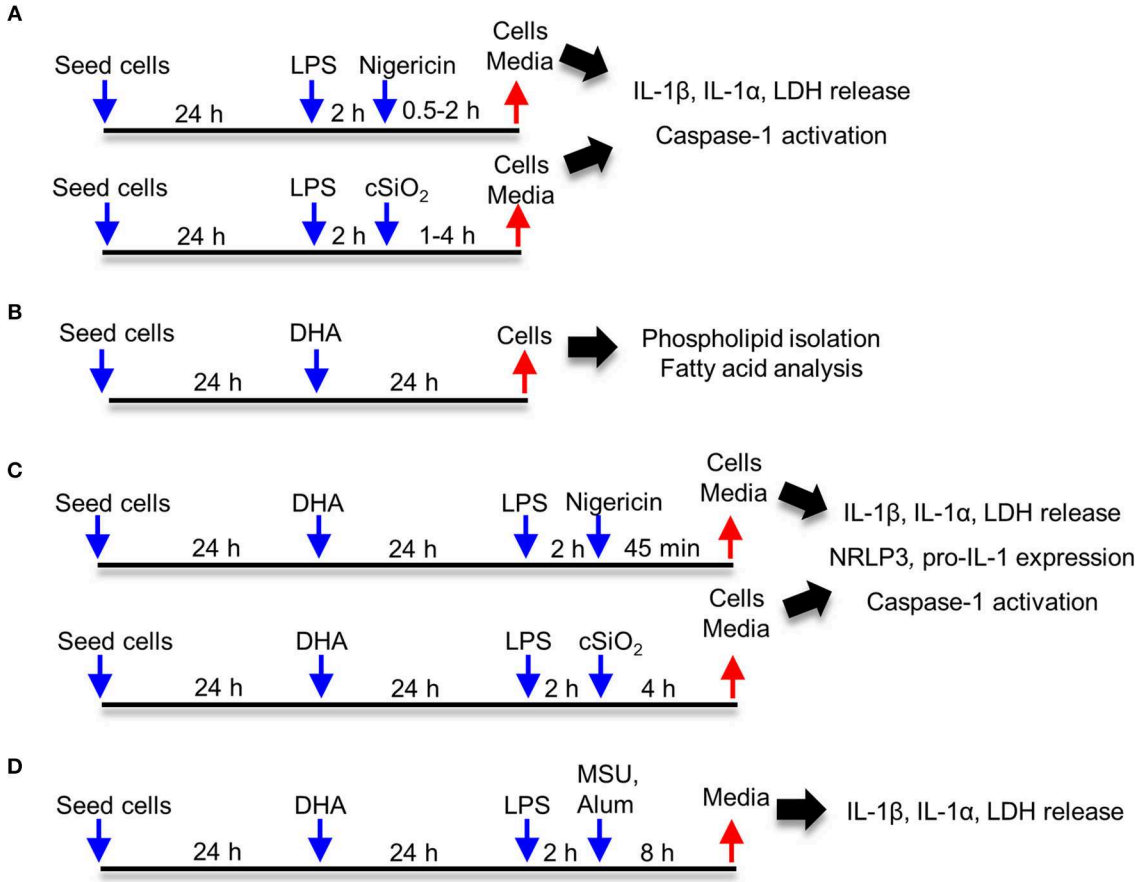

FIGURE 1 | Experimental design. Studies focused on **(A)** characterization of $cSiO_2$- and nigericin-induced inflammasome activation, IL-1 cytokine release and cell death in RAW-WT and RAW-ASC macrophages, **(B)** assessing effects of DHA supplementation on the fatty acid profile of membrane phospholipids, **(C)** determining how DHA impacts inflammasome activation, IL-1 cytokine release and cell death, and **(D)** assessing how DHA impacts inflammasome activation by monosodium urate (MSU) and alum crystals.

walled 24-well plate. After 24 h, cells were subjected to the treatments described above, with the exception that 15 μL of FAM-FLICA reagent (20x) was added 2 h before the end of incubation. Following treatment, plates were spun at 100 x g for 2 min to recover detached cells. Cells were gently washed with the provided wash buffer and centrifuged at 100 x g for 2 min three times. Cells were imaged with the EVOS FL Auto Cell Imaging System (Invitrogen Life Technologies) with 40x objective using the GFP light cube. For multi-well analysis, total green fluorescence intensity was measured at 492 ex and 520 em using surface scan mode of EnSpire™ Multilabel Plate Reader (PerkinElmer Inc., Waltham, MA). Total fluorescence intensity was normalized to total amount of protein as measured by Pierce™ BCA Protein Assay Kit (Thermo Fisher Scientific). Results from two separate experiments were combined and expressed as fold change relative to treatment control.

Cell Death

At the conclusion of the nigericin or $cSiO_2$ treatment periods, cell death was assessed by release of lactate dehydrogenase (LDH) as previously described (33). Briefly, 10% Triton X-100 (Millipore Sigma) was added to control wells designated for quantification of maximum kill (MK) at 2% (v/v) to induce maximum cell lysis. Media was collected from MK and sample wells and 50 μL media from each well added to an untreated, flat-bottomed 96-well plate. Serum-deprived RPMI was used as the sample blank and serum-deprived RPMI with 10% Triton-X was used as the MK blank. LDH reagent solution was prepared fresh as described (33) and 100 μL added to each well. Plates were incubated in the dark at room temperature for 15 min and read on a FilterMax F3 Multimode plate reader (Molecular Devices, San Jose, CA) at an absorbance wavelength of 492 nm. Cytotoxicity of samples was calculated as follows: $100\%*[(sample_{abs} - sample\ blank_{abs})/(MK_{abs} - MK\ blank_{abs})]$. Remaining cell culture medium was stored at −20°C until cytokine analysis.

PPARγ Transcription Factor Assay

Samples were prepared using a Nuclear Extraction Kit (Active Motif Inc., Carlsbad, CA) per the manufacturer's instructions. Protein content of the nuclear extracts was quantified by Pierce™ BCA Protein Assay Kit (Thermo Fisher Scientific). PPARγ activity in nuclear extracts was assessed using the TransAM®

PPARγ Transcription Factor ELISA kit (Active Motif Inc). Activity was expressed as fold-change relative to control.

qRT-PCR

Following 6 h incubation with 20 ng/mL LPS, RNA was extracted using RNeasy Mini spin columns provided with the RNeasy Mini Kit (Qiagen, Germantown, MD). Following extraction, reverse transcription was performed using a High Capacity RNA to cDNA Reverse Transcription Kit (Invitrogen Life Technologies). Quantitative real-time qPCR was performed using specific Taqman probes for selected genes involved in NLRP3 inflammasome

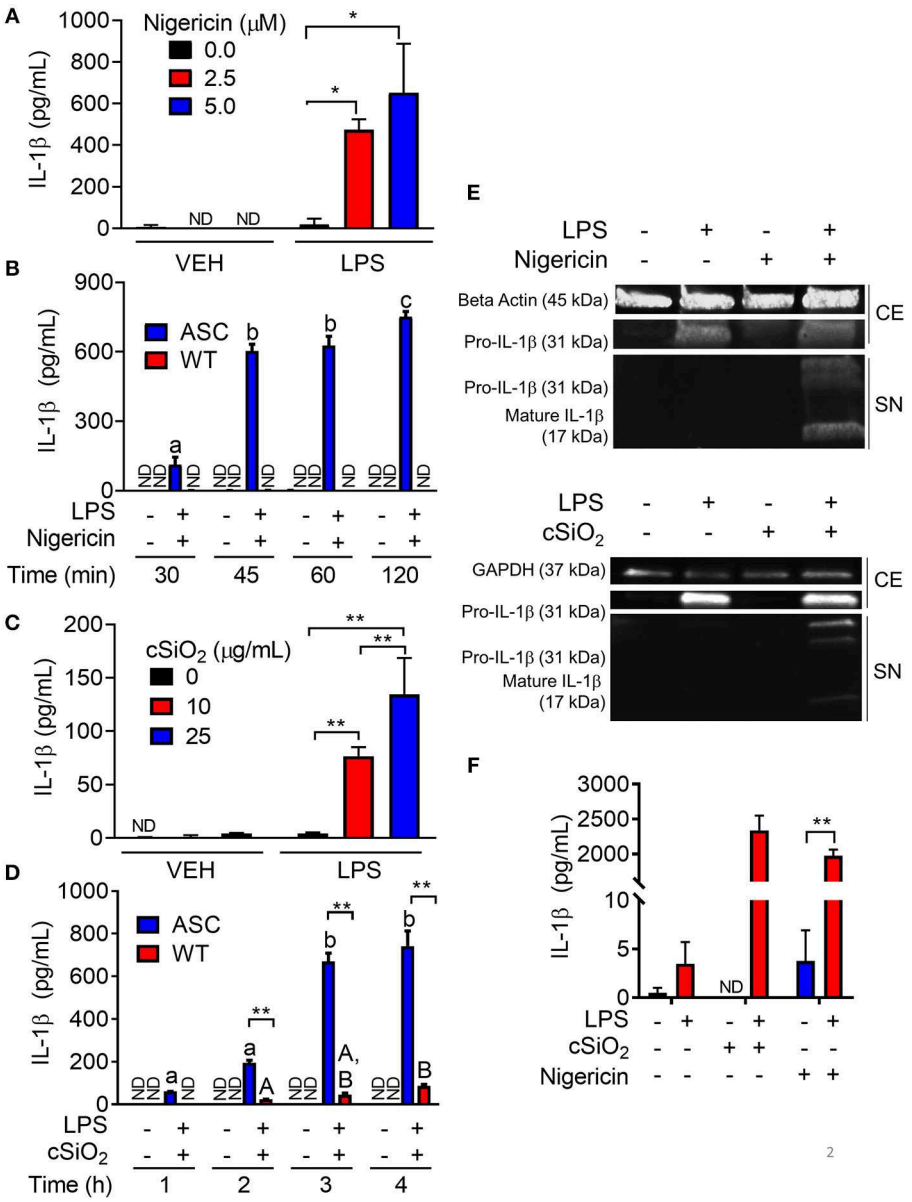

FIGURE 2 | Nigericin- and $cSiO_2$-induced IL-1β release are LPS- and ASC-dependent in RAW MΦs. **(A,C)** RAW-ASC cells were pretreated with 20 ng/ml LPS for 2 h, incubated with 0, 2.5, or 5.0 μM nigericin for 45 min **(A)**, or 0, 10, or 25 μg/ml $cSiO_2$ for 4 h **(C)**, and then release of IL-1β measured. **(B,D)** RAW-ASC and RAW-WT were pretreated with VEH or LPS for 2 h, incubated with VEH or 10 μM nigericin **(B)** or 25 μg/ml $cSiO_2$ **(D)**. IL-1β release was assessed at the indicated times. **(E)** Pro-IL-1β was present in the cell extracts (CE) of RAW-ASC MΦs treated with LPS, but only secreted into the supernatant (SN) with nigericin or $cSiO_2$ treatment. IL-1β in the supernatant contained both the precursor and cleaved forms. **(F)** Bone marrow-derived macrophages were pretreated with VEH or LPS (20 ng/ml) for 2 h, incubated with VEH or 5 μM nigericin or 25 μg/ml $cSiO_2$ and IL-1β release then assessed at 45 min or 4 h, respectively. Data presented as mean ± SEM, $n = 3$. ND = not detectable. Asterisks indicate significant differences between cell type **(B,D)** or treatment group **(A,C,E)** (*$p < 0.05$, **$p < 0.01$). Different letters indicate significant differences between treatment groups within each cell type **(B,D)** ($p < 0.05$). ELISA data are representative of three independent experiments. Western blots are representative of two independent experiments.

formation (*Nlrp3* Assay ID Mm00840904_m1, *Il1b* Assay ID Mm01336189_m1, *Il1a* Assay ID Mm00439620_m1, *Casp1* Assay ID Mm004438023_m1; Thermo Fisher Scientific) on the Applied Biosystems™ QuantStudio™ 7 real-time PCR system. Data were analyzed with Applied Biosystems™ Thermo Fisher Cloud using the RQ software and the relative quantification method. *Gapdh* (Assay ID Mm99999915_g1; Thermo Fisher Scientific) was used as the housekeeping gene. Relative copy number (RCN) for each gene was normalized to expression of *Gapdh* and calculated as described previously (34).

SDS-PAGE and Western Blot

RAW-ASC macrophages were lysed in RIPA buffer containing Halt Protease Inhibitor (RIPA-HPI; Thermo Fisher Scientific). To assess IL-1α in supernatant, protein was concentrated by precipitation with methanol and chloroform (35). Briefly, 600 μL of methanol:chloroform (4:1) was added to 600 μL media

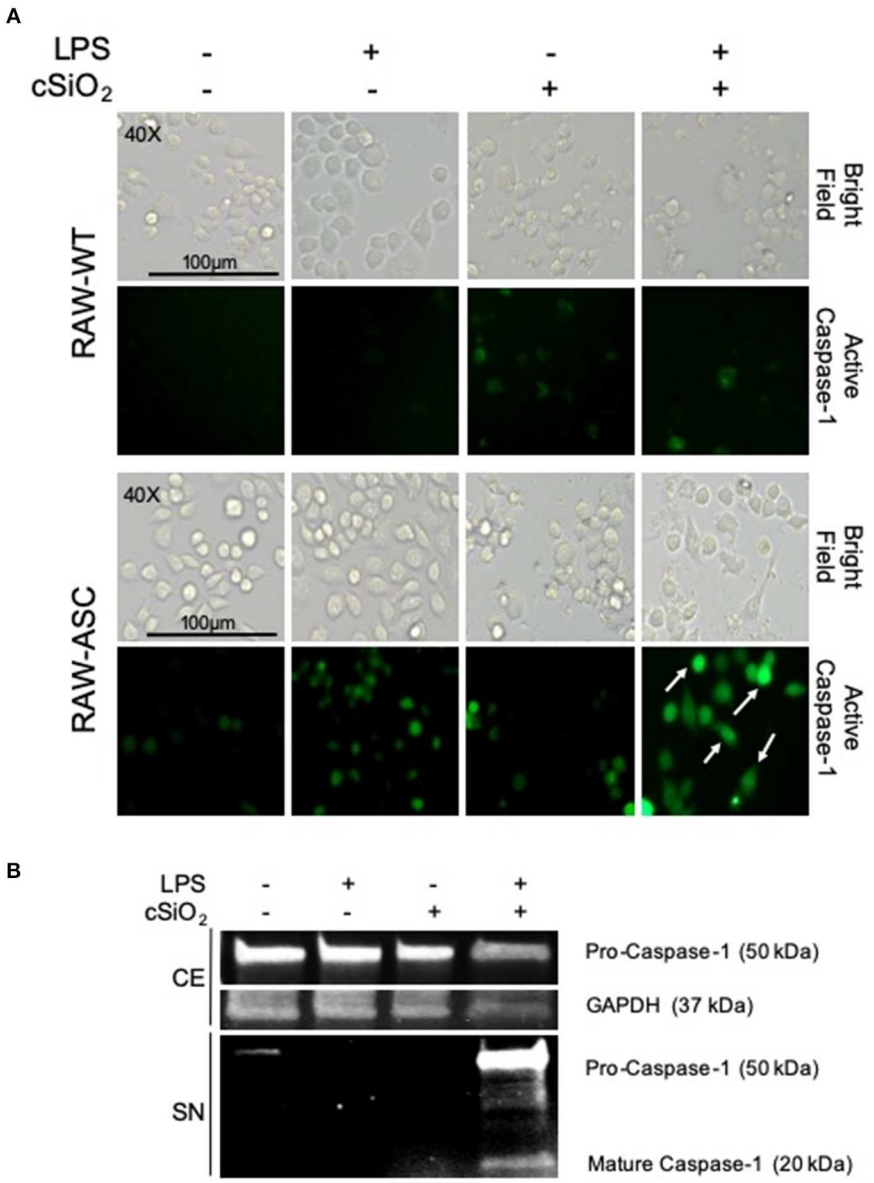

FIGURE 3 | $cSiO_2$-induced caspase-1 activation in RAW MΦs is LPS- and ASC-dependent. **(A)** RAW-WT and RAW-ASC cells were pretreated with VEH or 20 ng/ml LPS for 2 h and then incubated with VEH or 25 μg/ml $cSiO_2$ for 4 h. Caspase-1 activation was assessed using fluorescent inhibitor probe FAM-YVAD-FMK. Treatment with LPS and $cSiO_2$ induced minimal activation of caspase-1 in RAW-WT cells while RAW-ASC cells show robust activation of caspase-1 as indicated by green fluorescence (white arrows). Cells were imaged using an EVOS FL Auto Cell Imaging System; images representative of three independent experiments. **(B)** Pro-caspase-1 was constitutively expressed in RAW-ASC MΦs and detectable in the cell extract (CE). Pro-caspase-1 and cleaved, active caspase-1 (p20) were only present in the supernatant (SN) of cells treated with both LPS and $cSiO_2$; Western blots are representative of two independent experiments.

supernatant. Samples were centrifuged at 12,000 x g for 5 min and the upper methanol layer removed. Methanol (600 μL) was added, samples were vortexed and centrifuged again. Supernatant was removed, and the pellet was dried under a gentle stream of N_2. The pellet was then resuspended in 60 μL RIPA-HPI.

For assessment of NF-κB activation, nuclear and cytoplasmic extracts were prepared using a NE-PER Nuclear and Cytoplasmic

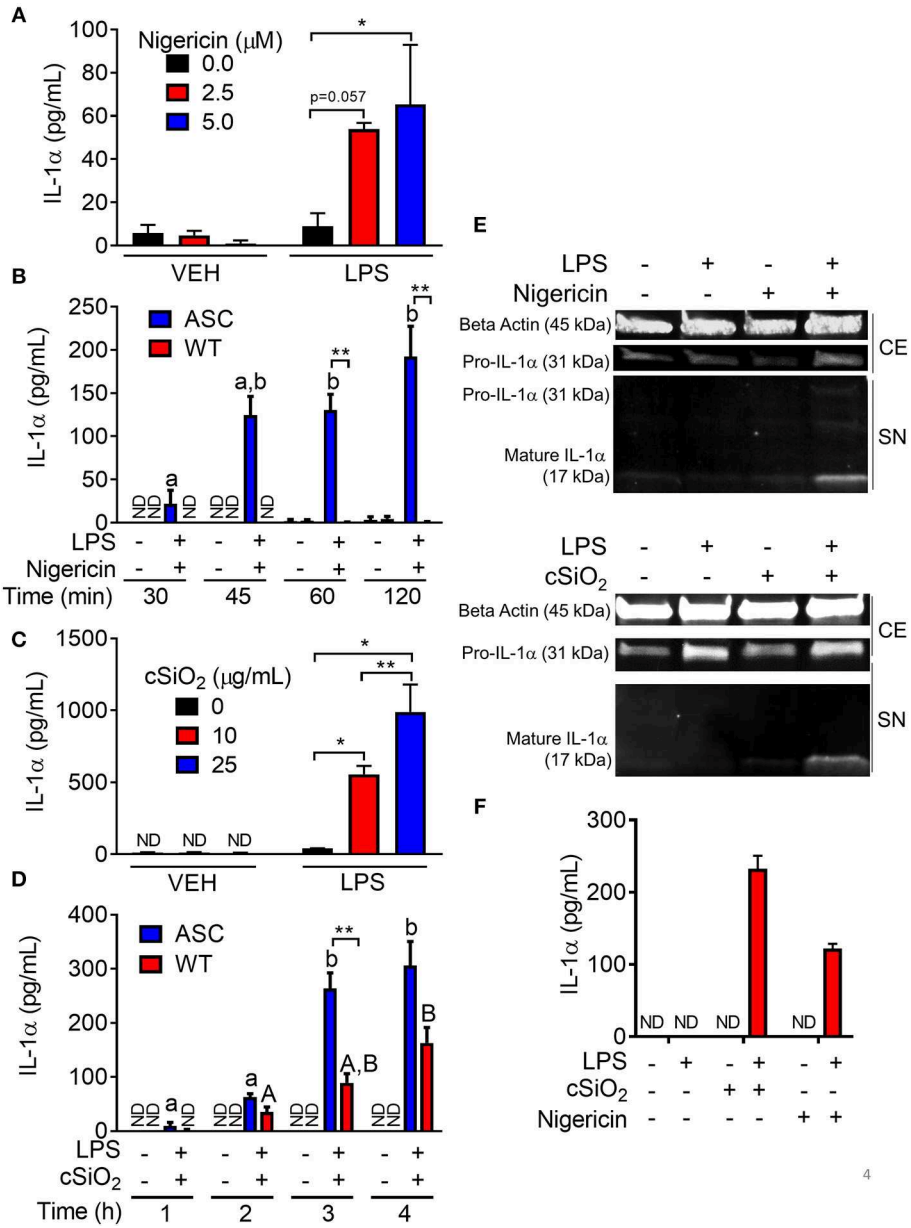

FIGURE 4 | Nigericin- and $cSiO_2$-induced IL-1α release is LPS- and ASC-dependent in RAW MΦs. **(A,D)** RAW-ASC cultures were pretreated with VEH or 20 ng/ml LPS for 2 h, incubated with 0, 2.5, or 5.0 μM nigericin for 45 min **(A)**, or 0, 10, or 25 μg/ml $cSiO_2$ for 4 h **(C)**, and then release of IL-1α measured. **(B,D)** RAW-ASC and RAW-WT were pretreated with VEH or LPS for 2 h, incubated with VEH, 10 μM nigericin **(B)**, or 25 μg/ml $cSiO_2$ **(D)** and release of IL-1α measured at the times indicated. **(E)** Pro-IL-1α was constitutively expressed and slightly upregulated in cell extracts (CE) of RAW-ASC MΦs treated with LPS, but only secreted into the supernatant (SN) with 5 μM nigericin or 25 μg/ml $cSiO_2$ treatment. Both pro-IL-1α and mature IL-1α were detected in the supernatant. To detect IL-1α in the supernatant, LPS priming was extended to 5 h and protein concentrated 10x by methanol-chloroform precipitation. **(F)** Bone marrow-derived macrophages were pretreated with VEH or LPS (20 ng/ml) for 2 h, incubated with VEH or 5 μM nigericin or 25 μg/ml $cSiO_2$ and IL-1α release then assessed at 45 min or 4 h, respectively. Data presented as mean ± SEM, $n = 3$. ND = not detectable. Asterisks indicate significant differences between cell type **(B,D)** or treatment group **(A,C,E)** (*$p < 0.05$, **$p < 0.01$). Different letters indicate significant differences between treatment groups within each cell type **(B,D)** ($p < 0.05$). ELISA data are representative of three independent experiments. Western blots are representative of two independent experiments.

Extraction Kit (Thermo Fisher Scientific) supplemented with Halt Protease Inhibitor according to the manufacturer's instructions and as previously described (36).

Protein lysates and supernatant concentrates were diluted in Laemmli sample buffer containing 5% β-mercaptoethanol and separated on a 4–20% gradient gel (Bio-Rad Laboratories, Hercules, CA) with 1x TGS buffer (Bio-Rad Laboratories). Protein was transferred to a Trans-Blot® Turbo™ RTA Mini low fluorescent PVDF membrane (Bio-Rad Laboratories) using Trans-Blot® Turbo™ gel transfer stacks (Bio-Rad Laboratories) and the Trans-Blot® Turbo™ Transfer Device (Bio-Rad Laboratories) as directed by the manufacturer. Efficient protein transfer was confirmed by staining membranes with a solution containing Coomassie Brilliant Blue R-250 Dye. The membranes were placed in an iBind Western Device (Thermo Fisher Scientific) and the primary and secondary antibody solutions and washes were added to the corresponding chambers. Dilutions of antibodies were made with the iBind Fluorescent Detection Solution Kit (Thermo Fisher Scientific) according to the manufacturer's protocol. The primary antibodies, namely goat anti-IL-1β (R&D Systems), rabbit anti-IL-1α (Cell Signaling Technology, Danvers, MA), rabbit anti-caspase-1 (p20) (Adipogen, San Diego, CA), mouse anti-IκBα (Cell Signaling Technology), rabbit anti-p-IKKα/β

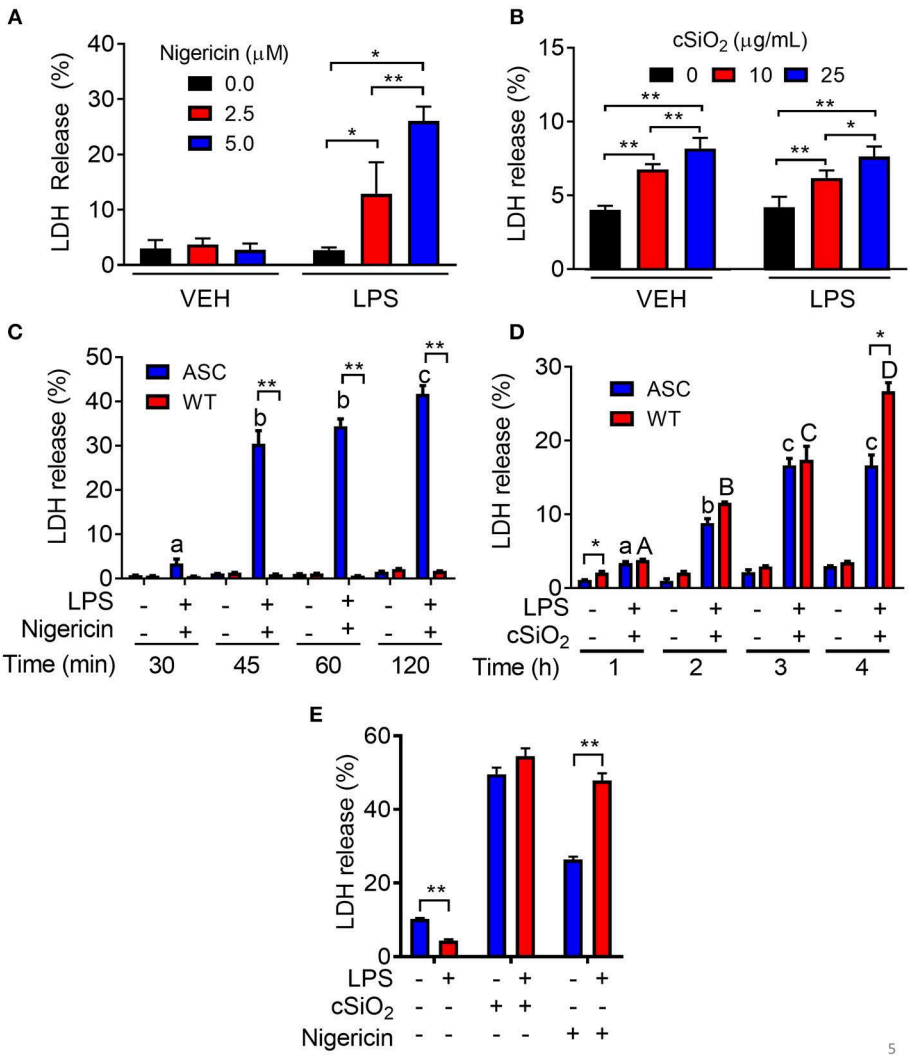

FIGURE 5 | Nigericin-induced cell death is LPS- and ASC-dependent while $cSiO_2$-induced cell death is LPS- and ASC-independent in RAW MΦs. **(A,C)** RAW-ASC cultures were pretreated with VEH or 20 ng/ml LPS for 2 h, incubated with 0, 2.5, or 5.0 μM nigericin for 45 min **(A)** or 0, 10, or 25 μg/ml $cSiO_2$ for 4 h **(C)**, and then LDH measured. **(B,D)** RAW-ASC and RAW-WT MΦs were pretreated with VEH or 20 ng/ml LPS for 2 h, incubated with VEH, 10 μM nigericin **(B)**, or 25 μM $cSiO_2$ **(D)** and then LDH release assessed at the indicated times. **(E)** Bone marrow-derived macrophages were pretreated with VEH or LPS (20 ng/ml) for 2 h, incubated with VEH or 5 μM nigericin or 25 μg/ml $cSiO_2$ and then LDH release assessed at 45 min or 4 h, respectively. Data presented as mean ± SEM, $n = 3$. ND = not detectable. Asterisks indicate significant differences between cell type **(B,D)** or treatment group **(A,C,E)** (*$p < 0.05$, **$p < 0.01$). Different letters indicate significant differences between treatment groups within each cell type **(B,D)** ($p < 0.05$). Representative of three independent experiments.

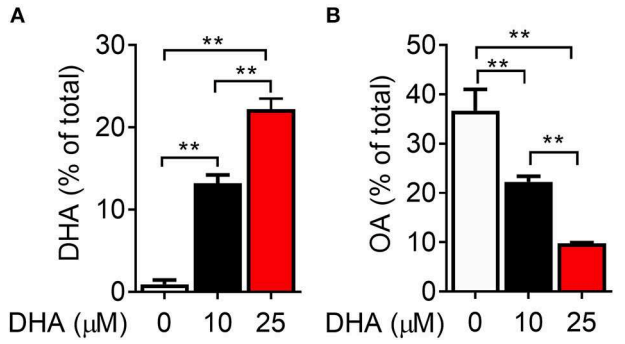

FIGURE 6 | DHA is incorporated into RAW-ASC MΦ phospholipids at the expense of oleic acid (OA). RAW-ASC cells were incubated in serum-deprived media containing DHA-BSA complexes or BSA vehicle for 24 h. Cell phospholipids were extracted and analyzed for fatty acid content by GLC. In non-supplemented conditions, the major unsaturated fatty acid in the cell membrane is oleic acid (OA), which is the primary fatty acid component of fetal bovine serum. Incubation with DHA increased membrane content of DHA **(A)** while decreasing the membrane content of OA **(B)**. See **Table 1** for complete fatty acid profile. Data presented as mean ± SEM, $n = 3$. Asterisks indicate significant difference ($^{**}p < 0.01$). Representative of two independent experiments.

(Cell Signaling Technology), and rabbit anti-NF-κB p65 (Cell Signaling Technology), were diluted at 1:1000 for cell lysates or 1:500 for supernatant and placed into the primary antibody chamber. Rabbit anti-GAPDH (Cell Signaling Technology) and rabbit anti-beta-actin (Cell Signaling Technology) were diluted 1:1000 and 1:2000, respectively, and used for normalization of proteins detected in the lysate or cytoplasmic fraction. Mouse anti-PCNA (Cell Signaling Technology) was diluted 1:1000 and used for normalization of proteins detected in the nuclear fraction. Similarly, the secondary antibodies (donkey anti-goat IRDye 800CW, goat anti-mouse 800CW, goat anti-rabbit 680RD) from LI-COR Biosciences System (LI-COR Biosciences, Lincoln, NE, USA) were diluted at 1:3000 and placed into their corresponding chamber. The membranes were left in the iBind system for >2.5 h at room temperature before scanning with the LI-COR Odyssey Infrared Imaging System (LI-COR Biosciences).

Data shown are mean percent of total FA ± SEM ($n = 8$ per group) as determined by GLC. FA levels significantly different from control (0 μM DHA) represented by asterisks ($^{*}p < 0.05$, $^{**}p < 0.01$).

Fatty Acid Analysis

Cells were seeded at a density of 1.5×10^6 cells per 100 mm dish. After 24 h in complete RPMI, wells were washed once with DPBS and media switched to serum-deprived RPMI supplemented with 25 μM DHA as described above. After 24 h, cells were washed once with DPBS, collected in ice-cold DPBS, and pelleted at 1,000 x g for 3 min. Cell pellets were resuspended in 1.4 mL ice-cold DPBS as previously described (37). Each sample was divided in half and stored in 1.6 mL screw-cap tubes in order to perform the phospholipid isolation in technical duplicates. Samples were then snap frozen and stored at −80°C until further analysis. Total lipids were extracted according to the method by Bligh and Dyer (38) and phospholipids were isolated by solid phase extraction as described previously (39). Isolated phospholipids were stored at −80°C in a 3:1 solution of hexane/isopropanol until methylation. The exogenous heptadecanoic acid, C17:0 (NuChek Prep, Elysian, MN), was added to isolated phospholipids as an internal standard. Samples were methylated using methanolic BF_3 (Millipore Sigma) as previously described (40). FAMEs were analyzed by gas chromatography using a Shimadzu GC equipped with a flame ionization detector. Samples were separated on a J&W DB-23 30 m capillary column (Agilent, Santa Clara, CA) with an inner diameter of 0.25 μm and a flow rate of 0.82 mL/min, with helium as the carrier gas. The injection temperature and detector temperature were 250°C and the column temperature ranged from 120 to 240°C. A 16-standard FAME mix (NuChek Prep) was used to identify peaks of interest.

TABLE 1 | DHA supplementation modulates phospholipid profile of RAW-ASC cells.

Fatty acid	Common name	DHA (μM)		
		0	10	25
C14:0	Myristic acid	2.94 ± 0.29	3.27 ± 0.28	4.90 ± 0.84**
C16:0	Palmitic acid	31.15 ± 3.10	31.34 ± 0.79	38.59 ± 1.25**
C16:1 ω-9	Palmitoleic acid	4.67 ± 1.04	3.13 ± 0.25	2.29 ± 0.50**
C18:0	Stearic acid	15.60 ± 9.05	22.03 ± 0.47	18.01 ± 1.21
C18:1 ω-9	Oleic acid	36.68 ± 4.32	22.23 ± 1.25**	9.77 ± 0.34**
C18:2 ω-6	Linoleic acid	0.63 ± 0.88	1.26 ± 0.11	0.78 ± 0.71
C20:2 ω-6	Eicosadienoic acid	4.16 ± 0.92	1.13 ± 0.68**	0.00 ± 0.00**
C20:4 ω-6	Arachidonic acid	3.27 ± 0.67	2.30 ± 0.47	1.80 ± 1.15
C20:5 ω-3	Eicosapentaenoic acid	0.00 ± 0.00	0.00 ± 0.00	1.13 ± 0.71
C22:4 ω-6	Adrenic acid	0.00 ± 0.00	0.15 ± 0.33	0.35 ± 0.79
C22:5 ω-3	ω3 docosapentaenoic acid	0.00 ± 0.00	0.17 ± 0.38	0.18 ± 0.40
C22:5 ω-6	ω6 docosapentaenoic acid	0.00 ± 0.00	0.14 ± 0.31	0.00 ± 0.00
C22:6 ω-3	Docosahexaenoic acid	0.91 ± 0.53	12.85 ± 0.49**	22.20 ± 1.42**
Total SFA		49.70 ± 5.81	55.44 ± 2.42*	60.63 ± 1.06**
Total MUFA		41.35 ± 5.29	25.05 ± 0.87**	11.88 ± 0.56**
Total ω-6		8.05 ± 1.02	5.77 ± 0.90*	3.71 ± 1.04**
Total ω-6		0.91 ± 0.53	13.73 ± 1.47**	23.77 ± 1.07**

*Data shown are mean percent of total FA ± SEM (n = 6 per group) as determined by GLC. FA levels significantly different from control (0 μM DHA) represented by asterisks (*p < 0.05, **p < 0.01).*

Statistical Analyses

Student's *t*-tests were used to compare two groups when applicable. If groups were determined non-parametric or determined to have unequal variance by the Shapiro-Wilk test for normality or the *F*-test for equal variance, respectively, they were analyzed using the Mann-Whitney U test. Comparison of multiple groups was accomplished by one-way ANOVA, and comparison of individual groups was accomplished using Tukey's

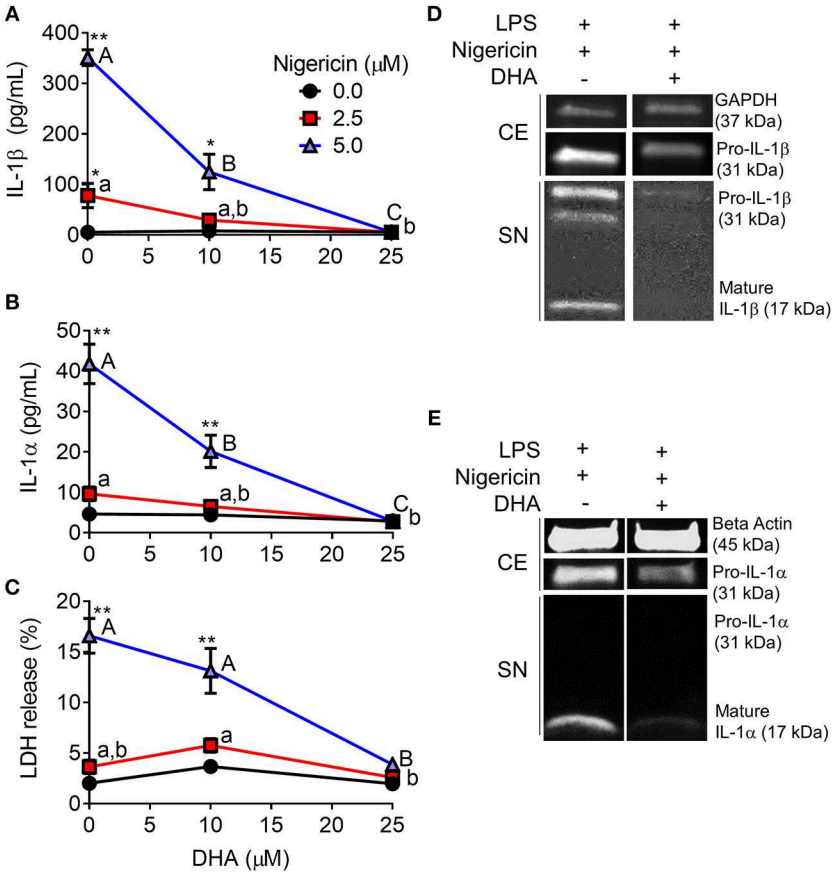

FIGURE 7 | DHA supplementation suppresses nigericin-induced IL-1β and IL-1α release and cell death in RAW-ASC MΦs. RAW-ASC cells were incubated in serum-deprived RPMI containing DHA (0, 10, or 25 μM) or VEH (BSA) for 24 h. Cells were pretreated with 20 ng/ml LPS for 2 h, incubated with 0, 2.5, or 5.0 μM nigericin for 45 min, and then release of **(A)** IL-1β, **(B)** IL-1α, and **(C)** LDH measured. The presence of mature **(D)** IL-1β and **(E)** IL-1α in the supernatant were determined by Western blotting. For Western blots of IL-1α, LPS priming was extended to 5 h and supernatant concentrated 10x by methanol-chloroform precipitation. Data presented as mean ± SEM, $n = 3$. Significant differences between DHA-supplemented groups represented as different letters (uppercase for 5 μM group, lowercase for 2.5 μM group). Significant differences from vehicle control at each DHA concentration represented by asterisks (*$p < 0.05$, **$p < 0.01$). ELISAs and LDH assay are representative of three independent experiments. Western blots are representative of two independent experiments.

test. If groups were determined non-parametric or determined to have unequal variance by the Shapiro-Wilk test for normality or the F-test equal variance, respectively, they were analyzed by the Kruskal-Wallis test. In this case, *post hoc* comparison of individual groups was accomplished using Dunn's test.

RESULTS

Nigericin- and $cSiO_2$- Induced IL-1β Release Is LPS- and ASC-Dependent

To confirm the efficacy of ASC transfection in conferring a functional inflammasome, the effects of the K^+ ionophore nigericin, a prototypical activator of the NLRP3 inflammasome, were compared in RAW-ASC and RAW-WT cells. Nigericin elicited marked IL-1β secretion in LPS-primed RAW-ASC cells, whereas unprimed RAW-ASC cells were unresponsive (**Figure 2A**). Robust IL-1β release was evident in LPS-primed RAW-ASC cells as early as 30 min after nigericin treatment (**Figure 2B**). IL-1β release from LPS-primed RAW-WT cells was negligible at all time points, verifying that they lacked inflammasome activity. As found with nigericin, $cSiO_2$ induced abundant IL-1β release in LPS-primed RAW-ASC cells within 1 h but not in RAW-WT or in unprimed RAW-ASC cells (**Figures 2C,D**). In response to both nigericin and $cSiO_2$, release of IL-1β by RAW-ASC cells included both the inactive precursor and the bioactive mature form (**Figure 2E**). Collectively, IL-1β release in response to either activating stimulus was dependent on the presence of a priming signal and a functional inflammasome. Under identical experimental conditions, primary BMDM likewise released IL-1β in an LPS-dependent manner in response to nigericin and $cSiO_2$ (**Figure 2F**) suggesting the RAW-ASC model was a relevant surrogate to investigate inflammasome activation in the macrophage.

$cSiO_2$-Induced Caspase-1 Activation Is LPS- and ASC-Dependent

During NLRP3 inflammasome activation, caspase-1 is post-translationally modified by cleavage to its mature, active form.

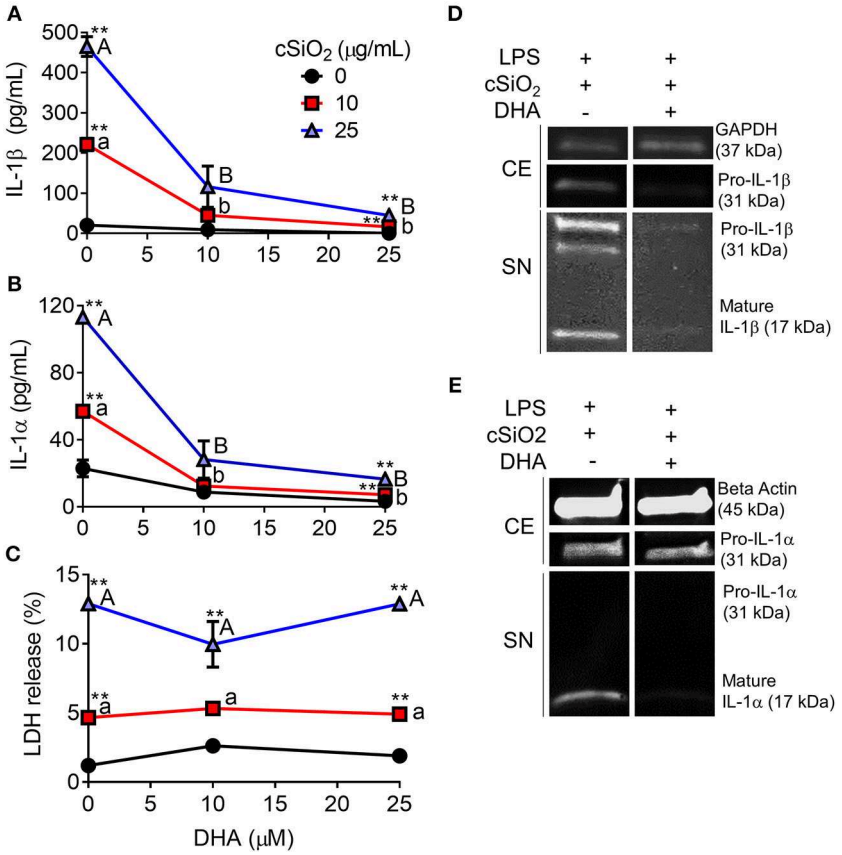

FIGURE 8 | DHA inhibits $cSiO_2$-induced IL-1β and IL-1α release but not cell death in RAW-ASC MΦs. RAW-ASC cells were incubated in serum-deprived RPMI containing DHA (0, 10, or 25 μM) or VEH (BSA) for 24 h. Cells were pretreated with 20 ng/ml LPS for 2 h, incubated with 0, 10, or 25 μg/ml $cSiO_2$ for 4 h, and then release of **(A)** IL-1α, **(B)** IL-1β, and **(C)** LDH measured. The presence of mature **(D)** IL-1β and **(E)** IL-1α in the supernatant were determined by Western blotting. For Western blots of IL-1α, LPS priming was extended to 5 h and supernatant concentrated 10x by methanol-chloroform precipitation. Data presented as mean ± SEM, $n = 3$. Significant differences between DHA-supplemented groups represented as different letters (uppercase for 5 μM group, lowercase for 2.5 μM group). Significant differences from vehicle control at each DHA concentration represented by asterisks (**$p < 0.01$). ELISAs and LDH assay are representative of three independent experiments. Western blots are representative of two independent experiments.

FAM-YVAD-FMK, a fluorescent dye that binds intracellularly to cleaved, active caspase-1, was used to compare $cSiO_2$-induced caspase-1 activation in RAW-ASC and RAW-WT cells. Caspase-1 was activated by $cSiO_2$ only in LPS-primed RAW-ASC cells, confirming inflammasome-dependent activation (**Figure 3A**). These results were confirmed by Western blot analysis of cleaved caspase-1 in the media supernatant in RAW-ASC cells treated with both LPS and $cSiO_2$ (**Figure 3B**). Consistent with these results, we observed the formation of ASC specks following LPS priming and $cSiO_2$ or nigericin treatment (**Figure S1A**).

Nigericin- and $cSiO_2$- Induced IL-1α Release Differ With Regard to LPS- and ASC-Dependence

Nigericin evoked a robust IL-1α response in LPS-primed RAW-ASC cells, but not unprimed cells (**Figure 4A**). The IL-1α response was detectable in supernatants of LPS-primed RAW-ASC cells within 30 min of nigericin addition but was not evident in LPS-primed RAW-WT supernatants up to 120 min following nigericin treatment (**Figure 4B**).

$cSiO_2$-induced IL-1α release in RAW-ASC cells also required LPS pretreatment (**Figure 4C**). In contrast to nigericin findings, IL-1α concentrations in culture supernatants of $cSiO_2$-treated RAW-WT cells were 30–50 percent of that observed in $cSiO_2$-treated RAW-ASC cells (**Figure 4D**). These results suggest that $cSiO_2$-induced release of some IL-1α occurs via mechanisms that do not involve NLRP3 inflammasome activation. IL-1α detected in the media of RAW-ASC cells was primarily the 17 kDa mature form (**Figure 4E**). Finally, as found in RAW-ASC cells, primary BMDM released IL-1α in response to nigericin and $cSiO_2$ in an LPS-dependent manner (**Figure 4F**).

Nigericin- but Not $cSiO_2$-Induced Cell Death Is Inflammasome-Dependent

Nigericin treatment induced LDH release in LPS-primed RAW-ASC cells but not in unprimed ones (**Figure 5A**). Concordant

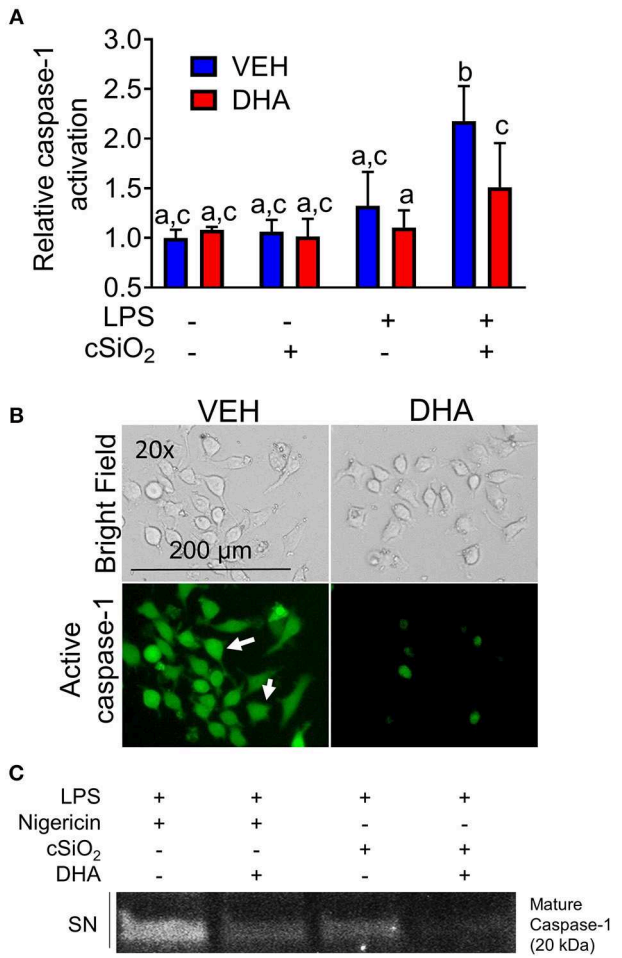

FIGURE 9 | DHA supplementation suppresses $cSiO_2$-induced caspase-1 activation in RAW-ASC MΦs. **(A)** RAW-ASC cells were incubated in serum-deprived RPMI containing DHA (25 μM) or VEH (BSA) for 24 h. Cultures were then primed with 20 ng/ml LPS for 2 h and incubated with or without 25 μg/ml $cSiO_2$ for 4 h. Caspase-1 activation was assessed using fluorescent probe FAM-YVAD-FMK. A fluorescent microplate assay indicated that DHA suppressed $cSiO_2$-induced caspase-1 activation. Fluorescence data pooled from two independent experiments and presented as mean ± SEM, $n = 6$. Significant differences between groups represented as different letters ($p < 0.05$). **(B)** Representative photomicrographs indicating that cells treated with LPS and $cSiO_2$ showed robust activation of caspase 1 as indicated by green fluorescence (white arrows) and this was attenuated by supplementation with DHA. Cells were imaged using an EVOS FL Auto Cell Imaging System. Images are representative of three independent experiments. **(C)** Western blot analysis confirmed that DHA suppressed both the cleavage and release of active caspase-1 (p20) into the supernatant. Western blot data are representative of two independent experiments.

with these findings, nigericin elicited LDH release in RAW-ASC but not RAW-WT cells following LPS priming (**Figure 5B**) suggesting that death was inflammasome-dependent and thus consistent with pyroptosis. Unlike nigericin, $cSiO_2$ induced LDH release in both LPS-primed and unprimed RAW-ASC cells (**Figure 5C**) and was largely equivalent in RAW-ASC and RAW-WT cells (**Figure 5D**), strongly indicating that $cSiO_2$-induced cell death is not strictly inflammasome dependent and pyroptotic. Consistent with our findings in RAW-ASC cells, nigericin-induced cell death in BMDM was LPS-dependent whereas $cSiO_2$-induced cell death was LPS-independent (**Figure 5E**).

DHA Is Efficiently Incorporated Into RAW-ASC Cell Phospholipids

Following 24 h pre-incubation with DHA, delivered as a complex with BSA, the fatty acid was dose-dependently incorporated into the phospholipid fraction of RAW-ASC cells (**Figure 6A**). This occurred largely at the expense of oleic acid (OA) (**Figure 6B**), the major unsaturated fatty acid in the fetal bovine serum present in the culture medium (41). Along with DHA incorporation, there were significant decreases in ω-9 palmitoleic acid and ω-6 eicosadienoic acid and a significant increase in ω-3 eicosapentaenoic acid, which can be formed by enzymatic retroconversion of DHA (**Table 1**).

DHA Inhibits Nigericin-Induced IL-1 Cytokine Release and Cell Death

When RAW-ASC cells were pretreated with DHA and then primed with LPS, nigericin-induced release of IL-1β (**Figure 7A**) and IL-1α (**Figure 7B**) were suppressed by the ω-3 fatty acid in a concentration-dependent manner. DHA's effects corresponded to decreased intracellular pro-IL-1β and pro-IL-1α, as well as diminished extracellular mature IL-1β and IL-1α (**Figures 7D,E**). Finally, DHA pretreatment blocked nigericin-induced LDH release (**Figure 7C**), suggesting that DHA inhibits pyroptotic cell death.

DHA Suppresses $cSiO_2$-Induced IL-1 Cytokine Release and Caspase-1 Activation but Not Cell Death

DHA concentration-dependently suppressed $cSiO_2$-induced release of both IL-1β (**Figure 8A**) and IL-1α (**Figure 8B**). Likewise, DHA inhibited $cSiO_2$-induced caspase-1 activation (**Figure 9**) and ASC speck formation (**Figure S1B**). DHA's inhibitory effects corresponded to reduced levels of intracellular pro-IL-1β and pro-IL-1α and extracellular mature IL-1β and IL-1α (**Figures 8D,E**). However, DHA did not affect cell death induced by $cSiO_2$ (**Figure 8C**), further suggesting that $cSiO_2$-induced cell death did not involve inflammasome activation and pyroptosis.

DHA Suppresses IL-1 Cytokine Release Triggered by Alum and MSU Crystals

Following priming with LPS, both alum (**Figures 10A,B**) and MSU (**Figures 10D,E**) induced robust release of both IL-1α and IL-1β. In both instances, release of IL-1 cytokines was ablated by supplementation with DHA. Unlike $cSiO_2$-induced LDH release, responses to alum and MSU were extremely modest, slightly potentiated by LPS priming, and negligibly affected by DHA (**Figures 10C,F**).

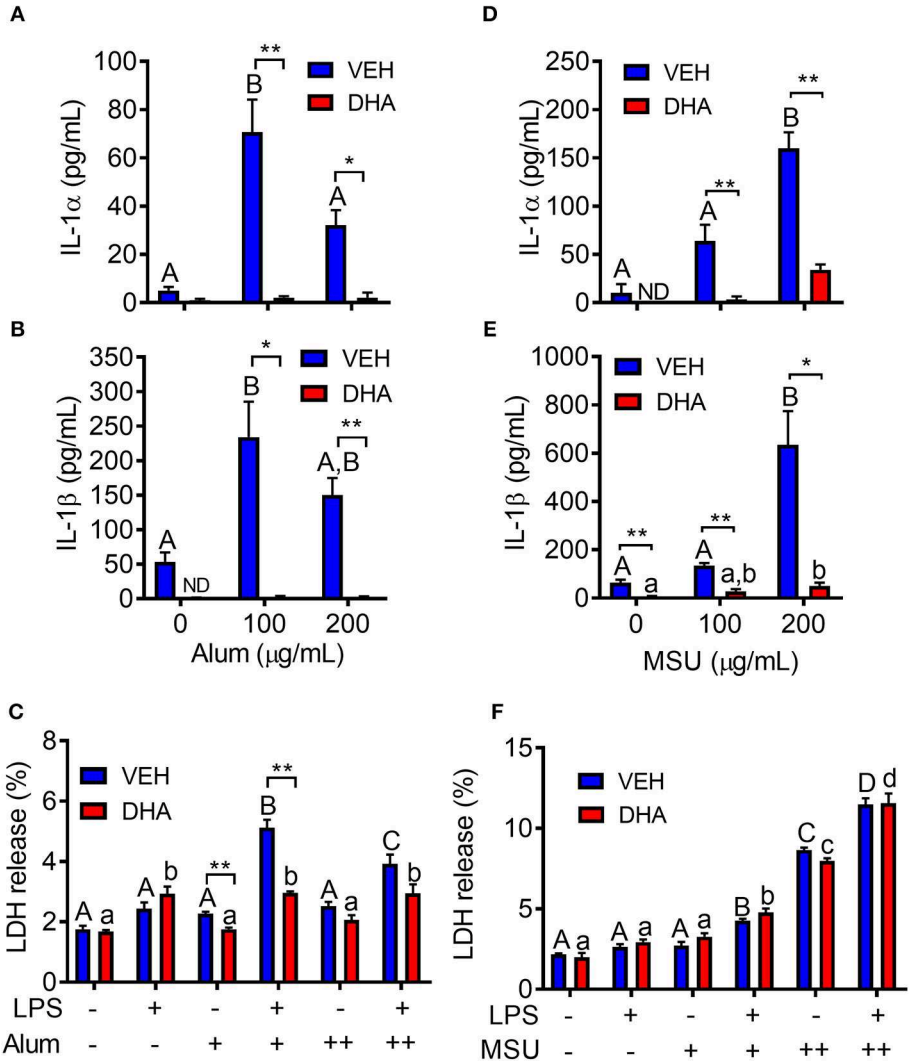

FIGURE 10 | Alum- and MSU crystal-induced IL-1 cytokine release is suppressed by DHA. RAW-ASC cells were incubated in serum-deprived RPMI containing DHA (25 μM) complexed with BSA or VEH (BSA only) for 24 h. Cells were pretreated with 20 ng/ml LPS for 2 h, incubated with 0 (-), 100 (+), or 200 (++) μg/ml alum **(A-C)** or MSU **(D–F)** for 8 h, and then release of IL-1α, **(A,D)**, IL-1β **(B,E)**, and LDH **(C,F)** measured. Data presented as mean ± SEM, $n = 3$. Asterisks indicate significant differences between DHA and BSA treated cells (*$p < 0.05$, **$p < 0.01$). Different letters indicate significant differences between treatment groups within each VEH treated cells (uppercase letters) or DHA treated cells (lowercase letters) ($p < 0.05$). Data representative of three independent experiments.

DHA Interferes With LPS Priming by Activating PPARγ

DHA pretreatment significantly suppressed LPS-induced expression of *Nlrp3* and *Il1b* (**Figure 11**). A similar trend ($p = 0.100$) of DHA inhibition was observed for LPS-induced *Il1a* mRNA expression. DHA potentially inhibits IL-1 cytokine and NLRP3 transcription by activating PPARγ, a well-known transrepressor of NF-κB (42). To test this possibility, PPARγ binding activity was measured in nuclear extracts of RAW-ASC cells treated with DHA or with the PPARγ agonist rosiglitazone as a positive control. Significantly more active PPARγ was detectable in nuclear extracts from the rosiglitazone- and DHA-treated cells than those from vehicle-treated cells (**Figure 12A**). Consistent with these findings, both rosiglitazone- and DHA-mediated suppression of IL-1 cytokine gene expression was suppressed in cells treated with the PPARγ antagonist SR16832 (**Figure 12B**). Although LPS treatment induced phosphorylation of IKKα/β, degradation of IκBα, NF-κB phosphorylation, and nuclear translocation of NF-κB (**Figure S2**), none of these effects were influenced by DHA.

DISCUSSION

Dysregulation of inflammasomes has been implicated as a contributing factor in lupus and other autoimmune diseases (43). Airway exposure to $cSiO_2$ triggers prolific inflammation in the lung and onset of localized and systemic autoimmunity in lupus-prone mice (2), but inclusion of DHA in the diet abrogates these

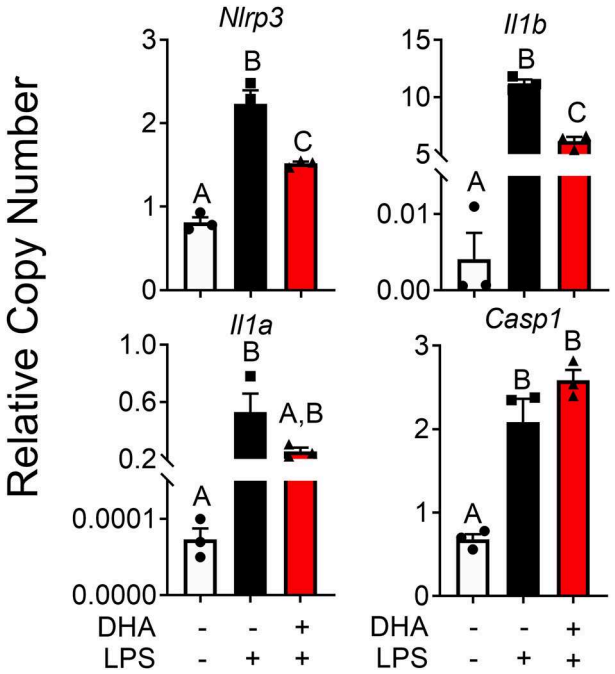

FIGURE 11 | DHA supplementation downregulates LPS-induced inflammasome gene expression and intracellular IL-1 cytokines in RAW-ASC cells. RAW-ASC cells were incubated in serum-deprived RPMI containing DHA (25 μM) or VEH (BSA) for 24 h. Cultures were then incubated with 20 ng/ml LPS for 6 h. Assessment of mRNA levels by qRT-PCR showed that LPS priming induced *Nlrp3*, *Casp1, Il1b*, and *Il1a* mRNA expression and upregulation of *Nlrp3, Il1b*, and *Il1a* was suppressed by DHA. Gene expression represented as copy number relative to *Gapdh.* Data presented as mean ± SEM, $n = 3$. Letters indicate significant differences between groups ($p<0.05$). Data are representative of two independent experiments.

effects (3, 4, 44). The early mechanisms for DHA's ameliorative actions are as yet unclear. To address this knowledge gap, we tested the hypothesis that DHA suppresses $cSiO_2$-induced NLRP3 inflammasome activation, IL-1 cytokine release, and cell death in the macrophage. Like BMDM, RAW-ASC cells were found to be capable of robust NLRP3 inflammasome activation, and therefore suitable surrogates to investigate DHA's effects on macrophage responses to $cSiO_2$. We report for the first time that DHA at physiologically relevant concentrations interferes with $cSiO_2$-induced inflammasome activation and release of mature IL-1α and IL-1β but not with cell death. As depicted in **Figure 13**, DHA likely acts at the level of priming (i.e., Signal 1), as evidenced by its suppression of LPS-induced *Nlrp3, Il1b,* and *Il1a* gene expression that influenced later responses to $cSiO_2$ or nigericin (Signal 2). Importantly, suppression by DHA was linked to increased PPARγ activity.

An early and critical response to airborne $cSiO_2$ exposure is robust release of IL-1 cytokines by AMΦs (16) Thus, it is noteworthy that DHA suppressed release of both mature IL-1α and IL-1β following treatment with $cSiO_2$ and other inflammasome activators (MSU, alum, and the canonical inflammasome inducer nigericin). Although IL-1α and IL-1β share many characteristics, there are distinctions in the mechanisms by which they are expressed, processed, and released. Pro-IL-1α is constitutively expressed in many cell types, including immune cells where it can be further upregulated by physiological stimuli, including oxidative stress, hormonal stimulation, and exposure to cytokines (including IL-1β and IL-1α itself) (15). Pro-IL-1β is primarily expressed by immune cells and is rapidly induced by inflammatory stimuli. Both exist as 31 kDa precursors that can be cleaved to 17–18 kDa mature forms (45). IL-1α is bioactive in both the precursor and mature forms, however, it has been reported that IL-1α activity is enhanced upon cleavage by calpains, which may be activated by $cSiO_2$-induced Ca^{2+} influx (46). IL-1β is only active in its mature form and can be cleaved by caspase-1 during inflammasome activation. IL-1β may also be cleaved in a caspase-independent manner by proteinases produced by other immune cell types (47). Additionally, both pro-IL-1α and pro-IL-1β released from dying cells can be processed by extracellular proteases (45).

Unlike most cytokines, IL-1 cytokines lack secretory sequences targeting them to the endoplasmic reticulum and Golgi apparatus for processing and release from the cell. Rather, mature IL-1β has been shown to be released through pores formed by gasdermin D (GSDMD) (48–50). Though it has not been confirmed experimentally, it is conceivable that mature IL-1α may also be released in this manner. During inflammasome activation, GSDMD is cleaved by caspase-1, whereupon the N-terminal fragment localizes to the cell membrane and oligomerizes to form pores (9). A further feature of GSDMD pores is their capacity to collapse the plasma membrane, causing lytic pyroptotic cell death and releasing additional alarmins and cytokines that act as priming signals for the NLRP3 inflammasome (9, 16, 47).

Since $cSiO_2$ clearance from the lung is very slow (51), the persistent presence of this particle elicits repeated cycles in AMΦs involving phagocytosis of free $cSiO_2$ → phagolysosome permeabilization → death → release of cell autoantigens and reemergence of free $cSiO_2$. Like $cSiO_2$, other exogenous and endogenous crystals (e.g., alum and MSU, respectively) also evoke phagolysosome permeabilization (8, 52, 53). These crystals elicit pyroptosis (54) as well as inflammasome-independent cell death via apoptotic and necrotic pathways (55, 56). Our data here suggest that crystal-induced death in RAW-ASC cells was, to a large extent, inflammasome-independent. The release of IL-1α during other types of death associated with inhalation of crystalline substances (9, 56–58) is consistent with our observation of this cytokine in cell supernatant following $cSiO_2$ treatment of LPS-treated RAW-WT cells.

Numerous preclinical and clinical studies show consuming long chain ω-3 PUFAs such as DHA and eicosapentaenoic acid (C20:5 ω-3; EPA) can reduce chronic inflammatory and autoimmune conditions (44, 59). Western diets tend to exclude these pro-resolving ω-3s and more typically contain high concentrations of proinflammatory ω-6 PUFAs like linoleic acid (C18:2 ω-6; LA) and arachidonic acid (C20:4 ω-6; ARA) found in plant- and animal-derived lipids. Americans consume many times more ω-6s than ω-3s, so tissue phospholipid fatty acids skew heavily toward ω-3 deficiency (60). Several marine algae proficiently catalyze formation of DHA and EPA. Oily

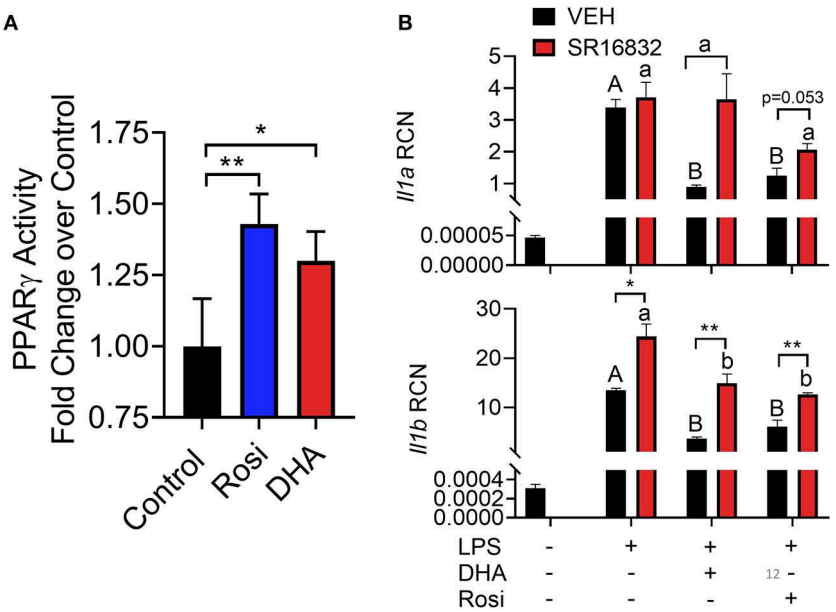

FIGURE 12 | (A) A TransAM™ PPARγ transcription factor assay was used to assess PPARγ activity in nuclear extracts of DHA (10 μM) and PPARγ agonist rosiglitazone (10 μM) treated RAW-ASC cells. Data presented as mean ± SEM, $n = 2$. Asterisks indicate significant relative to the control (*$p < 0.05$, **$p < 0.01$). **(B)** RAW-ASC cells were incubated in serum-deprived RPMI containing DHA (10 μM), rosiglitazone (10 μM), PPARγ antagonist SR16832 (100 nM), or VEH (BSA) for 24 h. Cultures were then incubated with 20 ng/ml LPS for 3.5 h. Assessment of mRNA levels by qRT-PCR showed that the PPARγ antagonist SR16832 blocked DHA and rosiglitazone-dependent suppression of LPS-induced gene expression. Gene expression represented as copy number relative to *Gapdh*. Asterisks indicate significant differences between DHA and BSA treated cells (*$p < 0.05$, **$p < 0.01$). Data presented as mean ± SEM, $n = 3$. Different letters indicate significant differences between treatment groups within VEH treated cells (uppercase letters) or SR16832 treated cells (lowercase letters) ($p < 0.05$). Representative of two independent experiments.

fish (e.g., salmon, mackerel) and small crustaceans (e.g., krill) bioconcentrate ω-3s into their membrane phospholipids by consuming the marine microalgae (61). Individuals can increase DHA and EPA tissue incorporation and correct ω-3 deficiency by consuming fish or dietary supplements with fish oil, krill oil, or microalgal oil.

Following dietary supplementation, DHA concentrations in the lung and other tissues in the lupus-prone NZBWF1 mouse correlate with decreased $cSiO_2$-triggered autoimmune pathogenesis (3, 4). Significantly, levels of *in vitro* DHA incorporation observed in the present study are similar to those found *in vivo* for mice fed diets supplemented with DHA, suggesting that *in vitro* concentrations of DHA (10 and 25 μM) used here are physiologically relevant. Our findings are consistent with prior reports that DHA suppresses NLRP3 inflammasome activation in other primary and transformed MΦ cell lines stimulated by nigericin (18, 62). The demonstration here that DHA suppresses expression of three NF-κB dependent genes is concordant with reports that activity of this transcription factor might be inhibited by ω-3 PUFAs, both *in vitro* and *in vivo* (59). Notably, our laboratory has previously shown that intranasally instilling mice with $cSiO_2$ upregulates many NF-κB targets, including but not limited to MCP-1, TNFα, BAFF, and IL-6. The expression of these genes is significantly reduced in animals supplemented with dietary DHA, suggesting involvement of this pathway *in vivo* (3, 4, 63).

Our finding here that DHA activates PPARγ is consistent with other studies in RAW 264.7 cells (64, 65) and in other macrophage cell lines (42). PPARγ's capacity to interfere with NF-κB-dependent gene expression (66) might partially explain DHA interference with IL-1 and NLRP3 gene expression. The exact mechanism of PPARγ-dependent inhibition of NF-κB appears to depend on the gene being upregulated. We found here that DHA did not impede nuclear translocation of NF-κB. A similar scenario has been observed for *iNos* expression in RAW 264.7 cells. In that case, PPARγ-dependent suppression of *iNos* does not impact NF-κB binding but rather represses LPS-induced *iNos* expression by preventing the recruitment of the proteasome machinery required to clear co-repressors from the *iNos* promoter (67). In a separate study in RAW 264.7 cells, activated PPARγ interacts directly with NF-κB to prevent it from binding to the *Il12* promoter (68). Other studies in human colonic cells and mouse embryonic fibroblast studies reveal that PPARγ has E3 ligase activity, and can induce degradation of NF-κB (69). Still others show that PPARγ promotes nuclear export of NF-κB in Caco-2 cells (70).

We cannot exclude the possibility of other mechanisms besides PPARγ that might contribute to our findings (71, 72). For example, ω-3 PUFAs have been shown to affect the physical properties of the cell membrane. Both TLR4 and IL-1R1 activation require the oligomerization of multiple receptors, a process that requires structural alteration of the plasma membrane (73, 74). Increased phospholipid ω-3 PUFA content reduces the formation of lipid rafts, thus suppressing inflammatory signaling pathways that depend on clustering of transmembrane receptors (73–75). Alternatively,

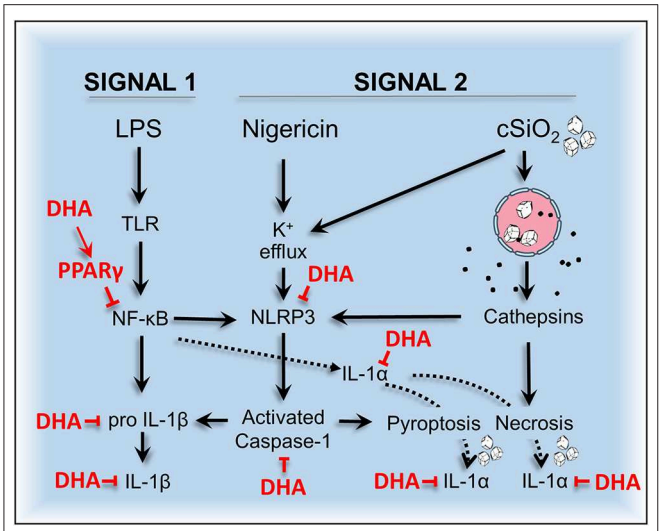

FIGURE 13 | Putative model for the protective effects of DHA against nigericin- and $cSiO_2$-induced inflammasome activation, IL-1 cytokine release, and death in MΦs. DHA inhibits nigericin- and $cSiO_2$-induced inflammasome activation as measured by IL-1β maturation and release and caspase-1 activation. DHA also suppresses nigericin- and $cSiO_2$-induced IL-1α cleavage and release and cell death. Cell death is wholly suppressed by DHA in nigericin-treated MΦs but only partially suppressed in $cSiO_2$-treated MΦs. Collectively, these inhibitory effects are linked to suppression of genes (*Nlrp3*, *Il1b*, and *Il1a*) regulated by the transcription factor NF-κB.

free DHA can be cleaved from the membrane and act as a ligand for anti-inflammatory receptors. *In vitro* studies reveal that DHA activates G-protein coupled receptors (GPCRs) FFAR1/GPR40 and FFAR4/GPR120 (18, 76). Previous studies indicate that activation of FFAR1/GPR40 and FFAR4/GPR120 by extracellular free DHA prevents TAB1 from binding TAK1, which is a necessary step in LPS-induced NF-κB activation (77). Finally, DHA-derived metabolites, many of which are termed specialized pro-resolving mediators (SPMs), are associated with the resolution of inflammation. Many reports of the bioactivity of SPMs support their potential to attenuate inflammasome activation (22, 78–82), potentially by binding to GPCRs involved in inhibiting NF-κB signaling (22, 81, 83–85). In general, these mechanisms culminate in inhibition of NF-κB, which we did not observe in our model. Accordingly, while outside the scope of this study, further clarification is needed to delineate the relative contributions of PPARγ-dependent and –independent mechanisms that might contribute to DHA-mediated suppression of IL-1 cytokine and NLRP3 gene expression.

Taken together, we have demonstrated that increasing the DHA content of membrane phospholipids suppresses $cSiO_2$-induced inflammasome activation and release of IL-1 cytokines and that these effects are potentially linked to PPARγ activation and interference with NF-κB-driven gene expression (**Figure 13**). Understanding how DHA and other ω-3 PUFAs influence crystal-mediated pathogenesis could potentially lead to harnessing dietary modulation of the lipidome as an intervention against chronic inflammatory and autoimmune diseases involving the inflammasome.

DATA AVAILABILITY

The raw data supporting the conclusions of this manuscript will be made available by the authors, without undue reservation, to any qualified researcher.

AUTHOR CONTRIBUTIONS

KW and JW: study design, data analyses/interpretation, and manuscript preparation. KG: data analysis/interpretation. LR: data analysis/interpretation and manuscript preparation. MB: optimization of RAW-ASC model and data analysis/interpretation. MG: data analysis/interpretation and generation of RAW-ASC model. AH: experimental design, data interpretation, manuscript writing, and project funding. JP: planning, coordination, oversight, manuscript preparation/submission, and project funding.

FUNDING

Research was funded by NIH ES027353 (JP and AH), NIH F31ES030593 (KW), NIH T32ES007255 (KW), Lupus Foundation of America (MB, JP, and KW), USDA National Institute of Food and Agriculture HATCH Project 1020129 (JP), and the Dr. Robert and Carol Deibel Family Endowment (JP).

ACKNOWLEDGMENTS

We would like to thank Dr. Hui-Ren Zhou, Augie Evered, and Elizabeth Ross for their excellent technical support and advice.

SUPPLEMENTARY MATERIAL

The Supplementary Material for this article can be found online at: https://www.frontiersin.org/articles/10.3389/fimmu.2019.02130/full#supplementary-material

Figure S1 | Visualization of ASC-CFP specks in RAW-ASC cells stimulated with LPS, nigericin and/or $cSiO_2$. Cells were incubated in serum-deprived media containing VEH (BSA) **(A)** or 25 μM DHA **(B)** for 24 h. Cells were then primed for 2 h with 500 ng/mL LPS and treated with 5 μM nigericin (45 min) or 25 μg/mL $cSiO_2$ (4 h). ASC specks (white arrows) were visualized using an EVOS FL Auto Cell Imaging System equipped with a CFP light cube. Photomicrographs representative of two independent experiments.

Figure S2 | Assessment of NF-κB activation. RAW-ASC cells were incubated in serum-deprived media containing the indicated concentration DHA or VEH (BSA) for 24 h. Cells were then treated with 20 ng/mL LPS and collected at the indicated times. Cell lysates were fractionated to obtain separate cytoplasmic and nuclear extracts. **(A)** NF-κB translocation was assessed by the presence of NF-κB in nuclear extracts. PCNA was used as a loading control. **(B)** Canonical NF-κB signaling was assessed by IκBα degradation in cytoplasmic extracts. Beta actin was used as a loading control. **(C)** Cells were treated with ng/mL LPS for 30 min. In the cytoplasm, phosphorylation of IKKα/β and degradation of IκBα were measured to assess activation of the NF-κB signaling pathway. In the nucleus, the NF-κB p65 subunit was measured to evaluate nuclear translocation. Actin and PCNA were used as cytoplasmic and nuclear loading controls, respectively.

Table S1 | List of products and reagents.

REFERENCES

1. Parks CG, Miller FW, Pollard KM, Selmi C, Germolec D, Joyce K, et al. Expert panel workshop consensus statement on the role of the environment in the development of autoimmune disease. *Int J Mol Sci*. (2014) 15:14269–97. doi: 10.3390/ijms150814269
2. Bates MA, Brandenberger C, Langohr I, Kumagai K, Harkema JR, Holian A, et al. Silica triggers inflammation and ectopic lymphoid neogenesis in the lungs in parallel with accelerated onset of systemic autoimmunity and glomerulonephritis in the lupus-prone NZBWF1 mouse. *PLoS ONE*. (2015) 10:e0125481. doi: 10.1371/journal.pone.0125481
3. Bates MA, Brandenberger C, Langohr, II, Kumagai K, Lock AL, Harkema JR, et al. Silica-triggered autoimmunity in lupus-prone mice blocked by docosahexaenoic acid consumption. *PLoS ONE*. (2016) 11:e0160622. doi: 10.1371/journal.pone.0160622
4. Bates MA, Akbari P, Gilley KN, Wagner JG, Li N, Kopec AK, et al. Dietary docosahexaenoic acid prevents silica-induced development of pulmonary ectopic germinal centers and glomerulonephritis in the lupus-prone NZBWF1 mouse. *Front Immunol*. (2018) 9:2002. doi: 10.3389/fimmu.2018.02002
5. Brown JM, Pfau JC, Pershouse MA, Holian A. Silica, apoptosis, and autoimmunity. *J Immunotoxicol*. (2005) 1:177–87. doi: 10.1080/15476910490911922
6. Hamilton RF, Thakur SA, Holian A. Silica binding and toxicity in alveolar macrophages. *Free Radic Biol Med*. (2008) 44:1246–58. doi: 10.1016/j.freeradbiomed.2007.12.027
7. Jessop F, Hamilton RF Jr, Rhoderick JF, Fletcher P, Holian A. Phagolysosome acidification is required for silica and engineered nanoparticle-induced lysosome membrane permeabilization and resultant NLRP3 inflammasome activity. *Toxicol Appl Pharmacol*. (2017) 318:58–68. doi: 10.1016/j.taap.2017.01.012
8. Hornung V, Bauernfeind F, Halle A, Samstad EO, Kono H, Rock KL, et al. Silica crystals and aluminum salts activate the NALP3 inflammasome through phagosomal destabilization. *Nat Immunol*. (2008) 9:847–56. doi: 10.1038/ni.1631
9. Frank D, Vince JE. Pyroptosis versus necroptosis: similarities, differences, and crosstalk. *Cell Death Diff*. (2018). 26:99–114. doi: 10.1038/s41418-018-0212-6
10. Cassel SL, Eisenbarth SC, Iyer SS, Sadler JJ, Colegio OR, Tephly LA, et al. The Nalp3 inflammasome is essential for the development of silicosis. *Proc Natl Acad Sci USA*. (2008) 105:9035–40. doi: 10.1073/pnas.0803933105
11. Reisetter AC, Stebounova LV, Baltrusaitis J, Powers L, Gupta A, Grassian VH, et al. Induction of inflammasome-dependent pyroptosis by carbon black nanoparticles. *J Biol Chem*. (2011) 286:21844–52. doi: 10.1074/jbc.M111.238519
12. Martinon F, Petrilli V, Mayor A, Tardivel A, Tschopp J. Gout-associated uric acid crystals activate the NALP3 inflammasome. *Nature*. (2006) 440:237–41. doi: 10.1038/nature04516
13. Duewell P, Kono H, Rayner KJ, Sirois CM, Vladimer G, Bauernfeind FG, et al. NLRP3 inflammasomes are required for atherogenesis and activated by cholesterol crystals. *Nature*. (2010) 464:1357–61. doi: 10.1038/nature08938
14. Bauernfeind FG, Horvath G, Stutz A, Alnemri ES, MacDonald K, Speert D, et al. Cutting edge: NF-kappaB activating pattern recognition and cytokine receptors license NLRP3 inflammasome activation by regulating NLRP3 expression. *J Immunol*. (2009) 183:787–91. doi: 10.4049/jimmunol.0901363
15. Di Paolo NC, Shayakhmetov DM. Interleukin 1alpha and the inflammatory process. *Nat Immunol*. (2016) 17:906–13. doi: 10.1038/ni.3503
16. Rabolli V, Badissi AA, Devosse R, Uwambayinema F, Yakoub Y, Palmai-Pallag M, et al. The alarmin IL-1alpha is a master cytokine in acute lung inflammation induced by silica micro- and nanoparticles. *Part Fibre Toxicol*. (2014) 11:69. doi: 10.1186/s12989-014-0069-x
17. Absher MP, Hemenway DR, Leslie KO, Trombley L, Vacek P. Intrathoracic distribution and transport of aerosolized silica in the rat. *Exp Lung Res*. (1992) 18:743–57. doi: 10.3109/01902149209031705
18. Yan Y, Jiang W, Spinetti T, Tardivel A, Castillo R, Bourquin C, et al. Omega-3 fatty acids prevent inflammation and metabolic disorder through inhibition of NLRP3 inflammasome activation. *Immunity*. (2013) 38:1154–63. doi: 10.1016/j.immuni.2013.05.015
19. Martinez-Micaelo N, Gonzalez-Abuin N, Pinent M, Ardevol A, Blay M. Dietary fatty acid composition is sensed by the NLRP3 inflammasome: omega-3 fatty acid (DHA) prevents NLRP3 activation in human macrophages. *Food Funct*. (2016) 7:3480–7. doi: 10.1039/C6FO00477F
20. Shen L, Yang Y, Ou T, Key CC, Tong SH, Sequeira RC, et al. Dietary PUFAs attenuate NLRP3 inflammasome activation via enhancing macrophage autophagy. *J Lipid Res*. (2017) 58:1808–21. doi: 10.1194/jlr.M075879
21. Duvall MG, Levy BD. DHA- and EPA-derived resolvins, protectins, and maresins in airway inflammation. *Eur J Pharmacol*. (2016) 785:144–55. doi: 10.1016/j.ejphar.2015.11.001
22. Lopategi A, Flores-Costa R, Rius B, Lopez-Vicario C, Alcaraz-Quiles J, Titos E, et al. Frontline science: specialized proresolving lipid mediators inhibit the priming and activation of the macrophage NLRP3 inflammasome. *J Leukoc Biol*. (2018). 105:22–36. doi: 10.1002/JLB.3HI0517-206RR
23. Raschke WC, Baird S, Ralph P, Nakoinz I. Functional macrophage cell lines transformed by Abelson leukemia virus. *Cell*. (1978) 15:261–7. doi: 10.1016/0092-8674(78)90101-0
24. Pelegrin P, Barroso-Gutierrez C, Surprenant A. P2X7 receptor differentially couples to distinct release pathways for IL-1beta in mouse macrophage. *J Immunol*. (2008) 180:7147–57. doi: 10.4049/jimmunol.180.11.7147
25. He WT, Wan H, Hu L, Chen P, Wang X, Huang Z, et al. Gasdermin D is an executor of pyroptosis and required for interleukin-1beta secretion. *Cell Res*. (2015) 25:1285–98. doi: 10.1038/cr.2015.139
26. Hara H, Tsuchiya K, Kawamura I, Fang R, Hernandez-Cuellar E, Shen Y, et al. Phosphorylation of the adaptor ASC acts as a molecular switch that controls the formation of speck-like aggregates and inflammasome activity. *Nat Immunol*. (2013) 14:1247–55. doi: 10.1038/ni.2749
27. Gavrilin MA, Mitra S, Seshadri S, Nateri J, Berhe F, Hall MW, et al. Pyrin critical to macrophage IL-1beta response to Francisella challenge. *J Immunol*. (2009) 182:7982–9. doi: 10.4049/jimmunol.0803073
28. Weischenfeldt J, Porse B. Bone Marrow-Derived Macrophages (BMM): isolation and applications. *CSH Protoc*. (2008) 2008:pdb prot5080. doi: 10.1101/pdb.prot5080
29. Biswas R, Trout KL, Jessop F, Harkema JR, Holian A. Imipramine blocks acute silicosis in a mouse model. *Part Fibre Toxicol*. (2017) 14:36. doi: 10.1186/s12989-017-0217-1
30. Bonilla DL, Ly LH, Fan YY, Chapkin RS, McMurray DN. Incorporation of a dietary omega 3 fatty acid impairs murine macrophage responses to *Mycobacterium tuberculosis*. *PLoS ONE*. (2010) 5:e10878. doi: 10.1371/journal.pone.0010878
31. Lynch RD. Utilization of polyunsaturated fatty acids by human diploid cells aging *in vitro*. *Lipids*. (1980) 15:412–20. doi: 10.1007/BF02534065
32. Wiesenfeld PW, Babu US, O'Donnell MW. Effect of long-chain fatty acids in the culture medium on fatty acid composition of WEHI-3 and J774A.1 cells. *Comp Biochem Physiol B Biochem Mol Biol*. (2001) 128:123–34. doi: 10.1016/S1096-4959(00)00305-5
33. Chan FK, Moriwaki K, De Rosa MJ. Detection of necrosis by release of lactate dehydrogenase activity. *Methods Mol Biol*. (2013) 979:65–70. doi: 10.1007/978-1-62703-290-2_7
34. Fahy RJ, Exline MC, Gavrilin MA, Bhatt NY, Besecker BY, Sarkar A, et al. Inflammasome mRNA expression in human monocytes during early septic shock. *Am J Respir Crit Care Med*. (2008) 177:983–8. doi: 10.1164/rccm.200703-418OC
35. Wessel D, Flugge UI. A method for the quantitative recovery of protein in dilute solution in the presence of detergents and lipids. *Anal Biochem*. (1984) 138:141–3. doi: 10.1016/0003-2697(84)90782-6
36. Choi HY, Lim JE, Hong JH. Curcumin interrupts the interaction between the androgen receptor and Wnt/beta-catenin signaling pathway in LNCaP prostate cancer cells. *Prostate Cancer Prostatic Dis*. (2010) 13:343–9. doi: 10.1038/pcan.2010.26
37. Dennis EA, Deems RA, Harkewicz R, Quehenberger O, Brown HA, Milne SB, et al. A mouse macrophage lipidome. *J Biol Chem*. (2010) 285:39976–85. doi: 10.1074/jbc.M110.182915
38. Bligh EG, Dyer WJ. A rapid method of total lipid extraction and purification. *Can J Biochem Physiol*. (1959) 37:911–7. doi: 10.1139/o59-099
39. Gurzell EA, Teague H, Duriancik D, Clinthorne J, Harris M, Shaikh SR, et al. Marine fish oils are not equivalent with respect to B-cell

membrane organization and activation. *J Nutr Biochem*. (2015) 26:369–77. doi: 10.1016/j.jnutbio.2014.11.005
40. Ostermann AI, Muller M, Willenberg I, Schebb NH. Determining the fatty acid composition in plasma and tissues as fatty acid methyl esters using gas chromatography - a comparison of different derivatization and extraction procedures. *Prostaglandins Leukot Essent Fatty Acids*. (2014) 91:235–41. doi: 10.1016/j.plefa.2014.10.002
41. Stoll LL, Spector AA. Changes in serum influence the fatty acid composition of established cell lines. *In vitro*. (1984) 20:732–8. doi: 10.1007/BF02618879
42. Ricote M, Glass CK. PPARs and molecular mechanisms of transrepression. *Biochim Biophys Acta*. (2007) 1771:926–35. doi: 10.1016/j.bbalip.2007.02.013
43. Kahlenberg JM, Kaplan MJ. The inflammasome and lupus: another innate immune mechanism contributing to disease pathogenesis? *Curr Opin Rheumatol*. (2014) 26:475–81. doi: 10.1097/BOR.0000000000000088
44. Pestka JJ, Vines LL, Bates MA, He K, Langohr I. Comparative effects of n-3, n-6 and n-9 unsaturated fatty acid-rich diet consumption on lupus nephritis, autoantibody production and CD4+ T cell-related gene responses in the autoimmune NZBWF1 mouse. *PLoS ONE*. (2014) 9:e100255. doi: 10.1371/journal.pone.0100255
45. Afonina IS, Muller C, Martin SJ, Beyaert R. Proteolytic processing of interleukin-1 family cytokines: variations on a common theme. *Immunity*. (2015) 42:991–1004. doi: 10.1016/j.immuni.2015.06.003
46. Zhang Y, Rong H, Zhang F-X, Wu K, Mu L, Meng J, et al. A Membrane potential- and calpain-dependent reversal of caspase-1 inhibition regulates canonical NLRP3 inflammasome. *Cell Rep*. (2018) 24:2356–69.e5. doi: 10.1016/j.celrep.2018.07.098
47. Dinarello CA. Overview of the IL-1 family in innate inflammation and acquired immunity. *Immunol Rev*. (2018) 281:8–27. doi: 10.1111/imr.12621
48. Ding J, Wang K, Liu W, She Y, Sun Q, Shi J, et al. Pore-forming activity and structural autoinhibition of the gasdermin family. *Nature*. (2016) 535:111–6. doi: 10.1038/nature18590
49. Liu X, Zhang Z, Ruan J, Pan Y, Magupalli VG, Wu H, et al. Inflammasome-activated gasdermin D causes pyroptosis by forming membrane pores. *Nature*. (2016) 535:153–8. doi: 10.1038/nature18629
50. Evavold CL, Ruan J, Tan Y, Xia S, Wu H, Kagan JC. The pore-forming protein gasdermin D regulates interleukin-1 secretion from living macrophages. *Immunity*. (2018) 48:35–44 e6. doi: 10.1016/j.immuni.2017.11.013
51. Kawasaki H. A mechanistic review of silica-induced inhalation toxicity. *Inhal Toxicol*. (2015) 27:363–77. doi: 10.3109/08958378.2015.1066905
52. Shirahama T, Cohen AS. Ultrastructural evidence for leakage of lysosomal contents after phagocytosis of monosodium urate crystals. A mechanism of gouty inflammation. *Am J Pathol*. (1974) 76:501–20.
53. Schorn C, Frey B, Lauber K, Janko C, Strysio M, Keppeler H, et al. Sodium overload and water influx activate the NALP3 inflammasome. *J Biol Chem*. (2011) 286:35–41. doi: 10.1074/jbc.M110.139048
54. Kovacs SB, Miao EA. Gasdermins: effectors of pyroptosis. *Trends Cell Biol*. (2017) 27:673–84. doi: 10.1016/j.tcb.2017.05.005
55. Joshi GN, Knecht DA. Silica phagocytosis causes apoptosis and necrosis by different temporal and molecular pathways in alveolar macrophages. *Apoptosis*. (2013) 18:271–85. doi: 10.1007/s10495-012-0798-y
56. Honarpisheh M, Foresto-Neto O, Desai J, Steiger S, Gomez LA, Popper B, et al. Phagocytosis of environmental or metabolic crystalline particles induces cytotoxicity by triggering necroptosis across a broad range of particle size and shape. *Sci Rep*. (2017) 7:15523. doi: 10.1038/s41598-017-15804-9
57. Desai J, Foresto-Neto O, Honarpisheh M, Steiger S, Nakazawa D, Popper B, et al. Particles of different sizes and shapes induce neutrophil necroptosis followed by the release of neutrophil extracellular trap-like chromatin. *Sci Rep*. (2017) 7:15003. doi: 10.1038/s41598-017-15106-0
58. England H, Summersgill HR, Edye ME, Rothwell NJ, Brough D. Release of interleukin-1α or interleukin-1β depends on mechanism of cell death. *J Biol Chem*. (2014) 289:15942–50. doi: 10.1074/jbc.M114.557561
59. Calder PC. Omega-3 fatty acids and inflammatory processes: from molecules to man. *Biochem Soc Trans*. (2017) 45:1105–15. doi: 10.1042/BST20160474
60. Lands B, Bibus D, Stark KD. Dynamic interactions of n-3 and n-6 fatty acid nutrients. *Prostaglandins Leukot Essent Fatty Acids*. (2017). 136:15–21. doi: 10.1016/j.plefa.2017.01.012
61. Adarme-Vega TC, Thomas-Hall SR, Schenk PM. Towards sustainable sources for omega-3 fatty acids production. *Curr Opin Biotechnol*. (2014) 26:14–8. doi: 10.1016/j.copbio.2013.08.003
62. Williams-Bey Y, Boularan C, Vural A, Huang NN, Hwang IY, Shan-Shi C, et al. Omega-3 free fatty acids suppress macrophage inflammasome activation by inhibiting NF-kappaB activation and enhancing autophagy. *PLoS ONE*. (2014) 9:e97957. doi: 10.1371/journal.pone.0097957
63. Bates MA, Benninghoff AD, Gilley KN, Holian A, Harkema JR, Pestka JJ. Mapping of dynamic transcriptome changes associated with silica-triggered autoimmune pathogenesis in the lupus-prone NZBWF1 mouse. *Front Immunol*. (2019) 10:632. doi: 10.3389/fimmu.2019.00632
64. Hwang JS, Kang ES, Ham SA, Yoo T, Lee H, Paek KS, et al. Activation of peroxisome proliferator-activated receptor gamma by rosiglitazone inhibits lipopolysaccharide-induced release of high mobility group box 1. *Mediators Inflamm*. (2012) 2012:352807. doi: 10.1155/2012/352807
65. Lin CF, Young KC, Bai CH, Yu BC, Ma CT, Chien YC, et al. Rosiglitazone regulates anti-inflammation and growth inhibition via PTEN. *Biomed Res Int*. (2014) 2014:787924. doi: 10.1155/2014/787924
66. Croasdell A, Duffney PF, Kim N, Lacy SH, Sime PJ, Phipps RP. PPARgamma and the innate immune system mediate the resolution of inflammation. *PPAR Res*. (2015) 2015:549691. doi: 10.1155/2015/549691
67. Pascual G, Fong AL, Ogawa S, Gamliel A, Li AC, Perissi V, et al. A SUMOylation-dependent pathway mediates transrepression of inflammatory response genes by PPAR-gamma. *Nature*. (2005) 437:759–63. doi: 10.1038/nature03988
68. Chung SW, Kang BY, Kim SH, Pak YK, Cho D, Trinchieri G, et al. Oxidized low density lipoprotein inhibits interleukin-12 production in lipopolysaccharide-activated mouse macrophages via direct interactions between peroxisome proliferator-activated receptor-gamma and nuclear factor-kappa B. *J Biol Chem*. (2000) 275:32681–7. doi: 10.1074/jbc.M002577200
69. Hou Y, Moreau F, Chadee K. PPARgamma is an E3 ligase that induces the degradation of NFkappaB/p65. *Nat Commun*. (2012) 3:1300. doi: 10.1038/ncomms2270
70. Kelly D, Campbell JI, King TP, Grant G, Jansson EA, Coutts AG, et al. Commensal anaerobic gut bacteria attenuate inflammation by regulating nuclear-cytoplasmic shuttling of PPAR-gamma and RelA. *Nat Immunol*. (2004) 5:104–12. doi: 10.1038/ni1018
71. Ricote M, Li AC, Willson TM, Kelly CJ, Glass CK. The peroxisome proliferator-activated receptor-gamma is a negative regulator of macrophage activation. *Nature*. (1998) 391:79–82. doi: 10.1038/34178
72. Castrillo A, Mojena M, Hortelano S, Bosca L. Peroxisome proliferator-activated receptor-gamma-independent inhibition of macrophage activation by the non-thiazolidinedione agonist L-796,449. Comparison with the effects of 15-deoxy-delta(12,14)-prostaglandin J(2). *J Biol Chem*. (2001) 276:34082–8. doi: 10.1074/jbc.M102472200
73. Lee JY, Sohn KH, Rhee SH, Hwang D. Saturated fatty acids, but not unsaturated fatty acids, induce the expression of cyclooxygenase-2 mediated through Toll-like receptor 4. *J Biol Chem*. (2001) 276:16683–9. doi: 10.1074/jbc.M011695200
74. Wong SW, Kwon MJ, Choi AM, Kim HP, Nakahira K, Hwang DH. Fatty acids modulate Toll-like receptor 4 activation through regulation of receptor dimerization and recruitment into lipid rafts in a reactive oxygen species-dependent manner. *J Biol Chem*. (2009) 284:27384–92. doi: 10.1074/jbc.M109.044065
75. Fuentes NR, Mlih M, Barhoumi R, Fan YY, Hardin P, Steele TJ, et al. Long-chain n-3 fatty acids attenuate oncogenic KRas-driven proliferation by altering plasma membrane nanoscale proteolipid composition. *Cancer Res*. (2018) 78:3899–912. doi: 10.1158/0008-5472.CAN-18-0324
76. Chang HY, Lee HN, Kim W, Surh YJ. Docosahexaenoic acid induces M2 macrophage polarization through peroxisome proliferator-activated receptor gamma activation. *Life Sci*. (2015) 120:39–47. doi: 10.1016/j.lfs.2014.10.014
77. Oh DY, Talukdar S, Bae EJ, Imamura T, Morinaga H, Fan W, et al. GPR120 is an omega-3 fatty acid receptor mediating potent anti-inflammatory and insulin-sensitizing effects. *Cell*. (2010) 142:687–98. doi: 10.1016/j.cell.2010.07.041
78. Hsiao HM, Thatcher TH, Levy EP, Fulton RA, Owens KM, Phipps RP, et al. Resolvin D1 attenuates polyinosinic-polycytidylic acid-induced inflammatory

signaling in human airway epithelial cells via TAK1. *J Immunol*. (2014) 193:4980–7. doi: 10.4049/jimmunol.1400313
79. Krishnamoorthy S, Recchiuti A, Chiang N, Yacoubian S, Lee CH, Yang R, et al. Resolvin D1 binds human phagocytes with evidence for proresolving receptors. *Proc Natl Acad Sci USA*. (2010) 107:1660–5. doi: 10.1073/pnas.0907342107
80. Hao H, Xu F, Hao J, He YQ, Zhou XY, Dai H, et al. Lipoxin A4 suppresses lipopolysaccharide-induced hela cell proliferation and migration via NF-kappaB pathway. *Inflammation*. (2015) 38:400–8. doi: 10.1007/s10753-014-0044-6
81. Bang S, Xie YK, Zhang ZJ, Wang Z, Xu ZZ, Ji RR. GPR37 regulates macrophage phagocytosis and resolution of inflammatory pain. *J Clin Invest*. (2018) 128:3568–82. doi: 10.1172/JCI 99888
82. White PJ, St-Pierre P, Charbonneau A, Mitchell PL, St-Amand E, Marcotte B, et al. Protectin DX alleviates insulin resistance by activating a myokine-liver glucoregulatory axis. *Nat Med*. (2014) 20:664–9. doi: 10.1038/nm.3549
83. Wendell SG, Golin-Bisello F, Wenzel S, Sobol RW, Holguin F, Freeman BA. 15-Hydroxyprostaglandin dehydrogenase generation of electrophilic lipid signaling mediators from hydroxy omega-3 fatty acids. *J Biol Chem*. (2015) 290:5868–80. doi: 10.1074/jbc.M114.635151
84. Chiang N, Serhan CN. Structural elucidation and physiologic functions of specialized pro-resolving mediators and their receptors. *Mol Aspects Med*. (2017) 58:114–29. doi: 10.1016/j.mam.2017.03.005
85. Norling LV, Headland SE, Dalli J, Arnardottir HH, Haworth O, Jones HR, et al. Proresolving and cartilage-protective actions of resolvin D1 in inflammatory arthritis. *JCI Insight*. (2016) 1:e85922. doi: 10.1172/jci.insight.85922

Conflict of Interest Statement: The authors declare that the research was conducted in the absence of any commercial or financial relationships that could be construed as a potential conflict of interest.

frontiers in Immunology

REVIEW
published: 27 September 2019
doi: 10.3389/fimmu.2019.02241

Therapeutic Potential of ω-3 Polyunsaturated Fatty Acids in Human Autoimmune Diseases

Xiaoxi Li[1,2†], Xinyun Bi[1†], Shuai Wang[1†], Zongmeng Zhang[1], Fanghong Li[1] and Allan Z. Zhao[1*]*

[1] The School of Biomedical and Pharmaceutical Sciences, Guangdong University of Technology, Guangzhou, China,
[2] Department of Immunology, Nanjing Medical University, Nanjing, China

The recognition of ω-3 polyunsaturated acids (PUFAs) as essential fatty acids to normal growth and health was realized more than 80 years ago. However, the awareness of the long-term nutritional intake of ω-3 PUFAs in lowering the risk of a variety of chronic human diseases has grown exponentially only since the 1980s (1, 2). Despite the overwhelming epidemiological evidence, many attempts of using fish-oil supplementation to intervene human diseases have generated conflicting and often ambiguous outcomes; null or weak supporting conclusions were sometimes derived in the subsequent META analysis. Different dosages, as well as the sources of fish-oil, may have contributed to the conflicting outcomes of intervention carried out at different clinics. However, over the past decade, mounting evidence generated from genetic mouse models and clinical studies has shed new light on the functions and the underlying mechanisms of ω-3 PUFAs and their metabolites in the prevention and treatment of rheumatoid arthritis, systemic lupus erythematosus (SLE), multiple sclerosis, and type 1 diabetes. In this review, we have summarized the current understanding of the effects as well as the underlying mechanisms of ω-3 PUFAs on autoimmune diseases.

Keywords: ω-3 polyunsaturated fatty acids, autoimmune diseases, inflammation, eicosanoids, mTOR-the mammalian target of rapamycin

OPEN ACCESS

Edited by:
Allen Jay Rosenspire, Wayne State University, United States

Reviewed by:
Philip Calder, University of Southampton, United Kingdom
Melissa Bates, Michigan Medicine, University of Michigan, United States

***Correspondence:**
Fanghong Li
fli@gdut.edu.cn
Allan Z. Zhao
azzhao@gdut.edu.cn

†These authors have contributed equally to this work

Specialty section:
This article was submitted to Autoimmune and Autoinflammatory Disorders, a section of the journal Frontiers in Immunology

Received: *26 April 2019*
Accepted: *04 September 2019*
Published: *27 September 2019*

Citation:
Li X, Bi X, Wang S, Zhang Z, Li F and Zhao AZ (2019) Therapeutic Potential of ω-3 Polyunsaturated Fatty Acids in Human Autoimmune Diseases. Front. Immunol. 10:2241. doi: 10.3389/fimmu.2019.02241

INTRODUCTION

Polyunsaturated fatty acids (PUFAs) can be divided into two major classes: ω-3 PUFAs and ω-6 PUFAs, with the primary structural difference at the positions of their double bonds on the carbon chain. ω-6 PUFAs have the first double bonds starting at the sixth carbon, while ω-3 PUFAs starting at the third carbon, from the methyl end of the carbon chain (the ω-carbon) (3). The two major ω-6 PUFAs that are typically consumed in the diet are linoleic acid (18:2; ω-6; LA) and arachidonic acid (20:4; ω-6; AA). Western diets are dominated by ω-6 PUFAs but contain only small amounts of ω-3 PUFAs with the ratio of ω-6/ω-3 reaching as high as 20–30 (4). The three major ω-3 PUFAs are α-linolenic acid (18:3; ω-3; α-LA), eicosapentaenoic acid (20:5; ω-3; EPA), and docosahexaenoic acid (22:6; ω-3; DHA). The α-LA (18:3; ω-3) should not be confused with γ-linolenic acid (GLA) that is also 18:3 but an ω-6 fatty acid. LA (precursor to the ω-6 series of fatty acids) and α-LA (precursor to the ω-3 series of fatty acids) are considered essential fatty acids because they cannot be synthesized in mammals. Starting with LA, mammals can sequentially synthesize GLA via Δ6-desaturase (Fads2) then AA through elongase and Δ5-desaturase (Fads1) (5–7). On the other hand, α-LA is converted to stearidonic acid (C18:4; ω-3) by Δ6-desaturase; stearidonic acid

is then elongated and converted to EPA via Δ5-desaturase. EPA add two carbons via elongase to form docosapentaenoic acid (22:5; ω-3; DPA), then add two more carbons via elongase followed by desaturation by Δ6-desaturase to produce tetracosahexaenoic acid (24:6; ω-3); the subsequent, removal of two carbons by β-oxidation yields DHA. Although Δ6-desaturase is widely considered as rate-limiting for the sequential synthesis from ALA to DHA (8–11), a recent study also revealed that elongase reactions (primarily mediated by elongase-5 in humans) were control points as well (12). These enzymatic constraints limit the tissue levels of EPA and DHA. Consequently, we still need to rely on dietary intake to meet the physiological demands of EPA and DHA.

The beneficial effects of ω-3 PUFAs are mediated by themselves as well as by their bioactive metabolites, such as resolvins, protectins, and maresins. Among them, the most studied anti-inflammation metabolites are resolvins which have two classes. E-series resolvins include RvE1, RvE2, and RvE3, all of which are synthesized from EPA by such enzymes as cytochrome P450 (CYP 450), cyclocygenase-2 (COX-2), and 15-lipoxygenase (15-LOX) (13, 14). The D series resolvins (RvD1–RvD6) are derived from DHA by such enzymes as COX-2, 12/15 LOX, and 5-LOX (13, 15–17). These metabolites from ω-3 PUFAs compete with those of ω-6 PUFAs to promote the resolution of the inflammatory cycle (18, 19), and have been increasingly recognized as the important players in the attenuation of inflammation and regulation of autoimmunity (18, 19).

Mounting evidence from both human and animal studies has demonstrated that ω-3 PUFAs, primarily EPA and DHA, can suppress inflammation and have beneficial roles in a variety of human diseases, including autoimmune diseases, diabetes, cancers, Alzheimer's disease (AD), and stroke (3, 20–26). Fish oil is the oil derived from the tissues of oily ocean fish. The main ω-3 PUFAs in fish oil are EPA and DHA. Researchers often use fish oil as the source of ω-3 PUFAs in clinical interventions. Although the effects of ω-3 PUFAs on these diseases have been extensively investigated in the past few decades, a series of recent studies involving the usage of a transgenic genetic model, fat-1 (or mfat-1) transgenic mice, have shed new light into the mechanisms underlying the protective effects of ω-3 PUFAs. The fat-1 transgenic mice, initially generated in Kang's lab (27) [and later the mfat-1 mouse model independently designed by our group (28)] carry a globally expressed *Caenorhabditis elegans* fat-1 transgene that encodes an ω-3 fatty acid desaturase. The FAT-1 enzyme can convert ω-6 PUFAs to the corresponding ω-3 forms by adding a double bond to the ω-3 position, thus allowing endogenous production of ω-3 PUFAs while reducing the ω-6: ω-3 ratio in tissues without special dietary adjustment (27, 28). The fat-1 transgenic model allows researchers to bypass the traditional lengthy dietary approach of feeding fish-oil to the animals, and have been widely applied to the studies related to autoimmune diseases, tumorigenesis, metabolic, and cardiovascular diseases, as well as neurological diseases (24, 27, 29, 30).

In this review, we choose to focus on the current understanding of the effects of ω-3 fatty acids on such debilitating diseases as rheumatoid arthritis (RA) (31), systemic lupus erythematosus (SLE) (32), type 1 diabetes (T1D) (33), and multiple sclerosis (MS) (34). Although there have been a large body of clinical research articles related to the application of ω-3 PUFAs in different indications, perhaps it should come with no surprise that not all published studies reached the same conclusions. The reasons behind such discrepancy are still unclear although different dose, source, and duration of ω-3 PUFAs treatment may have all played roles in the clinical outcomes. Unfortunately, many of these studies did not report the blood concentrations of EPA/DHA of the enrolled patients, making it difficult to evaluate if the enrolled patients for their studies have indeed gained sufficient EPA/DHA. Thus, for the benefit of readers, we have offered several formatted tables (by no means complete, but certainly representative) detailing the number of patients, dose, duration, and outcomes of each trial (**Tables 1–4**).

ω-3 PUFAS AND RHEUMATOID ARTHRITIS

Rheumatoid arthritis (RA) is a chronic autoimmune disease manifested by swollen and painful joints, bone erosion, and functional impairment. The joint lesions are characterized by infiltration of T lymphocytes, macrophages, and B lymphocytes into the synovium, as well as by synovial inflammation induced by PUFAs metabolites, cytokines, and matrix metalloproteinases (58–60). The intervention of RA with ω-3 PUFAs has attracted increasing attention. One of the earliest studies about ω-3 PUFAs' impact on rheumatoid arthritis was reported in Lancet in 1985 (35) (**Table 1**). In this pilot study, seventeen RA patients consumed a daily supplement of 1.8 g of EPA for 12 weeks. At the end of treatment, the EPA intervention significantly shortened morning stiffness time than the control group at 12 weeks and lessened the number of tender joints at 12 weeks from baseline. Several years following this study, Kremer et al. reported in 1990 that the number of tender joints significantly improved from baseline after both the low- and high-dose intervention with fish oil supplement (36) (**Table 1**). In addition to such beneficial effects, an ω-6 PUFAs-derived metabolite, leukotriene B4 (LTB_4), generated by the neutrophils of the fish oil-treated patients, decreased significantly (36) (**Table 1**). In a prospective study, sixty patients with active RA were enrolled in a randomized 12-week trial, who were given either fish oil supplement, or fish oil supplement with primrose evening oil (enriched in GLA), or no intervention (37) (**Table 1**). Daily supplementation of fish oil alone or in combination with primrose evening oil significantly improved the number of tender joints and visual analog scale (VAS) score. There was a sharp decline in the ratio of ω-6/ω-3 fatty acids in the plasma samples from the groups of subjects receiving fish oil, which was strongly linked to the clinical improvements. Beyer et al. reported in a nutrition study involving 78 RA patients, of which 58% had active RA, that consuming the recommended seafood intake was correlated with better RA disease outcome (38) (**Table 1**). In a separate study, sixteen patients received a daily dose of 2.04 g EPA and 1.32 g DHA for 12 weeks, the results also showed a significant reduction in joint swelling index and duration of early morning stiffness

TABLE 1 | Interventional studies with ω-3PUFAs in patients with rheumatoid arthritis (RA).

Study	*n*	Study design	Results
Kremer et al. (35)	37 patients with RA	17 patients took an experimental diet with a daily supplement of 1.8 g EPA for 12 weeks. 20 patients took a control diet with a lower polyunsaturated to saturated fat ratio and a placebo supplement for 12 weeks.	The experimental group had deteriorated significantly in patient and physician global evaluation of disease activity, pain assessment, and number of tender joints at 12th week and the following 1–2 months after stopping the diets.
Kremer et al. (36)	49 patients with active RA	20 patients consumed daily dietary supplements of 27 mg/kg EPA and 18 mg/kg DHA (low dose), 17 patients ingested 54 mg/kg EPA and 36 mg/kg DHA (high dose), and 12 patients ingested olive oil capsules containing 6.8 mg of oleic acid.	Significant decreases in the number of swollen joints were noted in the low and high-dose groups at weeks 12, 18, 24. Clinical benefits of dietary supplementation with ω-3 fatty acids are more commonly observed in patients consuming higher dosages of fish oil and olive oil is also associated with certain changes in immune function.
Veselinovic et al. (37)	60 patients with active RA	60 patients with active RA were involved in a prospective, randomized trial of a 12-week supplementation with fish oil (group I), fish oil with primrose evening oil (group II), or with no supplementation (group III). Clinical and laboratory evaluations were done at the beginning and at the end of the study.	The Disease Activity Score 28 (DAS 28 score), number of tender joints and visual analog scale (VAS) score decreased notably after supplementation in groups I and II ($p < 0.001$). In plasma phospholipids the n-6/n-3 fatty acids ratio declined from 15.47 ± 5.51 to 10.62 ± 5.07 ($p = 0.005$), and from 18.15 ± 5.04 to 13.50 ± 4.81 ($p = 0.005$) in groups I and II, respectively.
Beyer et al. (38)	78 RA patients (age 57 ± 12 y, disease duration 15 ± 11 y)	RA outpatients (age ≥35 y) were consecutively recruited. Rheumatologic clinical data were collected and periodontal status obtained. A food frequency questionnaire (FFQ) was used to estimate fish and supplement intake.	Seafood intake in accordance with nutritional recommendations was associated with better RA disease outcome ($P = 0.008$). An ω-3 index >8, present in 14% of the patients, correlated with a more desirable patient global health assessment scored on a visual analog scale (VAS; $P = 0.004$).
Van der Tempel et al. (39)	16 patients with RA	Patients were randomly allocated to receive each day either 12 capsules of fractionated fish oil (2.04 g DPA, 1.32 g DHA) or fractionated coconut oil flavored with fish aroma as placebo for 12 weeks.	Dietary fish oil supplementation is effective in suppressing joint swelling index and duration of early morning stiffness. Other clinical indices improved but did not reach statistical significance. The mean neutrophil leucotriene B4 production *in vitro* showed a reduction after 12 weeks of fish oil supplementation. Leucotriene B5 production rose to substantial quantities during fish oil treatment.
Lee et al. (40)	183 RA patients and 187 placebo-treated RA controls were included in this meta-analysis	The authors surveyed RCTs that examined the effects of ω-3 PUFAs on clinical outcomes in RA patients using MCCTR and by performing manual searches. Meta-analysis of RCTs was performed using fixed and random effects models.	The use ofω-3 PUFAs at dosages >2.7 g/day for >3 months reduces NSAID consumption by RA patients.
Espersen et al. (41)	32 patients with active RA	A 12-week double-blind, randomized study of dietary supplementation with ω-3 fatty acids (3.6 g per day) or placebo.	Dietary supplementation with ω-3 fatty acids results in significantly reduced plasma IL-1 beta levels in patients with rheumatoid arthritis, and the clinical status of the patients was improved in fish oil group.

NSAID, Non-steroidal anti-inflammatory drug; RA, Rheumatoid arthritis; DPA, Docosapentaenoic acid; RCTs, Randomized controlled trials; MCCTR, Medline and the cochrane controlled trials register; NSAID, Non-steroidal anti-inflammatory drugs; FFQ, Food-frequency questionnaire; DMARD, Disease-modifying anti-rheumatic drug; ACR, American college of rheumatology.

as well as a decrease of LTB4 production by the neutrophils isolated from patients' blood (39) (**Table 1**). A meta-analysis of 23 similar clinical studies revealed a fairly consistent finding that ω-3 PUFAs had a beneficial effect on joint swelling, pain and morning stiffness, and that there was a significant reduction in the required dose of steroidal anti-inflammatory drugs (40) (**Table 1**).

In an animal model study, fish-oil feeding in mice delayed the onset and reduced the incidence and severity of type II collagen-induced arthritis compared with the vegetable oil-fed group (61). In the susceptible DBA/1 mouse strain, daily intake of marine ω-3 PUFAs in the form of phospholipids delayed the onset of arthritis, decreased the severity, reduced paw swelling, and knee joint pathology in collagen-induced arthritis (62). Both EPA and DHA have also been shown to suppress *Streptococcal*-induced arthritis in rats, although EPA appeared to be more effective than DHA (63). As additional proof, endogenous production of ω-3 PUFAs in the fat-1 transgenic mice drastically attenuated arthritis as well as local and systemic levels of inflammatory cytokines following the establishment of RA, whereas the wild type control mice developed overt arthritis (64). Thus, in both animal models and patients, ω-3 PUFAs were able to decrease not only the incidence but also the severity of RA.

TABLE 2 | Interventional studies with ω-3 PUFAs in patients with systemic lupus erythematosus (SLE).

Study	*n*	Study design	Results
Clark et al. (42)	12 patients with SLE	12 patients took regular diet with two 1 g MaxEPA capsules (contained 180 mg EPA and 120 mg DHA) for 5 weeks, followed by a 5 weeks washout phase when no MaxEPA capsules were taken. Then the patients took six EPA capsules for 5 weeks.	Dietary supplementation with fish oil affects the mechanisms involved in inflammatory and atherosclerotic vascular disease in patients with lupus nephritis, including neutrophil leukotriene B4 release was reduced 78 and 42%, respectively, by the low and higher doses of fish oil. The higher fish oil dose induced a 38% decrease in triglyceride and a 39% reduction in VLDL cholesterol associated with a 28% rise in HDL, cholesterol. The fish oil had no effect on immune complex or anti-DNA antibody.
Westbergetal and Tarkowski (43)	17 patients with moderately active SLE	A double-blind, crossover study on the effect of MaxEPA (contained 180 mg EPA and 120 mg DHA), using olive oil as the control substance. 8/17 on MaxEPA, 2/17 on the control substance for 6 months.	MaxEPA had beneficial effects on the disease but short-lived.
Das et al. (44)	10 patients with newly diagnosed SLE	Patients were given orally 6 capsules of EPA/DHA (each contained EPA 27 mg, and DHA 24 mg) for 1 or 2 months. Some of these patients who had significant renal and/or other target organ involvement were given steroids initially for not more than I–2 months in addition to EPA/DHA. At the end of 1 or 2 months of therapy, steroids were withdrawn while patients continued to take EPA/DHA capsules.	Oral supplementation of EPA and DHA induced prolonged remission of SLE without any side-effects.
Duffy et al. (45)	52 patients with SLE	A double-blind, double placebo-controlled factorial trial for 24 weeks. One group received 3 g MaxEPA (contained 180 mg EPA and 120 mg DHA) and 3 mg copper, another 3 g MaxEPA and placebo copper, another 3 mg copper and placebo fish oil, and the fourth group received both placebo capsules.	Dietary supplementation with fish oil is beneficial in modifying symptomatic disease activity. There was a significant decline in SLAM-R score from 6.12 to 4.69 ($p < 0.05$) in those subjects taking fish oil compared to placebo. No significant effect on SLAM-R was observed in subjects taking copper.
Elkan et al. (46)	114 patients with SLE	In all 114 patients with SLE and 122 age- and sex-matched population-based controls answered a food frequency questionnaire (FFQ).	The low intake of ω-3 and high intake of carbohydrate among patients with SLE appear to be associated with worse disease activity, adverse serum lipids, and plaque presence.
Arriens et al. (47)	50 SLE patients	Fifty SLE patients were randomized 1:1 to fish oil supplementation or olive oil placebo, and blinded to their treatment group for 6 months.	Fish oil supplementation demonstrated improvement in PGA, RAND SF-36, and some circulating inflammatory markers of SLE patients.
Bello et al. (48)	85 SLE patients	SLE patients were randomly assigned to 3 g of ω-3 (Lovaza, GSK) vs. placebo for 12 weeks.	ω-3 did not improve endothelial function, disease activity, nor reduce inflammatory markers in SLE.

SLE, Systemic lupus erythematosus; VLDL, Very low density lipoprotein; HDL, High density lipoprotein; PGA, Physician global assessment; RAND SF-36, RAND 36-Item short form health survey version 1.0; SLAM-R, Systemic lupus activity measure.

The mechanisms underlying ω-3 PUFAs-initiated regulation of immunity in RA can be several. Most studies focused on molecular mediators, including cytokines, metabolites, and reactive oxygen species; others have interrogated the roles of immune cells such as T cells and antigen presenting cells. In the study by Espersen et al. (41) (**Table 1**), the level of interleukin-1β (IL-1β) in plasma was significantly suppressed in the patients who consumed fish oil by week 6 of the trial, and a further significant decrease was observed a few weeks later. Even in healthy volunteers, a clinical study involving supplementation of fish oil has demonstrated reduction in tumor necrosis factor-alpha (TNF-α), IL-1β, and interleukin-6 (IL-6) in endotoxin-stimulated monocytes cells (65), although the findings from a few other studies did not corroborate these results (66–68). Recently, interleukin-17 (IL-17) has been proposed to be a key cytokine in the onset and development of RA (69, 70). Studies using fish oil supplement found that DHA and EPA have anti-inflammation benefit by reducing the population of interferon-γ (IFN-γ) and IL-17-producing $CD4^+$ T cells in humans and animals (71–74). Thus, suppression of inflammatory cytokines is likely an important contributing factor to the amelioration of clinical signs and symptoms in RA patients. In cultured cells, studies also reported that EPA and DHA could inhibit the production of TNF-α, IL-1β, and IL-6, the classic panel of pro-inflammatory cytokines (75–78). The results derived from these clinical and cellular studies were also corroborated by similar findings in other animal models (24, 30). For example, the fat-1 transgenic mice showed strong anti-inflammatory effects that rendered tissues strongly resistant to cytokines (IL-1β and TNF-α)-induced cell death (24, 30). The inflammatory metabolites, prostaglandin E2 (PGE_2) and LTB_4, were sharply decreased in the tissues of the fat-1 mice. Endogenous production of ω-3 PUFAs also markedly attenuated cytokine-induced activation of nuclear

TABLE 3 | Interventional studies with ω-3 PUFAs in patients with type 1 diabetes (T1D).

Study	*n*	Study design	Results
Stene and Joner et al. (49)	545 subjects with childhood-onset T1D	Daily supplements with 5 mL of cod liver oil (0.6 g DHA, 0.4 g EPA, and 10 μg vitamin D) in the first year of life.	Significantly lower risk of type 1 diabetes in the first year of life with supplements of cod liver oil.
Norris et al. (50)	1770 children at increased risk for T1D	A longitudinal, observational study of children at increased risk for type1 diabetes with dietary intake of PUFAs (∼150 mg/day EPA+DHA) started at age 1 year. The mean age at follow-up was 6.2 years.	EPA/DHA supplement starting from the first year of life sharply lowered the incidence of islet autoimmunity and the titers of autoantibodies in children with a high risk of T1D.
Cadario et al. (51)	2 cases of T1D in pediatric subjects after a short clinical history of classic symptoms of overt disease	Supplements of vitamin D (1,000 IU/day) started just at the discharge and ω-3 (EPA + DHA 50–60 mg/kg/day, EnerZona ω-3).	Improved blood glucose control and progressively reduced in relation to blood glucose eat awakening. A small amount of basal insulin at bedtime was maintained. Vitamin D and ω-3 supplementation may represent a cost-effective strategy in T1D.
Chase et al. (52)	Beginning either in the last trimester of pregnancy (41 infants) or in the first 5 months after birth (57 infants). Infants had a first-degree relative with T1D	Mothers received DHA (800 mg/day) or corn/soy oil (800 mg/day) in the last trimester of pregnancy and continued on this same dose after delivery if breast-feeding. Formula-fed infants received formula with 10.2 mg DHA/ounce (treatment) or 3.4 mg DHA/ounce (control).	The levels of RBC DHA increased in treated infants. No statistically significant reductions in the production of the inflammatory cytokines. Reduced hsCRP level in breast-fed DHA-treated infants.

PUFAs, Polyunsaturated fatty acids; T1D, Type1 diabetes; DHA, Docosahexaenoic acid; EPA, Eicosapentaenoic acid; hsCRP, high-sensitivity C -reactive protein.

factor kappa-light-chain-enhancer of activated B cells (NF-κB) and extracellular signal–related kinase 1/2 (ERK1/2) (24, 30).

Our recent study and many other studies revealed that incubation of EPA and DHA with isolated human T cells could inhibit the proliferation of human T cells and their production of IL-2 (79–83). Similar findings were also made in the T-cells isolated from mice (80). *In vivo*, a dietary gain of ω-3 PUFAs has been shown to correct the imbalance of Th1 and Th2 ratios in such Th1-mediated autoimmune disease models as RA and EAE (84–86). Thus, both the proliferation and differentiation of T cells could be regulated by ω-3 PUFAs. EPA and DHA may have also influenced the function of antigen presenting cells. Studies derived from cultured cells have shown that the expression of major histocompatibility complex (MHC) II and antigen presentation via MHC II could be significantly reduced following the exposure to EPA and DHA (87–89). These findings are also supported by the observations in the mice fed fish-oil (90) or in humans with EPA/DHA supplementation (91). Taken together, these investigations supported the concept that ω-3 PUFAs can decrease levels of inflammatory cytokines, modulate T-cell differentiation, reduce antigen presentation via MHC II, and importantly correct a range of pathological conditions of RA.

ω-3 PUFAS AND SYSTEMIC LUPUS ERYTHEMATOSUS

In addition to the investigations of ω-3 PUFAs in the treatment for RA, there have also been a number of studies in animal models and clinical trials assessing the effects of dietary supplementation of ω-3 PUFAs in other autoimmune diseases, such as SLE (42, 92). SLE is a common autoimmune disorder with diverse clinical manifestations including inflammation, blood vessel abnormalities, and immune-complex deposition, which are all associated with autoantibodies against cellular components (93, 94). Since the earliest clinical trial in 1989 (**Table 2**), there have been seven major published clinical studies focusing on the relationship between ω-3 PUFAs and SLE (42–48) (**Table 2**). All but one of the clinical studies (48) (**Table 2**) reported beneficial effects, including the improvement in endothelial function, disease activity, or inflammatory markers following the implementation of ω-3 PUFAs in SLE patients. In all of the studies with positive outcomes, more than 12 weeks of intervention appeared to be necessary. In a recent randomized placebo-controlled 6-month trial involving fifty SLE patients (47) (**Table 2**), the patients who received ω-3 PUFAs intervention (2.25 g EPA and 2.25 g DHA) showed remarkable improvement in their scores derived from Physician Global Assessment (PGA) and RAND 36-Item Short Form Health Survey (RAND SF-36, Version 1.0). The circulating levels of several inflammatory markers, including IL-13 and IL-12, were significantly decreased (47) (**Table 2**). A clinical nutritional study of SLE patients found that dietary patterns low in ω-3 PUFAs and high in carbohydrates positively correlated with the severity of disease activity, adverse serum lipids, and the presence of plaque (46) (**Table 2**). A double-blind, double placebo-controlled factorial trial in 52 patients with SLE (45) (**Table 2**) reported a significant decline in SLAM-R score (revised Systemic Lupus Activity Measure) from 6.12 to 4.69 in the subjects receiving EPA/DHA compared to those on placebo. In the study carried out by Das and colleagues (44) (**Table 2**), daily oral supplementation of even moderate EPA and DHA (EPA 162 mg, DHA 144 mg) induced prolonged remission of SLE in ten patients. Furthermore, EPA and DHA also suppressed both T-cell proliferation and the production of IL-1, IL-2, as well as TNF-α *in vitro* and *in vivo* (44) (**Table 2**). A comparative clinical study compared fatty acid (FA) compositions in the red blood

TABLE 4 | Interventional studies with ω-3 PUFAs in patients with multiple sclerosis (MS).

Study	*n*	Study design	Results
Nordvik et al. (53)	16 newly diagnosed MS patients with EDSS < 6	Daily supplement with 5 ml fish oil (0.4 g EPA, 0.5 g DHA. 1.0 mg of vitamin A, 10 μg of vitamin D and 5.5 mg vitamin E). A vitamin B-complex (containing 2.25 mg of thiamin, 2.6 mg of riboflavin, 30 mg of niacin, 7 mg of pantothenic acid, 3 mg of pyridoxine, 150 μg of biotin, 100 μg of folic acid, 6 μg of cobalamin) and 200 mg of vitamin C (acid neutral).	ω-3 PUFAs supplementation given together with vitamins and dietary advice can improve clinical outcome in patients with newly diagnosed MS.
Kouchaki et al. (54)	53 patients with MS aged 18–55 y	Patients, aged 18–55 y, were matched for disease EDSS scores, gender, medications, BMI, and age ($n = 53$) and randomly received a combined 2 × 1,000 mg/d ω-3 fatty acid and 50,000 IU/biweekly cholecalciferol supplement or placebo for 12 week. The placebos were matched in color, shape, size, packaging, smell, and taste with supplements.	significant improvement in EDSS (β −0.18; 95% CI: −0.33, −0.04; $P = 0.01$) in patients taking ω-3 fatty acid plus vitamin D supplements compared with placebo.
Hoare et al. (55)	267 cases with FCD (aged 18–59) and 517 controls	Habitual dietary intake over the 12-month period prior to the study interview was collected from self-completion of the Cancer Council Victoria (CCV) Food Frequency Questionnaire (FFQ).	High intake of ω-3 PUFA and particularly that derived from fish rather than from plants was associated with a decreased risk of FCD.
Weinstock-Guttman et al. (56)	31 RRMS patients	Patients were randomized to two dietary interventions: the "Fish Oil" (FO) group received a low-fat diet (15% fat) with ω-3 FOs and the "Olive Oil" (OO) group received the AHA Step I diet (fat≤30%) with OO supplements. The primary outcome measure was the Physical Components Scale (PCS) of the Short Health Status Questionnaire (SF-36).	Clinical benefits favoring the FO group were observed on PCS/SF-36 ($P = 0.050$) and MHI ($P = 0.050$) at 6 months. Reduced fatigue was seen on the OO diet at 6 months ($P = 0.035$). The relapse rate decreased in both groups relative to the rates during the 1 year preceding the study: mean change in relapse rate in the FO group: −0.79 ± SD 1.12 relapses/year ($P = 0.021$) vs. −0.69 ± SD 1.11 ($P = 0.044$) in the OO group.
Torkildsen et al. (57)	92 patients aged 18–55 years with active relapsing-remitting multiple sclerosis, with a disability score equivalent to 5.0 or less on the Kurtzke EDSS	92 patients were randomized to ω-3 fatty acids ($n = 46$) or placebo capsules ($n = 46$). Administration of 1,350 mg of eicosapentaenoic acid and 850 mg of docosahexaenoic acid daily or placebo. After 6 months, all patients also received subcutaneously 44 μg of IFNβ-1α 3 times per week for another 18 months.	No differences were detected in fatigue or quality-of-life scores, and no safety concerns appeared.

PUFAs, Polyunsaturated fatty acids; DHA, Docosahexaenoic acid; EPA, Eicosapentaenoic acid; CNS, Central nervous system, FCD, a first clinical diagnosis of CNS demyelination; MS, Multiple sclerosis; RRMS, Relapsing/remitting multiple sclerosis; ATRA, All-trans retinoic acid; AOR, Adjusted odds ratio; CI, Confidence interval; EDSS, Expanded disability status scale; PCS, Physical components summary scale; SF-36, Short health status questionnaire; MHI, Mental health inventory; AHA, American heart association; IFNβ-1α, interferon beta–1 alpha.

cells (RBC) and plasma between the female SLE patients and age-matched females with a history of cardiovascular disease (CVD) or those SLE patients with no history of CVD (SLE+CVD and SLE-CVD) (5). The plasma levels of EPA and ω-3 index (EPA+DHA) were significantly lower in the SLE patients than the CVD controls. In RBC, the ratio of AA to EPA was also significantly higher in the SLE patients than in the controls. Thus, although there was no intervention with ω-3 PUFA supplement, these SLE patients clearly had altered plasma and RBC FA compositions favoring inflammation pathology (5). Following this study, Luca Navarini et al. analyzed fatty acids or metabolites in the plasma samples from SLE patients (95). RvD1, the main metabolic product of DHA, was found to be remarkably lower in the samples from SLE patients than those from the non-SLE controls (95), further supporting the potential of using ω-3 PUFAs and its metabolites in the clinical management of SLE.

Mounting evidence built in SLE animal models strongly supports the preventative and therapeutic benefits of ω-3 PUFAs against SLE. Although several SLE models have been widely used in published animal studies, we decided to focus on the results derived from NZB/NZW F1 mice (herein after named B/W F1) because it is a classic spontaneous SLE model with close resemblance to the development of human SLE. Fernandes et al. found that a diet rich in long chain ω-3 fatty acids (10%) delayed the onset, attenuated the severity of autoimmune diseases, and prolonged the survival of female B/W F1 mice (96). Such amelioration of autoimmune disease was mainly attributed to the elevation of transforming growth factor β1 (TGF-β1) and IL-4 as well as the reduction of pro-inflammatory cytokines IL-2 from the splenocytes of B/W F1 mice (96). Perhaps not surprisingly, in their following study, the analysis of fatty acids revealed significantly elevated EPA and DHA levels in the kidney tissue samples of the EPA/DHA-fed animals, and further confirmed the decreased expression of TGF-β1 played a key role in the development of SLE (97). In a separate independent study, the B/W F1 mice, after fed linseed-oil (containing 70% ω-3 PUFAs), showed lower titers of antibodies to DNA as well as cardiolipin and less severe kidney damage than the B/W F1 mice fed control diets (98). Consistent with these findings, Halade et al. found that

the concentrated EPA/DHA (Lovaza®) had a dose-dependent therapeutic effect on SLE progression: the diet containing 1% Lovaza extending maximal lifespan to 517 days; and the diet containing 4% Lovaza further prolonged both the median (502 d) and maximal (600 d) life span in B/W F1 mice compared to the same mice fed standard chow diet (301 d) (99). In addition, the diet containing 4% Lovaza significantly decreased anti-dsDNA antibodies, glomerulonephritis, and pro-inflammatory cytokines (IL-1β, IL-6, TNF-α) in the splenocytes. Notably, NF-κB activation and p65 nuclear translocation were also lowered by 4% Lovaza-containing diet when compared to that in the control diet. An independent study by Pestka et al. found that ω-3 PUFAs-enriched diets delayed the onset and markedly attenuated the severity of autoimmune glomerulonephritis, plasma autoantibodies, and proteinuria in the B/W F1 mice (100); importantly, such suppression of autoimmunity was found to correlate with a generalized reduction of $CD4^+$ T cell-specific gene expression in the kidneys and/or spleens of the SLE mice (100). Thus, daily oral supplementation of ω-3 PUFAs has shown promising therapeutic effects, even at low dosages, by suppressing glomerulonephritis and extending life span in patients and SLE-prone animals, most likely via reducing inflammatory cytokines. These studies further demonstrated that ω-3 PUFAs could alleviate the severity and slow the progression of SLE by regulating.

ω-3 PUFAS AND TYPE 1 DIABETES

T1D is a polygenic and organ-specific autoimmune disease, in which a certain subclass of T lymphocytes is involved in executing autoimmune attacks that lead to the destruction of pancreatic β cells (101, 102). Two recent large-scale clinical observational studies revealed clear preventative and therapeutic benefits against the development of T1D through early intervention with EPA/DHA-enriched agents to infants and children. Stene et al. initially reported in a large population-based case-control study that dietary supplement of cod-liver oil and vitamin D in the first year of life significantly reduced the incidence of childhood-onset T1D (49) (**Table 3**). In a separate longitudinal, observational study (part of the Diabetes Autoimmunity Study in the Young, DAISY), Norris and colleagues showed that EPA/DHA supplement starting from first year of life sharply lowered the incidence of islet autoimmunity and the titers of autoantibodies in children with high risk of T1D (50) (**Table 3**). In an attempt to treat a childhood onset T1D, Ricordi's group successfully normalized blood glucose and sharply reduced the dose of injected insulin to just once a day after a year and half of oral EPA/DHA and vitamin D supplement in an 8-year-old child (51) (**Table 3**). A multicenter, two-arm, randomized, double-blind pilot trial of DHA supplementation, beginning either in the last trimester of pregnancy (41 infants) or in the first 5 months after birth (57 infants) with a high genetic risk for T1D was conducted by Dr. Chase's group (52) (**Table 3**). There were no statistically significant reductions in the blood levels of inflammatory cytokines, such as IL-1β, TNF-α or interleukin-12 subunit p40 (IL-12p40). However, high-sensitivity C-reactive protein (hsCRP) was significantly lower in breast-fed DHA-treated infants compared to all formula-fed infants at age 12 months, suggesting that the nutritional matrix of breast milk, particularly the ones with increased DHA contents, has an anti-inflammatory effect (52) (**Table 3**).

A series of recent genetic and clinical studies have shed new light on the mechanisms and the therapeutic potential of ω-3 PUFAs in suppressing autoimmunity as well as protecting and enhancing islet functions. In animal studies, Otani et al. reported that low ratio of ω-6/ω-3 at 3.0 in the maternal diet during gestation and lactation delayed the onset of diabetes in NOD mice offspring (103). Their further study indicated that diet with a low ω-6/ω-3 ratio started immediately after the onset of overt diabetes prolonged survival of type 1 diabetes in NOD mice (104). However, a study by a different group failed to see a significant delay in the onset of diabetes with the supplementation of fish-oil (105). The author ascribed these results to the low power of statistical method and the possibility that EPA/DHA may have undergone oxidation after thawing from the −20°C storage condition (105). However, other factors, including the dosage and the concentrations of the administered EPA/DHA, should not be excluded.

The recent research coming from our own group revealed that elevation of cellular ω-3 PUFAs via the transgenic expression of fat-1 almost completely blocked the pancreatic β-cells from the attack of pro-inflammatory cytokines while significantly enhancing insulin secretion (30). These effects were primarily mediated via the reduction of PGE_2 secretion from the islets and β-cells, suggesting that the control of inflammation through reduction of ω-6 PUFAs and their metabolites was the main theme in the regulation of β-cell functions (30). These findings derived from the fat-1 transgenic model was also consistent with the results from earlier nutritional studies that dietary gain of marine ω-3 PUFAs could restore palmitate acid-or LA-impaired insulin secretion (106, 107).

In our latest published report using the spontaneous type 1 diabetic NOD mice, an EPA/DHA-enriched diet and a fat-1 gene therapy not only delayed the onset but also reversed the autoimmunity and diabetes (80). Both methods of treatment, provided as either a preventative or a therapeutic modality, significantly suppressed Th1 and Th17 cell populations, reduced the secreted levels of IFN-γ and IL-17, increased the proportion of Th2 and regulatory T cells (Tregs). Thus, EPA/DHA-initiated global changes in $CD4^+$ T-cells are likely the primary cellular mechanisms stalling the development of autoimmunity in T1D (80). Multiple molecular mechanisms may have contributed to the effects of ω-3 PUFAs on $CD4^+$ T-cell differentiation. In particular, the metabolites of PUFAs played critical roles in the modulation of immune system. For example, arachidonic acid (an ω-6 PUFA)-derived eicosanoids, synthesized through the activities of such enzymes as lipoxygenase, cyclooxygenase, and cytochrome P450, often have a pro-inflammatory effect (108). In contrast, EPA/DHA-derived eicosanoids and docosanoids are less inflammatory than those from ω-6 PUFAs (16). In our analysis, different eicosanoids and docosanoids played distinct roles in $CD4^+$ T-cell differentiation (80). Prostaglandin D3 (PGD3) (EPA-derived metabolite) had a strong inhibitory effect

on Th1 and Th17 differentiation and increased the percentage of Th2 and Treg.17, 18-dihydroxy-5Z,8Z,11Z,14Z-eicosatetraenoic acid (17,18-DiHETE), another EPA-derived metabolite, only decreased the population of Th17. One of the DHA-derived metabolites, resolvin D1 (RvD1), had a strong inhibitory effect on Th1 differentiation and promoted Th2 and Tregs differentiation. In contrast, the pro-inflammatory eicosanoids (synthesized from AA), such as 15-Hydroxyeicosatetraenoic acid (15-HETE) and 20-Hydroxyeicosatetraenoic acid (20-HETE), had exactly the opposite effects on naive $CD4^+$ T-cell differentiation than those of EPA/DHA-derived metabolites (80).

Olefsky' group has identified a receptor for ω-3 PUFA, which is G-protein coupled receptor 120 (GPR120), that can mediate at least in part the anti-inflammation effect of ω-3 PUFAs (103, 109). GPR120 couples to β-arrestin2 and inhibits TAK1 binding protein 1 (TAB1)-mediated activation of transforming growth factor-β activated kinase 1 (TAK1), providing a mechanism for inhibition of both the NF-κB related Toll-like receptor (TLR) signaling and TNF-α pro-inflammatory signaling (103, 109) (see the proposed model in **Figure 1**). Deficiency of GPR120 in mice and humans produced symptoms very similar to those of wild-type mice fed LOW ω-3 PUFA diets, including reduced energy expenditure, obesity, insulin resistance, and an elevated state of inflammation (114).

Our recent studies further revealed that the mTOR has emerged as an important signaling switch for ω-3 PUFA-regulated differentiation of $CD4^+$ T helper cells (110). In particular, application of rapamycin has been shown to inhibit the proliferation of T-cells and the differentiation to Th1 even in the presence of TCR co-stimulatory molecules, such as CD28 (82). T-cell specific mutation of mTOR gene or rapamycin treatment could suppress differentiation to Th17 cell (115). In contrast, rapamycin or diminution of mTOR activity promoted naive $CD4^+$ T cells differentiating into Tregs (115). EPA/DHA and ω-6 PUFAs (particularly AA) had the opposite effects on mTORC1 signaling pathway. EPA/DHA reduced phosphorylation of ribosomal protein S6, indicative of inhibition of mTORC1 activity, whereas AA increased S6 protein phosphorylation levels by activating mTORC1. Moreover, rapamycin, the inhibitor of mTOR, completely blocked the AA-induced Th1 differentiation. Thus, the totally opposite impact of ω-6- and ω-3 PUFAs on the regulation of mTOR complexes serves a molecular switch to dictate the differentiation fate of $CD4^+$ T cells following the treatment of PUFAs (80) (for a proposed working model, see **Figure 1**).

Interestingly, even in a chemically (*Streptozotocin*, STZ) induced diabetic model, the pancreatic enrichment of ω-3 PUFAs as a result of fat-1 expression could also prevent the development of diabetes (116). This dramatic effect was accompanied by the reduction of the expression of proinflammatory cytokine genes, the blockade of NF-κB activation, and a sharp suppression of proinflammatory PUFA-derived lipid mediators in the pancreas of the fat-1 mice (116). In contrast, the EPA-derived anti-inflammatory metabolites, lipoxin A4 (LXA4), and 18-hydroxy-5Z,8Z,11Z,14Z,16E-eicosapentaenoic acid (18-HEPE), were highly elevated in the STZ-treated fat-1 mice (116). Taken together, these clinical and animal studies have provided the hope that intervention with ω-3 PUFAs can be successfully applied to the prevention, and even therapeutic treatment of T1D. Additional studies are required to validate the effect of administration of ω-3 fatty acids on the progression of T1D.

Taken together, the reduction of ω-6 PUFAs and elevation of ω-3 PUFA intake are critical to the prevention and treatment of type 1 diabetes, which should help direct the future clinical intervention with EPA/DHA supplementation.

ω-3 PUFAS AND MULTIPLE SCLEROSIS

MS is a chronic autoimmune inflammatory disease of the brain and spinal cord in which immune cell infiltration promotes inflammation, demyelination, and neuroaxonal degeneration, leading to the damage of neuronal signaling (117, 118). At the initial stages of the disease, most patients experience reversible neurological dysfunction, which typically lasts several days or weeks. Over time, irreversible clinical, and cognitive deficits develop (119, 120).

ω-3 PUFAs have attracted a great deal of attention as the potential agents in the clinical management of MS owing to their anti-inflammatory, antithrombotic, antioxidant, and immunomodulatory functions (118, 121–123). Indeed, largely inspired by Swank's observation that a higher incidence of MS occurred in Norwegians with diets of higher levels of animal fats and dairy products than those with diets of higher amounts of fish, several clinical studies have been conducted with the focus on dietary supplements like vitamin D, polyunsaturated fatty acids or other specific diets (124). A Norwegian intervention study of the patients with newly diagnosed MS reported that a 2-year treatment regimen with 0.9 g/day supplement of long chain marine fatty acids and vitamins showed a significant reduction in the mean annual exacerbation rate and the mean expanded disability status scale (EDSS) as compared to the pre-study values (53) (**Table 4**). In a randomized, placebo-controlled clinical trial with EDSS score and inflammation as the primary outcomes, a significant improvement in EDSS compared with placebo was observed in the patients taking ω-3 fatty acid plus vitamin D supplements (54) (**Table 4**). In a multi-center incident case-control study (involving 267 cases and 517 controls) conducted in four regions of Australia, high intake of ω-3 PUFAs was strongly associated with a decreased risk of a first clinical diagnosis of central nervous system (CNS) demyelination (55) (**Table 4**). In a double-blind and randomized trial for the duration of 1 year, 27 relapsing-remitting MS (RRMS) patients were treated with the same doses of ω-3 PUFAs and olive oil (56) (**Table 4**). Patients were randomly divided into two groups: the ω-3 group with dietary fat intake restricted to <15% of the daily calorie intake and the olive oil group with dietary fat intake to <30%. The results showed no significant effect on relapse rate or clinical severity (EDSS) scores following the 12-month intervention. However, the patients with relapsing-remitting MS benefited from a low fat diet supplemented with ω-3 PUFAs as the mean change of relapse rate in the ω-3 group: −0.797 relapses/year ($P = 0.021$) vs. −0.69 ($P = 0.044$) in the olive oil control group (56) (**Table 4**). However,

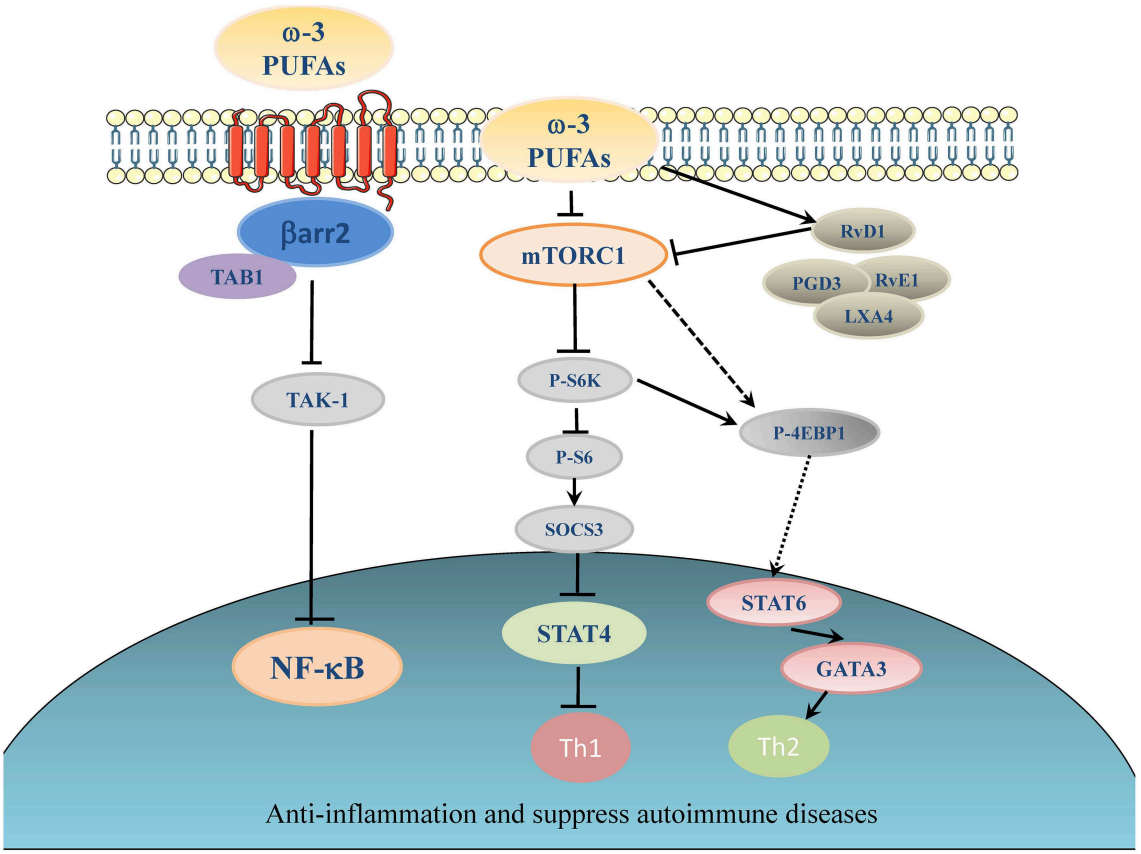

FIGURE 1 | Proposed working model of ω-3 PUFAs induced inhibitory effect on inflammation and autoimmunity. Elevation of ω-3 PUFAs can stimulate one of its major receptors, GPR120. GPR120 couples to β-arrestin2 and inhibit TAB1-mediated activation of TAK1, providing a mechanism for inhibition of NF-κB related pro-inflammatory signaling pathways in autoimmune disease (103, 109). ω-3 PUFAs and their metabolites suppress the activation of Th1 cells through inhibiting of mTORC1 (80, 110, 111), which in turn activates suppressor of cytokine signaling (SOCS) (112). ω-3 PUFAs can inhibit signal transducer and activator of transcription (STAT) 4 which is essential for the development of Th1 cells from naive $CD4^+$ T cells (113). In another signaling pathway, ω-3 PUFAs can dictate the differentiation toward Th2 cells by activating 4E-BP1 through dephosphorylation and then stimulate STAT6 (80).

not all clinical studies yielded positive outcomes. Torkildsen et al. evaluated the effect of ω-3 PUFAs on MS disease severity in a randomized, double-blind, and placebo-controlled trial (57) (**Table 4**). They applied 1,350 mg of EPA plus 850 mg of DHA daily in the treatment group with placebo as the control group for 6 months. Magnetic resonance imaging (MRI) was applied to quantify the number of new T1-weighted gadolinium-enhancing lesions during the first 6 months. Relapse rate, disability progression, fatigue, and quality of life were measured after 9 and 24 months. There was no difference between the ω-3 PUFAs and placebo groups during the first 6 months in the number of new gadolinium-enhancing MRI lesions, as well as in disease activity after 6 months or 24 months (57) (**Table 4**). It is still unclear about the discrepancy of outcomes in different trials although the dosage, the source and concentrations of EPA/DHA agents, the duration of the trial, and the methods of evaluation all could have led to the different results at the end of the trial.

Some of the positive clinical observations mentioned above prompted a series of cellular and animal research studies about the effects of ω-3 PUFAs on MS development. As described above, several different groups (including our own) have reported that ω-3 PUFAs could inhibit the activation of NF-κB via increasing the expression of PPARs (24, 30, 125–128), which in turn reduces the production of inflammatory markers. In a combinatorial treatment with DHA and all-trans-retinoic acid (a bioactive derivative of vitamin A), the expression of IL-17 and RORγt gene, which is vital for the initiation and progression of MS, was significantly attenuated in the PBMCs isolated from the patients with relapsing-remitting multiple sclerosis (129). Addition of EPA and DHA in cultured cells significantly decreased the production and activity of matrix metalloproteinase-9 (MMP-9) and inhibited the migration of human T cell derived from the PBMCs from MS patients, which implied the reduction of infiltrating capability of T-cells (130).

Kong et al. first reported in 2011 that dietary ω-3 fatty acids could suppress EAE in an animal model (73). Their extensive work showed that pretreatment of bone marrow-derived dendritic cells (DC) with DHA could prevent LPS-induced DC

maturation and weaken the stimulation of antigen-specific T cells (73). Consistent with these *in vitro* observations, the results from the animal model further demonstrated decreased numbers of IFNγ- and IL-17-producing $CD4^+$ T cells in both spleen and CNS (73). In another independent study, the mice with myelin oligodendrocyte glycoprotein (MOG)-induced EAE showed a significant delay in onset and amelioration in severity by DHA-enriched diet (131). In such context, the female mice were fed 4 weeks of either the control diet, or the diet containing 0.3 or 1.0% DHA in either phospholipid (PL) form or triacylglycerol (TAG) form pre-EAE induction and for 4 weeks post-EAE induction. The TAG-form DHA appeared to be effective in lower daily scores in the early phase of EAE during day 9–16 while PL-form DHA was effective in decreasing daily scores in the final outcome during day 23–28 (131). Increasing EPA content in the diet appeared to have the benefit similar to that of DHA-enriched diet. Unoda et al. found that EPA-enriched diet significantly lowered clinical EAE scores, and remarkably inhibited the production of IFN-γ and IL-17 (132). Consistent with these findings in the nutritional intervention studies, modeling of MS with cuprizone in the fat-1 mice revealed that endogenous production of ω-3 PUFAs strongly promoted remyelination after a toxic injury to CNS oligodendrocytes via modulation of the immune system (133, 134). Interestingly, some of the protective effects were mediated at least in part through EPA-derived lipid metabolites, such as 18-HEPE by acting directly on oligodendrocytes and neurons (133, 134). Taken together, the findings coming out of the clinical investigations and animal models provided the hope of applying high dose of EPA/DHA agents in the treatment of MS.

CONCLUSION

The promising findings coming from the cumulative research work over the last decade solidified the role of ω-3 PUFAs as a potential candidate to prevent or even treat such autoimmune diseases as type 1 diabetes, RA, SLE, MS. Undoubtedly, many of the beneficial effects of ω-3 PUFAs can be traced back to their anti-inflammation actions; however, other mechanisms, such as the regulation of mTOR activity may also be in place. Although still facing some technical issues, particularly clinical evaluation of efficacy and safety, the use of high dosages of EPA/DHA or fat-1 gene therapy to generate endogenousω-3 PUFAs have a huge potential in the clinical treatment of these debilitating diseases.

AUTHOR CONTRIBUTIONS

XB and XL wrote the manuscript. AZ oversaw the editing. XL, SW, ZZ, FL, and AZ revised the manuscript. All authors read and approved the final manuscript.

FUNDING

This work was supported by grants from the Guangdong Innovative Research Team Program (2016ZT06Y432 to AZ and FL), the National Natural Science Foundation of China (NSFC) (81630021 to AZ; 81372798 to FL; 81700690 to XB), the Special Grants of China Postdoctoral Science Fund (2018T110852 to XB), the Jiangsu Government Scholarship for Overseas Studies (to XL), and the National Key R&D Program of China (2018YFA0800603 to AZ).

REFERENCES

1. Dusheck J. Fish, fatty acids and physiology. *Sci News*. (1985) 128:252–4. doi: 10.2307/3970056
2. Holman RT. The slow discovery of the importance of omega 3 essential fatty acids in human health. *J Nutr*. (1998) 128 (2 Suppl):427S−33S. doi: 10.1093/jn/128.2.427S
3. Wall R, Ross RP, Fitzgerald GF, Stanton C. Fatty acids from fish: the anti-inflammatory potential of long-chain omega-3 fatty acids. *Nutr Rev*. (2010) 68:280–9. doi: 10.1111/j.1753-4887.2010.00287.x
4. Kang JX. The importance of omega-6/omega-3 fatty acid ratio in cell function. The gene transfer of omega-3 fatty acid desaturase. *World Rev Nutr Diet*. (2003) 92:23–36. doi: 10.1159/000073790
5. Aghdassi E, Ma DW, Morrison S, Hillyer LM, Clarke S, Gladman DD, et al. Alterations in circulating fatty acid composition in patients with systemic lupus erythematosus: a pilot study. *JPEN J Parenter Enteral Nutr*. (2011) 35:198–208. doi: 10.1177/0148607110386378
6. Jump DB. The biochemistry of n-3 polyunsaturated fatty acids. *J Biol Chem*. (2002) 277:8755–8. doi: 10.1074/jbc.R100062200
7. Kennedy EP. Biosynthesis of complex lipids. *Fed Proc*. (1961) 20:934–40.
8. Calder PC, Yaqoob P. Understanding omega-3 polyunsaturated fatty acids. *Postgrad Med*. (2009) 121:148–57. doi: 10.3810/pgm.2009.11.2083
9. Abedi E, Sahari MA. Long-chain polyunsaturated fatty acid sources and evaluation of their nutritional and functional properties. *Food Sci Nutr*. (2014) 2:443–63. doi: 10.1002/fsn3.121
10. Huang YS, Smith RS, Redden PR, Cantrill RC, Horrobin DF. Modification of liver fatty acid metabolism in mice by n-3 and n-6 delta 6-desaturase substrates and products. *Biochim Biophys Acta*. (1991) 1082:319–27. doi: 10.1016/0005-2760(91)90208-Y
11. Yamazaki K, Fujikawa M, Hamazaki T, Yano S, Shono T. Comparison of the conversion rates of alpha-linolenic acid. (18:3. (n - 3)) and stearidonic acid. (18:4. (n - 3)) to longer polyunsaturated fatty acids in rats. *Biochim Biophys Acta*. (1992) 1123:18–26. doi: 10.1016/0005-2760(92)90166-S
12. Gregory MK, Gibson RA, Cook-Johnson RJ, Cleland LG, James MJ. Elongase reactions as control points in long-chain polyunsaturated fatty acid synthesis. *PLoS ONE*. (2011) 6:e29662. doi: 10.1371/journal.pone.0029662
13. Serhan CN, Clish CB, Brannon J, Colgan SP, Chiang N, Gronert K. Novel functional sets of lipid-derived mediators with antiinflammatory actions generated from omega-3 fatty acids via cyclooxygenase 2-nonsteroidal antiinflammatory drugs and transcellular processing. *J Exp Med*. (2000) 192:1197–204. doi: 10.1084/jem.192.8.1197
14. Serhan CN, Gotlinger K, Hong S, Lu Y, Siegelman J, Baer T, et al. Anti-inflammatory actions of neuroprotectin D1/protectin D1 and its natural stereoisomers: assignments of dihydroxy-containing docosatrienes. *J Immunol*. (2006) 176:1848–59. doi: 10.4049/jimmunol.176.3.1848
15. Hong S, Gronert K, Devchand PR, Moussignac RL, Serhan CN. Novel docosatrienes and 17S-resolvins generated from docosahexaenoic acid in murine brain, human blood, and glial cells - Autacoids in anti-inflammation. *J Biol Chem*. (2003) 278:14677–87. doi: 10.1074/jbc.M300218200
16. Schmitz G, Ecker J. The opposing effects of n-3 and n-6 fatty acids. *Progress Lipid Res*. (2008) 47:147–55. doi: 10.1016/j.plipres.2007.12.004
17. Serhan CN, Petasis NA. Resolvins and protectins in inflammation resolution. *Chem Rev*. (2011) 111:5922–43. doi: 10.1021/cr100396c
18. Neuhofer A, Zeyda M, Mascher D, Itariu BK, Murano I, Leitner L, et al. Impaired local production of proresolving lipid mediators in obesity and 17-HDHA as a potential treatment for obesity-associated inflammation. *Diabetes*. (2013) 62:1945–56. doi: 10.2337/db12-0828

19. Watson JE, Kim JS, Das A. Emerging class of omega-3 fatty acid endocannabinoids & their derivatives. *Prostaglandins Other Lipid Mediat*. (2019) 143:106337. doi: 10.1016/j.prostaglandins.2019.106337
20. Fritsche K. Fatty acids as modulators of the immune response. *Annu Rev Nutr*. (2006) 26:45–73. doi: 10.1146/annurev.nutr.25.050304.092610
21. Kang JX, Liu A. The role of the tissue omega-6/omega-3 fatty acid ratio in regulating tumor angiogenesis. *Cancer Metastasis Rev*. (2013) 32:201–10. doi: 10.1007/s10555-012-9401-9
22. Maskrey BH, Megson IL, Rossi AG, Whitfield PD. Emerging importance of omega-3 fatty acids in the innate immune response: molecular mechanisms and lipidomic strategies for their analysis. *Molecul Nutr Food Res*. (2013) 57:1390–400. doi: 10.1002/mnfr.201200723
23. Terry P, Wolk A, Vainio H, Weiderpass E. Fatty fish consumption lowers the risk of endometrial cancer: a nationwide case-control study in Sweden. *Cancer Epidemiol Biomark Preven*. (2002) 11:143–5.
24. Li J, Li FR, Wei D, Jia W, Kang JX, Stefanovic-Racic M, et al. Endogenous omega-3 polyunsaturated fatty acid production confers resistance to obesity, dyslipidemia, and diabetes in mice. *Mol Endocrinol*. (2014) 28:1316–28. doi: 10.1210/me.2014-1011
25. Zhang W, Wang H, Zhang H, Leak RK, Shi Y, Hu X, et al. Dietary supplementation with omega-3 polyunsaturated fatty acids robustly promotes neurovascular restorative dynamics and improves neurological functions after stroke. *Exp Neurol*. (2015) 272:170–80. doi: 10.1016/j.expneurol.2015.03.005
26. Boston PF, Bennett A, Horrobin DF, Bennett CN. Ethyl-EPA in Alzheimer's disease–a pilot study. *Prostag Leukot Essential Fatty Acids*. (2004) 71:341–6. doi: 10.1016/j.plefa.2004.07.001
27. Kang JX, Wang J, Wu L, Kang ZB. Transgenic mice: fat-1 mice convert n-6 to n-3 fatty acids. *Nature*. (2004) 427:504. doi: 10.1038/427504a
28. Kang JX. Fat-1 transgenic mice: a new model for omega-3 research. *Prostag Leukotr Ess*. (2007) 77:263–7. doi: 10.1016/j.plefa.2007.10.010
29. Hudert CA, Weylandt KH, Lu Y, Wang J, Hong S, Dignass A, et al. Transgenic mice rich in endogenous omega-3 fatty acids are protected from colitis. *Proc Natl Acad Sci USA*. (2006) 103:11276–81. doi: 10.1073/pnas.0601280103
30. Wei D, Li J, Shen M, Jia W, Chen N, Chen T, et al. Cellular production of n-3 PUFAs and reduction of n-6-to-n-3 ratios in the pancreatic beta-cells and islets enhance insulin secretion and confer protection against cytokine-induced cell death. *Diabetes*. (2010) 59:471–8. doi: 10.2337/db09-0284
31. Miles EA, Calder PC. Influence of marine n-3 polyunsaturated fatty acids on immune function and a systematic review of their effects on clinical outcomes in rheumatoid arthritis. *Br J Nutr*. (2012) 107(Suppl 2):S171–84. doi: 10.1017/S0007114512001560
32. de Medeiros MCS, Medeiros JCA, de Medeiros HJ, Leitão JCGdC, Knackfuss MI. Dietary intervention and health in patients with systemic lupus erythematosus: a systematic review of the evidence. *Crit Rev Food Sci Nutri*. 17:1–8. doi: 10.1080/10408398.2018.1463966
33. Virtanen SM. Dietary factors in the development of type 1 diabetes. *Pediatr Diabet*. (2016) 17:49–55. doi: 10.1111/pedi.12341
34. Mische LJ, Mowry EM. The evidence for dietary interventions and nutritional supplements as treatment options in multiple sclerosis: a review. *Curr Treat Options Neurol*. (2018) 20:8. doi: 10.1007/s11940-018-0494-5
35. Kremer JM, Bigauoette J, Michalek AV, Timchalk MA, Lininger L, Rynes RI, et al. Effects of manipulation of dietary fatty acids on clinical manifestations of rheumatoid arthritis. *Lancet*. (1985) 1:184–7. doi: 10.1016/S0140-6736(85)92024-0
36. Kremer JM, Lawrence DA, Jubiz W, DiGiacomo R, Rynes R, Bartholomew LE, et al. Dietary fish oil and olive oil supplementation in patients with rheumatoid arthritis. Clinical and immunologic effects. *Arthr Rheumat*. (1990) 33:810–20. doi: 10.1002/art.1780330607
37. Veselinovic M, Vasiljevic D, Vucic V, Arsic A, Petrovic S, Tomic-Lucic A, et al. Clinical benefits of n-3 PUFA and. (sic)-linolenic acid in patients with rheumatoid arthritis. *Nutrients*. (2017) 9:E325. doi: 10.3390/nu9040325
38. Beyer K, Lie SA, Kjellevold M, Dahl L, Brun JG, Bolstad AI. Marine omega-3, vitamin D levels, disease outcome and periodontal status in rheumatoid arthritis outpatients. *Nutrition*. (2018) 55–56:116–24. doi: 10.1016/j.nut.2018.03.054
39. van der Tempel H, Tulleken JE, Limburg PC, Muskiet FA, van Rijswijk MH. Effects of fish oil supplementation in rheumatoid arthritis. *Ann Rheum Dis*. (1990) 49:76–80. doi: 10.1136/ard.49.2.76
40. Lee YH, Bae SC, Song GG. Omega-3 polyunsaturated fatty acids and the treatment of rheumatoid arthritis: a meta-analysis. *Arch Med Res*. (2012) 43:356–62. doi: 10.1016/j.arcmed.2012.06.011
41. Espersen GT, Grunnet N, Lervang HH, Nielsen GL, Thomsen BS, Faarvang KL, et al. Decreased interleukin-1 beta levels in plasma from rheumatoid arthritis patients after dietary supplementation with n-3 polyunsaturated fatty acids. *Clin Rheumatol*. (1992) 11:393–5. doi: 10.1007/BF02207200
42. Clark WF, Parbtani A, Huff MW, Reid B, Holub BJ, Falardeau P. Omega-3 fatty acid dietary supplementation in systemic lupus erythematosus. *Kidney Int*. (1989) 36:653–60. doi: 10.1038/ki.1989.242
43. Westberg G, Tarkowski A. Effect of MaxEPA in patients with SLE. A double-blind, crossover study. *Scand J Rheumatol*. (1990) 19:137–43. doi: 10.3109/03009749009102117
44. Das UN. Beneficial effect of eicosapentaenoic and docosahexaenoic acids in the management of systemic lupus erythematosus and its relationship to the cytokine network. *Prostag Leuk Essential Fatty Acids*. (1994) 51:207–13. doi: 10.1016/0952-3278(94)90136-8
45. Duffy EM, Meenagh GK, McMillan SA, Strain JJ, Hannigan BM, Bell AL. The clinical effect of dietary supplementation with omega-3 fish oils and/or copper in systemic lupus erythematosus. *J Rheumatol*. (2004) 31:1551–6.
46. Elkan AC, Anania C, Gustafsson T, Jogestrand T, Hafstrom I, Frostegard J. Diet and fatty acid pattern among patients with SLE: associations with disease activity, blood lipids and atherosclerosis. *Lupus*. (2012) 21:1405–11. doi: 10.1177/0961203312458471
47. Arriens C, Hynan LS, Lerman RH, Karp DR, Mohan C. Placebo-controlled randomized clinical trial of fish oil's impact on fatigue, quality of life, and disease activity in Systemic Lupus Erythematosus. *Nutr J*. (2015) 14:82. doi: 10.1186/s12937-015-0068-2
48. Bello KJ, Fang H, Fazeli P, Bolad W, Corretti M, Magder LS, et al. Omega-3 in SLE: a double-blind, placebo-controlled randomized clinical trial of endothelial dysfunction and disease activity in systemic lupus erythematosus. *Rheumatol Int*. (2013) 33:2789–96. doi: 10.1007/s00296-013-2811-3
49. Stene LC, Joner G. Use of cod liver oil during the first year of life is associated with lower risk of childhood-onset type 1 diabetes: a large, population-based, case-control study. *Am J Clin Nutr*. (2003) 78:1128–34. doi: 10.1093/ajcn/78.6.1128
50. Norris JM, Yin X, Lamb MM, Barriga K, Seifert J, Hoffman M, et al. Omega-3 polyunsaturated fatty acid intake and islet autoimmunity in children at increased risk for type 1 diabetes. *JAMA*. (2007) 298:1420–8. doi: 10.1001/jama.298.12.1420
51. Cadario F, Savastio S, Ricotti R, Rizzo AM, Carrera D, Maiuri L, et al. Administration of vitamin D and high dose of omega 3 to sustain remission of type 1 diabetes. *Eur Rev Med Pharmacol Sci*. (2018) 22:512–5. doi: 10.26355/eurrev_201801_14203
52. Chase HP, Boulware D, Rodriguez H, Donaldson D, Chritton S, Rafkin-Mervis L, et al. Effect of docosahexaenoic acid supplementation on inflammatory cytokine levels in infants at high genetic risk for type 1 diabetes. *Pediatr Diabet*. (2015) 16:271–9. doi: 10.1111/pedi.12170
53. Nordvik I, Myhr KM, Nyland H, Bjerve KS. Effect of dietary advice and n-3 supplementation in newly diagnosed MS patients. *Acta Neurol Scand*. (2000) 102:143–9. doi: 10.1034/j.1600-0404.2000.102003143.x
54. Kouchaki E, Afarini M, Abolhassani J, Mirhosseini N, Bahmani F, Masoud SA, et al. High-dose omega-3 fatty acid plus vitamin D3 supplementation affects clinical symptoms and metabolic status of patients with multiple sclerosis: a randomized controlled clinical trial. *J Nutr*. (2018) 148:1380–6. doi: 10.1093/jn/nxy116
55. Hoare S, Lithander F, van der Mei I, Ponsonby AL, Lucas R, Grp AI. Higher intake of omega-3 polyunsaturated fatty acids is associated with a decreased risk of a first clinical diagnosis of central nervous system demyelination: results from the ausimmune study. *Mult Scler J*. (2016) 22:884–92. doi: 10.1177/1352458515604380
56. Weinstock-Guttman B, Baier M, Park Y, Feichter J, Lee-Kwen P, Gallagher E, et al. Low fat dietary intervention with omega-3 fatty acid supplementation

in multiple sclerosis patients. *Prostag Leuk Essential Fatty Acids*. (2005) 73:397–404. doi: 10.1016/j.plefa.2005.05.024
57. Torkildsen O, Wergeland S, Bakke S, Beiske AG, Bjerve KS, Hovdal H, et al. omega-3 fatty acid treatment in multiple sclerosis. (OFAMS Study) a randomized, double-blind, placebo-controlled trial. *Arch Neurol-Chicago*. (2012) 69:1044–51. doi: 10.1001/archneurol.2012.283
58. Hoxha M. A systematic review on the role of eicosanoid pathways in rheumatoid arthritis. *Adv Med Sci*. (2018) 63:22–9. doi: 10.1016/j.advms.2017.06.004
59. McInnes IB, Schett G. Cytokines in the pathogenesis of rheumatoid arthritis. *Nat Rev Immunol*. (2007) 7:429–42. doi: 10.1038/nri2094
60. Tsokos GC. B cells, be gone — b-cell depletion in the treatment of rheumatoid arthritis. *New Engl J Med*. (2004) 350:2546–8. doi: 10.1056/NEJMp048114
61. Leslie CA, Gonnerman WA, Ullman MD, Hayes KC, Franzblau C, Cathcart ES. Dietary fish oil modulates macrophage fatty acids and decreases arthritis susceptibility in mice. *J Exp Med*. (1985) 162:1336–49. doi: 10.1084/jem.162.4.1336
62. Ierna M, Kerr A, Scales H, Berge K, Griinari M. Supplementation of diet with krill oil protects against experimental rheumatoid arthritis. *BMC Musculoskelet Disord*. (2010) 11:136. doi: 10.1186/1471-2474-11-136
63. Volker DH, FitzGerald PE, Garg ML. The eicosapentaenoic to docosahexaenoic acid ratio of diets affects the pathogenesis of arthritis in Lew/SSN rats. *J Nutr*. (2000) 130:559–65. doi: 10.1093/jn/130.3.559
64. Woo SJ, Lim K, Park SY, Jung MY, Lim HS, Jeon MG, et al. Endogenous conversion of n-6 to n-3 polyunsaturated fatty acids attenuates K/BxN serum-transfer arthritis in fat-1 mice. *J Nutr Biochem*. (2015) 26:713–20. doi: 10.1016/j.jnutbio.2015.01.011
65. Caughey GE, Mantzioris E, Gibson RA, Cleland LG, James MJ. The effect on human tumor necrosis factor alpha and interleukin 1 beta production of diets enriched in n-3 fatty acids from vegetable oil or fish oil. *Am J Clin Nutr*. (1996) 63:116–22. doi: 10.1093/ajcn/63.1.116
66. Finnegan YE, Minihane AM, Leigh-Firbank EC, Kew S, Meijer GW, Muggli R, et al. Plant- and marine-derived n-3 polyunsaturated fatty acids have differential effects on fasting and postprandial blood lipid concentrations and on the susceptibility of LDL to oxidative modification in moderately hyperlipidemic subjects. *Am J Clin Nutr*. (2003) 77:783–95. doi: 10.1093/ajcn/77.4.783
67. Miles EA, Banerjee T, Dooper MM, M'Rabet L, Graus YM, Calder PC. The influence of different combinations of gamma-linolenic acid, stearidonic acid and EPA on immune function in healthy young male subjects. *Br J Nutr*. (2004) 91:893–903. doi: 10.1079/BJN20041131
68. Kew S, Mesa MD, Tricon S, Buckley R, Minihane AM, Yaqoob P. Effects of oils rich in eicosapentaenoic and docosahexaenoic acids on immune cell composition and function in healthy humans. *Am J Clin Nutr*. (2004) 79:674–81. doi: 10.1093/ajcn/79.4.674
69. Rosu A, Margaritescu C, Stepan A, Musetescu A, Ene M. IL-17 patterns in synovium, serum and synovial fluid from treatment-naive, early rheumatoid arthritis patients. *Rom J Morphol Embryol*. (2012) 53:73–80.
70. Moon YM, Yoon BY, Her YM, Oh HJ, Lee JS, Kim KW, et al. IL-32 and IL-17 interact and have the potential to aggravate osteoclastogenesis in rheumatoid arthritis. *Arthritis Res Ther*. (2012) 14:R246. doi: 10.1186/ar4089
71. Qin S, Wen J, Bai XC, Chen TY, Zheng RC, Zhou GB, et al. Endogenous n-3 polyunsaturated fatty acids protect against imiquimod-induced psoriasis-like inflammation via the IL-17/IL-23 axis. *Mol Med Rep*. (2014) 9:2097–104. doi: 10.3892/mmr.2014.2136
72. Ye P, Li J, Wang S, Xie A, Sun W, Xia J. Eicosapentaenoic acid disrupts the balance between Tregs and IL-17+ T cells through PPARγ nuclear receptor activation and protects cardiac allografts. *J Surg Res*. (2012) 173:161–70. doi: 10.1016/j.jss.2010.08.052
73. Kong W, Yen JH, Ganea D. Docosahexaenoic acid prevents dendritic cell maturation, inhibits antigen-specific Th1/Th17 differentiation and suppresses experimental autoimmune encephalomyelitis. *Brain Behav Immun*. (2011) 25:872–82. doi: 10.1016/j.bbi.2010.09.012
74. Allen MJ, Fan YY, Monk JM, Hou TY, Barhoumi R, McMurray DN, et al. n-3 PUFAs reduce T-helper 17 cell differentiation by decreasing responsiveness to interleukin-6 in isolated mouse splenic CD4. (+) T cells. *J Nutr*. (2014) 144:1306–13. doi: 10.3945/jn.114.194407
75. Babcock TA, Novak T, Ong E, Jho DH, Helton WS, Espat NJ. Modulation of lipopolysaccharide-stimulated macrophage tumor necrosis factor-alpha production by omega-3 fatty acid is associated with differential cyclooxygenase-2 protein expression and is independent of interleukin-10. *J Surg Res*. (2002) 107:135–9. doi: 10.1006/jsre.2002.6498
76. Novak TE, Babcock TA, Jho DH, Helton WS, Espat NJ. NF-kappa B inhibition by omega−3 fatty acids modulates LPS-stimulated macrophage TNF-alpha transcription. *Am J Physiol Lung Cell Mol Physiol*. (2003) 284:L84–9. doi: 10.1152/ajplung.00077.2002
77. Zhao Y, Joshi-Barve S, Barve S, Chen LH. Eicosapentaenoic acid prevents LPS-induced TNF-alpha expression by preventing NF-kappaB activation. *J Am Coll Nutr*. (2004) 23:71–8. doi: 10.1080/07315724.2004.10719345
78. Trebble T, Arden NK, Stroud MA, Wootton SA, Burdge GC, Miles EA, et al. Inhibition of tumour necrosis factor-α and interleukin 6 production by mononuclear cells following dietary fish-oil supplementation in healthy men and response to antioxidant co-supplementation. *Br J Nutr*. (2003) 90:405–12. doi: 10.1079/BJN2003892
79. Pompos LJ, Fritsche KL. Antigen-driven murine CD4+ T lymphocyte proliferation and interleukin-2 production are diminished by dietary. (n-3) polyunsaturated fatty acids. *J Nutr*. (2002) 132:3293–300. doi: 10.1093/jn/132.11.3293
80. Bi X, Li F, Liu S, Jin Y, Zhang X, Yang T, et al. omega-3 polyunsaturated fatty acids ameliorate type 1 diabetes and autoimmunity. *J Clin Invest*. (2017) 127:1757–71. doi: 10.1172/JCI87388
81. Meydani SN, Endres S, Woods MM, Goldin BR, Soo C, Morrill-Labrode A, et al. Oral. (n-3) fatty acid supplementation suppresses cytokine production and lymphocyte proliferation: comparison between young and older women. *J Nutr*. (1991) 121:547–55. doi: 10.1093/jn/121.4.547
82. Soyland E, Nenseter MS, Braathen L, Drevon CA. Very long chain n-3 and n-6 polyunsaturated fatty acids inhibit proliferation of human T-lymphocytes *in vitro*. *Eur J Clin Invest*. (1993) 23:112–21. doi: 10.1111/j.1365-2362.1993.tb00750.x
83. Terada S, Takizawa M, Yamamoto S, Ezaki O, Itakura H, Akagawa KS. Suppressive mechanisms of EPA on human T cell proliferation. *Microbiol Immunol*. (2001) 45:473–81. doi: 10.1111/j.1348-0421.2001.tb02647.x
84. Mizota T, Fujita-Kambara C, Matsuya N, Hamasaki S, Fukudome T, Goto H, et al. Effect of dietary fatty acid composition on Th1/Th2 polarization in lymphocytes. *JPEN J Parent Enteral Nutr*. (2009) 33:390–6. doi: 10.1177/0148607108325252
85. Sierra S, Lara-Villoslada F, Comalada M, Olivares M, Xaus J. Dietary fish oil n-3 fatty acids increase regulatory cytokine production and exert anti-inflammatory effects in two murine models of inflammation. *Lipids*. (2006) 41:1115–25. doi: 10.1007/s11745-006-5061-2
86. Suzuki D, Furukawa K, Kimura F, Shimizu H, Yoshidome H, Ohtsuka M, et al. Effects of perioperative immunonutrition on cell-mediated immunity, T helper type 1. (Th1)/Th2 differentiation, and Th17 response after pancreaticoduodenectomy. *Surgery*. (2010) 148:573–81. doi: 10.1016/j.surg.2010.01.017
87. Khair-el-Din TA, Sicher SC, Vazquez MA, Wright WJ, Lu CY. Docosahexaenoic acid, a major constituent of fetal serum and fish oil diets, inhibits IFN gamma-induced Ia-expression by murine macrophages *in vitro*. *J Immunol*. (1995) 154:1296–306.
88. Hughes DA, Pinder AC. N-3 polyunsaturated fatty acids modulate the expression of functionally associated molecules on human monocytes and inhibit antigen-presentation *in vitro*. *Clin Exp Immunol*. (1997) 110:516–23. doi: 10.1046/j.1365-2249.1997.4351455.x
89. Hughes DA, Pinder AC, Piper Z, Johnson IT, Lund EK. Fish oil supplementation inhibits the expression of major histocompatibility complex class II molecules and adhesion molecules on human monocytes. *Am J Clin Nutr*. (1996) 63:267–72. doi: 10.1093/ajcn/63.2.267
90. Calder PC. Polyunsaturated fatty acids alter the rules of engagement. *Future Lipidol*. (2007) 2:27–30. doi: 10.2217/17460875.2.1.27

91. Hughes DA, Pinder AC. n-3 polyunsaturated fatty acids inhibit the antigen-presenting function of human monocytes. *Am J Clin Nutr*. (2000) 71 (Suppl 1):357S−60S. doi: 10.1093/ajcn/71.1.357s
92. Jolly CA, Muthukumar A, Avula CP, Troyer D, Fernandes G. Life span is prolonged in food-restricted autoimmune-prone. (NZB x NZW)F. (1) mice fed a diet enriched with. (n-3) fatty acids. *J Nutr*. (2001) 131:2753–60. doi: 10.1093/jn/131.10.2753
93. Yaniv G, Twig G, Shor DB, Furer A, Sherer Y, Mozes O, et al. A volcanic explosion of autoantibodies in systemic lupus erythematosus: a diversity of 180 different antibodies found in SLE patients. *Autoimmun Rev*. (2015) 14:75–9. doi: 10.1016/j.autrev.2014.10.003
94. Rose T, Dorner T. Drivers of the immunopathogenesis in systemic lupus erythematosus. *Best Pract Res Clin Rheumatol*. (2017) 31:321–33. doi: 10.1016/j.berh.2017.09.007
95. Navarini L, Bisogno T, Margiotta DPE, Piccoli A, Angeletti S, Laudisio A, et al. Role of the specialized proresolving mediator resolvin D1 in systemic lupus erythematosus: preliminary results. *J Immunol Res*. (2018). doi: 10.1155/2018/5264195
96. Fernandes G, Bysani C, Venkatraman JT, Tomar V, Zhao W. Increased TGF-beta and decreased oncogene expression by omega-3 fatty acids in the spleen delays onset of autoimmune disease in B/W mice. *J Immunol*. (1994) 152:5979–87.
97. Chandrasekar B, Troyer DA, Venkatraman JT, Fernandes G. Dietary omega-3 lipids delay the onset and progression of autoimmune lupus nephritis by inhibiting transforming growth factor beta mRNA and protein expression. *J Autoimmun*. (1995) 8:381–93. doi: 10.1006/jaut.1995.0030
98. Reifen R, Blank M, Afek A, Kopilowiz Y, Sklan D, Gershwin ME, et al. Dietary polyunsaturated fatty acids decrease anti-dsDNA and anti-cardiolipin antibodies production in idiotype induced mouse model of systemic lupus erythematosus. *Lupus*. (1998) 7:192–7. doi: 10.1191/096120398678919985
99. Halade GV, Williams PJ, Veigas JM, Barnes JL, Fernandes G. Concentrated fish oil. (Lovaza. (R)) extends lifespan and attenuates kidney disease in lupus-prone short-lived. (NZBxNZW)F1 mice. *Exp Biol Med*. (2013) 238:610–22. doi: 10.1177/1535370213489485
100. Pestka JJ, Vines LL, Bates MA, He K, Langohr I. Comparative effects of n-3, n-6 and n-9 unsaturated fatty acid-rich diet consumption on lupus nephritis, autoantibody production and CD4+ T cell-related gene responses in the autoimmune NZBWF1 mouse. *PLoS ONE*. (2014) 9:e100255. doi: 10.1371/journal.pone.0100255
101. Wallberg M, Cooke A. Immune mechanisms in type 1 diabetes. *Trends Immunol*. (2013) 34:583–91. doi: 10.1016/j.it.2013.08.005
102. Lehuen A, Diana J, Zaccone P, Cooke A. Immune cell crosstalk in type 1 diabetes. *Nat Rev Immunol*. (2010) 10:501–13. doi: 10.1038/nri2787
103. Kagohashi Y, Abiru N, Kobayashi M, Hashimoto M, Shido O, Otani H. Maternal dietary n-6/n-3 fatty acid ratio affects type 1 diabetes development in the offspring of non-obese diabetic mice. *Congen Anom*. (2010) 50:212–20. doi: 10.1111/j.1741-4520.2010.00296.x
104. Kagohashi Y, Otani H. Diet with a low n-6/n-3 essential fatty acid ratio when started immediately after the onset of overt diabetes prolongs survival of type 1 diabetes model NOD mice. *Congen Anom*. (2010) 50:226–31. doi: 10.1111/j.1741-4520.2010.00289.x
105. Schmid S, Koczwara K, Schwinghammer S, Lampasona V, Ziegler AG, Bonifacio E. Delayed exposure to wheat and barley proteins reduces diabetes incidence in non-obese diabetic mice. *Clin Immunol*. (2004) 111:108–18. doi: 10.1016/j.clim.2003.09.012
106. Winzell MS, Pacini G, Ahren B. Insulin secretion after dietary supplementation with conjugated linoleic acids and n-3 polyunsaturated fatty acids in normal and insulin-resistant mice. *Am J Physiol Endocrinol Metabol*. (2006) 290:E347–54. doi: 10.1152/ajpendo.00163.2005
107. Kato T, Shimano H, Yamamoto T, Ishikawa M, Kumadaki S, Matsuzaka T, et al. Palmitate impairs and eicosapentaenoate restores insulin secretion through regulation of SREBP-1c in pancreatic islets. *Diabetes*. (2008) 57:2382–92. doi: 10.2337/db06-1806
108. Patterson E, Wall R, Fitzgerald GF, Ross RP, Stanton C. Health implications of high dietary omega-6 polyunsaturated fatty acids. *J Nutr Metabol*. (2012) 2012:539426. doi: 10.1155/2012/539426
109. Oh da Y, Walenta E, Akiyama TE, Lagakos WS, Lackey D, Pessentheiner AR, et al. A Gpr120-selective agonist improves insulin resistance and chronic inflammation in obese mice. *Nat Med*. (2014) 20:942–7. doi: 10.1038/nm.3614
110. Chi H. Regulation and function of mTOR signalling in T cell fate decisions. *Nat Rev Immunol*. (2012) 12:325–38. doi: 10.1038/nri3198
111. Delgoffe GM, Pollizzi KN, Waickman AT, Heikamp E, Meyers DJ, Horton MR, et al. The kinase mTOR regulates the differentiation of helper T cells through the selective activation of signaling by mTORC1 and mTORC2. *Nat Immunol*. (2011) 12:295–303. doi: 10.1038/ni.2005
112. White CA, Nicola NA. SOCS3. *JAK-STAT*. (2013) 2:e25045. doi: 10.4161/jkst.25045
113. Powell JD, Pollizzi KN, Heikamp EB, Horton MR. Regulation of immune responses by mTOR. *Ann Rev Immunol*. (2012) 30:39–68. doi: 10.1146/annurev-immunol-020711-075024
114. Ichimura A, Hirasawa A, Poulain-Godefroy O, Bonnefond A, Hara T, Yengo L, et al. Dysfunction of lipid sensor GPR120 leads to obesity in both mouse and human. *Nature*. (2012) 483:350–4. doi: 10.1038/nature10798
115. Delgoffe GM, Kole TP, Zheng Y, Zarek PE, Matthews KL, Xiao B, et al. The mTOR kinase differentially regulates effector and regulatory T cell lineage commitment. *Immunity*. (2009) 30:832–44. doi: 10.1016/j.immuni.2009.04.014
116. Bellenger J, Bellenger S, Bataille A, Massey KA, Nicolaou A, Rialland M, et al. High pancreatic n-3 fatty acids prevent STZ-induced diabetes in fat-1 mice: inflammatory pathway inhibition. *Diabetes*. (2011) 60:1090–9. doi: 10.2337/db10-0901
117. Frischer JM, Bramow S, Dal-Bianco A, Lucchinetti CF, Rauschka H, Schmidbauer M, et al. The relation between inflammation and neurodegeneration in multiple sclerosis brains. *Brain*. (2009) 132(Pt 5):1175–89. doi: 10.1093/brain/awp070
118. Harbige LS, Sharief MK. Polyunsaturated fatty acids in the pathogenesis and treatment of multiple sclerosis. *Br J Nutr*. (2007) 98(Suppl 1):S46–53. doi: 10.1017/S0007114507833010
119. Lublin FD, Reingold SC, Cohen JA, Cutter GR, Sørensen PS, Thompson AJ, et al. Defining the clinical course of multiple sclerosis. *Neurology*. (2014) 83:278–86. doi: 10.1212/WNL.0000000000000560
120. Dendrou CA, Fugger L, Friese MA. Immunopathology of multiple sclerosis. *Nat Rev Immunol*. (2015) 15:545–58. doi: 10.1038/nri3871
121. Riccio P. The molecular basis of nutritional intervention in multiple sclerosis: a narrative review. *Complement Ther Med*. (2011) 19:228–37. doi: 10.1016/j.ctim.2011.06.006
122. Farooqui AA, Horrocks LA, Farooqui T. Modulation of inflammation in brain: a matter of fat. *J Neurochem*. (2007) 101:577–99. doi: 10.1111/j.1471-4159.2006.04371.x
123. Calder PC. n-3 polyunsaturated fatty acids, inflammation, and inflammatory diseases. *Am J Clin Nutr*. (2006) 83(Suppl 6):1505S−19S. doi: 10.1093/ajcn/83.6.1505S
124. Roy LSwank OL. Multiple sclerosis in rural norway — its geographic and occupational incidence in relation to nutrition. *N Engl J Med*. (1952) 246:721–8. doi: 10.1056/NEJM195205082461901
125. Rossi A, Kapahi P, Natoli G, Takahashi T, Chen Y, Karin M, et al. Anti-inflammatory cyclopentenone prostaglandins are direct inhibitors of I kappa B kinase. *Nature*. (2000) 403:103–8. doi: 10.1038/47520
126. Li H, Ruan XZ, Moorhead JF, Powis SH, Fernando R, Wheeler DC, et al. omega 3 Polyunsaturated fatty acids. (PUFA) inhibit NF-kappa B activity in LPS-Stimulated proximal tubular cells by PPAR γ activation. *J Am Soc Nephrol*. (2003) 14:85a–a.
127. Derecka K, Sheldrick EL, Wathes DC, Abayasekara DRE, Flint APF. A PPAR-independent pathway to PUFA-induced COX-2 expression. *Mol Cell Endocrinol*. (2008) 287:65–71. doi: 10.1016/j.mce.2008.02.015
128. Zuniga J, Cancino M, Medina F, Varela P, Vargas R, Tapia G, et al. N-3 PUFA supplementation triggers PPAR-α activation and PPAR-α/NF-κ B interaction: anti-inflammatory implications in liver ischemia-reperfusion injury. *PLoS ONE*. (2011) 6:e28502. doi: 10.1371/journal.pone.0028502
129. Mousavi Nasl-Khameneh A, Mirshafiey A, Naser Moghadasi A, Chahardoli R, Mahmoudi M, Parastouei K, et al. Combination treatment of docosahexaenoic acid. (DHA) and all-trans-retinoic

acid. (ATRA) inhibit IL-17 and RORγt gene expression in PBMCs of patients with relapsing-remitting multiple sclerosis. *Neurol Res*. (2018) 40:11–7. doi: 10.1080/01616412.2017.1382800

130. Shinto L, Marracci G, Mohr DC, Bumgarner L, Murchison C, Senders A, et al. Omega-3 fatty acids for depression in multiple sclerosis: a randomized pilot study. *PLoS ONE*. (2016) 11:e0147195. doi: 10.1371/journal.pone.0147195
131. Adkins Y, Soulika AM, Mackey B, Kelley DS. Docosahexaenoic acid. (22:6n-3) ameliorated the onset and severity of experimental autoimmune encephalomyelitis in mice. *Lipids*. (2019) 54:13–23. doi: 10.1002/lipd.12130
132. Unoda K, Doi Y, Nakajima H, Yamane K, Hosokawa T, Ishida S, et al. Eicosapentaenoic acid. (EPA) induces peroxisome proliferator-activated receptors and ameliorates experimental autoimmune encephalomyelitis. *J Neuroimmunol*. (2013) 256:7–12. doi: 10.1016/j.jneuroim.2012.12.003
133. Siegert E, Paul F, Rothe M, Weylandt KH. The effect of omega-3 fatty acids on central nervous system remyelination in fat-1 mice. *BMC Neurosci*. (2017) 18:19. doi: 10.1186/s12868-016-0312-5
134. Endo J, Arita M. Cardioprotective mechanism of omega-3 polyunsaturated fatty acids. *J Cardiol*. (2016) 67:22–7. doi: 10.1016/j.jjcc.2015.08.002

Conflict of Interest: The authors declare that the research was conducted in the absence of any commercial or financial relationships that could be construed as a potential conflict of interest.

frontiers in Immunology

SYSTEMATIC REVIEW
published: 01 October 2019
doi: 10.3389/fimmu.2019.02349

The Impact of Obesity on Thyroid Autoimmunity and Dysfunction: A Systematic Review and Meta-Analysis

*Rong-hua Song[1], Bin Wang[2], Qiu-ming Yao[2], Qian Li[2], Xi Jia[2] and Jin-an Zhang[1]**

[1] Department of Endocrinology & Rheumatology, Shanghai University of Medicine & Health Sciences Affiliated Zhoupu Hospital, Shanghai, China, [2] Department of Endocrinology, Jinshan Hospital of Fudan University, Shanghai, China

Background: To help inform decision making in the clinical setting, we carried out a systematic review and meta-analysis to estimate the association of thyroid disease risks with obesity.

Methods: Pubmed, Embase, Web of Science, Cochrane database and Google Scholar electronic databases were searched from inception to October 31, 2018 without language restrictions to explore the relationship between thyroid disorders and obesity. The relative risk (RR) or odds risk (OR) for thyroid disorders were pooled using the SPSS and STATA software.

Results: A total of 22 studies were included in the study. (1) Meta-analysis showed that obesity was significantly associated with an increased risk of hypothyroidism (RR = 1.86, 95% CI 1.63–2.11, $P < 0.001$). Meta-analyses after stratification further showed that obese population had increased risks of overt hypothyroidism (RR = 3.21, 95% CI 2.12–4.86, $P < 0.001$) and subclinical hypothyroidism (RR = 1.70, 95% CI 1.42–2.03, $P < 0.001$). (2) Further meta-analysis also showed obesity was clearly associated with Hashimoto's thyroiditis (RR = 1.91, 95% CI 1.10–3.32, $P = 0.022$), but not with Graves' disease. (3) In the meta-analysis of antibodies, obesity was correlated with positive thyroid peroxidase antibody (TPOAb) (RR = 1.93, 95% CI 1.31–2.85, $P = 0.001$), but not with positive thyroglobulin antibody (TGAb).

Conclusions: Obesity was significantly related to hypothyroidism, HT, and TPOAb, implying that prevention of obesity is crucial for thyroid disorders.

Systematic Review Registration: PROSPERO: CRD42018096897.

Keywords: obesity, thyroid disease, thyroid autoimmunity, thyroid dysfunction, hypothyroidism, systematic review, meta-analysis

OPEN ACCESS

Edited by:
James J. Pestka, Michigan State University, United States

Reviewed by:
Weiping Teng, The First Hospital Affiliated of China Medical University, China
Rita S. Strakovsky, Michigan State University, United States

***Correspondence:**
Jin-an Zhang
zhangjinan@hotmail.com

Specialty section:
This article was submitted to Autoimmune and Autoinflammatory Disorders, a section of the journal Frontiers in Immunology

Received: *16 December 2018*
Accepted: *17 September 2019*
Published: *01 October 2019*

Citation:
Song R, Wang B, Yao Q, Li Q, Jia X and Zhang J (2019) The Impact of Obesity on Thyroid Autoimmunity and Dysfunction: A Systematic Review and Meta-Analysis. Front. Immunol. 10:2349. doi: 10.3389/fimmu.2019.02349

INTRODUCTION

Since the rise of obesity epidemic worldwide, obesity has gained increasing attention and been regarded as a significant public health challenge globally for its wide-ranging adverse consequences on human health such as increased risks of diabetes (1), cardiovascular disease (2), and cancers (3).

The incidence of thyroid disorders, which mainly include thyroid dysfunctions and autoimmune thyroid diseases (AITDs), is increasing in these years. Thyroid dysfunctions include

hyperthyroidism and hypothyroidism (4), both of which can be categorized into subclinical (only with changes in TSH) and overt stages (with changes in both TSH and thyroid hormones). AITDs, one of the most common autoimmune diseases, are characterized by autoantibodies against thyroid antigens, such as TSH receptor antibody (TRAb), thyroid peroxidase antibody (TPOAb), and thyroglobulin antibody (TGAb). They have two principal subtypes: Graves' disease (GD) and Hashimoto's thyroiditis (HT), which hold different clinical manifestations though have similar immunogenetic mechanisms (5). Patients with thyroid disorders also have a high risk of other non-thyroid diseases, such as cardiovascular diseases, cancer, obesity, and adverse pregnancy outcomes (6–9). Patients with thyroid dysfunctions or Graves' disease need long-term medical therapy or surveillance to optimize prognosis (10, 11). Identifying risk factors for thyroid disorders may help clinicians recognize individuals at risk for or with subclinical thyroid disorders and provide immediate treatment to improve patients' outcomes, and is crucial for elucidating the underlying pathophysiological mechanisms of these thyroid disorders.

Although previous studies have revealed that immune dysfunction, environmental elements and genetic factors all contribute to the pathogenesis of thyroid disorders, their pathology is not yet completely clear. It is well-known that obesity is associated with changes in hormones including thyroid-stimulating hormone (TSH) and thyroid hormones and is accompanied by several endocrine and metabolic diseases (12, 13). In clinic, it is well-known that hypothyroidism may induce obesity, so we propose a hypothesis that the relationship between obesity and thyroid disease may be bidirectional. Furthermore, if this relationship is bidirectional and if obesity indeed influences the risk of thyroid disorders, it is still incompletely elucidated how obesity influences the risk of thyroid dysfunctions and impacts the risk of thyroid autoimmunity. Although some studies have reported that obesity may be associated with dysfunctions of thyroid immunity and thyroid gland (14–16), these results are not entirely the same and even controversial. In addition, some of these studies have a relatively small sample size. Therefore, in this study, we conducted a systematic review and meta-analysis with aims to review the influence of obesity on thyroid diseases and uncover their association.

METHODS

Registration

This systematic review and meta-analysis was conducted in accordance with the PRISMA guideline (17) and has been registered in the International Prospective Register of Systemic Reviews (PROSPERO, www.crd.york.ac.uk/PROSPERO, CRD42018096897).

Literature Search

Pubmed, Embase, Web of Science, Cochrane database, and Google Scholar were searched from inception to October 31, 2018. The search in Pubmed used the following criteria: (obese OR obesity OR overweight) AND (thyroid autoimmunity

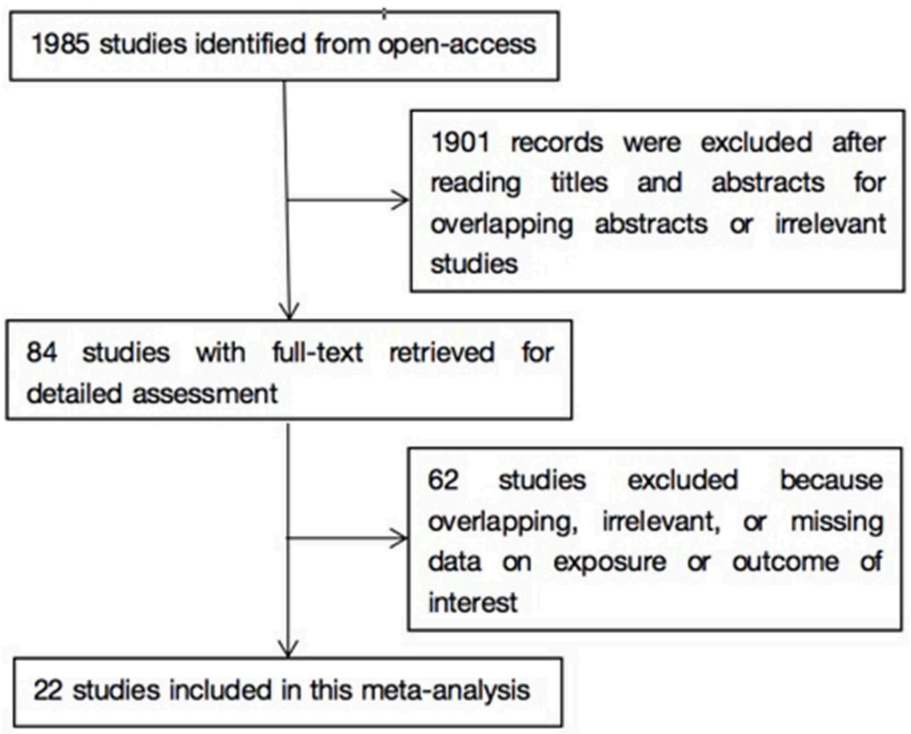

FIGURE 1 | Flow chart of study selection in this meta-analysis.

TABLE 1 | Characteristics of studies included in the meta-analysis.

References	Design	Country	Participants	Subgroup	Outcomes (positive diagnostic criteria of antibodies)	Adjusted matched factors	Quality
Rimm et al. (23)	Cross-sectional	USA	73,532 weight-conscious women	Adults	Hypothyroidism	None	6
Stichel et al. (24)	Case-control	Germany	290 obese and 280 healthy children	Children	SCH, TPOAb (>200 U/ml), TGAb (>100 U/ml)	Age	7
Knudsen et al. (25)	Cross-sectional	Denmark	4,082 eligible individuals after excluding subjects with previous or present overt thyroid dysfunction	Adults	SCH	Age, sex, region of inhabitancy, and tobacco smoking	8
Holm et al. (26)	Cohort	USA	115,109 women aged 25 to 42 at entry	Adults	GD	Age, duration of oral contraceptive use, age at menarche, parity, recent pregnancy, menopausal status, smoking status, alcohol intake, and physical activity level	9
Bhowmick et al. (14)	Case-control	USA	308 children with obesity and 286 non-obese children	Children	SCH	Age	8
Asvold et al. (27)	Cross-sectional	Norway	27,097 individuals older than 40 year of age who were without previously known thyroid disease	Adults	SCH, overt hypothyroidism	Age and smoking status	8
Gopinath et al. (28)	Cohort	Australia	951 participants without thyroid dysfunction	Adults	Hypothyroidism, overt hypothyroidism, SCH	Age and gender	9
Marzullo et al. (15)	Case-control	Italy	165 obese and 118 lean subjects	Adults	Hypothyroidism, overt hypothyroidism, SCH, HT, TPOAb (>35 IU/L), TGAb (>40 IU/L)	Age and gender	7
Dekelbab et al. (16)	Case-control	USA	191 obese and 125 non-obese children (younger than 18 years old)	Children	SCH	Age and gender	7
Somwaru et al. (29)	Cohort	USA	5,888 community-dwelling individuals aged 65 years and older	Adults	Hypothyroidism	Age, gender, race, education, and CHD at baseline	9
Hemminki et al. (30)	Cohort	Sweden	29,665 patients hospitalized for obesity and 367,459 individuals never hospitalized for obesity	Adults	GD, HT	Standardized incidence ratios (SIRs)	9
Ittermann et al. (33)	Cross-sectional	Germany	6,435 children (ages 3–10) and 5,918 adolescents (ages 11–17) from the "The German Health Interview and Examination Survey for Children and Adolescents" (KiGGS)	Children	Hyperthyroidism, hypothyroidism	Age, sex, smoking status, and environmental tobacco smoke	8
Ong et al. (31)	Cohort	UK	1,277 women and 1,185 men	Children	TPOAb (>100 IU/ml), hypothyroidism	None	9
Marwaha et al. (32)	Cross-sectional	India	13,691 children in the age group of 5–18 years	Children	SCH	None	8
Han et al. (34)	Cross-sectional	China	6,303 pregnant women	Adults	hypothyroidism, Overt hypothyroidism, TPOAb (>34 IU/ml), TGAb (>115 IU/ml)	Age, gestational weeks, TPOAb, TgAb, and UIC (stepwise manner)	8

(Continued)

TABLE 1 | Continued

References	Design	Country	Participants	Subgroup	Outcomes (positive diagnostic criteria of antibodies)	Adjusted matched factors	Quality
Ghergherehchi and Hazhir (35)	Case-control	Iran	190 children who were overweight and obese and 133 children without obesity of the same age and sex were evaluated	Children	SCH	Age and sex	7
Korevaar et al. (36)	Cross-sectional	Netherlands	9,767 women during early pregnancy (≤18 week)	Adults	Overt hypothyroidism	Age, smoking, parity, ethnicity, and gestational age	8
Garcia-Garcia et al. (37)	Cross-sectional	Spain	1,317 healthy subjects aged 2–16 years	Children	SCH, HT	None	7
Amouzegar et al. (37)	Cohort	Iran	5,783 individuals were followed for 6 years	Adults	Overt hypothyroidism, SCH	Age, gender, smoking, waist circumference, and TPOAb	9
Valdes et al. (39)	Cross-sectional	Spain	3,928 individuals free of thyroid disease	Adults	SCH	Age, sex, smoking status, and UI concentrations	8
Ornaghi et al. (40)	Cross-sectional	Italy	309 pregnant patients	Adults	Hypothyroidism	Maternal age, parity, ethnicity, pre-gestational diabetes, use of antihypertensive medication before and during pregnancy, LDA prophylaxis, and GA at delivery	8
Wang et al. (42)	Cross-sectional	China	2,808 individuals	Adults	Hypothyroidism, SCH, HT, TPOAb (>34 IU/L), TGAb (>50 IU/L)	Age, gender, smoking, diabetes, uric acid, salt type and urinary iodine concentration	9

SCH, subclinical hypothyroidism.

OR Hashimoto's thyroiditis OR Graves' disease OR Graves hyperthyroidism OR hyperthyroidism OR hypothyroidism OR TPOAb OR TGAb OR thyroid peroxidase antibodies OR thyroid peroxidase antibody OR thyroglobulin antibodies OR thyroglobulin antibody OR thyroiditis). No restrictions were applied on language or publication period. Reference lists of eligible studies and reviews were also screened to identify more details.

Eligibility Criteria

Inclusion criteria were as follows: (1) observational studies including cohort studies, cross-sectional studies and case-control studies; (2) studies comparing the risk of thyroid disorders of obese patients, who were defined as people with body mass index (BMI) $\geq$ 30 kg/m^2 (in western population) or 28 kg/m^2 (in eastern population), and normal controls, who were defined as people with 18.5 $\leq$ BMI $<$ 24.9 kg/m^2, or providing risk estimates for the associations of thyroid disorders with obesity; (3) studies analyzing thyroid disorders including hyperthyroidism, hypothyroidism, or AITDs; (4) studies providing risk estimates with 95% CI for the associations of thyroid disorders, such as relative risk (RR) and odds ratio (OR), or providing other data that could be transformed into risk estimates. Studies against any item of the eligibility criteria were excluded. Case reports and studies containing overlapping data were also excluded. Studies using overweight (24 $\leq$ BMI $<$ 28 kg/m^2), but not obesity (BMI $\geq$ 28 kg/m^2) as the exposure were also excluded. The primary outcomes were the risk of thyroid autoimmunity, hypothyroidism or hyperthyroidism among obese patients and the secondary outcomes were the risk of AITDs, TPOAb positive, and TGAb positive among obese patients.

Data Extraction

Data extraction was conducted using the extraction form, which mainly included study characteristics (the first author, publication year, design, country), participant characteristics (number, subgroups), outcomes (types of thyroid diseases), and adjusted matched factors.

Quality Assessment

Quality assessment of included studies was conducted using Newcastle-Ottawa scale (NOS) based on participant selection (4 points), exposure evaluation (2 points), outcome evaluation, and confounders adjustment (3 points) (18). Studies scoring 5 or less were considered to have sub-optimal quality, and studies scoring 6 or higher were considered in good quality.

Data Analysis

The pooled relative risk (RR) with 95% CI was used to evaluate the impact of obesity on the risk of thyroid autoimmunity and dysfunctions. To account for heterogeneity among included studies, data were pooled using random-effect meta-analysis (19). Heterogeneity was assessed using the I^2 statistic, and $I^2 > 40\%$ was considered high heterogeneity (20). Subgroup analysis was conducted based on types of thyroid autoimmunity, hypothyroidism and hyperthyroidism.

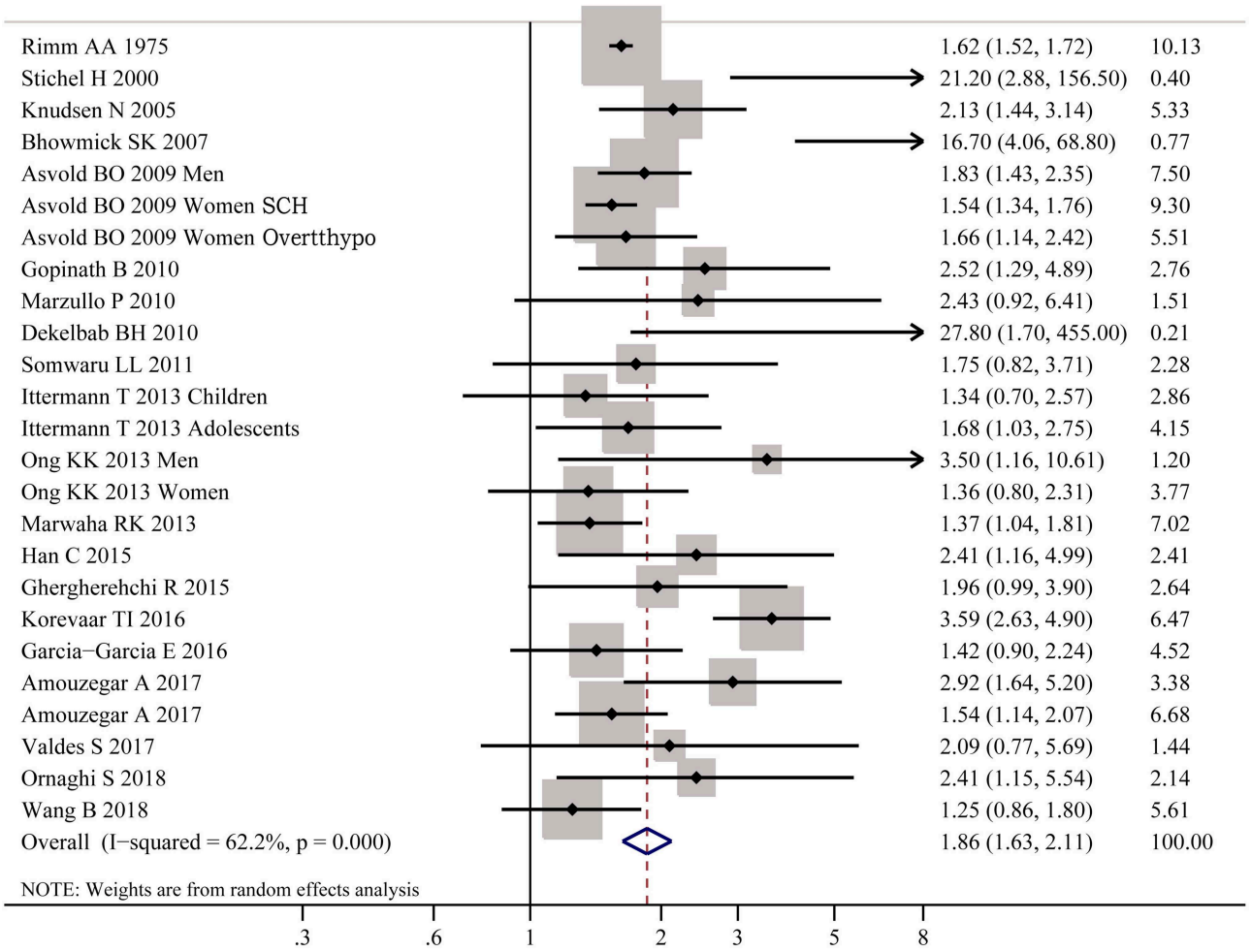

FIGURE 2 | Forest plot for the risk of the whole hypothyroid disorders in obesity. SCH, subclinical hypothyroidism; Overtthypo, overt hypothyroidism.

Sensitivity analysis was conducted by excluding low-quality studies. Publication bias was assessed by the Begg's funnel plot and Egger's test (21). Trim-and-fill method was utilized when publication bias existed (22). All analyses were conducted in SPSS (version 25, IBMCorp) and STATA (version 12.0, StataCorp), and $P < 0.05$ was considered statistically significant.

RESULTS

Search Results

As shown in **Figure 1**, literature search yielded 1985 related papers. After further careful abstracts viewing, 84 studies with full-text publications were retrieved for detailed assessment. After eliminating 62 papers with unrelated or ambiguous results, 22 papers were further analyzed in detail (14–16, 23–41). **Table 1** lists the abstract items of the final 22 papers, including publication year, design, country or region, sample size, source of study sample, outcomes, adjusted matched factors, and quality assessment score.

Obesity and Thyroid Dysfunctions

As shown in **Figure 2**, meta-analysis of the 22 studies indicated that obesity was significantly associated with the increased risk of hypothyroidism (OR = 1.86; 95% CI 1.63–2.11, $P < 0.001$). Further meta-analysis of 6 studies on hypothyroidism (shown in **Figure 3**) showed that patients with BMI $\geq$ 28 kg/m^2 had an increased risk of overt hypothyroidism (OR = 3.21, 95% CI 2.12–4.86, $P < 0.001$). Likewise, meta-analysis of 14 studies on subclinical hypothyroidism (SCH) also showed that obese population had an 70% increased risk of subclinical hypothyroidism (OR = 1.70, 95% CI 1.42–2.03, $P < 0.001$). However, meta-analysis of studies on hyperthyroidism showed no significant association between obesity and an increased risk of hyperthyroidism ($P > 0.05$).

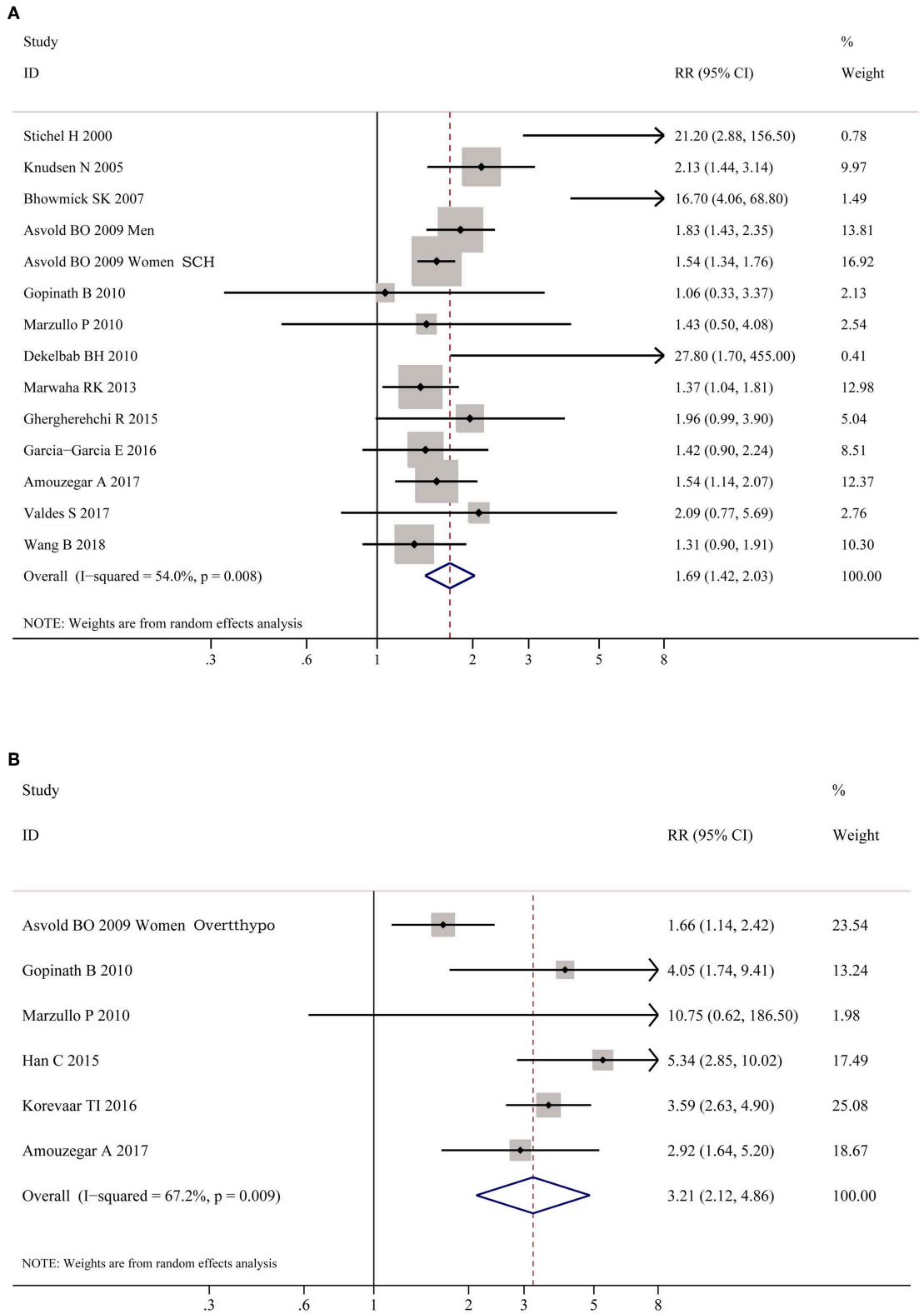

FIGURE 3 | Forest plots for the risk of hypothyroid disorders in obesity. **(A)** Forest plot for the risk of overt hypothyroidism in obesity patients. **(B)** Forest plot for the risk of subclinical hypothyroidism in obesity patients. SCH, subclinical hypothyroidism; Overtthypo, overt hypothyroidism.

Obesity and Thyroid Autoimmunity

Table 2 shows the pooled estimates of AITDs risk in obese patients. Although obese patients had increased risk of AITDs, the difference was not statistically significant ($P = 0.077$). Similarly, meta-analysis of two studies on GD showed that obese population had no increased risk of GD ($P = 0.852$). But, there was a significant association between HT and obesity (OR = 1.91; 95% CI 1.10–3.32, $P = 0.022$), as shown in **Figure 4**. As shown in **Table 2** and **Figure 5**, meta-analysis of thyroid antibodies (TGAb and TPOAb) revealed that there was a significant association between TPOAb positive and obesity (OR = 1.93; 95% CI 1.31–2.85, $P = 0.001$), but no such an association between TGAb positive and obesity. The risks of HT and TPOAb in obese population were increased by 91 and 93%, respectively.

TABLE 2 | Meta-analysis of association of obesity with thyroid disorders.

Analyses	No. of studies	I^2 (%)	*P*-value	RR	95% CI
AITDs	6	91.5	0.077	1.56	0.95–2.54
GD	2	90.4	0.852	0.94	0.51–1.75
HT	5	85.3	0.022	1.91	1.10–3.32
Hyperthyroidism	3	77.8	0.409	0.79	0.46–1.38
Hypothyroidism	20	62.2	0.000	1.86	1.63–2.11
Overt hypothyroidism	6	67.2	0.000	3.21	2.12–4.86
Subclinical hypothyroidism	14	54.0	0.000	1.70	1.42–2.03
TGAb	4	45.1	0.161	1.45	0.86–2.43
TPOAb	5	43.9	0.001	1.93	1.31–2.85

DISCUSSION

Obesity and thyroid disorders are two common conditions and there is an intriguing relationship between these two entities. Although available data have uncovered the relationship between thyroid disorder and body weight status, their results are inconsistent. For example, researchers have previously found that obese individuals have higher serum TSH levels (42, 43), while others have found no significant differences (44, 45). The aim of our study is to analyze these results systemically and also to reveal casual relationship between obesity and thyroid disorders.

A total of 22 researches with a size large enough were included in the present study. Clinically, it is easy to find that patients with hyperthyroidism often lose a lot of weight and regain it after remission. In contrast, patients with hypothyroidism often gain some weight and lose modest weight after thyroid hormone replacement. Therefore, it is a common sense that obesity is often regarded to be secondary to hypothyroidism (8). And the mechanisms by which hypothyroidism causes weight increase is supposed to be achieved via altered energy expenditure and appetite (41, 46).

Until recently, there have been more novel views identifying that thyroid disorders could well be secondary to obesity

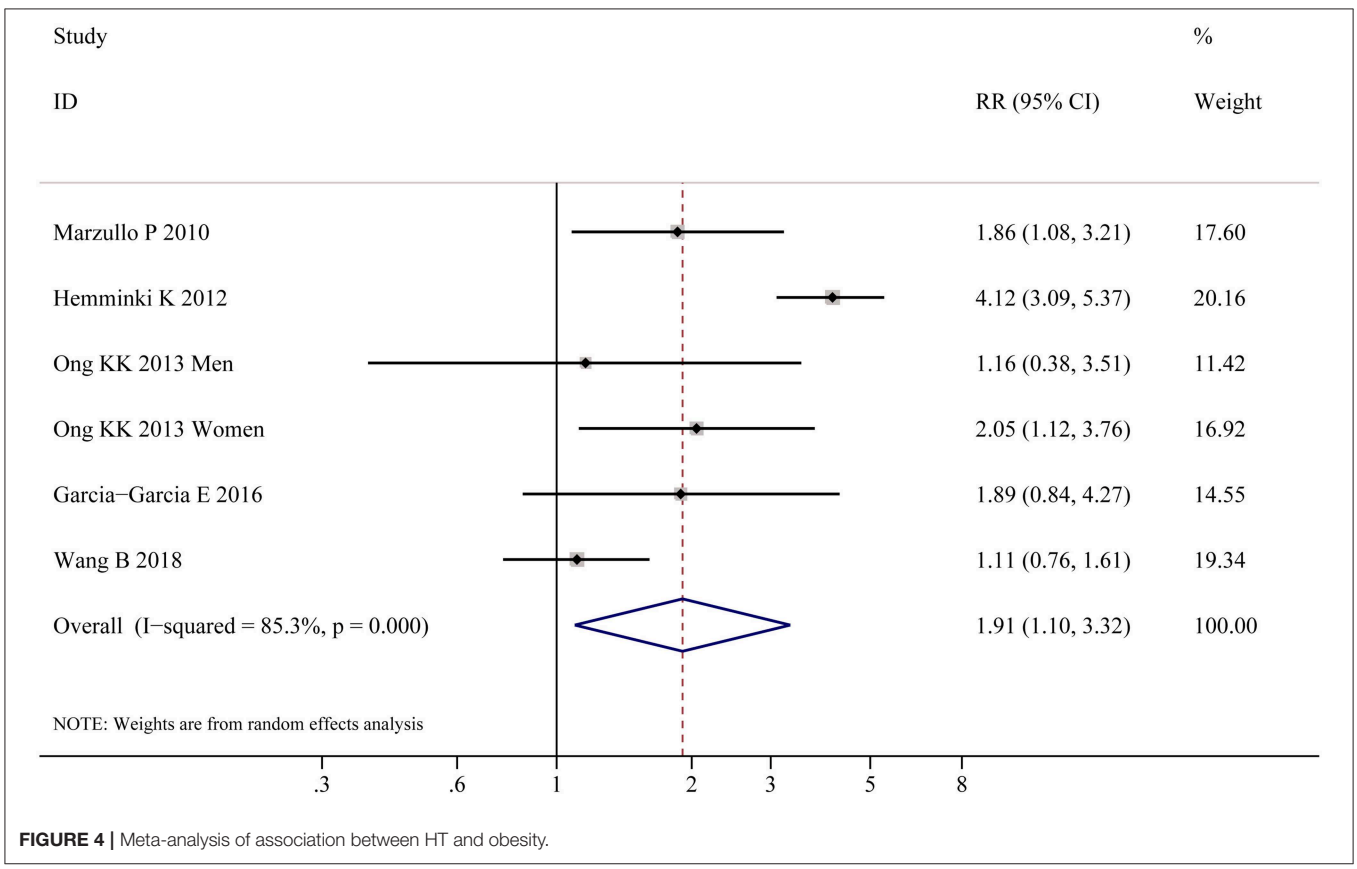

FIGURE 4 | Meta-analysis of association between HT and obesity.

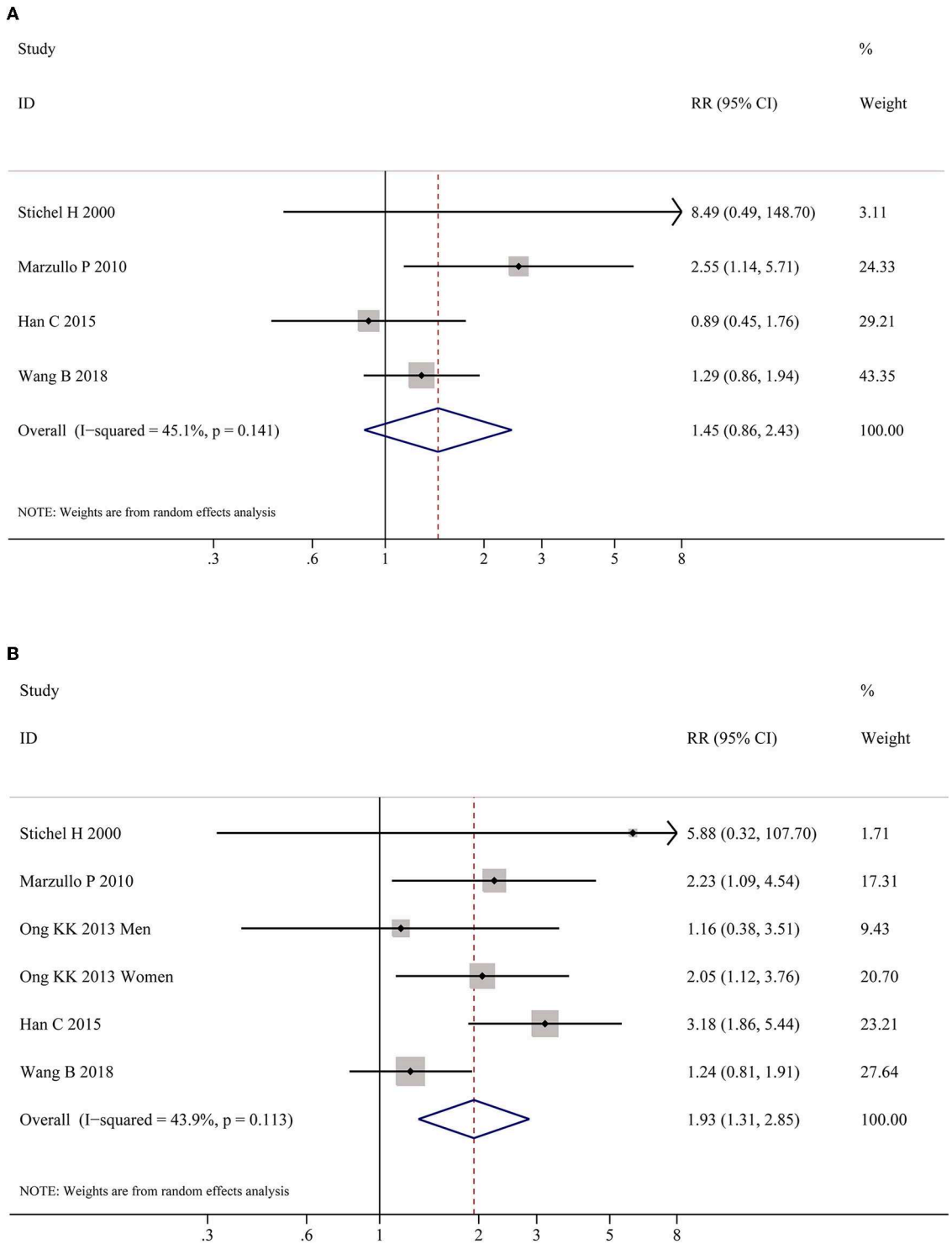

FIGURE 5 | Meta-analysis of association between thyroid auto-antibodies and obesity. **(A)** Association between positive TGAb and obesity. **(B)** Association between positive TPOAb and obesity patients.

(47). Our meta-analysis showed that obesity was significantly associated with increased risks of hypothyroidism, including overt hypothyroidism and subclinical hypothyroidism, and could be accompanied by at least 1.86-fold increase of developing hypothyroidism. These results are concordant with other studies showing that lower levels of FT3 and FT4 or higher level of

TSH are associated with high body weight (15, 25, 32, 48). The parthenogenesis of this relation is not yet entirely revealed, but some explanations have been proposed. Obesity is a chronic low-grade inflammation process; thus the cytokines and other inflammatory markers produced by over-loading adipose tissue, such as interleukin-1 (IL-1), IL-6, and tumor necrosis factor alpha (TNF-alpha), will be increased (46). These increased inflammatory cytokines may inhibit the mRNA expression of symporter sodium/iodide, then influence iodide uptake activity of human thyroid cells (49). These cytokines can also induce vasodilation and elevated permeability of blood vessels of thyroid gland, thus bringing morphological and functional changes in thyroid (46, 49). Leptin, a factor produced by adipocytes, also plays a role in chronic inflammation may result in the morphological changes in thyroid, and may also restrain the expressions of soidium/iodide symporter and thyroglobulin, thus inducing the changes of thyroid hormone levels in obese people (50). Some other studies found that this chronic inflammation status in obesity may also affect thyroid function by modulating the expression and activity of deiodinases (51, 52). The above researches may partially explain the mechanisms by which obesity may induce hypothyroidism (13, 49–53). Nevertheless, the etiology for the correlation of obesity and hypothyroidism still needs to be further elucidated in more in-depth studies.

Moreover, our meta-analysis also found the obese population had increased odds for thyroid autoimmunity. It is well-known that autoimmune diseases are caused by both genetic and immune pathogenesis. Our results are in accordance with previous reports showing that adiposity is a risk factor for many autoimmune inflammatory diseases, such as type 1 diabetes, multiple sclerosis, rheumatoid arthritis, and psoriatic arthritis (54–57). The mechanisms linking obesity and autoimmune disease are unclear. Some studies suggest that adipokines may play a vital role in immune disorders (58, 59). Adipokines, including leptin and interleukin-6, could mediate immune and inflammatory responses. Adipose tissue is crucial for maintaining normal immune function for humans (60, 61). Similarly, other observational researches also provide evidence that dysfunction in adipokines is associated with thyroid autoimmunity (62, 63). Meanwhile, meta-analysis of thyroid antibodies showed the correlation between TPOAb positive and obesity, and obesity is associated with a 93% increased risk of developing positive TPOAb. Leptin, which is mainly produced by adipocytes, is identified to mediate the immune system and contribute to increased production of TPOAb by shifting T helper balance toward to T helper 1 (Th1) cells phenotype and inhibiting the function of regulatory T (Treg) cells (64, 65). Autoimmune thyroiditis, mainly HT, is believed to be the main cause of hypothyroidism in iodine-sufficient regions, and thyroid auto-antibodies (TPOAb and TGAb) are the hallmarks of this disease (66). This may be another interpretation to explain the mechanism why obesity induces hypothyroidism.

Holm has reported that obesity may reduce the risk of hyperthyroidism (26). However, our meta-analysis including both Holm's study and another one showed no relationship between hyperthyroidism and GD with obesity. We speculate that this discrepancy is due to limited GD cases to reveal a fact in heterogeneous populations. In future, much larger and more ethnic researches are warranted.

In this study, we demonstrate the association between obesity and thyroid disorders, indicating that obesity may be a contributing factor for hypothyroidism, HT and positive TPOAb, and suggest that thyroid functions in obese population needs extra attention. So by synthesizing our present study and some other researches (13, 47, 49–53, 58–65), it seems reasonable to suggest that the relationship between obesity and thyroid disease is bidirectional; of course, it needs more studies to be elucidated. The present study still has some limitations. For instance, abnormal weight including overweight and underweight were barely explored. Additionally, most studies only explored the association between obesity and thyroid disorders, and barely investigated whether thyroid dysfunction is the cause or consequence of obesity, which needs further prospective cohort and causality studies to investigate.

In conclusion, obesity is significantly associated with hypothyroidism, HT and TPOAb, indicating that prevention of obesity is crucial for thyroid disorders.

AUTHOR CONTRIBUTIONS

BW designed the study and generated the hypotheses. BW and RS extracted the data. RS analyzed the data and wrote the first draft of the report, with support from QY, QL, and XJ. JZ and BW both revised the manuscript. All authors participated in interpreting the data and critically reviewed the paper.

FUNDING

The present work has received fundings from the National Natural Science Foundation of China (Grant No. 81800696, 81873636 and 81670722) and Science and Technology Development Fund of Pudong New District Minsheng Scientific Research (Medical and Health) Project (No. PKJ2018-Y39).

REFERENCES

1. Riobo Servan P. Obesity and diabetes. *Nutr Hosp*. (2013) 28(Suppl. 5):138–43. doi: 10.3305/nh.2013.28.sup5.6929
2. Mitchell AB, Cole JW, McArdle PF, Cheng YC, Ryan KA, Sparks MJ, et al. Obesity increases risk of ischemic stroke in young adults. *Stroke*. (2015) 46:1690–2. doi: 10.1161/STROKEAHA.115.008940
3. Afshin A, Forouzanfar MH, Reitsma MB, Sur P, Estep K, Lee A, et al. Health effects of overweight and obesity in 195 Countries over 25 years. *N Engl J Med*. (2017) 377:13–27. doi: 10.1056/NEJMoa1614362
4. Taylor PN, Albrecht D, Scholz A, Gutierrez-Buey G, Lazarus JH, Dayan CM, et al. Global epidemiology of hyperthyroidism and hypothyroidism. *Nat Rev Endocrinol*. (2018) 14:301–16. doi: 10.1038/nrendo.2018.18

5. Tomer Y. Mechanisms of autoimmune thyroid diseases: from genetics to epigenetics. *Annu Rev Pathol*. (2014) 9:147–56. doi: 10.1146/annurev-pathol-012513-104713
6. Baumgartner C, da Costa BR, Collet TH, Feller M, Floriani C, Bauer DC, et al. Thyroid function within the normal range, subclinical hypothyroidism, and the risk of atrial fibrillation. *Circulation*. (2017) 136:2100–16. doi: 10.1161/CIRCULATIONAHA.117.028753
7. Journy NMY, Bernier MO, Doody MM, Alexander BH, Linet MS, Kitahara CM. Hyperthyroidism, hypothyroidism, and cause-specific mortality in a large cohort of women. *Thyroid*. (2017) 27:1001–10. doi: 10.1089/thy.2017.0063
8. Biondi B. Thyroid and obesity: an intriguing relationship. *J. Clin. Endocrinol. Metab.* (2010) 95:3614–17. doi: 10.1210/jc.2010-1245
9. Cooper DS, Laurberg P. Hyperthyroidism in pregnancy. *Lancet Diab Endocrinol*. (2013) 1:238–49. doi: 10.1016/S2213-8587(13)70086-X
10. Burch HB, Cooper DS. Management of graves disease: a review. *JAMA*. (2015) 314:2544–54. doi: 10.1001/jama.2015.16535
11. Antonelli A, Ferrari SM, Corrado A, Di Domenicantonio A, Fallahi P. Autoimmune thyroid disorders. *Autoimmun Rev*. (2015) 14:174–80. doi: 10.1016/j.autrev.2014.10.016
12. Kopelman PG. Hormones and obesity. *Baillieres Clin Endocrinol Metab*. (1994) 8:549–75. doi: 10.1016/S0950-351X(05)80286-1
13. Pearce EN. Thyroid hormone and obesity. *Curr Opin Endocrinol Diabetes Obes*. (2012) 19:408–13. doi: 10.1097/MED.0b013e328355cd6c
14. Bhowmick SK, Dasari G, Levens KL, Rettig KR. The prevalence of elevated serum thyroid-stimulating hormone in childhood/adolescent obesity and of autoimmune thyroid diseases in a subgroup. *J Natl Med Assoc*. (2007) 99:773–6. doi: 10.1016/S0929-6646(07)60013-8
15. Marzullo P, Minocci A, Tagliaferri MA, Guzzaloni G, Di Blasio A, De Medici C, et al. Investigations of thyroid hormones and antibodies in obesity: leptin levels are associated with thyroid autoimmunity independent of bioanthropometric, hormonal, and weight-related determinants. *J Clin Endocrinol Metab*. (2010) 95:3965–72. doi: 10.1210/jc.2009-2798
16. Dekelbab BH, Abou Ouf HA, Jain I. Prevalence of elevated thyroid-stimulating hormone levels in obese children and adolescents. *Endocr Pract*. (2010) 16:187–90. doi: 10.4158/EP09176.OR
17. Moher D, Liberati A, Tetzlaff J, Altman DG. Preferred reporting items for systematic reviews and meta-analyses: the PRISMA statement. *BMJ*. (2009) 339:b2535. doi: 10.1136/bmj.b2535
18. Margulis AV, Pladevall M, Riera-Guardia N, Varas-Lorenzo C, Hazell L, Berkman ND, et al. Quality assessment of observational studies in a drug-safety systematic review, comparison of two tools: the Newcastle-Ottawa Scale and the RTI item bank. *Clin Epidemiol*. (2014) 6:359–68. doi: 10.2147/CLEP.S66677
19. DerSimonian R, Laird N. Meta-analysis in clinical trials. *Control Clin Trials*. (1986) 7:177–88. doi: 10.1016/0197-2456(86)90046-2
20. Higgins JP, Thompson SG, Deeks JJ, Altman DG. Measuring inconsistency in meta-analyses. *BMJ*. (2003) 327:557–60. doi: 10.1136/bmj.327.7414.557
21. Egger M, Davey Smith G, Schneider M, Minder C. Bias in meta-analysis detected by a simple, graphical test. *BMJ*. (1997) 315:629–34. doi: 10.1136/bmj.315.7109.629
22. Peters JL, Sutton AJ, Jones DR, Abrams KR, Rushton L. Performance of the trim and fill method in the presence of publication bias and between-study heterogeneity. *Stat Med*. (2007) 26:4544–62. doi: 10.1002/sim.2889
23. Rimm AA, Werner LH, Yserloo BV, Bernstein RA. Relationship of ovesity and disease in 73,532 weight-conscious women. *Public Health Rep*. (1975) 90:44–51.
24. Stichel H, l'Allemand D, Gruters A. Thyroid function and obesity in children and adolescents. *Horm Res*. (2000) 54:14–9. doi: 10.1159/000063431
25. Knudsen N, Laurberg P, Rasmussen LB, Bulow I, Perrild H, Ovesen L, et al. Small differences in thyroid function may be important for body mass index and the occurrence of obesity in the population. *J Clin Endocrinol Metab*. (2005) 90:4019–24. doi: 10.1210/jc.2004-2225
26. Holm IA, Manson JE, Michels KB, Alexander EK, Willett WC, Utiger RD. Smoking and other lifestyle factors and the risk of Graves' hyperthyroidism. *Arch Intern Med*. (2005) 165:1606–11. doi: 10.1001/archinte.165.14.1606
27. Asvold BO, Bjoro T, Vatten LJ. Association of serum TSH with high body mass differs between smokers and never-smokers. *J Clin Endocrinol Metab*. (2009) 94:5023–7. doi: 10.1210/jc.2009-1180
28. Gopinath B, Wang JJ, Kifley A, Wall JR, Eastman CJ, Leeder SR, et al. Five-year incidence and progression of thyroid dysfunction in an older population. *Intern Med J*. (2010) 40:642–9. doi: 10.1111/j.1445-5994.2009.02156.x
29. Somwaru LL, Arnold AM, Cappola AR. Predictors of thyroid hormone initiation in older adults: results from the cardiovascular health study. *J Gerontol A Biol Sci Med Sci*. (2011) 66:809–14. doi: 10.1093/gerona/glr063
30. Hemminki K, Li X, Sundquist J, Sundquist K. Risk of asthma and autoimmune diseases and related conditions in patients hospitalized for obesity. *Ann Med*. (2012) 44:289–95. doi: 10.3109/07853890.2010.547515
31. Ong KK, Kuh D, Pierce M, Franklyn JA. Childhood weight gain and thyroid autoimmunity at age 60–64 years: the 1946 British birth cohort study. *J Clin Endocrinol Metab*. (2013) 98:1435–42. doi: 10.1210/jc.2012-3761
32. Marwaha RK, Tandon N, Garg MK, Ganie MA, Narang A, Mehan N, et al. Impact of body mass index on thyroid functions in Indian children. *Clin Endocrinol*. (2013) 79:424–8. doi: 10.1111/cen.12148
33. Ittermann T, Thamm M, Schipf S, John U, Rettig R, Volzke H. Relationship of smoking and/or passive exposure to tobacco smoke on the association between serum thyrotropin and body mass index in large groups of adolescents and children. *Thyroid*. (2013) 23:262–8. doi: 10.1089/thy.2012.0110
34. Han C, Li C, Mao J, Wang W, Xie X, Zhou W, et al. High body mass index is an indicator of maternal hypothyroidism, hypothyroxinemia, and thyroid-peroxidase antibody positivity during early pregnancy. *Biomed Res Int*. (2015) 2015:351831. doi: 10.1155/2015/351831
35. Ghergherehchi R, Hazhir N. Thyroid hormonal status among children with obesity. *Ther Adv Endocrinol Metab*. (2015) 6:51–5. doi: 10.1177/2042018815571892
36. Korevaar TI, Nieboer D, Bisschop PH, Goddijn M, Medici M, Chaker L, et al. Risk factors and a clinical prediction model for low maternal thyroid function during early pregnancy: two population-based prospective cohort studies. *Clin Endocrinol*. (2016) 85:902–9. doi: 10.1111/cen.13153
37. Garcia-Garcia E, Vazquez-Lopez MA, Garcia-Fuentes E, Galera-Martinez R, Gutierrez-Repiso C, Garcia-Escobar I, et al. Thyroid function and thyroid autoimmunity in relation to weight status and cardiovascular risk factors in children and adolescents: a population-based study. *J Clin Res Pediatr Endocrinol*. (2016) 8:157–62. doi: 10.4274/jcrpe.2687
38. Amouzegar A, Ghaemmaghami Z, Beigy M, Gharibzadeh S, Mehran L, Tohidi M, et al. Natural course of euthyroidism and clues for early diagnosis of thyroid dysfunction: tehran thyroid study. *Thyroid*. (2017) 27:616–25. doi: 10.1089/thy.2016.0409
39. Valdes S, Maldonado-Araque C, Lago-Sampedro A, Lillo-Munoz JA, Garcia-Fuentes E, Perez-Valero V, et al. Reference values for TSH may be inadequate to define hypothyroidism in persons with morbid obesity: Di@bet.es study. *Obesity*. (2017) 25:788–93. doi: 10.1002/oby.21796
40. Ornaghi S, Algeri P, Todyrenchuk L, Vertemati E, Vergani P. Impact of excessive pre-pregnancy body mass index and abnormal gestational weight gain on pregnancy outcomes in women with chronic hypertension. *Pregnancy Hypertens*. (2018) 12:90–5. doi: 10.1016/j.preghy.2018.04.005
41. Santini F, Marzullo P, Rotondi M, Ceccarini G, Pagano L, Ippolito S, et al. Mechanisms in endocrinology: the crosstalk between thyroid gland and adipose tissue: signal integration in health and disease. *Eur J Endocrinol*. (2014) 171:R137–52. doi: 10.1530/EJE-14-0067
42. Wang B, Song R, He W, Yao Q, Li Q, Jia X, et al. Sex differences in the associations of obesity with hypothyroidism and thyroid autoimmunity among chinese adults. *Front Physiol*. (2018) 9:1397. doi: 10.3389/fphys.2018.01397
43. Matzen LE, Kvetny J, Pedersen KK. TSH, thyroid hormones and nuclear-binding of T3 in mononuclear blood cells from obese and non-obese women. *Scand J Clin Lab Invest*. (1989) 49:249–53. doi: 10.1080/00365518909089090
44. Strata A, Ugolotti G, Contini C, Magnati G, Pugnoli C, Tirelli F, et al. Thyroid and obesity: survey of some function tests in a large obese population. *Int J Obes*. (1978) 2:333–40.
45. Duntas L, Hauner H, Rosenthal J, Pfeiffer EF. Thyrotropin releasing hormone (TRH) immunoreactivity and thyroid function in obesity. *Int J Obes*. (1991) 15:83–7.

46. Fontenelle LC, Feitosa MM, Severo JS, Freitas TE, Morais JB, Torres-Leal FL, et al. Thyroid function in human obesity: underlying mechanisms. *Horm Metab Res*. (2016) 48:787–94. doi: 10.1055/s-0042-121421
47. Sanyal D, Raychaudhuri M. Hypothyroidism and obesity: an intriguing link. *Indian J Endocrinol Metab*. (2016) 20:554–7. doi: 10.4103/2230-8210.183454
48. Rotondi M, Leporati P, La Manna A, Pirali B, Mondello T, Fonte R, et al. Raised serum TSH levels in patients with morbid obesity: is it enough to diagnose subclinical hypothyroidism? *Eur J Endocrinol*. (2009) 160:403–8. doi: 10.1530/EJE-08-0734
49. Longhi S, Radetti G. Thyroid function and obesity. *J Clin Res Pediatr Endocrinol*. (2013) 5(Suppl. 1):40–4. doi: 10.4274/jcrpe.856
50. Isozaki O, Tsushima T, Nozoe Y, Miyakawa M, Takano K. Leptin regulation of the thyroids: negative regulation on thyroid hormone levels in euthyroid subjects and inhibitory effects on iodide uptake and Na + /I- symporter mRNA expression in rat FRTL-5 cells. *Endocr J*. (2004) 51:415–23. doi: 10.1507/endocrj.51.415
51. Jakobs TC, Mentrup B, Schmutzler C, Dreher I, Köhrle J. Proinflamma- tory cytokines inhibit the expression and function of human type I 5′-deiodinase in HepG2 hepatocarcinoma cells. *Eur J Endocrinol*. (2002) 146:559–66. doi: 10.1530/eje.0.1460559
52. Kwakkel J, Surovtseva OV, Vries EM, Stap J, Fliers E, Boelen A. A novel role for the thyroid hormone-activating enzyme type 2 deiodinase in the inflammatory response of macrophages. *Endocrinology*. (2014) 155:2725–34. doi: 10.1210/en.2013-2066
53. Radetti G, KleonW, Buzi F, Crivellaro C, Pappalardo L, diIorgi N, et al. Thyroid function and structure are affected in childhood obesity. *J Clin Endocrinol Metab*. (2008) 93:4749–54. doi: 10.1210/jc.2008-0823
54. Verbeeten KC, Elks CE, Daneman D, Ong KK. Association between childhood obesity and subsequent Type 1 diabetes: a systematic review and meta-analysis. *Diabet Med*. (2011) 28:10–8. doi: 10.1111/j.1464-5491.2010.03160.x
55. Hedstrom AK, Olsson T, Alfredsson L. High body mass index before age 20 is associated with increased risk for multiple sclerosis in both men and women. *Mult Scler*. (2012) 18:1334–6. doi: 10.1177/1352458512436596
56. Gremese E, Tolusso B, Gigante MR, Ferraccioli G. Obesity as a risk and severity factor in rheumatic diseases (autoimmune chronic inflammatory diseases). *Front Immunol*. (2014) 5:576. doi: 10.3389/fimmu.2014.00576
57. Russolillo A, Iervolino S, Peluso R, Lupoli R, Di Minno A, Pappone N, et al. Obesity and psoriatic arthritis: from pathogenesis to clinical outcome and management. *Rheumatology*. (2013) 52:62–7. doi: 10.1093/rheumatology/kes242
58. Vieira-Potter VJ. Inflammation and macrophage modulation in adipose tissues. *Cell Microbiol*. (2014) 16:1484–92. doi: 10.1111/cmi.12336
59. Hino J, Nakatani M, Arai Y, Tsuchida K, Shirai M, Miyazato M, et al. Overexpression of bone morphogenetic protein-3b (BMP-3b) in adipose tissues protects against high-fat diet-induced obesity. *Int J Obes*. (2017) 41:483–8. doi: 10.1038/ijo.2017.15
60. Lourenco EV, Liu A, Matarese G, La Cava A. Leptin promotes systemic lupus erythematosus by increasing autoantibody production and inhibiting immune regulation. *Proc Natl Acad Sci USA*. (2016) 113:10637–42. doi: 10.1073/pnas.1607101113
61. Abella V, Scotece M, Conde J, Pino J, Gonzalez-Gay MA, Gomez-Reino JJ, et al. Leptin in the interplay of inflammation, metabolism and immune system disorders. *Nat Rev Rheumatol*. (2017) 13:100–9. doi: 10.1038/nrrheum.2016.209
62. Teixeira PF, Cabral MD, Silva NA, Soares DV, Braulio VB, Couto AP, et al. Serum leptin in overt and subclinical hypothyroidism: effect of levothyroxine treatment and relationship to menopausal status and body composition. *Thyroid*. (2009) 19:443–50. doi: 10.1089/thy.2007.0393
63. Drobniak A, Kanecki K, Grymowicz M, Radowicki S. Serum leptin concentration in women of reproductive age with euthyroid autoimmune thyroiditis. *Gynecol Endocrinol*. (2016) 32:128–31. doi: 10.3109/09513590.2015.1092512
64. Procaccini C, Carbone F, Galgani M. Obesity and susceptibility to autoimmune diseases. *Expert Rev. Clin. Immunol*. (2011) 7:287–94. doi: 10.1586/eci.11.18
65. Fresno M, Alvarez R, Cuesta N. Toll-like receptors, inflammation, metabolism and obesity. *Arch Physiol Biochem*. (2011) 117:151–64. doi: 10.3109/13813455.2011.562514
66. Karakosta P, Alegakis D, Georgiou V. Thyroid dysfunction and autoantibodies in early pregnancy are associated with increased risk of gestational diabetes and adverse birth outcomes. *J Clin Endocrinol Metab*. (2012) 97:4464–72. doi: 10.1210/jc.2012-2540

Conflict of Interest: The authors declare that the research was conducted in the absence of any commercial or financial relationships that could be construed as a potential conflict of interest.

The reviewer RS and handling editor declared their shared affiliation.

frontiers in Immunology

ORIGINAL RESEARCH
published: 01 October 2019
doi: 10.3389/fimmu.2019.02336

Silica Exposure Differentially Modulates Autoimmunity in Lupus Strains and Autoantibody Transgenic Mice

Mary H. Foster[1,2], Jeffrey R. Ord[1], Emma J. Zhao[1], Anastasiya Birukova[1], Lanette Fee[1,2], Francesca M. Korte[1], Yohannes G. Asfaw[3], Victor L. Roggli[4], Andrew J. Ghio[5], Robert M. Tighe[1,2] and Amy G. Clark[1,2]*

[1] Department of Medicine, Duke University Health System, Durham, NC, United States, [2] Durham VA Medical Center, Durham, NC, United States, [3] Division of Laboratory Animal Resources, Duke University Medical Center, Durham, NC, United States, [4] Department of Pathology, Duke University Health System, Durham, NC, United States, [5] National Health and Environmental Effects Research Laboratory, US Environmental Protection Agency, Chapel Hill, NC, United States

OPEN ACCESS

Edited by:
James J. Pestka,
Michigan State University,
United States

Reviewed by:
Andrij Holian,
University of Montana, United States
Melissa Bates,
University of Michigan, United States

***Correspondence:**
Mary H. Foster
mary.h.foster@dm.duke.edu

Specialty section:
This article was submitted to Autoimmune and Autoinflammatory Disorders, a section of the journal Frontiers in Immunology

Received: 20 April 2019
Accepted: 16 September 2019
Published: 01 October 2019

Citation:
Foster MH, Ord JR, Zhao EJ, Birukova A, Fee L, Korte FM, Asfaw YG, Roggli VL, Ghio AJ, Tighe RM and Clark AG (2019) Silica Exposure Differentially Modulates Autoimmunity in Lupus Strains and Autoantibody Transgenic Mice. Front. Immunol. 10:2336. doi: 10.3389/fimmu.2019.02336

Inhalational exposure to crystalline silica is linked to several debilitating systemic autoimmune diseases characterized by a prominent humoral immune component, but the mechanisms by which silica induces autoantibodies is poorly understood. To better understand how silica lung exposure breaks B cell tolerance and unleashes autoreactive B cells, we exposed both wildtype mice of healthy C57BL/6 and lupus-prone BXSB, MRL, and NZB strains and mice carrying an autoantibody transgene on each of these backgrounds to instilled silica or vehicle and monitored lung injury, autoimmunity, and B cell fate. Silica exposure induced lung damage and pulmonary lymphoid aggregates in all strains, including in genetically diverse backgrounds and in autoantibody transgenic models. In wildtype mice strain differences were observed in specificity of autoantibodies and site of enhanced autoantibody production, consistent with genetic modulation of the autoimmune response to silica. The unique autoantibody transgene reporter system permitted the *in vivo* fate of autoreactive B cells and tolerance mechanisms to be tracked directly, and demonstrated the presence of transgenic B cells and antibody in pulmonary lymphoid aggregates and bronchoalveolar lavage fluid, respectively, as well as in spleen and serum. Nonetheless, B cell enumeration and transgenic antibody quantitation indicated that B cell deletion and anergy were intact in the different genetic backgrounds. Thus, silica exposure sufficient to induce substantial lung immunopathology did not overtly disrupt central B cell tolerance, even when superimposed on autoimmune genetic susceptibility. This suggests that silica exposure subverts tolerance at alternative checkpoints, such as regulatory cells or follicle entry, or requires additional interactions or co-exposures to induce loss of tolerance. This possibility is supported by results of differentiation assays that demonstrated transgenic autoantibodies in supernatants of Toll-like receptor (TLR)7/TLR9-stimulated splenocytes harvested from silica-exposed,

but not vehicle-exposed, C57BL/6 mice. This suggests that lung injury induced by silica exposure has systemic effects that subtly alter autoreactive B cell regulation, possibly modulating B cell anergy, and that can be unmasked by superimposed exposure to TLR ligands or other immunostimulants.

Keywords: silica, humoral autoimmunity, B cell tolerance, lupus, autoantibody transgene

INTRODUCTION

Autoimmune diseases afflict 10–20% of the US population, often striking young adults and destroying vital organs. Abnormal activation of self-reactive B cells and T cells precipitates spontaneous immune attack on the body. Current therapies can dampen the immune response but do so non-specifically and risk serious side effects. There is an urgent need for safer treatments, but their development will require a better understanding of underlying disease pathogenesis. Considerable evidence indicates that autoimmune responses originate from interaction of environmental triggers with disease susceptibility genes, but little is known about the cellular or molecular basis of this interaction. In particular there is a paucity of information about the mechanism by which environmental agents lead to loss of autoimmune regulation, the fundamental defect in these diseases.

Inhalational exposure to crystalline silica dust (silicon dioxide) has been convincingly linked to human autoimmunity (1). Silica is an abundant natural mineral used commercially in multiple industrial applications and in professions where grinding processes produce silica dust. In addition, there is silica exposure in numerous occupations with manipulation of crustal sources (e.g., agriculture and mining). Numerous case series, case-control, and other epidemiological studies link silica exposure to systemic lupus erythematosus (SLE), anti-neutrophil cytoplasmic autoantibody (ANCA)-associated vasculitis (AAV), rheumatoid arthritis (RA), and systemic sclerosis (SSC), reviewed in (1–5). These chronic relapsing autoimmune diseases cause considerable disability, have life threatening consequences, and currently afford limited opportunities for treatment.

A common and remarkable feature of each of these autoimmune diseases is a prominent autoantibody (autoAb) component. Each disease has a characteristic profile of circulating autoAbs that serves as a biomarker to facilitate diagnosis, prognostication, and disease monitoring and that informs treatment decisions. The appearance of high affinity autoAbs often precedes clinical disease, suggesting their importance early in the disease process (6). Considerable experimental data indicate that the autoAbs mediate tissue destruction and play a critical role in disease pathogenesis (7). AutoAbs to nuclear and other self-antigens deposit in and damage kidneys or bind to and deplete blood cells in SLE (8–10); IgG reacting with type II collagen, citrullinated proteins, and Ig itself (rheumatoid factor) destroys peripheral joints in RA (11); IgG bound to neutrophil myeloperoxidase and proteinase3 triggers small blood vessel injury in ANCA vasculitis (12, 13); and antibodies to nuclear antigens and cell membrane receptors facilitate skin and organ fibrosis in SSC (14–16). The common feature in these autoimmune diseases is activation of autoreactive B cells that have escaped B cell tolerance to generate autoAbs.

To understand how inhalation of silica dust leads to breach of immune tolerance and induction of humoral autoimmunity, we took advantage of a preclinical model system developed in part to better mirror the outbred human situation. This unique mouse reporter system was previously generated to study gene-environment interactions in SLE. For this purpose, a lupus autoAb was expressed as a transgene (Tg) in the non-autoimmune C57BL/6 (B6) strain as well as in multiple classic lupus strains (MRL, NZB, BXSB) (17–20). Each lupus strain carries a different constellation of lupus susceptibility genes, such that they *collectively* mirror the genetic complexity of human lupus. Moreover, the selected strains develop clinical and immunological features and incorporate genetic susceptibility relevant to multiple silica-linked diseases: MRL mice develop delayed lupus nephritis, whereas their MRL/lpr congenic counterparts develop aggressive kidney disease and RA-like arthritis (21); a subset develop anti-myeloperoxidase (MPO) autoAb similar to those observed in ANCA vasculitis (22). NZB mice develop IFNα-receptor-dependent lupus with delayed nephritis and severe autoAb-mediated autoimmune hemolytic anemia (23, 24). NZB carry major risk alleles for severe nephritis (25). The BXSB strain carries an aberrant macrophage receptor with collagenous structure (MARCO) and develops nephritis that is accelerated in the presence of the Y-chromosome-linked autoimmune acceleration (*Yaa*) locus that includes a TLR7 duplication (26, 27).

In mice of these strains carrying the autoAb Tg, the fate of Tg autoreactive B cells, Ab, and tolerance phenotypes can be tracked and quantified. The IgMa Tg was originally constructed from the dominant Ig heavy chain of an IgG autoAb derived from a nephritic MRL/lpr mouse (28). The index IgG binds to laminin, a multifunctional glycoprotein expressed in basement membranes and a target of autoAbs implicated in SLE, blistering dermatoses, reproductive failure, and other disorders (29–34). A prominent subset of Tg autoAbs also crossreacts with DNA (28), a prototypical target antigen in SLE. In healthy B6 mice, these autoreactive Tg B cells are stringently regulated by central deletion, anergy (a state of functional unresponsiveness), and receptor editing (17, 18), tolerance phenotypes that are readily measured and have been stable for over 1.5 decades of study

Abbreviations: ANCA, anti-neutrophil cytoplasmic autoantibody; AAV, ANCA-associated vasculitis; autoAb, autoantibody; BALF, bronchoalveolar lavage fluid; MPO, myeloperoxidase; RA, rheumatoid arthritis; SLE, systemic lupus erythematosus; SSC, systemic sclerosis; Tg, transgene/transgenic; TLS, tertiary lymphoid structures.

in our mouse colony. Thus, the autoAb Tg permits reliable tracking of key tolerance checkpoints using a single disease-relevant autoAb. In the studies described herein, the autoAb Tg system is leveraged to study and quantitate effects of silica exposure on B cell tolerance, under the influence of genetically distinct healthy and disease-prone backgrounds.

MATERIALS AND METHODS

Mice

To study wildtype mice, young adult female autoimmune NZB, BXSB, and MRL mice and healthy C57BL/6 (B6) mice were purchased from Jackson Labs and used between 1.6 and 3 months of age. Generation and characterization of the LamH IgMa+ autoAb Tg was previously described (17, 18). The autoAb Tg was crossed onto the B6 strain a minimum of 21 generations and onto NZB/BINJ (NZB), BXSB, and MRL strains between 9 and 21 generations, and carried as a hemizygote (19). Experimental autoAb Tg mice were bred in our colony and included adult male and female mice between 4.3 and 11.7 months of age, with mice of similar age, primarily littermates, assigned to silica and vehicle instillation within a strain. Mice were housed in microisolators in a specific pathogen-free facility with a 14:10-h light/dark cycle. The care and use of all experimental animals were in accordance with institutional guidelines, and all studies and procedures were approved by the local Institutional Animal Care and Use Committees and conform to institutional standards and to the National Institutes of Health guide for the care and use of laboratory animals.

Silica Administration

Heat sterilized endotoxin-free crystalline silica (Min-U-Sil-5 crystalline silica) was administered once by oropharyngeal instillation as a suspension in sterile phosphate-buffered saline, at 0.2 mg/gm, as described (35, 36). This dose of silica was chosen to ensure that it overcomes pulmonary clearance mechanisms and results in substantial lung delivery and response, including lung inflammation, recruitment of pulmonary lymphocytes, and induction of tertiary lymphoid structures, as observed in our pilot studies and described in investigation into silica-related lung and immune injury using intratracheal or transoral instillations of 5–10 mg silica (37–39). Saline alone was administered as control.

Tissue and Organ Harvest and Preparation

Wildtype mice were sacrificed at 1, 2, or 3 months after silica instillation for analysis of the whole lung lavage fluid and blood and organ harvest. AutoAb transgenic mice were sacrificed at times indicated in the text. Following CO_2 euthanasia, blood was collected from the inferior vena cava and serum stored at −20°C. In some mice the descending aorta was transected and organs perfused with saline via the right ventricle. Spleens were removed into culture media. The trachea was exposed and cannulated with PE-60 tubing (Clay Adams, NJ) and lungs lavaged with PBS and bronchoalveolar lavage fluid (BALF) collected (40). The right lung was removed and single cell suspensions for cell culture and flow cytometry obtained by tissue fragmentation in 1 ml RPMI medium using a blade, followed by digestion at 37°C for 40 min after addition of 5 ml solution containing 1 mg/ml collagenase and 0.2 mg/ml DNase 1, with reaction stoppage by addition of cold 120 mM EDTA and cell collection through a 70 μm strainer prior to ACK red cell lysis. The left lung was isolated, inflated to a pressure of 20 cm H_2O with 10% formalin, removed, and immersed in fixative for immunohistochemistry (IHC).

Quantitation of Lymphocyte Subsets by Flow Cytometry

For flow cytometry, freshly isolated red blood cell-depleted lung or spleen cell suspensions were Fcgamma Receptor blocked and stained using fluorescence (FL)-labeled Ig, and isotype controls, for CD45 (leukocytes), CD19 (B cells), CD3 (T cells), IgMa (Ig Tg), and IgMb (endogenous Ig) as previously described (19, 20). Data were acquired using FACScalibur or FACSCanto machines (BD Biosciences, San Jose, CA), and data were analyzed using FlowJo software (Ashland, OR).

BALF Cell Counts and Evaluation of Lung Injury and Tertiary Lymphoid Structures (TLS)

Cells from the BALF were isolated using centrifugation (1,500 rpm, 15 min) and the supernatant was stored at −80°C. The cells underwent red cell lysis (ACK lysis solution) and were counted using a Cellometer K2 (Nexcelom Bioscience, Laurence, MA). Total cell counts were obtained and normalized to the BALF lavage volume. Cells were then immobilized by cytospin and stained with Diff-Quik staining solution to obtain differential counts. Histological analysis was performed on H&E or PAS stained tissue. Lung injury was scored on a 5-point scale that incorporated inflammation, edema, hemorrhage, necrosis, and fibrosis across whole lung sections (41) by an experienced veterinary diagnostician (YA) blinded to study group, using a Nikon photomicroscope and images acquired using an NIS-Elements Nikon camera. To identify deposited silica particles, lung H&E sections were examined with a polarizing attachment as previously described (42). For lung direct IF and quantitation of lymphoid structures, 10% formalin inflated/fixed whole lungs were oriented similarly in cassettes for paraffin embedding, and sectioned (5 μm), with one full-size section from within the first 250 μm of tissue used for counting. This was based on a pilot study examining silica-exposed lungs ($n = 3$) at multiple (5) depths through the lung, which showed that while the average % lung area containing TLS and TLS composition (B/T cell ratios) were similar at all depths, the overall lung section size decreased after a depth of 250 μm. Lung sections were deparaffinized, heated in 10 mM citrate buffer (pH 6.0) to expose antigen, and stained with anti-B220 (B cells) and anti-CD3e (T cells) using appropriate blocking buffer, then labeled using species-specific TRITC-(B cells) or FITC-(T cells) labeled secondary Ab, and counterstained with DAPI (nuclei). Mouse spleen sections served as a positive staining control. For quantitation of TLS: whole lung sections were scanned at the Alafi Neuroimaging Core (Washington University, St. Louis, MO) and NDP Viewer software (Hamamatsu) used for data collection. Images were gridded and each block assessed for TLS, which we defined as

a group of 10+ adjacent B and/or T cells. Where indicated, perimeter, area, and B/T cell composition of each TLS were recorded using the Freehand annotation tool. Total TLS area is normalized to overall lung area for the entire lung section, measured using the Freehand tool. Slides were scored by an investigator blinded to study group.

Cell Culture

For autoAb measurement assays, lung and spleen cell preparations were RBC-depleted and cells plated in 48- or 96-well plates containing one million cells/mL in RPMI 1640 medium (Sigma, St. Louis. MO) containing 10% heat inactivated fetal bovine serum (HI-FBS), plus 2 mM additional L-glutamine, 100 U/mL Penicillin-Streptomycin, 1X MEM Non-essential Amino Acids, 10 mM HEPES Buffer, pH 7.6, and 1 mM Sodium Pyruvate (all additives from Gibco, Waltham MA). To test for the capacity of superimposed environmental stimuli (microbial products) to enhance autoAb production by B cells from silica-exposed wildtype mice and to test for defective or reversible anergy in B cells from autoAb Tg mice, a subset of cell cultures were stimulated with either 50 μg/mL lipopolysaccharide (LPS, TLR4 agonist, Sigma) or a combination of 2 μg/mL resiquimod (R848, TLR7 agonist, Sigma) and 1 μg/mL ODN 1668 CpG oligos (CpG, TLR9 agonist, Invivogen, San Diego, CA). Cells were cultured for 7–8 days in 5% CO_2, 37°C. Collected culture supernatants were stored with 0.01% sodium azide as a preservative at −20°C until assay.

Ig and AutoAb Quantitation by ELISA

ELISA was used to detect lupus-associated anti-DNA and vasculitis-associated anti-MPO autoAb in wildtype mice, and to detect lupus-associated anti-laminin and anti-DNA autospecificities encoded by the Tg in autoAb Tg mice. Total Ig and Ig Tg (IgMa+) concentration in serum, BALF, and culture supernatants was determined by ELISA, as described (17, 19). To detect autoAb, Immulon 2 HB plates (Thermo Scientific, Waltham, MA) were coated overnight at 4°C with antigen diluted in PBS, including ssDNA prepared by phenol chloroform extraction of calf thymus DNA (Worthington Biochemicals, Lakewood, NJ) (43) at 4.5 or 45 μg/mL, human leukocyte MPO (Sigma Aldrich, St. Louis, MO, or Lee Biosolutions, Maryland Heights, MO) at 0.02 or 0.2 U/mL, laminin from Engelbreth-Holm-Swarm mouse sarcoma (Sigma) at 10 μg/mL in PBS, or with diluent (PBS) only. Plates were blocked for at least 60 min with 3% BSA (Sigma) in PBS, incubated with samples for minimum 60 min, then labeled with goat-anti-mouse Ig-alkaline phosphatase or mouse-anti-mouse-IgMa-biotin-conjugated antibody (BD Pharmingen, San Diego, CA) followed by alkaline-phosphatase conjugated streptavidin (Southern Biotech, Birmingham, AL). Bound Ig were detected with phosphatase substrate (Sigma) and OD405 recorded on Emax microplate reader (Molecular Devices) using SoftMax software. Results for binding to antigen were recorded as OD on antigen minus OD on wells coated with diluent only, after subtraction of OD blank (determined for dilution buffer without Ig). Controls include anti-ssDNA IgG H241 (44), anti-MPO mAb clone CLB-MPO-1/1 (Sigma Aldrich), anti-laminin IgG H50 (45), anti-laminin IgM A10C (28), and anti-laminin/anti-DNA transfectant IgM LamH/Vk8Jk5 (18). Unless otherwise indicated, serum was diluted 1:20 in PBS/0.1% BSA for ELISA assays, and BALF and cell culture supernatants were assayed undiluted.

Statistical Analysis

Data management and statistical analysis were performed using JMP software (SAS, Cary, NC). Differences between silica- and vehicle-exposed mice within each strain were assessed using Wilcoxon each pair, with $p < 0.05$ considered significant. Differences between silica-exposed mice across all strains were evaluated using Kruskal-Wallis rank sums test and the multiple comparisons Steel-Dwass All Pairs test was used to determine which pairs were significant. To examine the capacity of silica exposure to abrogate deletional tolerance in autoAb Tg mice, sample size determination was performed to estimate the minimum number of animals per group that could significantly differentiate high level deletion (measured as low spleen B cell counts) from a non-deletional phenotype in each strain. Using reference values (mean and standard deviation) from our published data (17–19) that includes experimental groups containing mean 25.9 mice/group (range 11–48), *a priori* power analyses suggested that 3 mice/group could attain statistical significance of $p < 0.05$ with a 90% probability.

RESULTS

Lung Injury and Inflammation in Diverse Backgrounds After Silica Exposure

To first determine if silica instillation induced lung injury and lymphoid cell accumulation in mice of the different autoimmune genetic susceptibilities, adult wildtype female mice of each background (B6, BXSB, MRL, NZB) were given a single exposure of 0.2 mg/gm (∼3–6 mg/mouse) crystalline silica or vehicle (saline) at age 3 months (NZB, B6, MRL) or 1.6 months (BXSB) and analyzed at 1, 2, or 3 months post-exposure. Three time points were chosen for harvest because the effect of this exposure on lung injury and survival in the different backgrounds was unknown. At harvest mice ranged from 3.6 to 6 months old, depending on the month post-exposure. Results showed that all exposed mice survived until the predefined harvest date, at which time mice exposed to silica showed extensive lung injury, whereas vehicle-exposed lungs showed minimal damage (**Figures 1A,B**). Lung histopathological examination revealed leukocyte infiltration, granuloma formation, alveolar proteinosis, lymphoid collections, edema, and scattered hemorrhage in silica-exposed mice in each strain (**Figure 1A**). Lung injury was observed at each time point tested, with no correlation between lung injury score and months post-exposure (not shown). Extensive lung injury was already observed by the 1 month time point (**Figure S.1**). Among all silica-exposed mice, no significant differences were found in lung score between the four strains (Kruskal-Wallis test, ChiSquare = 2.59, $p = 0.46$, $df = 3$). Polarizing light microscopy of lung tissue on H&E stained sections revealed multiple small birefringent particles in lungs of mice exposed to silica, whereas lungs of most mice exposed to vehicle demonstrated only scattered background birefringence.

Silica particles were concentrated in pulmonary nodules and granulomas (**Figure 1C**), and in some animals were scattered throughout lung parenchyma. In contrast, silica particles were generally absent from lymphoid collections.

Silica exposure was associated with leukocytic infiltration of bronchoalveolar space and lungs in each strain. BALF from silica-exposed mice contained significantly more leukocytes than BALF from their vehicle-exposed counterparts (**Figure 1D**). A Kruskal-Wallis test also showed a significant difference in BALF leukocyte counts between silica-exposed mice of different strains (**Table 1**). Adjustment for multiple comparisons showed that both BXSB and MRL silica-exposed mice had significantly higher BALF leukocyte counts than did B6 or NZB silica-exposed mice (Steel-Dwass All Pairs method, $p < 0.05$ each pair), whereas there were no significant differences between MRL vs. BXSB or NZB vs. B6 silica-exposed groups. Whereas, macrophages dominated BALF cell composition in vehicle-exposed mice (range 96% to 100% of BALF cells in B6, BXSB and NZB mice, $n = 16$; range 60–99% of BALF cells in MRL, $n = 6$), neutrophils constituted a significantly greater proportion of BALF cells in silica-exposed mice of each strain: % neutrophils, median (IQR), 15% (12.5) for B6, 15% (19) for BXSB, 36% (21.5) for MRL, and 32% (19.5) for NZB, all $p < 0.05$ vs. their vehicle-exposed counterparts. Lymphocytes comprised a small percentage of BALF cells in all strains (not shown).

Flow cytometry of dissociated whole lung revealed that silica-exposed BXSB and MRL mice had significant enrichment for CD45+ leukocytes and CD19+ B cells in their lungs compared to their vehicle-exposed counterparts (**Figure 1E**). Lung leukocyte counts also differed according to strain among all silica-exposed mice, though in a pattern different from that observed for BALF: silica-exposed BXSB lungs contained significantly fewer leukocytes than lungs of silica-exposed MRL or NZB mice (**Table 1**). For CD19+ B cell counts, a trend was observed for fewer B cells in silica-exposed NZB vs. BXSB lungs ($p = 0.05$ by Steel-Dwass All Pairs).

Lung Lymphoid Structures

Immunostaining revealed aggregates of B cells and T cells, similar to TLS, scattered in the lungs of wildtype mice exposed to silica (**Figure 2A**). Many TLS-like aggregates consisted of a B cell-dominant central region with an adjacent or surrounding collection of T cells, and numerous clusters abutted small blood vessels or bronchioles (**Figure 2B**). Lymphoid aggregates were delineated and quantified on gridded scanned images of whole lung sections (**Figure 2C**). TLS were identified in lungs of silica-exposed mice of each strain but were rarely observed in their vehicle-exposed counterparts. This difference was statistically significant for B6, BXSB, and MRL mice, measured both as total number (**Figure 2D**) and as total lymphoid area as percent of total lung area (**Figure 2E**). For NZB there was a trend toward an increased number of lung TLS in silica- vs. vehicle-exposed mice.

Among silica-exposed mice differences between strains were also observed, with silica-exposed MRL demonstrating a significantly higher TLS count than their BXSB or NZB counterparts and significantly higher TLS percent area than silica-exposed B6 mice (**Table 1**). Among silica-exposed mice, there was no correlation between TLS count and duration post-exposure ($p = 0.7966$). TLS area did increase with post-exposure duration (Spearman's rho, $p = 0.0485$), primarily in BXSB and MRL mice.

AutoAb in Lungs and Serum

Anti-DNA IgM and IgG autoAb were significantly higher in BALF of silica-exposed mice compared to their vehicle-exposed counterparts for the B6, BXSB, and MRL strains (**Figures 3A,B**). Silica-exposed B6 and MRL also had higher BALF IgM levels compared to vehicle exposed mice (**Figure 3C**). Conversely, anti-DNA Ig levels in NZB BALF did not vary by exposure (**Figures 3A–C**), although there was a trend to higher levels of anti-DNA IgG in BALF of silica-exposed NZB. IgM antibodies to MPO, a major target antigen in ANCA vasculitis, were significantly elevated in BALF of silica- compared to vehicle-exposed BXSB mice (**Figure 3D**). Low levels of anti-MPO IgG were detected in BALF of several silica-exposed mice of other strains; however, overall levels did not exceed those in their vehicle-exposed counterparts. Among all silica-exposed mice, B6 had significantly lower levels of BALF autoAb than other strains, including less anti-DNA IgM than silica-exposed mice in each of the lupus strains, less anti-DNA IgG than silica-exposed MRL and BXSB, and less anti-MPO than exposed BXSB (**Table 1**).

Isolated lung cells from exposed B6, MRL and NZB mice were cultured with or without ligands to TLRs to assess silica-related responsivity, with and without the additional environmental (TLR) stimulus. Ligand to TLR4 or a mixture of ligands to TLR7 and TLR9 were used, based on our prior experience demonstrating additive effect of TLR7 and 9 ligands in unmasking reversible anergy in NZB lupus (20). Both TLR solutions induced anti-DNA IgM, including from lung cells of both silica- and vehicle-exposed mice; the highest levels of anti-DNA IgM were induced by TLR7/9 ligand combination (not shown). Quantitation of anti-DNA IgG revealed significantly higher levels in supernatants of lung cells harvested from silica-exposed MRL mice and co-cultured with TLR7/9 ligands compared to similarly cultured lung cells from vehicle-exposed MRL mice (**Figure 3E**). In contrast, recovery of TLR7/9-induced IgG anti-DNA was not increased in lung cultures from silica- vs. vehicle-exposed B6 or NZB mice (**Figure 3E**). Among all silica-exposed mice (B6, MRL, and NZB), anti-DNA IgG production by TLR7/9-stimulated lung cells was significantly higher for MRL compared to B6 or NZB (**Table 1**). For MRL mice, there were trends toward higher spontaneous (in the absence of TLR ligand additive) and TLR4 ligand-induced IgG anti-DNA levels in cultures of lung cells derived from silica- compared to vehicle-exposed mice ($p = 0.0972$ and $p = 0.0987$, respectively, not shown). Among all silica-exposed mice, levels of TLR4-stimulated anti-DNA IgG were significantly higher for MRL compared to B6 and NZB (**Table 1**).

Elevated levels of IgM anti-MPO were detected in supernatants of TLR7/TLR9 stimulated cultured lung cells from 2 of 9 silica-exposed, vs. 0 of 6 vehicle-exposed, B6 mice; however, overall anti-MPO autoAb levels did not significantly exceed those in vehicle-exposed counterparts (not shown). Ig

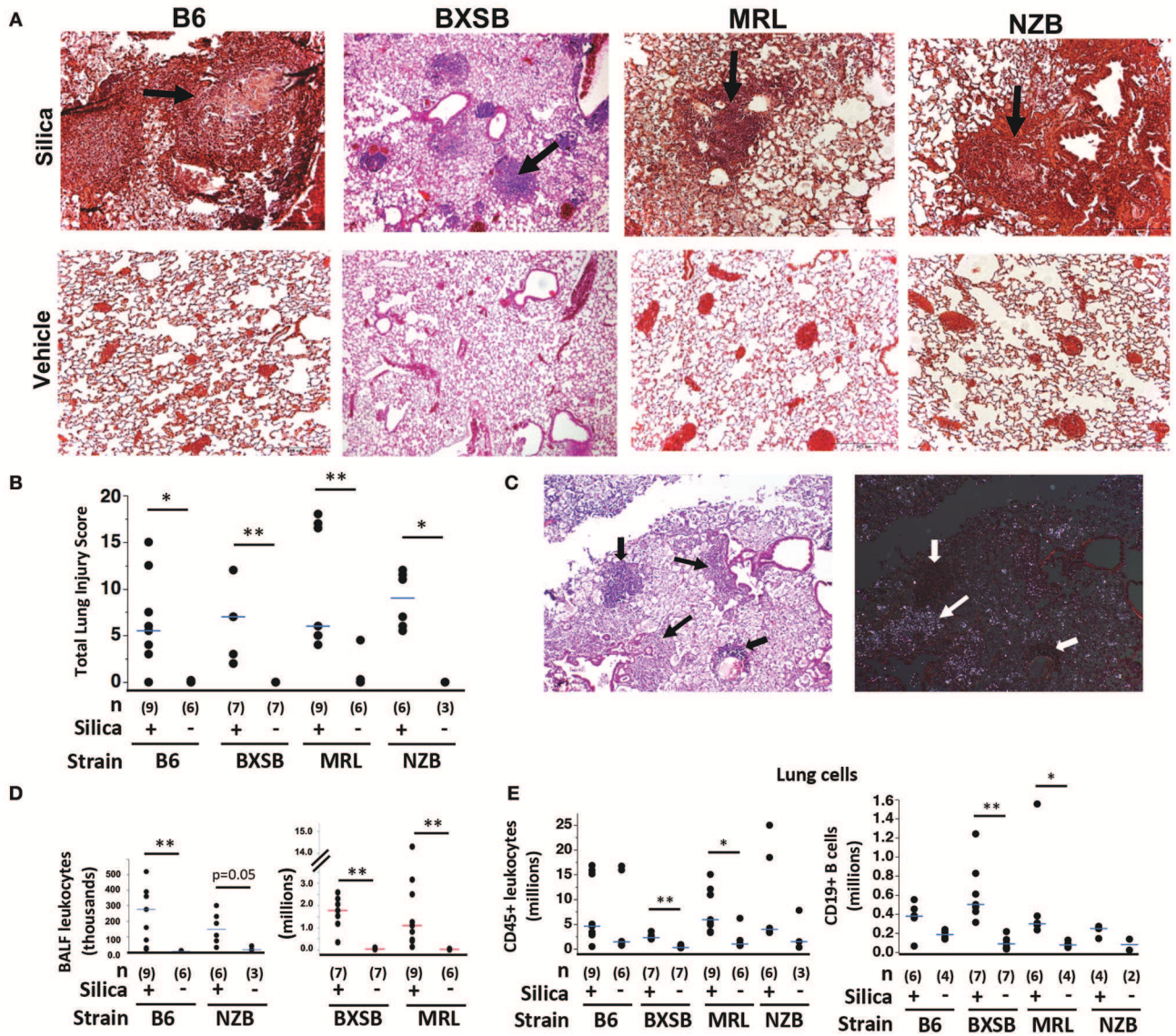

FIGURE 1 | Lung injury and inflammation in diverse wildtype mouse strains after exposure to crystalline silica. **(A)** Representative sections of lung from mice of indicated strain 2 months (MRL) or 3 months (B6, BXSB, NZB) after instillation of silica or vehicle; H&E, original magnification ×40. Arrows indicate granulomas. **(B)** Lung injury composite scores for mice of each strain after exposure to silica or vehicle. **(C)** Localization of silica particles in a representative H&E stained section of lung tissue from an MRL mouse 1 month after silica instillation, viewed by conventional (left) or polarizing (right) light microscopy; thin arrows indicate granulomas, thick arrows indicate lymphoid collections. **(D)** Leukocytes in BAL fluid, counted using Diffquick. **(E)** CD45+ leukocytes (left) and CD45+ CD19+ B cells (right) in whole lung cell isolates of mice after exposure were quantitated by flow cytometry, gated on live cells. For data in scatterplots, lungs were harvested 1, 2, and 3 months post-exposure for each group, except for BXSB for which lungs were harvested at 2 or 3 months post-exposure. Each symbol represents an individual mouse, with tissue harvested at 1, 2, or 3 months after exposure; the median for each group is indicated by the bar; $^{*}p < 0.05$ and $^{**}p < 0.01$ for silica- vs. vehicle-exposed mice of same strain, Wilcoxon rank sum test.

reactive with alpha3(IV)NC1 collagen, the target antigen in Goodpasture's Disease/anti-glomerular basement membrane nephritis, diseases with serologic and clinical overlap with ANCA vasculitis, were detected in several supernatants of TLR7/TLR9-stimulated cultured lung cells from MRL and B6 mice, including cells from vehicle- as well as silica-exposed subjects (not shown).

Mice of all strains had detectable serum IgM and IgG anti-ssDNA. Anti-DNA IgM and IgG levels did not differ significantly between silica- and vehicle-exposed mice at tested dilutions with the exception of NZB anti-DNA IgG levels, which were significantly higher in silica-exposed mice (**Figure 3F**). Among silica-exposed mice, serum anti-DNA IgG levels in MRL significantly exceeded those in B6 and BXSB (and likely exceeded those in NZB, noting that MRL serum was tested at 5-fold greater dilution) (**Figure 3F** and **Table 1**); levels in NZB serum also exceeded those in BXSB (**Table 1**).

TABLE 1 | Differences between silica-exposed wildtype mice of diverse autoimmune genetic backgrounds.

	Si-exposed strain								Kruskal-Wallis			Steel-Dwass all pairs
	B6		BXSB		MRL		NZB		Chi square	*df*	*p*-value	*p*-value
Parameter	**Median**	**IQR[a]**	**Median**	**IQR**	**Median**	**IQR**	**Median**	**IQR**				
BALF LEUKOCYTE COUNT (THOUSANDS)[b]												
	275	322	1,772	1124	1,096	2,406	147	185	17.77	3	0.0005	<0.05, BXSB vs. B6 & NZB <0.05, MRL vs. B6 & NZB
LUNG CD45+ LEUKOCYTE COUNT (MILLIONS)[b]												
	4.6	12.6	2.3	0.7	5.9	7.3	4.0	16.8	11.62	3	0.0088	<0.05, BXSB vs. MRL & NZB
LUNG TLS COUNT[c]												
	51	34	29	28	70	46	14.5	20.3	15.55	3	0.0014	<0.05, MRL vs. BXSB <0.01, MRL vs. NZB
LUNG TLS AREA %[c]												
	0.79	0.84	1.11	1.76	1.47	0.91	0.47	1.23	10.03	3	0.0183	<0.05, MRL vs. B6
BALF autoAb LEVELS (OD405)[d]												
α-DNA IgM	0.262	0.255	0.965	0.928	1.386	1.223	0.635	0.340	19.85	3	0.0002	<0.01, B6 vs. MRL <0.05, B6 vs. BXSB & NZB
α-DNA IgG	0.058	0.056	0.445	0.661	1.510	1.452	0.273	0.616	20.63	3	0.0001	<0.01, B6 vs. MRL & BXSB
α-MPO IgM	0.000	0.005	0.079	0.094	0.003	0.047	0.008	0.026	12.97	3	0.0047	<0.01, B6 vs. BXSB
LUNG CELL CULTURE (TLR LIGAND STIMULATED) ANTI-DNA IgG (OD405)[d]												
TLR7/9	0.011	0.029	–	–	0.312	0.910	0.000	0.013	16.10	2	0.0003	<0.01, MRL vs. B6 & NZB
TLR4	0.000	0.003	–	–	0.100	0.307	0.000	0.014	16.08	2	0.0003	<0.001, MRL vs. B6 <0.05, MRL vs. NZB
SERUM ANTI-DNA IgG (OD405)[d]												
	0.553	0.572	0.278	0.362	2.965	2.536	2.045	1.727	21.35	3	<0.0001	<0.01, MRL vs. B6 & BXSB <0.05, NZB vs. BXSB

[a] *BALF, bronchoalveolar lavage fluid; IQR, interquartile range; df, degrees of freedom; MPO, myeloperoxidase; Si, silica; TLR, toll-like receptor; TLS, tertiary lymphoid structures.*
[b] *BALF leukocyte counts were determined by Cellometer K2 and lung counts by flow cytometry.*
[c] *Lung TLS count and % area were quantified on gridded images of scanned whole lung sections stained for B and T cells.*
[d] *Autoantibodies in undiluted BALF and lung cell culture supernatants and in sera diluted 1:100, except for MRL sera diluted 1:500, were measured using ELISA.*

A few mice of different strains had detectable serum anti-MPO Ig, without a discernable difference based on exposure. Splenocytes from all strains and from mice exposed both to silica and vehicle produced IgM anti-ssDNA in culture, with increased levels after TLR ligand stimulation. TLR4 ligand induced the highest level of IgG anti-DNA from MRL splenocytes, although induced levels did not differ significantly between exposure groups (not shown). BXSB splenocytes uniquely produced high levels of IgM anti-MPO after TLR ligand stimulation; however, levels did not vary based on exposure (not shown).

Silica Exposure in AutoAb Tg Mice

A major goal of these studies was to directly assess the impact of silica instillation on autoreactive B cell fate and pathogenic autoAb production. For this purpose, we took advantage of an established autoAb Tg reporter system in which B6, NZB, MRL, and BXSB mice carry the LamH IgMa autoAb Tg (17, 18). LamH encodes a dominant Ig heavy chain that generates Ig reactive with laminin and DNA. Expression of the autoAb Tg enriches for B cells with this autospecificity that can be readily tracked using allotypic or idiotypic markers. This model permits measurement of major tolerance mechanisms: deletion is quantitated using spleen B cell counts; anergy can be assessed in part by autoAb production and B cell response to TLR4 stimulation; and receptor inclusion or editing can be measured by expression of endogenous Ig chains. This overcomes some limitations of dissecting mechanisms in wildtype mice with highly diverse polyclonal B cell populations and specificities in which tracking the fate of individual B cells is difficult.

For these experiments, adult autoAb Tg mice were given a single exposure of 0.2 mg/gm (∼3–6 mg/mouse) crystalline silica or vehicle (saline) and analyzed after 3.5–7 weeks. AutoAb Tg mice were age-matched to silica vs. vehicle exposure within each strain using littermates (Tg+ mice are not age-matched across strains because between-strain comparison was not a primary goal of this study that measures effects of silica exposure on B cell tolerance mechanisms). Ages are reported for individual autoAb Tg mice in **Table S.1**. Older adult mice were included, as we rationalized that breach of tolerance, if present, may be more likely detected in older individuals. All autoAb Tg mice were exposed on the same date, and within each autoAb Tg strain mice in the two exposure groups were harvested on the same date. B6-Tg, BXSB-Tg, and MRL-Tg mice were

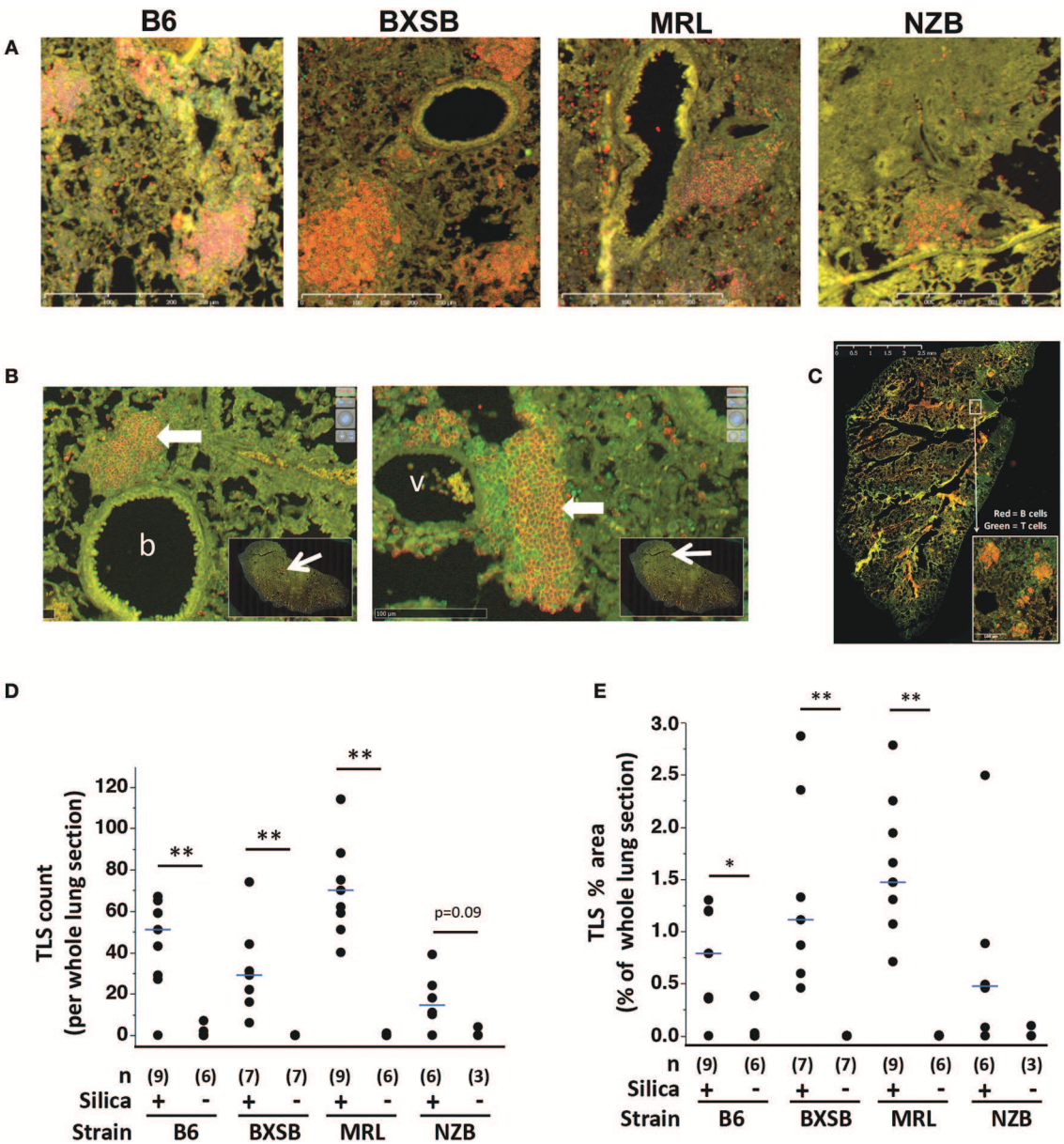

FIGURE 2 | Tertiary lymphoid structures (TLS) in lungs of wildtype mice exposed to silica. **(A)** Representative sections of lung from mice of indicated strain 2 months (MRL) or 3 months (B6, BXSB, NZB) after instillation of silica or vehicle, stained with anti-B220 (B cells, red) and anti-CD3e (T cells, green), original magnification ×100. **(B)** Representative peribronchiolar (left) and perivascular (right) tertiary lymphoid structures (thick arrows), from the lung of an MRL mouse 1 month after silica exposure; b, bronchiole; v, vessel. The insets show the whole lung section, with the area of magnification outlined by the red box at the tip of the arrow. **(C)** Representative whole lung section scanned after staining with fluorescein-conjugated anti-mouse-CD19 (B cells, red) or anti-mouse-CD3e (T cells, green). The inset shows four TLS. TLS were counted and TLS area quantitated across the entire lung section. **(D)** TLS number per whole lung section; and **(E)** TLS area as percentage of area of whole lung section. For scatterplots each symbol represents an individual mouse; the median for each group is indicated by the bar; $^{*}p < 0.05$ and $^{**}p < 0.01$ for silica- vs. vehicle-exposed mice of same strain, Wilcoxon rank sum test.

harvested 1.5–1.75 months after silica exposure, a time point based on results in wildtype mice, in which extensive lung inflammation and TLS were already observed by 1 month after silica instillation. A similar post-exposure duration was planned for NZB-Tg mice; however due to weight loss and death of 3 NZB-Tg mice within 3 weeks post-exposure, the remaining NZB-Tg were harvested at this time point and are included in this report.

Lung injury was observed in all autoAb Tg mice exposed to silica, and included inflammation, necrosis, fibrosis, alveolar proteinosis, and edema, whereas vehicle-exposed lungs showed no or minimal injury (**Figure S.2A**). Immunostaining revealed

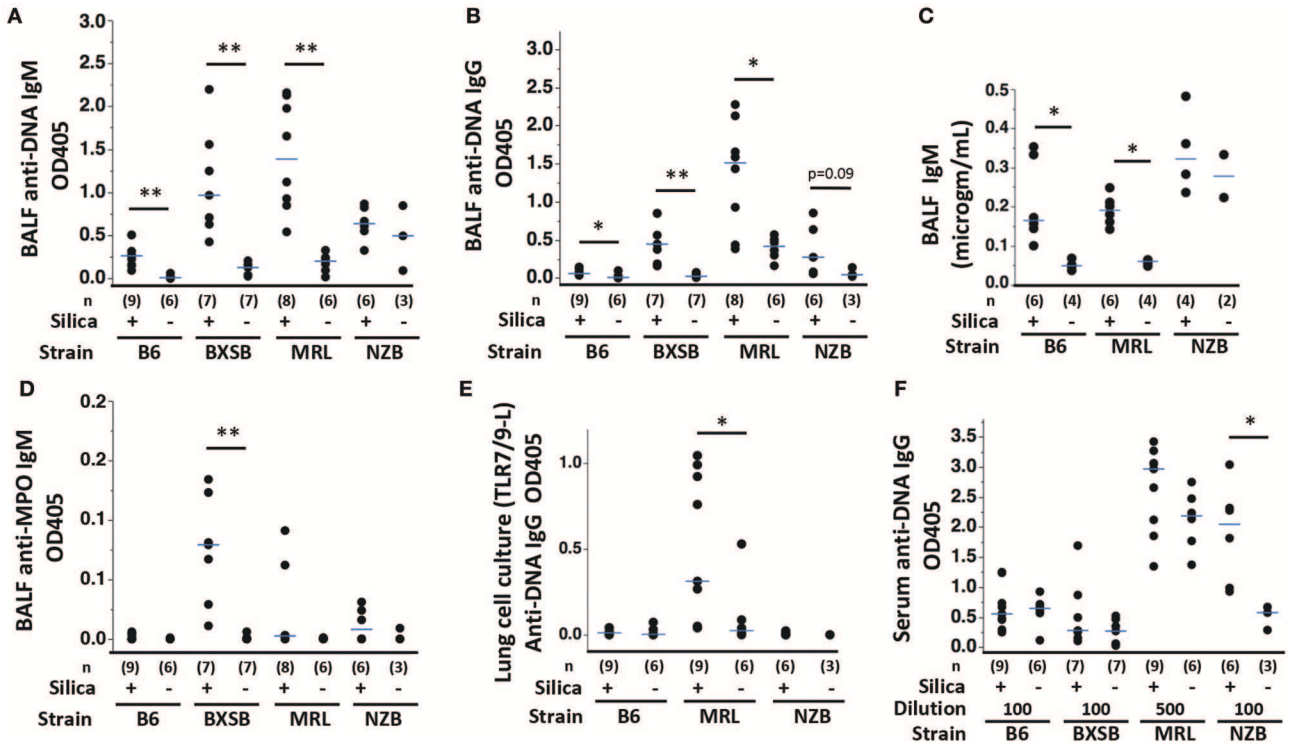

FIGURE 3 | Autoantibody production in wildtype mice of diverse genetic backgrounds exposed to silica. **(A)** Anti-ssDNA IgM; **(B)** Anti-ssDNA IgG; **(C)** IgM concentration; and **(D)** Anti-MPO IgM levels in bronchoalveolar lavage fluid (BALF) from wildtype mice 1–3 months after exposure to silica or vehicle. Autoantibody levels were measured as OD405 for binding to antigen minus binding to diluent-only using undiluted BALF in duplicate. **(E)** Anti-ssDNA IgG levels in supernatants derived from lung cells cultured with a mixture of TLR7 and TLR9 ligands R848 and CpG oligos, from mice of indicated exposure and strain. **(F)** Anti-ssDNA IgG levels in serum diluted 1/100 or 1/500, as indicated. Each symbol represents an individual mouse; the median for each group is indicated by the bar; $^{*}p < 0.05$ and $^{**}p < 0.01$ for silica- vs. vehicle-exposed mice of same strain, Wilcoxon rank sum test.

aggregates of B and T cells consistent with TLS scattered in the lungs of the silica-exposed subset in each strain (**Figures S.2B,C**). Overall TLS counts per whole lung section (58.7 ± 29.8, mean ± SD, $n = 12$) in the silica-exposed autoAb Tg mice were comparable to TLS counts in wildtype mice (45.1 ± 30.1, $n = 31$). Similar to the case in wildtype mice, numerous lymphoid clusters were located adjacent to small blood vessels or bronchioles (**Figure S.2D**). Semiquantitative assessment of TLS composition identified a relatively low proportion of B cells within lymphoid clusters in autoAb Tg mice on the MRL and NZB backgrounds (**Figure S.2E**). Flow cytometric analysis confirmed that B cells expressing the Tg+ allotype IgMa were represented among lung infiltrating B cells (**Figure S.2F**).

Tolerance Phenotypes in Silica-Exposed AutoAb Tg Mice

Despite evidence of extensive lung injury and TLS formation in silica-exposed adult autoAb Tg mice across a range of ages and autoimmune backgrounds, overt breach of B cell tolerance was not detected in any mouse. The total number of splenic B cells was very low in all autoAb Tg mice studied (5.7 ± 3.4 million, mean ± SD, $n = 25$), regardless of exposure or background strain (values for individual mice by strain are shown in **Figure 4A**). In each of the four strains, the mean number of B cells per spleen in Tg+ mice was very similar to that previously reported in our colonies. Spleen B cell counts (millions, mean ± SD) by autoAb Tg strain were 4.9 ± 2.8 for B6, 8.8 ± 4.3 for BXSB, 4.9 ± 1.7 for MRL, and 3.9 ± 1.3 for NZB. This compares to historical mean counts of 6.0, 10.6, 5.6, and 3.6 million, respectively, for these autoAb Tg strains (17, 19). We observed similar consistency in spleen B cell number among different cohorts of B6 Tg+ mice in our colonies evaluated many years apart (17–19, 46). Historically the spleen B cell count in unmanipulated autoAb Tg+ mice represented a 76–89% reduction in the total number of splenic B cells compared to non-Tg (wildtype) counterparts, in which average B cell counts ranged from 18.2 million in NZB to 60.6 million in BXSB (19). Although age-matched non-Tg littermates were not evaluated simultaneously in the current study, preventing direct comparison of autoAb Tg+ and non-Tg spleen B cell counts, spleen B cell counts of the commercially-acquired adult wildtype mice exposed to silica or vehicle and described in the current study ($n = 53$) were comparable to historical values (**Figure 4A**). Within each strain, spleen B cell counts were highly significantly lower in autoAb Tg mice compared to wildtype mice for B6, BXSB and MRL, and significant with $p = 0.0027$ for NZB (**Figure 4A**). For all

silica-exposed autoAb Tg mice, mean spleen B cell count was 5.3 ± 3.5 million ($n = 12$). Collectively, the findings support the notion that a large number of B cells in the autoAb Tg+ mice undergo deletional tolerance and that exposure to silica and its associated lung inflammation does not promote a major breach in this central regulation.

The number of splenic B cells did not differ between silica- and vehicle-exposed groups in any autoAb Tg strain (**Figure S.3A**), nor did the number of splenic B cells in silica-exposed autoAb Tg mice differ between strains (Kruskal-Wallis test, ChiSquare $= 3.62$, $p = 0.3061$, $df = 3$). The number of mice per individual exposure group is small, however, and a larger number of subjects will be needed to detect lesser, partial, or subtle defects in deletional regulation, if present.

The functional status of the residual Tg B cells was assessed by quantitating Ig production, an indicator of B cell activation and differentiation. For this purpose, levels of serum Tg-encoded IgM and autoAbs were measured in B6-Tg, BXSB-Tg, and NZB-Tg mice, in which Tg allotype IgMa is readily distinguished from endogenous IgMb (levels are not reported for MRL mice, in which endogenous IgM is j-allotype that crossreacts with IgMa, such that differentiation of Tg from endogenous Ig is not possible using anti-allotype reagents). Serum IgMa concentrations ranged from 1.2 to 30.5 μg/mL (**Figure 4B**), similar to the low levels we previously observed in LamH autoAb Tg mice and 10- to 100-fold lower than normal serum IgM concentrations in wildtype mice (47). Serum levels of Tg anti-laminin autoAb were very low (**Figure 4C**), consistent with ongoing regulation of the residual Tg anti-laminin B cells that escaped deletion. Anti-ssDNA autoAb encoded by Tg IgMa were detected in serum, indicating that at least a subset of residual Tg-encoded B cells are activated *in vivo* (**Figure 4D**). Low levels of Tg IgMa were detected in BALF (range 0.001–0.178 μg/mL), with a trend toward higher levels in silica compared to vehicle-exposed mice in B6 and BXSB strains (not shown). Whereas, trace amounts of anti-DNA IgMa were detected in BALF from several mice, no anti-laminin IgMa was detected. Collectively, these findings are consistent with preservation of anergy in residual (non-deleted) anti-laminin Tg B cells, despite exposure to silica.

Another hallmark of anergy in autoAb Tg models is failure of TLR4 ligand LPS to induce Tg autoAb from cultured splenic B cells. In the current experiments sufficient spleen cells were available from B6-Tg and BXSB-Tg mice to assay effects of TLR ligand stimulation. Only low levels of Tg anti-laminin IgMa were induced regardless of silica exposure of the donor autoAb Tg mouse (**Figure 4E**). This finding supports preservation of anergy in the residual Tg B cells. Surprisingly, stimulation with a combination of TLR7/TLR9 ligands induced substantial levels of Tg anti-laminin autoAb. In B6-Tg mice, there was a trend for greater anti-laminin Tg Ig production by TLR7/9-stimulated B cells from silica- compared to vehicle-exposed mice, despite plating of similar numbers of B cells (**Figure 4E**). A similar trend was seen for TLR7/9 induction of Tg anti-DNA autoAb from silica-exposed B6 B cells (**Figure S.4**).

There is also evidence that the Tg B cells are regulated in part by receptor editing, as previously described for this model (18). Flow cytometric analysis of lung cells using allotype-specific anti-sera confirmed the presence of IgMa+ Tg B cells among lung leukocytes in B6-Tg, BXSB-Tg, and NZB-Tg strains (**Figure S.2F**). In all autoAb Tg mice the percent of lung CD45+CD19+ B cells that are IgMa+ was low (range 3.2–38.9%), a finding not accounted for by endogenous IgMb staining (**Figure S.2F**). This suggests downregulation of surface IgM, a feature frequently seen in B cell anergy. In the spleen, surface Tg (IgMa) expression on CD19+ B cells varied inversely with that of endogenous IgMb (**Figure S.3B**), with lowest IgMa levels in B6-Tg mice and only a low frequency of double positive cells (range 0.7–5.7% of CD19+ cells, not shown). This suggests that editing including heavy chain allelic inclusion is operative, particularly in the B6 strain.

DISCUSSION

Results from silica exposure in mice of genetically diverse backgrounds, including non-autoimmune B6 and autoimmune-prone BXSB, MRL, and NZB strains, substantiate silica's universal capacity to induce pulmonary injury and lymphoid aggregates and demonstrate strain-specific effects on humoral autoimmunity and B cell tolerance. We detected strain differences in autoAb specificity and in the site of enhanced autoAb production, consistent with genetic modulation of the autoimmune response to silica. Using an autoAb Tg reporter system to track the *in vivo* fate of autoreactive Tg B cells, we were able to measure several tolerance mechanisms within the different strains after exposure to a silica dose capable of inducing severe lung injury and TLS in each strain. We observed gross preservation of autoreactive B cell regulation in each autoAb Tg strain: spleen B cells remained markedly depleted in all Tg strains, consistent with intact central immune tolerance, and the residual population of autoAb Tg B cells contributed only low to modest levels of serum Tg IgMa and minimal Tg anti-laminin Ig, regardless of exposure. These tolerance phenotypes mirror those previously reported for unmanipulated mice bearing this autoAb Tg (17, 18), and indicate that silica exposure alone does not overtly disrupt central B cell tolerance. This suggests that silica exposure subverts tolerance at alternative checkpoints, such as regulatory cells or follicle entry, or requires additional interactions or co-exposures to induce loss of tolerance.

It is interesting to note that autoAb Tg B cells localize to lungs of silica-exposed mice in each strain, as demonstrated by flow cytometry and immunohistochemistry, and aggregate in TLS-like clusters. The potential of these B cells to increase local production of autoAb after silica exposure and resulting lung inflammation in B6 and BXSB mice is suggested by the trend toward increased levels of Tg Ig in BALF of silica-exposed mice in these strains; nonetheless, BALF levels of Tg IgMa remain low and anti-DNA and anti-laminin Ig levels are negligible in this setting.

Systemic Effects of Silica on Autoimmune Regulation

An unexpected finding was the induction of substantial levels of anti-laminin autoAb Tg by splenocytes harvested from B6 mice

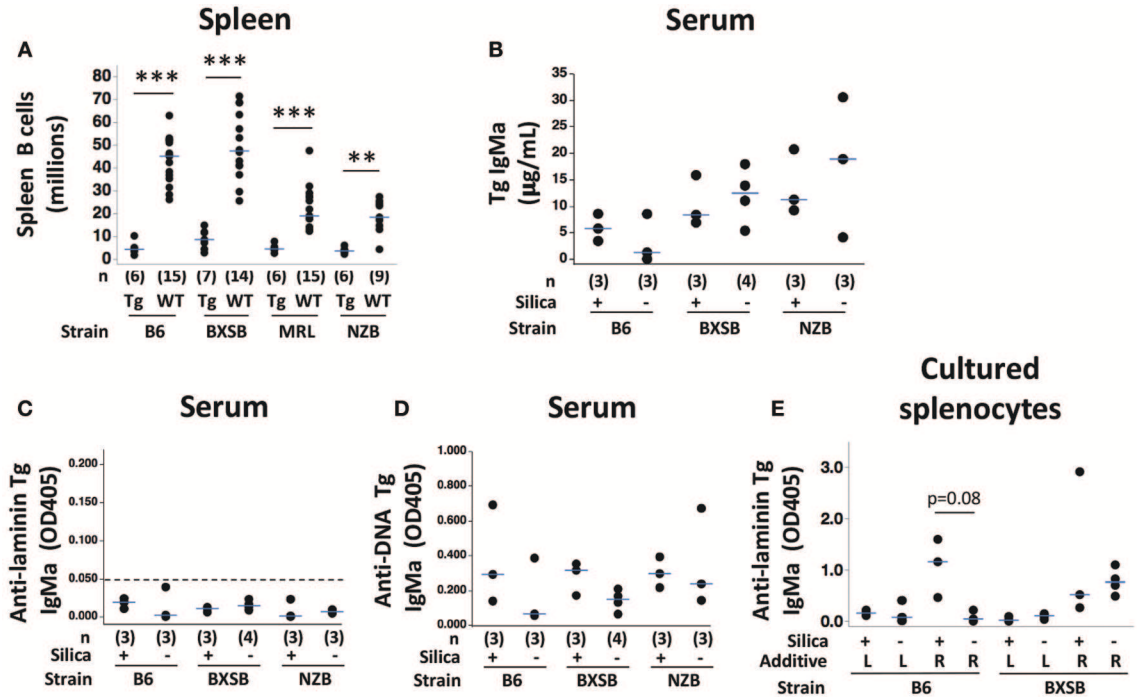

FIGURE 4 | Autoreactive B cell regulation in autoantibody transgenic (autoAb Tg) mice with or without exposure to crystalline silica. **(A)** Spleen CD19+ B cell numbers as determined by flow cytometric analysis in autoAb Tg and WT mice. Within an indicated strain, silica and vehicle-exposed mice are pooled for each genotype; $^{**}p < 0.01$, $^{***}p < 0.001$ for autoAb Tg vs. wildtype mice of the same strain, Wilcoxon rank sum test. **(B)** Serum IgMa (Tg) concentration, determined using a standard curve; **(C)** serum anti-laminin Tg autoAb, with cutoff for laminin-binding positivity at an OD of 0.050 indicated by the dashed line; and **(D)** serum anti-ssDNA Tg autoAb. Concurrent mean OD405 for positive control Tg-expressing IgM monoclonal antibodies are 0.208 for anti-laminin Ig A10C and 0.352 for anti-DNA Ig LamH/Vk8Jk5 (not shown). Antigen binding was tested in serum at 1/20 dilution in duplicate, measured as OD405 on antigen after subtraction of OD405 for binding on diluent-coated wells. **(E)** Level of anti-laminin Tg IgMa autoAb in supernatants of spleen cells from exposed mice stimulated 7–8 days with indicated additive: L, lipopolysaccharide (TLR4 ligand); R, R848 (TLR7 ligand) in combination with CpG oligos (TLR9 ligand). Undiluted supernatants were tested in duplicate; $n = 3$ mice/strain. Concurrent OD405 for positive control monoclonal antibody was 0.974 for anti-laminin H50 IgG.

exposed to silica and co-cultured with ligands to intracellular TLR7 and TLR9. The capacity of the TLR ligands to elicit anti-laminin Ig from Tg B cells from non-autoimmune B6 mice is surprising, because on this background the autoAb Tg is stringently regulated by deletion, editing, and anergy, a tolerance phenotype that has been remarkably stable for over 1.5 decades of study in our mouse colony. Tg anti-laminin Ig have rarely been detected in or recovered from B6 autoAb Tg mice (17, 18). In the current study, the induction of anti-laminin Tg Ig is not observed with splenocytes from vehicle-exposed autoAb Tg B6 mice, and the difference in autoAb production is not explained by differences in B cell numbers, which are equal in the two groups of B6 mice. This suggests that silica-exposed B6 mice have a unique population of autoreactive splenic B cells that can be activated by TLR7/9 ligands and that are not present in their vehicle-exposed counterparts. This supports the notion that the injury induced by silica inhalation has systemic, not just local, effects that subtly alter autoreactive B cell regulation and that can be unmasked by superimposed exposure to TLR ligands. Some potential differences may have been missed in the current study because of the low sample size; these can be tested in a larger follow up study.

A plausible explanation for the subtle deregulated autoimmunity revealed in the spleen B cell differentiation assays is that the systemic immune and cytokine milieu created by silica-induced lung inflammation modulates B cell anergy and promotes generation of a population of reversibly anergic B cells. The phenotype observed in silica-exposed B6 splenic B cells is reminiscent of the reversible anergy previously observed among NZB autoAb Tg B cells, which respond to TLR ligands with production of autoAb Tg, in contrast to anergic B cells in other strains (19). As previously reported, the NZB reversible anergy phenotype is revealed by both TLR4 and TLR7/9 stimulation and is also observed in B cells from autoAb Tg NZB F1 progeny (20), but not in anergic B cells from autoAb Tg B6 or BXSB mice (19). Whereas, the NZB phenotype is genetically-determined and likely cell intrinsic, the cause of development of a TLR7/9 reversible anergy in B cells from silica-exposed B6 mice is unclear and may well involve a distinct mechanism.

Study of models of B cell anergy in non-autoimmune-prone mice suggest that maintenance of anergy in healthy cells centers on mechanisms that block TLR ligands from inducing autoAb secretion (48–51). Known mechanisms involve altered MAPK activation or function, in some cases accompanied by altered B cell receptor and/or TLR trafficking and exclusion from late

endosomes (site of activation of endosomal TLRs). Increased basal p-ERK, blocked p-ERK nuclear import, and decreased JNK activation have been described. These mechanisms are consistent with central roles of Ras/MAPK pathways in B cell tolerance, TLR signaling, and activation of Blimp-1 (52, 53), the transcriptional regulator that induces plasma cell differentiation and Ig secretion after BCR/TLR stimulation. In this regard, MAPK activation is described in human lung epithelial cells exposed to crystalline silica in culture (54); however, direct exposure seems an unlikely cause of silica-modulated anergy in splenic B cells. Rather exposure of developing or anergic B cells to the sustained systemic proinflammatory milieu created during non-resolving lung inflammation is a more likely culprit. Potential candidates to mediate a breach of B cell anergy include endogenous TLR ligands—such as extracellular matrix components or high-mobility group box 1 (HMGB1) protein—released from injured lung tissue or cells and that can reach high systemic levels in patients with chronic inflammation (55). In this regard, TLR signaling has been shown to reverse anergy in human autoreactive chronic lymphocytic leukemia B cells (56).

It is possible that silica exposure and lung injury interfere with B cell regulation by other mechanisms. A systemic effect on the fate of developing B cells in the bone marrow is plausible. Proinflammatory factors, including interferon and tumor necrosis factor (TNF), have a profound impact on and direct reprogramming in hematopoietic stem cell fate (57). It is thus notable that TNF-α is elevated in plasma of silica-exposed (NZBxNZW)F1 lupus mice (58). Subsequent modulation of B cell signaling thresholds could alter tolerance induction and deletion and allow a small subset of normally censored autoreactive B cells to escape to the periphery. Alternatively, the pulmonary and systemic proinflammatory milieu induced by silica exposure could interfere with extrinsic B cell regulation. This has been observed for some anergic B cells, in which Blimp-1 induction and autoAb secretion is suppressed by dendritic- or macrophage-derived suppressive factors, such as IL6, sCD40L, or TNFα (59–61). This is possible in the assays reported here, which used spleen cell, not isolated B cell, cultures. It is plausible that in some settings silica-induced innate cell activation shifts the balance of secreted factors to release cytokine-mediated B cell suppression. This suggests a milieu distinct from that described in silicosis, in which IL6 and TNF-α levels are typically increased (62).

The relevance of these findings to human autoimmunity will require further study. Epidemiological studies link autoimmunity to occupational exposure to inhaled silica dust. For practical reasons, we and others have modeled silica pulmonary exposure using bolus instillations rather than chronic dust inhalation. The dose administered in our studies (3–6 mg/mouse) is similar to the cumulative dose of 4 mg/mouse, administered by 4 weekly intranasal instillations, used by Bates and colleagues (58), who calculated that 4 mg was the mouse equivalent of one-half of a human lifetime occupational exposure based on recommended exposure limits. This and similar bolus exposures lead to lung injury, TLS, and autoantibody production in mice, suggesting that the protocols provide useful models to study mechanisms of silica-induced autoimmunity. Ultimately, however, relevance of mechanisms to silica-induced injury in humans will require study of alternative exposures, inhalation in particular, and optimized models, including human lung and immune organoids and animals with humanized immune systems, genes, and cytokines.

Local Autoimmune Regulation After Silica Instillation

The role of the induced pulmonary TLS-like structures in modulating B cell autoimmunity in these strains remains unclear and will require further study, as the role may vary in wildtype vs. autoAb Tg strains. Silica-induced pulmonary TLS in mice is well-described (39, 58, 63–65), and the enhanced humoral autoimmunity described here parallels the findings of Brown, Bates, and Mayeux in lupus-prone New Zealand Mixed 2410 and (NZBxNZW)F1 (BWF1) strains and diversity outbred mice (39, 58, 64). TLS are functional and can provide a microenvironment for local B cell and helper T cell interactions, foreign antigen-driven immune responses, and local antibody production (66–69). TLS may also promote autoimmunity. Autoreactive B cells were detected in ectopic germinal centers of salivary gland from patients with Sjogren's syndrome, suggesting that TLS lack normal regulatory checkpoints, such as follicular exclusion found in secondary lymphoid organs (70). Moreover, synovial TLS dissected from RA patients' joints produce human anti-citrullinated-protein IgG when transplanted into scid mice (71, 72).

There is evidence for a role for lung TLS in promoting local autoAb production in the wildtype mice in the present study, although with strain-specific differences. Silica exposure led to significantly elevated levels of anti-DNA Ig in BALF in all strains except NZB, in which it trended toward significance. Levels of anti-DNA Ig in silica-exposed B6 mouse BALF were nonetheless quite low, relative to their autoimmune counterparts (**Figures 3A,B** and **Table 1**). Conversely, levels of BALF anti-DNA Ig in silica-exposed MRL mice significantly exceeded those in other silica-exposed strains. Whereas, it is possible that these high BALF levels in MRL derive from elevated serum anti-DNA levels, the recovery of significantly more anti-DNA IgG from TLR-stimulated lung cells of silica-exposed MRL mice compared to other strains (**Figure 3E**) suggests that abundant IgG is produced locally.

Anti-MPO Ig were also detected in BALF of silica-exposed mice, although with a different strain distribution. Levels of anti-MPO Ig in BALF from BXSB mice significantly exceeded levels in other silica-exposed strains. This strain restriction was unexpected, in that we initially screened for autoAb to MPO, a major autoAb specificity linked to ANCA vasculitis, both because of the association of silica exposure with ANCA vasculitis in humans and because of reports of detection of anti-MPO Ig in subsets of MRL/lpr mice (22) as well as in the derivative autoimmune SCG/Kj strain (73, 74). These results suggest that BXSB as well as MRL genes contribute to anti-MPO production in SCG/Kj mice. We did not observe anti-MPO Ig in silica-exposed B6 mice, a strain in which B cell responses to self-MPO are difficult to induce in the absence of genetic manipulation of antigen expression (75).

The role of TLS in autoAb Tg mice is likely more complicated and more challenging to dissect. The autoAb Tg is highly useful for tracking B cells of known autospecificity and tolerance mechanisms that control them, considerations that guided the choice of model for this study. However, introduction of an Ig Tg by design generates a relatively homogeneous B cell population, with elimination of much of the endogenous B cell population by allelic exclusion. An autoAb Tg further skews the repertoire, particularly if regulation markedly depletes and inactivates B cells, as is the case with the autoAb Tg under study here. B cell repertoire restriction also impacts T cell numbers, immunity, and subset distribution. Because functional, activated B cells and T cells may be critical for initiation, organization, and maintenance of TLS (76), this process may be disrupted in autoAb Tg mice. Moreover, the influence of anergic or regulatory B cells on TLS biology is less clear. Nonetheless it is of note that our silica-exposed autoAb Tg mice develop multiple TLS-like structures in their lungs.

In summary, our findings collectively suggest that silica exposure and subsequent sustained lung inflammation lead to strain-specific modulation of humoral autoimmunity that includes subtle effects on B cell tolerance. The type of autoAb induced varies by autoimmune genetic susceptibility and by site of autoAb production, as revealed by local production of anti-MPO autoAb in silica-exposed BXSB lung. However, silica exposure alone is insufficient to overtly disrupt B cell deletional or anergric tolerance, even at doses capable of inducing striking lung injury and TLS formation in multiple autoimmune backgrounds. Evidence is provided that superimposed exposure to TLR ligands may collaborate with silica-induced immune aberrations to promote autoAb production. Future studies can define the local and systemic immune phenotypes induced by silica exposure, including the pulmonary immune response in autoAb Tg mice, and further dissect the cellular and molecular basis of aberrant tolerance after silica exposure and role of synergistic environmental susceptibility, the results of which may inform design of inhaled or systemic immunotherapies.

DATA AVAILABILITY STATEMENT

All datasets generated for this study are included in the manuscript/**Supplementary Files**.

ETHICS STATEMENT

This study was carried out in accordance with the recommendations of the National Institutes of Health guide for the care and use of laboratory animals. The protocol was approved by the Institutional Animal Care and Use Committees of Duke University and the DVAMC.

AUTHOR CONTRIBUTIONS

MF, RT, AG, and AC contributed to conception and design of the study. JO, EZ, AB, FK, LF, and AC performed the experiments. YA scored the lung histopathology. VR reviewed and documented the lung pathology and silica deposition. MF, JO, LF, and AC performed the statistical analyses. MF wrote the first and revision drafts of the manuscript. All authors contributed to manuscript revision, read, and approved the submitted version.

FUNDING

Research reported in this publication was supported by the National Institute of Environmental Health Sciences (NIEHS) under award numbers R01ES027873 and R21ES024451 (MF), Duke University Undergraduate Research grant (JO and EZ), and a Wellesley undergraduate internship (FK). As a Duke Cancer Institute member, MF acknowledges support from the Duke Cancer Institute as part of the P30 Cancer Center Support Grant (Grant ID: P30 CA014236). The content is solely the responsibility of the authors and does not necessarily represent the official views of the National Institutes of Health. We thank the following Shared Resources of the Duke Cancer Institute: Flow Cytometry Shared Resource and DNA Analysis Facility. We thank Gary London at the Hope Center Alafi Neuroimaging Core for his careful attention to detail and accuracy. The Alafi neuroimaging core was supported by the Hope Center Alafi Neuroimaging Lab and a P30 Neuroscience Blueprint Interdisciplinary Center Core award to Washington University (P30 NS057105) and an NIH Shared Instrumentation Grant (S10 RR027552).

ACKNOWLEDGMENTS

We thank J. Michael Cook, Ph.D. for help with flow cytometry, Julie Fuller of the Duke Substrate Services Core & Research Support resource for help with histopathology, the Duke and DVAMC Animal Care Facilities staff for their attentive care of their charges, and the Duke Department of Biostatistics and Bioinformatics for statistical guidance.

SUPPLEMENTARY MATERIAL

The Supplementary Material for this article can be found online at: https://www.frontiersin.org/articles/10.3389/fimmu.2019.02336/full#supplementary-material

REFERENCES

1. Miller FW, Alfredsson L, Costenbader KH, Kamen DL, Nelson LM, Norris JM, et al. Epidemiology of environmental exposures and human autoimmune diseases: findings from a National Institute of Environmental Health Sciences Expert Panel Workshop. *J Autoimmun.* (2012) 39:259–71. doi: 10.1016/j.jaut.2012.05.002
2. Parks CG, Conrad K, Cooper GS. Occupational exposure to crystalline silica and autoimmune disease. *Environ Health Perspect.* (1999) 107:793–802. doi: 10.1289/ehp.99107s5793
3. de Lind van Wijngaarden RA, van Rijn L, Hagen EC, Watts RA, Gregorini G, Tervaert JW, et al. Hypotheses on the etiology of antineutrophil cytoplasmic autoantibody associated vasculitis: the cause is hidden, but the result is known. *Clin J Am Soc Nephrol.* (2008) 3:237–52. doi: 10.2215/CJN.03550807

4. Chen M, Kallenberg CG. The environment, geoepidemiology and ANCA-associated vasculitides. *Autoimmun Rev.* (2010) 9:A293–8. doi: 10.1016/j.autrev.2009.10.008
5. Dospinescu P, Jones GT, Basu N. Environmental risk factors in systemic sclerosis. *Curr Opin Rheumatol.* (2013) 25:179–83. doi: 10.1097/BOR.0b013e32835cfc2d
6. Rawlings DJ, Metzler G, Wray-Dutra M, Jackson SW. Altered B cell signalling in autoimmunity. *Nat Rev Immunol.* (2017) 17:421–36. doi: 10.1038/nri.2017.24
7. Ludwig RJ, Vanhoorelbeke K, Leypoldt F, Kaya Z, Bieber K, McLachlan SM, et al. Mechanisms of autoantibody-induced pathology. *Front Immunol.* (2017) 8:603. doi: 10.3389/fimmu.2017.00603
8. Mannik M, Merrill CE, Stamps LD, Wener MH. Multiple autoantibodies form the glomerular immune deposits in patients with systemic lupus erythematosus. *J Rheumatol.* (2003) 30:1495–504. Available online at: http://www.jrheum.org/content/30/71495
9. Bonanni A, Vaglio A, Bruschi M, Sinico RA, Cavagna L, Moroni G, et al. Multi-antibody composition in lupus nephritis: isotype and antigen specificity make the difference. *Autoimmun Rev.* (2015) 14:692–702. doi: 10.1016/j.autrev.2015.04.004
10. Skare T, Picelli L, Dos Santos TAG, Nisihara R. Direct antiglobulin (Coombs) test in systemic lupus erythematosus patients. *Clin Rheumatol.* (2017) 36:2141–4. doi: 10.1007/s10067-017-3778-3
11. Nandakumar KS. Targeting IgG in arthritis: disease pathways and therapeutic avenues. *Int J Mol Sci.* (2018) 19:E677. doi: 10.3390/ijms19030677
12. Gibelin A, Maldini C, Mahr A. Epidemiology and etiology of Wegener granulomatosis, microscopic polyangiitis, Churg-Strauss syndrome and Goodpasture syndrome: vasculitides with frequent lung involvement. *Semin Respir Crit Care Med.* (2011) 32:264–73. doi: 10.1055/s-0031-1279824
13. Hilhorst M, van Paassen P, Tervaert JW. Proteinase 3-ANCA vasculitis versus myeloperoxidase-ANCA vasculitis. *J Am Soc Nephrol.* (2015) 26:2314–27. doi: 10.1681/ASN.2014090903
14. Grassegger A, Pohla-Gubo G, Frauscher M, Hintner H. Autoantibodies in systemic sclerosis (scleroderma): clues for clinical evaluation, prognosis and pathogenesis. *Wien Med Wochenschr.* (2008) 158:19–28. doi: 10.1007/s10354-007-0451-5
15. Baroni SS, Santillo M, Bevilacqua F, Luchetti M, Spadoni T, Mancini M, et al. Stimulatory autoantibodies to the PDGF receptor in systemic sclerosis. *N Engl J Med.* (2006) 354:2667–76. doi: 10.1056/NEJMoa052955
16. Kill A, Riemekasten G. Functional autoantibodies in systemic sclerosis pathogenesis. *Curr Rheumatol Rep.* (2015) 17:34. doi: 10.1007/s11926-015-0505-4
17. Rudolph EH, Congdon KL, Sackey FN, Fitzsimons MM, Foster MH. Humoral autoimmunity to basement membrane antigens is regulated in C57BL/6 and MRL/MpJ mice transgenic for anti-laminin Ig receptors. *J Immunol.* (2002) 168:5943–53. doi: 10.4049/jimmunol.168.11.5943
18. Brady GF, Congdon KL, Clark AG, Sackey FN, Rudolph EH, Radic MZ, et al. Kappa editing rescues autoreactive B cells destined for deletion in mice transgenic for a dual specific anti-laminin Ig. *J Immunol.* (2004) 172:5313–21. doi: 10.4049/jimmunol.172.9.5313
19. Clark AG, Fan Q, Brady GF, Mackin KM, Coffman ED, Weston ML, et al. Regulation of basement membrane-reactive B cells in BXSB, (NZBxNZW)F1, NZB, and MRL/lpr lupus mice. *Autoimmunity.* (2013) 46:188–204. doi: 10.3109/08916934.2012.746671
20. Clark AG, Buckley ES, Foster MH. Altered toll-like receptor responsiveness underlies a dominant heritable defect in B cell tolerance in autoimmune New Zealand Black mice. Eur J Immunol. (2018) 48:492-7. doi: 10.1002/eji.201747287
21. O'Sullivan FX, Fassbender HG, Gay S, Koopman WJ. Etiopathogenesis of the rheumatoid arthritis-like disease in MRL/l mice. I. The histomorphologic basis of joint destruction. *Arthritis Rheum.* (1985) 28:529–36. doi: 10.1002/art.1780280511
22. Harper JM, Thiru S, Lockwood CM, Cooke A. Myeloperoxidase autoantibodies distinguish vasculitis mediated by anti-neutrophil cytoplasm antibodies from immune complex disease in MRL/Mp-lpr/lpr mice: a spontaneous model for human microscopic angiitis. *Eur J Immunol.* (1998) 28:2217–26.
23. Santiago-Raber ML, Baccala R, Haraldsson KM, Choubey D, Stewart TA, Kono DH, et al. Type-I interferon receptor deficiency reduces lupus-like disease in NZB mice. *J Exp Med.* (2003) 197:777–88. doi: 10.1084/jem.20021996
24. DeHeer DH, Edgington TS. Evidence for a B lymphocyte defect underlying the anti-X anti-erythrocyte autoantibody response of NZB mice. *J Immunol.* (1977) 118:1858–63.
25. Morel L. Genetics of SLE: evidence from mouse models. *Nat Rev Rheumatol.* (2010) 6:348–57. doi: 10.1038/nrrheum.2010.63
26. Rogers NJ, Lees MJ, Gabriel L, Maniati E, Rose SJ, Potter PK, et al. A defect in Marco expression contributes to systemic lupus erythematosus development via failure to clear apoptotic cells. *J Immunol.* (2009) 182:1982–90. doi: 10.4049/jimmunol.0801320
27. Santiago-Raber M-L, Kikuchi S, Borel P, Uematsu S, Akira S, Kotzin BL, et al. Evidence for genes in addition to Tlr7 in the Yaa translocation linked with acceleration of systemic lupus erythematosus. *J Immunol.* (2008) 181:1556–62. doi: 10.4049/jimmunol.181.2.1556
28. Fitzsimons MM, Chen H, Foster MH. Diverse endogenous light chains contribute to basement membrane reactivity in nonautoimmune mice transgenic for an anti-laminin Ig heavy chain. *Immunogenetics.* (2000) 51:20–9. doi: 10.1007/s002510050004
29. Ben-Yehuda A, Rasooly L, Bar-Tana R, Breuer G, Tadmor B, Ulmansky R, et al. The urine of SLE patients contains antibodies that bind to the laminin component of the extracellular matrix. *J Autoimmun.* (1995) 8:279–91. doi: 10.1006/jaut.1995.0021
30. Amital H, Heilweil M, Ulmansky R, Szafer F, Bar-Tana R, Morel L, et al. Treatment with a laminin-derived peptide suppresses lupus nephritis. *J Immunol.* (2005) 175:5516–23. doi: 10.4049/jimmunol.175.8.5516
31. Groth S, Vafia K, Recke A, Dahnrich C, Zillikens D, Stocker W, et al. Antibodies to the C-terminus of laminin gamma1 are present in a distinct subgroup of patients with systemic and cutaneous lupus erythematosus. *Lupus.* (2012) 21:1482–3. doi: 10.1177/0961203312460113
32. Inagaki J, Kondo A, Lopez LR, Shoenfeld Y, Matsuura E. Pregnancy loss and endometriosis: pathogenic role of anti-laminin-1 autoantibodies. *Ann N Y Acad Sci.* (2005) 1051:174–84. doi: 10.1196/annals.1361.059
33. Wolff PG, Kuhl U, Schultheiss HP. Laminin distribution and autoantibodies to laminin in dilated cardiomyopathy and myocarditis. *Am Heart J.* (1989) 117:1303–9. doi: 10.1016/0002-8703(89)90410-9
34. Foster MH. Basement membranes and autoimmune diseases. *Matrix Biol.* (2017) 57–58:149–68. doi: 10.1016/j.matbio.2016.07.008
35. Ghio AJ, Jaskot RH, Hatch GE. Lung injury after silica instillation is associated with an accumulation of iron in rats. *Am J Physiol.* (1994) 267:L686–92. doi: 10.1152/ajplung.1994.267.6.L686
36. Ghio AJ, Tong H, Soukup JM, Dailey LA, Cheng WY, Samet JM, et al. Sequestration of mitochondrial iron by silica particle initiates a biological effect. *Am J Physiol Lung Cell Mol Physiol.* (2013) 305:L712–24. doi: 10.1152/ajplung.00099.2013
37. Huaux F, Louahed J, Hudspith B, Meredith C, Delos M, Renauld JC, et al. Role of interleukin-10 in the lung response to silica in mice. *Am J Respir Cell Mol Biol.* (1998) 18:51–9. doi: 10.1165/ajrcmb.18.1.2911
38. Barbarin V, Nihoul A, Misson P, Arras M, Delos M, Leclercq I, et al. The role of pro- and anti-inflammatory responses in silica-induced lung fibrosis. *Respir Res.* (2005) 6:112. doi: 10.1186/1465-9921-6-112
39. Mayeux JM, Escalante GM, Christy JM, Pawar RD, Kono DH, Pollard KM. Silicosis and silica-induced autoimmunity in the diversity outbred mouse. *Front Immunol.* (2018) 9:874. doi: 10.3389/fimmu.2018.00874
40. Tighe RM, Birukova A, Yaeger MJ, Reece SW, Gowdy KM. Euthanasia- and lavage-mediated effects on bronchoalveolar measures of lung injury and inflammation. *Am J Respir Cell Mol Biol.* (2018) 59:257–66. doi: 10.1165/rcmb.2017-0357OC
41. Pinchai N, Perfect BZ, Juvvadi PR, Fortwendel JR, Cramer RA Jr, Asfaw YG, et al. Aspergillus fumigatus calcipressin CbpA is involved in hyphal growth and calcium homeostasis. *Eukaryot Cell.* (2009) 8:511–9. doi: 10.1128/EC.00336-08
42. McDonald JW, Roggli VL. Detection of silica particles in lung tissue by polarizing light microscopy. *Arch Pathol Lab Med.* (1995) 119:242–6.

43. Madaio M, Hodder S, Schwartz R, Stollar B. Responsiveness of autoimmune and normal mice to nucleic acid antigens. *J Immunol.* (1984) 132:872.
44. Ali R, Dersimonian H, Stollar BD. Binding of monoclonal anti-native DNA autoantibodies to DNA of varying size and conformation. *Mol Immunol.* (1985) 22:1415–22. doi: 10.1016/0161-5890(85)90065-3
45. Foster MH, Sabbaga J, Line SRP, Thompson KS, Barrett KJ, Madaio MP. Molecular analysis of nephrotropic anti-laminin antibodies from an MRL/lpr autoimmune mouse. *J Immunol.* (1993) 151:814–24.
46. Clark AG, Weston ML, Foster MH. Lack of galectin-1 or galectin-3 alters B cell deletion and anergy in an autoantibody transgene model. *Glycobiology.* (2013) 23:893–903. doi: 10.1093/glycob/cwt026
47. Cascalho M, Ma A, Lee S, Masat L, Wabl M. A quasi-monoclonal mouse. *Science.* (1996) 272:1649–52. doi: 10.1126/science.272.5268.1649
48. Rui L, Vinuesa C, Blasioli J, Goodnow C. Resistance to CpG DNA-induced autoimmunity through tolerogenic B cell antigen receptor ERK signaling. *Nat Immunol.* (2003) 4:594–600. doi: 10.1038/ni924
49. Rui L, Healy JI, Blasioli J, Goodnow CC. ERK signaling is a molecular switch integrating opposing inputs from B cell receptor and T cell cytokines to control TLR4-driven plasma cell differentiation. *J Immunol.* (2006) 177:5337–46. doi: 10.4049/jimmunol.177.8.5337
50. O'Neill SK, Veselits ML, Zhang M, Labno C, Cao Y, Finnegan A, et al. Endocytic sequestration of the B cell antigen receptor and toll-like receptor 9 in anergic cells. *Proc Natl Acad Sci USA.* (2009) 106:6262–7. doi: 10.1073/pnas.0812922106
51. Lee SR, Rutan JA, Monteith AJ, Jones SZ, Kang SA, Krum KN, et al. Receptor cross-talk spatially restricts p-ERK during TLR4 stimulation of autoreactive B cells. *J Immunol.* (2012) 189:3859–68. doi: 10.4049/jimmunol.1200940
52. Teodorovic LS, Babolin C, Rowland SL, Greaves SA, Baldwin DP, Torres RM, et al. Activation of Ras overcomes B-cell tolerance to promote differentiation of autoreactive B cells and production of autoantibodies. *Proc Natl Acad Sci USA.* (2014) 111:E2797–806. doi: 10.1073/pnas.1402159111
53. Yasuda T, Kometani K, Takahashi N, Imai Y, Aiba Y, Kurosaki T. ERKs induce expression of the transcriptional repressor Blimp-1 and subsequent plasma cell differentiation. *Sci Signal.* (2011) 4:ra25. doi: 10.1126/scisignal.2001592
54. Tomaru M, Matsuoka M. The role of mitogen-activated protein kinases in crystalline silica-induced cyclooxygenase-2 expression in A549 human lung epithelial cells. *Toxicol Mech Methods.* (2011) 21:513–9. doi: 10.3109/15376516.2011.568982
55. Yu L, Wang L, Chen S. Endogenous toll-like receptor ligands and their biological significance. *J Cellular and Mol Med.* (2010) 14:2592–603. doi: 10.1111/j.1582-4934.2010.01127.x
56. Ntoufa S, Papakonstantinou N, Apollonio B, Gounari M, Galigalidou C, Fonte E, et al. B cell anergy modulated by TLR1/2 and the miR-17 approximately 92 cluster underlies the indolent clinical course of chronic lymphocytic leukemia stereotyped subset #4. *J Immunol.* (2016) 196:4410–7. doi: 10.4049/jimmunol.1502297
57. Pietras EM. Inflammation: a key regulator of hematopoietic stem cell fate in health and disease. *Blood.* (2017) 130:1693–8. doi: 10.1182/blood-2017-06-780882
58. Bates MA, Brandenberger C, Langohr I, Kumagai K, Harkema JR, Holian A, et al. Silica triggers inflammation and ectopic lymphoid neogenesis in the lungs in parallel with accelerated onset of systemic autoimmunity and glomerulonephritis in the lupus-prone NZBWF1 mouse. *PLoS ONE.* (2015) 10:e0125481. doi: 10.1371/journal.pone.0125481
59. Kilmon MA, Rutan JA, Clarke SH, Vilen BJ. Low-affinity, Smith antigen-specific B cells are tolerized by dendritic cells and macrophages. *J Immunol.* (2005) 175:37–41. doi: 10.4049/jimmunol.175.1.37
60. Kilmon MA, Wagner NJ, Garland AL, Lin L, Aviszus K, Wysocki LJ, et al. Macrophages prevent the differentiation of autoreactive B cells by secreting CD40 ligand and interleukin-6. *Blood.* (2007) 110:1595–602. doi: 10.1182/blood-2006-12-061648
61. Gilbert MR, Wagner NJ, Jones SZ, Wisz AB, Roques JR, Krum KN, et al. Autoreactive preplasma cells break tolerance in the absence of regulation by dendritic cells and macrophages. *J Immunol.* (2012) 189:711–20. doi: 10.4049/jimmunol.1102973
62. Vanhee D, Gosset P, Boitelle A, Wallaert B, Tonnel AB. Cytokines and cytokine network in silicosis and coal workers' pneumoconiosis. *Eur Respir J.* (1995) 8:834–42.
63. Davis GS, Leslie KO, Hemenway DR. Silicosis in mice: effects of dose, time, and genetic strain. *J Environ Pathol Toxicol Oncol.* (1998) 17:81–97.
64. Brown JM, Archer AJ, Pfau JC, Holian A. Silica accelerated systemic autoimmune disease in lupus-prone New Zealand mixed mice. *Clin Exp Immunol.* (2003) 131:415–21. doi: 10.1046/j.1365-2249.2003.02094.x
65. Bates MA, Akbari P, Gilley KN, Wagner JG, Li N, Kopec AK, et al. Dietary docosahexaenoic acid prevents silica-induced development of pulmonary ectopic germinal centers and glomerulonephritis in the lupus-prone NZBWF1 mouse. *Front Immunol.* (2018) 9:2002. doi: 10.3389/fimmu.2018.02002
66. Moyron-Quiroz JE, Rangel-Moreno J, Hartson L, Kusser K, Tighe MP, Klonowski KD, et al. Persistence and responsiveness of immunologic memory in the absence of secondary lymphoid organs. *Immunity.* (2006) 25:643–54. doi: 10.1016/j.immuni.2006.08.022
67. Maglione PJ, Xu J, Chan J. B cells moderate inflammatory progression and enhance bacterial containment upon pulmonary challenge with *Mycobacterium tuberculosis*. *J Immunol.* (2007) 178:7222–34. doi: 10.4049/jimmunol.178.11.7222
68. GeurtsvanKessel CH, Willart MA, Bergen IM, van Rijt LS, Muskens F, Elewaut D, et al. Dendritic cells are crucial for maintenance of tertiary lymphoid structures in the lung of influenza virus-infected mice. *J Exp Med.* (2009) 206:2339–49. doi: 10.1084/jem.20090410
69. Randall TD. Bronchus-associated lymphoid tissue (BALT) structure and function. *Adv Immunol.* (2010) 107:187–241. doi: 10.1016/B978-0-12-381300-8.00007-1
70. Le Pottier L, Devauchelle V, Fautrel A, Daridon C, Saraux A, Youinou P, et al. Ectopic germinal centers are rare in Sjogren's syndrome salivary glands and do not exclude autoreactive B cells. *J Immunol.* (2009) 182:3540–7. doi: 10.4049/jimmunol.0803588
71. Croia C, Serafini B, Bombardieri M, Kelly S, Humby F, Severa M, et al. Epstein-Barr virus persistence and infection of autoreactive plasma cells in synovial lymphoid structures in rheumatoid arthritis. *Ann Rheum Dis.* (2013) 72:1559–68. doi: 10.1136/annrheumdis-2012-202352
72. Corsiero E, Bombardieri M, Carlotti E, Pratesi F, Robinson W, Migliorini P, et al. Single cell cloning and recombinant monoclonal antibodies generation from RA synovial B cells reveal frequent targeting of citrullinated histones of NETs. *Ann Rheum Dis.* (2016) 75:1866–75. doi: 10.1136/annrheumdis-2015-208356
73. Kinjoh K, Kyogoku M, Good R. Genetic selection for crescent formation yields mouse strain with rapidly progressive glomerulonephritis and small vessel vasculitis. *Proc Natl Acad Sci USA.* (1993) 90:3413–7. doi: 10.1073/pnas.90.8.3413
74. Neumann I, Birck R, Newman M, Schnulle P, Kriz W, Nemoto K, et al. SCG/Kinjoh mice: a model of ANCA-associated crescentic glomerulonephritis with immune deposits. *Kidney Int.* (2003) 64:140–8. doi: 10.1046/j.1523-1755.2003.00061.x
75. Xiao H, Heeringa P, Hu P, Liu Z, Zhao M, Aratani Y, et al. Antineutrophil cytoplasmic autoantibodies specific for myeloperoxidase cause glomerulonephritis and vasculitis in mice. *J Clin Invest.* (2002) 110:955–63. doi: 10.1172/JCI200215918
76. Alsughayyir J, Pettigrew GJ, Motallebzadeh R. Spoiling for a fight: B lymphocytes as initiator and effector populations within tertiary lymphoid organs in autoimmunity and transplantation. *Front Immunol.* (2017) 8:1639. doi: 10.3389/fimmu.2017.01639

Conflict of Interest: The authors declare that the research was conducted in the absence of any commercial or financial relationships that could be construed as a potential conflict of interest.

frontiers in Immunology

REVIEW
published: 10 January 2020
doi: 10.3389/fimmu.2019.03094

Environmental Exposures and Autoimmune Diseases: Contribution of Gut Microbiome

M. Firoze Khan and Hui Wang*

Department of Pathology, University of Texas Medical Branch at Galveston, Galveston, TX, United States

Environmental agents have been gaining more attention in recent years for their role in the pathogenesis of autoimmune diseases (ADs). Increasing evidence has linked environmental exposures, including trichloroethene (TCE), silica, mercury, pristane, pesticides, and smoking to higher risk for ADs. However, potential mechanisms by which these environmental agents contribute to the disease pathogenesis remains largely unknown. Dysbiosis of the gut microbiome is another important environmental factor that has been linked to the onset of different ADs. Altered microbiota composition is associated with impaired intestinal barrier function and dysregulation of mucosal immune system, but it is unclear if gut dysbiosis is a causal factor or an outcome of ADs. In this review article, we first describe the recent epidemiological and mechanistic evidences linking environmental/occupational exposures with various ADs (especially SLE). Secondly, we discuss how changes in the gut microbiome composition (dysbiosis) could contribute to the disease pathogenesis, especially in response to exposure to environmental chemicals.

Keywords: environmental agents, autoimmune diseases, microbiome, oxidative stress, dysbiosis

OPEN ACCESS

Edited by:
Allen Jay Rosenspire, Wayne State University, United States

Reviewed by:
Çagla Tükel, Temple University, United States
Janine Adele Lamb, University of Manchester, United Kingdom

****Correspondence:***
M. Firoze Khan
mfkhan@utmb.edu

Specialty section:
This article was submitted to Autoimmune and Autoinflammatory Disorders, a section of the journal Frontiers in Immunology

Received: *27 September 2019*
Accepted: *18 December 2019*
Published: *10 January 2020*

Citation:
Khan MF and Wang H (2020) Environmental Exposures and Autoimmune Diseases: Contribution of Gut Microbiome. Front. Immunol. 10:3094. doi: 10.3389/fimmu.2019.03094

INTRODUCTION

Autoimmune diseases (ADs), such as systemic lupus erythematosus (SLE), autoimmune hepatitis (AIH), rheumatoid arthritis (RA), and systemic sclerosis (SSc), are chronic and potentially life-threatening inflammatory disorders. The etiology of ADs is complex and mostly unknown, but it is evident that such diseases are influenced by genetic, hormonal and environmental factors (1–4). The most challenging aspect of autoimmunity is to identify the early events that trigger immune dysregulation and autoimmunity (5). In recent years, increasing attention has been paid to define the contribution of environmental agents in the pathogenesis of ADs. The environmental factors account for up to 70% of all ADs (1, 6). Strong evidence exists linking environmental agents, including solvents, crystalline silica, mercury, pesticides, pristine, and cigarette smoking with the development of various ADs (7). However, significant knowledge gaps remain regarding potential cellular, molecular, and immunological mechanisms by which environmental agents contribute to the disease pathogenesis.

In addition to physical and environmental agents that can trigger and perpetuate an autoimmune response, gut microbiome can also play critical role in such responses. Dysbiosis of gut, oral, and skin microbiome has been linked to auto-inflammation and tissue damages in susceptible individuals (8). Thus, the human microbiome changes could be a significant contributory factor in autoimmunity as an altered microbial composition can induce inflammation

and loss of immune tolerance (9). The composition and stability of gut microbiome not only help with the nutrient absorption but also regulate mucosal immune system, therefore, dysbiosis can result in multiple ADs (10).

In this review article, we first describe the latest epidemiological and mechanistic evidences linking environmental/occupational exposures with various ADs (especially SLE). Further, we discuss how changes in the gut microbiome composition (dysbiosis) could contribute to the pathogenesis of ADs, especially in response to xenobiotics.

ENVIRONMENTAL TOXICANTS IN AUTOIMMUNE DISEASES

It is well-accepted that both genetic and environmental factors influence the pathogenesis of ADs. Environmental factors could play critical roles in the etiology and pathogenesis of ADs such as SLE, RA, inflammatory bowel disease, and AIH. Although several environmental agents are implicated in the pathogenesis of ADs via numerous mechanisms, below we discuss the more prominent ones which are not only known to induce/exacerbate autoimmunity but also have oxidative stress (OS) as one common mechanism, and participate in the pathogenesis of ADs (**Figure 1**):

MERCURY

Mercury (Hg) is a well-established environmental toxicant and its exposure in humans is associated with markers of inflammation and autoimmunity (11), which are generally characterized by pro-inflammatory cytokines, lymphoproliferation, immune complex deposition, autoantibody generation and tissue damage. *In vivo* studies using autoimmune-prone murine models report that exposure to inorganic Hg leads to lupus-like syndrome. Studies in animals reveal significant differences in autoimmunity and inflammatory markers among different stains, suggesting genetic regulation of mercury-induced auto-inflammatory responses (12). Hg-induced autoimmunity (HgIA) was found to be a novel type I IFN-independent model of systemic autoimmunity and suggested the contribution of TLR and NF-kB signaling in the generation of autoantibodies (13).

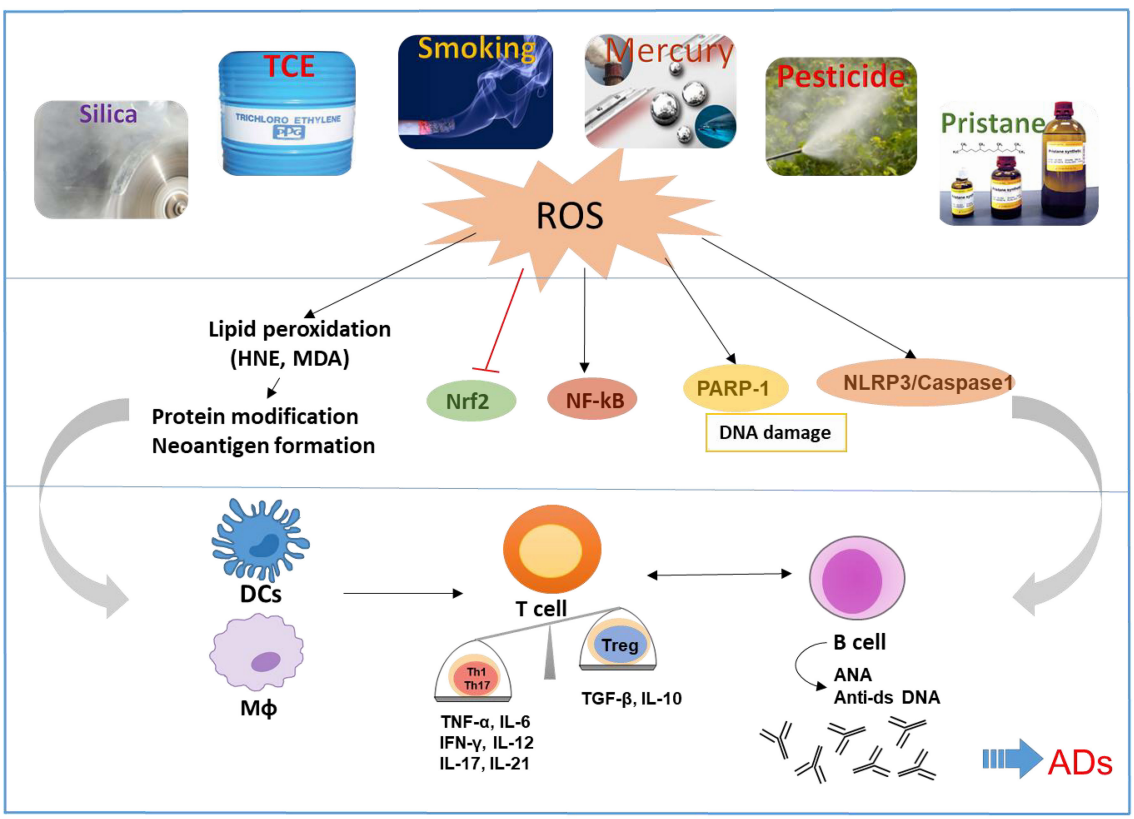

FIGURE 1 | Schematic presentation of the proposed mechanistic pathways linking environmental agents to the development of ADs. Environmental agents are associated with the development of ADs in susceptible hosts. OS appears to be a common mechanism of many environmental agents that contribute to ADs. OS-mediated disturbance of nuclear factor erythroid 2-related factor 2 (Nrf2) and induction of NF-kB, Poly (ADP-ribose) polymerase 1 (PARP1), and NLR family pyrin domain containing 3 (NLRP3) can cause activation of both innate and adaptive immune systems, resulting in pro-inflammatory cytokines and production of autoantibodies, leading to tissue damage in ADs. Reactive oxygen species (ROS) and lipid peroxidation-derived reactive aldehydes (i.e., HNE and MDA) have the potential to cause protein medications and neoantigen formation, which will activate antigen presentation cells including dendritic cells (DCs) and macrophages (MΦ), that consequently promote activation of T and B cells.

B cell activation factor of the tumor necrosis family (BAFF) is required for B cell activation, and BAFF blockage reduces disease activity in $HgCl_2$-treated susceptible A.SW mice (14). In an effort to delineate the mechanism responsible for Hg-mediated autoimmunity, phosphorylation was evaluated in Wehi-231 cells (an immature B-cell model) after different doses of Hg exposure. The study suggested that cytoskeletal proteins are susceptible to Hg exposure and their phosphorylation may alter B cell function and development (15). Mechanistic evidence was also provided to suggest that Hg can alter phosphorylation status of SYK, which is a critical protein in B cell receptor (BCR) signaling (16). In human T cells, both methyl mercuric chloride and inorganic Hg induce mitochondrial dysfunction and glutathione depletion (17), leading to generation of reactive oxygen species (ROS) and apoptotic caspases (18). Another study using A.SW mice showed significantly lower Bank 1 (B-cell scaffold protein with ankyrin repeats 1) gene expression and higher NF-kB, TLR-9, IL-6, and TNF-α after Hg exposure, supporting the roles of Bank1 (produced mainly in B cells) and NF-kB as the key regulators of antinucleolar antibodies in HgIA (19).

PESTICIDES

While pesticide use is associated with systemic ADs, the role of specific pesticides in the development of systemic autoimmunity is not established. Twelve individuals chronically exposed to chlorpyrifos were found to have higher rate of autoimmunity, evident from increased levels of autoantibodies against smooth muscle, brush border, thyroid gland, myelin, and antinuclear antibodies (ANA). Among them, two individuals were diagnosed with either SLE or SLE-like symptoms (20), suggesting a need for more thorough examination of the potential of chlorpyrofos in inducing an autoimmune response. SLE patients exposed to pesticide mixtures and living in rural areas were found to have over 3.5 times more oxidative DNA damage than those living in the city, suggesting usefulness of DNA damage and oxidative stress in the characterization of individual risk to ADs (21). In an *in vivo* study, exposure to organochlorine pesticide chlordecone with estrogenic effects in ovariectomized female (NZB x NZW) F1 mice resulted in accelerated appearance of SLE disease (22). A dose-dependent early appearance of anti-dsDNA antibodies was observed following chlordecone exposure. Furthermore, chlordecone exposure in these mice increased TNF-α, IFN-γ, IL-2, and GM-CSF secretion by CD4 T cells (23).

In a study involving 668 male farmers, ANA was examined in relation to lifetime use of 46 pesticides. Moderate to higher ANA levels were associated with lifetime pesticide exposure, with higher positivity with the use of cyclodiene organochlorine insecticides (24). These studies support the notion that certain organochlorine insecticides are associated with increased risk to develop ADs.

PRISTANE

Pristane, which is a mineral oil component, is associated with RA and SLE. Exposure to pristane causes lupus-like disease that is characterized by interferon(IFN)-I-dependent autoantibody production, inflammatory cytokines and renal diseases in susceptible mouse models (25). Pristane-induced autoimmune responses are mainly attributed to apoptosis generated autoantigens, stimulating the immune system to produce cytokines (IFN α and β) and autoantibodies, that consequently can lead to breakdown of immune tolerance (26).

Induction of pristane-induced autoantibodies has been shown to be dependent on the inflammatory cytokines as protective effects on nephritis and autoantibodies were observed in INF-$\gamma^{-/-}$, IL-$6^{-/-}$, IL-$12^{-/-}$, and IL-$17^{-/-}$ mice (27–29). Innate pattern-recognition receptors recognize self-antigens from damaged cells, among which toll like receptors (TLRs) are activated and lead to type I IFN production in pristane-induced lupus models (30). MiRNAs (miRNA-132-3p, miRNA-106-5p, miRNA-27b-3p, and miRNA-25-3P) are involved in the susceptibility of pristane-induced arthritis (PIA), and miRNA-26a is negatively correlated to TLR3 expression ameliorating PIA in rats (31, 32). PIA development has been highly associated with the microflora (33), and recent studies provide further evidence that immunoregulatory probiotics effectively enhance Tregs and decrease inflammatory Th1/Th17 in pristane-induced lupus model (34, 35). Mechanistically, the contribution of Th17 in pristane-induced lupus relies on IL-6/STAT3-induced RFX1 and epigenetic regulations (36). Pristane injected intraperitoneally in C57BL/6J mice induced macrophage activation, OS (increased superoxide anion and reduced antioxidant enzymes), and Th1/Th2 imbalance, which were attenuated by chloroquine (37). These studies suggest a potential role for OS in pristane-mediated autoimmune responses. However, more detailed studies are needed to establish the role of OS, microbiome and other mechanisms in pristane-mediated ADs.

SILICA

Among the environmental and occupational agents associated with immune dysregulation, silica is considered a notable risk factor due to its widespread exposure. Silica exposure has been linked with various ADs including SLE, RA, and systemic sclerosis (38, 39). Silica exposure in humans led to elevated autoantibodies such as ANA, anti-topoisomerase I and anti-Fas antibodies, indicating its potential to elicit an autoimmune response (40, 41).

Lupus-prone NZ-2410 mice exposed to silica exhibited increased autoantibodies, circulating immune complex, renal deposits of C3, and proteinuria (42). Silica exposure generated pro-inflammatory cytokines, impaired alveolar macrophage function, and resulted in accumulation of apoptotic self-antigens, leading to autoimmune response (43). Recent study using the genetically heterogeneous diversity outbred mice confirmed exacerbation of ADs after silica exposure with increased serum IgM, IgG, ANA, and anti-ENA (RNP and Sm) levels (44). Mechanistically, silica may contribute to an autoimmune response via OS and inflammation involving NLRP3 inflammasome and STING activation (45–47).

SMOKING

Linking smoking with autoimmunity, especially its role in the pathogenesis of ADs has been a subject of great interest (48). Smoking causes OS, which can induce DNA demethylation, and upregulation of inflammatory genes, thereby leading to lupus-like disease (48). There is strong epidemiological evidence linking cigarette smoking (CS) and the risk of SLE incidence (49). A case-control study found a link between CS and SLE as evident from an increased level of anti-dsDNA antibodies in the current smokers (50). CS and hypoxia can both lead to increased OS which can potentially lead to generation of autoreactive T cells and autoantibodies, inhibition in Treg activity and enhanced expression of pro-inflammatory mediators (51). Studies conducted in RA patients suggest a strong association between lung pathology and CS (52). CS exposure is associated with lung injury and systemic hypoxia, leading to increased incidence of Crohn's disease in chronic obstructive pulmonary disease patients (53). Therefore, smoking and hypoxia may synergistically act as potent environmental risk factors for the inflammation and ADs. Survivin, a protein which enhances antigen presentation and production of autoantibodies, is considered as a diagnostic biomarker of RA and several other ADs. As a key regulator of cell apoptosis, survivin level correlates with reduced apoptosis and increased inflammation in multiple autoimmune disorders (54). Comparison of survivin levels between smokers and non-smokers of RA and healthy subjects suggest that nicotine contributes to autoimmunity by inducing the non-exhausted PD-1^{-}IL-7R^{+} CD8^{+} T cells resulting in the release of survivin, and that potentially presents a new mechanism for smoke-mediated RA pathogenesis (55).

Smoking influences intestinal microbiome by altering its composition. This interaction is associated with the progression of intestinal and systemic diseases (56). Future studies, especially on the role of gene-environment interactions, epigenetics, metabolomics, microbiome and OS-related mechanisms, along with extensive epidemiological studies should lead to a better understanding of the role of smoking in the pathogenesis of ADs.

TRICHLOROETHENE

Trichloroethene (trichloroethylene, TCE) is an environmental pollutant and widely used industrial solvent. It is evident from a series of case reports that occupational TCE exposure is a contributing factor for multiple ADs, including SLE, scleroderma, and AIH (57–59). Khan and colleagues were first to demonstrate that TCE exposure causes an early induction/exacerbation of autoimmune response in female MRL+/+ mice (60). These novel observations were further substantiated by other investigators (61, 62) as well as our follow-up studies (63–65). Chronic studies in female MRL+/+ mice have also demonstrated that TCE exposure causes induction of AIH via CD4+ T cell activation (66–68) and SLE-like disease (69).

Khan et al. also proposed the role of OS in TCE-mediated autoimmunity based on their novel observation of increased anti-malondialdehyde (MDA) antibodies in MRL +/+ mice exposed to TCE (70). TCE-mediated generation of lipid peroxidation-derived aldehydes (LPDAs) [i.e., 4-hydroxynonenal (HNE) and MDA] (64, 70), can cause endogenous macromolecule modifications, leading to formation of neoantigens, and thus, contributing to SLE. These LPDAs have also been shown to contribute to TCE-mediated autoimmunity via Th1/Th17 activation (71). Role of OS in TCE-mediated autoimmunity is well-supported by studies using an antioxidant NAC and iNOS-null MRL+/+ mice, resulting in an improvement of autoimmune responses (63, 72). Furthermore, protein oxidation (carbonylation and nitration) also seems to contribute to the induction of TCE-mediated autoimmunity (65, 73). The oxidative modification of proteins may alter immunogenicity of self-antigens, and may generate an autoimmune response by stimulating T cells (65).

Oxidative DNA damage and resulting poly(ADP-ribose)polymerase-1 (PARP-1) activation could be another mechanism by which OS could contribute to TCE-mediated autoimmunity. In fact, TCE treatment in MRL+/+ mice led to increased 8-OHdG, PARP-1, caspases and elevated anti-ssDNA antibodies, and these changes were attenuated by NAC supplementation (74). Further support to role of OS in TCE-mediated autoimmunity was also evident from observed activation of hepatic pro-inflammatory NLRP3 and IL-1β production (75).

In addition, the pathogenesis of SLE is linked with dysfunctional T cells, B cells, natural Killer cells, dendritic cells, macrophages, and neutrophils. TCE and its metabolites have been shown to stimulate splenic CD4+ T cells toward Th1 and Th17 responses, which could be involved in the development of SLE (62, 71, 76). TCE exposure alters DNA methylation in CpG sites of ifng gene promoter of effector/memory CD4 T cells, resulting in altered T cell signaling and lineage differentiation (77). More recently, TCE exposure was shown to cause significant hepatic T cell infiltration, especially CD44+CD62L-CD8 effector T cells, and imbalance between Tregs (decreased) and Th17 cells (increased). Furthermore, a dramatic increase in hepatic DCs and NKs was noticed after TCE exposure. TCE-induced hepatic immune dysregulation was effectively blunted by antioxidant NAC supplementation, suggesting a critical role for OS in TCE-mediated immune cell infiltration and their activation in SLE/AIH exposure (75).

GUT MICROBIOTA IN THE PATHOGENESIS OF ADs: CAUSE OR CONSEQUENCE OF THE DISEASE?

Human gut microbiota is composed of ∼100 trillion microorganisms from over 500 genera of bacteria from two main phyla, namely Bacteroidetes and Firmicutes (78–80). The impact of gut microbiome dysbiosis in the pathogenesis of ADs is evident from an increasing number of studies, both in animal models and humans (81). These studies support the striking linkage of altered microbiota composition with the onset of several autoimmune disorders, including SLE (82), multiple sclerosis (83), RA (84), systemic sclerosis (85),

inflammatory bowel disease (IBD) and ulcerative colitis (86). Despite the evidence for an association of gut dysbiosis with several ADs, the mechanisms by which intestinal microbiota may affect these diseases are not well-known. Therefore, characterization and manipulation of microbiome could thus represent a potential therapeutic strategy for the improvement and potentially complete restoration of the normal immune system in different ADs.

The pathogenesis of one of the most prominent ADs, SLE, is not completely understood. However, environmental (infections, chemicals/drugs, ultraviolet light), hormonal and genetic factors could potentially contribute to SLE flares (87). More importantly, whether gut microbiome modification is a causal factor or an outcome of lupus remains unknown (88). Therefore, more mechanistic studies are required to delineate the casual effect of the gut microbiota in autoimmune- prone mouse models or humans with diverse manifestations of SLE.

Recent studies suggest that alterations in the gut microbial composition and function may be correlated with SLE disease activity. In fact, SLE patients have a lower Firmicutes/Bacteroidetes ratio and abundance of several genera (89, 90). Reduction in the abundance of Lactobacillaceae and increase in Lachnospiraceae were also observed in patients with SLE (91). Increases in *Ruminococcus gnavus* of Lachnospiraceae family, elevated serum sCD14 and higher levels of fecal secretory IgA and calprotectin levels were also reported in female SLE patients (92). Increased serum levels of endotoxin lipopolysaccharide (LPS) in SLE patients, possibly due to leaky gut, suggest that chronic microbial translocation can contribute to pathogenesis of SLE (93, 94). Similarly, bacterial amyloid/DNA complex was shown to stimulate autoimmune responses, including the production of type I IFN and autoantibodies in lupus-prone NZBxW/F1 mice (95, 96). In young lupus-prone mice, marked depletion of lactobacilli and increases in Lachnospiraceae were observed compared to age-matched healthy controls. Dietary intervention with retinoic acid restored lactobacilli with improved symptoms. The results thus show the dynamic changes in the gut microbiota in murine lupus and suggest the use of retinoic acid as dietary supplement to relieve inflammatory flares in lupus patients (97, 98). A comparison of gut microbiota between mice strains (NZB/W F1, MRL/lpr, and SNF1) and a cohort of SLE patients showed gut microbiota in different mouse models were more diverse as disease progressed, while the diversity was lower in SLE patients with active disease (82). However, the exact role of either symbiotic or pathogenic microbes in this disease has yet to be elucidated.

ENVIRONMENTAL AGENTS AND GUT MICROBIOME

Exposure to various environmental chemicals on a regular basis can cause gut microbiome dysbiosis. Environmental chemical-induced intestinal microbiome alternations might lead to systemic effects in the host (99). Despite involvement of several environmental agents in the pathogenesis of ADs (7), very little is known on their impact to microbiota and the role of subsequent dysbiosis on disease initiation/progression.

TCE exposure, which is known to induce/exacerbate SLE in both experimental animals and humans, is also reported to cause alterations in the gut microbiome with increased abundance of genus Bifidobacterium and bacterial family Enterobacteriaceae as well as lower abundance of the genus Bacteroides and Lactobacillus in MRL+/+ mice at a high but occupationally relevant TCE dose compared to controls (100). Smoking affects the microbiome composition in animal models and humans. Decreased Actinobacteria and Firmicutes phyla as well as the genera Bifidobacteria and Lactococcus, but increased Proteobacteria and Bacteroidetes phyla were reported in smokers (56). Beneficial role of Lactobacillus probiotics was also observed in pristane-induced lupus model through reduction of Th1, Th17, and cytotoxic T lymphocytes (34). Studies suggest that interactions between host and commensal microbiome, as well as infectious microorganisms, including bacteria, viruses and parasites, can influence the outcome of ADs (101–105). The observed changes in microbiome due to environmental agents are important findings and deserve a more careful and thorough evaluation of their role, especially in terms of establishing a cause-and-effect relationship.

MECHANISTIC APPROACHES ELUCIDATING THE CONTRIBUTION OF GUT MICROBIOME TO ADs

Despite implications of gut microbiota in the pathogenesis of ADs, molecular mechanisms by which microbiota influences immune responses remain largely unknown. However, a few approaches using probiotics, antibiotics, bacterial metabolites, and antioxidants resulting in alleviation of some of the immune dysregulations are described here.

EFFECT OF PROBIOTICS

Probiotics, defined as live microorganisms, provide beneficial effects on the host when administrated in adequate amounts, can effectively prevent or treat immune-mediated diseases. Probiotics have been effective in multiple ADs in animal models and clinical trials (106, 107). In a study aimed to delineate the contribution of microbiota in disease pathogenesis, it was noticed that oral Lactobacillus administration in MRL/lpr mice exerted anti-inflammatory effects by restoring intestinal barrier function, suppressing pro-inflammatory cytokines, and improving the ratio of Treg vs. Th17 cells, thereby attenuating kidney inflammation. The study suggests how modulation of gut microbiota can regulate immune responses in lupus (89). Studies aimed in evaluating the effects of Lactobacillus rhamnosus and Lactobacillus delbrueckii in pristane-induced BALB/c mouse model of

SLE showed that the immune-regulatory probiotics led to reduction in autoantibodies, decreased population of Th1-Th17 cells and reduced IFN-γ and IL-17, suggesting the usefulness of these probiotics in the management of SLE (35). Further studies clarifying if probiotics function as immunosuppressive agents or by regulating or restoring the gut microbiome composition will be necessary in evaluating the contribution of the gut microbiome in the pathogenesis of auto-inflammatory diseases.

EFFECT OF ANTIBIOTICS

Despite the use of antibiotics that generates an adverse impact on gut microbiota, there is plenty of evidence to suggest that antibiotics have a positive impact on ADs. Oral administration of antibiotics in MRL/lpr mice improved the disease by decreasing inflammatory cytokines (i.e., IL-17) and increasing anti-inflammatory IL-10 (89). Through the modification of gut microbiota, antibiotics may cause profound alterations of the gut epithelial barrier, mucosal immune cells and even enteric neural system. Low-dose penicillin treatment in mice suppressed IL-17 in intestinal tissues and decreased Th17 cells in small intestine lamina due to eradication of segmented filamentous bacteria (SFB) (108), suggesting that the therapeutic role of antibiotics in autoimmunity is probably through modifying the autoimmune-prone bacteria such as SFB. Gut microbiota and increased intestinal permeability have been reported in both experimental animal models and SLE patients (90, 109). Furthermore, translocation of gut *Enterococcus gallinarum* to the liver can induce autoimmune responses in (NZW × BXSB) F1 hybrid mice. This study further showed that antibiotic treatment inhibited *Enterococcus gallinarum* growth and T cell response, relieving the autoimmune manifestations (110). Treatment of vancomycin reshaped the gut microbiome composition and improved intestinal barrier function by increasing the tight junction proteins (Occludin, ZO-1) (89). Traditional standard treatments for autoimmunity have been immunosuppressive medications that dampen the immune system non-specifically and alter the gut microbiome composition (111, 112). Furthermore, microbiome-drug interactions also provide mechanistic insight into the role of gut microbiota in drug efficacy and toxicity (113).

IMPACT OF MICROBIAL METABOLITES

Microbial metabolites can also contribute to the pathogenesis of ADs. Short-chain fatty acids (SCFAs), such as acetate, propionate and butyrate are produced by fermentation of non-digestible carbohydrates (114). SCFAs exhibit immune-regulatory functions by inhibiting NF-kB signaling and inflammatory cytokines (115). In non-obese diabetic (NOD) strain, supplementation of microbial metabolites acetate and butyrate provided protection against type 1 diabetes by enhancing gut integrity, decreasing diabetogenic cytokines, inhibiting autoreactive T cell, and inducing Treg functions (116). Additionally, SCFA ameliorates experimental allergic encephalomyelitis (EAE) disease symptoms by increasing level of Treg cells in the gut (117). SCFAs function as inhibitors of histone deacetylases (HDACs) to induce anti-inflammatory environment (118). Thus, induction of SCFA-producing bacteria and restoring Treg function could be an effective approach to counter autoreactive T cells in ADs.

IMPACT OF OXIDATIVE STRESS

In recent years, OS has been considered as potential triggering mechanism by which microbiota influences the immune responses and ADs. Macrophages and neutrophils produce abundant ROS as a microbicidal response. The NADPH oxidase, Nox2, catalyzes "oxidative burst" in phagocytes. Nox2 is also found in many non-phagocytic cell types, with colonic epithelial cells expressing high level of Nox2, where they likely mediate ROS production and contribute to host defense system (78, 119–121). It was recently reported that specific taxa of intestinal bacteria stimulate ROS production within enterocytes, among which Lactobacilli have a greater potential to induce ROS with enhanced ability to penetrate the mucus layer in gut injury model (122).

A large body of evidence suggests that probiotics reduce OS, inflammation, and intestinal permeability. Consumption of Dahi, a traditional Indian fermented milk enriched in Lactobacillus acidophilus and Lactobacillus casei, apparently reduces lipid peroxidation (123). Contribution of OS was also apparent from the study where intake of fructose caused CYP2E1-dependent protein nitration of intestinal junctional proteins, resulting in increased gut leakiness, endotoxemia and liver fibrosis (124). On the other hand, lactobacilli induced Nrf2 signaling (125, 126), which could be a mechanism by which probiotic bacteria may elicit beneficial effects on disease states including ADs.

Fecal microbiota transplantation (FMT), a strategy to transfer fecal microbiome from health donor into patient's gut, is a successful therapy in Clostridium difficile infection and is under investigation for other ADs (127). FMT was highly effective in a mouse model of necrotizing enterocolitis through the modulation of oxidative stress, altered microbiota and reduced colon inflammation (128). Fecal microbiome from SLE patients can induce Th17 cell differentiation *in vitro* and promote inflammation (129). A recent study also shows that the fecal microbiome from SLE mice can induce autoimmune responses in germ-free C57BL/6J mice, evidenced by induction of anti-dsDNA antibodies, inflammatory response and SLE susceptibility genes (130). Interestingly, Mu et al. (89) found that MRL-to-MRL/lpr cecal microbiome transplantation showed protective effect in SLE disease marker as evident from significantly reduced level of anti-dsDNA antibodies, possibly due to increased abundance of Lactobacillales. These studies suggest that functional analyses of microbiome dysbiosis and ROS-dependent outcomes related to disease progression will be a challenging future work, especially delineating their roles in the pathogenesis of ADs.

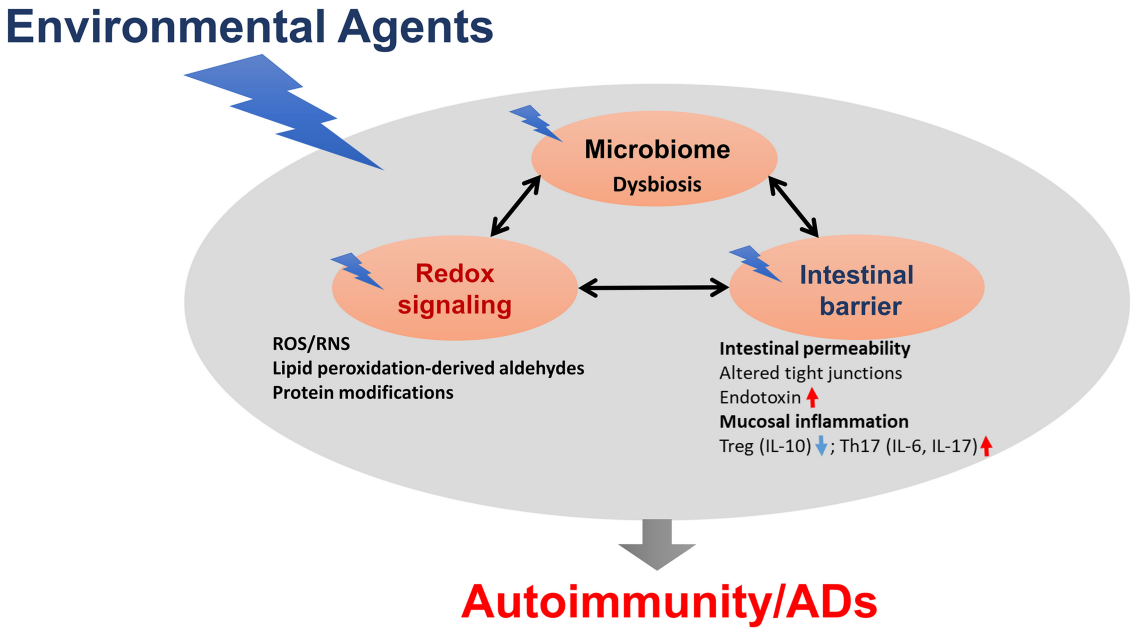

FIGURE 2 | The proposed link between gut dysbiosis and ADs in genetically susceptible individuals. Chemical-induced gut microbiome dysbiosis can alter intestinal barrier function, mucosal inflammation and immunity, resulting in increased translocation of bacteria, or its metabolites, such as circulating endotoxin lipopolysaccharides (LPS), thus promoting systemic aberrant auto-inflammatory responses, and eventually leading to ADs.

CONCLUSIONS AND FUTURE DIRECTIONS

Based on evidences presented, it is becoming clear that environmental agents can trigger autoimmunity in susceptible individuals. It would be important to delineate how different environmental agents lead to different disease phenotype. Studies conducted in animal models suggest a number of potential mechanisms, including OS, epigenetic modifications, systemic inflammation, inflammatory cytokines, and hormonal triggers, some of which are shared by other environmental agents. However, one mechanism which appears most common among these agents is OS, as depicted in **Figure 1**. Environmental agent-mediated OS is pivotal in the pathogenesis of ADs and many such agents indeed participate through this mechanism. More in-depth studies to delineate the molecular and cellular pathways by which OS contributes to autoimmunity, especially the redox-immune interactions, ROS scavenger antioxidants, and exploring OS-mediated protein/DNA modifications in generating neoantigens, will provide critical information on OS-mediated autoimmunity (7).

Microbiome dysbiosis is another very important environmental factor which can contribute to various ADs, although precise mechanistic links between the microbiome and ADs remain largely unknown (**Figure 2**). Clearly, gut microbiome dysbiosis is well-documented in the pathogenesis of ADs, and host-microbiome studies will further clarify mechanisms underlying how microbiome dysbiosis affects the disease progression. Further studies are needed to clarify whether chemical-induced gut microbiome dysbiosis can alter intestinal barrier function and mucosal immune responses, resulting in increased translocation of bacteria or its metabolites, such as circulating endotoxin LPS or bacterial amyloid/DNA complex, thus promoting systemic aberrant auto-inflammatory responses and ADs (**Figure 2**). In addition, it remains very uncertain whether gut microbiome is a causative factor or a consequence of the disease, which necessitates more thoughtful approaches, including colonization of germ-free mice with gut microbiome associated with the disease which might offer more insight into the role of these bacteria in the disease pathogenesis. Use of FMT could thus provide a great future avenue to control inflammation in AD patients. Application of microbiota-derived probiotics also holds great promise for future clinical improvements of these inflammatory diseases. Furthermore, promoting the induction of anti-inflammatory Tregs and reducing pro-inflammatory/pathogenic Th17 cell responses might be a great strategy for the prevention of autoimmunity/ADs.

AUTHOR CONTRIBUTIONS

MK and HW wrote the manuscript.

FUNDING

This work was supported by RO1 grants [ES016302 and ES026887] from the National Institute of Environmental Health Sciences (NIEHS), NIH, and its contents are solely the responsibility of the authors and do not necessarily represent the official views of the NIEHS, NIH.

REFERENCES

1. Zhao CN, Xu Z, Wu GC, Mao YM, Liu LN, Qian W, et al. Emerging role of air pollution in autoimmune diseases. *Autoimmun Rev.* (2019) 18:607–14. doi: 10.1016/j.autrev.2018.12.010
2. Vojdani A. A Potential link between environmental triggers and autoimmunity. *Autoimmune Dis.* (2014) 2014:437231. doi: 10.1155/2014/437231
3. Selmi C, Lu Q, Humble MC. Heritability versus the role of the environment in autoimmunity. *J Autoimmun.* (2012) 39:249–52. doi: 10.1016/j.jaut.2012.07.011
4. Fishbein AB, Fuleihan RL. The hygiene hypothesis revisited: does exposure to infectious agents protect us from allergy? *Curr Opin Pediatr.* (2012) 24:98–102. doi: 10.1097/MOP.0b013e32834ee57c
5. Pollard KM, Hultman P, Kono DH. Toxicology of autoimmune diseases. *Chem Res Toxicol.* (2010) 23:455–66. doi: 10.1021/tx9003787
6. Vojdani A, Pollard KM, Campbell AW. Environmental triggers and autoimmunity. *Autoimmune Dis.* (2014) 2014:798029. doi: 10.1155/2014/798029
7. Khan MF, Wang G. Environmental agents, oxidative stress and autoimmunity. *Curr Opin Toxicol.* (2018) 7:22–7. doi: 10.1016/j.cotox.2017.10.012
8. Dehner C, Fine R, Kriegel MA. The microbiome in systemic autoimmune disease: mechanistic insights from recent studies. *Curr Opin Rheumatol.* (2019) 31:201–7. doi: 10.1097/BOR.0000000000000574
9. De Luca F, Shoenfeld Y. The microbiome in autoimmune diseases. *Clin Exp Immunol.* (2019) 195:74–85. doi: 10.1111/cei.13158
10. Li B, Selmi C, Tang R, Gershwin ME, Ma X. The microbiome and autoimmunity: a paradigm from the gut-liver axis. *Cell Mol Immunol.* (2018) 15:595–609. doi: 10.1038/cmi.2018.7
11. Crowe W, Allsopp PJ, Watson GE, Magee PJ, Strain JJ, Armstrong DJ, et al. Mercury as an environmental stimulus in the development of autoimmunity - a systematic review. *Autoimmun Rev.* (2017) 16:72–80. doi: 10.1016/j.autrev.2016.09.020
12. Pollard KM, Cauvi DM, Toomey CB, Hultman P, Kono DH. Mercury-induced inflammation and autoimmunity. *Biochim Biophys Acta Gen Subj.* (2019) 1863:129299. doi: 10.1016/j.bbagen.2019.02.001
13. Pollard KM, Escalante GM, Huang H, Haraldsson KM, Hultman P, Christy JM, et al. Induction of systemic autoimmunity by a xenobiotic requires endosomal TLR trafficking and signaling from the late endosome and endolysosome but not type I IFN. *J Immunol.* (2017) 199:3739–47. doi: 10.4049/jimmunol.1700332
14. Zheng Y, Gallucci S, Gaughan JP, Gross JA, Monestier M. A role for B cell-activating factor of the TNF family in chemically induced autoimmunity. *J Immunol.* (2005) 175:6163–8. doi: 10.4049/jimmunol.175.9.6163
15. Carruthers NJ, Rosenspire AJ, Caruso JA, Stemmer PM. Low level $Hg^{(2+)}$ exposure modulates the B-cell cytoskeletal phosphoproteome. *J Proteomics.* (2018) 173:107–14. doi: 10.1016/j.jprot.2017.11.026
16. Caruso JA, Carruthers N, Shin N, Gill R, Stemmer PM, Rosenspire A. Mercury alters endogenous phosphorylation profiles of SYK in murine B cells. *BMC Immunol.* (2017) 18:37. doi: 10.1186/s12865–017-0221–0
17. Shenker BJ, Guo TL, Shapiro IM. Low-level methylmercury exposure causes human T-cells to undergo apoptosis: evidence of mitochondrial dysfunction. *Environ Res.* (1998) 77:149–59. doi: 10.1006/enrs.1997.3816
18. Shenker BJ, Pankoski L, Zekavat A, Shapiro IM. Mercury-induced apoptosis in human lymphocytes: caspase activation is linked to redox status. *Antioxid Redox Signal.* (2002) 4:379–89. doi: 10.1089/15230860260196182
19. Alkaissi H, Havarinasab S, Nielsen JB, Soderkvist P, Hultman P. Bank1 and NF-kappaB as key regulators in anti-nucleolar antibody development. *PLoS ONE.* (2018) 13:e0199979. doi: 10.1371/journal.pone.0199979
20. Thrasher JD, Madison R, Broughton A. Immunologic abnormalities in humans exposed to chlorpyrifos: preliminary observations. *Arch Environ Health.* (1993) 48:89–93. doi: 10.1080/00039896.1993.9938400
21. Simoniello MF, Contini L, Benavente E, Mastandrea C, Roverano S, Paira S. Different end-points to assess effects in systemic lupus erythematosus patients exposed to pesticide mixtures. *Toxicology.* (2017) 376:23–9. doi: 10.1016/j.tox.2016.08.003
22. Sobel ES, Gianini J, Butfiloski EJ, Croker BP, Schiffenbauer J, Roberts SM. Acceleration of autoimmunity by organochlorine pesticides in (NZB x NZW)F1 mice. *Environ Health Perspect.* (2005) 113:323–8. doi: 10.1289/ehp.7347
23. Wang F, Sobel ES, Butfiloski EJ, Roberts SM. Comparison of chlordecone and estradiol effects on splenic T-cells in (NZBxNZW)F(1) mice. *Toxicol Lett.* (2008) 183:1–9. doi: 10.1016/j.toxlet.2008.08.020
24. Parks CG, Santos ASE, Lerro CC, DellaValle CT, Ward MH, Alavanja MC, et al. Lifetime pesticide use and antinuclear antibodies in male farmers from the agricultural health study. *Front Immunol.* (2019) 10:1476. doi: 10.3389/fimmu.2019.01476
25. Reeves WH, Lee PY, Weinstein JS, Satoh M, Lu L. Induction of autoimmunity by pristane and other naturally occurring hydrocarbons. *Trends Immunol.* (2009) 30:455–64. doi: 10.1016/j.it.2009.06.003
26. Calvani N, Caricchio R, Tucci M, Sobel ES, Silvestris F, Tartaglia P, et al. Induction of apoptosis by the hydrocarbon oil pristane: implications for pristane-induced lupus. *J Immunol.* (2005) 175:4777–82. doi: 10.4049/jimmunol.175.7.4777
27. Richards HB, Satoh M, Shaw M, Libert C, Poli V, Reeves WH. Interleukin 6 dependence of anti-DNA antibody production: evidence for two pathways of autoantibody formation in pristane-induced lupus. *J Exp Med.* (1998) 188:985–90. doi: 10.1084/jem.188.5.985
28. Richards HB, Satoh M, Jennette JC, Croker BP, Yoshida H, Reeves WH. Interferon-gamma is required for lupus nephritis in mice treated with the hydrocarbon oil pristane. *Kidney Int.* (2001) 60:2173–80. doi: 10.1046/j.1523–1755.2001.00045.x
29. Summers SA, Odobasic D, Khouri MB, Steinmetz OM, Yang Y, Holdsworth SR, et al. Endogenous interleukin (IL)-17A promotes pristane-induced systemic autoimmunity and lupus nephritis induced by pristane. *Clin Exp Immunol.* (2014) 176:341–50. doi: 10.1111/cei.12287
30. Smith N, Rodero MP, Bekaddour N, Bondet V, Ruiz-Blanco YB, Harms M, et al. Control of TLR7-mediated type I IFN signaling in pDCs through CXCR4 engagement-a new target for lupus treatment. *Sci Adv.* (2019) 5:eaav9019. doi: 10.1126/sciadv.aav9019
31. Fernandes JG, Borrego A, Jensen JR, Cabrera WHK, Correa MA, Starobinas N, et al. miRNA expression and interaction with genes involved in susceptibility to pristane-induced arthritis. *J Immunol Res.* (2018) 2018:1928405. doi: 10.1155/2018/1928405
32. Jiang C, Zhu W, Xu J, Wang B, Hou W, Zhang R, et al. MicroRNA-26a negatively regulates toll-like receptor 3 expression of rat macrophages and ameliorates pristane induced arthritis in rats. *Arthritis Res Ther.* (2014) 16:R9. doi: 10.1186/ar4435
33. Thompson SJ, Elson CJ. Susceptibility to pristane-induced arthritis is altered with changes in bowel flora. *Immunol Lett.* (1993) 36:227–31. doi: 10.1016/0165–2478(93)90057–9
34. Mardani F, Mahmoudi M, Esmaeili SA, Khorasani S, Tabasi N, Rastin M. *In vivo* study: Th1-Th17 reduction in pristane-induced systemic lupus erythematosus mice after treatment with tolerogenic Lactobacillus probiotics. *J Cell Physiol.* (2018) 234:642–9. doi: 10.1002/jcp.26819
35. Khorasani S, Mahmoudi M, Kalantari MR, Lavi Arab F, Esmaeili SA, Mardani F, et al. Amelioration of regulatory T cells by *Lactobacillus delbrueckii* and *Lactobacillus rhamnosus* in pristane-induced lupus mice model. *J Cell Physiol.* (2019) 234:9778–86. doi: 10.1002/jcp.27663
36. Zhao M, Tan Y, Peng Q, Huang C, Guo Y, Liang G, et al. IL-6/STAT3 pathway induced deficiency of RFX1 contributes to Th17-dependent autoimmune diseases via epigenetic regulation. *Nat Commun.* (2018) 9:583. doi: 10.1038/s41467–018-02890–0
37. Ouyang Q, Huang Z, Wang Z, Chen X, Ni J, Lin L. Effects of pristane alone or combined with chloroquine on macrophage activation, oxidative stress, and TH1/TH2 skewness. *J Immunol Res.* (2014) 2014:613136. doi: 10.1155/2014/613136
38. Lee S, Hayashi H, Mastuzaki H, Kumagai-Takei N, Otsuki T. Silicosis and autoimmunity. *Curr Opin Allergy Clin Immunol.* (2017) 17:78–84. doi: 10.1097/ACI.0000000000000350
39. Pollard KM. Silica, silicosis, and autoimmunity. *Front Immunol.* (2016) 7:97. doi: 10.3389/fimmu.2016.00097
40. Wu P, Miura Y, Hyodoh F, Nishimura Y, Hatayama T, Hatada S, et al. Reduced function of CD4+25+ regulatory T cell fraction in

silicosis patients. *Int J Immunopathol Pharmacol.* (2006) 19:357–68. doi: 10.1177/039463200601900212
41. Takata-Tomokuni A, Ueki A, Shiwa M, Isozaki Y, Hatayama T, Katsuyama H, et al. Detection, epitope-mapping and function of anti-Fas autoantibody in patients with silicosis. *Immunology.* (2005) 116:21–9. doi: 10.1111/j.1365–2567.2005.02192.x
42. Brown JM, Archer AJ, Pfau JC, Holian A. Silica accelerated systemic autoimmune disease in lupus-prone New Zealand mixed mice. *Clin Exp Immunol.* (2003) 131:415–21. doi: 10.1046/j.1365–2249.2003.02094.x
43. Pfau JC, Brown JM, Holian A. Silica-exposed mice generate autoantibodies to apoptotic cells. *Toxicology.* (2004) 195:167–76. doi: 10.1016/j.tox.2003.09.011
44. Mayeux JM, Escalante GM, Christy JM, Pawar RD, Kono DH, Pollard KM. Silicosis and silica-induced autoimmunity in the diversity outbred mouse. *Front Immunol.* (2018) 9:874. doi: 10.3389/fimmu.2018.00874
45. Benmerzoug S, Rose S, Bounab B, Gosset D, Duneau L, Chenuet P, et al. STING-dependent sensing of self-DNA drives silica-induced lung inflammation. *Nat Commun.* (2018) 9:5226. doi: 10.1038/s41467–018-07425–1
46. Dostert C, Petrilli V, Van Bruggen R, Steele C, Mossman BT, Tschopp J. Innate immune activation through Nalp3 inflammasome sensing of asbestos and silica. *Science.* (2008) 320:674–7. doi: 10.1126/science.1156995
47. Cassel SL, Eisenbarth SC, Iyer SS, Sadler JJ, Colegio OR, Tephly LA, et al. The Nalp3 inflammasome is essential for the development of silicosis. *Proc Natl Acad Sci USA.* (2008) 105:9035–40. doi: 10.1073/pnas.0803933105
48. Perricone C, Versini M, Ben-Ami D, Gertel S, Watad A, Segel MJ, et al. Smoke and autoimmunity: the fire behind the disease. *Autoimmun Rev.* (2016) 15:354–74. doi: 10.1016/j.autrev.2016.01.001
49. Speyer CB, Costenbader KH. Cigarette smoking and the pathogenesis of systemic lupus erythematosus. *Expert Rev Clin Immunol.* (2018) 14:481–7. doi: 10.1080/1744666X.2018.1473035
50. Freemer MM, King TE Jr, Criswell LA. Association of smoking with dsDNA autoantibody production in systemic lupus erythematosus. *Ann Rheum Dis.* (2006) 65:581–4. doi: 10.1136/ard.2005.039438
51. Hussain MS, Tripathi V. Smoking under hypoxic conditions: a potent environmental risk factor for inflammatory and autoimmune diseases. *Mil Med Res.* (2018) 5:11. doi: 10.1186/s40779–018-0158–5
52. Doyle JJ, Eliasson AH, Argyros GJ, Dennis GJ, Finger DR, Hurwitz KM, et al. Prevalence of pulmonary disorders in patients with newly diagnosed rheumatoid arthritis. *Clin Rheumatol.* (2000) 19:217–21. doi: 10.1007/s100670050160
53. Fricker M, Goggins BJ, Mateer S, Jones B, Kim RY, Gellatly SL, et al. Chronic cigarette smoke exposure induces systemic hypoxia that drives intestinal dysfunction. *JCI Insight.* (2018) 3:94040. doi: 10.1172/jci.insight.94040
54. Gravina G, Wasen C, Garcia-Bonete MJ, Turkkila M, Erlandsson MC, Toyra Silfversward S, et al. Survivin in autoimmune diseases. *Autoimmun Rev.* (2017) 16:845–55. doi: 10.1016/j.autrev.2017.05.016
55. Wasen C, Turkkila M, Bossios A, Erlandsson M, Andersson KM, Ekerljung L, et al. Smoking activates cytotoxic $CD8^{(+)}$ T cells and causes survivin release in rheumatoid arthritis. *J Autoimmun.* (2017) 78:101–10. doi: 10.1016/j.jaut.2016.12.009
56. Savin Z, Kivity S, Yonath H, Yehuda S. Smoking and the intestinal microbiome. *Arch Microbiol.* (2018) 200:677–84. doi: 10.1007/s00203–018-1506–2
57. Ordaz JD, Damayanti NP, Irudayaraj JMK. Toxicological effects of trichloroethylene exposure on immune disorders. *Immunopharmacol Immunotoxicol.* (2017) 39:305–17. doi: 10.1080/08923973.2017.1364262
58. Kilburn KH, Warshaw RH. Prevalence of symptoms of systemic lupus erythematosus (SLE) and of fluorescent antinuclear antibodies associated with chronic exposure to trichloroethylene and other chemicals in well water. *Environ Res.* (1992) 57:1–9. doi: 10.1016/S0013–9351(05)80014–3
59. Cooper GS, Makris SL, Nietert PJ, Jinot J. Evidence of autoimmune-related effects of trichloroethylene exposure from studies in mice and humans. *Environ Health Perspect.* (2009) 117:696–702. doi: 10.1289/ehp.11782
60. Khan MF, Kaphalia BS, Prabhakar BS, Kanz MF, Ansari GA. Trichloroethene-induced autoimmune response in female MRL +/+ mice. *Toxicol Appl Pharmacol.* (1995) 134:155–60. doi: 10.1006/taap.1995.1179
61. Griffin JM, Blossom SJ, Jackson SK, Gilbert KM, Pumford NR. Trichloroethylene accelerates an autoimmune response by Th1 T cell activation in MRL +/+ mice. *Immunopharmacology.* (2000) 46:123–37. doi: 10.1016/S0162–3109(99)00164–2
62. Gilbert KM, Griffin JM, Pumford NR. Trichloroethylene activates CD4+ T cells: potential role in an autoimmune response. *Drug Metab Rev.* (1999) 31:901–16. doi: 10.1081/DMR-100101945
63. Wang G, Wang J, Ma H, Ansari GA, Khan MF. N-Acetylcysteine protects against trichloroethene-mediated autoimmunity by attenuating oxidative stress. *Toxicol Appl Pharmacol.* (2013) 273:189–95. doi: 10.1016/j.taap.2013.08.020
64. Wang G, Ansari GA, Khan MF. Involvement of lipid peroxidation-derived aldehyde-protein adducts in autoimmunity mediated by trichloroethene. *J Toxicol Environ Health A.* (2007) 70:1977–85. doi: 10.1080/15287390701550888
65. Wang G, Wang J, Ma H, Khan MF. Increased nitration and carbonylation of proteins in MRL+/+ mice exposed to trichloroethene: potential role of protein oxidation in autoimmunity. *Toxicol Appl Pharmacol.* (2009) 237:188–95. doi: 10.1016/j.taap.2009.03.010
66. Gilbert KM, Przybyla B, Pumford NR, Han T, Fuscoe J, Schnackenberg LK, et al. Delineating liver events in trichloroethylene-induced autoimmune hepatitis. *Chem Res Toxicol.* (2009) 22:626–32. doi: 10.1021/tx800409r
67. Gilbert KM, Reisfeld B, Zurlinden TJ, Kreps MN, Erickson SW, Blossom SJ. Modeling toxicodynamic effects of trichloroethylene on liver in mouse model of autoimmune hepatitis. *Toxicol Appl Pharmacol.* (2014) 279:284–93. doi: 10.1016/j.taap.2014.07.003
68. Blossom SJ, Pumford NR, Gilbert KM. Activation and attenuation of apoptosis of CD4+ T cells following *in vivo* exposure to two common environmental toxicants, trich2loroacetaldehyde hydrate and trichloroacetic acid. *J Autoimmun.* (2004) 23:211–20. doi: 10.1016/j.jaut.2004.06.007
69. Cai P, Konig R, Boor PJ, Kondraganti S, Kaphalia BS, Khan MF, et al. Chronic exposure to trichloroethene causes early onset of SLE-like disease in female MRL +/+ mice. *Toxicol Appl Pharmacol.* (2008) 228:68–75. doi: 10.1016/j.taap.2007.11.031
70. Khan MF, Wu X, Ansari GA. Anti-malondialdehyde antibodies in MRL+/+ mice treated with trichloroethene and dichloroacetyl chloride: possible role of lipid peroxidation in autoimmunity. *Toxicol Appl Pharmacol.* (2001) 170:88–92. doi: 10.1006/taap.2000.9086
71. Wang G, Wang J, Fan X, Ansari GA, Khan MF. Protein adducts of malondialdehyde and 4-hydroxynonenal contribute to trichloroethene-mediated autoimmunity via activating Th17 cells: dose- and time-response studies in female MRL+/+ mice. *Toxicology.* (2012) 292:113–22. doi: 10.1016/j.tox.2011.12.001
72. Wang G, Wakamiya M, Wang J, Ansari GA, Firoze Khan M. iNOS null MRL+/+ mice show attenuation of trichloroethene-mediated autoimmunity: contribution of reactive nitrogen species and lipid-derived reactive aldehydes. *Free Radic Biol Med.* (2015) 89:770–6. doi: 10.1016/j.freeradbiomed.2015.10.402
73. Wang G, Wang J, Luo X, Ansari GA, Khan MF. Nitrosative stress and nitrated proteins in trichloroethene-mediated autoimmunity. *PLoS ONE.* (2014) 9:e98660. doi: 10.1371/journal.pone.0098660
74. Wang G, Ma H, Wang J, Khan MF. Contribution of poly(ADP-ribose)polymerase-1 activation and apoptosis in trichloroethene-mediated autoimmunity. *Toxicol Appl Pharmacol.* (2019) 362:28–34. doi: 10.1016/j.taap.2018.10.012
75. Wang H, Wang G, Liang Y, Du X, Boor PJ, Sun J, et al. Redox regulation of hepatic NLRP3 inflammasome activation and immune dysregulation in trichloroethene-mediated autoimmunity. *Free Radic Biol Med.* (2019) 143:223–31. doi: 10.1016/j.freeradbiomed.2019.08.014
76. Cai P, Konig R, Khan MF, Qiu S, Kaphalia BS, Ansari GA. Autoimmune response in MRL+/+ mice following treatment with dichloroacetyl chloride or dichloroacetic anhydride. *Toxicol Appl Pharmacol.* (2006) 216:248–55. doi: 10.1016/j.taap.2006.05.010
77. Gilbert KM, Blossom SJ, Reisfeld B, Erickson SW, Vyas K, Maher M, et al. Trichloroethylene-induced alterations in DNA methylation were enriched in polycomb protein binding sites in effector/memory $CD4^{(+)}$ T cells. *Environ Epigenet.* (2017) 3:dvx013. doi: 10.1093/eep/dvx013
78. Neish AS, Jones RM. Redox signaling mediates symbiosis between the gut microbiota and the intestine. *Gut Microbes.* (2014) 5:250–3. doi: 10.4161/gmic.27917

79. Morgan XC, Segata N, Huttenhower C. Biodiversity and functional genomics in the human microbiome. *Trends Genet.* (2013) 29:51–8. doi: 10.1016/j.tig.2012.09.005
80. Rahbar Saadat Y, Hejazian M, Bastami M, Hosseinian Khatibi SM, Ardalan M, Zununi Vahed S. The role of microbiota in the pathogenesis of lupus: dose it impact lupus nephritis? *Pharmacol Res.* (2019) 139:191–8. doi: 10.1016/j.phrs.2018.11.023
81. Gianchecchi E, Fierabracci A. Recent advances on microbiota involvement in the pathogenesis of autoimmunity. *Int J Mol Sci.* (2019) 20:283. doi: 10.3390/ijms20020283
82. Luo XM, Edwards MR, Mu Q, Yu Y, Vieson MD, Reilly CM, et al. Gut microbiota in human systemic lupus erythematosus and a mouse model of lupus. *Appl Environ Microbiol.* (2018) 84:e02288–17. doi: 10.1128/AEM.02288–17
83. Kirby TO, Ochoa-Reparaz J. The gut microbiome in multiple sclerosis: a potential therapeutic avenue. *Med Sci.* (2018) 6:E69. doi: 10.3390/medsci6030069
84. Maeda Y, Kurakawa T, Umemoto E, Motooka D, Ito Y, Gotoh K, et al. Dysbiosis contributes to arthritis development via activation of autoreactive t cells in the intestine. *Arthritis Rheumatol.* (2016) 68:2646–61. doi: 10.1002/art.39783
85. Bellocchi C, Volkmann ER. Update on the gastrointestinal microbiome in systemic sclerosis. *Curr Rheumatol Rep.* (2018) 20:49. doi: 10.1007/s11926–018-0758–9
86. Clemente JC, Manasson J, Scher JU. The role of the gut microbiome in systemic inflammatory disease. *BMJ.* (2018) 360:j5145. doi: 10.1136/bmj.j5145
87. Moulton VR, Suarez-Fueyo A, Meidan E, Li H, Mizui M, Tsokos GC. Pathogenesis of human systemic lupus erythematosus: a cellular perspective. *Trends Mol Med.* (2017) 23:615–35. doi: 10.1016/j.molmed.2017.05.006
88. de Oliveira GLV, Leite AZ, Higuchi BS, Gonzaga MI, Mariano VS. Intestinal dysbiosis and probiotic applications in autoimmune diseases. *Immunology.* (2017) 152:1–12. doi: 10.1111/imm.12765
89. Mu Q, Zhang H, Liao X, Lin K, Liu H, Edwards MR, et al. Control of lupus nephritis by changes of gut microbiota. *Microbiome.* (2017) 5:73. doi: 10.1186/s40168–017-0300–8
90. Hevia A, Milani C, Lopez P, Cuervo A, Arboleya S, Duranti S, et al. Intestinal dysbiosis associated with systemic lupus erythematosus. *MBio.* (2014) 5:e01548–14. doi: 10.1128/mBio.01548–14
91. Katz U, Zandman-Goddard G. Drug-induced lupus: an update. *Autoimmun Rev.* (2010) 10:46–50. doi: 10.1016/j.autrev.2010.07.005
92. Azzouz D, Omarbekova A, Heguy A, Schwudke D, Gisch N, Rovin BH, et al. Lupus nephritis is linked to disease-activity associated expansions and immunity to a gut commensal. *Ann Rheum Dis.* (2019) 78:947–56. doi: 10.1136/annrheumdis-2018–214856
93. Shi L, Zhang Z, Yu AM, Wang W, Wei Z, Akhter E, et al. The SLE transcriptome exhibits evidence of chronic endotoxin exposure and has widespread dysregulation of non-coding and coding RNAs. *PLoS ONE.* (2014) 9:e93846. doi: 10.1371/journal.pone.0093846
94. Ogunrinde E, Zhou Z, Luo Z, Alekseyenko A, Li QZ, Macedo D, et al. A link between plasma microbial translocation, microbiome, and autoantibody development in first-degree relatives of systemic lupus erythematosus patients. *Arthritis Rheumatol.* (2019) 71:1858–68. doi: 10.1002/art.40935
95. Tursi SA, Lee EY, Medeiros NJ, Lee MH, Nicastro LK, Buttaro B, et al. Bacterial amyloid curli acts as a carrier for DNA to elicit an autoimmune response via TLR2 and TLR9. *PLoS Pathog.* (2017) 13:e1006315. doi: 10.1371/journal.ppat.1006315
96. Gallo PM, Rapsinski GJ, Wilson RP, Oppong GO, Sriram U, Goulian M, et al. Amyloid-DNA composites of bacterial biofilms stimulate autoimmunity. *Immunity.* (2015) 42:1171–84. doi: 10.1016/j.immuni.2015.06.002
97. Zhang H, Liao X, Sparks JB, Luo XM. Dynamics of gut microbiota in autoimmune lupus. *Appl Environ Microbiol.* (2014) 80:7551–60. doi: 10.1128/AEM.02676–14
98. Abdelhamid L, Luo XM. Retinoic acid, leaky gut, and autoimmune diseases. *Nutrients.* (2018) 10:E1016. doi: 10.3390/nu10081016
99. Rosenfeld CS. Gut dysbiosis in animals due to environmental chemical exposures. *Front Cell Infect Microbiol.* (2017) 7:396. doi: 10.3389/fcimb.2017.00396
100. Khare S, Gokulan K, Williams K, Bai S, Gilbert KM, Blossom SJ. Irreversible effects of trichloroethylene on the gut microbial community and gut-associated immune responses in autoimmune-prone mice. *J Appl Toxicol.* (2019) 39:209–20. doi: 10.1002/jat.3708
101. Neuman H, Mor H, Bashi T, Givol O, Watad A, Shemer A, et al. Helminth-based product and the microbiome of mice with lupus. *mSystems.* (2019) 4:e00160-18. doi: 10.1128/mSystems.00160–18
102. Versini M, Jeandel PY, Bashi T, Bizzaro G, Blank M, Shoenfeld Y. Unraveling the hygiene hypothesis of helminthes and autoimmunity: origins, pathophysiology, and clinical applications. *BMC Med.* (2015) 13:81. doi: 10.1186/s12916–015-0306–7
103. Mu Q, Zhang H, Luo XM. SLE: Another autoimmune disorder influenced by microbes and diet? *Front Immunol.* (2015) 6:608. doi: 10.3389/fimmu.2015.00608
104. Francis L, Perl A. Infection in systemic lupus erythematosus: friend or foe? *Int J Clin Rheumtol.* (2010) 5:59–74. doi: 10.2217/ijr.09.72
105. Tursi SA, Tukel C. Curli-containing enteric biofilms inside and out: matrix composition, immune recognition, and disease implications. *Microbiol Mol Biol Rev.* (2018) 82:e00028–18. doi: 10.1128/MMBR.00028–18
106. Zamani B, Golkar HR, Farshbaf S, Emadi-Baygi M, Tajabadi-Ebrahimi M, Jafari P, et al. Clinical and metabolic response to probiotic supplementation in patients with rheumatoid arthritis: a randomized, double-blind, placebo-controlled trial. *Int J Rheum Dis.* (2016) 19:869–79. doi: 10.1111/1756–185X.12888
107. Uusitalo U, Liu X, Yang J, Aronsson CA, Hummel S, Butterworth M, et al. Association of early exposure of probiotics and islet autoimmunity in the TEDDY study. *JAMA Pediatr.* (2016) 170:20–8. doi: 10.1001/jamapediatrics.2015.2757
108. Jin S, Zhao D, Cai C, Song D, Shen J, Xu A, et al. Low-dose penicillin exposure in early life decreases Th17 and the susceptibility to DSS colitis in mice through gut microbiota modification. *Sci Rep.* (2017) 7:43662. doi: 10.1038/srep43662
109. Yacoub R, Jacob A, Wlaschin J, McGregor M, Quigg RJ, Alexander JJ. Lupus: The microbiome angle. *Immunobiology.* (2018) 223:460–5. doi: 10.1016/j.imbio.2017.11.004
110. Manfredo Vieira S, Hiltensperger M, Kumar V, Zegarra-Ruiz D, Dehner C, Khan N, et al. Translocation of a gut pathobiont drives autoimmunity in mice and humans. *Science.* (2018) 359:1156–61. doi: 10.1126/science.aar7201
111. Maseda D, Zackular JP, Trindade B, Kirk L, Roxas JL, Rogers LM, et al. Nonsteroidal anti-inflammatory drugs alter the microbiota and exacerbate clostridium difficile colitis while dysregulating the inflammatory response. *MBio.* (2019) 10:e02282–18. doi: 10.1128/mBio.02282–18
112. Yildirim-Toruner C, Diamond B. Current and novel therapeutics in the treatment of systemic lupus erythematosus. *J Allergy Clin Immunol.* (2011) 127:303–12. doi: 10.1016/j.jaci.2010.12.1087
113. Guthrie L, Kelly L. Bringing microbiome-drug interaction research into the clinic. *EBioMedicine.* (2019) 44:708–15. doi: 10.1016/j.ebiom.2019.05.009
114. Alexander C, Swanson KS, Fahey GC, Garleb KA. Perspective: physiologic importance of short-chain fatty acids from nondigestible carbohydrate fermentation. *Adv Nutr.* (2019) 10:576–89. doi: 10.1093/advances/nmz004
115. Luhrs H, Gerke T, Muller JG, Melcher R, Schauber J, Boxberge F, et al. Butyrate inhibits NF-kappaB activation in lamina propria macrophages of patients with ulcerative colitis. *Scand J Gastroenterol.* (2002) 37:458–66. doi: 10.1080/003655202317316105
116. Marino E, Richards JL, McLeod KH, Stanley D, Yap YA, Knight J, et al. Gut microbial metabolites limit the frequency of autoimmune T cells and protect against type 1 diabetes. *Nat Immunol.* (2017) 18:552–62. doi: 10.1038/ni.3713
117. Haghikia A, Jorg S, Duscha A, Berg J, Manzel A, Waschbisch A, et al. Dietary fatty acids directly impact central nervous system autoimmunity via the small intestine. *Immunity.* (2015) 43:817–29. doi: 10.1016/j.immuni.2015.09.007
118. Chang PV, Hao L, Offermanns S, Medzhitov R. The microbial metabolite butyrate regulates intestinal macrophage function via histone deacetylase inhibition. *Proc Natl Acad Sci USA.* (2014) 111:2247–52. doi: 10.1073/pnas.1322269111
119. Lambeth JD. NOX enzymes and the biology of reactive oxygen. *Nat Rev Immunol.* (2004) 4:181–9. doi: 10.1038/nri1312

120. Lambeth JD, Neish AS. Nox enzymes and new thinking on reactive oxygen: a double-edged sword revisited. *Annu Rev Pathol.* (2014) 9:119–45. doi: 10.1146/annurev-pathol-012513–104651
121. Ogier-Denis E, Mkaddem SB, Vandewalle A. NOX enzymes and Toll-like receptor signaling. *Semin Immunopathol.* (2008) 30:291–300. doi: 10.1007/s00281–008-0120–9
122. Jones RM, Luo L, Ardita CS, Richardson AN, Kwon YM, Mercante JW, et al. Symbiotic lactobacilli stimulate gut epithelial proliferation via Nox-mediated generation of reactive oxygen species. *EMBO J.* (2013) 32:3017–28. doi: 10.1038/emboj.2013.224
123. Gomes AC, Bueno AA, de Souza RG, Mota JF. Gut microbiota, probiotics and diabetes. *Nutr J.* (2014) 13:60. doi: 10.1186/1475–2891-13–60
124. Cho YE, Kim DK, Seo W, Gao B, Yoo SH, Song BJ. Fructose promotes leaky gut, endotoxemia, and liver fibrosis through ethanol-inducible cytochrome P450–2E1-mediated oxidative and nitrative stress. *Hepatology.* (2019). doi: 10.1002/hep.30652. [Epub ahead of print].
125. Jones RM, Desai C, Darby TM, Luo L, Wolfarth AA, Scharer CD, et al. Lactobacilli modulate epithelial cytoprotection through the Nrf2 pathway. *Cell Rep.* (2015) 12:1217–25. doi: 10.1016/j.celrep.2015.07.042
126. Jones RM, Neish AS. Redox signaling mediated by the gut microbiota. *Free Radic Biol Med.* (2017) 105:41–7. doi: 10.1016/j.freeradbiomed.2016.10.495
127. Weingarden AR, Vaughn BP. Intestinal microbiota, fecal microbiota transplantation, and inflammatory bowel disease. *Gut Microbes.* (2017) 8:238–52. doi: 10.1080/19490976.2017.1290757
128. Li X, Li X, Shang Q, Gao Z, Hao F, Guo H, et al. Fecal microbiota transplantation (FMT) could reverse the severity of experimental necrotizing enterocolitis (NEC) via oxidative stress modulation. *Free Radic Biol Med.* (2017) 108:32–43. doi: 10.1016/j.freeradbiomed.2017.03.011
129. Lopez P, de Paz B, Rodriguez-Carrio J, Hevia A, Sanchez B, Margolles A, et al. Th17 responses and natural IgM antibodies are related to gut microbiota composition in systemic lupus erythematosus patients. *Sci Rep.* (2016) 6:24072. doi: 10.1038/srep24072
130. Ma Y, Xu X, Li M, Cai J, Wei Q, Niu H. Gut microbiota promote the inflammatory response in the pathogenesis of systemic lupus erythematosus. *Mol Med.* (2019) 25:35. doi: 10.1186/s10020–019-0102–5

Conflict of Interest: The authors declare that the research was conducted in the absence of any commercial or financial relationships that could be construed as a potential conflict of interest.

frontiers in Immunology

ORIGINAL RESEARCH
published: 21 August 2020
doi: 10.3389/fimmu.2020.01796

Requisite Omega-3 HUFA Biomarker Thresholds for Preventing Murine Lupus Flaring

Kathryn A. Wierenga[1,2*], *Rita S. Strakovsky*[2,3], *Abby D. Benninghoff*[4], *Lichchavi D. Rajasinghe*[2,3], *Adam L. Lock*[5], *Jack R. Harkema*[2,6] *and James J. Pestka*[2,3,7*]

[1] *Department of Biochemistry and Molecular Biology, Michigan State University, East Lansing, MI, United States,* [2] *Institute for Integrative Toxicology, Michigan State University, East Lansing, MI, United States,* [3] *Department of Food Science and Human Nutrition, Michigan State University, East Lansing, MI, United States,* [4] *Department of Animal, Dairy and Veterinary Sciences and USTAR Applied Nutrition Research, Utah State University, Logan, UT, United States,* [5] *Department of Animal Science, Michigan State University, East Lansing, MI, United States,* [6] *Department of Pathobiology and Diagnostic Investigation, Michigan State University, East Lansing, MI, United States,* [7] *Department of Microbiology and Molecular Genetics, Michigan State University, East Lansing, MI, United States*

OPEN ACCESS

Edited by:
Lisa G. Rider,
National Institute of Environmental Health Sciences (NIEHS), United States

Reviewed by:
Carlo Chizzolini,
Université de Genève, Switzerland
Andras Perl,
Upstate Medical University, United States

***Correspondence:**
Kathryn A. Wierenga
royerkat@msu.edu
James J. Pestka
pestka@msu.edu

Specialty section:
This article was submitted to Autoimmune and Autoinflammatory Disorders, a section of the journal Frontiers in Immunology

Received: *07 May 2020*
Accepted: *06 July 2020*
Published: *21 August 2020*

Citation:
Wierenga KA, Strakovsky RS, Benninghoff AD, Rajasinghe LD, Lock AL, Harkema JR and Pestka JJ (2020) Requisite Omega-3 HUFA Biomarker Thresholds for Preventing Murine Lupus Flaring. Front. Immunol. 11:1796. doi: 10.3389/fimmu.2020.01796

Lupus is a systemic autoimmune disease typified by uncontrolled inflammation, disruption of immune tolerance, and intermittent flaring – events triggerable by environmental factors. Preclinical and clinical studies reveal that consumption of the marine ω-3 highly unsaturated fatty acids (HUFAs) eicosapentaenoic acid (EPA) and docosahexaenoic acid (DHA) might be used as a precision nutrition intervention to lessen lupus symptoms. The anti-inflammatory and pro-resolving effects of ω-3 HUFAs are inextricably linked to their presence in membrane phospholipids. The ω-3 HUFA score, calculated as [100 × (ω-3 HUFAs/(ω-3 HUFAs + ω-6 HUFAs))] in red blood cells (RBCs), and the Omega-3 Index (O3I), calculated as [100 × ((DHA+EPA)/total fatty acids)] in RBCs, are two biomarkers potentially amenable to relating tissue HUFA balance to clinical outcomes in individuals with lupus. Using data from three prior preclinical DHA supplementation studies, we tested the hypothesis that the ω-3 HUFA score and the O3I inversely correlate with indicators of autoimmune pathogenesis in the $cSiO_2$-triggered lupus flaring model. The three studies employed both low and high fat rodent diets, as well as more complex diets emulating the U.S. dietary pattern. The ω-3 HUFA scores in RBCs were comparatively more robust than the O3I at predicting HUFA balances in the kidney, liver, spleen, and lung. Importantly, increases in both the ω-3 HUFA score (>40%) and the O3I (>10%) were strongly associated with suppression of $cSiO_2$-triggered (1) expression of interferon-regulated genes, proinflammatory cytokine production, leukocyte infiltration, and ectopic lymphoid structure development in the lung, (2) pulmonary and systemic autoantibody production, and (3) glomerulonephritis. Collectively, these findings identify achievable ω-3 HUFA scores and O3I thresholds that could be targeted in future human intervention studies querying how ω-3 HUFA consumption influences lupus and other autoimmune diseases.

Keywords: systemic lupus erythematosus, NZBWF1, ω-3 fatty acid, Omega-3 Index, highly unsaturated fatty acid, silica, docosahexaenoic acid, precision nutrition

INTRODUCTION

Systemic lupus erythematosus (lupus) is a prototypic, multifaceted autoimmune disease characterized by uncontrolled inflammation, disruption of self-tolerance, and intermittent episodes of disease flaring often triggered by environmental factors (1). Lupus-associated autoimmune pathogenesis elicits irreversible damage in the kidney and other organs, sometimes culminating in death. The overactive immune response in lupus is typically managed with glucocorticoids, which have deleterious effects associated with long-term use, including organ damage, osteoporosis, diabetes, and increased risk of cardiovascular disease (2, 3). Both animal and human studies indicate that consumption of marine ω-3 highly unsaturated fatty acids (HUFAs) docosahexaenoic acid (DHA) and eicosapentaenoic acid (EPA) may potentially alleviate the severity of chronic inflammatory and autoimmune diseases [reviewed in (4–6)], suggesting this precision nutrition approach might be a steroid-sparing intervention for lupus.

Human studies support the contention that ω-3 HUFA consumption may benefit lupus patients. In observational studies, low ω-3 HUFA intake is associated with exacerbated disease activity, adverse serum lipids, and atherosclerotic plaques in lupus patients (7), and a recent study by the Michigan Lupus Epidemiology and Surveillance (MiLES) program reported that positive patient-reported outcomes were associated with high consumption of ω-3 fatty acids and low dietary ω-6:ω-3 ratios (8). Most intervention trials implementing ω-3 HUFA supplementation in lupus patients report lessening of symptoms (9–18). However, there is variability across studies with some trials failing to show positive results. Key limiting factors contributing to disparities among investigations in humans include inadequate patient numbers; lack of consideration of effects of concurrent pharmacotherapies; variability in ω-3 HUFA dosages, sources, and supplementation durations; and failure to monitor ω-3 HUFA tissue levels in patients. This final point is immensely critical because the pro-resolving and anti-inflammatory properties of dietary ω-3 HUFAs are inextricably linked to the extent of their presence in the cell membrane (19). Importantly, pro-inflammatory ω-6 HUFAs, generated by elongation of shorter chain ω-6 polyunsaturated fatty acids (PUFAs), that dominate the typical Western diet compete with ω-3 HUFAs for occupancy at the sn2 position of phospholipids, thereby diminishing their anti-inflammatory and pro-resolving effects (19). In clinical studies, many factors influence the efficiency ω-3 HUFA incorporation, including patient compliance, individual differences in absorption, genetic variation in lipid metabolizing genes, and consumption of competing ω-6 PUFAs (20). Accordingly, for any clinical trial of marine ω-3 HUFA supplementation, it is essential to measure the balance of ω-3 HUFA levels both at baseline and throughout the study.

Animal models of lupus are an essential tool for understanding how gene-environment interactions influence development of the disease in humans. The NZBWF1 mouse is genetically predisposed to the development of autoimmune disease and has been widely used for over five decades as a preclinical lupus model for investigating mechanisms of disease pathogenesis, effects of environmental exposures, and efficacy of pharmacological and immunotherapeutic interventions (21). Female NZBWF1 mice spontaneously develop lupus at around 7 months of age, much earlier than males, and rarely live past 12 months (22, 23), mimicking the sex bias observed in human lupus. Inclusion of marine ω-3 HUFAs in the diet delays lupus onset and extends survival in this strain (24–29). Our laboratory has recently developed a novel model for lupus flaring involving intranasal instillation of female NZBWF1 mice with crystalline silica ($cSiO_2$). Frequent, high exposure to $cSiO_2$ particles in occupations such as construction, mining, and farming is etiologically linked to multiple human autoimmune diseases, including lupus (30–33). In this model, autoimmune disease is triggered 3 months earlier than vehicle-treated controls, as reflected in the lung by pro-inflammatory and interferon-regulated gene (IRG) upregulation, mononuclear cell infiltration, ectopic lymphoid structure (ELS) neogenesis, and autoantibody production. In the kidney, we see concurrent induction of glomerulonephritis (34, 35). Importantly, dietary supplementation with the ω-3 HUFA docosahexaenoic acid (DHA) ameliorates $cSiO_2$-triggered lupus flaring in female NZBWF1 mice (35–38), and this intervention is effective against the background of three unique diets (36–38).

The ω-3 HUFA score (39) and the Omega-3 Index (O3I) (40) are two interrelated red blood cell (RBC) biomarkers potentially applicable for associating tissue HUFA balance with disease outcomes in both preclinical and clinical studies. The ω-3 HUFA score reflects the total ω-3 HUFAs as a % of total HUFAs (ω-3, ω-6, and ω-9 HUFAs), while the O3I is the sum of DHA and EPA as a percent of total fatty acids. The goal of the present study was to test the hypothesis that the ω-3 HUFA score and the O3I inversely correlate with indicators of inflammation and autoimmune pathogenesis during $cSiO_2$-triggered lupus flaring in NZBWF1 mice. Data used to test this hypothesis were drawn from three unique DHA supplementation studies recently published by our laboratory (36–38) that employed both purified mouse diets, as well as more complex diets reflecting Western eating patterns. Our findings indicate that increases in both the O3I and the ω-3 HUFA score were strongly associated with suppression of autoimmune pathogenesis in this preclinical mouse model of toxicant-triggered lupus flaring. Importantly, these preclinical results identify the ω-3 HUFA score and O3I thresholds potentially required for successful intervention against lupus and other autoimmune diseases.

MATERIALS AND METHODS

Experimental Design

Data used for this study were collected from our previously published investigations based on three DHA feeding studies (35–38) (see **Supplementary Data**). Each study used female NZBWF1 mice obtained from Jackson Laboratories (Bar Harbor, ME). Female mice were used in these studies due to the sexual dimorphism observed in both human lupus and the NZBWF1 mouse model (21). Experimental protocols were designed and performed in accordance with National Institutes of Health

guidelines and approved by the Institutional Animal Care and Use Committee at Michigan State University (AUF#01/15-021-00; AUF# PROTO201800113). Upon arrival, mice were randomly assigned to experimental groups and housed four per cage with access to food and water provided *ad libitum*. Animal facilities were maintained at constant temperature (21–24°C) and humidity (40–55%) with a 12 h light/dark cycle. One animal in Study 3 was euthanized for health concerns unrelated to $cSiO_2$ exposure or lupus development (38).

Experimental diets contained specified amounts of DHA against unique dietary backgrounds as summarized in **Table 1**. Study 1 used a modified high fat American Institute of Nutrition-93G diet (HF-AIN-93G) containing 134 g fat/kg diet (30% kcal fat), formulated with corn oil (10 g/kg), soybean oil (64 g/kg), and high-oleic safflower oil (60 g/kg) (35, 36). High-oleic safflower oil was substituted with 10, 30, or 60 g/kg microalgal oil containing 40% (w/w) DHA (DHASCO, provided by Dr. Kevin Hadley, Martek Biosciences Corporation, Columbia, MD). The resulting experimental diets yielded 0.4, 1.2, or 2.4% (w/w) DHA, respectively. Analyses were only performed on animals fed diets containing 0, 0.4, and 1.2% (w/w) DHA because no additional protection was seen when comparing the 1.2% (w/w) DHA diet to the 2.4% (w/w) DHA diet. Furthermore, animals fed the 2.4% (w/w) DHA diet achieved an ω-3 HUFA score of ∼90%, which is much higher than those achieved in the other studies and beyond levels observed in humans (41). Study 2 employed the AIN-93G diet containing 70 g fat/kg diet (17% kcal fat), composed of corn oil (10 g/kg) and high-oleic safflower oil (60 g/kg) (37). High-oleic safflower oil was replaced with 10 or 25 g/kg DHASCO to yield experimental diets containing 0.4 and 1% (w/w) DHA, respectively. Study 3 utilized a modified total Western diet (MTWD) and a MTWD with 40% less saturated fats and ω-6 HUFAs (MTWD ↓SF.ω-6) (38). Both MTWDs contained 164 g fat/kg diet (34.5% kcal fat), composed of soybean oil, anhydrous milk fats, olive oil, lard, beef tallow, corn oil, cholesterol, and high-oleic safflower oil. Olive oil was replaced by 30 g/kg DHASCO to achieve 1.2% (w/w) DHA.

In each study, groups of female mice (n = 7–8/group) were initiated on experimental diets at age 6 wk and maintained on those same diets until experiment termination. To limit oxidation of dietary lipids, diets were prepared every 2 weeks, vacuum-sealed and stored at −20°C, and provided fresh every 1–2 days. Two weeks later (age 8 wk), mice were anesthetized with 4% isoflurane and intranasally instilled with 1 mg $cSiO_2$ (Min-U-Sil-5, 1.5–2.0 μm average particle size, U.S. Silica, Berkeley Springs, WV) in 25 μL PBS or PBS vehicle (VEH) every week for 4 weeks. The total amount of $cSiO_2$ provided over the course of the experiment (4 mg per mouse) was chosen to approximate half of a recommended human lifetime exposure as established by the Occupational Safety and Health Administration (34). Mice were euthanized by intraperitoneally injecting 56 mg/kg BW sodium pentobarbital 11–13 weeks after the final $cSiO_2$ exposure. Selected tissue analyses were conducted as described for Study 1 (36), Study 2 (35, 37), and Study 3 (38). These included fatty acid profiling (RBC, lung, kidney, spleen, liver), IRG expression (lung), pro-inflammatory cytokines (bronchioalveolar lavage fluid [BALF]), lymphocyte infiltration (lung), ELS development (lung), pulmonary and systemic autoantibody expression (BALF, plasma), and glomerulonephritis (kidney).

Fatty Acid Analyses

Experimental diets from Studies 1, 2, and 3, tissues from Studies 1 and 3, and RBCs from Study 1 were analyzed by GLC at Michigan State University as described previously using a GC2010 Gas Chromatograph (Shimadzu, Columbia, MD) equipped with a CP-Sil 88 WCOT (wall-coated open tubular) fused-silica column (100 m × 0.25 mm i.d. × 0.2-μm film thickness; Varian Inc., Lake Forest, CA) with hydrogen as carrier gas (36). A standard cocktail of fatty acids characteristic of erythrocytes was used to identify phospholipid fatty acids, which were quantified as a percentage of total identified fatty acids after response factor correction. Analysis of RBCs from Studies 2 and 3 was performed by OmegaQuant Analytics, LLC (Sioux Falls, SD), an independent CLIA-certified laboratory.

To verify fatty acid compositions, final diets were analyzed by gas liquid chromatography (GLC) as described above and presented in **Table 2**. The dietary fatty acid composition was used to calculate predicted RBC $\omega - 3$ HUFA scores. We used a modification of Lands' equation (41) as follows, where HC3 = 3.0, HC6 = 0.70, PC3 = 0.0555, PC6 = 0.0441, HI3 = 0.005, CO = 5.0, and Ks = 0.175.

$$\begin{aligned} &Predicted\ \omega - 3\ HUFA\ Score = \\ &100 - \left(\frac{100}{1 + (HC6/en\%H6)\,(1 + en\%H3/HC3)} + \right. \\ &\left. \frac{100}{1 + (PC6/en\%H6)\,(1 + en\%P3/PC3 + en\%H3/HI3 + \ en\%O/CO + en\%P6/KS)}\right) \end{aligned} \quad (1)$$

En%P6 was the en% of linoleic acid (C18:2n6), en%P3 was the en% of alpha-linolenic acid, en%H6 was the en% of arachidonic acid (C20:4n6), and en%H3 was the en% of EPA (C20:5n3), DPA (C22:5n6), and DHA (C22:6n3). En%O (other fatty acids) was calculated for each diet by subtracting en%P6, P3, H6, and H3 from the total en% of fat in the diet. In diet formulations with no measurable arachidonic acid, EPA, DPA, or DHA, the values for en%H6 or H3 were replaced with 0.001, a value much smaller than the estimated en%H6 or H3 in the Western diet.

Determination of the RBC ω-3 HUFA Score and the O3I

The ω-3 HUFA score and O3I were determined for RBCs and all available tissues of each animal. The ω-3 HUFA score is the sum of EPA (C20:5n3), DPA (C22:5n3), and DHA (C22:6n3) as a percentage of the most abundant HUFAs (C20:5n3,

TABLE 1 | Composition of experimental diets.

Basal diet	**Experimental diets**									
	Study 1[36]			**Study 2[37]**			**Study 3[38]**			
	HF AIN-93G			**AIN-93G**			**MTWD**		**MTWD ↓SF.ω-6**	
DHA (en%)	**0%**	**0.96%**	**2.40%**	**0%**	**0.87%**	**2.62%**	**0%**	**2.63%**	**0%**	**2.63%**
DHA (%w/w)	**0%**	**0.40%**	**1.20%**	**0%**	**0.40%**	**1%**	**0%**	**1%**	**0%**	**1%**
Macronutrient	***(g/Kg)***									
Carbohydrates										
Corn starch	366	366	366	398	398	398	230	230	230	230
Maltodextrin (Dyetrose)	121	121	121	132	132	132	70	70	70	70
Sucrose	92	92	92	100	100	100	257	257	257	257
Cellulose	46	46	46	50	50	50	30	30	30	30
kcal (% of total)	53.3	53.3	53.3	63.2	63.2	63.2	49.4	49.4	49.4	49.4
Proteins										
Casein	184	185	184	200	200	200	190	190	190	190
L-cysteine	3	3	3	3	3	3	3	3	3	3
kcal (% of total)	16.7	16.7	16.7	19.7	19.7	19.7	16.1	16.1	16.1	16.1
Fats										
Soybean oil	64	64	64	-	-	-	29	29	6	6
Anhydrous milkfat	-	-	-	-	-	-	36	36	7	7
Olive oil[a,b]	-	-	-	-	-	-	30	0	138	108
Lard	-	-	-	-	-	-	28	28	6	6
Beef tallow	-	-	-	-	-	-	25	25	5	5
Corn oil[a,c]	10	10	10	10	10	10	16	16	3	3
Cholesterol	-	-	-	-	-	-	0.4	0.4	0.5	0.5
High-oleic safflower oil[a,d]	60	50	30	60	50	35	-	-	-	-
DHA-enriched algal oil[a,e]	0	10	30	0	10	25	0	30	0	30
kcal (% of total)	30.0	30.0	30.0	17.1	17.1	17.1	34.5	34.5	34.5	34.5
Other										
AIN93G mineral mix	32	32	32	35	35	35	41	41	41	41
AIN93G vitamin mix	19	19	19	10	10	10	12	12	12	12
Choline bitartrate	2	2	2	3	3	3	3	3	3	3
TBHQ antioxidant	0.01	0.01	0.01	0.01	0.01	0.01	0.03	0.03	0.03	0.03

[a] *Based on oil composition reported by manufacturer.*
[b] *Olive oil contained 678 g/kg oleic acid and 84 g/kg linoleic acid, as reported by the USDA, FDC ID 748648.*
[c] *Corn oil contained 612 g/kg linoleic acid and 26 g/kg oleic acid.*
[d] *High-oleic safflower oil contained 750 g/kg oleic acid and 140 g/kg linoleic acid.*
[e] *Algal oil contained 395 g/kg DHA and 215 g/kg oleic acid, as reported by manufacturer.*

C22:5n3, C22:6n3, C20:3n6, C20:4n6, C22:4n6, C22:5n6, C20:3n9) (39).

$$\omega - 3\ HUFA\ Score = \frac{100\% * (20:5n3\ +\ 22:5n3\ +\ 22:6n3)}{Total\ HUFA} \quad (2)$$

The O3I was calculated by taking the sum of EPA and DHA as a percent of total fatty acids (40). In tissues, this value is referred to as EPA + DHA.

$$Omega - 3\ Index\ (O3I) = \frac{100\% * (20:5n3\ +\ 22:6n3)}{Total\ FA} \quad (3)$$

Data Analysis and Statistics

All correlations to inflammatory endpoints used ω-3 HUFA scores and O3Is measured in RBCs. Data were analyzed using Graph Pad Prism 8.0.0 (GraphPad Software, San Diego, CA, www.graphpad.com). Inflammatory endpoints that were undetectable were replaced with half of the minimum value for the individual endpoint. The robust regression and outlier removal (ROUT) method was used to identified outliers, which were excluded from further analysis ($Q = 0.5\%$). For all endpoints, <10% of data points were identified as outliers. Where appropriate, non-normal data were $\log_{10}$ transformed and analyzed using linear regression. To account for experimental and methodological differences, all log transformed

TABLE 2 | Fatty acid profiles of experimental diets as determined by gas-liquid chromatography.

	Basal diet	**Experimental diets**								
		Study 1[36]			**Study 2[37]**			**Study 3[38]**		
		HF AIN-93G			**AIN-93G**			**MTWD**	**MTWD ↓SF.ω-6**	
	DHA (en%)	**0%**	**0.96%**	**2.40%**	**0%**	**0.87%**	**2.62%**	**0%**	**2.63%**	**0%**	**2.63%**
	DHA (%w/w)	**0%**	**0.40%**	**1.20%**	**0%**	**0.40%**	**1%**	**0%**	**1%**	**0%**	**1%**
Common name	**Chemical formula**	***(% of total fatty acids)***									
Lauric	C12:0	0.07 ± 0.00	0.30 ± 0.06	0.75 ± 0.03	0.04 ± 0.00	0.62 ± 0.00	1.42 ± 0.07	0.65 ± 0.01	1.49 ± 0.03	0.14 ± 0.01	0.83 ± 0.01
Myristic	C14:0	0.18 ± 0.01	0.97 ± 0.21	2.57 ± 0.11	0.16 ± 0.01	1.79 ± 0.02	4.15 ± 0.21	2.87 ± 0.06	5.54 ± 0.05	0.53 ± 0.01	2.51 ± 0.02
Pentadecanoic	C15:0	0.03 ± 0.00	0.03 ± 0.00	0.03 ± 0.00	0.03 ± 0.00	0.02 ± 0.00	0.03 ± 0.00	0.29 ± 0.00	0.30 ± 0.00	0.07 ± 0.00	0.06 ± 0.00
Palmitic	C16:0	8.31 ± 0.12	8.94 ± 0.33	10.05 ± 0.11	5.64 ± 0.04	6.82 ± 0.02	7.79 ± 0.02	22.24 ± 0.16	22.24 ± 0.05	10.87 ± 0.06	11.00 ± 0.01
Palmitoleic	C16:1ω7	0.09 ± 0.00	0.18 ± 0.02	0.34 ± 0.01	0.08 ± 0.00	0.41 ± 0.00	0.86 ± 0.03	0.13 ± 0.01	0.10 ± 0.00	0.13 ± 0.01	0.12 ± 0.01
Strearic	C18:0	2.61 ± 0.04	2.58 ± 0.07	2.47 ± 0.03	0.03 ± 0.00	0.04 ± 0.00	0.04 ± 0.00	8.49± 0.04	8.26 ± 0.03	3.61 ± 0.03	3.37 ± 0.01
Oleic	C18:1ω9	46.36 ± 0.87	42.55 ± 2.21	35.56 ± 1.05	71.08 ± 0.13	62.40 ± 0.08	53.26 ± 0.50	39.19 ± 0.38	29.00 ± 0.08	72.63 ± 0.08	64.41 ± 0.03
Linoleic	C18:2ω6	36.55 ± 0.70	36.09 ± 1.14	34.51 ± 0.70	19.17 ± 0.10	18.94 ± 0.01	15.08 ± 0.79	21.07 ± 0.21	20.62 ± 0.18	8.57 ± 0.04	7.82 ± 0.04
Arachidic	C20:0	0.32 ± 0.01	0.31 ± 0.01	0.28 ± 0.00	0.31 ± 0.00	0.28 ± 0.00	0.24 ± 0.00	0.21 ± 0.03	0.17 ± 0.01	0.29 ± 0.00	0.28 ± 0.01
Alpha-linolenic	C18:3ω3	3.15 ± 0.08	3.25 ± 0.08	3.26 ± 0.09	0.36 ± 0.01	0.37 ± 0.00	0.32 ± 0.01	1.90 ± 0.03	1.81 ± 0.04	0.93 ± 0.01	0.87 ± 0.02
Behenic	C22:0	0.28 ± 0.01	0.28 ± 0.01	0.28 ± 0.01	0.22 ± 0.00	0.21 ± 0.00	0.20 ± 0.00	0.10 ± 0.01	0.11 ± 0.01	0.10 ± 0.01	0.11 ± 0.00
Lignoceric	C24:0	0.13 ± 0.01	0.12 ± 0.01	0.12 ± 0.00	0.14 ± 0.00	0.13 ± 0.00	0.12 ± 0.00	0.04 ± 0.01	0.05 ± 0.01	0.03 ± 0.00	0.05 ± 0.00
Eicosapentaenoic	C20:5ω3	0.00 ± 0.00	0.00 ± 0.00	0.01 ± 0.00	0.00 ± 0.00	0.09 ± 0.00	0.20 ± 0.01	0.00 ± 0.00	0.13 ± 0.00	0.00 ± 0.00	0.10 ± 0.01
Docosahexaenoic	C22:6ω3	0.00 ± 0.00	2.47 ± 0.74	7.74 ± 0.43	0.00 ± 0.00	5.40 ± 0.05	14.20 ± 0.65	0.00 ± 0.00	7.09 ± 0.20	0.00 ± 0.00	6.34 ± 0.08
Total saturated fat		12.1 ± 0.2	13.7 ± 0.7	16.8 ± 0.2	8.3 ± 0.1	11.5 ± 0.1	15.4 ± 0.1	35.28 ± 0.21	38.84 ± 0.05	15.80 ± 0.08	18.39 ± 0.02
Total MUFA		47.8 ± 0.9	44.0 ± 2.2	37.1 ± 1.1	71.9 ± 0.1	63.5 ± 0.1	54.7 ± 0.5	41.74 ± 0.36	31.49 ± 0.10	74.70 ± 0.10	66.49 ± 0.01
Total ω-6 PUFA		36.7 ± 0.7	36.1 ± 1.14	34.6 ± 0.7	19.2 ± 0.1	18.9 ± 0.1	15.1 ± 0.8	21.07 ± 0.21	20.62 ± 0.18	8.57 ± 0.04	7.82 ± 0.04
Total ω-3 PUFA		3.2 ± 0.1	5.8 ± 0.9	11.1 ± 0.4	0.4 ± 0.00	5.9 ± 0.1	14.7 ± 0.1	1.90 ± 0.03	9.04 ± 0.19	0.93 ± 0.01	7.31 ± 0.05
ω-6:ω-3 ratio		11.6 ± 0.3	6.4 ± 0.9	3.12 ± 0.13	52.8 ± 1.3	3.2 ± 0.0	1.0 ± 0.1	11.07 ± 0.10	2.28 ± 0.07	9.24 ± 0.13	1.12 ± 0.01

MUFA, monounsaturated fatty acid; PUFA, polyunsaturated fatty acid.

inflammatory/autoimmune endpoints were standardized prior to performing correlations across multiple experiments. When the best-fit values of the slope and y-intercept were not significantly different between experiments, raw data from each experiment were combined and re-analyzed to obtain a single linear regression model. Correlation analyses were performed on raw data using Spearman's Correlation due to non-normality of the data (per Shapiro-Wilk Test, $p < 0.05$). For correlations to autoantibody classes and subtypes, autoantibody groups were determined based on location and function of cognate autoantigens. Within a given group, signal intensities for individual autoantibodies were normalized and summed to obtain a group score for each animal, as described previously (42). The score was used to perform correlation analyses against the RBC ω-3 HUFA score. In analyses comparing diet groups, data are presented as mean ± SEM with $n = 7–8$ mice per group. To compare the O3I and ω-3 HUFA scores of animals positive or negative for nephritis, the non-parametric Mann-Whitney Rank Sum test was used. A $p < 0.05$ was considered statistically different for all study outcomes.

RESULTS

DHA Supplementation Dose-Dependently Increases ω-3 HUFA Score Uniformly Across RBC and Tissues

The effects of substituting various amounts of DHA-rich microalgal oil for high oleic acid safflower oil (HF AIN-93G, Study 1; AIN-93G, Study 2) or olive oil in (MTWD and MTWD ↓SF.ω6, Study 3) on resultant tissue and RBC ω-3 HUFA scores were compared. Regardless of diet, increasing the DHA content up to 2.6 en% (human equivalent dose of ~5 g/day) dose-dependently increased RBC ω-3 HUFA scores (**Figure 1A**). These increases closely correlated ($R^2 = 0.93–0.99$, $p < 0.05$) with predicted ω-3 HUFA scores calculated from diet composition using Lands' equation (**Figure 1B**). ω-3 HUFA scores were relatively consistent across all tissues, both for basal and DHA-supplemented diets (**Figures 2A,C**). DHA-dependent increases in RBC ω-3 HUFA score closely correlated ($p < 0.001$) with those in lung ($r_s = 0.87$), spleen ($r_s = 0.84$), and kidney ($r_s = 0.72$) for Study 1 (**Figures 2A,B**), and in lung ($r_s = 0.90$), spleen ($r_s = 0.89$), liver ($r_s = 0.86$), and kidney ($r_s = 0.95$) for Study 3 (**Figures 2C,D**). Using the O3I as a measure of fatty acid content resulted in lower and more varied correlations ($r_s = 0.27–0.88$, **Figures S2B,D**).

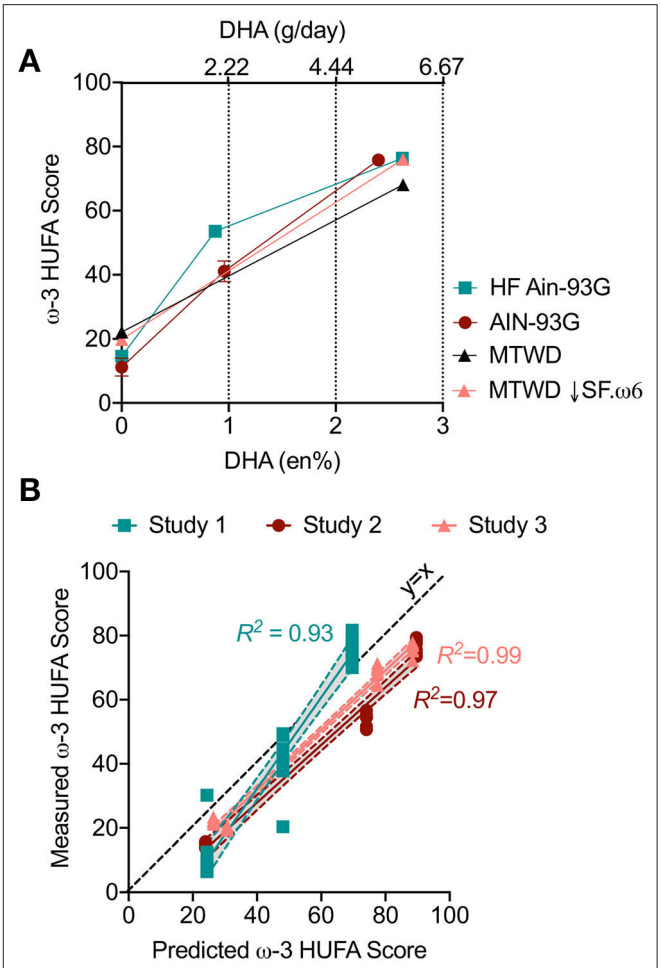

FIGURE 1 | RBC ω-3 High unsaturated fatty acid (HUFA) score increases with DHA intake in NZBWF1 mice and can be predicted based on diet composition in $cSiO_2$-treated NZBWF1 mice. Animals were fed different diets for Studies 1 (HF AIN-93G), 2 (AIN-93G), and 3 (MTWD and MTWD ↓SF.ω6) with or without DHA (see **Table 1**) as indicated by individually colored lines and symbols. At experiment termination, red blood cells (RBCs) were analyzed for fatty acids by GLC. **(A)** Increasing en% of DHA in the diet elevated omega-3 HUFA score similarly across all experimental diets. Data presented as mean ± SEM. **(B)** The ω-3 HUFA score is predictable based on the en% of major ω-3 and ω-6 fatty acids using Lands' equation. Individual animals represented by individual data points. For all regression analyses, R^2 is reported next to the corresponding line and $p < 0.001$ Shaded bands around regression lines represent 95% confidence intervals.

Elevated RBC ω-3 HUFA Scores Negatively Correlate With Interferon Regulated Gene (IRG) Expression in the Lung

Elevated IRG expression is highly associated with flaring and increased disease severity in lupus (43). It was demonstrated in Studies 2 and 3 that IRG expression is upregulated in $cSiO_2$-exposed NZBWF1 mice and that this is suppressed by DHA supplementation (35, 38). Here, an IFN score was generated by combining the autoscaled expression of 12 IRGs measured in animals fed AIN-93G, MTWD, and MTWD ↓SF.ω6 (38). Resultant IFN scores negatively correlated with ω-3 HUFA scores ($R^2 = 0.29$, $p < 0.0001$, **Figure 3A**). This negative correlation is illustrated for representative IRGs including *Isg15* ($R^2 = 0.32$, $p < 0.0001$, **Figure 3B**), *Psmb8* ($R^2 = 0.32$, $p < 0.0001$, **Figure 3C**), *Irf7* ($R^2 = 0.26$, $p < 0.0001$, **Figure 3D**), and *Oasl1* ($R^2 = 0.30$, $p < 0.0001$, **Figure 3E**). Overall, the autoscaled plots indicate that ω-3 HUFA scores above 40% were associated with reduced IRG scores and individual gene expression (**Figure 3**).

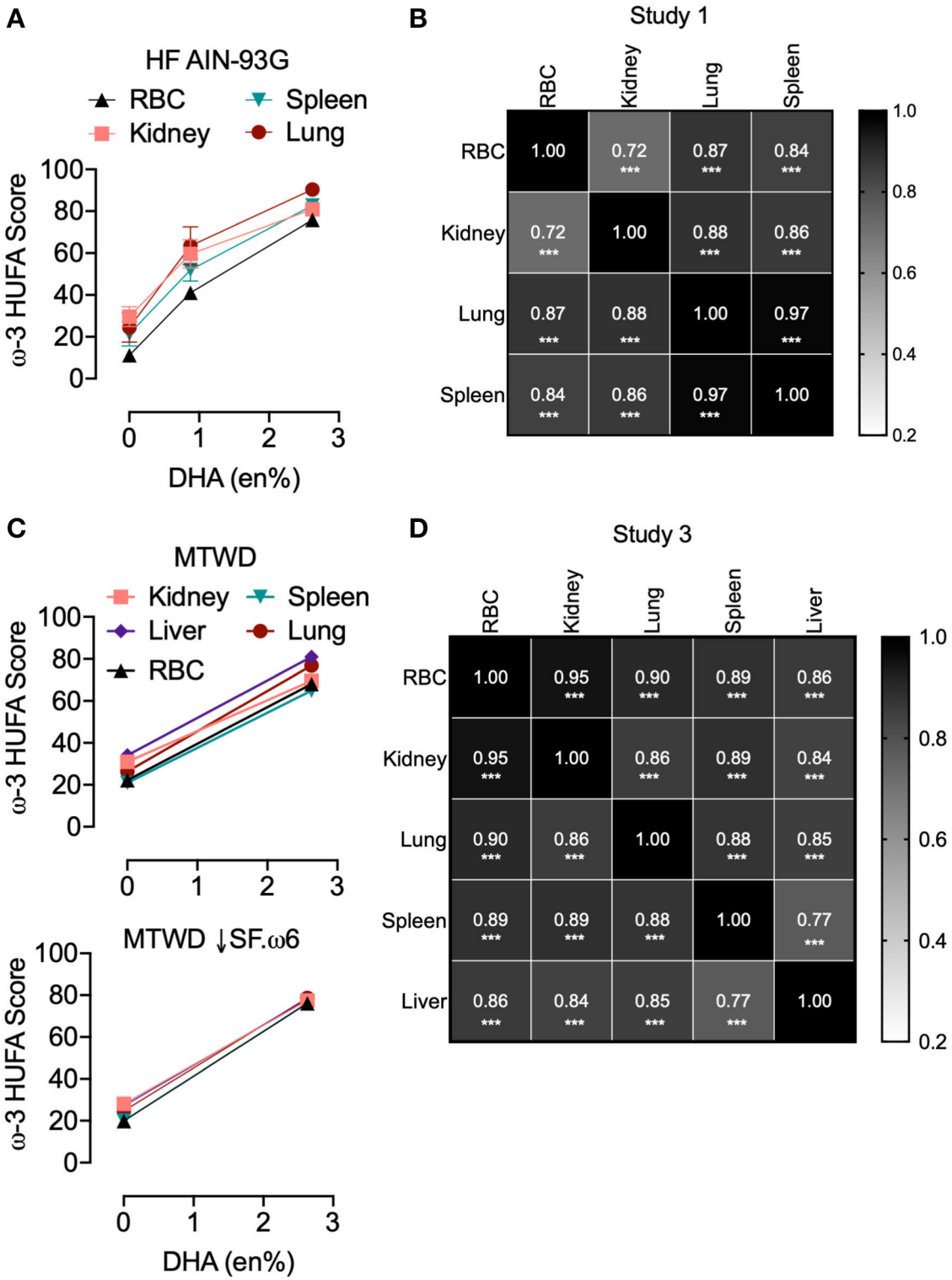

FIGURE 2 | ω-3 HUFA scores are consistent across multiple tissues in $cSiO_2$-treated NZBWF1 mice. Mouse tissues from **(A,B)** Study 1 (HF AIN-93G diet) and **(C,D)** Study 3 (MTWD and MTWD ↓SF.ω6 diets) were analyzed separately to assess the impact of DHA in tissue fatty acid incorporation. Study 2 is not included because only RBCs were analyzed in this study. **(A,C)** ω-3 HUFA scores increased similarly across tissues with DHA supplementation. Data presented as mean ± SEM. **(B,D)** Pearson's correlation was used to assess correlations between the ω-3 HUFA score across different tissues (***$p < 0.001$).

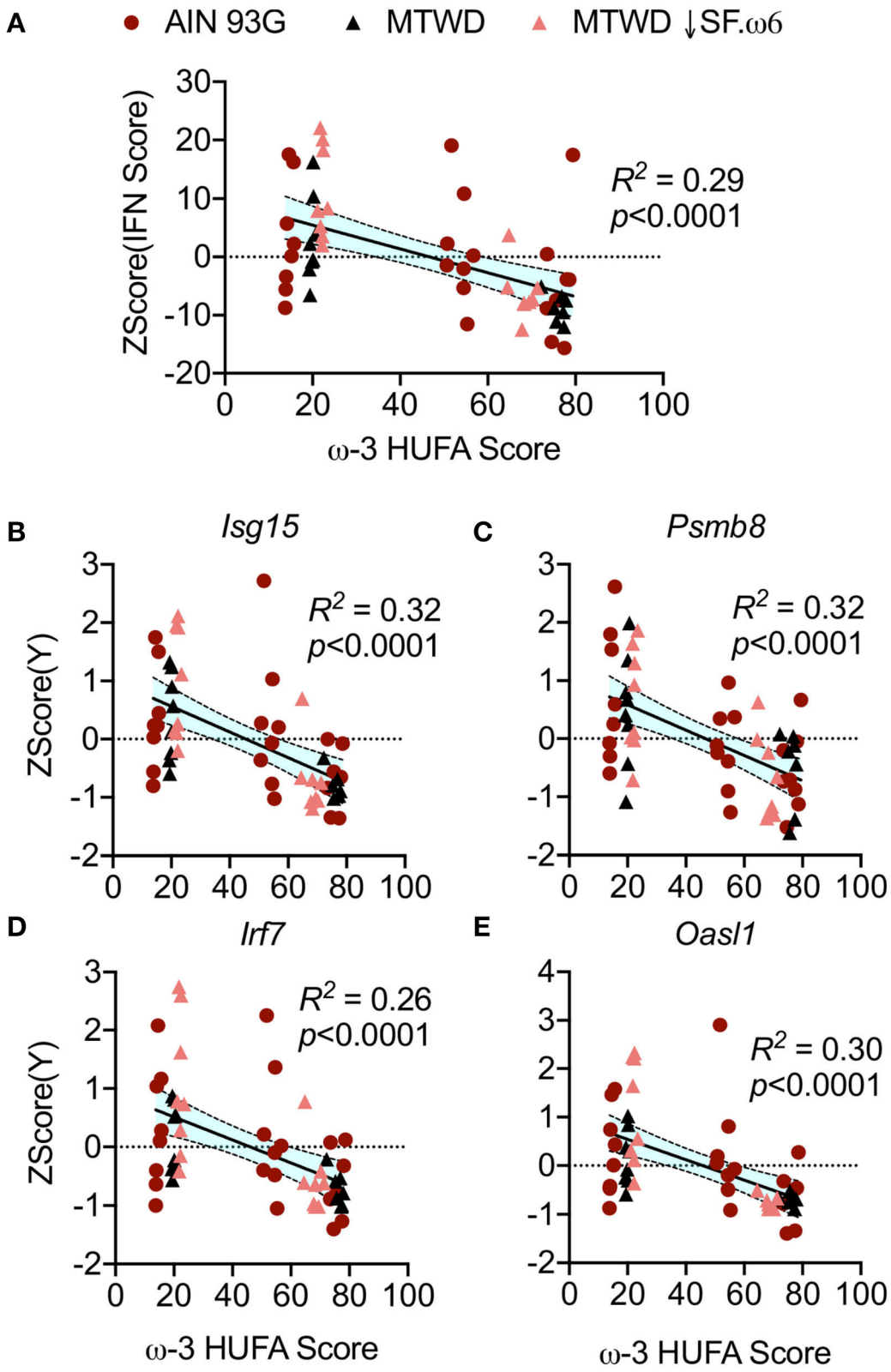

FIGURE 3 | RBC ω-3 HUFA score negatively correlates with IFN regulated gene expression in $cSiO_2$-triggered NZBWF1 mice. **(A)** An IFN score was calculated to include 12 IFN-related genes significantly induced by $cSiO_2$ exposure (*Ccl7, Zbp1, Ifi44, Ifit1, Irf7, Isg15, Mx1, Oas2, Oasl1, IPsmb8, Rsad2, Siglec1*). These genes

(Continued)

FIGURE 3 | were presented as fold-change relative to vehicle-instilled animals. Missing values and outliers were handled as described in the Methods section. Expression was standardized by autoscaling (subtracting the mean expression of the gene and dividing by the standard deviation of the expression of the gene). Then, standardized scores of all genes for an individual sample were summed to achieve the IFN score **(B–E)**. Representative genes used in the calculation of the IFN score including **(B)** *Isg15*, **(C)** *Psmb8*, **(D)** *Irf7*, and **(E)** *Oasl1* reflect the trend observed in the combined IFN score. All values were plotted against the ω-3 HUFA score and the resulting data analyzed by simple linear regression. Regression coefficients were considered statistically significant at $p < 0.05$. Shaded bands around regression lines represent 95% confidence intervals.

Higher RBC ω-3 HUFA Scores Correspond to Reduced Pro-inflammatory Cytokines and Leukocyte Infiltration in BALF

Intranasal instillation of $cSiO_2$ elicits local sterile inflammation in the lungs of NZBWF1 mice that is associated with elevated proinflammatory cytokines, chemokines, and mononuclear cell influx, all of which can be suppressed by DHA supplementation (36–38). Here it was found that IL-6 ($R^2 = 0.26$, $p = 0.0001$, **Figure 4A**), MCP-1 ($R^2 = 0.29$, $p < 0.0001$, **Figure 4B**), and TNFα ($R^2 = 0.39$, $p < 0.0001$, **Figure 4C**) concentrations in the BALF were negatively correlated with the ω-3 HUFA score. Consistent with these findings, numbers of macrophages ($R^2 = 0.40$, $p < 0.0001$, **Figure 5A**), lymphocytes ($R^2 = 0.35$, $p < 0.0001$, **Figure 5B**), and neutrophils ($R^2 = 0.12$, $p = 0.0029$, **Figure 5C**) in BALF also negatively correlated with the ω-3 HUFA score in all three studies. Though some R^2 values are relatively low, there is a consistent negative linear relationship with all endpoints assessed. Consonant with IRG expression, reductions in these inflammatory responses was most apparent when ω-3 HUFA scores exceeded 40% (**Figures 4**, **5**).

Increased RBC ω-3 HUFA Scores Are Associated With Reduced Ectopic Lymphoid Structure (ELS) Neogenesis and Autoantibody Production

Central to $cSiO_2$-triggered autoimmunity in NZBWF1 mice is the appearance of ELS in the lung composed of germinal center-like organization of B- and T-cells (36). These structures promote the development of autoreactive plasma cells and the production of autoantibodies. Notably, their formation is suppressed by DHA supplementation (36–38). Consistent with those observations, very strong, negative linear correlations were observed between the ω-3 HUFA score and $CD3^+$ ($R^2 = 0.45$, $p < 0.0001$) and $CD45R^+$ ($R^2 = 0.62$, $p < 0.0001$) lung tissue in Studies 1, 2, and 3 (**Figures 6A,B**). Similar correlations were observed for anti-dsDNA in BALF ($R^2 = 0.35$, $p < 0.0001$) and plasma ($R^2 = 0.24$, $p < 0.0001$) as measured by ELISA (**Figures 6C,D**). Again, ω-3 HUFA scores over 40% were associated with reduced ELS development and anti-dsDNA production (**Figure 6**). A further feature of Study 2 was the use of high throughput autoantigen microarray for in-depth analysis of autoantibodies relative to specificity and isotype (44). Robust negative correlations were found between ω-3 HUFA score and IgG and IgM autoantibodies in both BALF and plasma with specificity for a broad range of host antigens (most r_s values between −0.4 and −0.6, significance indicated by asterisks) (**Figure 7**).

Higher RBC ω-3 HUFA Scores Were Associated With Delayed Disease Progression

Early glomerulonephritis onset and production of autoantibodies is a critical outcome of $cSiO_2$-triggered systemic autoimmunity that was prevented by dietary DHA supplementation in Studies 1, 2, and 3 (36–38). We defined lupus disease progression in animals as the presence of renal lesions combined with elevated plasma anti-dsDNA IgG in $cSiO_2$-treated animals compared to the mean of the vehicle-treated group ($p < 0.05$). This is reflective of the SLICC criteria published in 2013, which stated that combination of biopsy confirmed nephritis in the presence of either ANA or anti-dsDNA antibodies is sufficient for classification of SLE in humans (45). Mice negative for both renal lesions and plasma anti-dsDNA IgG had significantly higher ω-3 HUFA scores (median of 69.18, 95% CI 54.46–74.59) compared to animals positive for both endpoints (median of 21.43, 95% CI 19.44–30.21) (**Figure 6E**). Consistent with the above findings for inflammation and autoimmunity indicators, ω-3 HUFA scores below ∼40% were associated with disease progression.

Higher O3I Were Associated With Reduced Autoimmune Pathogenesis

O3Is for Study 1 increased with en% DHA in the diet to a much lesser extent than those for Studies 2 and 3 (**Figure S1**). When assessing DHA's effects on the O3I in tissues, responses followed the rank order of kidney > lung > spleen > RBC for Study 1, whereas for Study 3 the rank order was RBC > kidney > lung > spleen > liver (**Figures S2A,C**). Previous reports of the RBC O3I for animals fed similar diets were much more similar to those observed in studies 2 and 3 (in the range of 6–14%) (46). Together these observations suggest that there were methodological issues with the fatty acid analysis in Study 1, possibly due to fatty acid decomposition. Therefore, correlation analyses between O3Is and inflammation and autoimmunity indicators were performed only for Studies 2 and 3.

O3Is significantly correlated with decreased IFN scores (**Figure 8A**) and with downregulated expression of the representative IRGs *Isg15* ($R^2 = 0.28$, $p < 0.0001$, **Figure 8B**), *Psmb8* ($R^2 = 0.32$, $p < 0.0001$, **Figure 8C**), *Irf7* ($R^2 = 0.25$, $p = 0.0001$, **Figure 8D**), and *Oasl1* ($R^2 = 0.30$, $p < 0.0001$, **Figure 8E**). Furthermore, high O3Is were strongly associated with suppression of $cSiO_2$-triggered increases in numbers of macrophages ($R^2 = 0.33$, $p < 0.0001$, **Figure 9A**) and lymphocytes ($R^2 = 0.40$, $p < 0.0001$, **Figure 9B**) in BALF, as well as decreased ELS neogenesis in the lung as reflected by B-cell ($R^2 = 0.52$, $p < 0.0001$, **Figure 9C**) and T-cell ($R^2 = 0.45$, $p < 0.0001$, **Figure 9D**) accumulation. Importantly, autoscaled

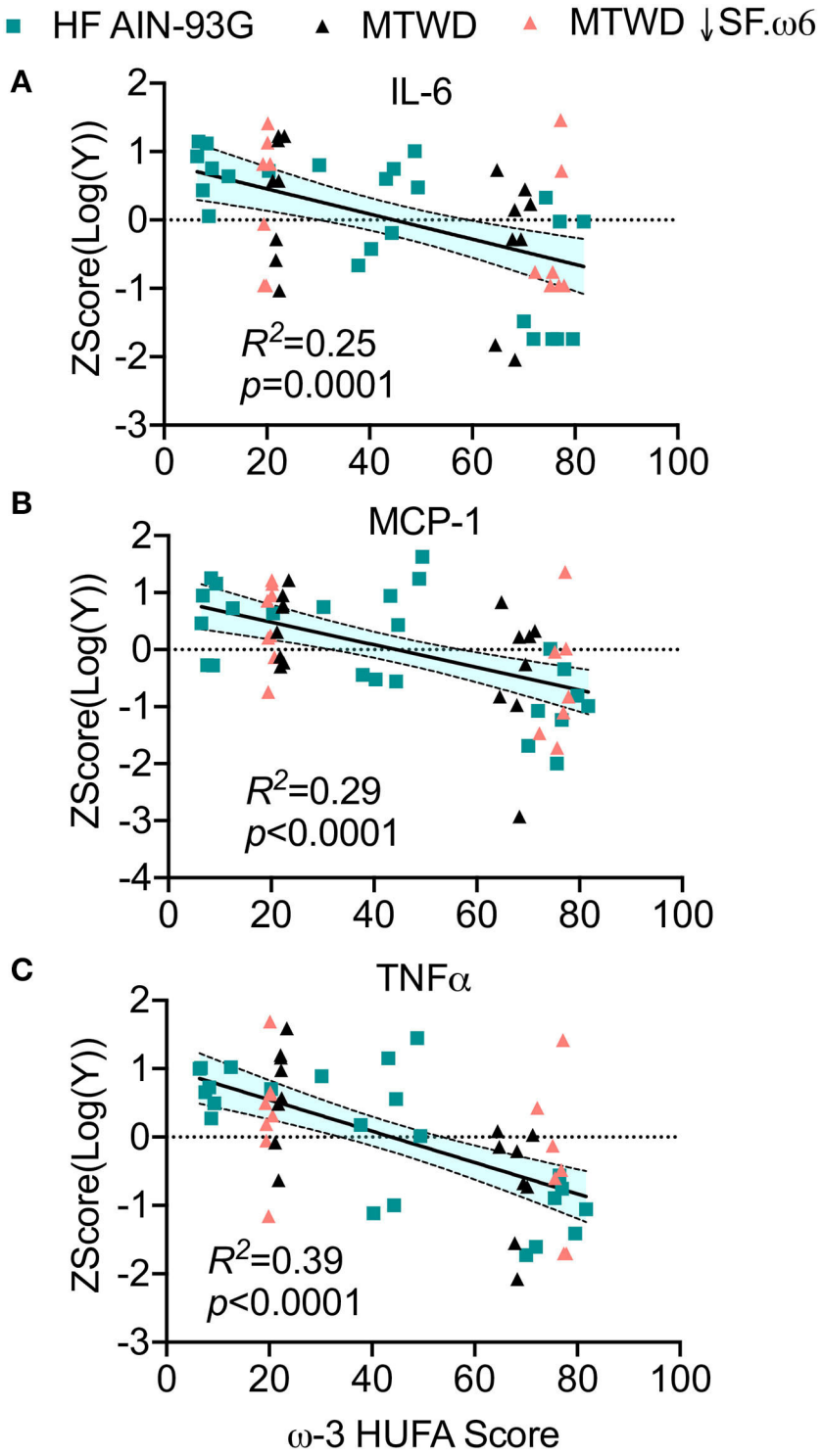

FIGURE 4 | Increasing RBC ω-3 HUFA score corresponds to reduced inflammatory cytokines in the lung alveolar fluid of $cSiO_2$-triggered NZBWF1 mice. Bronchoalveolar fluid (BALF) was analyzed for the proinflammatory cytokines **(A)** IL-6, **(B)** MCP-1, and **(C)** TNFα by ELISA in Study 1 and by a multiplexed bead based assay in Study 3. To compare across experiments, data was linearized by $\log_{10}$ transformation and standardized by autoscaling. The normalized and standardized data were plotted against the ω-3 HUFA score for each animal. When each diet was assessed individually, the resultant linear models were not found to be significantly different from one another, indicating that the data sets could be combined and analyzed simultaneously. The combined data were analyzed by a simple linear regression and goodness of fit presented as R^2. Regression coefficients were considered statistically significant at $p < 0.05$. Shaded bands around regression lines represent 95% confidence intervals.

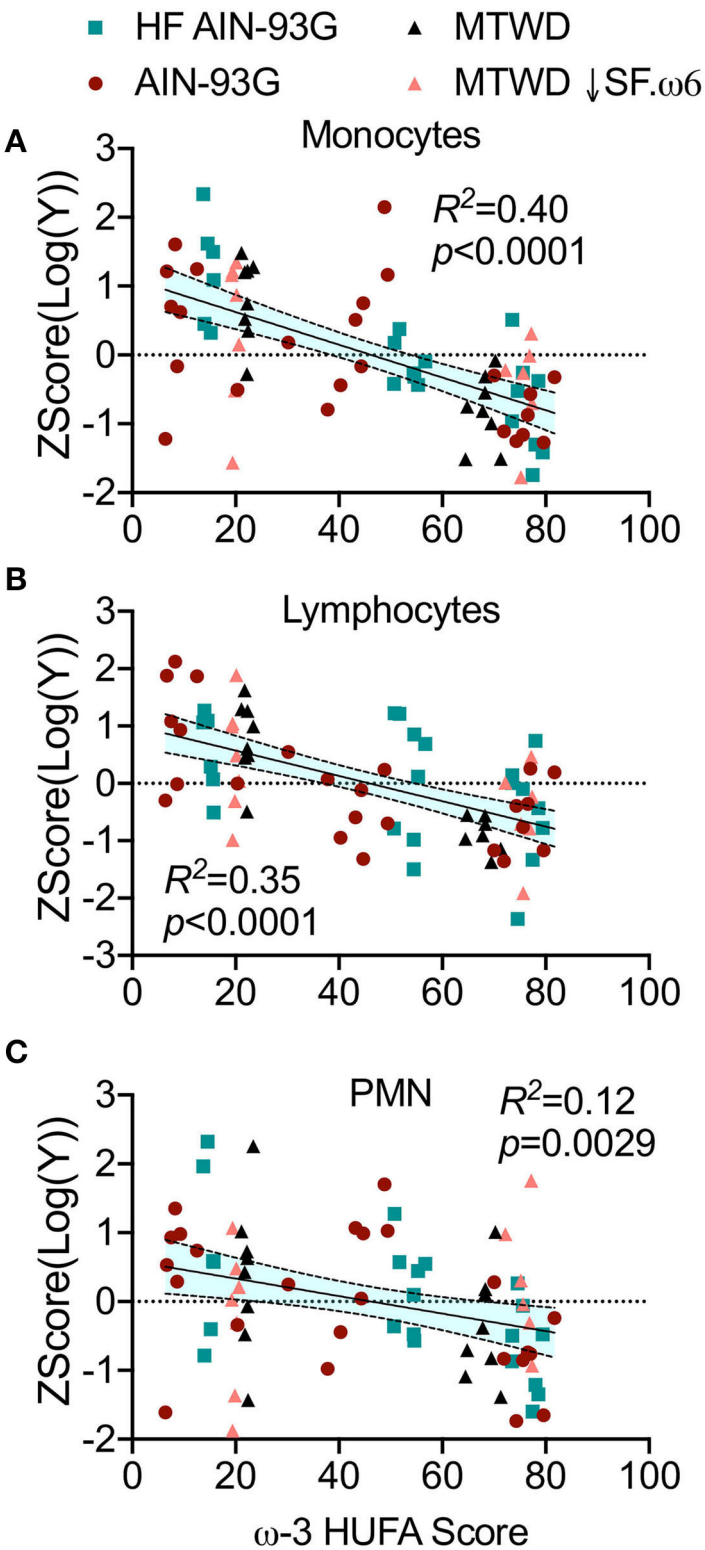

FIGURE 5 | Elevated RBC ω-3 HUFA scores are associated with reduced mononuclear cell infiltration into lung alveolar fluid of $cSiO_2$-triggered NZBWF1 mice. BALF was assessed for **(A)** macrophages, **(B)** lymphocytes, and **(C)** neutrophils by differential cell counts, as determined by morphological assessment of 200 total cells on cytological slides. Counts between diet groups were normalized by log transformation and standardized by autoscaling. The normalized and standardized data was plotted against the ω-3 HUFA score for each animal. The data was analyzed by a simple linear regression and goodness of fit presented as R^2. Regression coefficients were considered statistically significant at $p < 0.05$. Shaded bands around regression lines represent 95% confidence intervals.

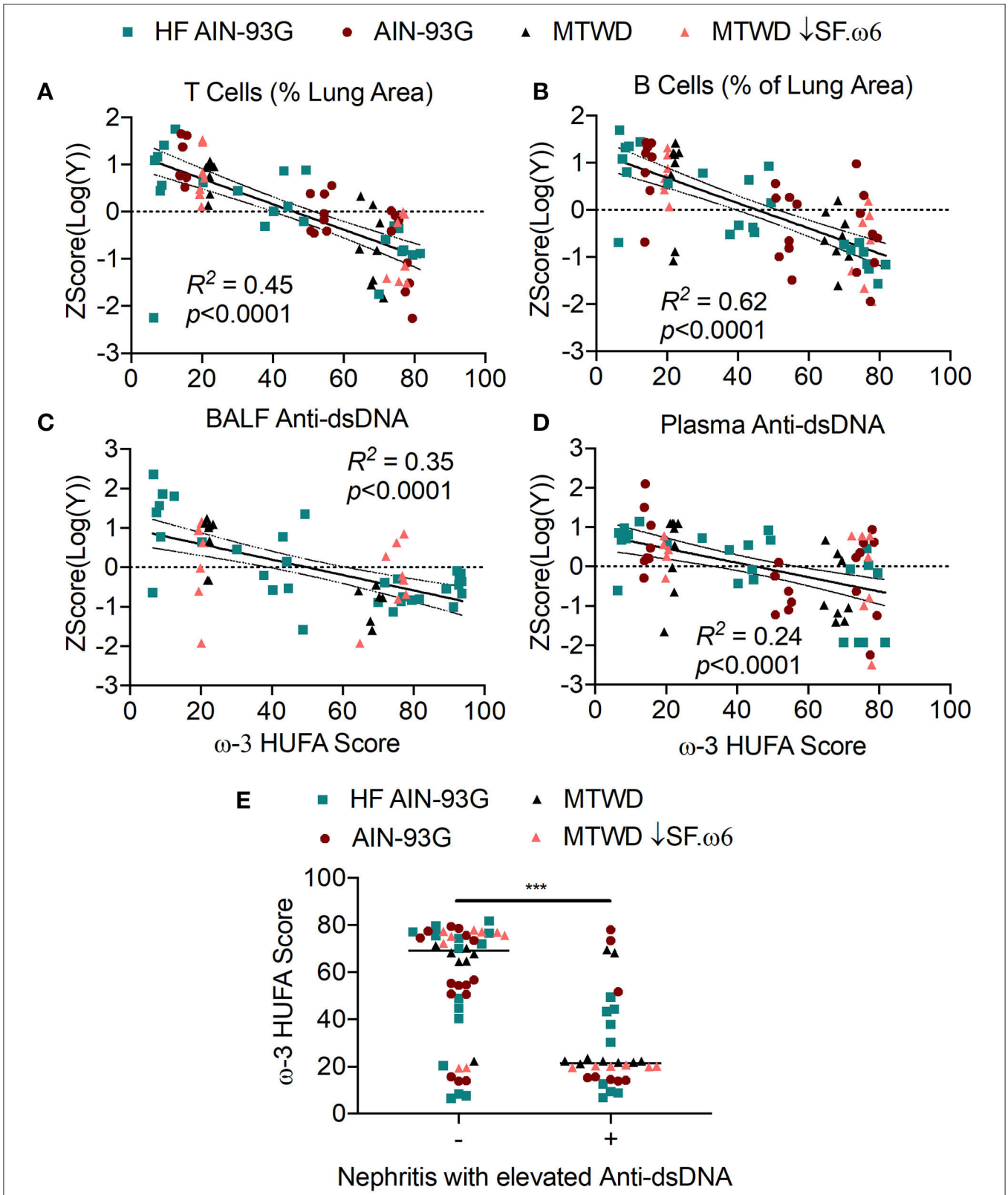

FIGURE 6 | High RBC ω-3 HUFA scores correspond with suppression of ectopic lymphoid structure (ELS) neogenesis, anti-dsDNA response, and disease progression in $cSiO_2$-triggered NZBWF1 mice. **(A,B)** ELS neogenesis was assessed by measuring the volume density of **(A)** T cells ($CD3^+$) and **(B)** B cells ($CD45R^+$),

(Continued)

FIGURE 6 | respectively, in the bronchial and perivascular regions of the lung. Anti-dsDNA was measured in **(C)** BALF and **(D)** plasma by ELISA. Percent area covered by T or B cells and anti-dsDNA levels and were $\log_{10}$ transformed to normalize followed by autoscaling to standardize across experiments. These values were plotted against the ω-3 HUFA score and the resulting data analyzed by simple linear regression. Goodness of fit of the linear regression was presented as R^2. Regression coefficients were considered statistically significant at $p < 0.05$. Shaded bands around regression lines represent 95% confidence intervals. **(E)** Mice positive for renal lesions and elevated plasma anti-dsDNA IgG (significantly different from mean of the Veh-treated group, $p < 0.05$) had significantly lower median ω-3 HUFA scores than mice in the the group negative for these endpoints, as assessed by the non-parametric Mann-Whitney *U*-test (***$p < 0.001$). Quantification of renal histopathology score was based on the following scoring criteria: No proteinosis, normal glomeruli (0); multifocal segmental proliferative glomerulonephritis (1); multifocal segmental proliferative glomerulonephritis and occasional glomerular sclerosis and crescent formation (2); diffuse global segmental proliferative glomerulonephritis (3). Animals receiving any score ≥1 were categorized as positive for renal lesions.

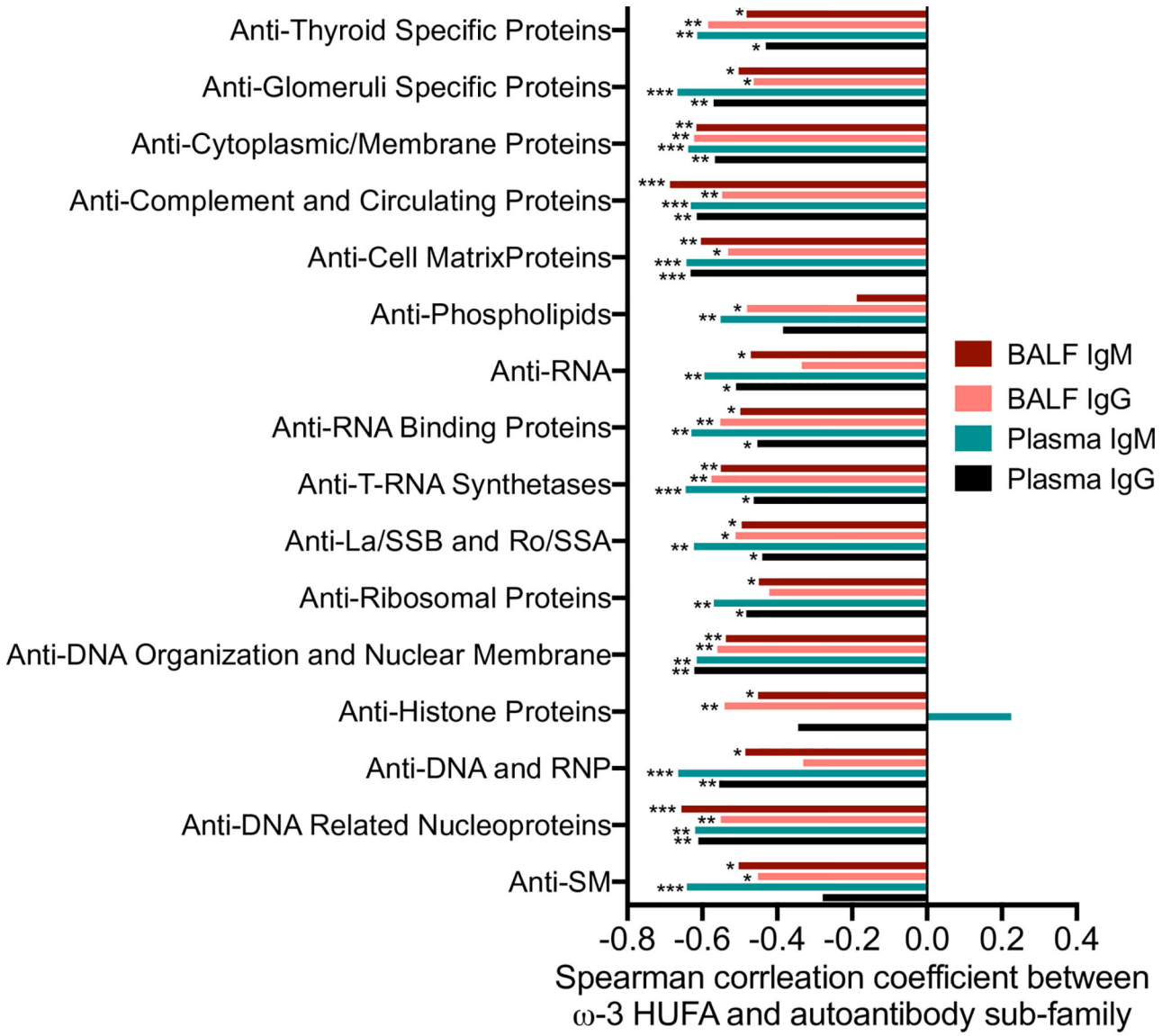

FIGURE 7 | Increased RBC ω-3 HUFA scores correlate with reductions in a broad array of autoantibodies relative to specificity and isotype in the plasma and BALF of $cSiO_2$-treated NZBWF1 mice. Autoantigen coated protein arrays were used for profiling four isotypes of autoantibody (IgG, IgM, IgA, and IgE) in plasma and BALF in Study 2. The final intensity value of each autoantibody was expressed as an autoantibody score. Individual autoantibodies were grouped according to the function of their cognate antigens (group names shown on y-axis) as described in the Methods section. The scores of each autoantibody in this group were combined to obtain an overall score for each group. This score was related to the ω-3 HUFA score using Spearman's correlation coefficient. *$p < 0.05$, **$p < 0.01$, ***$p < 0.001$.

plots consistently suggested that O3Is above 10% were associated with reduced IRG expression, leukocyte infiltration, and ELS development (**Figures 8**, **9**). Lastly, O3Is were significantly lower in mice (median of 5.44, 95% CI 5.30–5.85) that showed development of lupus as indicated by renal lesions and elevated anti-dsDNA compared to mice negative for both of these endpoints (median of 17.48, 95% CI 14.83–19.67) (**Figure 9E**).

Correlations between inflammation/leukocyte infiltration indicators and RBC ω-3 HUFA scores and O3I for individual animals in Studies 1, 2, and 3 were assessed by Spearman's correlation analysis. Both ω-3 HUFA scores and the O3I were found to similarly negatively correlate with most endpoints in each study, suggesting that both biomarkers were comparable in predicting DHA's disease-preventive effects (**Figure 10**). The only endpoint that showed an opposing trend was the number of PMN measured in the BALF. These differences may be due to the fact that the animals in each experiment were sacrificed at slightly different times post $cSiO_2$ instillation. It appears that animals sacrificed at later dates show an increasing strength in the correlation between ω-3 content and PMN (study 3 sacrificed at 11 weeks, study 2 sacrificed at 13 weeks, study 1 sacrificed at 12 weeks). This may be due to increased disease severity leading to more pronounced neutrophil infiltration between treatment groups.

DISCUSSION

Murine lupus models typically display gradual increases in autoantibodies prior to glomerulonephritis and thus mimic quiescent disease prior to flaring-associated organ damage (47). Here, airway exposure to $cSiO_2$ was used to mimic flaring in NZBWF1 mice by promoting persistent sterile inflammation, cell death, robust expression of IRGs, and development of autoantibody-producing ELS in the lung (34–36). These autoantibodies and resultant immune complexes can accumulate in the kidney, accelerating glomerulonephritis (48–50). We report here for the first time that increasing two biomarkers of ω-3 HUFA tissue content, the ω-3 HUFA score and the O3I, by dietary DHA supplementation is highly associated with suppression of $cSiO_2$-triggered lupus flaring. Benchmark thresholds for these biomarkers were further identified that may be highly relevant to future clinical use of ω-3 HUFA supplementation as an intervention against lupus and other autoimmune diseases.

As has been reviewed previously (51), autoimmune disease onset and progression following $cSiO_2$ inhalation likely begins with unresolvable inflammation and rampant cell death in the lung, overwhelming the ability of alveolar macrophages to clear autoantigen-containing debris by efferocytosis (52). The presence of host nucleic acids released from dying cells may stimulate a type I IFN response (53, 54). Type I IFNs, including IFN-α, promote autoantigen presentation to infiltrating B- and T-cells and induce the release of additional cytokines such as B-cell activating factor (BAFF) (55, 56), the target of the monoclonal antibody drug Benlysta, approved for treatment of adult lupus in 2011 and pediatric lupus in 2019. BAFF stimulates the maturation of B-cells into autoantibody-producing plasma cells. The resultant DNA-containing immune complexes induce further release of IFN-α, sustaining this cycle (43). Marine ω-3s and their metabolites attenuate multiple steps of this putative pathway, resulting in protection against $cSiO_2$-triggered autoimmunity. Several studies indicate that DHA is capable of blocking key inflammatory pathways and promoting a more pro-resolving phenotype in macrophages, which enhances their ability to efferocytose dying cells, thereby preventing aberrant production of type 1 IFNs, pro-inflammatory cytokines, and chemokines (57–59). Together, these inhibitory actions could dampen the subsequent inflammatory and downstream autoimmune responses. As shown here, increasing both the ω-3 HUFA score or the O3I correlated with reductions in IRG, cytokine, chemokine expression, B- and T-cell infiltration, autoantibody production, and glomerulonephritis induced by $cSiO_2$ exposure.

In 2020, the National Institutes of Health announced at 10 years strategic plan focusing on precision nutrition—a "holistic approach to developing comprehensive and dynamic nutritional recommendations relevant to both individual and population health" (https://www.niddk.nih.gov/about-niddk/strategic-plans-reports/strategic-plan-nih-nutrition-research). Selection of dietary lipids would be central to the development on an individual's precision nutrition plan. The strong correlations between the ω-3 biomarkers and inflammatory endpoints suggest that the balance between ω-3 and ω-6 fatty HUFAs in the cell membrane is critical to promoting inflammation or resolution (60). At the translational level, there are a variety of factors that will influence the incorporation of dietary HUFAs into the cell membrane of individuals. ω-3 and ω-6 HUFAs compete for incorporation into the membrane phospholipids at the sn2 position, thus increasing the levels of ω-6 fatty acids in the diet will reduce the ω-3 HUFA incorporation in the tissue and vice versa (19). It has also been shown that the bioavailability of ω-3 supplements is enhanced when provided with a meal rich in other fats (61). Finally, single nucleotide polymorphisms (SNPs) in lipid metabolizing genes are associated with altered levels of various fatty acids observed in the RBCs and tissues (62, 63), and variations in lipid metabolizing genes are associated with the efficacy of ω-3 supplementation in cardiovascular disease (CVD) (64). Therefore, in preclinical and clinical ω-3 HUFA intervention studies, it is vital to measure of the balance of ω-3 and ω-6 HUFAs.

Measuring an individual's tissue HUFA status can be readily accomplished with low-cost commercial tests that are performed using dried blood spots (65). The alteration of RBC ω-3 and ω-6 fatty acids observed following dietary interventions is reflected in multiple tissues (**Figure 2**, **Figure S2**). Similarly, other studies have shown membrane fatty acid profiles of various immune cells, including monocytes, macrophages, T-cells, and B-cells, are also influenced by ω-3 supplementation (66). Of the two biomarkers studied, the O3I (i.e., DHA + EPA as a percent of total erythrocyte fatty acids) has been extensively validated in human clinical studies and is more widely implemented. A critical advantage of the O3I is the wealth of literature utilizing

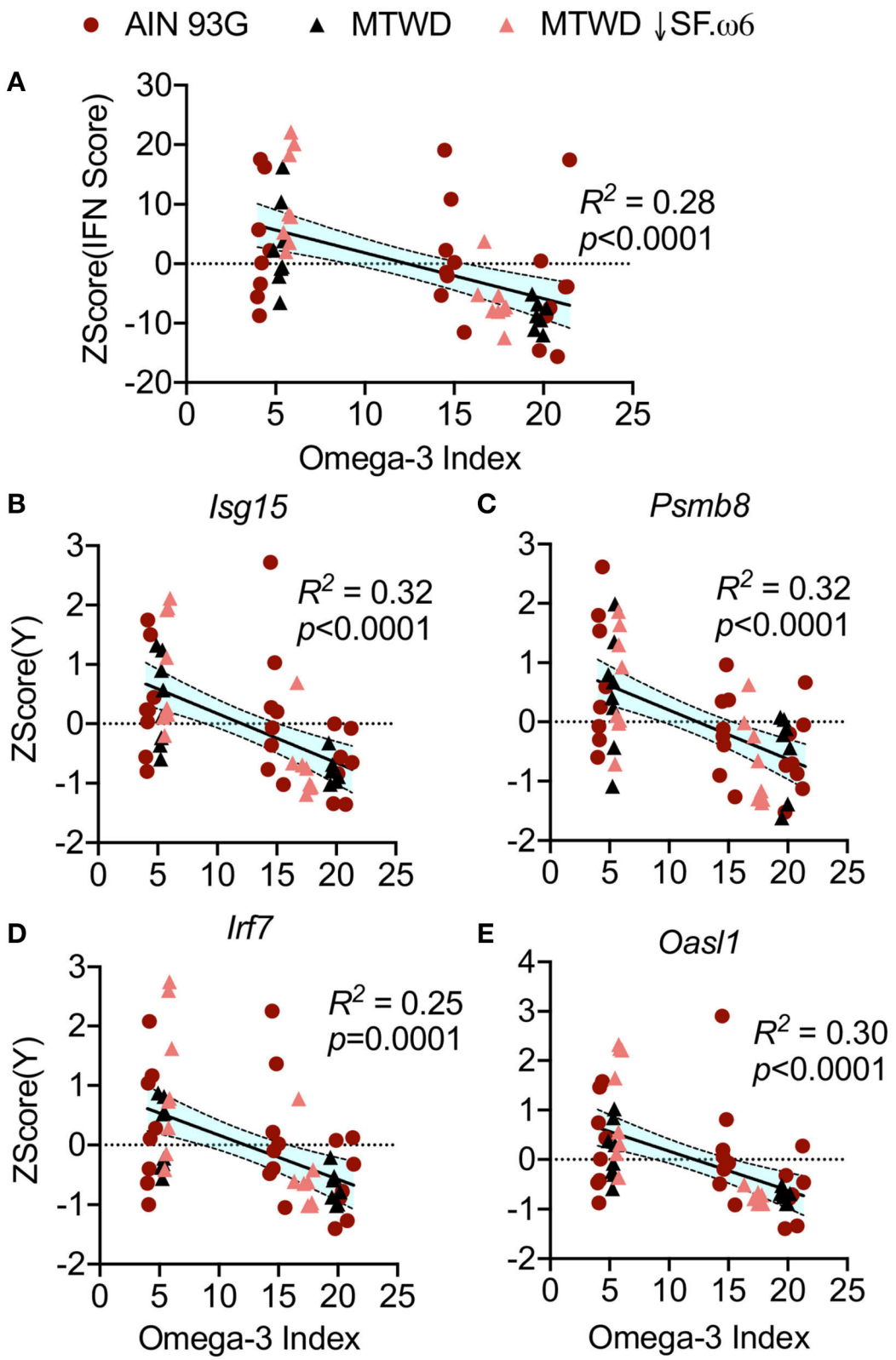

FIGURE 8 | The Omega-3 Index (O3I) negatively correlates with IRG expression in $cSiO_2$-triggered NZBWF1 mice. The IFN scores **(A)** and expression of **(B)** *Isg15*, **(C)** *Psmb8*, **(D)** *Irf7*, and **(E)** *Oasl1* expression were calculated as described in **Figure 3**. The autoscaled IFN scores and the expression of each gene was plotted against the O3I and the resulting data analyzed by simple linear regression. Regression coefficients were considered statistically significant at $p < 0.05$. Shaded bands around regression lines represent 95% confidence intervals.

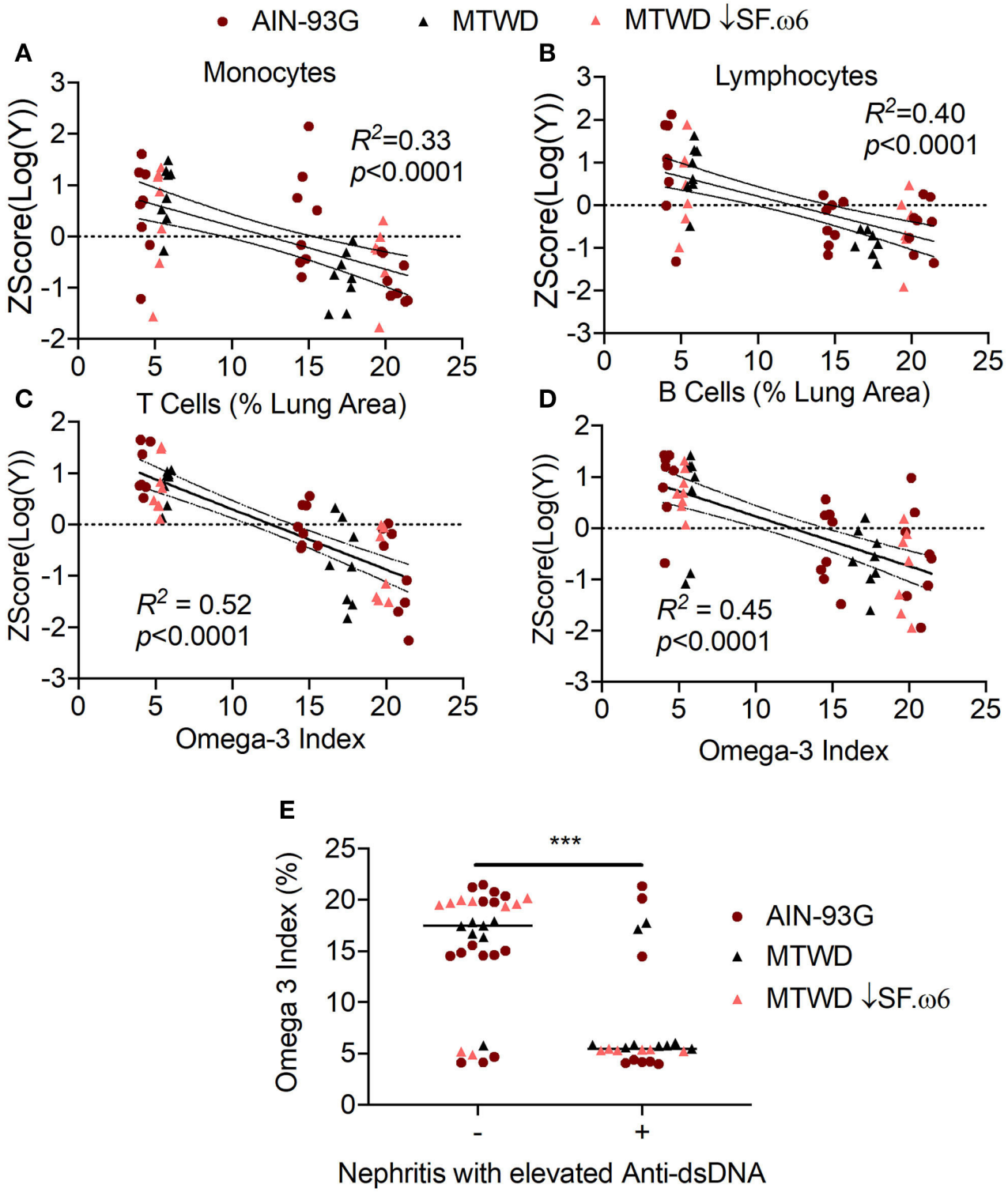

FIGURE 9 | Heightened O3Is correspond with suppression of leukocyte infiltration, ELS development, and disease progression in $cSiO_2$-triggered NZBWF1 mice. **(A)** Macrophage and **(B)** lymphocyte infiltration, as well as **(C)** B-cell, and **(D)** T-cell positive lung tissue were negatively correlated with the O3I. **(E)** Mice positive for renal lesions and elevated plasma anti-dsDNA IgG (significantly different from mean of the Veh-treated group, $p < 0.05$) had significantly lower median Omega-3 Indexes than mice in the the group negative for these endpoints, as assessed by the non-parametric Mann-Whitney *U*-test (***$p < 0.001$). For **(A–D)**, data were analyzed by a simple linear regression and goodness of fit presented as R^2. Regression coefficients were considered statistically significant at $p < 0.05$. Shaded bands around regression lines represent 95% confidence intervals.

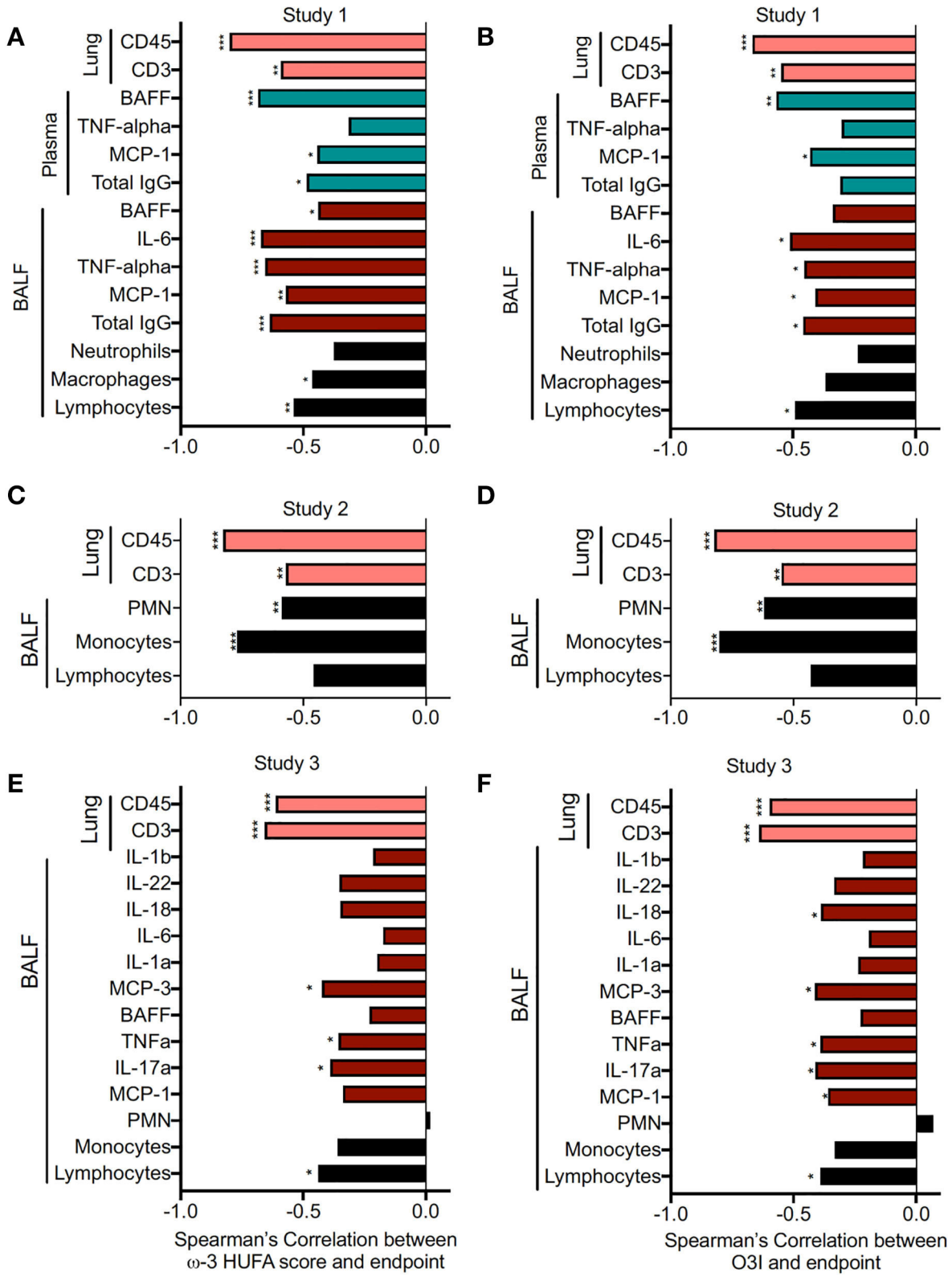

FIGURE 10 | RBC ω-3 HUFA score and O3I both negatively correlate with inflammatory/autoimmune indicators and pulmonary immune cell infiltration. Correlation between inflammatory endpoints and RBC ω-3 HUFA scores and O3Is for individual animals was assessed by Spearman's correlation coefficient, due to non-normal distribution of samples. Many endpoints in Study 1 (HF AIN-93G diet) **(A,B)**, Study 2 (AIN-93G diet) **(C,D)**, and Study 3 (MTWD and MTWD ↓SF.ω6 diets) **(E,F)** were significantly negatively correlated with both the omega-3 HUFA score **(A,C,E)** and the O3I **(B,D,F)**. $^{*}p < 0.05$, $^{**}p < 0.01$, $^{***}p < 0.001$.

this biomarker, which was proposed for use as a risk factor for CVD in 2004. The widespread use of this biomarker has allowed for meta-analyses to identify O3I levels that show protection against a variety of disease endpoints, particularly in the field of cardiovascular and coronary heart disease. In instances where storage conditions, extraction protocols, and analytical techniques remain consistent across studies and samples, the O3I is preferable because it can be understood in the context of previous studies. If inconsistencies among these factors are a concern, defining fatty acid levels using the ω-3 HUFA score might be more advantageous.

A major advantage of the ω-3 HUFA score is its consistency across tissues and blood fractions and recalcitrance to differences in storage conditions and analytical techniques. Since HUFAs have similar chemical properties, they are degraded at similar rates (19). This appeared to be critical factor in our studies, where we found that ω-3 HUFA scores in RBCs were similarly impacted by en% DHA across all three studies, whereas the O3I was less robust (**Figure S1**). This observation is supported by a previous study that investigated the stability of dried blood spot fatty acids over the course of 4 weeks when stored at 4 and −20°C. Bell et al. observed a 15–30% decrease in individual HUFAs stored at 4°C for 28 days, while the ω-3 HUFA score decreased by only 8% (67). Because our samples were stored and processed under different conditions among experiments, we favored the use of the ω-3 HUFA score for this study. With the ω-3 HUFA score, we saw slightly higher correlations in many of the endpoints assessed, which may be in part due to the reduced variability observed in the HUFA score compared to the O3I. Another advantage shown here (**Figure 1B**) and previously (41) is that the ω-3 HUFA score can be predicted from dietary fat intake, making it an important tool when developing personalized nutritional interventions. Finally, focusing on the HUFA pool gives the clinician insight into the potential for the generation of anti-inflammatory ω-3 and proinflammatory ω-6 HUFA metabolites (19, 68).

There are multiple mechanisms by which ω-3 and ω-6 HUFAs directly influence inflammatory pathways in the cell (69). First, by increasing membrane fluidity and impeding lipid raft formation, DHA and EPA can interfere with activation of transmembrane receptors associated with inflammatory signaling (70). Second, both extracellular and intracellular phospholipases can cleave HUFAs from the membrane (71, 72). Resultant free DHA and EPA may activate transmembrane receptors or intracellular receptors associated with suppressing proinflammatory signaling (73, 74). Specifically, ω-3 HUFAs have been shown to antagonize TLR activation (75, 76) and interfere with NF-kB-dependent transcription by activating PPARγ (58, 77). Third, both DHA and EPA are metabolized to form specialized pro-resolving mediators (SPMs) such as maresins, resolvins, protectins, and anti-inflammatory epoxide metabolites (78, 79). SPMs inhibit inflammatory signaling (80, 81) and promote efferocytosis of dead cells (82, 83), both of which are critical to halting autoimmune disease pathogenesis.

Besides competing for cell membrane incorporation, ω-3 HUFAs can inhibit ω-6 HUFA metabolism to downstream proinflammatory eicosanoids (e.g., thromboxanes, prostaglandins, and leukotrienes) (19). Lipid metabolites derived from the arachidonic acid cascade have primarily inflammatory actions, especially during acute inflammation. Shifting the HUFA balance to favor ω-3 HUFAs rather than ω-6 HUFAs, such as arachidonic acid, may enhance the pro-resolving phenotype promoted by ω-3 derived lipid mediators. A recent study demonstrated that the plasma and red blood cell levels of ω-3 HUFAs were highly correlated with the production of downstream lipid mediators (79). Similarly, supplementation with EPA and DHA led to a decrease in ω-6 HUFAs, namely arachidonic acid, as well as decreased ω-6 HUFA-derived metabolites.

It is likely that the anti-inflammatory actions of ω-3 HUFAs and their downstream metabolites are at play in the inflammatory processes driving lupus symptoms. Among lupus patients, higher ω-3 HUFA levels or more frequent consumption of fish correlate with reduced disease activity (8, 84). In 2011, it was reported that lupus patients had lower amounts of ω-3 HUFAs in RBC and plasma than observed in healthy controls (85), and a subsequent study showed a negative correlation between adipose ω-3 levels and disease activity (7). More recently, it was shown that individuals with lupus had decreased levels of plasma resolvin D1, an anti-inflammatory metabolite of DHA, as compared to healthy controls (86). To date, there has been no extensive study of the membrane fatty acid content or plasma lipidome of lupus patients. Investigation in this area is necessary to elucidate potential benefit of ω-3 supplementation in human patients.

The majority of clinical trials utilizing ω-3 fatty acid supplementation to combat disease have been specific to CVD. Over the past three decades, randomized control trials (RCTs) have produced inconclusive results, with some showing benefit and others not. There are a variety of potential reasons for this inconsistency, as thoroughly reviewed by Rice et al. (87). Reasons include, among other things, insufficient dose of ω-3 HUFAs and inadequate duration of supplementation. Analysis of the results of some CVD studies reveal that that there can be significant overlap in the O3I in treatment vs. control group at trial completion, which would explain why researchers did not observe any effect with supplementation (88, 89). Additionally, there is a lack of consistency in measuring the fatty acid content in trial participants. The authors concluded that assessment of the ω-3 status of study participants, both at baseline and throughout the study, is critical to implementing an effective nutritional intervention. A recently published large scale RCT showing positive results with EPA supplementation met many of the suggestions put forth by Rice et al. (87): (i) the EPA dose given (4 g/day) was ∼4-fold greater than other contemporaneous trials, (ii) the study had an average duration of 4.9 years, (iii) the baseline EPA levels were identical between the placebo and treatment group, and (iv) the plasma EPA content at 1 year was 5-fold higher than at baseline (90). This study, as well as other recent RCTs showing beneficial effects of ω-3 supplementation have been reviewed in detail by O'Keefe et al. (91).

Compared to CVD, there have been very few trials investigating the impact of ω-3 supplementation on lupus outcomes, all of which have very few subjects ($n < 100$) (**Table 3**). Recent reviews on this subject (5, 92) reveal that approximately half of the clinical trials performed employing

TABLE 3 | Summary of ω-3 HUFA intervention trials in lupus patients.

Year	Author	FA dose (EPA+DHA)	Supplementation type	N	Trial duration	Measured fatty acids	Fatty acids reported	Result
1989	Clark et al. (9)	1.8 g, 5.4 g	MaxEPA fish oil capsules	12	5 wk	Yes—platelets	ARA, EPA, DHA	Decreased Triglycerides and cholesterol
1991	Walton et al. (11)	5.6 g	MaxEPA fish oil capsules	27	12 wk	Yes—RBCs	not reported	Improved disease status
1993	Clark et al. (10)	4.4 g	MaxEPA fish oil capsules	21	1 yr	Yes—Platelets	ARA, EPA, DHA	Improvement, but not in renal function or disease activity
2004	Duffy et al. (12)	0.9 g	MaxEPA fish oil capsules	52	24 wk	Yes—Platelets	EPA, DHA	Improved disease status
2005	Nakamura et al. (17)	1.8 g	EPA, ethyl esters	6	3 mo	Yes—Plasma PL	LA, DGLA, ARA, ALA, EPA, DPA, DHA	Decreased oxidative stress (8-isoprostane)
2008	Wright et al. (18)	3 g	Omacor, EPA/DHA methyl esters	60	24 wk	Yes—Platelets	ARA, EPA, DHA	Decreased SLAM-R, BILAG, FMD, isoprostanes
2013	Bello et al. (14)	3 g	Lovaza, EPA/DHA ethyl esters	85	12 wk	No	-	No change
2015	Arriens et al. (13)	4.5g	Metagenics fish oil capsules	32	6 mo	No	-	Improved disease status
2015	Lozovoy et al. (16)	300 mg	Fish oil capsules (no brand)	62	4 mo	No	-	Decreased SLEDAI, increased adiponectin, decreased leptin
2017	Borges et al. (15)	1.28 g	Naturalis HiOmega3 fish oil capsules	49	12 wk	No	-	Decreased CRP

ARA, arachidonic acid; EPA, eicosapentaenoic acid; DHA, docosahexaenoic acid; LA, linoleic acid; DGLA, dihomo-gamma linoleic acid; ALA, alpha linolenic acid; DPA, docosapentaenoic acid; SLAM-R, systemic lupus activity measure—revised; BILAG, British Isles lupus assessment group; FMD, flow mediated dilation; SLEDAI, systemic lupus erythematosus disease activity index; CRP, C-reactive protein; PL, phospholipid.

ω-3 supplementation in lupus patients report a reduction in disease activity (11–13, 16, 18, 93). Many studies that did not observe a reduction in disease activity reported improvements in other areas, such as a reduction in serum triglycerides (9, 10) or biomarkers of inflammation and oxidative stress (9, 15). A critical impediment to evaluating the efficacy of ω-3 supplementation in these trials is the inconsistency in measuring and reporting the ω-3 levels in subjects. Among lupus studies reporting fatty acid levels, there is variability in units used for reporting [mol% (9, 10), wt% (17, 18, 85), mg/mL (12)], the source [platelets (9, 10, 12, 18), RBCs (11, 85), plasma phospholipids (17, 85)], and the fatty acids reported. To more definitively identify ω-3 levels that are protective against lupus symptoms and flaring requires frequent measurement and consistent reporting of ω-3 status in human patients, in addition to more robust clinical trials.

The recent studies identifying the protective effects of ω-3 supplementation in CVD support the potential benefit for a similar dietary intervention in lupus. Notably, patients with lupus have an increased risk of myocardial infarction and CVD mortality relative to the general population (94). A key mechanism proposed to link these chronic diseases is increased oxidative stress (95, 96). A 2012 clinical trial with >700 participants reported that 4 g/day IPE (iscosapent ethyl, an ethyl ester of EPA) for 12 weeks significantly decreased plasma oxLDL (97), an oxidized biomarker implicated in CVD. Similarly, urinary F2 isoprostanes, produced by the non-enzymatic oxidation of arachidonic acid and a widely accepted marker for oxidative stress, were decreased by supplementation with 4 g/day of either DHA or EPA in a study of 59 hypertensive patients with type 2 diabetes (98) A specific member of the F2-isoprostane family, 8-isoprostane, was found to be decreased in with ω-3 supplementation in lupus patients, as measured in both the platelets and urine (**Table 3**) (17, 18).

In the present study, O3Is above 10% and ω-3 HUFA scores >40% appeared to be associated with absence of disease progression. This is consistent with studies showing decreased mortality from cardiovascular disease in populations where the ω-3 HUFA score is >40% (99) and associating increased ω-3 HUFA scores to a reduction in chronic pain (100). In 2004, Harris and von Schacky proposed that an O3I > 8% was associated with decreased risk of death from CHD, while O3I < 4% was associated with increased risk (101), based on a small clinical trial of 57 subjects. In 2017, a meta-analysis of 10 cohort studies, with a combined n > 27,505, confirmed these cutoffs (102). Because

there are far fewer clinical studies investigating the role of ω-3 HUFAs in rheumatic disease, and even fewer that present enough fatty acid information to calculate the ω-3 HUFA score, it is difficult to identify a protective ω-3 HUFA score or O3I for lupus. However, a study performed in patients with rheumatoid arthritis showed that increasing the ω-3 HUFA score from ∼30 to ∼40% resulted in decreased joint swelling, pain, various inflammatory markers, and NSAID and glucocorticoid use (103).

Providing sufficient levels of ω-3 supplementation is paramount to achieving ω-3 HUFA levels capable of reducing symptoms involved in lupus flares. A recent study presented an equation to predict the change in the O3I using the baseline O3I and the supplemented dose of EPA and DHA (104). These findings suggested that individuals with a baseline O3I around 4%, a level typical for many individuals consuming a Western diet, would require 1,500 mg/day EPA + DHA for 13 weeks to achieve an O3I of 8%. Though many ω-3 supplementation trials in lupus patients use doses >1,500 mg/day, the results presented herein suggest that a human equivalent dose of ∼5 g/day may be necessary to provide protection against a variety of lupus associated endpoints. Consumption of 5 g/day ω-3 HUFAs has been determined as safe by the European Food Safety Authority after analyzing the impact of ω-3 HUFAs on endpoints such as bleeding time, immune function, and changes in blood LDL-cholesterol (105).

A potential limitation of this study is the limited range of doses of DHA provided (0, 2, and 5 g/day human equivalent dose), which may contribute to the relatively low R^2 value observed between the ω-3 biomarkers and some inflammatory endpoints. Additional intermediate doses of DHA, and corresponding intermediate ω-3 levels, may allow for a more accurate regression model. Other informative modifications to the diet would include using EPA as the primary source of dietary ω-3 HUFAs, providing ω-3 HUFAs as phospholipids rather than triglycerides, or varying levels of ω-6 fatty acids to determine the extent to which ω-6 HUFAs impact levels of ω-3 biomarkers and lupus-associated inflammatory endpoints. Finally, it should be recognized that DHA was administered here prophylactically. Since the most severe lupus symptoms are episodic and associated with flaring, the study design of our experiments is most relevant to periods of disease remission achievable by treatment with glucocorticoids, antimalarials, and immunosuppressants—drugs that have many adverse side effects (106). ω-3 supplementation might be amenable as a substitute or adjunct therapy for these strong drugs to prevent flaring and prolong the quiescent state. However, the prophylaxis model does not mimic the human situation where ω-3 supplementation is provided after the onset of overt symptoms. Thus, further research is needed on the effects of ω-3 supplementation to treat ongoing lupus flares.

To summarize, we demonstrated with this study that both ω-3 HUFA scores and O3Is of mice fed a wide range of diets supplemented with DHA could be related to numerous lupus-associated inflammatory endpoints. This determination is highly relevant to current and future trials investigating the effect of ω-3 supplementation in inflammatory and autoimmune diseases. Our results suggest that measurement of RBC ω-3 levels allows clinicians and administrators of randomized clinical trials to assess the efficacy of the supplementation strategy employed, as well as confirming compliance. Precision nutritional interventions can be designed to reduce consumption of ω-6 fatty acids while simultaneously supplementing with ω-3 HUFAs, with the objective of achieving an ω-3 HUFA score or O3I that may protect against lupus flaring and autoimmune disease progression.

DATA AVAILABILITY STATEMENT

All datasets presented in this study are included in the article/**Supplementary Material**.

ETHICS STATEMENT

The animal study was reviewed and approved by The Institutional Animal Care and Use Committee at Michigan State University (AUF#01/15-021-00; AUF# PROTO201800113).

AUTHOR CONTRIBUTIONS

KW: investigation, data curation, data analysis/interpretation, figure preparation, manuscript preparation, and project funding. RS, AB, LR, JH: data analysis/interpretation and manuscript preparation. AL: tissue, red blood cells, and diet fatty acid analysis. JP: initial study design, manuscript preparation, supervision, and project funding. All authors contributed to the article and approved the submitted version.

FUNDING

This research was funded by NIH ES027353 (JP), NIH F31ES030593 (KW), NIH T32ES007255 (KW), Lupus Foundation of America (JP, KW), USDA National Institute of Food and Agriculture Hatch Projects 1020129 (JP) and UTA-01407 and UTA-01456 (AB), and the Dr. Robert and Carol Deibel Family Endowment (JP).

ACKNOWLEDGMENTS

We would like to thank Jason Polreis and Bill Harris of OmegaQuant for their assistance in the red blood cell analysis, Elizabeth Ross for assistance in manuscript preparation, and Melissa Bates and Kristen Gilley for coordination of the animal studies.

SUPPLEMENTARY MATERIAL

The Supplementary Material for this article can be found online at: https://www.frontiersin.org/articles/10.3389/fimmu.2020.01796/full#supplementary-material

Supplementary Data Sheet 1 | Supplementary Figures S1 and S2.

Supplementary Table 1 | Microsoft Excel table of RBC fatty acid composition.

Supplementary Table 2 | Excel tables containing data from studies 1–3 used to perform generate graphs presented herein.

REFERENCES

1. Durcan L, O'Dwyer T, Petri M. Management strategies and future directions for systemic lupus erythematosus in adults. *Lancet.* (2019) 393:2332–43. doi: 10.1016/S0140-6736(19)30237-5
2. Ruiz-Irastorza G, Danza A, Khamashta M. Glucocorticoid use and abuse in SLE. *Rheumatology.* (2012) 51:1145–53. doi: 10.1093/rheumatology/ker410
3. Davidson JE, Fu Q, Rao S, Magder LS, Petri M. Quantifying the burden of steroid-related damage in SLE in the hopkins lupus cohort. *Lupus Sci Med.* (2018) 5:e000237. doi: 10.1136/lupus-2017-000237
4. Calder PC. Omega-3 fatty acids and inflammatory processes: from molecules to man. *Biochem Soc Trans.* (2017) 45:1105–15. doi: 10.1042/BST20160474
5. Li X, Bi X, Wang S, Zhang Z, Li F, Zhao AZ. Therapeutic potential of omega-3 polyunsaturated fatty acids in human autoimmune diseases. *Front Immunol.* (2019) 10:2241. doi: 10.3389/fimmu.2019.02241
6. Pestka JJ. n-3 polyunsaturated fatty acids and autoimmune-mediated glomerulonephritis. *Prostaglandins Leukot Essent Fatty Acids.* (2010) 82:251–8. doi: 10.1016/j.plefa.2010.02.013
7. Elkan AC, Anania C, Gustafsson T, Jogestrand T, Hafstrom I, Frostegard J. Diet and fatty acid pattern among patients with SLE: associations with disease activity, blood lipids and atherosclerosis. *Lupus.* (2012) 21:1405–11. doi: 10.1177/0961203312458471
8. Charoenwoodhipong P, Harlow SD, Marder W, Hassett AL, McCune WJ, Gordon C, et al. Dietary omega polyunsaturated fatty acid intake and patient-reported outcomes in systemic lupus erythematosus: the michigan lupus epidemiology & surveillance (MILES) program. *Arthritis Care Res.* (2019) 72:874–81. doi: 10.1002/acr.23925
9. Clark WF, Parbtani A, Huff MW, Reid B, Holub BJ, Falardeau P. Omega-3 fatty acid dietary supplementation in systemic lupus erythematosus. *Kidney Int.* (1989) 36:653–60. doi: 10.1038/ki.1989.242
10. Clark WF, Parbtani A, Naylor CD, Levinton CM, Muirhead N, Spanner E, et al. Fish oil in lupus nephritis: clinical findings and methodological implications. *Kidney Int.* (1993) 44:75–86. doi: 10.1038/ki.1993.215
11. Walton AJ, Snaith ML, Locniskar M, Cumberland AG, Morrow WJ, Isenberg DA. Dietary fish oil and the severity of symptoms in patients with systemic lupus erythematosus. *Ann Rheum Dis.* (1991) 50:463–6. doi: 10.1136/ard.50.7.463
12. Duffy EM, Meenagh GK, McMillan SA, Strain JJ, Hannigan BM, Bell AL. The clinical effect of dietary supplementation with omega-3 fish oils and/or copper in systemic lupus erythematosus. *J Rheumatol.* (2004) 31:1551–6. Available online at: https://www.jrheum.org/content/31/8/1551
13. Arriens C, Hynan LS, Lerman RH, Karp DR, Mohan C. Placebo-controlled randomized clinical trial of fish oil's impact on fatigue, quality of life, and disease activity in systemic lupus erythematosus. *Nutr J.* (2015) 14:82. doi: 10.1186/s12937-015-0068-2
14. Bello KJ, Fang H, Fazeli P, Bolad W, Corretti M, Magder LS, et al. Omega-3 in SLE: a double-blind, placebo-controlled randomized clinical trial of endothelial dysfunction and disease activity in systemic lupus erythematosus. *Rheumatol Int.* (2013) 33:2789–96. doi: 10.1007/s00296-013-2811-3
15. Borges MC, Santos FM, Telles RW, Andrade MV, Correia MI, Lanna CC. Omega-3 fatty acids, inflammatory status and biochemical markers of patients with systemic lupus erythematosus: a pilot study. *Rev Bras Reumatol.* (2016) 57:526–34. doi: 10.1016/j.rbre.2016.09.014
16. Lozovoy MA, Simao AN, Morimoto HK, Scavuzzi BM, Iriyoda TV, Reiche EM, et al. Fish oil N-3 fatty acids increase adiponectin and decrease leptin levels in patients with systemic lupus erythematosus. *Mar Drugs.* (2015) 13:1071–83. doi: 10.3390/md13021071
17. Nakamura N, Kumasaka R, Osawa H, Yamabe H, Shirato K, Fujita T, et al. Effects of eicosapentaenoic acids on oxidative stress and plasma fatty acid composition in patients with lupus nephritis. *In Vivo.* (2005) 19:879–82. doi: 10.1007/s11745-006-5079-5
18. Wright SA, O'Prey FM, McHenry MT, Leahey WJ, Devine AB, Duffy EM, et al. A randomised interventional trial of omega-3-polyunsaturated fatty acids on endothelial function and disease activity in systemic lupus erythematosus. *Ann Rheum Dis.* (2008) 67:841–8. doi: 10.1136/ard.2007.077156
19. Lands B, Bibus D, Stark KD. Dynamic interactions of n-3 and n-6 fatty acid nutrients. *Prostaglandins Leukot Essent Fatty Acids.* (2018) 136:15–21. doi: 10.1016/j.plefa.2017.01.012
20. de Groot RHM, Meyer BJ. ISSFAL official statement number 6: the importance of measuring blood omega-3 long chain polyunsaturated fatty acid levels in research. *Prostaglandins Leukot Essent Fatty Acids.* (2019) 157:102029. doi: 10.1016/j.plefa.2019.102029
21. Crampton SP, Morawski PA, Bolland S. Linking susceptibility genes and pathogenesis mechanisms using mouse models of systemic lupus erythematosus. *Dis Model Mech.* (2014) 7:1033–46. doi: 10.1242/dmm.016451
22. Gelfand MC, Steinberg AD. Therapeutic studies in NZB-W mice. II. Relative efficacy of azathioprine, cyclophosphamide and methylprednisolone. *Arthritis Rheum.* (1972) 15:247–52. doi: 10.1002/art.1780150305
23. Gelfand MC, Steinberg AD, Nagle R, Knepshield JH. Therapeutic studies in NZB-W mice. I. Synergy of azathioprine, cyclophosphamide and methylprednisolone in combination. *Arthritis Rheum.* (1972) 15:239–46. doi: 10.1002/art.1780150304
24. Jolly CA, Muthukumar A, Avula CP, Troyer D, Fernandes G. Life span is prolonged in food-restricted autoimmune-prone (NZB x NZW)F(1) mice fed a diet enriched with (n-3) fatty acids. *J Nutr.* (2001) 131:2753–60. doi: 10.1093/jn/131.10.2753
25. Chandrasekar B, Troyer DA, Venkatraman JT, Fernandes G. Dietary omega-3 lipids delay the onset and progression of autoimmune lupus nephritis by inhibiting transforming growth factor beta mRNA and protein expression. *J Autoimmun.* (1995) 8:381–93. doi: 10.1006/jaut.1995.0030
26. Jeng KC, Fernandes G. Effect of fish oil diet on immune response and proteinuria in mice. *Proc Natl Sci Counc Repub China B.* (1991) 15:105–10.
27. Halade GV, Rahman MM, Bhattacharya A, Barnes JL, Chandrasekar B, Fernandes G. Docosahexaenoic acid-enriched fish oil attenuates kidney disease and prolongs median and maximal life span of autoimmune lupus-prone mice. *J Immunol.* (2010) 184:5280–6. doi: 10.4049/jimmunol.0903282
28. Halade GV, Williams PJ, Veigas JM, Barnes JL, Fernandes G. Concentrated fish oil (Lovaza (R)) extends lifespan and attenuates kidney disease in lupus-prone short-lived (NZBxNZW)F1 mice. *Exp Bio Med.* (2013) 238:610–22. doi: 10.1177/1535370213489485
29. Pestka JJ, Vines LL, Bates MA, He K, Langohr I. Comparative effects of n-3, n-6 and n-9 unsaturated fatty acid-rich diet consumption on lupus nephritis, autoantibody production and CD4+ T cell-related gene responses in the autoimmune NZBWF1 mouse. *PLoS ONE.* (2014) 9:e100255. doi: 10.1371/journal.pone.0100255
30. Gomez-Puerta JA, Gedmintas L, Costenbader KH. The association between silica exposure and development of ANCA-associated vasculitis: systematic review and meta-analysis. *Autoimmun Rev.* (2013) 12:1129–35. doi: 10.1016/j.autrev.2013.06.016
31. Makol A, Reilly MJ, Rosenman KD. Prevalence of connective tissue disease in silicosis (1985–2006)—a report from the state of michigan surveillance system for silicosis. *Amer J Ind Med.* (2011) 54:255–62. doi: 10.1002/ajim.20917
32. Parks CG, Cooper GS. Occupational exposures and risk of systemic lupus erythematosus: a review of the evidence and exposure assessment methods in population- and clinic-based studies. *Lupus.* (2006) 15:728–36. doi: 10.1177/0961203306069346
33. Parks CG, Cooper GS. Occupational exposures and risk of systemic lupus erythematosus. *Autoimmunity.* (2005) 38:497–506. doi: 10.1080/08916930500285493
34. Bates MA, Brandenberger C, Langohr I, Kumagai K, Harkema JR, Holian A, et al. Silica triggers inflammation and ectopic lymphoid neogenesis in the lungs in parallel with accelerated onset of systemic autoimmunity and glomerulonephritis in the lupus-prone NZBWF1 mouse. *PLoS ONE.* (2015) 10:e0125481. doi: 10.1371/journal.pone.0125481
35. Bates MA, Benninghoff AD, Gilley KN, Holian A, Harkema JR, Pestka JJ. Mapping of dynamic transcriptome changes associated with silica-triggered autoimmune pathogenesis in the lupus-prone NZBWF1 mouse. *Front Immunol.* (2019) 10:632. doi: 10.3389/fimmu.2019.00632
36. Bates MA, Brandenberger C, Langohr, II, Kumagai K, Lock AL, et al. Silica-triggered autoimmunity in lupus-prone mice

blocked by docosahexaenoic acid consumption. *PLoS ONE.* (2016) 11:e0160622. doi: 10.1371/journal.pone.0160622
37. Bates MA, Akbari P, Gilley KN, Wagner JG, Li N, Kopec AK, et al. Dietary docosahexaenoic acid prevents silica-induced development of pulmonary ectopic germinal centers and glomerulonephritis in the lupus-prone NZBWF1 mouse. *Front Immunol.* (2018) 9:2002. doi: 10.3389/fimmu.2018.02002
38. Gilley KN, Wierenga KA, Chauhan PS, Wagner JG, Lewandowski RP, Ross EA, et al. Influence of total western diet on docosahexaenoic acid suppression of silica-triggered lupus flaring in NZBWF1 mice. *PLoS ONE.* (2020) 15:e0233183. doi: 10.1371/journal.pone.0233183
39. Stark KD. The percentage of n-3 highly unsaturated fatty acids in total HUFA as a biomarker for omega-3 fatty acid status in tissues. *Lipids.* (2008) 43:45–53. doi: 10.1007/s11745-007-3128-3
40. Harris WS. The omega-3 index: clinical utility for therapeutic intervention. *Curr Cardiol Rep.* (2010) 12:503–8. doi: 10.1007/s11886-010-0141-6
41. Strandjord SE, Lands B, Hibbeln JR. Validation of an equation predicting highly unsaturated fatty acid (HUFA) compositions of human blood fractions from dietary intakes of both HUFAs and their precursors. *Prostag Leukotr Ess Fatty Acids.* (2018) 136:171–6. doi: 10.1016/j.plefa.2017.03.005
42. Rajasinghe L, Quan L, Bates M, Akbari P, Harkema J, Pestka J. Docosahexaenoic acid (DHA) suppresses broad spectrum of pathogenic autoantibodies elicited in murine model of lupus flaring. In: *Nutritional Immunology Inflammation. American Society of Nutrition's 2019 Annual Meeting.* Baltimore, MD. (2019). doi: 10.1093/cdn/nzz049.OR12-03-19
43. Chasset F, Arnaud L. Targeting interferons and their pathways in systemic lupus erythematosus. *Autoimmun Rev.* (2018) 17:44–52. doi: 10.1016/j.autrev.2017.11.009
44. Rajasinghe LD, Li QZ, Zhu C, Yan M, Chauhan SP, Wierenga KA, et al. Omega-3 fatty acid intake suppresses induction of diverse autoantibody repertoire by crystalline silica in lupus-prone mice. *Autoimmunity.* (2020) 2020–0061.
45. Petri M, Orbai AM, Alarcon GS, Gordon C, Merrill JT, Fortin PR, et al. Derivation and validation of the systemic lupus international collaborating clinics classification criteria for systemic lupus erythematosus. *Arthritis Rheum.* (2012) 64:2677–86. doi: 10.1002/art.34473
46. Fenton JI, Gurzell EA, Davidson EA, Harris WS. Red blood cell PUFAs reflect the phospholipid PUFA composition of major organs. *Prostag Leukot Essent Fatty Acids.* (2016) 112:12–23. doi: 10.1016/j.plefa.2016.06.004
47. Sang A, Yin Y, Zheng YY, Morel L. Animal models of molecular pathology systemic lupus erythematosus. *Prog Mol Biol Transl Sci.* (2012) 105:321–70. doi: 10.1016/B978-0-12-394596-9.00010-X
48. Brown JM, Archer AJ, Pfau JC, Holian A. Silica accelerated systemic autoimmune disease in lupus-prone New Zealand mixed mice. *Clin Exp Immunol.* (2003) 131:415–21. doi: 10.1046/j.1365-2249.2003.02094.x
49. Beamer CA, Holian A. Antigen-presenting cell population dynamics during murine silicosis. *Am J Respir Cell Mol Biol.* (2007) 37:729–38. doi: 10.1165/rcmb.2007-0099OC
50. Pfau JC, Brown JM, Holian A. Silica-exposed mice generate autoantibodies to apoptotic cells. *Toxicology.* (2004) 195:167–76. doi: 10.1016/j.tox.2003.09.011
51. Wierenga KA, Harkema JR, Pestka JJ. Lupus, silica, and dietary omega-3 fatty acid interventions. *Toxicol Pathol.* (2019) 47:1004–11. doi: 10.1177/0192623319878398
52. Gilberti RM, Joshi GN, Knecht DA. The phagocytosis of crystalline silica particles by macrophages. *Am J Respir Cell Mol Biol.* (2008) 39:619–27. doi: 10.1165/rcmb.2008-0046OC
53. McNab F, Mayer-Barber K, Sher A, Wack A, O'Garra A. Type I interferons in infectious disease. *Nat Rev Immunol.* (2015) 15:87–103. doi: 10.1038/nri3787
54. Crow MK, Olferiev M, Kirou KA. Type I interferons in autoimmune disease. *Annu Rev Pathol.* (2019) 14:369–93. doi: 10.1146/annurev-pathol-020117-043952
55. Jacob N, Guo S, Mathian A, Koss MN, Gindea S, Putterman C, et al. B Cell and BAFF dependence of IFN-alpha-exaggerated disease in systemic lupus erythematosus-prone NZM 2328 mice. *J Immunol.* (2011) 186:4984–93. doi: 10.4049/jimmunol.1000466
56. Lopez P, Scheel-Toellner D, Rodriguez-Carrio J, Caminal-Montero L, Gordon C, Suarez A. Interferon-alpha-induced B-lymphocyte stimulator expression and mobilization in healthy and systemic lupus erythmatosus monocytes. *Rheumatology.* (2014) 53:2249–58. doi: 10.1093/rheumatology/keu249
57. Wierenga KA, Wee J, Gilley KN, Rajasinghe LD, Bates MA, Gavrilin MA, et al. Docosahexaenoic acid suppresses silica-induced inflammasome activation and IL-1 cytokine release by interfering with priming signal. *Front Immunol.* (2019) 10:2130. doi: 10.3389/fimmu.2019.02130
58. Chang HY, Lee H-N, Kim W, Surh Y-J. Docosahexaenoic acid induces M2 macrophage polarization through peroxisome proliferator-activated receptor gamma activation. *Life Sci.* (2015) 120:39–47. doi: 10.1016/j.lfs.2014.10.014
59. Gutierrez S, Svahn SL, Johansson ME. Effects of omega-3 fatty acids on immune cells. *Int J Mol Sci.* (2019) 20:5028. doi: 10.3390/ijms20205028
60. Mason RP, Libby P, Bhatt DL. Emerging mechanisms of cardiovascular protection for the omega-3 fatty acid eicosapentaenoic acid. *Arterioscler Thromb Vasc Biol.* (2020) 40:1135–47. doi: 10.1161/ATVBAHA.119.313286
61. Schuchardt JP, Hahn A. Bioavailability of long-chain omega-3 fatty acids. *Prostag Leukot Essent Fatty Acids.* (2013) 89:1–8. doi: 10.1016/j.plefa.2013.03.010
62. Martinelli N, Girelli D, Malerba G, Guarini P, Illig T, Trabetti E, et al. FADS genotypes and desaturase activity estimated by the ratio of arachidonic acid to linoleic acid are associated with inflammation and coronary artery disease. *Am J Clin Nutr.* (2008) 88:941–9. doi: 10.1093/ajcn/88.4.941
63. Schaeffer L, Gohlke H, Muller M, Heid IM, Palmer LJ, Kompauer I, et al. Common genetic variants of the FADS1 FADS2 gene cluster and their reconstructed haplotypes are associated with the fatty acid composition in phospholipids. *Hum Mol Genet.* (2006) 15:1745–56. doi: 10.1093/hmg/ddl117
64. Madden J, Williams CM, Calder PC, Lietz G, Miles EA, Cordell H, et al. The impact of common gene variants on the response of biomarkers of cardiovascular disease (CVD) risk to increased fish oil fatty acids intakes. *Annu Rev Nutr.* (2011) 31:203–34. doi: 10.1146/annurev-nutr-010411-095239
65. Johnston DT, Deuster PA, Harris WS, Macrae H, Dretsch MN. Red blood cell omega-3 fatty acid levels and neurocognitive performance in deployed U.S. servicemembers. *Nutr Neurosci.* (2013) 16:30–8. doi: 10.1179/1476830512Y.0000000025
66. Fritsche K. Important differences exist in the dose-response relationship between diet and immune cell fatty acids in humans and rodents. *Lipids.* (2007) 42:961–79. doi: 10.1007/s11745-007-3106-9
67. Bell JG, Mackinlay EE, Dick JR, Younger I, Lands B, Gilhooly T. Using a fingertip whole blood sample for rapid fatty acid measurement: method validation and correlation with erythrocyte polar lipid compositions in UK subjects. *Br J Nutr.* (2011) 106:1408–15. doi: 10.1017/S0007114511001978
68. Browning LM, Walker CG, Mander AP, West AL, Madden J, Gambell JM, et al. Incorporation of eicosapentaenoic and docosahexaenoic acids into lipid pools when given as supplements providing doses equivalent to typical intakes of oily fish. *Am J Clin Nutr.* (2012) 96:748–58. doi: 10.3945/ajcn.112.041343
69. Calder PC. Omega-3 polyunsaturated fatty acids and inflammatory processes: nutrition or pharmacology? *Br J Clin Pharmacol.* (2013) 75:645–62. doi: 10.1111/j.1365-2125.2012.04374.x
70. Wong CK, Wong PT, Tam LS, Li EK, Chen DP, Lam CW. Activation profile of Toll-like receptors of peripheral blood lymphocytes in patients with systemic lupus erythematosus. *Clin Exp Immunol.* (2010) 159:11–22. doi: 10.1111/j.1365-2249.2009.04036.x
71. Norris PC, Dennis EA. Omega-3 fatty acids cause dramatic changes in TLR4 and purinergic eicosanoid signaling. *Proc Natl Acad Sci USA.* (2012) 109:8517–22. doi: 10.1073/pnas.1200189109
72. Norris PC, Dennis EA. A lipidomic perspective on inflammatory macrophage eicosanoid signaling. *Adv Biol Regul.* (2014) 54:99–110. doi: 10.1016/j.jbior.2013.09.009
73. Li X, Yu Y, Funk CD. Cyclooxygenase-2 induction in macrophages is modulated by docosahexaenoic acid via interactions with free fatty acid receptor 4 (FFA4). *FASEB J.* (2013) 27:4987–97. doi: 10.1096/fj.13-235333
74. Yan Y, Jiang W, Spinetti T, Tardivel A, Castillo R, Bourquin C, et al. Omega-3 fatty acids prevent inflammation and metabolic disorder through inhibition of NLRP3 inflammasome activation. *Immunity.* (2013) 38:1154–63. doi: 10.1016/j.immuni.2013.05.015

75. Hwang DH, Kim JA, Lee JY. Mechanisms for the activation of Toll-like receptor 2/4 by saturated fatty acids and inhibition by docosahexaenoic acid. *Eur J Pharmacol.* (2016) 785:24–35. doi: 10.1016/j.ejphar.2016.04.024
76. Weatherill AR, Lee JY, Zhao L, Lemay DG, Youn HS, Hwang DH. Saturated and polyunsaturated fatty acids reciprocally modulate dendritic cell functions mediated through TLR4. *J Immunol.* (2005) 174:5390–7. doi: 10.4049/jimmunol.174.9.5390
77. Ricote M, Glass CK. PPARs and molecular mechanisms of transrepression. *Biochim Biophys Acta.* (2007) 1771:926–35. doi: 10.1016/j.bbalip.2007.02.013
78. Serhan CN, Yang R, Martinod K, Kasuga K, Pillai PS, Porter TF, et al. Maresins: novel macrophage mediators with potent antiinflammatory and proresolving actions. *J Exp Med.* (2009) 206:15–23. doi: 10.1084/jem.20081880
79. Ostermann AI, Schebb NH. Effects of omega-3 fatty acid supplementation on the pattern of oxylipins: a short review about the modulation of hydroxy-, dihydroxy-, and epoxy-fatty acids. *Food Funct.* (2017) 8:2355–67. doi: 10.1039/C7FO00403F
80. Sham HP, Walker KH, Abdulnour R-EE, Krishnamoorthy N, Douda DN, Norris PC, et al. 15-epi-lipoxin A(4), resolvin D2, and resolvin D3 induce NF-kappa B regulators in bacterial pneumonia. *Immunol.* (2018) 200:2757–66. doi: 10.4049/jimmunol.1602090
81. Titos E, Rius B, Lopez-Vicario C, Alcaraz-Quiles J, Garcia-Alonso V, Lopategi A, et al. Signaling and immunoresolving actions of resolvin D1 in inflamed human visceral adipose tissue. *J Immunol.* (2016) 197:3360–70. doi: 10.4049/jimmunol.1502522
82. Chiang N, Fredman G, Backhed F, Oh SF, Vickery T, Schmidt BA, et al. Infection regulates pro-resolving mediators that lower antibiotic requirements. *Nature.* (2012) 484:524–U152. doi: 10.1038/nature11042
83. Fredman G, Hellmann J, Proto JD, Kuriakose G, Colas RA, Dorweiler B, et al. An imbalance between specialized pro-resolving lipid mediators and pro-inflammatory leukotrienes promotes instability of atherosclerotic plaques. *Nat Commun.* (2016) 7:12859. doi: 10.1038/ncomms12859
84. Vordenbaumen S, Sokolowski A, Kutzner L, Rund KM, Dusing C, Chehab G, et al. Erythrocyte membrane polyunsaturated fatty acid profiles are associated with systemic inflammation and fish consumption in systemic lupus erythematosus: a cross-sectional study. *Lupus.* (2020) 29:554–9. doi: 10.1177/0961203320912326
85. Aghdassi E, Ma DW, Morrison S, Hillyer LM, Clarke S, Gladman DD, et al. Alterations in circulating fatty acid composition in patients with systemic lupus erythematosus: a pilot study. *JPEN J Parenter Enteral Nutr.* (2011) 35:198–208. doi: 10.1177/0148607110386378
86. Navarini L, Bisogno T, Margiotta DPE, Piccoli A, Angeletti S, Laudisio A, et al. Role of the specialized proresolving mediator resolvin D1 in systemic lupus erythematosus: preliminary results. *J Immunol Res.* (2018) 2018:5264195. doi: 10.1155/2018/5264195
87. Rice HB, Bernasconi A, Maki KC, Harris WS, von Schacky C, Calder PC. Conducting omega-3 clinical trials with cardiovascular outcomes: proceedings of a workshop held at ISSFAL 2014. *Prostagl Leukot Essent Fatty Acids.* (2016) 107:30–42. doi: 10.1016/j.plefa.2016.01.003
88. James MJ, Sullivan TR, Metcalf RG, Cleland LG. Pitfalls in the use of randomised controlled trials for fish oil studies with cardiac patients. *Br J Nutr.* (2014) 112:812–20. doi: 10.1017/S0007114514001408
89. Farquharson AL, Metcalf RG, Sanders P, Stuklis R, Edwards JR, Gibson RA, et al. Effect of dietary fish oil on atrial fibrillation after cardiac surgery. *Am J Cardiol.* (2011) 108:851–6. doi: 10.1016/j.amjcard.2011.04.036
90. Bhatt DL, Steg PG, Miller M, Brinton EA, Jacobson TA, Ketchum SB, et al. Cardiovascular risk reduction with icosapent ethyl for hypertriglyceridemia. *N Engl J Med.* (2019) 380:11–22. doi: 10.1056/NEJMoa1812792
91. O'Keefe EL, Harris WS, DiNicolantonio JJ, Elagizi A, Milani RV, Lavie CJ, et al. Sea change for marine omega-3s: randomized trials show fish oil reduces cardiovascular events. *Mayo Clin Proc.* (2019) 94:2524–33. doi: 10.1016/j.mayocp.2019.04.027
92. Akbar U, Yang M, Kurian D, Mohan C. Omega-3 fatty acids in rheumatic diseases: a critical review. *J Clin Rheumatol.* (2017) 23:330–9. doi: 10.1097/RHU.0000000000000563
93. Das UN. Beneficial effect of eicosapentaenoic and docosahexaenoic acids in the management of systemic lupus erythematosus and its relationship to the cytokine network. *Prostag Leukot Essent Fatty Acids.* (1994) 51:207–13. doi: 10.1016/0952-3278(94)90136-8
94. Piranavan P, Perl A. Management of cardiovascular disease in patients with systemic lupus erythematosus. *Expert Opin Pharmacother.* (2020) 5:75–100. doi: 10.1080/14656566.2020.1770227
95. Liu Y, Kaplan MJ. Cardiovascular disease in systemic lupus erythematosus: an update. *Curr Opin Rheumatol.* (2018) 30:441–8. doi: 10.1097/BOR.0000000000000528
96. Perl A. Oxidative stress in the pathology and treatment of systemic lupus erythematosus. *Nat Rev Rheumatol.* (2013) 9:674–86. doi: 10.1038/nrrheum.2013.147
97. Bays HE, Ballantyne CM, Braeckman RA, Stirtan WG, Soni PN. Icosapent ethyl, a pure ethyl ester of eicosapentaenoic acid: effects on circulating markers of inflammation from the MARINE and ANCHOR studies. *Am J Cardiovasc Drugs.* (2013) 13:37–46. doi: 10.1007/s40256-012-0002-3
98. Mori TA, Puddey IB, Burke V, Croft KD, Dunstan DW, Rivera JH, et al. Effect of omega 3 fatty acids on oxidative stress in humans: GC-MS measurement of urinary F2-isoprostane excretion. *Redox Rep.* (2000) 5:45–6. doi: 10.1179/rer.2000.5.1.45
99. Lands WE. Diets could prevent many diseases. *Lipids.* (2003) 38:317–21. doi: 10.1007/s11745-003-1066-0
100. Ramsden CE, Faurot KR, Zamora D, Suchindran CM, Macintosh BA, Gaylord S, et al. Targeted alteration of dietary n-3 and n-6 fatty acids for the treatment of chronic headaches: a randomized trial. *Pain.* (2013) 154:2441–51. doi: 10.1016/j.pain.2013.07.028
101. Harris WS, Von Schacky C. The Omega-3 index: a new risk factor for death from coronary heart disease? *Prev Med.* (2004) 39:212–20. doi: 10.1016/j.ypmed.2004.02.030
102. Del Gobbo LC, Imamura F, Aslibekyan S, Marklund M, Virtanen JK, Wennberg M, et al. Omega-3 polyunsaturated fatty acid biomarkers and coronary heart disease: Pooling project of 19 cohort studies. *JAMA Intern Med.* (2016) 176:1155–66. doi: 10.1001/jamainternmed.2016.2925
103. Adam O, Beringer C, Kless T, Lemmen C, Adam A, Wiseman M, et al. Anti-inflammatory effects of a low arachidonic acid diet and fish oil in patients with rheumatoid arthritis. *Rheumatol Int.* (2003) 23:27–36. doi: 10.1007/s00296-002-0234-7
104. Walker RE, Jackson KH, Tintle NL, Shearer GC, Bernasconi A, Masson S, et al. Predicting the effects of supplemental EPA and DHA on the omega-3 index. *Am J Clin Nutr.* (2019) 110:1034–40. doi: 10.1093/ajcn/nqz161
105. EFSA Panel on Dietetic Products NaAN. Scientific opinion related to the tolerable upper intake level of eicosapentaenoic acid (EPA), docosahexaenoic acid (DHA) and docosapentaenoic acid (DPA). *EFSA J.* (2012) 10:1–48. doi: 10.2903/j.efsa.2012.2815
106. Anders HJ, Saxena R, Zhao MH, Parodis I, Salmon JE, Mohan C. Lupus nephritis. *Nat Rev Dis Primers.* (2020) 6:7. doi: 10.1038/s41572-019-0141-9

Conflict of Interest: The authors declare that the research was conducted in the absence of any commercial or financial relationships that could be construed as a potential conflict of interest.

frontiers in Immunology

ORIGINAL RESEARCH
published: 30 October 2020
doi: 10.3389/fimmu.2020.590444

Serological Evidence for the Association Between Epstein-Barr Virus Infection and Sjögren's Syndrome

Jingxiu Xuan[1,2†], Zhiqian Ji[1†], Bin Wang[1†], Xiaoli Zeng[1], Rongjuan Chen[1,2], Yan He[1,2], Peishi Rao[1,2], Puqi Wu[1,2] and Guixiu Shi[1,2]*

[1] Department of Rheumatology and Clinical Immunology, The First Affiliated Hospital of Xiamen University, Xiamen, China,
[2] Department of Science & Technology, Xiamen Key Laboratory of Rheumatology and Clinical Immunology, Xiamen, China

Background: Exposure to Epstein-Barr virus (EBV) infection has been hypothesized to be an important risk factor for multiple rheumatic diseases, but the serological evidence so far for its role in Sjögren's syndrome (SjS) is not clearly established yet. This study aimed to assess the seroepidemiological associations of antibodies to EBV with SjS.

Methods: A seroepidemiological study containing 119 patients with SjS and 65 healthy controls was first performed, in which the associations of SjS with four commonly studied EBV antibodies including IgM-anti-viral capsid antigen (anti-VCA) antibody, IgG-anti-VCA antibody, IgG-anti-early antigen (anti-EA) antibody, and IgG-anti-EBV nuclear antigen 1 (anti-EBNA1) antibody were evaluated. A systematic review and meta-analysis of eligible seroepidemiological studies was also carried out, and data syntheses were performed using random-effect meta-analysis.

Results: In the case-control study, the patients with SjS had both a significantly higher prevalence of IgG-anti-EA antibody positivity (31.9% vs. 3.1%, $P < 0.001$) and high titers of IgG-anti-EA antibody ($P < 0.001$) than healthy controls. The titer of IgG-anti-VCA antibody was significantly increased in the patients with SjS compared with healthy controls ($P < 0.001$). IgG-anti-EA antibody seropositive patients with SjS had lower levels of both C3 ($P = 0.002$) and C4 ($P = 0.02$), and the titer of IgG-anti-EA antibody was inversely related to the levels of both C3 ($r = -0.31$, $P < 0.001$) and C4 ($r = -0.20$, $P = 0.03$). A total of 14 eligible studies on the serological associations between EBV infection and SjS were finally included into the meta-analysis, which suggested obvious associations of SjS with IgM-anti-VCA antibody [Odds ratio (OR) = 5.77, 95%CI 1.73–19.25, $P = 0.004$] and IgG-anti-EA antibody (OR = 9.97, 95%CI 4.58-21.67, $P < 0.00001$).

Conclusions: The findings from this study provide strong serological evidence for the association between EBV infection and SjS. SjS has obvious associations with IgM-anti-VCA antibody and IgG-anti-EA antibody. IgG-anti-EA antibody is linked to low levels of C3 and C4 in the patients with SjS, the significance of which needs to be addressed in further studies.

Keywords: Epstein-Barr virus, Sjögren's syndrome, systematic review, associations, meta-analysis

OPEN ACCESS

Edited by:
Allen Jay Rosenspire, Wayne State University, United States

Reviewed by:
Gunnar Houen, Statens Serum Institut (SSI), Denmark
William Lee, Wadsworth Center, United States

****Correspondence:***
Guixiu Shi
gshi@xmu.edu.cn

[†]These authors have contributed equally to this work

Specialty section:
This article was submitted to Autoimmune and Autoinflammatory Disorders, a section of the journal Frontiers in Immunology

Received: *01 August 2020*
Accepted: *09 October 2020*
Published: *30 October 2020*

Citation:
Xuan J, Ji Z, Wang B, Zeng X, Chen R, He Y, Rao P, Wu P and Shi G (2020) Serological Evidence for the Association Between Epstein-Barr Virus Infection and Sjögren's Syndrome. Front. Immunol. 11:590444. doi: 10.3389/fimmu.2020.590444

INTRODUCTION

Sjögren's syndrome (SjS) is a complex and heterogeneous rheumatic disease (1). SjS is characterized by autoantibody production and lymphocyte infiltration in exocrine glands such as salivary and lacrimal glands (2, 3). Exocrine glandular injuries induced by autoimmune attacks can gradually cause dryness of eyes and mouth (1). Like systemic lupus erythematosus (SLE) and rheumatoid arthritis (RA), the pathogenesis of SjS involves a complex interplay between genetic, immune and environmental factors, and the underlying molecular mechanisms remain to be defined (4–7). Though many studies have explored possible treatments of SjS, effective targeted therapies for SjS are still lacking (8, 9). Further studies are needed to elucidate SjS pathogenesis and find possible therapeutic targets.

Infections such as Epstein-Barr virus (EBV) infection have been proposed as one of the environmental triggers of SjS (10, 11). EBV is a common herpes virus affecting more than 90% of the total population worldwide (12). The possible roles of EBV infection in rheumatic diseases have been postulated for many years, and it has proven to be an important environmental trigger of several autoimmune diseases such as SLE and multiple sclerosis (MS) (13–16). Like SLE, a possible link between EBV infection and SjS has also been proposed for many years (17, 18). Increased prevalence of EBV infection and elevated viral loads in salivary glands had been reported in patients with SjS (19–21). There were also some studies exploring the serological evidence for the pathogenic role of EBV infection in SjS, and associations of SjS with EBV antibodies such as IgM-anti-viral capsid antigen (anti-VCA) antibody, IgG-anti-VCA antibody, IgG-anti-early antigen (anti-EA) antibody and IgG-anti-EBV nuclear antigen 1 (anti-EBNA1) antibody had been studied. However, the findings from these various studies were inconsistent (22–28). Therefore, the serological evidence for the contribution of EBV infection to the pathophysiology of SjS is not firmly established. To further explore the link between EBV antibodies and SjS, we performed an original seroepidemiological case-control study at first. We then carried out a systematic review and meta-analysis of available seroepidemiological studies on the associations between antibodies to EBV and SjS.

METHODS

Participants

A seroepidemiological study using case-control design was performed to evaluate the association between EBV infection and SjS, in which the associations of SjS with EBV antibodies were analyzed. 119 patients with SjS were recruited in The First Affiliated Hospital of Xiamen University from June 2018 to December 2019. SjS was diagnosed according to the 2016 American College of Rheumatology (ACR) and the European League Against Rheumatism (EULAR) classification criteria for SjS (29). 65 healthy controls without autoimmune diseases were randomly recruited from individuals receiving routine medical examination in our hospital, whose age and gender matched SjS patients. The mean age of the SjS patients was 51.2 ± 15.7 years, and the mean age of the healthy controls was 50.7 ± 11.1 years (**Supplementary Table 1**). This study was approved by the Medical Ethics Committee at The First Affiliated Hospital of Xiamen University (KY202015-034). Written informed consent was obtained from all participants.

Clinical Assessment

The disease activity of SjS patients was evaluated by the EULAR Sjögren's syndrome disease activity index (ESSDAI) (30). Clinical data such as age, gender, disease history, clinical manifestations and treatment drugs were collected. Outcomes of laboratory tests such as anti-SSA/Ro, anti-SSB/La, C3, and C4 were also recorded.

Detection of EBV Antibodies

Sera from SjS patients and healthy controls were stored at -80°C. Four commonly used antibodies to EBV including IgM-anti-VCA antibody, IgG-anti-VCA antibody, IgG-anti-EA antibody and IgG-anti-EBNA1 antibody were analyzed. EBV antibodies were detected by using commercial enzyme-linked immunosorbent assay (ELISA) kits according to the manufacturer's instructions (EUROIMMUN, Germany). The cut-off values for positivity of IgG-anti-VCA antibody, IgG-anti-EA antibody and IgG-anti-EBNA1 antibody were defined as 22 RU/ml, and the cut-off value for IgM-anti-VCA antibody positivity was defined as a ratio of $OD_{Patient}/OD_{Standard}$ or $OD_{Control}/OD_{Standard}$ more than 1.1.

Statistical Analysis

Quantitative variables were shown as mean ± standard deviation (SD) or median with interquartile range (IQR). Categorical variables were shown as counts with percentages. Differences in quantitative data between groups were compared by student's t-test or Mann-Whitney U test when necessary. Differences in categorical variables between groups were compared by Chi-square or Fischer's exact tests. Odds ratios (OR) with 95% confidence intervals (95%CI) were calculated to evaluate the associations between EBV antibodies and SjS. Data analyses were performed using GraphPad (Version 7.0, GraphPad Software, California, USA) and STATA (Version 12.0, StataCorp, Texas, USA). All tests were two-sided, and outcomes were considered statistically significant at $P < 0.05$.

Systematic Review and Meta-Analysis

A systematic review and meta-analysis was performed to evaluate the relationship between antibodies to EBV and patients with SjS. We searched Pubmed and China National

Abbreviations: anti-EA, anti-early antigen; anti-EBNA1, anti-EBV nuclear antigen 1; anti-VCA, anti-viral capsid antigen; CR2, complement receptor type 2; CNKI, China National Knowledge Infrastructure; EBV, Epstein-Barr virus; ELISA, enzyme-linked immunosorbent assay; ELS, ectopic lymphoid structures; ESSDAI, European League Against Rheumatism Sjögren's syndrome disease activity index; IF, immunofluorescence; IFN-α, interferon-α; IQR, interquartile range; MS, multiple sclerosis; OR, Odds ratios; pDC, plasmacytoid dendritic cells; RA, rheumatoid arthritis; RF, rheumatoid factor; SD, standard deviation; SGECs, salivary glandular epithelial cells; SjS, Sjögren's syndrome; SLE, systemic lupus erythematosus; TLR-9, Toll-like receptor 9; 95%CI, 95% confidence interval.

Knowledge Infrastructure (CNKI) from inception to May 16, 2020, to identify epidemiological studies on the serological associations between antibodies to EBV and SjS. We also searched the reference citations of those included studies to identify more possible articles. The following terms were used in the literature search: (Epstein-Barr virus OR EBV OR human herpesvirus 4 OR HHV-4) AND (Sjogren's syndrome OR Sjögren's syndrome OR Sjogren syndrome OR Sjögren syndrome). No language restriction was applied. Articles concerning the epidemiological associations of anti-EBV antibodies with SjS were reviewed. Studies eligible into the systematic review met the following criteria: 1) Clinical observational studies such as cohort studies, cross-sectional studies or case-control studies; 2) Participants contained at least 10 SjS patients; 3) Reporting data on the serological associations of EBV antibodies with SjS; 4) EBV antibodies were examined using recommended clinical laboratory methods such as immunofluorescence (IF) or ELISA; 5) Data did not overlap with other included studies. Studies not meeting the above eligible criteria were all excluded. Studies that did not specify the type of anti-EBV antibodies or did not provide usable data were excluded.

Two authors independently extracted data from eligible studies such as authors, country, sample size, types of EBV antibodies, laboratory methods, diagnostic criteria of SjS, cut-off values of seropositivity, and risk estimates with 95%CIs. Discrepancies in the data extracted by those two authors were resolved *via* group discussions among all authors.

Heterogeneity among included studies was assessed using the I^2-statistic, and I^2 more than 50% suggested high heterogeneity (31). To reduce the impact of heterogeneity on the pooled risk estimates, meta-analysis was performed by DerSimonian and Laird's random-effect model (32). Publication bias was assessed by funnel plot. Review Manager (Version 5.2; Cochrane, London, United Kingdom) was used in statistical analyses, and P values less than 0.05 were considered statistically significant.

RESULTS

Case-Control Study

The clinical characteristics of SjS patients and healthy controls in the case-control study are shown in **Supplementary Table 1**. There was no obvious difference in age and gender between SjS patients and healthy controls (P > 0.05). The mean ESSDAI of those 119 SjS patients was 2.1 ± 1.5.

Compared with healthy subjects, SjS patients had both a significantly higher prevalence of IgG-anti-EA antibody positivity (31.9% vs. 3.1%, P < 0.001) and higher titers of IgG-anti-EA antibody (P < 0.001; **Table 1**). There was no obvious difference in the prevalence of IgM-anti-VCA antibody, IgG-anti-VCA antibody and IgG-anti-EBNA1 antibody between SjS patients and controls (P > 0.05; **Table 1**). However, the titer of IgG-anti-VCA antibody was significantly increased in SjS patients compared to healthy controls (P < 0.001; **Table 1**, **Figures 1A–C**). The titer of anti-EBNA1 IgG antibody was marginally increased in SjS patients than healthy controls (P = 0.07; **Table 1**).

TABLE 1 | Associations between EBV antibodies and SjS in the case-control study.

EBV antibodies	SjS (n=119)	Controls (n=65)	P value
IgM-anti-VCA antibody			
Positivity (n, %)	3(2.5%)	0(0.0%)	0.55
IgG-anti-VCA antibody			
Antibody titers	166(123–200)	121(88–162)	**<0.001***
Positivity (n, %)	117(98.3%)	62(95.4%)	0.35
IgG-anti-EA antibody			
Antibody titers	9(4–56)	3(2–4)	**<0.001***
Positivity (n, %)	38(31.9%)	2(3.1%)	**<0.001***
IgG-anti-EBNA1 antibody			
Antibody titers	128(69–186)	100(54–160)	0.07
Positivity (n, %)	107(89.9%)	56(86.2%)	0.44

**Bold values suggested statistically significant findings.*

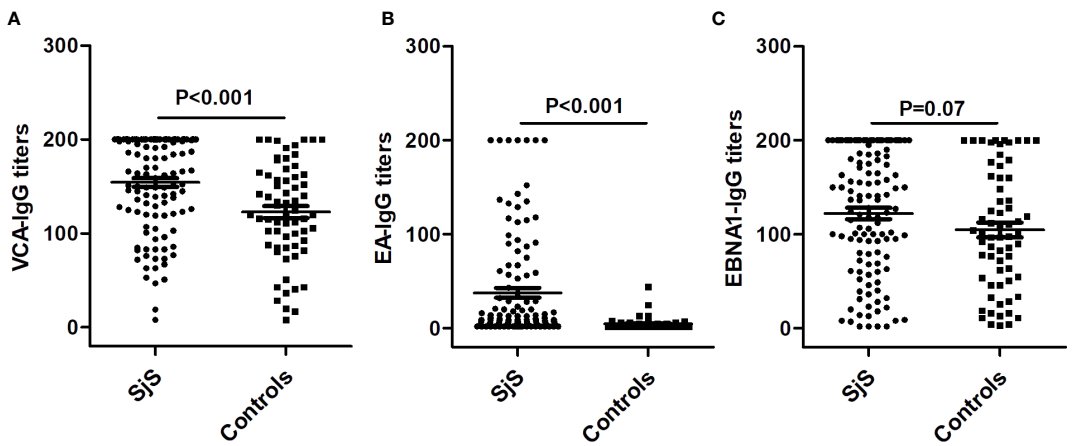

FIGURE 1 | Differences in the titers of IgG-anti-VCA antibody, IgG-anti-EA antibody and IgG-anti-EBNA1 antibody between SjS patients and healthy controls. **(A)** The difference in the titers of IgG-anti-VCA antibody between SjS patients and healthy controls. **(B)** The difference in the titers of IgG-anti-EA antibody between SjS patients and healthy controls. **(C)** The difference in the titers of IgG-anti-EBNA1 antibody between SjS patients and healthy controls.

The clinical characteristics of SjS patients stratified by seropositivity status of EBV antibodies were then analyzed. As shown in the supplementary tables (**Supplementary Tables 2–5**), IgG-anti-EA antibody seropositive patients with SjS had lower levels of both C3 (P = 0.002) and C4 (P = 0.02). Among those 119 SjS patients, the titer of IgG-anti-EA antibody was inversely related to the levels of C3 (r = -0.31, P < 0.001) and C4 (r = -0.20, P = 0.03), and a marginally significant inverse correlation between IgG-anti-VCA antibody titer and C3 level was also observed (r = -0.17, P = 0.06) (**Table 2**). The titers of other EBV antibodies were not significantly related to the levels of C3 and C4 except for the marginally significant correlation between IgG-anti-VCA antibody and C3 level (P = 0.06; **Table 2**). The disease activity of SjS patients evaluated by ESSDAI was not significantly correlated with EBV antibodies (P > 0.05; **Table 2**).

TABLE 2 | Correlations of EBV antibodies with clinical characteristics of SjS patients.

EBV antibodies	Spearman r	P value
IgG-anti-VCA antibody		
Age	0.16	0.08
ESSDAI	0.08	0.39
C3	-0.17	0.06
C4	-0.08	0.39
IgG-anti-EA antibody		
Age	0.08	0.37
ESSDAI	0.09	0.31
C3	-0.31	**<0.001***
C4	-0.20	**0.03***
IgG-anti-EBNA1 antibody		
Age	-0.05	0.58
ESSDAI	0.07	0.48
C3	-0.07	0.46
C4	-0.10	0.29

**Bold values suggested statistically significant findings.*

Systematic Review and Meta-Analysis

A total of 261 publications were found in the literature search. 224 studies were excluded after the initial evaluation by reading titles and abstracts. The rest of 37 studies were evaluated in details by reading full-texts, and 24 studies were further excluded as they did not analyze the epidemiological associations of EBV antibodies with SjS. Finally, 13 published studies focusing on the serological association between EBV infection and SjS were identified (22–28, 33–38). Among those 13 published studies, nine studies reported outcomes on IgG-anti-VCA antibody, seven studies reported outcomes on IgM-anti-VCA antibody, 6 studies reported outcomes on IgG-anti-EA antibody, and nine studies reported outcomes on IgG-anti-EBNA1 antibody (**Table 3**). Together with the present case-control study, a total of 14 available studies on the serological association between EBV infection and SjS were finally included into the meta-analysis (**Table 3**).

Obvious heterogeneity was found among those eight studies on the association between IgM-anti-VCA antibody and SjS (I^2 = 59%; **Figures 2A–D**). Meta-analysis of those eight studies suggested that IgM-anti-VCA antibody was significantly associated with SjS (Pooled OR = 5.77, 95%CI 1.73-19.25, P = 0.004) (**Figure 2A**). Obvious heterogeneity was also found among those seven studies on the association between IgG-anti-EA antibody and SjS (I^2 = 62%), and meta-analysis of those seven studies revealed an obvious association between IgG-anti-EA antibody and SjS (Pooled OR = 9.97, 95%CI 4.58-21.67, P < 0.00001) (**Figure 2C**). However, obvious associations of SjS with IgG-anti-EBNA1 antibody and IgG-anti-VCA antibody were not found (P > 0.05; **Figures 2B, D**).

Funnel plots in this meta-analysis suggested low risk of publication bias, and all those 4 funnel plots were nearly symmetric (**Figure 3**).

TABLE 3 | Summarization of 14 studies focusing on the serological association between EBV infection and SjS.

Study	Country	Participants	Detection method	EBV antibodies
Venables PJ 1985 (22)	UK	26 SjS patients and 26 healthy controls	Indirect IF	IgG-anti-VCA antibody
Yamaoka K 1988 (33)	Japan	26 SjS patients and 15 healthy controls	Indirect IF	IgG-anti-VCA and IgM-anti-VCA antibodies
Venables PJ 1989 (25)	UK	20 SjS patients and 35 healthy controls	ELISA	IgG-anti-EBNA1 antibody
Inoue N 1991 (23)	Japan	32 SjS patients and 38 healthy controls	ELISA	IgG-anti-EBNA1 antibody
Yang J 1991 (34)	China	95 SjS patients and 8 healthy controls	Indirect IF	IgG-anti-VCA, IgM-anti-VCA and IgG-anti-EBNA1 antibodies
Marchini B 1994 (24)	Italy	12 SjS patients and 20 healthy controls	ELISA	IgG-anti-EBNA1 antibody
Toda I 1994 (26)	Japan	62 SjS patients and 47 healthy controls	Indirect IF	IgG-anti-VCA, IgG-anti-EA, and IgG-anti-EBNA1 antibodies
Gao C 2010 (35)	China	29 SjS patients and 44 healthy controls	ELISA	IgM-anti-VCA, IgG-anti-VCA and IgG-anti-EA antibodies
Li H 2014 (36)	China	75 SjS patients and 74 healthy controls	ELISA	IgM-anti-VCA, IgG-anti-VCA and IgG-anti-EA antibodies
Yang L 2015 (37)	China	39 SjS patients and 22 healthy controls	ELISA	IgG-anti-EBNA1 antibody
Zhang L 2019 (38)	China	72 SjS patients and 60 healthy controls	ELISA	IgM-anti-VCA, IgG-anti-VCA, IgG-anti-EA and IgG-anti-EBNA1 antibodies
Pasoto SG 2013 (27)	Brazil	100 SjS patients and 89 healthy controls	ELISA	IgM-anti-VCA, IgG-anti-VCA, IgG-anti-EA and IgG-anti-EBNA1 antibodies
Kivity S 2014 (28)	Israel	82 SjS patients and 139 healthy controls	Multiplexed assay	IgM-anti-VCA, IgG-anti-VCA, IgG-anti-EA and IgG-anti-EBNA1 antibodies
Present study	China	119 SjS patients and 65 healthy controls	ELISA	IgM-anti-VCA, IgG-anti-VCA, IgG-anti-EA and IgG-anti-EBNA1 antibodies

IF, immunofluorescence; ELISA, enzyme linked immunosorbent assay; SjS, Sjögren's syndrome; VCA, viral capsid antigen; EA, early antigen; EBNA1, EBV nuclear antigen 1.

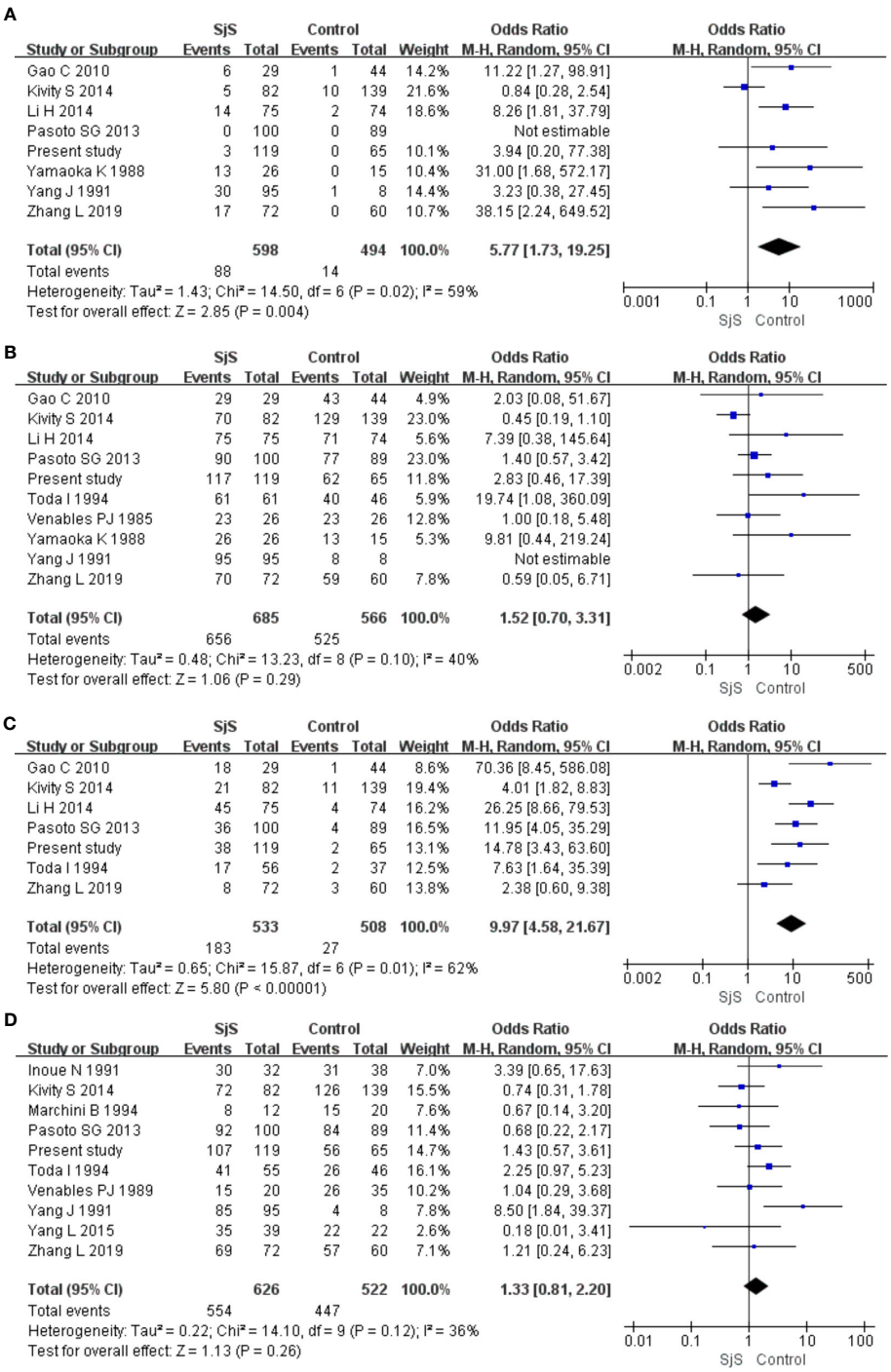

FIGURE 2 | Forest plots in the meta-analysis of the associations between EBV antibodies and SjS. **(A)** Forest plot in the meta-analysis of the association between IgM-anti-VCA antibody and SjS. **(B)** Forest plot in the meta-analysis of the association between IgG-anti-VCA antibody and SjS. **(C)** Forest plot in the meta-analysis of the association between IgG-anti-EA antibody and SjS. **(D)** Forest plot in the meta-analysis of the association between IgG-anti-EBNA1 antibody and SjS.

DISCUSSION

Though EBV infection has been hypothesized to be a possible risk factor of SjS in a long term, prior studies have revealed conflicting results and the serological evidence is not yet definitely established (**Table 3**). For instance, half of those published studies on the association between IgM-anti-VCA antibody and SjS did not detect an obvious correlation, which

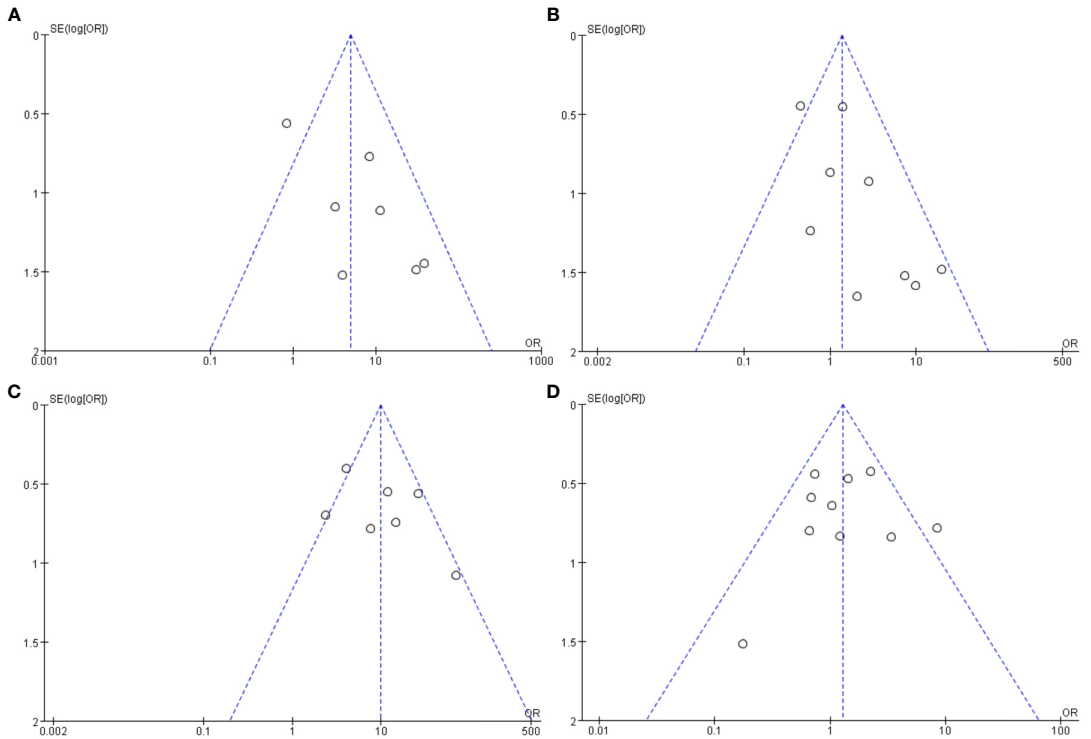

FIGURE 3 | Funnel plots in the meta-analysis of the associations between EBV antibodies and SjS. **(A)** Funnel plot in the meta-analysis on IgM-anti-VCA antibody. **(B)** Funnel plot in the meta-analysis on IgG-anti-VCA antibody. **(C)** Funnel plot in the meta-analysis on IgG-anti-EA antibody. **(D)** Funnel plot in the meta-analysis on IgG-anti-EBNA1 antibody.

may result from the low statistical power caused by the limited sample size. In the present study, we assessed the serological association between antibodies to EBV and SjS through both an original case-control study and a meta-analysis. The meta-analysis included a total of 14 studies, and could provide a more robust evaluation of the associations between antibodies to EBV and SjS by increasing sample size and statistical power. An obvious association of SjS with IgG-anti-EA antibody was observed in both our case-control study and the meta-analysis, and an obvious association of SjS with IgM-anti-VCA antibody was confirmed in the meta-analysis. However, IgG-anti-VCA antibody and IgG-anti-EBNA1 antibody were not associated with SjS in either the case-control study or the meta-analysis. Therefore, the above findings provide serological evidence for the association between EBV infection and SjS, and also scrutinize the different associations of SjS with different antibodies to EBV.

Multiple factors such as genetic factors, immunological abnormality and environmental risk factors are involved in the development of rheumatic diseases, and EBV infection has been proposed as an important environmental risk factor (39, 40). A meta-analysis by Hanlon et al. found that patients with SLE had significantly higher rates of IgG-anti-VCA antibody, IgA-anti-VCA antibody and IgG-anti-EA antibody than controls, but not IgG-anti-EBNA1 antibody (41). A recent study by Jog et al. revealed that EBV serological reactivation was associated with the probability of transitioning to SLE in at-risk individuals (42). A meta-analysis by Kudaeva et al. reported that the patients with RA had obviously higher rates of IgG-anti-VCA and IgG-anti-EA antibodies than controls, but not for IgG-anti-EBNA1 antibody (43). Therefore, there is compelling serological evidence for EBV infection as an important risk factor of SLE and RA. Our study revealed the obvious associations of SjS with IgM-anti-VCA antibody and IgG-anti-EA antibody *via* a systematic review and meta-analysis of 14 available studies, which added the evidence of EBV infection as an important environmental risk factor for SjS development.

There are some possible explanations for the discrepancy in the associations of SjS with different EBV antibodies. Molecular mimicry has been suggested to be a key mechanism underlying the role of EBV infection in triggering autoimmune diseases (44, 45). The sequence similarities or homologous peptides between human proteins and EBV viral proteins are different across those EBV viral antigens, and immune responses to different EBV viral antigens are distinct (46, 47). Different EBV viral antigens may have distinct cross reactivity with different autoantigens, and thus trigger the immune system to produce specific antibodies with distinct pathogenicity in SjS etiology, which may lead to the discrepancy in the associations of SjS with different EBV antibodies (48, 49). In addition, the non-significant associations of SjS with other EBV antibodies may result from the low statistical power caused by the relatively small sample size. For instance, though our study and one prior study indicated that the titer of IgG-anti-VCA antibody was

significantly increased in patients with SjS compared with healthy controls (50), IgG-anti-VCA antibody positivity was not associated with SjS in both the original case-control study and the meta-analysis. Both patients with SjS and healthy controls have been found to have a high prevalence of IgG-anti-VCA antibody positivity (over 90%), and the sample size required to detect a significant association between IgG-anti-VCA antibody positivity and SjS in an epidemiological study is undoubtedly increased. To provide a more accurate estimate of the associations of SjS with EBV antibodies, further epidemiological studies on a large-scale are recommended.

An intriguing finding in our study is the inverse association between the titer of IgG-anti-EA antibody and the levels of C3 ($r = -0.31$, $P < 0.001$) and C4 ($r = -0.20$, $P = 0.02$) (**Table 2**). Low C3 or C4 levels can reflect disease severity of the patients with SjS, and are related to disease progression and poor outcomes (51–53). The lower levels of C3 and C4 in IgG-anti-EA antibody seropositive patients with SjS suggest that IgG-anti-EA antibody may have the possibility of promoting the progression of SjS by exhausting C3 and C4. Wilson et al. found that the serum cryoprecipitates from SjS patients contained autoantibodies to La and rheumatoid factor (RF) as well as complement proteins C3 and C4, which could activate classical complement pathway or alternative complement pathway (54). A key possible mechanism for the decreased C3 and C4 is the activation of complement system during EBV infection. In absence of antibodies, complement system may be activated with viral surface molecules and polysaccharides *via* alternative and mannose-lectin pathways during innate immunity (55, 56). In the presence of antibodies, antigen-antibody complexes formed by EBV antigens bound by antibodies can further activate complement system (57–59). Both C3 and C4 are the key components of the complement system, and can be exhausted by EBV-induced activation of the complement system. Furthermore, higher levels of IgG-anti-VCA antibody and IgG-anti-EA antibody have been proposed as indicators of chronic or frequent EBV reactivation, and EBV reactivation is intensively involved in the progression of EBV-related diseases (60–63). Frequent EBV reactivation can promote the production of EBV-related antibodies, which can further exhaust circulating complement proteins and result in decreased C3 and C4.

EBV can infect a variety of cell types such as B cells, epithelial cells, T cells and dendritic cells (64, 65). Published studies have revealed that high EBV viral loads and EBV-related antibodies exist in salivary glandular epithelial cells (SGECs) and saliva of SjS patients, and EBV antigens such as the lytic cycle antigen EA/D also exist in the SGECs of SjS patients (19, 66–68). Additionally, MHC-II molecules and viral early antigen have been found to be inappropriately expressed in SGECs of SjS patients, which may lead to vicious immune responses and promote the chronic inflammation in SGECs during SjS development (69). These studies imply that EBV can infect SGECs and trigger immune damages to salivary epithelium, which may promote the autoimmune processes in SjS pathogenesis.

EBV infection may be involved in SjS pathogenesis by promoting the activation of autoreactive B and T cells. EBV can infect B cells *via* envelope gp350/220 binding to the complement receptor type 2 (CR2) on B cells and *via* gp42 interacting with HLA class II molecules on B cells (64, 70, 71). The binding of the complex of C3d and EBV or antigen-antibody complexes to B cells brings CD19 into proximity of BCR-associated kinases, and the cytoplasmic tail of CD19 rapidly becomes tyrosine-phosphorylated, which can further promote the proliferation and activation of B cells (72–75). Some EBV proteins such as LMP2A and LMP1 have proven to prevent infected B cells from apoptosis and thus promote the progression of autoimmunity (76–79). Some studies have suggested that EBV can alter the differentiation and interrupt the normal function of T cells through different mechanisms, which may contribute to autoimmunity development (80–83). Therefore, EBV infection can cause the abnormal activation of B cells and/or T cells, which can further result in loss of immune tolerance and the development of autoimmunity (84–87). In SjS, active EBV infection has been found to be related to ectopic lymphoid structures (ELS) in the glandular tissues of SjS patients, suggesting that it may drive local autoimmune response and the activation of autoreactive B cells during the progression of SjS (88, 89).

There are other explanations for the roles of EBV infection in the pathogenesis of SjS (11). One explanation is molecular mimicry between EBV proteins and self antigens, which may promote the development of SjS through inducing the formation of cross-reactive autoantibodies to both pathogens and self-antigens (90–93). For instance, a study by Navone et al. found that antibodies to EBV could recognize autoantigens such as alpha-fodrin and tear lipocalin (94). Moreover, EBV can directly regulate innate immune cells such as dendritic cells (95, 96). An activated interferon-α (IFN-α) signature pathway is involved in the autoimmune process of SjS, and EBV DNA and RNA have been reported to activate plasmacytoid dendritic cells (pDC) through engagement of Toll-like receptor 9 (TLR-9) and TLR-7, and then increase IFN-α production (95, 96). To date, there is no confirming evidence to verify the pathogenic role of EBV in SjS pathogenesis, and the link remains to be further elaborated.

Several limitations exist in the present study. A major limitation is the retrospective case-control design in those included studies, which was unable to adequately evaluate the causality between antibodies to EBV and SjS. Further studies using a prospective design are recommended. Besides, the sample size of some included studies was limited, and owing to the limited sample size of recruited participants, the influence of other confounding factors such as treatment drugs on the associations of anti-EBV antibodies with SjS was not excluded. Finally, the cut-off values determining seropositivity of anti-EBV antibodies were different among the included studies, which may result in obvious heterogeneity in the meta-analysis and impair the strength of the findings.

In summary, the findings from this study provide strong serological evidence for the association between EBV infection and SjS. Moreover, anti-EA-IgG antibody is likely linked to low levels of C3 and C4 in patients with SjS. More efforts in addressing the roles of EBV infection in SjS and the underlying molecular mechanisms are needed.

DATA AVAILABILITY STATEMENT

The raw data supporting the conclusions of this article will be made available by the authors, without undue reservation.

ETHICS STATEMENT

The studies involving human participants were reviewed and approved by Medical Ethics Committee at The First Affiliated Hospital of Xiamen University. The patients/participants provided their written informed consent to participate in this study.

AUTHOR CONTRIBUTIONS

GS and JX designed the study and wrote the manuscript. ZJ and BW analyzed data and wrote the manuscript. XZ, RC, PR, YH, and PW collected samples and data. All authors contributed to the article and approved the submitted version.

FUNDING

This work was supported by grants from the National Natural Science Foundation of China (Grant No. 81971536 and No. U1605223) to GS, the First Affiliated Hospital of Xiamen University Projects for Young Scholar, China Funding (No. XYY2016013) to ZJ, and the National Natural Science Foundation of China (No.81701556) to YH.

ACKNOWLEDGMENTS

All authors would like to thank the researchers for their data used in meta-analysis in this work.

SUPPLEMENTARY MATERIAL

The Supplementary Material for this article can be found online at: https://www.frontiersin.org/articles/10.3389/fimmu.2020.590444/full#supplementary-material

REFERENCES

1. Mariette X, Criswell LA. Primary Sjogren's Syndrome. *N Engl J Med* (2018) 378(10):931–9. doi: 10.1056/NEJMcp1702514
2. Martin-Nares E, Hernandez-Molina G. Novel autoantibodies in Sjogren's syndrome: A comprehensive review. *Autoimmun Rev* (2019) 18(2):192–8. doi: 10.1016/j.autrev.2018.09.003
3. Mavragani CP, Moutsopoulos HM. Sjogren's syndrome. *Annu Rev Pathol* (2014) 9:273–85. doi: 10.1146/annurev-pathol-012513-104728
4. Psianou K, Panagoulias I, Papanastasiou AD, de Lastic AL, Rodi M, Spantidea PI, et al. Clinical and immunological parameters of Sjogren's syndrome. *Autoimmun Rev* (2018) 17(10):1053–64. doi: 10.1016/j.autrev.2018.05.005
5. Fessler J, Fasching P, Raicht A, Hammerl S, Weber J, Lackner A, et al. Lymphopenia in primary Sjogren's syndrome is associated with premature aging of naive CD4+ T cells. *Rheumatology* (2020). doi: 10.1093/rheumatology/keaa105
6. Bjork A, Mofors J, Wahren-Herlenius M. Environmental factors in the pathogenesis of primary Sjogren's syndrome. *J Internal Med* (2020) 287 (5):475–92. doi: 10.1111/joim.13032
7. Lucchesi D, Coleby R, Pontarini E, Prediletto E, Rivellese F, Hill DG, et al. Impaired IL-27 Mediated Control of CD4+ T Cell Function Impacts on Ectopic Lymphoid Structure Formation in Patients with Sjogren's Syndrome. *Arthritis Rheumatol* (2020). doi: 10.1002/art.41289
8. Felten R, Scher F, Sibilia J, Gottenberg JE, Arnaud L. The pipeline of targeted therapies under clinical development for primary Sjogren's syndrome: A systematic review of trials. *Autoimmun Rev* (2019) 18(6):576–82. doi: 10.1016/j.autrev.2018.12.008
9. Ramos-Casals M, Brito-Zeron P, Bombardieri S, Bootsma H, De Vita S, Dorner T, et al. EULAR recommendations for the management of Sjogren's syndrome with topical and systemic therapies. *Ann Rheum Dis* (2020) 79 (1):3–18. doi: 10.1136/annrheumdis-2019-216114
10. Bjork A, Thorlacius GE, Mofors J, Richardsdotter Andersson E, Ivanchenko M, Tingstrom J, et al. Viral antigens elicit augmented immune responses in primary Sjogren's syndrome. *Rheumatology* (2020) 59(7):1651–61. doi: 10.1093/rheumatology/kez509
11. Maslinska M. The role of Epstein-Barr virus infection in primary Sjogren's syndrome. *Curr Opin Rheumatol* (2019) 31(5):475–83. doi: 10.1097/BOR.0000000000000622
12. Smatti MK, Al-Sadeq DW, Ali NH, Pintus G, Abou-Saleh H, Nasrallah GK. Epstein-Barr Virus Epidemiology, Serology, and Genetic Variability of LMP-1 Oncogene Among Healthy Population: An Update. *Front Oncol* (2018) 8:211. doi: 10.3389/fonc.2018.00211
13. Belbasis L, Bellou V, Evangelou E, Ioannidis JP, Tzoulaki I. Environmental risk factors and multiple sclerosis: an umbrella review of systematic reviews and meta-analyses. *Lancet Neurol* (2015) 14(3):263–73. doi: 10.1016/S1474-4422(14)70267-4
14. Draborg AH, Jorgensen JM, Muller H, Nielsen CT, Jacobsen S, Iversen LV, et al. Epstein-Barr virus early antigen diffuse (EBV-EA/D)-directed immunoglobulin A antibodies in systemic lupus erythematosus patients. *Scand J Rheumatol* (2012) 41(4):280–9. doi: 10.3109/03009742.2012.665944
15. Toussirot E, Roudier J. Epstein-Barr virus in autoimmune diseases. *Best Pract Res Clin Rheumatol* (2008) 22(5):883–96. doi: 10.1016/j.berh.2008.09.007
16. Almohmeed YH, Avenell A, Aucott L, Vickers MA. Systematic review and meta-analysis of the sero-epidemiological association between Epstein Barr virus and multiple sclerosis. *PloS One* (2013) 8(4):e61110. doi: 10.1371/journal.pone.0061110
17. Harley JB, Zoller EE. Editorial: What caused all these troubles, anyway? Epstein-Barr virus in Sjogren's syndrome reevaluated. *Arthritis Rheumatol* (2014) 66(9):2328–30. doi: 10.1002/art.38725
18. Miyasaka N, Saito I, Haruta J. Possible involvement of Epstein-Barr virus in the pathogenesis of Sjogren's syndrome. *Clin Immunol Immunopathol* (1994) 72(2):166–70. doi: 10.1006/clin.1994.1124
19. Karameris A, Gorgoulis V, Iliopoulos A, Frangia C, Kontomerkos T, Ioakeimidis D, et al. Detection of the Epstein Barr viral genome by an in situ hybridization method in salivary gland biopsies from patients with secondary Sjogren's syndrome. *Clin Exp Rheumatol* (1992) 10(4):327–32.
20. Tateishi M, Saito I, Yamamoto K, Miyasaka N. Spontaneous production of Epstein-Barr virus by B lymphoblastoid cell lines obtained from patients with Sjogren's syndrome. Possible involvement of a novel strain of Epstein-Barr virus in disease pathogenesis. *Arthritis Rheum* (1993) 36(6):827–35. doi: 10.1002/art.1780360614
21. Mariette X, Gozlan J, Clerc D, Bisson M, Morinet F. Detection of Epstein-Barr virus DNA by in situ hybridization and polymerase chain reaction in salivary gland biopsy specimens from patients with Sjogren's syndrome. *Am J Med* (1991) 90(3):286–94. doi: 10.1016/0002-9343(91)80007-9
22. Venables PJ, Ross MG, Charles PJ, Melsom RD, Griffiths PD, Maini RN. A seroepidemiological study of cytomegalovirus and Epstein-Barr virus in rheumatoid arthritis and sicca syndrome. *Ann Rheum Dis* (1985) 44 (11):742–6. doi: 10.1136/ard.44.11.742

23. Inoue N, Harada S, Miyasaka N, Oya A, Yanagi K. Analysis of antibody titers to Epstein-Barr virus nuclear antigens in sera of patients with Sjogren's syndrome and with rheumatoid arthritis. *J Infect Dis* (1991) 164(1):22–8. doi: 10.1093/infdis/164.1.22
24. Marchini B, Dolcher MP, Sabbatini A, Klein G, Migliorini P. Immune response to different sequences of the EBNA I molecule in Epstein-Barr virus-related disorders and in autoimmune diseases. *J Autoimmun* (1994) 7 (2):179–91. doi: 10.1006/jaut.1994.1014
25. Venables PJ, Baboonian C, Horsfall AC, Halliday D, Maini RN, Teo CG, et al. The response to Epstein-Barr virus infection in Sjogren's syndrome. *J Autoimmun* (1989) 2(4):439–48. doi: 10.1016/0896-8411(89)90173-x
26. Toda I, Ono M, Fujishima H, Tsubota K. Sjogren's syndrome (SS) and Epstein-Barr virus (EBV) reactivation. *Ocul Immunol Inflammation* (1994) 2(2):101–9. doi: 10.3109/09273949409057066
27. Pasoto SG, Natalino RR, Chakkour HP, Viana Vdos S, Bueno C, Leon EP, et al. EBV reactivation serological profile in primary Sjogren's syndrome: an underlying trigger of active articular involvement? *Rheumatol Int* (2013) 33 (5):1149–57. doi: 10.1007/s00296-012-2504-3
28. Kivity S, Arango MT, Ehrenfeld M, Tehori O, Shoenfeld Y, Anaya JM, et al. Infection and autoimmunity in Sjogren's syndrome: a clinical study and comprehensive review. *J Autoimmun* (2014) 51:17–22. doi: 10.1016/j.jaut.2014.02.008
29. Shiboski CH, Shiboski SC, Seror R, Criswell LA, Labetoulle M, Lietman TM, et al. American College of Rheumatology/European League Against Rheumatism classification criteria for primary Sjogren's syndrome: A consensus and data-driven methodology involving three international patient cohorts. *Ann Rheum Dis* (2017) 76(1):9–16. doi: 10.1136/annrheumdis-2016-210571
30. Seror R, Ravaud P, Bowman SJ, Baron G, Tzioufas A, Theander E, et al. EULAR Sjogren's syndrome disease activity index: development of a consensus systemic disease activity index for primary Sjogren's syndrome. *Ann Rheum Dis* (2010) 69(6):1103–9. doi: 10.1136/ard.2009.110619
31. Higgins JP, Thompson SG, Deeks JJ, Altman DG. Measuring inconsistency in meta-analyses. *BMJ* (2003) 327(7414):557–60. doi: 10.1136/bmj.327.7414.557
32. DerSimonian R, Laird N. Meta-analysis in clinical trials. *Controlled Clin Trials* (1986) 7(3):177–88. doi: 10.1016/0197-2456(86)90046-2
33. Yamaoka K, Miyasaka N, Yamamoto K. Possible involvement of Epstein-Barr virus in polyclonal B cell activation in Sjogren's syndrome. *Arthritis Rheum* (1988) 31(8):1014–21. doi: 10.1002/art.1780310812
34. Yang J, Zhang N, Zeng Y, Dong Y, Li H, Han R, et al. [Possible etiological relations between Sjogren's syndrome and Epstein-Barr virus]. *Zhonghua Yi Xue Za Zhi* (1991) 71(3):131–5. 10.
35. Gao C, Xin M, Liu X, Chao Y, Luo B. Detection and Significance of Epstein Barr Virus Markers in Peripheral Blood of Patients with Primary Sjogren's Syndrome. *Prog Modern Biomed* (2010) 10(20):3900–2.
36. Li H, Wang J, Wang L. Analysis of the situation of EB virus infection in patients with Sjögren's syndrome. *Chin J Nosocomiol* (2014) 24(24):6154–5.
37. Yang L, Fu P. Expression of EBNA1 and EBNA2 in the labial salivary gland of patients with sicca syndrome. *J Clin Dermatol* (2015) 44(2):73–7.
38. Zhang L, Wang R, Zhou Y, Zhang G. Correlation between Epstein-Barr virus and Sjögren's syndrome. *Chin Remedies Clinics* (2019) 19(4):556–9.
39. Bo M, Erre GL, Niegowska M, Piras M, Taras L, Longu MG, et al. Interferon regulatory factor 5 is a potential target of autoimmune response triggered by Epstein-barr virus and Mycobacterium avium subsp. paratuberculosis in rheumatoid arthritis: investigating a mechanism of molecular mimicry. *Clin Exp Rheumatol* (2018) 36(3):376–81.
40. Berti A, Felicetti M, Peccatori S, Bortolotti R, Guella A, Vivaldi P, et al. EBV-induced lymphoproliferative disorders in rheumatic patients: A systematic review of the literature. *Joint Bone Spine* (2018) 85(1):35–40. doi: 10.1016/j.jbspin.2017.01.006
41. Hanlon P, Avenell A, Aucott L, Vickers MA. Systematic review and meta-analysis of the sero-epidemiological association between Epstein-Barr virus and systemic lupus erythematosus. *Arthritis Res Ther* (2014) 16(1):R3. doi: 10.1186/ar4429
42. Jog NR, Young KA, Munroe ME, Harmon MT, Guthridge JM, Kelly JA, et al. Association of Epstein-Barr virus serological reactivation with transitioning to systemic lupus erythematosus in at-risk individuals. *Ann Rheum Dis* (2019) 78 (9):1235–41. doi: 10.1136/annrheumdis-2019-215361
43. Kudaeva FM, Speechley MR, Pope JE. A systematic review of viral exposures as a risk for rheumatoid arthritis. *Semin Arthritis Rheum* (2019) 48(4):587–96. doi: 10.1016/j.semarthrit.2018.03.011
44. Tengvall K, Huang J, Hellström C, Kammer P, Biström M, Ayoglu B, et al. Molecular mimicry between Anoctamin 2 and Epstein-Barr virus nuclear antigen 1 associates with multiple sclerosis risk. *Proc Natl Acad Sci U S A* (2019) 116(34):16955–60. doi: 10.1073/pnas.1902623116
45. Csorba K, Schirmbeck LA, Tuncer E, Ribi C, Roux-Lombard P, Chizzolini C, et al. Anti-C1q Antibodies as Occurring in Systemic Lupus Erythematosus Could Be Induced by an Epstein-Barr Virus-Derived Antigenic Site. *Front Immunol* (2019) 10:2619. doi: 10.3389/fimmu.2019.02619
46. Capone G, Calabro M, Lucchese G, Fasano C, Girardi B, Polimeno L, et al. Peptide matching between Epstein-Barr virus and human proteins. *Pathog Dis* (2013) 69(3):205–12. doi: 10.1111/2049-632X.12066
47. Bo M, Niegowska M, Eames HL, Almuttaqi H, Arru G, Erre GL, et al. Antibody response to homologous epitopes of Epstein-Barr virus, Mycobacterium avium subsp. paratuberculosis and IRF5 in patients with different connective tissue diseases and in mouse model of antigen-induced arthritis. *J Transl Autoimmun* (2020) 3:100048. doi: 10.1016/j.jtauto.2020.100048
48. Agmon-Levin N, Dagan A, Peri Y, Anaya JM, Selmi C, Tincani A, et al. The interaction between anti-Ro/SSA and anti-La/SSB autoantibodies and anti-infectious antibodies in a wide spectrum of auto-immune diseases: another angle of the autoimmune mosaic. *Clin Exp Rheumatol* (2017) 35(6):929–35.
49. Sanosyan A, Daien C, Nutz A, Bollore K, Bedin AS, Morel J, et al. Discrepancy of Serological and Molecular Patterns of Circulating Epstein-Barr Virus Reactivation in Primary Sjogren's Syndrome. *Front Immunol* (2019) 10:1153. doi: 10.3389/fimmu.2019.01153
50. Suzuki M, Nagata S, Hiramatsu K, Takagi I, Ito H, Kitao S, et al. Elevated levels of soluble Fc epsilon RII/CD23 and antibodies to Epstein-Barr virus in patients with Sjogren's syndrome. *Acta Otolaryngol Suppl* (1996) 525:108–12.
51. Flores-Chavez A, Kostov B, Solans R, Fraile G, Maure B, Feijoo-Masso C, et al. Severe, life-threatening phenotype of primary Sjogren's syndrome: clinical characterisation and outcomes in 1580 patients (GEAS-SS Registry). *Clin Exp Rheumatol* (2018) 36 Suppl 112(3):121–9.
52. Nocturne G, Virone A, Ng WF, Le Guern V, Hachulla E, Cornec D, et al. Rheumatoid Factor and Disease Activity Are Independent Predictors of Lymphoma in Primary Sjogren's Syndrome. *Arthritis Rheumatol* (2016) 68 (4):977–85. doi: 10.1002/art.39518
53. Brito-Zeron P, Kostov B, Fraile G, Caravia-Duran D, Maure B, Rascon FJ, et al. Characterization and risk estimate of cancer in patients with primary Sjogren syndrome. *J Hematol Oncol* (2017) 10(1):90. doi: 10.1186/s13045-017-0464-5
54. Wilson M, Arroyave C, Miles L, Tan E. Immune reactants in cryoproteins. Relationship to complement activation. *Ann Rheum Dis* (1977) 36(6):540–8. doi: 10.1136/ard.36.6.540
55. Christensen T, Petersen T, Thiel S, Brudek T, Ellermann-Eriksen S, Møller-Larsen A. Gene-environment interactions in multiple sclerosis: innate and adaptive immune responses to human endogenous retrovirus and herpesvirus antigens and the lectin complement activation pathway. *J Neuroimmunol* (2007) 183(1-2):175–88. doi: 10.1016/j.jneuroim.2006.09.014
56. Mold C, Bradt BM, Nemerow GR, Cooper NR. Epstein-Barr virus regulates activation and processing of the third component of complement. *J Exp Med* (1988) 168(3):949–69. doi: 10.1084/jem.168.3.949
57. Weis JH, Morton CC, Bruns GA, Weis JJ, Klickstein LB, Wong WW, et al. A complement receptor locus: genes encoding C3b/C4b receptor and C3d/Epstein-Barr virus receptor map to 1q32. *J Immunol* (1987) 138(1):312–5.
58. Wands JR, Perrotto JL, Isselbacher KJ. Circulating immune complexes and complement sequence activation in infectious mononucleosis. *Am J Med* (1976) 60(2):269–72. doi: 10.1016/0002-9343(76)90436-8
59. Vivanco F, Muñoz E, Vidarte L, Pastor C. The covalent interaction of C3 with IgG immune complexes. *Mol Immunol* (1999) 36(13-14):843–52. doi: 10.1016/s0161-5890(99)00105-4
60. Gulley ML. Molecular diagnosis of Epstein-Barr virus-related diseases. *J Mol Diagn* (2001) 3(1):1–10. doi: 10.1016/S1525-1578(10)60642-3
61. Cardenas-Mondragon MG, Torres J, Sanchez-Zauco N, Gomez-Delgado A, Camorlinga-Ponce M, Maldonado-Bernal C, et al. Elevated Levels of Interferon-gamma Are Associated with High Levels of Epstein-Barr Virus

Reactivation in Patients with the Intestinal Type of Gastric Cancer. *J Immunol Res* (2017) 2017:7069242. doi: 10.1155/2017/7069242
62. Christian LM, Iams JD, Porter K, Glaser R. Epstein-Barr virus reactivation during pregnancy and postpartum: effects of race and racial discrimination. *Brain Behav Immun* (2012) 26(8):1280–7. doi: 10.1016/j.bbi.2012.08.006
63. Masuda S, Mori M, Arai K, Uzawa A, Muto M, Uchida T, et al. Epstein-Barr virus persistence and reactivation in neuromyelitis optica. *J Neurol Neurosurg Psychiatry* (2015) 86(10):1137–42. doi: 10.1136/jnnp-2014-308095
64. Hutt-Fletcher L. Epstein-Barr virus entryl. *J Virol* (2007) 81(15):7825–32. doi: 10.1128/JVI.00445-07
65. Crawford D. Biology and disease associations of Epstein-Barr virus. *Philos Trans R Soc Lond B Biol Sci* (2001) 356(1408):461–73. doi: 10.1098/rstb.2000.0783
66. Wen S, Shimizu N, Yoshiyama H, Mizugaki Y, Shinozaki F. Takada K.Association of Epstein-Barr virus (EBV) with Sjögren's syndrome: differential EBV expression between epithelial cells and lymphocytes in salivary glands. *Am J Pathol* (1996) 149(5):1511–7.
67. Tonoyan L, Vincent-Bugnas S, Olivieri CV, Doglio A. New Viral Facets in Oral Diseases: The EBV Paradox. *Int J Mol Sci* (2019) 20(23):5861. doi: 10.3390/ijms20235861
68. Fox RI, Pearson G, Vaughan JH. Detection of Epstein-Barr virus-associated antigens and DNA in salivary gland biopsies from patients with Sjogren's syndrome. *J Immunol* (1986) 137(10):3162–8.
69. Venables PJ, Teo CG, Baboonian C, Griffin BE, Hughes RA. Persistence of Epstein-Barr virus in salivary gland biopsies from healthy individuals and patients with Sjögren's syndrome. *Clin Exp Immunol* (1989) 75(3):359–64.
70. Fingeroth JD, Weis JJ, Tedder TF, Strominger JL, Biro PA, Fearon DT. Epstein-Barr virus receptor of human B lymphocytes is the C3d receptor CR2. *Proc Natl Acad Sci U S A* (1984) 81(14):4510–4. doi: 10.1073/pnas.81.14.4510
71. Li Q, Turk SM, Hutt-Fletcher LM. The Epstein-Barr virus (EBV) BZLF2 gene product associates with the gH and gL homologs of EBV and carries an epitope critical to infection of B cells but not of epithelial cells. *J Virol* (1995) 69(7):3987–94. doi: 10.1128/JVI.69.7.3987-3994.1995
72. Kudo T, Tachibana T. Phenotype characteristics of human B cells studied by Epstein-Barr virus infection. II. C3 receptor switching during human B cell differentiation. *Immunol Lett* (1984) 8(6):343–8. doi: 10.1016/0165-2478(84)90022-1
73. Hutt-Fletcher LM. Synergistic activation of cells by Epstein-Barr virus and B-cell growth factor. *J Virol* (1987) 61(3):774–81. doi: 10.1128/JVI.61.3.774-781.1987
74. Masucci MG, Szigeti R, Ernberg I, Hu CP, Torsteinsdottir S, Frade R, et al. Activation of B lymphocytes by Epstein-Barr virus/CR2 receptor interaction. *Eur J Immunol* (1987) 17(6):815–20. doi: 10.1002/eji.1830170613
75. van Noesel CJ, Lankester AC, van Schijndel GM, van Lier RA. The CR2/CD19 complex on human B cells contains the src-family kinase Lyn. *Int Immunol* (1993) 5(7):699–705. doi: 10.1093/intimm/5.7.699
76. Portis T, Longnecker R. Epstein-Barr virus (EBV) LMP2A mediates B-lymphocyte survival through constitutive activation of the Ras/PI3K/Akt pathway. *Oncogene* (2004) 23(53):8619–28. doi: 10.1038/sj.onc.1207905
77. Price AM, Dai J, Bazot Q, Patel L, Nikitin PA, Djavadian R, et al. Epstein-Barr virus ensures B cell survival by uniquely modulating apoptosis at early and late times after infection. *Elife* (2017) 6:e22509. doi: 10.7554/eLife.22509
78. Pender MP. Infection of autoreactive B lymphocytes with EBV, causing chronic autoimmune diseases. *Trends Immunol* (2003) 11):584–8. doi: 10.1016/j.it.2003.09.005
79. Croia C, Serafini B, Bombardieri M, Kelly S, Humby F, Severa M, et al. Epstein-Barr virus persistence and infection of autoreactive plasma cells in synovial lymphoid structures in rheumatoid arthritis. *Ann Rheum Dis* (2013) 72(9):1559–68. doi: 10.1136/annrheumdis-2012-202352
80. Paterson RL, Kelleher C, Amankonah TD, Streib JE, Xu JW, Jones JF, et al. Model of Epstein-Barr virus infection of human thymocytes: expression of viral genome and impact on cellular receptor expression in the T-lymphoblastic cell line, HPB-ALL. *Blood* (1995) 85(2):456–64. doi: 10.1182/blood.V85.2.456.bloodjournal852456
81. Long Y, Zhao X, Xia C, Liu X, Fan C, Liu C. Infection of Epstein-Barr Virus is Associated with the Decrease of Helios(+)FoxP3(+)Regulatory T Cells in Active Ulcerative Colitis Patients. *Immunol Invest* (2020). doi: 10.1080/08820139.2020.1723021
82. Salloum N, Hussein HM, Jammaz R, Jiche S, Uthman IW, Abdelnoor AM, et al. Epstein-Barr virus DNA modulates regulatory T-cell programming in addition to enhancing interleukin-17A production via Toll-like receptor 9. *PloS One* (2018) 13(7):e0200546. doi: 10.1371/journal.pone.0200546
83. Tirotta E, Duncker P, Oak J, Klaus S, Tsukamoto MR, Gov L, et al. Epstein-Barr virus-induced gene 3 negatively regulates neuroinflammation and T cell activation following coronavirus-induced encephalomyelitis. *J Neuroimmunol* (2013) 254(1-2):110–6. doi: 10.1016/j.jneuroim.2012.10.005
84. Babcock GJ, Hochberg D, Thorley-Lawson AD. The expression pattern of Epstein-Barr virus latent genes in vivo is dependent upon the differentiation stage of the infected B cell. *Immunity* (2000) 13(4):497–506. doi: 10.1016/s1074-7613(00)00049-2
85. Adler B, Schaadt E, Kempkes B, Zimber-Strobl U, Baier B, Bornkamm GW. Control of Epstein-Barr virus reactivation by activated CD40 and viral latent membrane protein 1. *Proc Natl Acad Sci U S A* (2002) 99(1):437–42. doi: 10.1073/pnas.221439999
86. Nagata K, Kumata K, Nakayama Y, Satoh Y, Sugihara H, Hara S, et al. Epstein-Barr Virus Lytic Reactivation Activates B Cells Polyclonally and Induces Activation-Induced Cytidine Deaminase Expression: A Mechanism Underlying Autoimmunity and Its Contribution to Graves' Disease. *Viral Immunol* (2017) 30(3):240–49. doi: 10.1089/vim.2016.0179
87. Wang H, Nicholas MW, Conway KL, Sen P, Diz R, Tisch RM, et al. EBV latent membrane protein 2A induces autoreactive B cell activation and TLR hypersensitivity. *J Immunol* (2006) 177(5):2793–802. doi: 10.4049/jimmunol.177.5.2793
88. Croia C, Astorri E, Murray-Brown W, Willis A, Brokstad KA, Sutcliffe N, et al. Implication of Epstein-Barr virus infection in disease-specific autoreactive B cell activation in ectopic lymphoid structures of Sjogren's syndrome. *Arthritis Rheumatol* (2014) 66(9):2545–57. doi: 10.1002/art.38726
89. Onuora S. Connective tissue diseases: Epstein-Barr virus in Sjogren's syndrome salivary glands drives local autoimmunity. *Nat Rev Rheumatol* (2014) 10(7):384. doi: 10.1038/nrrheum.2014.97
90. Vaughan JH, Nguyen MD, Valbracht JR, Patrick K, Rhodes GH. Epstein-Barr virus-induced autoimmune responses. II. Immunoglobulin G autoantibodies to mimicking and nonmimicking epitopes. Presence in autoimmune disease. *J Clin Invest* (1995) 95(3):1316–27. doi: 10.1172/JCI117782
91. Vaughan JH, Valbracht JR, Nguyen MD, Handley HH, Smith RS, Patrick K, et al. Epstein-Barr virus-induced autoimmune responses. I. Immunoglobulin M autoantibodies to proteins mimicking and not mimicking Epstein-Barr virus nuclear antigen-1. *J Clin Invest* (1995) 95(3):1306–15. doi: 10.1172/JCI117781
92. Hung T, Pratt GA, Sundararaman B, Townsend MJ, Chaivorapol C, Bhangale T, et al. The Ro60 autoantigen binds endogenous retroelements and regulates inflammatory gene expression. *Science* (2015) 350(6259):455–9. doi: 10.1126/science.aac7442
93. Cusick MF, Libbey JE, Fujinami RS. Molecular mimicry as a mechanism of autoimmune disease. *Clin Rev Allergy Immunol* (2012) 42(1):102–11. doi: 10.1007/s12016-011-8293-8
94. Navone R, Lunardi C, Gerli R, Tinazzi E, Peterlana D, Bason C, et al. Identification of tear lipocalin as a novel autoantigen target in Sjogren's syndrome. *J Autoimmun* (2005) 25(3):229–34. doi: 10.1016/j.jaut.2005.09.021
95. Quan TE, Roman RM, Rudenga BJ, Holers VM, Craft JE. Epstein-Barr virus promotes interferon-alpha production by plasmacytoid dendritic cells. *Arthritis Rheum* (2010) 62(6):1693–701. doi: 10.1002/art.27408
96. Gujer C, Murer A, Müller A, Vanoaica D, Sutter K, Jacque E, et al. Plasmacytoid dendritic cells respond to Epstein-Barr virus infection with a distinct type I interferon subtype profile. *Blood Adv* (2019) 3(7):1129–44. doi: 10.1182/bloodadvances.2018025536

Conflict of Interest: The authors declare that the research was conducted in the absence of any commercial or financial relationships that could be construed as a potential conflict of interest.

Advantages of publishing in Frontiers

OPEN ACCESS
Articles are free to read for greatest visibility and readership

FAST PUBLICATION
Around 90 days from submission to decision

HIGH QUALITY PEER-REVIEW
Rigorous, collaborative, and constructive peer-review

TRANSPARENT PEER-REVIEW
Editors and reviewers acknowledged by name on published articles

Frontiers
Avenue du Tribunal-Fédéral 34
1005 Lausanne | Switzerland

Visit us: www.frontiersin.org
Contact us: frontiersin.org/about/contact

REPRODUCIBILITY OF RESEARCH
Support open data and methods to enhance research reproducibility

DIGITAL PUBLISHING
Articles designed for optimal readership across devices

FOLLOW US
@frontiersin

IMPACT METRICS
Advanced article metrics track visibility across digital media

EXTENSIVE PROMOTION
Marketing and promotion of impactful research

LOOP RESEARCH NETWORK
Our network increases your article's readership